SENSITIVITY OF THE HAZEN PLATEAU AND NORTH COAST, ELLESMERE ISLAND, NUNAVUT, CANADA TO CLIMATE CHANGE

A Dissertation Presented

by

CARSTEN BRAUN

Submitted to the Graduate School of the
University of Massachusetts Amherst in partial fulfillment
of the requirements for the degree of

DOCTOR OF PHILOSOPHY

May 2006

Department of Geosciences

UMI Number: 3216942

Copyright 2006 by
Braun, Carsten

All rights reserved.

INFORMATION TO USERS

The quality of this reproduction is dependent upon the quality of the copy submitted. Broken or indistinct print, colored or poor quality illustrations and photographs, print bleed-through, substandard margins, and improper alignment can adversely affect reproduction.

In the unlikely event that the author did not send a complete manuscript and there are missing pages, these will be noted. Also, if unauthorized copyright material had to be removed, a note will indicate the deletion.

UMI®

UMI Microform 3216942
Copyright 2006 by ProQuest Information and Learning Company.
All rights reserved. This microform edition is protected against unauthorized copying under Title 17, United States Code.

ProQuest Information and Learning Company
300 North Zeeb Road
P.O. Box 1346
Ann Arbor, MI 48106-1346

© Copyright by Carsten Braun 2006

All Rights Reserved

SENSITIVITY OF THE HAZEN PLATEAU AND NORTH COAST, ELLESMERE ISLAND, NUNAVUT, CANADA TO CLIMATE CHANGE

A Dissertation Presented

by

CARSTEN BRAUN

Approved as to style and content by:

Raymond S. Bradley, Chair

William D. McCoy, Member

Robert M. DeConto, Member

Douglas R. Hardy, Member

Jonathan Machta, Member

Michael L. Williams, Department Head
Department of Geosciences

ACKNOWLEDGMENTS

This research project was supported by a U.S. National Science Foundation Grant (OPP-9819362) to the University of Massachusetts. Additional financial support was provided by the Graduate School of the University of Massachusetts, by the Department of Geosciences, by the Isenberg School of Management, by the Geological Society of America, by the Everywoman's Center, by the UMass Police Department, and by Parks Canada (Nunavut Field Unit).

ABSTRACT

SENSITIVITY OF THE HAZEN PLATEAU AND NORTH COAST, ELLESMERE ISLAND, NUNAVUT, CANADA TO CLIMATE CHANGE

MAY 2006

CARSTEN BRAUN, B.S., UNIVERSITY OF FREIBURG

M.S., UNIVERSITY OF MASSACHUSETTS AMHERST

Ph.D., UNIVERSITY OF MASSACHUSETTS AMHERST

Directed by: Professor Raymond S. Bradley

The objective of this study is to test the hypothesis that the Hazen Plateau and North Coast of Ellesmere Island, Nunavut, Canada are two environmentally-sensitive area where relatively slight changes in meteorological conditions can lead to dramatic changes in snow and firn extent in the short-term, and to a systematic shift in the regional glaciation level in the long-term. The study represents an integrated program of field measurements, data analysis, and data modeling to determine the nature of the land-atmosphere-snow and ice interactions and to quantify the sensitivity of snow and ice cover on the Hazen Plateau and along the North Coast to climate change. The glaciers along the northern coast of Ellesmere Island, specifically the Ward Hunt Ice Rise and Ice Shelf, are today not in equilibrium with climatic conditions and will disappear at some point in the near future unless climatic conditions deteriorate dramatically. Dynamical stresses related to wind, wave, and tidal action may further accelerate this process, as open water conditions on the Arctic Ocean become more prevalent. Mass losses occurring at the bottom of the floating ice shelf are more significant in terms of its stability than the associated surface mass losses. The Hazen Plateau ice caps have experienced considerable marginal recession and significant overall mass loss since at least 1959. The sensitivity of these ice caps to changes in climate is enhanced by the low amounts of winter snow accumulation, the absence of iceflow, and their small vertical relief. They are also out-of-equilibrium with modern climate and considered to be relicts of past climatic conditions with reduced summer melt and/or increased snowfall.

TABLE OF CONTENTS

LIST OF TABLES

LIST OF FIGURES

CHAPTER 1

INTRODUCTION

One of the many key issues surrounding past and future climate change is the role of the Arctic under a climate warming scenario, since the high-latitude temperature response to increased greenhouse gas concentrations is expected to be greater (= polar amplification) than the response of the mid- and low latitudes (e.g. Sellers, 1973; Holland and Bitz, 2003; Bigelow *et al.*, 2003; Barnett *et al.*, 2005; Chapin III *et al.*, 2005; Meehl *et al.*, 2005; Siegenthaler *et al.*, 2005; Winton, 2006). Ohmura (2000; his Equation 3) showed elegantly that the net temperature change in cold climates (e.g. high latitudes or high altitudes) is greater for the same magnitude of change in the surface energy balance (e.g. due to increased concentrations of greenhouse gases) than the temperature change in warmer climates (e.g. mid- or low-latitudes) (cf. Bintanja and Oerlemans, 1995). The particular climatic sensitivity of high-latitude climates is additionally explained by the operation of two positive (and synergistic) feedback processes (Barry, 1996; Walsh *et al.*, 2002; Holland and Bitz, 2003; Bigelow *et al.*, 2003; Hall, 2004; Rial *et al.*, 2004):

- Changes in the thermal inertia (albedo) of the ocean (surface), as a consequence of changes in Arctic Ocean sea ice extent, thickness, and duration (e.g. Robock, 1983; Johannessen *et al.*, 2004).
- Changes in the albedo of the adjacent land surface as a consequence of changes in snow cover extent and duration (e.g. Robock. 1980; Chapin III *et al.*, 2005).

For example, higher air temperatures can reduce the extent of highly reflective sea ice or snow cover, which in turn increases the absorption of atmospheric energy at the Earths surface, which in turn leads to further sea-ice and snow cover reduction. Thus, a positive feedback loop is established. Overall, the climatic variability caused by sea ice variations (and the associated albedo-temperature feedback) appears to be about twice (Robock, 1983; Bintanja and Oerlemans, 1995) or perhaps 5-8 times (Harvey, 1988) as large as for snow cover variations on land. However, exposure of large areas of the Arctic Ocean

with cold open water, which has a high capacity for CO_2 absorption, could become in turn a significant sink for atmospheric CO_2, thus mitigating 'Global Warming' (Laxon *et al.*, 2003) to some extent. More recently, Feddema *et al.* (2005) reported on the interactions and feedbacks between changes in global land cover/land use and climate for the 21st century.

1.1 A Short History of High Arctic Climate and Glaciation

The term 'Little Ice Age' was originally coined by Matthes (1939) with reference to the re-growth of glaciers in the Sierra Nevada of California, following their disappearance during the Early Holocene. The so-called 'Little Ice Age' (~1250 to 1900) (Koerner, 1989a; Bradley *et al.*, 2003) was characterized by the coldest summers of the entire Holocene (Koerner and Fisher, 1990) and instrumental and paleoclimatic records indicate that the coldest part of the 'Little Ice Age' (~1550 to 1900) was about 1.0 to 3.0°C colder than the 20th century (Williams, 1978a; Dowdeswell, 1995; Dowdeswell *et al.*, 1997; Dowdeswell and Hagen, 2003). As a result, many glaciers in the Canadian High Arctic (and elsewhere around the world, e.g. Luckman, 2000; Nesje and Dahl, 2003; Grove, 2001; 2004; Matthews and Briffa, 2005) expanded in size and volume to reach a distinct Holocene maximum towards the end of the 'Little Ice Age' (Koerner, 1989a; Dowdeswell *et al.*, 1997; Koerner and Fisher, 2002, Miller *et al.*, 2005).

Thorarinsson (1940) offered a detailed and comprehensive review of global changes in glacier extent as documented in the scientific literature since the turn of the century and came to the following four generalized conclusions:

1. "The majority of the glaciers in practically every glacier district around the world are now receding, i.e. the present glacier shrinkage is a universal phenomena."
2. "The marginal variations of the glaciers in recent centuries have in all probability been more or less concurrent all over the world."
3. "Since the middle or latter half of the 19th century the glaciers have thus been retreating from positions equal to or approximating their maximum extent in historical times."
4. "The great total recession of the glaciers has taken place in several stages of ever increasing intensity, interrupted by intervals of stagnation or advance."

At least the first two conclusions are strikingly similar to those of the most recent comprehensive global glacier mass balance survey based on measurements collected over the last four decades (Dyurgerov, 2002). Geoff Hattersley-Smith, arguably the dean of modern Canadian High Arctic

glaciology, quoted the following two statements from a lecture given by H.W. Ahlmann in 1953, who was (at that time) "the foremost authority to point out the probable connexion between recent climatic fluctuations and the recent recession of the glaciers around the northernmost Atlantic" (Hattersley-Smith, 1960a).

> "...increased ablation, consequent upon the increase in temperature, has played the fundamental role in the recession of glaciers..."

Ahlmann (1953) continued to note that:

> "It is probable that the rise in spring and autumn temperatures, i.e. the lengthening of the ablation season has been of particular importance." (cf. Ahlman, 1936)

This idea had been put forward already by Kinger (1940), who commented on the connection between glacier recession and relatively high temperatures during the early parts of the 20th century. It is important to remember that Kinger (1940), Thorarinsson (1940), and Ahlmann (1953) were referring to the global recession of glaciers between about 1850 and 1950 (i.e. since the end of the 'Little Ice Age'). Geoff Hattersley-Smith himself was clearly impressed and concerned by the amount of recent glacier recession and mass loss he witnessed upon first visiting the northern coast of Ellesmere Island in 1953 (Hattersley-Smith, 1954; Hattersley-Smith *et al.*, 1955). He was also notably pessimistic about the future survival of glaciers in the Canadian High Arctic:

> "From the present gradual wastage deduced from surface observations, it is concluded that only a slight amelioration of climate would be extremely destructive to the [Ward Hunt] ice shelf. For example, continual mild seasons, like that of 1954, would cause the whole of the present mass of the ice shelf to melt in about 80 years." (Hattersley-Smith *et al.*, 1955)

Fortunately, the comparatively warm climatic conditions of the 1950s and early 1960s did not persist much longer, and in fact much of the Canadian High Arctic experienced overall colder summers, increased precipitation, positive glacier mass balance, and glacier expansion between the mid-1960s and mid-1970s (Bradley and Miller, 1972; Bradley, 1973; Bradley and England, 1978; Alt, 1987; Braun *et al.*, 2004a, b). For example, Hattersley-Smith and Serson (1970) reached the following much more optimistic

conclusion regarding the mass balance regime of the Ward Hunt Ice Rise and Ice Shelf at that particular time:

> "Quite small deviations from mean summer temperature appear to determine whether the mass balance is positive or negative, and for this reason neither the ice rise nor the ice shelf should be considered a relict glacial feature."

Hattersley-Smith and Serson (1973) also came to this upbeat assessment regarding the glaciologic 'health' of the larger St. Patrick Bay ice cap on the Hazen Plateau and the future of glaciation on north-eastern Ellesmere Island in general:

> "It now appears to be in a healthy state and is spreading laterally as well as thickening...If the trend to cooler summers continues, extension of snow banks and development of thin ice caps may be expected in the general region south-west of Alert."

Finally, Bradley and England (1978) summarized the current climatic conditions in the Canadian High Arctic and their influence on glacier mass balance as follows:

> "These conditions [during the mid-1960s to mid-1970s] resulted in much reduced net mass losses on glaciers in the region after 1963 than in the preceding period. No evidence for a return to pre-1963 conditions is yet apparent."

Yet, these more favorable climatic conditions for glaciation did not persist for much longer, and the overall cumulative mass balance of the monitored Canadian High Arctic glaciers has been highly negative now for the last 40 years or so, with a consistent turn towards more negative values during the 1990s (Koerner, 1995, 2001; Dowdeswell *et al.*, 1997; Serreze *et al.*, 2000; Braun *et al.*, 2004a, b).

These selected examples highlight the possible pitfalls associated with future predictions based on a relatively short temporal perspective (cf. Chapter 5). It is entirely possible that the most recent 10 to 15 years of climate change represent merely an unusual phase of variability, as recorded before in terms of glacier mass balance and climate during the comparatively warm 1930s, 1940s, 1950s and early 1960s (Diamond, 1960; Hattersley-Smith, 1969; Holdsworth, 1984; Warren, 1990; Bengtsson *et al.*, 2004; Johannessen *et al.*, 2004). Bengtsson *et al.* (2004) noted, for example, that present warming in the Arctic has just now reached the peak warming values of the 1940s (cf. Davies and Krinsley, 1962; Warren,

1990). On the other hand, such an interpretation must be balanced against the significant and widespread environmental changes already underway in the Arctic and elsewhere (e.g. Serreze *et al.*, 2000; Comiso, 2002a, b, 2003; Kuhry *et al.*, 2002; Serreze *et al.*, 2003; Wang and Key, 2003; ACIA, 2005; Burgess and Sharp, 2004; Hinzman *et al.*, 2005; Overpeck *et al.*, 2005; Raper and Braithwaite, 2006) and the consistency of climate model predictions for a continued, and probably accelerated, warming at high latitudes (e.g. Houghton *et al.*, 2001; Walsh and Timlin, 2003; Johannessen *et al.*, 2004) in the foreseeable future. Nevertheless, superimposed on this overall climate warming is a high degree of multi-year internal climatic variability (Bengtsson *et al.*, 2004), which may overwhelm the long-term signal at times (e.g. Kahl *et al.*, 1993).

1.2 Hypothesis, Objectives, and Strategy

I hypothesize that the Hazen Plateau and North Coast of Ellesmere Island, Nunavut, Canada are two environmentally-sensitive zones where relatively slight changes in meteorological conditions can lead to dramatic changes in snow and firn extent in the short-term, and to a systematic shift in the regional glaciation level in the long-term. I conducted an integrated program of field measurements, data analysis, and data modeling to test this hypothesis and to determine the nature of the associated land-atmosphere-snow and ice interactions. My basic research objective was to quantitatively evaluate the sensitivity of snow and ice cover on the Hazen Plateau and along the North Coast to climate change. This project was originally conceived by R.S. Bradley and D.R. Hardy and funded by a U.S. National Science Foundation Grant (OPP-9819362) to the University of Massachusetts. Thus, the original grant proposal narrative provides the basic scientific framework for this project.

The research strategy consisted of four complementary tasks and is reflected in the formal organization of this thesis (Section 1.3). First, it was necessary to conduct a thorough review of the available scientific literature to provide a thematic and geographic context for this research (Chapter 2). Second, it was necessary to create a temporal context for the short-term data collected during this project by developing suitable mass balance histories for the Hazen Plateau and North Coast of Ellesmere Island (Chapters 3 and 4). Third, it was necessary to define the modern climatic conditions for the two study areas (Chapter 5). Finally, simple modeling experiments were used to quantitatively explore the

sensitivity of snow and ice cover on the Hazen Plateau and along the North Coast of Ellesmere Island to climate change (Chapter 6).

1.3 Thesis Organization

- Chapter 1 Introduction
- Chapter 2 Glaciation of the Hazen Plateau and North Coast, Ellesmere Island, Nunavut, Canada
- Chapter 3 Mass Balance and Area Changes of four High Arctic Plateau Ice Caps, 1959-2002 (Braun *et al.*, 2001, 2004a)
- Chapter 4 Surface Mass Balance of the Ward Hunt Ice Rise and Ice Shelf, Ellesmere Island, Nunavut, Canada (Braun *et al.*, 2004b)
- Chapter 5 Climatology of the Hazen Plateau and North Coast, Ellesmere Island, Nunavut, Canada
- Chapter 6 Sensitivity of the Hazen Plateau and North Coast to Climate Change
- Chapter 7 Summary and Conclusions

CHAPTER 2

GLACIATION OF THE HAZEN PLATEAU AND NORTH COAST, ELLESMERE ISLAND, NUNAVUT, CANADA

Chapter 2 describes the glaciation of northern Ellesmere Island in the context of its sensitivity to current, future, and past climate change. In essence, it represents a comprehensive, albeit subjective, review of the relevant scientific literature. Section 2.1 gives a brief geographic introduction of the Hazen Plateau and North Coast of Ellesmere Island. A more elaborate description of the geography and mass balance history of the Hazen Plateau ice caps (unofficial name) and Ward Hunt Ice Rise and Ice Shelf is provided in Chapter 3 and 4 (i.e. Braun *et al.*, 2004a, b). Section 2.2 presents and discusses a selection of 'geographic analogues' around the world with the goal of highlighting some of the specific climatic and geographic factors relevant in the context of glaciation and its climatic sensitivity. Section 2.3 focuses on how glaciation of a particular locality might be achieved from a broad conceptual point of view, using the two opposing models proposed by Flint (1943) and Ives *et al.* (1975). Both models are entirely qualitative, but offer important insights into the processes and feedbacks associated with the onset of glaciation, especially with regard to the interactions between local/regional topography, local/regional climate, and the initiation, expansion, and eventual demise of permanent snow and ice cover as a function of climate change. Such processes, interactions, and feedbacks have to be incorporated into any more quantitative attempts to model the changes of snow and ice extent at any particular location as a result of climate change. Section 2.4, finally, discusses the climatic sensitivity of glaciers and the interactions between external forcing (e.g. climate and topography) and internal factors (e.g. glacier mass balance and ice flow). It is obvious that products of climate change have a profound effect on glaciers – however, the exact type(s) of response(s), and associated rate(s) of change, is (are) very much determined by the specific sensitivity of a given glacier to such external changes.

2.1 Glaciation of the Hazen Plateau and North Coast, Ellesmere Island, Nunavut, Canada

Northern Ellesmere Island (Fig. 2.1) can be subdivided into four different physiographic regions, based on their broad geographical similarities: 1) The Hazen Plateau (Fig. 2.2, 2.3); 2) the Grantland Mountains; 3) the Lake Hazen Basin; and 4) the North Coast (Fig. 2.4) (Humphreys *et al.*, 1936; Bednarski, 1994). Today, much of the region is protected within Quttinirpaaq (formerly Ellesmere Island) National Park, the northernmost national park in North America. The northern boundary of the Grantland Mountains (unofficial name) is defined by the northern coast of Ellesmere Island (Fig. 2.4), forming an narrow apron between Ellesmere Island and the Arctic Ocean. The Grantland Mountains are covered by large ice caps and valley glaciers up to 900 m thick (Hattersley-Smith *et al.*, 1969) which are penetrated by isolated summits forming nunataks. The main backbone of the Grantland Mountains is the U.S. Range / British Empire Range (Moore *et al.*, 1936). This NE-SW trending topographic divide reaches elevations over 2000 m above sea level (asl) and separates the main valley glaciers that flow towards the Arctic Ocean from those flowing towards the Lake Hazen basin (Fig. 2.1).

Glaciation along the northern coast of Ellesmere Island includes several large outlet glaciers draining the large Grantland Mountains ice caps, small low-elevation ice rises and plateau ice caps, and the only ice shelves (cf. Chapter 4) found today in the northern hemisphere (Fig. 2.4, 2.5) (Gray, 1994). Most of the Hazen Plateau is currently unglacierized, with the exception of several small, stagnant ice caps (cf. Chapter 3) along its southwest and southeast margin (Fig. 2.2, 2.3). In contrast, the Grantland Mountains are covered by the largest and thickest ice cap in the Northern Hemisphere, second only to the Greenland Ice Sheet (Bednarski, 1994). Small, stagnant ice caps/ice rises persist today, either on the high-elevation plateau areas of northern Ellesmere Island (Hazen Plateau) or at low elevation in close proximity to the Arctic Ocean (North Coast), presumably because of increased moisture availability and reduced ablation due to frequent fog and low-level clouds (Koerner, 1979).

2.1.1 The Hazen Plateau of Ellesmere Island

The Hazen Plateau, Ellesmere Island, Canada (Fig. 2.2, 2.3) forms a large upland plateau region, gently rising from about 175 m asl near Lake Hazen to over 1000 m asl along the northeast coast of Ellesmere Island (see also Fig. 2.6). This large plateau surface is essentially unglaciated today, except for

two pairs of small, thin, and stagnant ice caps (Hazen Plateau ice caps, unofficial name) along its southeastern margin. Murray and Simmons Ice Cap together range in elevation between about 960 and 1100 m asl. The St. Patrick Bay ice caps (unofficial name) are located about 110 km to the northeast at slightly lower elevation (~750 to 900 m asl), possibly related to the influence of local moisture sources from nearby Nares Strait/Kane Basin (Hattersley-Smith and Serson, 1973).

The Hazen Plateau ice caps exist today almost at the same elevation as adjacent ice-free plateau areas. This peculiar juxtaposition of ice-free and ice-covered plateau areas, for no immediately apparent reason, indicates that the main plateau surface is relatively close to the regional equilibrium-line altitude (ELA) or glaciation level (Miller *et al.*, 1975). The glacial history of the Hazen Plateau is still largely unknown today, although localized permanent ice cover may have persisted throughout the entire Holocene at selected favorable, high-elevation locations (Smith, 1999; 2002). However, it is also possible that the Hazen Plateau ice caps did not survive the Holocene Climatic Optimum and instead re-formed on the plateau more recently, perhaps during the so-called main phase of the 'Little Ice Age' (~1600 to 1900) (Koerner, 1989a, 2002; Koerner and Fisher, 2002; Bradley *et al.*, 2003). The Hazen Plateau ice caps apparently reached their Holocene maximum extent and were several times larger during the so-called 'Little Ice Age' (Braun *et al.*, 2004a). Dyke (1983), Edlund (1985), and Dowdeswell and Dowdeswell (2004) have described similar ice-cap expansions during the 'Little Ice Age' on northern Somerset, western Melville Island, and Bylot Island. The Hazen Plateau ice caps probably maintained their maximum Neoglacial extents as late as around 1925 (cf. Hattersley-Smith, 1969; Bengtsson *et al.*, 2004), but experienced considerable marginal recession and significant overall mass losses since at least 1959 (Braun *et al.*, 2004a). There is additional evidence from snow-pit and firn-core studies (Hattersley-Smith, 1963; 1969), and instrumental climate records, for further elevated summer temperatures (~1 to 2°C), increased glacier melting, and glacier recession in the period from about 1925 to 1961 (Diamond, 1960; Davies and Krinsley, 1962; Holdsworth, 1984; Koerner, 1996, 2001; Bengtsson *et al.*, 2004; Johannessen *et al.*, 2004). This suggests overall more negative glacier mass balances in the Canadian High Arctic and northern Greenland during the first part of the 20th century, compared to the last 40 years of direct glaciological measurements (Fristrup, 1951; Koerner, 1996). However, Bengtsson *et al.* (2004) noted more recently that present warming in the Arctic has now surpassed the peak warming values of the

1940s (cf. Davies and Krinsley, 1962; Warren, 1990). The regional ELA is located today, on average, above the summits of the ice caps and the plateau surface, indicating that they are out-of-equilibrium with current climatic conditions, and thus represent relict ice features on an otherwise unglaciated plateau surface (Bradley and Serreze, 1987a; Braun *et al.*, 2004a). Thus, the regional glaciation level, as determined by the presence of 'permanent' ice cover (Miller *et al.*, 1975), is in reality not in equilibrium with modern climate (Williams *et al.*, 1978b) and rather represents a 'paleo'-glaciation level.

Nevertheless, relatively small changes in climate can lead to significant changes in the extent of snow and ice cover on the Hazen Plateau. For example, the Hazen Plateau ice caps experienced predominantly positive mass balance years and ice cap expansion from the mid-1960s to mid-1970s, a time period characterized by reduced summer melt and perhaps increased precipitation throughout much of the Canadian High Arctic (Braun *et al.*, 2004a, and references therein).

2.1.2 The North Coast of Ellesmere Island

Ice shelves in the Canadian High Arctic are typically formed from in-situ accumulations of multiyear landfast sea ice, surface snow accumulations, and basal freezing of seawater, with only minor direct mass input from associated upstream land glaciers (as opposed to the 'typical' Antarctic-type ice shelf) (Hattersley-Smith *et al.*, 1955; Vincent *et al.*, 2001; Jeffries, 2002). Debenham (1954), for example, argued that the ice shelf represents "some unusual form of sea ice". The ice shelves along Ellesmere Island's north coast probably formed initially some 3000 to 4000 years ago (Jeffries and Krouse, 1984; Evans and England, 1992; Jeffries, 1994) as climatic conditions in the High Arctic deteriorated from the early/mid Holocene warm phase (Bradley, 1990). The High Arctic ice shelves were first described as 'paleocrystic ice' by the Nares expeditions, although the Eskimo word 'sikussak' (i.e. very old ice) appears to be roughly equivalent (Koch, 1926). The entire northern coastline of the island (Fig. 2.1, 2.5) appears to have been fringed by a continuous ice shelf some 500 km in length as late as the turn of the century (Hattersley-Smith, 1960a; Vincent *et al.*, 2001). The map presented by Koch (1926; his Fig. 1) shows paleocrystic ice also extending all the way around the northern tip of Greenland at that time. There is also some evidence to suggest that ice shelf-like features existed along the eastern coast of Ellesmere Island and western coast of Greenland in the early 20th century (Wright, 1940). This larger

Ellesmere Ice Shelf progressively disintegrated over the course of the 20th century and today only about 10 percent remains (Vincent *et al.*, 2001), the largest remnant being the Ward Hunt Ice Shelf (Fig. 2.4). The ice shelf fractured into two distinct pieces just to the south of Ward Hunt Island between 2000 and 2002, after experiencing some 20 years of relative stability (Mueller *et al.*, 2003). The causes behind the disintegration of the Ellesmere and Ward Hunt ice shelves over the last 100 years are still a subject of debate (cf. Section 2.2.2.5), but are likely a combination of several mechanisms, including wind/wave/tidal action, pressure by Arctic Ocean pack ice, and recent climate change (Scambos *et al.*, 2000; Vincent *et al.*, 2001; Mueller *et al.*, 2003). The Ward Hunt Ice Rise (Fig. 2.4) is between 40 and 100 m thick and probably formed only within the last ~1500 years when the ice shelf thickened and grounded on the isostatically-uplifted seafloor north of Ward Hunt Island (Lyons and Ragle, 1962; Lyons *et al.*, 1972) (cf. Section 2.2.2.5).

2.1.3 The Glaciation Level of northern Ellesmere Island

The lowest glaciation levels (= the lowest elevation at which ice can persist on a given landscape; Ahlmann, 1948) and glacier equilibrium line altitudes (ELAs, i.e. the boundary between the accumulation area and ablation area where the mass balance is zero) in the Northern Hemisphere are found today along the northern coast of Ellesmere Island (Miller *et al.,* 1975; Andrews and Barry, 1978), as manifested by low-elevation, coastal ice caps/ice rises and marine ice shelves (such as the Ward Hunt Ice Rise and Ice Shelf; see also Fig. 2.4, 2.6). Frequent fog and low stratus clouds, associated with dominant airflow from the Arctic Ocean, lead to reduced summer ablation in its immediate vicinity (Hattersley-Smith, 1954; Sagar, 1962; Lister, 1962; Paterson, 1969; Hattersley-Smith and Serson, 1970; Koerner, 1979). At the same time, the Arctic Ocean also represents a significant local moisture source (Bradley and Eischeid, 1985; Jeffries and Krouse, 1984; 1987), leading to increased precipitation along the coast relative to the more interior, continental areas of Ellesmere Island (Miller *et al.*, 1975; Koerner, 1979; Edlund and Alt, 1989). This combination of (1) reduced summer melt and (2) enhanced snow accumulation thus appears to be responsible for the very low glacier ELAs along the northern coast of Ellesmere Islands (cf. Miller *et al.*, 1975; Koerner, 1979; Maxwell, 1981; Hardy, 1996) and the existence of the Ward Hunt Ice Rise and Ice Shelf (Braun *et al.*, 2004b).

However, this 'Arctic Ocean Effect' (Braun *et al.*, 2004b) is limited to only a narrow zone right along the coastline (Hattersley-Smith, 1960a). By contrast, the highest ice margins and ELAs in the Canadian High Arctic (800 to 1000 m asl) occur just on the other side of the British Empire / U.S. Range, on the dry continental plateau highlands of northeastern Ellesmere Island (Hazen Plateau, Fig. 2.6) (Miller *et al.*, 1975; Koerner, 1979; England, 1986a). There, snow accumulation is much lower, and summer ablation plays a dominant role in annual glacier mass balance (Braun *et al.*, 2004a). This steep regional glaciation gradient presumably reflects a correspondingly sharp climatic gradient, specifically in terms of snow accumulation and summer melt. Accumulation (ablation) appears to decrease (increase) with horizontal and vertical distance from the Arctic Ocean, as the frequency of fog and stratus cloud conditions and associated temperature inversions decreases towards the interior and high-elevation parts of Ellesmere Island (cf. Humlum, 1985, Lie *et al.*, 2003a, b). It is important to note that the existence of these gradients is largely inferential; detailed, comprehensive measurements of glacier mass balance, modern climate, and paleoclimate do not (yet) exist across these (inferred) gradients and transitions.

2.2 Geographic Analogues for the Hazen Plateau and North Coast: A Review of the Literature

Section 2.2 describes and discusses what may be considered as 'geographic analogues' for the Hazen Plateau and North Coast and their current snow and ice cover, based on a comprehensive survey of the available scientific literature. There is, in reality, of course no such thing as a 100 percent geographic analogue on Earth – there are always important or subtle differences in the specific geographic characteristics of different areas or regions around the globe. However, it is precisely these geographic differences that make the concept of geographic analogues useful when trying to characterize the geography of an area of interest (e.g. the Hazen Plateau or North Coast of Ellesmere Island) (cf. Matthews and Briffa, 2005; Blöschl, 2006). Previous scientific studies of the Hazen Plateau ice caps (e.g. Braun *et al.*, 2004a) and Ward Hunt Ice Rise and Ice Shelf (e.g. Braun *et al.*, 2004b) are summarized in greater detail in Chapter 3 and Chapter 4.

2.2.1 Geographic Analogues for the Hazen Plateau

2.2.1.1 The Barnes Ice Cap (Baffin Island, Canada)

The Barnes Ice Cap (Fig. 2.5) is today perhaps the closest glaciologic analogue to the Hazen Plateau ice caps in the Canadian High Arctic. The Barnes Ice Cap is located on the broad north-central Baffin Island plateau and probably represents the last contiguous remnant of the former Laurentide Ice Sheet (Ward, 1954; Dyke and Prest, 1987; Andrews, 2002). Baird *et al.* (1952; Page 3) provided the following interesting description of the first glaciologic investigation of the Barnes Ice Cap (in 1950):

> "We were satisfied, however, that we should be up in the accumulation area, and a few days after the camp was set up [~1 June 1950] we began to dig a pit, IAI. Only a few minutes work revealed less than a metre of snow on solid ice. It was obvious that there was no firn here. This was disconcerting." See Orvig (1954; his Fig. 41) for a photograph of this first snow pit on the Barnes Ice Cap.

These were literally the same circumstances and feelings we experienced on Murray and Simmons Ice Cap upon the start of this project on 26 May 1999. It is also worth noting that Hattersley-Smith (1954) described the same situation on the Ward Hunt Ice Shelf. Baird *et al.* (1952; Page 4) continued their initial description and survey of the Barnes Ice Cap by remarking:

> "It occurred to us then that owing to the great cold of the ice and the briefness of the summer season, the snow cover was normally dissipated each year, but a large portion of it was 'superimposed' on the existing ice surface as melting took place; that somewhere on the ice cap was a line corresponding to the firn line where this 'superimposed' ice showed a net gain during the year, and that therefore above this was a true accumulation area."

Baird *et al.* (1952; Page 9) concluded their initial glaciologic description of the Barnes Ice Cap by defining the four basic characteristics of what they considered to represent a typical 'Baffin Type' glacier or ice cap (cf. Ives, 1962):

> "The conditions requisite for such 'Baffin Type' glaciers would seem to be (a) insufficient altitude to reach the local firn line, (b) great residual cold in the ice, (c) light precipitation, and (d) the usual Arctic climatic environment of short cool summers and long cold winters."

This original definition was later expanded upon by Paterson (1969), based on his work on the Meighen Ice Cap (Section 2.2.1.6) to include the following four more specific glaciologic and topographic features of a 'Baffin Type' glacier or ice cap (cf. Falconer, 1966; Gellatly *et al.*, 1987):

- No obvious signs of past or present ice movement (e.g. no crevasses).
- Thin and gently sloping ice margins.
- No evidence of glacial erosion or deposition in the surrounding ice-free areas.
- Formation of superimposed ice is the normal mode of mass accumulation each year.

Baird *et al.* (1952) and Ward (1954) hypothesized that most of the 'Baffin Type' glaciers in the Canadian High Arctic are "survivals from before the post-glacial climatic optimum, since it is difficult to reconcile their reappearance since this time in the light of present-day low precipitation." (cf. Smith, 1999; 2002). On the other hand, Koerner (1968, 1989a) and Koerner and Fisher (2002) concluded that the Meighen Ice Cap and many of the smaller ice caps in the Canadian High Arctic have only developed since the end of the post-glacial climatic optimum (i.e. within the past 3000 to 4000 years or less). In fact, many of the smallest ice caps (such as the Hazen Plateau ice caps) appear to have only (re)formed (again) during the so-called 'Little Ice Age', some 200 to 300 years ago (Koerner, 2002).

The early glaciological studies conducted in the 1950s and 1960s (e.g. Orvig, 1951; Baird *et al.*, 1952; Ward and Orvig, 1953; Orvig, 1954; Løken and Andrews, 1966) all indicated that the Barnes Ice Cap was in "near equilibrium with present climate" (Jacobs *et al.*, 1997) – it was maintaining itself primarily through the formation of superimposed ice, even though climatic conditions at that time would not have allowed the initiation of a new ice cap at this particular location on Baffin Island. More recent work during the 1990s (e.g. Jacobs *et al.*, 1992; 1997) however clearly demonstrated that the Barnes Ice Cap is today actually in a state of "sustained decay under present climate" (Jacobs *et al.*, 1997), characterized by extensive marginal recession and significant overall mass losses since the late 19th century (i.e. since the end of the 'Little Ice Age').

2.2.1.1.1 Recent Glacial History of the Barnes Ice Cap

Ives (1962) presented geomorphic evidence (e.g. lichen-free zones and trim lines), suggesting that the Barnes Ice Cap was significantly larger during the 'Little Ice Age', when up to 70 percent of the surrounding plateau surface was covered by thin, permanent ice and snow cover (cf. Chapter 6). Dyke (1983), Edlund (1985), and Dowdeswell and Dowdeswell (2004) described similar evidence for ice-cap expansion during the 'Little Ice Age' on northern Somerset, western Melville Island, and Bylot Island, whereas Christiansen (1998) described increased nivation activity in northeast Greenland during the same time period. This 'Baffin Type' of glaciation (Baird *et al.*, 1952) is typically cold-based and therefore not very erosive – thus it "leaves little permanent record of its former existence" (cf. Falconer, 1966; England, 1986b; Rea *et al.*, 1998). This once extensive snow and ice cover has progressively disappeared since the end of the 'Little Ice Age' and today only about two percent of the north-central Baffin Island plateau are glacierized. Ives (1962) hypothesized that this reduction of snow and ice cover represented a considerable reduction in the 'average' surface albedo during the snow-free parts of the summer (= positive feedback process, Ives *et al.*, 1975; Koerner, 1980a).

Andrews *et al.* (1976) compared the spatial distribution of permanent snow and ice cover on the north-central Baffin Island plateau during the 'Little Ice Age' with that of today, using lichen-free areas and trim lines visible on satellite imagery to delineate the extent of snow and ice cover during the 'Little Ice Age'. Their study indicated that the regional snowline (or glaciation level) fell by about 100 to 300 m during the 'Little Ice Age' (cf. Locke and Locke, 1977; Andrews and Barry, 1978; Williams, 1978b) – thus extensive parts of the north-central Baffin Island plateau (above ~500 to 600 m asl) were covered by thin, but extensive permanent snow cover (cf. Chapter 6). This drop in glaciation level also corresponded to a drop in summer temperature of about 1.5°C (Williams, 1978b). Andrews *et al.* (1976) argued that the climatic deterioration during the 'Little Ice Age' had the potential (in terms of its amplitude) to push North America into a full glaciation. However, the duration of the 'Little Ice Age' was insufficient and thus it has to be considered an 'abortive glaciation' (cf. Flohn, 1974; Ives *et al.*, 1975; Stroeven *et al.*, 2002) in the context of Quaternary glaciations. It should be mentioned that Koerner (1980b) challenged the interpretation (perennial snow/ice cover) of the evidence (lichen-free zones) (cf. Chapter 6) and its climatic implications (cf. Wolken *et al.*, 2005).

Falconer (1962) presented evidence based on repeat aerial photography from the 1950s for a continued shrinkage of several small ice caps (cf. Section 2.2.1.2) in the vicinity of the Barnes Ice Cap since the end of the 'Little Ice Age'. The amount of their marginal recession between 1949 and 1958 was about 180 m. These ice caps are very similar in their size and shape to the Hazen Plateau ice caps. Unfortunately, the earliest available aerial photographs of the Hazen Plateau are from 1959; there are no aerial photographs available from 1949 (Braun *et al.*, 2004a).

2.2.1.1.2 Snowmelt and Ablation on the Barnes Ice Cap

Jacobs (1991) provided this interesting and relevant description of the surface conditions on the summit of the Barnes Ice Cap at about 1100 m asl on 24 July 1991:

> "The surface was wet but firm, with approximately 0.4 m of loose, coarse-grained ice crystals overlying more solid ice [= weathering crust, cf. Müller and Keeler, 1969]. There were numerous shallow puddles and small channels with slight drainage to the west."

Jacobs (1991) description fits perfectly the late summer surface conditions encountered on all four Hazen Plateau ice caps between 1999 and 2001, and on the Ward Hunt Ice Rise and Ice Shelf in 2002 and 2003. Pictures of the Barnes Ice Cap summit area from 24 July 1991 (Jacobs, 1991; his Fig. 6, 7, and 8) look exactly like the late summer summits of the Hazen Plateau ice caps (1999 to 2001) and the surface of the Ward Hunt Ice Rise and Ice Shelf in 2002 and 2003. Sagar (1966; his Fig. 17) showed similar pictures of slush hollows and incipient stream channels on the summit of the Barnes Ice Cap (~1075 m asl) from mid-July 1962. Baird *et al.* (1952, Pages 18 to 20) also included beautiful pictures of the Barnes Ice Cap from 1950, which are strikingly similar to those of the modern Hazen Plateau ice caps and the Ward Hunt Ice Rise and Ice Shelf.

Orvig (1951, 1954) discussed and compared the glacial-meteorological observations conducted on the two large Baffin Island ice caps (Barnes and Penny Ice Cap; Fig. 2.5). Orvig (1951) provided the following elegant description of the typical snowmelt process on the Barnes Ice Cap during the summer season:

> "During the ablation season melt water trickled down [into the snowpack] and part froze on to the old impervious ice surface [= superimposed ice formation], while the rest became slush or flowed into hollows and formed lakes. Old depressions in the ice formed river channels whence the slush discharged to the edge." See Ward and Orvig (1953; Page 162) for a detailed description and photographs of these so-called 'slushers' and Glen (1941 a, b) for another detailed description of the summer melting process and associated photographs.

Air temperature measurements above the melting ice cap surface showed that the Barnes Ice Cap acted as a 'temperature stabilizer' (Orvig, 1951, 1954), attempting to lower the air temperature directly above it down to 0°C, its own surface temperature during the summer ablation season. Thus, only a relatively small amount of energy is available for melt and ablation by way of sensible heat flux. However, in his conclusion, Orvig (1951, 1954) stated that "the Barnes Ice Cap is too small to cause a large degree of cooling and direct self-preserving effects through increased precipitation". In his view, the ice caps and glaciers on Baffin Island exercise only very little direct control over the climate of the surrounding land (e.g. in terms of temperature and cloud cover), even after the surrounding land becomes snow-free during the summer (cf. Arnold, 1965). This does not imply that air temperatures over the surrounding land are not higher – but the higher temperatures are caused by the lower albedo of the bare land surface (= more absorbed radiation), rather than the ice cap itself (cf. Chapter 5). After the surrounding land becomes partly snow-covered again in mid-August, the air temperature difference between the ice cap and the nearby land becomes negligible. The formation and accumulation of superimposed ice, however, means that the Barnes Ice Cap is "self-preserving in an unusual sense". Orvig (1951, 1954) agreed with the assertion of Baird *et al.* (1952) and Løken and Andrews (1966) that the Barnes and Penny ice cap were formed prior to the post-glacial climatic optimum, since modern levels of precipitation are insufficient for a reappearance of permanent ice since that time at this particular location (cf. Chapter 6).

Parts of the southern Barnes Ice Cap are surrounded today (= 1961) by several unglaciated plateau hilltops of equal or even greater elevation than its ice margin (Løken and Andrews, 1966). If the post-glacial climatic optimum deterioration in climate would have been responsible for the re-formation of the present Barnes Ice Cap, then those hilltops should also be glaciated today (Løken and Andrews, 1966). The absence of ice cover thus suggests that the a proto-Barnes Ice Cap must have existed during the post-glacial climatic optimum as the subsequent climatic deterioration was insufficient to redevelop

an ice cap (Løken and Andrews, 1966). On the other hand, this close juxtaposition of ice-free and ice-covered terrain may simply reflect the influence of a 'Manley-Type' threshold elevation and size necessary (Manley, 1955) for glacier formation and survival (cf. Whalley *et al.*, 1989).

2.2.1.1.3 Mass Balance of the Barnes Ice Cap

Hooke *et al.* (1987) presented a simple and elegant mass balance model for the Barnes Ice Cap. They were able to show that winter precipitation (as measured at a nearby weather station) was not correlated at all with the annual net mass balance of the ice cap. The inter-annual variations and absolute magnitude of winter precipitation and winter mass balance were fortunately so small in comparison to the annual balance (cf. Table 2.2) that they simply treated winter precipitation/winter mass balance as a constant and attributed all variability in the annual mass balance data solely to the summer balance (cf. Bradley and England, 1978). Hooke *et al.* (1987) found that mean summer air temperature fluctuations alone (measured at the same nearby weather station) was able to explain 87 percent of the annual mass balance variations of the Barnes Ice Cap (n = 17 years) (cf. Wild *et al.*, 2003). Hooke *et al.* (1987) therefore concluded that ablation season duration and intensity are the two primary controls on the annual mass balance of the Barnes Ice Cap today (cf. Hattersley-Smith *et al.*, 1961).

2.2.1.2 The Tiger Ice Cap (Baffin Island)

The geographic setting of the small Tiger Ice Cap (unofficial name), located on the northern Baffin Island plateau (Fig. 2.5), has been eloquently described by Falconer (1966) and appears to be literally a perfect analogue for the Hazen Plateau ice caps on northern Ellesmere Island today. The Tiger Ice Cap in 1961 measured about 2 by 3 km in size, with an inferred maximum ice thickness of no more than 30 m. Its surface had a gentle slope and Falconer (1966) described the shape of the ice margin as 'feathered' (cf. Glen, 1941a), rather than abrupt or steep. All other geographic and glaciologic characteristics of the Tiger Ice Cap described by Falconer (1966) are also characteristic for the Hazen Plateau ice caps and Ward Hunt Ice Rise and Ice Shelf, and have been directly observed between 1999 and 2003:

- "Two smaller adjacent ice patches were once part of Tiger Ice Cap but have become detached by progressive melting." A similar process is currently on-going along the western lobe of Simmons Ice Cap.
- "There was considerable amount of meltwater runoff on the surface and quantities of slush were being carried down to the margin in numerous meltwater runnels." (cf. Ward and Orvig, 1953)
- "The surface layer consisted of 10 cm of water-saturated, loosely-bonded white ice crystals from 2 to 5 cm in diameter. Below this was much harder white to blue ice which was difficult to chop with an ice axe." (= weathering crust; cf. Müller and Keeler, 1969)
- "Cryoconite pitting occurred all over the surface; the holes contained very fine, presumably windblown, sediment." (cf. Hattersley-Smith and Serson, 1970, 1973)
- "There are no crevasses and no other sign of ice motion was seen." (cf. Paterson, 1969)
- "The area exposed by recession displays well-preserved ground features primarily in the form of large tundra polygons, some up to 50 meters in diameter." (cf. Whalley *et al.*, 1981)

Falconer (1966) concluded that the Tiger Ice Cap represents a slowly decaying remnant of a once more extensive, thin, and static ice cap or ice sheet. The direct effects of this larger ice mass on the underlying ground (e.g. glacial erosion) "appears to have been negligible or protective" (cf. Glen, 1941a; Kleman, 1994). However, "this protective function is partly offset by the release of seasonal meltwater, which causes marginal erosion, landslips, and mass movements in saturated surface material" (Falconer, 1966).

2.2.1.3 The Gilman Glacier (Ellesmere Island)

Glacier mass balance observations and meteorological measurements on the Gilman Glacier (cf. Moore *et al.*, 1936) and surrounding ice masses from 1957 to 1961 (Fig. 2.1, 2.5) were sponsored by the Defense Research Board of Canada. These measurements provide a useful reference for the Hazen Plateau ice caps, as they occurred at similar elevations and within a very similar climatic environment. Furthermore, the Gilman Glacier is located only about 80 km to the north of the Hazen Plateau ice caps.

2.2.1.3.1 Measurements/Observations from 1957 to 1959

Hattersley-Smith (1960b) and Hattersley-Smith *et al.* (1961) reported on the comprehensive mass balance measurements conducted on the Gilman Glacier between 1957 and 1959 (Table 2.1), as well as on reconnaissance studies on several smaller ice masses in the vicinity of the Gilman Glacier.

Lotz and Sagar (1962) noted that the only other glacial-meteorological studies in the Canadian High Arctic (at the time) had been carried out on two much more maritime ice caps (Barnes Ice Cap and Penny Ice Caps, Baffin Island, Fig. 2.5), which receive over 70 cm summer snowfall. In addition, localized fog and low stratus cloud cover reduced incoming solar radiation about 70 percent of the time during the summer melt season on the Barnes and Penny Ice Cap. The climate on the Gilman Glacier (and Hazen Plateau in general), in contrast, is very continental, with comparatively little annual or summer precipitation and much more frequent clear-sky conditions (cf. Chapter 5).

Spring snow depth on the Gilman Glacier varied spatially, yet the mean snow depth and water equivalent of the winter snow pack for the three years (1957, 1958, and 1959) was very similar (Table 2.1). Summer ice ablation was about one order of magnitude greater than winter accumulation, which implies that changes in summer melt have a much greater effect on annual mass balance of the Gilman Glacier than changes in winter accumulation (cf. Bradley and England, 1978; Hooke *et al.*, 1987). Consequently, Hattersley-Smith *et al.* (1961) concluded that ablation season length and intensity largely control the mass balance of the Gilman Glacier. Hattersley-Smith (1960b) also described the presence of an exceptionally hard and dense wind-packed snow layer near the bottom of the winter snow pack in 1959 on the Gilman Glacier and Lake Hazen (Table 2.1). This unusual layer appears to be analogous to the 'Dole-Layer' (unofficial term) discovered in many places across Murray Ice Cap in 2000.

An ablation stake transect from about 800 to 1200 m asl revealed an approximately linear relationship between ablation and elevation in 1958 (Hattersley-Smith *et al.*, 1961; Mercer, 1961a) (this elevation range covers approximately the vertical extent of the modern Hazen Plateau ice caps). Lotz and Sagar (1962) also noted an almost perfect correlation between high daily (maximum) air temperature and high daily ice ablation. Ablation was much greater (almost double) near the margins of the Gilman Glacier than towards the center of the glacier, as also seen on Murray and Simmons Ice Cap, because of localized turbulent heat transfer from the nearby bare ground and the presence of wind-blown dust. The mean ELA of the Gilman Glacier was at about 1200 m asl in 1957 and 1958 (Table 2.1), similar to the ELA in northernmost Greenland (Fristrup, 1951). Reconnaissance surveys of two other (unspecified) glaciers on north-eastern Ellesmere Island also indicated an ELA of about 1200 m asl in those two years. Accumulation between about 1450 and 2000 m asl on the Gilman Glacier was by firn formation. Between

about 1280 and 1450 m asl, mass accumulation typically consisted of firn and inter-layered superimposed ice. Accumulation exclusively by superimposed ice only occurred in a narrow zone between the ELA (~1200 m asl) and 1280 m asl (Hattersley-Smith, 1960c; Hattersley-Smith *et al.* (1961).

Hattersley-Smith *et al.* (1961) also qualitatively assessed the mass balance regime of a small ice dome in the vicinity of the Gilman Glacier, which, based on their description, appears to be very similar to the Hazen Plateau ice caps. They concluded that the ELA of this ice dome lies currently above its summit in most years (i.e. it has typically no accumulation area). Hence, each year with net ablation "...appears to be uncovering ice formed in a recent slightly colder period" (Hattersley-Smith *et al.*, 1961), presumably during the so-called 'Little Ice Age'.

Lotz and Sagar (1962) offered this elegant and quite fitting description of the typical summer weather conditions on the Gilman Glacier:

> "The summer weather on the Gilman Glacier presents a contrasting picture between the pre-melt and the melt season. Before late June, the continuous snow cover, high incoming solar radiation and high albedos, coupled with light winds and stable air temperatures carry the glacier landscape of winter to summer. When the summer heat begins to clear the land of snow, high relative humidities, fog and low cloud, low insolation, and low albedo contribute to, or prevent, the decay of the glacier surface."

> "The decrease in solar radiation during August, coupled with any increase in albedo brought about by falls of snow, would effectively end ablation on the Gilman Glacier."

2.2.1.3.2 Measurements/Observations in 1960 and 1961

Sagar (1964) summarized the glaciological and meteorological observation on the Gilman Glacier conducted at 1660 m asl over the 1961 summer melt season. Snow depth in late May/early June was about 50 cm, with a snow density of about 0.3, yielding a mean winter snow accumulation of about 150 mm weq. Summer snowfall added about 35 mm weq or about 23 percent (snow density 0.05 to 0.15) for a total budget-year accumulation of 185 mm weq at about 1660 m asl.

Glacier ice ablation across the Gilman Glacier was once again directly and systematically related to air temperature during the melt season (cf. Lotz and Sagar, 1962). Sagar (1964) thus concluded, based on five years of in-situ measurements, that the mass balance of the Gilman Glacier is highly sensitive to variations in summer ablation. In contrast, annual mass accumulation (Table 2.1) on the glacier is fairly

constant from year-to-year (cf. Bradley and England, 1978; Hooke *et al.*, 1987). Thus, only small changes in summer melt season temperature (e.g. mean air temperature in June and July) had a critical effect on the annual mass balance of the Gilman Glacier (Sagar, 1964).

Hattersley-Smith (1969) combined the mass balance measurements and climatological observations on the Gilman Glacier with traditional geomorphic field mapping across northern Ellesmere Island and concluded that the glaciers and ice caps on northern Ellesmere Island, and specifically on the Hazen Plateau, are generally receding today (= 1969), after reaching their maximum neoglacial extent perhaps as late as 1925, similar to many glaciers in Scandinavia (Nesje and Dahl, 2003) and along the coast of Greenland (Weidick, 1984). He also noted, based on indirect evidence, that only small changes (i.e. reductions) in summer temperature, if sustained for a number of years, would lead to significant glacier advances and ice-cap growth on the Hazen Plateau. He further speculated that the ice caps on the Hazen Plateau have re-formed sometime within the last 4000 years, possibly during the 'Little Ice Age' (cf. Koerner, 1989a; 2002), similar to some of the low-elevation ice masses located today along the northern coast of Ellesmere Island (Fig. 2.4). In contrast, Smith (1999, 2002) argued that localized permanent ice cover may have persisted throughout the entire Holocene at selected favorable, high-elevation locations on the Hazen Plateau.

2.2.1.4 Quviagivaa Glacier (Ellesmere Island)

Wolfe and English (1995) presented simple mass balance measurements conducted on Quviagivaa Glacier (~4.7 km^2, 560 to 1250 m asl) over the 1992/1993 mass balance year (Fig. 2.5). Point measurements of snow depth and snow density were spatially-integrated across the entire glacier using hand-drawn snow water equivalent contours. Snow accumulation was not primarily a function of glacier elevation, but instead very much influenced by glacier topography (i.e. sheltered vs. exposed or convex vs. concave locations) interacting with snow drifting. Summer ablation measurements were spatially-distributed across the glacier using a well-defined linear ablation gradient, determined using an elevation transect consisting of 12 ablation stake. Net annual mass balance was not determined as the difference between winter and summer balances, but instead by hand-drawing of an 'equi-ablation' map for the glacier. Wolfe and English (1995) justified their rather unconventional approach (cf. Østrem and

Brugman, 1991) by the lack of a well-defined accumulation gradient and the "familiarity of the authors with patterns of melt on the glacier".

Wolfe and English (1995) also described interesting localized spatial patterns of snow accumulation and ablation along the margins of the glacier, similar to those seen on Murray and Simmons Ice Cap between 1999 and 2001. Furthermore, they noted a marked recession of the glacier margin (~50 m) since 1959 (based on a qualitative comparison with available aerial photographs, cf. Braun *et al.*, 2004a) and a recession of about 200 m and lowering of about 40 m since the end of the 'Little Ice Age' (based on well-defined trim lines surrounding the modern glacier terminus). The 1992/1993 net mass balance of Quviagivaa Glacier was highly negative, and the glacier supported only a tiny accumulation area (accumulation area ratio = 0.06). Reconnaissance visits to several other glaciers in the Sawtooth Range of Ellesmere Island revealed that "most showed weathered glacier ice from snout to summit, suggesting an entire surface of net ablation." (Wolfe and English, 1995).

2.2.1.5 White and Baby Glacier (Axel Heiberg Island)

Glacier mass balance measurements on Axel Heiberg Island. Nunavut, Canada (Fig. 2.5) were initiated in 1959 by the Jacobsen-McGill Arctic Research Expedition (Müller, 1962). The measurement program was maintained by McGill University, Montreal, and later by ETH, Zürich, until the death of the principal investigator, Fritz Müller. Thereafter the measurement series were interrupted before being resumed in 1982 by Trent University. Two glaciers are currently involved: White Glacier, on which measurements are available for the balance years 1959/60 to 1978/79 and 1982/83 to current; and the nearby (much smaller) Baby Glacier, on which measurements are available for 1959/60 to 1976/77 and 1989/90 to current.

The White Glacier is a 'typical' High Arctic valley glacier on Axel Heiberg Island (according to Müller, 1962), extending in elevation from 56 to 1782 m asl, and is considered as being "representative of the Canadian High Arctic" in general (Cogley *et al.*, 1996). Its annual mass balance is, on average, highly negative (Table 2.2), but no statistically significant trend is evident in the annual mass balance series so far (Cogley *et al.*, 1996). Cogley *et al.* (1996) argued that (climatically) plausible trend values are currently not detectable, as uncertainties in the annual mass balance estimates due to measurement

technique and error are on the order of 200 to 250 mm weq/year (cf. Cogley and Adams, 1998; Cogley, 2004). However, the average annual balance during the 1990s (–273 mm weq/year) was clearly the most negative of the four decadal averages on record (cf. Braun *et al.*, 2004a). Oerlemans and Reichert (2000) found that the mass balance of the White Glacier responds solely to changes in summer temperature, and is essentially unaffected by (winter) precipitation changes (cf. Bradley and England, 1978; Hooke *et al.*, 1987).

According to Müller (1962), Baby Glacier is "a small remnant glacier", with "its small ice mass in close proximity to the equilibrium line". Adams *et al.* (1998) reviewed the long mass balance measurements on the Baby Glacier, Axel Heiberg, Canada, available from 1959 to 1992 (with some gaps, Table 2.2). This small glacier is located today very close to the median elevation of the regional ELA (~975 m asl), which, together with its small altitudinal range (~300 m), means that even small changes in the regional ELA can literally put the entire Baby Glacier either above, or below, the regional ELA (cf. Hoelzle *et al.*, 2003). Adams *et al.* (1998) also noted that several years of positive balances can be easily offset by a single large negative mass balance year (cf. Koerner, 1980a). This temporal pattern is the result of relatively consistent, but low, winter snow accumulation from year-to-year, and, in contrast, much more variable and greater summer ablation. The average annual mass balance of the Baby Glacier, therefore, is highly negative today (Table 2.2). The average annual balance during the 1990s (–266 mm weq/year) was significantly more negative than the long-term average (cf. Braun *et al.*, 2004a). Adams *et al.* (1998) considered the (smaller) Baby Glacier as much more sensitive to climatic variations than its close, but much larger, neighbor the White Glacier (cf. Section 2.4.4.4).

Adams *et al.* (1998) also stressed the peculiar topographic characteristics of the Baby Glacier in the context of its mass balance and climatic sensitivity. For example, relatively deep snow typically accumulates upon and around the glacier terminus and along its lower sides, which locally reduces annual net ablation in what normally would be a high ablation zone (cf. Blatter and Kappenberger, 1988; Wolfe and English, 1995). Flatter sections near the top of the glacier, on the other hand, favor the formation and accumulation of superimposed ice, as meltwater drainage is impeded by the small surface slope (cf. Hattersley-Smith, 1960c; Koerner, 1970) (also Chapter 6).

2.2.1.6 The Meighen Ice Cap (Meighen Island, Canada)

Paterson (1969) described and discussed the mass balance and flow (or rather lack thereof) of the Meighen Ice Cap, Meighen Island (Fig. 2.5). The Meighen Ice Cap is a fairly large (~85 km^2), low-elevation ice cap, extending only from about 50 to 250 m asl. This ice cap is stagnant (i.e. no obvious signs of past or present ice movement), thus the surrounding ice-free areas show little or no evidence of past or current glacial erosion or deposition (cf. Falconer, 1966; Kleman, 1994). Paterson (1969) discussed the sensitivity of such a stagnant ice cap relative to changes in climate and mass balance in contrast to more dynamic glaciers:

> "Small stagnant ice caps such as the Meighen Ice Cap are sometimes said to be sensitive indicators of climatic changes, in the sense that small changes in climate may produce relatively large changes in the position of the margin of the ice cap. While this is true, an active glacier and a stagnant ice cap do not respond in the same way to changes in mass balance. The terminus of an active glacier responds to changes in the mass balance of the whole glacier. There is a time lag before the full effects of a mass balance change are apparent at the terminus. And the complete adjustment of a glacier to a mass balance change may require tens or even hundreds of years (Nye, 1963). On the other hand, in an ice cap in which flow is insignificant, the change in position of the margin during one year depends only on the net balance at that point on the margin for that year. If the net balance is positive, the margin will 'advance'; if the net balance is negative, the margin will 'retreat'. In this argument we assume that the margins are wedge-shaped, not vertical. This completes the response of the ice cap to that year's mass balance. Again, the average net balance of a stagnant ice cap may be zero year after year but the margins will continue to retreat. The margins will only advance when the whole ice cap lies in the accumulation area."

Arnold (1965) additionally stressed the importance of superimposed ice formation on the Meighen Ice Cap in the context of its total mass accumulation each year. The drainage of meltwater and rainwater is impeded by the small surface slope of the ice cap and therefore tends to percolate into the snow pack and refreeze into a solid layer of superimposed ice at the snow/ice interface. Arnold (1965) also concluded, based on unpublished micro-meteorological studies on and around the ice cap, that the Meighen Ice Cap exerted only a very limited temperature cooling effect on the surrounding ice-free land (cf. Orvig, 1951, 1954).

2.2.1.7 Glaciation of Phillips Inlet (Ellesmere Island, Canada)

Rea *et al.* (1998) qualitatively described the current plateau glaciation on and around Phillips Inlet, northwestern Ellesmere Island, Canada (Fig. 2.1) in the context of Manley's theory of a non-linear relationship between plateau summit breadth/altitude above the regional firnline and its ability to serve as a focal point for the initiation of glaciation (Manley, 1955; see below). Rea *et al.* (1998) argued that the dissected, high-elevation plateaus of northern Ellesmere Island indeed provide for "an ideal collection area for permanent snow fields at the onset of glacial conditions". During the early/advanced stages of local/regional glaciation, these cold-based plateau ice fields then begin to discharge warm-based outlet glaciers into pre-existing valleys (Whalley *et al.*, 1995). As glaciation proceeds, the plateau ice fields and their associated outlet glaciers become eventually overwhelmed by a large regional ice sheet. During deglaciation, the high-elevation plateau areas, however, will probably loose their ice cover before the less-sensitive and thicker outlet glaciers in the fjords and low-lying areas begin their retreat and eventual disappearance (Evans *et al.*, 2002). Such a situation may have occurred on the Hazen Plateau during the so-called 'Holocene Climatic Optimum' (~10 to 8 kyrs ago; Bradley, 1990), when the high-elevation plateau may have become deglaciated well before the valley/fjord that is now occupied by the two Murray Lakes became ice-free.

2.2.1.8 Selected Examples from Scandinavia

The chronology of glacier variations during the Holocene in Scandinavia more-or-less mirrors the situation in the Canadian High Arctic (e.g. Karlen, 1988; Bogen *et al.*, 1989; Chinn *et al.*, 2005; and references therein). The majority of the Scandinavian glaciers probably disappeared during the Early-Holocene and re-established themselves during the Late Holocene to reach their Holocene maxima during the so-called 'Little Ice Age'. Interestingly, the 'Little Ice Age' in Scandinavia appears to have lasted until about 1920 (Nesje and Dahl, 2003), very similar to the situation on northern Ellesmere Island (Hattersley-Smith, 1969) and coastal Greenland (Weidick, 1984). Only some of the high-elevation glaciers or ice caps in the more continental mountain regions of Scandinavia are thought to have survived throughout the entire Holocene (e.g. Rosqvist and Østrem, 1989, see below).

2.2.1.8.1 Messel (1971)

Messel (1971) provided a comprehensive description of the mass and energy balance of Omnsbreen Glacier in southern Norway. The geographical similarities between this glacier and the modern-day Hazen Plateau ice caps (Fig. 2.2, 2.3) are striking. Messel (1971) considered Omnsbreen a 'climatically dead' glacier, out-of-equilibrium with current climatic conditions. Omnsbreen represented also a 'dynamically dead' glacier, with no evidence of current ice flow. Omnsbreen Glacier had a total vertical relief of only 110 m and Messel (1971) described its surface topography as "flat and even" (again, very similar to the Hazen Plateau ice caps and Ward Hunt Ice Rise and Ice Shelf).

Its current survival is prolonged to some extent by topographically-induced accumulation of wind-blown snow and superimposed ice formation (Omnsbreen Glacier was located inside a local topographic depression, much like the smaller St.Patrick Bay ice cap; Fig. 2.3; cf. Bradley and Serreze, 1987b). Messel (1971) concluded that Omnsbreen Glacier represented a relict of a once active and expansive ice mass, which had its center and greatest thickness at or near the glaciers present location. Geomorphic evidence indicates that the Omnsbreen Glacier was considerably larger, and about 70 m thicker, during the peak of the 'Little Ice Age' (~1750) in southern Norway.

2.2.1.8.2 Whalley *et al.* (1981)

Whalley *et al.* (1981) described eloquently the different periglacial features found today near the modern margin of a receding plateau ice cap (Balgesvarri Ice Cap), Lyngen Peninsula, northern Norway. The similarities between their description and the modern Hazen Plateau surface uncovered by the receding Hazen Plateau ice caps are striking. This small ice cap has a maximum thickness of less than 60 m and is cold/dry-based (at least today). Whalley *et al.* (1981) documented pronounced changes in surface color, surface texture, weathering rinds, and lichen cover of the surficial materials, indicating significant retreat of the ice cap margins since the end of the 'Little Ice Age' (~1750 to 1900) (see Koerner, 1980b for an alternative interpretation of similar evidence). The retreating plateau ice cap is also uncovering very well-preserved sorted stone circles, which had to be formed prior to being overrun by the advancing ice cap. A similar process has been described on Baffin Island (Fig. 2.5) by Falconer (1962, 1966) and Ives (1962). Whalley *et al.* (1981) hypothesized that the uncovered sorted stone circles were

formed originally during the so-called 'Medieval Warm Period', prior to the 'Little Ice Age' (cf. Falconer, 1966; Kleman, 1994).

2.2.1.8.3 Gellatly *et al.* (1987)

Gellatly *et al.* (1987) noted the conspicuous absence of glacial moraines around the receding margins of three small plateau ice caps on the Lyngen Peninsula, northern Norway (including the aforementioned Balgesvarri Ice Cap, Whalley *et al.*, 1981). They also found no other evidence of basal sliding (e.g. glacial striations) in the surrounding area, which implies that these cold/dry-based thermal conditions have persisted at least since the end of the 'Little Ice Age' (~1750 to 1900). Instead, these small, thin, dry-based ice caps (which are today frozen to their beds) appear to "melt away largely in situ" (cf. Bradley and Serreze, 1987a) and "leave negligible evidence of their former presence" (cf. Falconer, 1966; Paterson, 1969; England, 1986b; Kleman, 1994).

2.2.1.8.4 Gellatly *et al.* (1989)

Gellatly *et al.* (1989) described the modern plateau and associated valley glaciation of the Bergsfjord Peninsula in northern Norway. The plateau ice caps on the Bergsfjord Peninsula occupy today what Gellatly *et al.* (1989) considered a 'critical altitudinal threshold' between 900 and 1200 m asl, and appear to be therefore particularly sensitive to recent climate change. The associated outlet and valley glaciers, fed by these plateau ice caps, are also dramatically affected, primarily through changes in ice supply when the plateau ice caps shrink and expand in response to climate change (Gellatly *et al.*, 1986).

Overall, only the largest high plateau areas in northern Norway are currently able to support permanent ice cover in the form of small plateau ice caps, which Gellatly *et al.* (1989) interpreted to reflect the control or influence of an elevation/area threshold as originally proposed by Manley (1955). On the Bergsfjord Peninsula, extensive plateau ice caps are able persist today a few hundred meters lower in elevation than elsewhere in northern Norway, as the larger plateau summit areas on the Bergsfjord Peninsula are able to compensate for the lower overall elevation of the plateau surface (cf. Manley, 1955).

2.2.1.8.5 Whalley *et al.* (1989)

Whalley *et al.* (1989) provided a comprehensive review of the effects of climatic and topographic controls on glacier changes in northern Norway. There, some of the highest plateau summits do not currently support permanent ice cover, while other plateau summits in the vicinity of similar or slightly lower elevation, on the other hand, are currently glacierized by thin, stagnant ice. This was again (cf. Gellatly *et al.*, 1989) interpreted to reflect the control of a 'Manley –Type' threshold topographic elevation and area necessary for glacier growth (Manley, 1955): A mountain or plateau hilltop might very well be high enough in elevation to be above the regional snow line to permit glaciation, but glacier development is nonetheless impeded by its limited size and available area for snow accumulation. Whalley *et al.* (1989) therefore concluded that local or regional differences in the glaciation level may sometimes be due to subtle topographic, rather than pronounced climatic, differences (cf. Andrews *et al.*, 1970).

2.2.1.8.6 Rosqvist and Østrem (1989)

Rosqvist and Østrem (1989) discussed the mass balance of Riukojietna Ice Cap, northern Sweden, in the context of its overall glaciologic sensitivity to climate change. This small plateau ice cap, and its surrounding plateau topography, is an almost perfect analogue for the Hazen Plateau ice caps (Braun *et al.*, 2004a) on northern Ellesmere Island.

Riukojietna Ice Cap reached a distinct Holocene maximum size at the beginning of the 20th century, which corresponds to the end of the so-called 'Little Ice Age' in this part of Scandinavia. Since that time, the surface of the entire ice cap has remained largely below the regional glaciation level, causing significant marginal recession and associated mass and volume loss. The ice cap today has no accumulation area, and its annual mass balance is primarily a function of summer climatic conditions (Pohjola *et al.*, 2005). Riukojietna Ice Cap could not reform again under current climatic conditions after a disappearance, unless a significant deterioration in climate would lower the regional glaciation level by about 150 m. Its small vertical extent (~300 m) and highly non-linear area-elevation distribution make the ice cap very sensitive to climatic fluctuations, as ELA variations of only 100 m can put large parts of the

ice cap either above, or below, the ELA or glaciation level (cf. Ives *et al.*, 1975; Adams *et al.*, 1998; Hoelzle *et al.*, 2003).

2.2.1.8.7 Nyberg and Lindh (1990)

Nyberg and Lindh (1990) hypothesized that the mass balance of what they refer to as 'marginal' glacial features in the Abisko Mountains, northern Sweden is primarily governed by the accumulation of wind-drifted snow (cf. Christiansen, 1998). Furthermore, they argued that the annual snow accumulation on these glacial features is strongly influenced by the available upwind snow fetch area. Many of these 'glacier-like' features in the Abisko Mountains occur today some 200 m below the regional glaciation level (~1500 m asl), because they receive enhanced snow accumulation (i.e. they act as 'snow traps', cf. Humlum (1997), see below). The overall geographic setting is very similar to that of the Hazen Plateau today and the glacial features described by Nyberg and Lindh (1990) are very similar to the Hazen Plateau ice caps. They are typically between 20 and 30 m thick and their size each year is directly related to contemporary climatic variability. There is also geomorphic evidence for more extensive snow, and thicker ice cover in the area (up to 50 m thick) in the past during the 'Little Ice Age'.

2.2.1.8.8 Grudd (1990)

Grudd (1990) discussed the mass balance of two very small glaciers in the Kebnekaise massif of northern Sweden, and compared their records to long-term mass balance measurements at two much larger glaciers nearby. He concluded that the two smaller glaciers responded much more sensitively to climatic changes because of their much shorter response times. They can thus provide information about the duration and magnitude of short-term or minor climatic fluctuations (cf. Ballantyne, 1990). In contrast, the response of the larger glaciers is too 'sluggish' to show any significant (i.e. measurable) changes in ice extent or area in response to short-term and rapid climate change (cf. Hubbard, 1997; Chinn, 1999; Cia *et al.*, 2005).

2.2.1.8.9 Gordon *et al.* (1995)

Gordon *et al.* (1995) described the plateau glaciation of Lyngsdalen, Troms, Norway, and its response to 20th century climate change. They showed that plateau glaciers above about 1500 m asl have not changed appreciably in recent years, whereas the existence of plateau ice caps below about 1400 m asl is today only marginal, and highly dependent on variations in their annual net mass balance. This very narrow altitudinal range, together with the small thickness of these plateau ice caps, means that their response to any short-term changes in climate is very rapid – small changes in weather or climate can literally put the entire ice cap (and surrounding plateau area) either above or below the ELA (cf. Ives *et al.*, 1975; Adams *et al.*, 1998; Hoelzle *et al.*, 2003). Gordon *et al.* (1995) concluded that the existence of such a critical and narrow 'altitudinal threshold' (in this case 1400 to 1500 m asl) means that a single glacier alone cannot be used as a reliable indicator of the glacier-climate-topography relationships in a given area or region (cf. Williams, 1978b; Humlum, 1997; Lie *et al.*, 2003a, b).

2.2.1.8.10 Whalley *et al.* (1995)

Whalley *et al.* (1995) discussed the interaction between plateau and valley glaciation in northern Norway in response to climate change over the last 100 years. Their conceptual, qualitative model complements the ice sheet initiation model proposed by Ives *et al.* (1975) (cf. Section 2.3.2) and describes the formation and growth of plateau ice caps, formation of associated valley and outlet glaciers, and their eventual retreat and decay as the ELA first lowers and then later rises during a given climatic cycle (for example the 'Little Ice Age'). The modern glacial conditions in northern Norway are very similar to those on the Hazen Plateau, with the ELA located on average well-above the plateau ice caps and the plateau surface. This situation actually makes these plateau ice caps somewhat less sensitive to climate change according to Whalley *et al.* (1995) – they basically constitute stagnant ice bodies which continually waste away passively (cf. Bradley and Serreze, 1987a; Gellatly *et al.*, 1987). A more sensitive situation with respect to climate change would occur if the ELA is, on average, located at about the same elevation as the plateau ice caps or plateau surface – in such a case, even small or rapid changes in climate (i.e. small changes in the ELA) would have a very dramatic effect on the annual mass balance of

those ice caps by significantly changing the relative proportions of the ablation and accumulation area (Ives *et al.*, 1975; Adams *et al.*, 1998; Hoelzle *et al.*, 2003).

2.2.1.8.11 Humlum (1997)

Humlum (1997) described the climatic and topographic controls on glaciation of the Söderasen Upland in southern Sweden during the Younger Dryas. He showed that increases in snowfall alone were not able to re-initiate glaciation, because the majority of the snowfall on the Söderasen Upland is immediately removed again by intense snow drifting. He argued instead that glaciation of this location can only begin in topographically-sheltered areas (which he refers to as 'snow traps' and 'radiation shelters'), where snow accumulation is augmented locally by snow drift deposition. This topography-wind-radiation interaction led to a peculiar regional pattern of the ELA during the Younger Dryas: the local ELA of the Söderasen Upland was perhaps as low as 100 m asl, whereas the regional ELA or glaciation level in southern Sweden was much higher at about 500 m asl (cf. Sissons, 1979; Dahl and Nesje, 1992).

2.2.1.8.12 Evans *et al.* (2002)

Evans *et al.* (2002) beautifully described the glaciation and deglaciation of the Bergsfjord Peninsula, northern Norway, during the last glacial-interglacial cycle:

> "From a glaciological perspective, the deglaciation and downwasting of plateau icefields is manifest as an inwards retreat towards the plateau, where a local ice cover may be maintained even during interglacials. This is likely to have been a common situation wherever plateau icefields occurred and was certainly the case on the Bergsfjord Peninsula in north Norway during the Weichselian deglaciation as the ice sheet margin retreated southwards. The high plateaux act as ice accumulation centres feeding outlet glaciers down steep valley-heads towards the main fjords, where many terminated as calving marine snouts. Where such plateaux are high and wide enough [cf. Manley, 1955], they still support an ice cover at the present time."

The retreat of these plateau ice field outlet glaciers is often a highly non-linear process, once the 'feeder icefalls' at the plateau lip disintegrate and thus separate the outlet glaciers from their supporting ice field above (cf. Golledge and Hubbard, 2005). Such a situation may very well have occurred during

the last deglaciation on the Hazen Plateau (e.g. 'proto'-Murray Ice Cap and its associated outlet glacier inside what is today the Murray Lake valley).

2.2.1.8.13 Carrivick and Brewer (2004)

Carrivick and Brewer (2004) provided an interesting GIS-based assessment of small glacier (~0.2 to 6 km^2) ELAs in northern Sweden. They argued that the response of a glacier to any (external) temperature shift will be primarily determined by its size and area-elevation distribution (cf. Section 2.4.5.4). Plateau ice caps, with relatively small slope angles, are therefore only particularly sensitive to small climatic changes if a large proportion of their mass and area is situated close to the regional ELA. Conversely, glaciers with more vertical relief are generally less sensitive to climatic perturbations. Carrivick and Brewer (2004) thus cautioned against over-interpreting the perhaps dramatic response of a single glacier to climatic change without taking into account its specific topographic and glaciologic characteristics (cf. Furbish and Andrews, 1984; Gordon *et al.*, 1995; Chinn, 1999; Lie *et al.*, 2003a, b).

A similar situation exists today on the large and small ice caps in the Canadian High Arctic. Bradley (1973, 1975) noted an approximately linear relationship between glacier ELA and July atmospheric freezing level in the Canadian High Arctic (cf. Miller *et al.*, 1975). Taking into account the non-linear area-elevation distribution of the ice caps, a linear change in climate (e.g. +1°C summer warming) would lead to a non-linear change in overall ice cap mass balance and thus non-linear ice cap expansion or recession over time (Koerner, 1979; 1980a).

2.2.1.8.14 Matthews (2005)

Matthews (2005) provided a comprehensive review of 'Little Ice Age' glacier variations in Jotunheimen, southern Norway, which represents the highest mountain range in northern Europe and today supports about 300 cirque and valley glaciers and small ice caps. These very continental glaciers are more influenced by their summer balance than their winter balance in contrast to the maritime glaciers in western Norway (Nesje *et al.*, 1995). Matthews (2005) argued that glacier advances that are summer temperature controlled are likely to occur/have occurred synchronously throughout the entire region, whereas spatially-restrictive events are probably linked to more localized winter precipitation variations.

2.2.1.9 An Example from Iceland

Brown and Ward (1996) discussed the interactions between local topography, snow patch development, and subsequent glacier/ice cap formation in southern Iceland. They noted that, at the regional/global scale, glacierization is usually associated with high elevations and/or high latitudes, as this favors snow accumulation through increased solid precipitation and limits ablation through lower temperatures (e.g. Munro, 1991; Sugden *et al.*, 2002). Yet, at the same time within those high-elevation regions, topographically-sheltered locations often offer more favorable conditions for snow accumulation at the more local level (cf. Dahl and Nesje, 1992; Humlum, 1997; Glazirin and Escher-Vetter, 1998). Strong winds tend to scour snow away from high, exposed plateau summits and this wind-drifted snow then tends to accumulate in lee-side hollows or other available 'snow traps' (cf. Kerr, 1993; Humlum, 1997), often well-below the elevation of the main plateau surface. Deeper and steeper valleys also offer protection from solar radiation ('radiation shelters') and thus experience less ablation than more exposed plateau summits (Humlum, 1997).

On the other hand, Brown and Ward (1996) found that the existence of semi-permanent or perennial snow fields in southern Iceland is also strongly influenced by the proximity to existing (larger) ice caps, which provide a precipitation shadow and localized cold air drainage. These ice caps therefore provide a suitable micro-climate with wind, air temperature, and precipitation anomalies, promoting the existence of snow fields in their vicinity. This may be regarded as a localized positive feedback mechanism for glaciation, similar to the snow/ice-albedo-temperature feedback (cf. Ives *et al.*, 1975; Koerner, 1980a, Section 2.3.2).

2.2.1.10 Selected Examples from Svalbard

2.2.1.10.1 Hagen and Liestol (1990)

Hagen and Liestol (1990), in a short paper summarizing the long-term glacier mass balance measurements on Svalbard, emphasized the importance of superimposed ice formation on many Svalbard glaciers in the context of their annual mass balance. Superimposed ice often contributes an additional 10 to 30 percent to the annual mass accumulation on the glacier. They also noted a high linear correlation

between summer glacier ablation and melting degree-day totals from June to September ($R^2 = 0.77$) on Svalbard. Simple degree-day models can therefore be used to give "very reliable results of the ablation in the summer season" (Hagen *et al.*, 1999) (cf. Chapter 6).

2.2.1.10.2 Ziaja (2001)

Ziaja (2001) discussed glacial recession and thinning in two different areas of southern Spitsbergen, Svalbard, Norway during the 20th century and found distinct spatial differences in the amount of ice loss between the central and southern parts of the island. For example, glacial recession and thinning in the central part of the island was more than double that in the southern part of the island. He suggested that the greater and more direct exposure of the southern parts of the island to humid maritime air masses is more beneficial for glacier survival than the higher elevation or latitude of the central parts of the island. A similar contrast exists today on northern Ellesmere Island between the maritime North Coast (e.g. Paterson, 1969; Braun *et al.*, 2004b) and the very continental, high-elevation Hazen Plateau (e.g. Miller *et al.*, 1975; Braun *et al.*, 2004a).

2.2.1.10.3 Hagen *et al.* (2003)

Hagen *et al.* (2003) first described and quantified the net mass balance of all monitored glaciers and ice caps on Svalbard. They then calculated net annual mass balance vs. altitude curves for thirteen different sub-regions in Svalbard and combined them with a digital elevation model to determine net glacier mass balance as a function of elevation and area (Hagen *et al.*, 2003; their Fig. 7). This exercise showed that the modern ELA is located today very close to the bulk of the glacier area in Svalbard. ELA shifts of only a few tens of meters can therefore have a large effect on Svalbard's total glacier mass balance (cf. Andrews *et al.*, 1976; Koerner, 1979; Adams *et al.*, 1998; Hoelzle *et al.*, 2003).

2.2.1.10.4 Pälli *et al.* (2003)

Pälli *et al.* (2003) described changes in glacier volume and extent in southern Svalbard over the last 100 years. Two of the larger outlet glaciers in the area (Hornbreen and Hambergbreen) included two large ice caps upstream at the end of the 19th century. Today, both glaciers have retreated by about 15 km

and lost their associated 'feeder' ice caps. The glaciers are situated today well-below the local ELA. They thus represent flat, thin, low-elevation glacial remnants that are very sensitive to climate change, similar to the Ward Hunt Ice Rise and Ice Shelf. Overall, the retreat of these two glaciers, and the disappearance of their associated ice caps, appear to be linked to the overall climate warming since the end of the 'Little Ice Age'.

2.2.1.11 Examples from Greenland

Fristrup (1951) provided an interesting summary of the Danish Pearyland Expedition between 1947 and 1950 to northernmost Greenland. Mass balance observation focused on the Chr. Erichsen Brae, which represented a "typical glacier cap" between 1100 and 1300 m asl. On this glacier, the amount of melting exceeded the amount of accumulation each year, thus "exposing very beautiful cryoconite holes" up to 40 cm (!) in depth. Trigonometric surveying of the glacier revealed no ice flow or movement, thus Fristrup (1951) concluded that the glacier "is a mass of dead ice which diminishes every year" and "[all] the glaciers at present time are masses of dead ice". The front of the Chr. Erichsen Brae retreated about 40 m each year between 1947 and 1950. Furthermore he noted, "All the glacier tongues seem to be retreating at the present time, according to the amelioration of the climate." (cf. Section 2.1.1).

Weidick (1984) provided a comprehensive overview of current glaciation and glaciation changes in Greenland, focusing on the time interval following the 'Little Ice Age'. This paper is by now some 20 years old, yet the main conclusions are still very relevant in the context of glacier behavior and climatic variability in the High Arctic. The margin of the Greenland Ice sheet apparently reached its 'Little Ice Age' maximum position around 1880 to 1890, with a minor re-advance occurring around 1920 (cf. Koch, 1926). This was "followed by a great retreat, which has, however, slowed down in recent decades" (Weidick, 1984). Davies and Krinsley (1962) determined that a more-or-less identical post-'Little Ice Age' sequence also applies to smaller glaciers and ice caps surrounding the northern Greenland Ice Sheet margin. For example, the terminus of the Petermann Glaciers appears to have not receded appreciably between 1876 and 1922 (Davies and Krinsley (1962). This chronology matches (almost) perfectly the sequence of events at the end of the 'Little Ice Age' proposed by Hattersley-Smith (1963; 1969) for northern Ellesmere Island (cf. Section 2.1.1). Weidick (1984) concluded that the 'Little Ice Age'

maximum of 1880/1890 was a response to the "culmination of cold conditions 100-200 years earlier" and that the margin of the Greenland Ice Sheet will continue to retreat "unless the climate returns to the cold conditions of the coldest periods of the Little Ice Age".

Warren (1990) compared the fluctuations of glaciers along the west coast of Greenland between 1942 and 1985, a time interval that covers the climatic transition from the relatively warm early 20th century through a time of gradual cooling (his Fig. 2). He found a strong contrast between the response of calving and non-calving glaciers. Non-calving glaciers responded directly and linearly, albeit with variable time lags, to the external climatic forcing (mainly summer temperature). In contrast, topographic 'pinning points' often created stable positions for calving glaciers within the fjords, regardless of climatic variability.

2.2.2 Geographic Analogues for the North Coast

The lowest glaciation levels in the Northern Hemisphere are found today along the northern coast of Ellesmere Island, as defined by low elevation, coastal ice caps and marine ice shelves (Miller *et al.*, 1975). Most of the Earth's ice shelves are located today in Antarctica, where they are almost all seaward extensions of the vast Antarctic Ice Sheet. In contrast, the Ellesmere Island ice shelves are several orders of magnitude smaller than their more famous Antarctic counterparts.

The ice cover along the northern coast of Ellesmere Island is today comprised of a series of small floating ice shelves (Fig. 2.1, Fig. 2.4) and associated grounded ice rises (Hattersley-Smith *et al.*, 1955; Ragle *et al.*, 1964; Lyons *et al.*, 1972) in topographically-suitable locations. The difference between an ice cap and an ice rise is that an ice rise is "surrounded either by an ice shelf, or partly by an ice shelf and partly by sea and/or ice-free land" (Armstrong and Roberts, 1956). In the words of Hindmarsh (1993):

> "Parts of ice shelves frequently ground on shoals and small islands, giving rise to ice rumples and ice rises. These features are believed to have a disproportionate influence on the mechanics and deformation of ice shelves."

In essence, the grounded portion of the (otherwise floating) Ward Hunt Ice Shelf comprises today the Ward Hunt Ice Rise (Lyons and Ragle, 1962) (Fig. 2.4), which leads to interesting implications

in terms of their respective dynamics (e.g. Weertman, 1957) and thus sensitivities and responses to climatic change (cf. Chapter 6). The (possible) (in)stability of the Earth's ice shelves has received increased scientific and public attention in recent years (e.g. Mueller *et al.*, 2003; Rignot *et al.*, 2004, Scambos *et al.*, 2004, Thomas *et al.*, 2004), since the ice shelves are believed by some to provide an important 'footing' or 'buttress' for some of the large inland glaciers in Antarctica (Hindmarsh, 1993; Dupont and Alley, 2005).

2.2.2.1 The Meighen Ice Cap (Meighen Island, Canada)

Paterson (1969) noted that the elevation of the Meighen Ice Cap (~40 to 270 m asl; Fig. 2.5) is "abnormally low" for glaciers and ice caps in the Canadian High Arctic, which in turn implies that "accumulation on the Meighen Ice Cap must be abnormally high, or ablation abnormally low, or both". Paterson (1969) found no evidence to suggest that mass accumulation on the ice cap was much greater compared to the other High Arctic glaciers (Table 2.2), but showed that summer ablation was perhaps as much as three times lower. He thus concluded that:

> "Low ablation, perhaps resulting from the high frequency of fog during the summer, is probably the main reason for the existence of the Meighen Ice Cap. Present values of ablation are, however, still too high to maintain it. If the net mass balance were to remain at the value it has averaged since 1959, the ice cap would disappear in a few hundred years."

The exact same conclusions were reached by Hattersley-Smith and Serson (1970) with respect to the climatic conditions, mass balance, and future survival prospects of the Ward Hunt Ice Shelf and Ice Rise. Arnold (1965), for example, determined that a 2.8°C decrease in mean summer temperature would be required for the Meighen Ice Cap to achieve a positive annual mass balance (assuming that winter accumulation would remain unchanged at about 150 mm weq). In contrast, winter accumulation would have to increase by about 500 percent (to about 900 mm weq) to achieve a positive mass balance under unchanged summer melt conditions. Arnold (1965) also stressed the importance of superimposed ice formation on the Meighen Ice Cap, both as a source of (additional) mass each year and as a sink for melt energy during the summer melt season (cf. Chapter 6).

2.2.2.2 Storöyjökulen Ice Cap (Svalbard)

Jonsson (1982) described the current climatic conditions and mass balance of a low-elevation, coastal ice cap (Storöyjökulen) on Svalbard. His basic objective was to qualitatively assess how such a large ice mass can exist under present-day climatic conditions at or near sea level. Jonsson (1982) concluded:

> "The reason for the existence of Storöyjökulen, although its highest point is only 239 m asl and its winter balance is very small, seems to be a combination of cold ice and a cloud-covered summit plateau with frequent summer snowfalls and summer air temperatures most often below zero degrees."

Rime, frozen hoar frost, and frozen fog precipitation during the summer increased annual accumulation by as much as 10 percent, in addition to indirectly inhibiting melt through the associated albedo effect (cf. Hattersley-Smith, 1960a). Superimposed ice formation also played a critical role in ice cap survival by directly increasing annual mass accumulation and indirectly reducing ablation. In fact, mass accumulation on Storöyjökulen Ice Cap is today (almost) exclusively in the form of superimposed ice (Jonsson and Hansson, 1990). Most meltwater and rain water refreezes within the snow pack on the flat, poorly-drained ice cap summit plateau. In other words: the winter snow cover is gradually transformed into a layer of superimposed ice during each summer melt season, rather than melting and immediately forming runoff (cf. Chapter 6). Jonsson (1982) also noted the striking similarities between the climatic and glaciologic conditions on Storöyjökulen and the Meighen Ice Cap (Fig. 2.5) in the Canadian High Arctic (cf. Paterson, 1969).

Summer temperatures in coastal locations (such as Storöyjökulen), which are surrounded by sea ice for much of the year, show relatively little variability (Jonsson and Hansson, 1990), especially when compared to very continental locations such as the Hazen Plateau of Ellesmere Island. Therefore, one might expect a relatively weak correlation between summer temperatures and net annual mass balance at coastal sites (Jonsson and Hansson, 1990). Lotz (1961a, b) commented precisely on the absence of strong correlation between air temperature and ablation on the Ward Hunt Ice Shelf in 1959 and noted:

> "This is strikingly at variance with Sagar's conclusions [Sagar, 1962] on the [very strong] relation between ablation and meteorological factors [air temperature] on Gilman Glacier."

Instead, mean annual temperature might be of greater importance for coastal glaciers or ice caps, as superimposed ice can only form as long as the underlying ice surface is sufficiently cold (Ward and Orvig, 1953; Woodward *et al.*, 1997). In addition, annual precipitation and the length of the summer ablation season may also be of importance (Jonsson and Hansson, 1990).

2.2.2.3 Austfonna Ice Cap (Svalbard)

Bamber *et al.* (2004) reported on the recent 'anomalous' growth of the Austfonna Ice Cap, eastern Svalbard, which is the largest ice cap (~8200 km^2) today in the Eurasian Arctic, ranging in elevation between 0 and 800 m asl. Recent airborne laser altimetry measurements indicated a thickening and growth of the central part of this ice cap between 1996 and 2002. This period of mass gain coincided with reductions in sea ice cover in the adjacent Barents Sea, which Bamber *et al.* (2004) argued led to increased moisture availability and precipitation in eastern Svalbard. Krabill *et al.* (2000) also noted localized positive ice elevation changes for a small ice cap in north-east Greenland in the vicinity of an offshore polynya. More recently, Davis *et al.* (2005) and Johannessen *et al.* (2005) also reported a thickening of the interior parts of the East Antarctic and Greenland Ice Sheets in response to recent climate change, even though the margins of the Greenland Ice Sheet continue to thin at present (Krabill *et al.*, 2004).

2.2.2.4 The Laika Ice Cap (Coburg Island, Canada)

Blatter and Kappenberger (1988) reported on the mass balance and thermal regime of the Laika Ice Cap, Coburg Island, Nunavut, Canada (Fig. 2.5). Laika Ice Cap is a small ice field (~10 km^2), extending from close to sea level to an altitude of about 530 m asl. Its overall mass balance is highly negative today, with annual mass accumulation (in the form of superimposed ice) limited to only a small area near the summit of the ice cap. The ice cap experiences an Arctic-maritime climate, which is characterized by enhanced precipitation, stronger winds, and reduced net radiation "than is normal in that latitude of the Canadian Arctic" (Blatter and Kappenberger, 1988). Consequently, large parts of Coburg Island are currently ice-covered, despite the lack of significant vertical relief on the island. Geomorphic

evidence suggests that the Laika Ice Cap was considerably thicker, and larger, at some point in the recent past, possibly during the 'Little Ice Age' (cf. Wolfe and English, 1995; Braun *et al.*, 2004a).

2.2.2.5 The (floating) Ward Hunt Ice Shelf: A Special Case

Mueller *et al.* (2003) have linked recent fracturing, calving, and thinning of the floating Ward Hunt Ice Shelf (Fig. 2.4) directly to recent increases in summer air temperature. However, Doake *et al.* (1998) have shown that floating ice shelves may only have a limited number of stable configurations and thus may be subject to rapid retreat or irreversible break-up once the ice shelf front retreats behind such a stable configuration (cf. Weidick, 1984; Warren, 1990; Vaughan and Doake, 1996; Cooke *et al.*, 2005). This implies that the rate of observed glaciological change for an ice shelf (e.g. retreat, fracturing, thinning, calving, etc.) is not necessarily a direct/linear function of (concurrent) climate change, but instead a dynamically-controlled process also governed by the surrounding and/or underlying topography (Thomas, 1973; Warren, 1990; Hindmarsh, 1993; Knight, 1998). It is also important to note that these are not actually new ideas with respect to the long-term stability of the Ward Hunt Ice Shelf (e.g. Hattersley-Smith, 1960a), despite generating considerable public interest in recent years. For example, Koenig *et al.* (1952) wrote over 50 years ago:

> "It is possible that the fringe of shelf ice on the north coast of Ellesmere Island is only able to maintain its present hold through the presence of small off-shore islands, which it has swamped and to which it is firmly anchored. In some of the air photographs small islands can actually be seen in the process of emerging through the shelf ice."

> "Wind action, tide action, and pressure from the pack may cause cracks to develop in the ice shelf, and so hasten the ultimate calving of ice islands."

On the other hand, sea ice cover on the Arctic Ocean may actually have a stabilizing effect on the ice shelf (van der Veen, 2002a) by buttressing and supporting the floating front of the Ward Hunt Ice Shelf (Fig. 2.4). Reduced Arctic Ocean sea ice extent (e.g. Comiso, 2002a, b) thus may make the ice shelf more susceptible to fracturing and calving, which in turn could hasten its ultimate collapse.

Hattersley-Smith (1960a) argued that even the present levels of low annual precipitation and snow accumulation are perfectly sufficient to allow for a (slow) growth and thickening of the Ward Hunt

Ice Rise and Ice Shelf – all that is really required today to achieve a positive mass balance year is a shortening of the summer melt season. He further noted that the ice shelves and ice rises along the northern coast of Ellesmere Island are today especially sensitive to even small changes in summer temperature, as summer temperatures are currently barely above freezing to begin with. Thus, even a slight lowering of summer temperatures would cause much of the summer precipitation to fall as snow (rather than rain), dramatically limiting melting and ablation (via the snow/ice-albedo-temperature feedback process). On the other hand, Hattersley-Smith *et al.* (1955) came to a slightly different conclusion with respect to the long-term survival of the Ward Hunt Ice Shelf just five years earlier:

> "From the present gradual wastage deduced from surface observations, it is concluded that only a slight amelioration of climate would be extremely destructive to the ice shelf. For example, continual mild seasons, like that of 1954, would cause the whole of the present mass of the ice shelf to melt in about 80 years."

It is worth noting that the long surface mass balance record for the Ward Hunt Ice Shelf (Braun *et al.*, 2004b) does not provide any information about mass gains or losses occurring at the bottom of the floating ice shelf through melting and/or accretion of sea water (Hattersley-Smith and Serson, 1970). Recent evidence from the ice shelves along the Antarctic Peninsula suggested that mass losses at the bottom of ice shelves related to warmer ocean water temperatures might be more significant than surface mass balance in terms of overall ice shelf mass balance and stability (Shepherd *et al.*, 2003; Braun *et al.*, 2004b; Grosfeld and Sandhäger, 2004; Scambos *et al.*, 2004; Smedsrud *et al.*, 2006) (cf. Chapter 6), but this notion was already discussed by Debenham (1954) and Wexler (1960) some 50 years ago.

2.2.3 Synopsis

Miller *et al.* (1975) were the first to comprehensively describe and map the steep glaciation level and ELA gradients across northern Ellesmere Island (Fig. 2.6), which are ultimately a function of (winter) snow accumulation and summer melt patterns interacting with the regional topography of the island (cf. Humlum, 1985). However, it is important to recognize that the glaciation level, as determined by ice extent depicted on topographic maps, reflects only a 'snap shot' of glaciation that is also a function of the

climate of the preceding decades to centuries, depending on the climatic sensitivity of the ice masses (Bradley, 1972; Williams, 1978b).

It is clear that the Hazen Plateau and northern coast of Ellesmere Island represent two very different geographic environments, yet, at the same time, there are also some notable and quite unexpected similarities in terms of their climate and glaciation:

1. Summer temperatures are quite similar (Fig. 2.6), despite the very large difference in elevation (~1000 m) (cf. Chapter 5).
2. They both represent very marginal environments for the existence of glaciers, at least today.

It appears that the Hazen Plateau ice caps can persist today, despite the (relatively) warm and dry climate, only at the highest (= coldest) elevations of the Hazen Plateau. Their annual mass balance is therefore almost exclusively a function of ablation season length and intensity (Braun *et al.*, 2004a). The Ward Hunt Ice Rise and Ice Shelf, in contrast, can today only persist directly at sea level because of the unique climatic conditions brought about by their close proximity to the Arctic Ocean (= 'Arctic Ocean Effect', cf. Chapter 4). Their annual mass balance is also strongly controlled by summer melting (Braun *et al.*, 2004b), however, winter and summer precipitation may play a more significant role. In addition, the survival of the Hazen Plateau ice caps and the Ward Hunt Ice Rise/Ice Shelf appears to be intimately linked to the formation and temporary accumulation of superimposed ice each melt season (Bednarski, 1994), which reduces net ablation by providing a (temporary) mass buffer during each summer melt season.

The glaciers, ice caps, and ice shelves on the Hazen Plateau and along northern coast of Ellesmere Island are today all experiencing highly negative mass balances, indicating that they are currently adjusting their overall geometry to match the rapidly changing climatic conditions of today. Unfortunately, this adjustment process to a new equilibrium condition will probably involve their complete disappearance over the next 50 to 100 years or so (Braun *et al.*, 2004a, b).

2.3 Initiation of Glaciation

Flint (1943, the theory of 'Highland Origin and Windward Growth') and Ives *et al.* (1975, the theory of 'Instantaneous Glacierization') have proposed two somewhat competing 'Big-Picture' theories to conceptually explain the onset of glaciation and ice sheet formation at high elevations in response to climate change. Both theories, and their respective differences, have been 'tested' and 'expanded' upon over the years through the collection of in-situ geographic evidence (e.g. Williams, 1978a; Whalley *et al.*, 1989; Whalley *et al.*, 1995; Brown and Ward, 1996; Humlum, 1997), which directly illustrates how climatic change is expressed through snow and ice cover changes on the landscape, and larger-scale modeling studies (e.g. Andrews and Mahaffy, 1976; Andrews and Barry, 1978; Mengel *et al.*, 1988; Marsiat, 1995; Pollard and Thompson, 1997; Marshall and Clarke, 1999; Oerlemans, 2002; Bintanja *et al.*, 2002; Lie *et al.*, 2003a, b; Pollard and DeConto, 2005; Ruddiman *et al.*, 2005), which were focused on the more quantitative interactions of climate change at a variety of time scales and associated glacier and ice sheet formation. In addition, Stroeven *et al.* (2002) provided an interesting and concise overview of ice sheet nucleation and inception from a more conceptual point of view. Loewe (1971) and Denton and Hughes (1981) proposed two (complementary) ice sheet initiation theories focused on the existence of large, flat areas near (the receding) sea level as suitable sites for ice sheet formation (cf. Souchez, 1997).

2.3.1 The Hazen Plateau and North Coast of Ellesmere Island in the Context of Global Glaciation

The prevailing climate at the equilibrium line altitude (ELA) of a glacier is typically considered as 'just sufficient' to sustain its permanent existence (e.g. Ohmura *et al.*, 1992). This makes annual precipitation at the ELA a useful proxy for annual snow accumulation (i.e. mass addition to the glacier) and mean summer temperature at the ELA a useful proxy for ablation (i.e. glacier mass loss) (Dugdale, 1972; Sutherland, 1984; Ohmura *et al.*, 1992; Humlum, 1997; Benn and Lehmkuhl, 2000; Zeeberg and Forman, 2001; Lie *et al.*, 2003a). Annual precipitation and summer temperature together can therefore provide a useful generalized picture of the climatic conditions required to sustain the existence of a permanent glacier or ice cap at any given location (Fig. 2.7).

It is quite obvious that the climate of the Hazen Plateau today is (1) too dry and (2) too warm to support permanent plateau ice cover on the basis of a global glacier dataset (Fig. 2.7; red solid circle). Given today's 'current' summer temperatures, annual precipitation would have to at least triple to initiate glaciation on the plateau. Or, given 'current' levels of annual precipitation, summer temperatures would have to decrease by about 1 to 2°C to allow for the existence of permanent and healthy glaciers on the Hazen Plateau. The climate along the northern coast of Ellesmere Island today (blue solid circle) appears to be only slightly more conducive (i.e. colder and wetter) for permanent ice cover in terms of summer temperature and annual precipitation (Fig. 2.7). It is interesting to note that summer temperatures were in fact about 1 to 2°C colder than today in the Canadian High Arctic (Hattersley-Smith, 1963; Koerner, 1989a) during the so-called 'Little Ice Age' (open circles), and there is some evidence for more extensive snow and ice cover on the Hazen Plateau (Braun *et al.*, 2004a) and along the northern coast of Ellesmere Island (Hattersley-Smith and Serson, 1970; Braun *et al.*, 2004b).

If the prevailing climate at the glacier ELA is indeed adequate for its continued survival (Ohmura *et al.*, 1992), then any incipient glaciation of any given (unglaciated) locality requires the existence (i.e. lowering) of a snowline or glacier ELA at the terrain surface (Andrews and Barry, 1978; Williams, 1979; Humlum, 1997; Benn and Lehmkuhl, 2000; Bromwich *et al.*, 2002; Hock *et al.*, 2002; Sugden *et al.*, 2002; Pollard and DeConto, 2005). Based on this argument, it seems therefore necessary to lower the regional snowline or glacier ELA (which is today on average above the surface of the Hazen Plateau; Braun *et al.*, 2004a) down to the elevation of the Hazen Plateau, either by increasing annual snowfall/snow accumulation and/or by lowering summer temperatures (cf. Lie *et al.*, 2003a, b) (Fig. 2.8). The same basic argument is also applicable for the initiation of glaciation along the northern coast of Ellesmere Island (Hattersley-Smith, 1960a).

2.3.2 The Theory of 'Instantaneous Glacierization'

Ives (1957) and Ives *et al.* (1975) theory of 'Instantaneous Glacierization' essentially argues that a climatic deterioration (for example an increase in snowfall and/or decrease of summer temperature) would lead to an overall lowering of the regional snowline relative to the land surface (Fig. 2.8). Once the snowline (or equilibrium line, cf. Koerner, 1980a) lowers down to the elevation of certain 'sensitive'

plateau areas (e.g. Baffin Island plateau or Hazen Plateau, Fig. 2.5) these plateaus would be quasi-instantly covered by a thin, but perennial snow cover. Such large snow-covered, high-albedo, high-elevation areas would then begin to 'modify' their own surrounding climate (cf. Brooks, 1924; Barry *et al.*, 1975; Andrews and Mahaffy, 1976; Williams, 1978b; Bromwich *et al.*, 2002; Stroeven *et al.*, 2002) through efficient positive feedback processes (for example snow/ice-albedo-temperature feedback; Koerner, 1980a; Birchfield and Wertman, 1983; Bintanja and Oerlemans, 1995; Hall, 2004; Winton, 2006) to the point where they become quasi self-sustaining. In essence, these positive feedback processes serve to amplify the initial climatic forcing and turn snow/ice cover from merely a passive result of climatic variability into an active component of climate change that promotes and amplifies its own initiation, expansion, and survival (cf. North, 1984; Kerr, 1993; Rial *et al.*, 2004; Chapin III *et al.*, 2005; Pollard and DeConto, 2005).

True glaciation can then start with the formation of small glaciers and ice caps at high elevations (cf. Brown and Ward, 1996; Koerner, 1989b; Koerner and Fisher, 2002), which gradually thicken (cf. Lamb and Woodroffe, 1970), and eventually expand to form large continental ice sheets (cf. Andrews and Mahaffy, 1976). This expansion, in turn, is promoted by additional positive feedback processes (Payne *et al.*, 1989; Ogura and Abe-Ouchi, 2001; Sugden *et al.*, 2002; Pollard and DeConto, 2005). This process eventually reverses itself at the end of a glacial cycle when the ice sheet decays back slowly to small remnant plateau ice caps (e.g. Barnes Ice Cap, Baffin Island or Hazen Plateau ice caps, Ellesmere Island), although this reversal may exhibit a series of hysteresis effects due to a variety of different feedback processes (Loewe, 1971; Pollard and DeConto, 2005). In this context, Ives *et al.* (1975) considered the 'Little Ice Age' an 'abortive glaciation' and hypothesized that a more sustained (i.e. longer) climatic deterioration could have pushed the entire region (and North America as a whole) into such an 'instantaneous glacierization' (cf. Andrews *et al.*, 1972). Whalley *et al.* (1995) took the basic model or concept proposed by Ives *et al.* (1975) one step further and introduced a complementary model that qualitatively describes the formation and growth of plateau ice caps, formation and growth of associated valley and outlet glaciers, and their eventual retreat and decay as the ELA first lowers, and later rises again, during a given climatic cycle (for example during the so-called 'Little Ice Age').

2.3.2.1 Some Considerations

Ives *et al.* (1975) theory of 'Instantaneous Glacierization' requires the existence of climatically-sensitive areas, specifically the highest elevations of large, high-latitude plateau areas (e.g. Baffin Island plateau, Baffin Island or Hazen Plateau, Ellesmere Island, Fig. 2.5), as initial sites for glacial development (e.g. Brooks, 1924; Andrews and Barry, 1978; Birchfield *et al.*, 1982; Pollard and Thompson, 1997; Marshall and Clarke, 1999; Bintanja *et al.*, 2002; Marshall, 2002; Ruddiman *et al.*, 2005). This choice follows the basic argument first presented by Manley (1955): "The narrower a summit, the greater its height must be above the firnline to retain a snow cover". In other words (according to Manley, 1955), a glaciated plateau summit has to be both high and large enough to allow for sufficient snow accumulation to occur – if the plateau summit is too small or narrow, the remaining snow, not already removed by wind drifting, will be too thin to persist through the summer melt season (e.g. Humlum, 1997). Whalley *et al.* (1989) discussed the effects of climatic and topographic control on glacier changes in northern Norway, where some of the highest plateau summits currently do not support permanent ice cover. Yet, other nearby plateau summits of similar, or even lower, elevation are currently glacierized by thin, stagnant ice cover. This appears to reflect the presence of a 'Manley-Type' topographic elevation and area 'threshold' necessary for glacier initiation and development in this region (cf. Gellatly *et al.*, 1989).

Rea *et al.* (1998) described contemporary plateau ice fields and associated geomorphologic evidence of past glacial activity from north-western Ellesmere Island (Phillips Inlet) (Fig. 2.1). They concluded that the initially-formed plateau ice caps became 'overwhelmed' at some point by a larger, regional ice sheet, which imprinted its own geomorphologic signature on top of that of the earlier plateau glaciation, which is consistent with Ives *et al.* (1975) theory of 'Instantaneous Glacierization'. But they also argued that the highest parts of the plateau were deglaciated before the less sensitive and thicker outlet glaciers in the fjords and other low-lying areas began to retreat and disappear at the end of a glacial cycle. Their argument is consistent with the notion that low-elevation, topographically-sheltered locations are sometimes more conducive for glacier initiation and survival than high-elevation, exposed locations (Brown and Ward, 1996).

Williams (1978b) attempted to test the second notion central to Ives *et al.* (1975) theory of 'Instantaneous Glacierization' that increased snow cover would lead locally, and regionally, to reduced air temperatures, increased precipitation, and changes in the overall atmospheric circulation patterns through a variety of different positive feedback processes (cf. Brooks, 1924; Barry *et al.*, 1975). He concluded:

> "All of these changes occurred [in the Canadian High Arctic] in the October mean patterns of 1971-75, apparently in response to increased early-October snow-cover extent. Similar effects could be expected in summer at the onset of continental glaciation, but of course it cannot be assumed that these effects would be quantitatively identical to the results of this study."

However, Williams (1978b) also cautioned against over-interpreting the results of his simple assessment (cf. Andrews and Barry, 1978):

> "They [the observed changes] would probably depend not only on the snow cover, but also on sea ice, sea surface temperatures, and the general circulation, which would be different in the summer especially with whatever change was responsible for the snow-cover expansion in the first place."

At a much smaller scale, Bradley and Serreze (1987b) were able to show that even very small plateau ice caps can have a measurable cooling effect on the lower atmosphere relative to the surrounding snow- and ice-free tundra. On the other hand, Orvig (1951, 1954) argued, without the benefits of boundary layer soundings, that even the much larger Barnes Ice Cap on Baffin Island (Fig. 2.5) is still too small to induce positive feedback processes effective and extensive enough to play a significant role in its own preservation. Arnold (1965) also concluded, based on unpublished micro-meteorological studies on and around the ice cap, that the Meighen Ice Cap only exerted a very limited cooling effect on the surrounding land surface.

At a much larger scale, Birchfield *et al.* (1982) and Birchfield and Wertman (1983) concluded that the presence of high-latitude and mid-latitude plateaus increases the climatic sensitivity and provides a suitable inception point for an ice sheet (cf. Kerr, 1993). Most large-scale modeling studies (e.g. Pollard and Thompson, 1997; Marshall and Clarke, 1999) predicted ice sheet nucleation occurring both on the north-central Baffin Island plateau and Ellesmere Islands Hazen Plateau at the start of the last glacial cycle. However, more recent studies by Bintanja *et al.* (2002) and Ruddiman *et al.* (2005) were not able

to form ice initially on northern Ellesmere Island because of the lack of precipitation (cf. England and Bradley, 1978; Chapter 6).

2.3.3 The Theory of 'Highland Origin and Windward Growth'

Flint's (1943) theory of 'Highland Origin and Windward Growth' argued that the Laurentide Ice Sheet instead originated in the coastal mountains of Labrador-Ungava and Baffin Island, where a climatic deterioration would first lead to the formation of thick snow banks in topographically-sheltered locations and small, localized cirque glaciers. These glaciers would then slowly increase in size and begin to grow westward (towards the source of precipitation, cf. Sugden *et al.*, 2002), gradually expanding and thicken to continental ice sheet proportions. This process eventually reverses itself at the end of a glacial cycle, when the ice sheet decays back eastward to leave small remnant cirque glaciers and permanent snow banks stranded in the coastal mountains.

2.3.3.1 Some Considerations

Flint (1943) theory of 'Highland Origin and Windward Growth' also requires the existence of climatically-sensitive areas, which in this case are not the highest elevations of large, high-latitude plateau areas, but instead topographically-sheltered locations that enhance local snow accumulation and reduce melting. It is interesting to note that Brown and Ward (1996) argued that the availability of such 'snow traps' and 'radiation shelters' (Humlum, 1997; Glazirin and Escher-Vetter, 1998) is progressively reduced over the course of many glacial-interglacial cycles as the landscape gradually matures from a fluvially-dissected to an ice-moulded topography (cf. Oerlemans, 2002).

Humlum (1997) described the climatic and topographic controls on glaciation of the Söderasen Upland in southern Sweden during the Younger Dryas and showed that increases in snowfall alone are not able to initiate glaciation, because the majority of snowfall on the exposed upland is immediately removed again by snow drifting. He argued instead that glaciation can only begin in topographically-sheltered areas ('snow traps' and 'radiation shelters'), where snow accumulation is augmented locally by snow drift deposition, and melting is reduced locally by topographic shading. This led to a peculiar regional ELA pattern during the Younger Dryas in southern Sweden: The local ELA of the Söderasen

Upland was perhaps as low as 100 m asl, whereas the regional ELA or glaciation level elsewhere in southern Sweden was at about 500 m asl (Humlum, 1997). Sissons (1979) also argued that regional patterns of glacier advances during the Younger Dryas in the Scottish Highlands are best explained by a combination of snow-bearing winds and snow-blowing winds, rather than air temperature changes.

Basal ice formation (cf. Chapter 6) may provide an additional positive feedback process by further enhancing net mass accumulation in suitable locations. Basal ice typically forms at the base of thick snow drifts and snow banks during the spring snowmelt season and may not entirely melt during the summer, especially in suitable locations, for example 'snow traps' and 'radiation shelters' (Humlum, 1997). Snowfall in the subsequent fall and winter will then cover the newly-formed basal ice and in the following spring, an additional layer of basal ice will be superimposed on the year-old basal ice (Woo *et al.*, 1982). A continuation of this process over several years may help to establish a 'semi-permanent' snow bank, which has a core consisting of a series of multi-year basal ice layers (Østrem, 1963). This process may continue and lead to the initiation of permanent, localized, ice cover at those suitable locations, consistent with Flint's (1943) theory of 'Highland Origin and Windward Growth'.

2.3.4 Synopsis

In reality, the two 'Big-Picture' theories proposed by Flint (1943) and Ives *et al.* (1975) do not appear to be mutually exclusive – in fact they seem to be very much complementary (e.g. Flint, 1971) and can occur at the same time and space, or in temporal succession, depending on the specific local and regional topographic and climatic circumstances (e.g. Andrews *et al.*, 1970; Kerr, 1993; Whalley *et al.*, 1995; Rea *et al.*, 1998; Fredin, 2002; Sugden *et al.*, 2002). Marshall (2002), for example, showed that glacier inception/formation can occur at a number of independent sites across the globe, controlled by the amount of local/regional climate cooling and the specifics of the local/regional topography. Brown and Ward (1996) described the overall dependence of glacierization and geography as follows:

> "At the regional level, glacierization is associated with high elevation, as this encourages accumulation through increased precipitation and discourages ablation due to lower temperatures...However, within mountainous regions, at a local level topographic lows often represent more favorable conditions for snow accumulation."

Oerlemans (1991/1992) argued that the potential location of glacier or ice cap is largely determined by the available topography of a given region. However, once an ice body forms, it creates locally colder climatic conditions, thereby providing a positive feedback process that promotes its continued growth and survival (cf. Section 2.4.2). The ultimate size, shape, or elevation of the glacier or ice cap is therefore much less dependent on the available topography than its original inception. For example, Pollard and DeConto (2005) noted a pronounced hysteresis effect in Antarctic ice sheet growth and decay related to the so-called 'height-mass balance' feedback process (cf. Kerr, 1993). The basic idea that it is much easier to maintain an ice mass than to initiate one was already noted by Loewe (1971):

> "Once established, an ice sheet grows to higher and generally colder levels; it will tend to preserve itself. Hence, the conditions which allow an ice sheet to start will generally be more stringent than those which allow its survival."

It is also important to note that the geomorphic evidence visible today on the landscape represents an 'integration' of many past types (e.g. cold-based or warm-based) or phases of successive glaciation or deglaciation (e.g. snow fields, plateau glaciation, formation of outlet/valley glaciers, continental ice sheets, etc.), each one imprinting its own distinct geographic signature on top of the older ones (Dahl *et al.*, 1997; Rea *et al.*, 1998). Brown and Ward (1996) and Oerlemans (2002) have also argued that glaciation initiation may become more and more difficult to achieve as the landscape gradually matures from a fluvially-dissected to an ice-moulded topography over time (cf. Glasser, 1995).

Ives *et al.* (1975) theory of 'Instantaneous Glacierization' implies that strong secondary positive feedback processes (e.g. snow/ice-albedo-temperature feedback) supplement and enhance the initial external climate forcing to achieve the eventual full-scale glaciation of a large area or entire region. It is, however, difficult to imagine how such a self-sustaining system could establish itself, except, as postulated by Ives *et al.* (1975), in large climatically-sensitive areas, such as the interior Baffin Island plateau and Hazen Plateau of Ellesmere Island (Fig. 2.5) (cf. Andrews and Barry, 1978; Birchfield and Wertman, 1983). In addition, Koerner (1980a) questioned the precise mechanics of the theory of 'Instantaneous Glacierization', especially with respect to the existence of a non-linear, self-amplifying jump in the rate of albedo change. Flint's (1943) theory, in contrast, operates (at least initially) at much smaller spatial scales (e.g. 'snow traps' and 'radiation shelters') and it is difficult to imagine how such

small-scale processes can be directly linked to the initiation of continental ice sheets. In this context, it is an interesting thought experiment to imagine the 'most' sensitive geographic/topographic environment for glacier inception and survival: large high-elevation basins with a sudden increase in precipitation (Kerr, 1993; his Fig. 7), such as those that confine the North and South Patagonian Icefields (Sugden *et al.*, 2002; Hubbard *et al.*, 2005).

Dahl and Nesje (1992) noted an interesting difference between the climatic sensitivity of cirque and plateau glaciers, which is relevant in the context of the two 'Big-Picture' theories proposed by Flint (1943) and Ives *et al.* (1975). Cirque glaciers are often able to exist well-below the regional glaciation level, since their mass accumulation is enhanced by snow drifting and avalanching (cf. Andrews *et al.*, 1970; Williams, 1978a; Kuhn, 1995; Porter, 2001). As such, they respond more sensitively to changes in precipitation than plateau glaciers. However, Dahl and Nesje (1992) also showed considerably larger ELA depressions for plateau glaciers than for cirque glaciers during the Younger Dryas and 'Little Ice Age' in western and central Norway. This implies that plateau glaciers responded much more sensitively to changes in climate, given that annual precipitation and ablation season temperatures probably both decreased during these two time periods.

Brown and Ward (1996) presented examples and field evidence for both 'Big-Picture' theories from literally the same geographic area in southern Iceland (cf. Andrews *et al.*, 1970). Their work suggests that any glaciation begins ultimately with the formation and expansion of small snow fields in suitable locations. These locations are defined by subtle interactions between climate and the (currently available) local topography (cf. Manley, 1955). This topographic and climatic control decreases in importance as glaciation proceeds and glaciers increase in size (Oerlemans, 1991/1992; 2002). Whalley *et al.* (1995) effectively linked the two 'Big-Picture' theories together, by considering high-elevation plateau glaciation and associated lower elevation valley/cirque glaciation as separate, but mutually-dependent systems (cf. Evans *et al.*, 2002). The climatic sensitivity of the combined system (plateau and associated valley/cirque glaciation) is however primarily a function of the size of the plateau glaciers, which provide much of the required mass input (i.e. accumulation area) to the rest of the system (Dahl and Nesje, 1992; Whalley *et al.*, 1995).

2.4 Sensitivity of Glaciers to Climate Change

The basic premise of this study is the underlying hypothesis that the Hazen Plateau and North Coast are both environmentally-sensitive regions, where relatively slight changes in meteorological conditions can lead to significant changes in snow and firn extent in the short-term, and to a systematic shift in the regional glaciation level in the long-term (Fig. 2.8). The connection between glacier variations, weather, and climate were probably noted for the first time by Walcher (1773) (after Hoinkes, 1968; Hock, 2005). The question of climatic sensitivity of a particular glacier or region is obviously relevant in the context of climate change research. In essence, the glacier acts as a (non-linear) low-pass filter with respect to the associated climatic variability (Raper *et al.*, 1996) while at the same time also introducing a (variable) time lag between climate forcing and glacier response. A particularly sensitive glacier or region will most likely show a relatively larger, faster, or earlier response to even a small climatic perturbation, which may not (yet) have a discernable effect on a less sensitive glacier or region (e.g. Grudd, 1990; Hubbard, 1997; Cia *et al.*, 2005; Jansson *et al.*, 2005). On the other hand, it is also important to not over-interpret the perhaps dramatic response (i.e. retreat) of a single, highly sensitive, glacier or region (Furbish and Andrews, 1984; Gordon *et al.*, 1995; Burgess and Sharp, 2004) in a regional or global context. These considerations are also quite relevant in the context of paleoclimatic reconstructions based on proglacial lake sediments (e.g. Leonard, 1986; Braun *et al.*, 2000; Hardy *et al.*, 1996; Lewis *et al.*, 2002; Smith *et al.*, 2004; Jansson *et al.*, 2005) or glacier mass balance reconstructions based on paleoclimatic proxy records (e.g. Larocque and Smith, 2005).

2.4.1 Static vs. Dynamic Sensitivity of a Glacier

The static sensitivity or response of a glacier is defined as its immediate change in mass balance in response to a change in an external climatic parameter (e.g. temperature or precipitation). The dynamic sensitivity or response of a glacier additionally incorporates changes in glacier geometry occurring in response to the initial or continued mass balance perturbation. The difference between static and dynamic sensitivity/response is best illustrated with a simple thought experiment of a glacier initially in equilibrium with current climatic conditions (after Braithwaite and Zhang, 1999) (Fig. 2.9). Here, temperatures (T1) are abruptly increased (Δt) and then held constant at a new higher value ($T2 = T1 + \Delta t$)

for an extended period of time. The mean specific mass balance of the glacier will change abruptly (= short-term or static sensitivity/response) and then slowly decays back to zero (= long-term or dynamic sensitivity/response) as the glacier adjusts its own geometry to match the new climatic conditions and attains equilibrium again (cf. Greene, 2005).

It is useful here to discuss this simple thought experiment in a more comprehensive manner. An increase in air temperature during the melt season will obviously have a direct effect on the ablation of snow and ice during the melt season. In addition, the melt season will become longer and the higher air temperatures may also reduce the proportion of melt season precipitation falling as snow (Ohmura *et al.*, 1992). The warming may also be accompanied by an overall increase in precipitation, which is obviously only beneficial for the survival of the glacier if it is in the form of snow (e.g. Fujita and Ageta, 2000). The relative importance of the increases in ablation and increases in accumulation will depend on local conditions, but typically the increases in ablation will completely overwhelm the effect of increased precipitation/accumulation, and thus the net change in glacier mass balance in response to a climate warming will be negative (Braithwaite *et al.*, 2002; Oerlemans, 2005). In addition, there are several interrelated indirect effects influencing the overall mass balance of a given glacier or ice cap:

- The size of the ablation area will gradually increase, as the ELA rises in elevation in response to a climate warming. The albedo of exposed glacier ice is much lower than the albedo of snow, resulting in a positive feedback loop between the initial warming and glacier ablation.
- The lowering of the glacier surface (in elevation) due to increased ablation, will, in turn, lead to increased further melting (due to air temperature gradients with elevation; Braithwaite and Raper, 2002; Pollard and DeConto, 2005).
- The lowering of the glacier surface (in elevation) may also reduce overall snow accumulation on the glacier (due to precipitation gradients with elevation/temperature; e.g. Chinn *et al.*, 2005).

However, the dynamic response of the glacier (i.e. retreat of the terminus) begins to compensate for the negative mass balance perturbation by gradually reducing the size of the ablation area (= negative feedback process). This negative feedback process is initially weak, but becomes more and more significant as the glacier adjusts its geometry to a new equilibrium condition (van de Wal and Oerlemans, 1994; Raper *et al.*, 2000; Pollard and DeConto, 2005; Ridley *et al.*, 2005) (Fig. 2.9). Johannesson *et al.* (1989) related this exponential decay function to the ratio of maximum glacier thickness and mass balance at the glacier terminus. The initial and resultant mass balance of the glacier are the same (zero), while the respective glacier geometries and climatic conditions may be drastically different (Elsberg *et al.*, 2001; Harrison *et al.*, 2001).

The complete solution of the glacier-climate interaction problem obviously should include the dynamic sensitivity of the glaciers. However, the static sensitivity alone already captures the primary forcing of glacier variations by climate (Tangborn, 1980; Ohmura *et al.*, 1996a; Braithwaite and Zhang, 1999; Greene *et al.*, 1999; Braithwaite and Raper, 2002). It is therefore common practice to focus the discussion of glacier climate sensitivity on their static sensitivity (e.g. Oerlemans and Fourtin, 1992; Oerlemans, 1993; Gregory and Oerlemans, 1998; Braithwaite and Zhang, 1999; 2000; Braithwaite *et al.*, 2002; De Woul and Hock, 2004; Raper and Braithwaite, 2006), although a few studies have attempted to quantitatively incorporate dynamic changes in glacier geometry as well (e.g. Oerlemans *et al.*, 1998; Oerlemans, 2005).

2.4.2 External Forcing vs. Internal Modulation

Climatic changes, combined with local meteorological conditions, exert perhaps the most fundamental control on glacier mass balance, yet glacier fluctuations in response to any external forcing are additionally modulated by a wide range of internal factors that influence both the mass balance and dynamic response of a glacier (for example glacier location, size, type, shape, altitude, dynamics, and thermal regime) (Fig. 2.10). Therefore, glaciers even within a single area or region may behave somewhat differently even under the same general climatic conditions (e.g. Church, 1924; Mercer, 1961b; Andrews *et al.*, 1970; Williams, 1978b; Furbish and Andrews, 1984; Warren, 1990; Gordon *et al.*, 1995; Allen, 1997; Luckman, 2000; Abdalati *et al.*, 2004; Lehmkuhl and Owen, 2005). For example, the mass balance

of plateau ice caps is often less influenced by wind-drifted snow accumulation than that of valley or cirque glaciers within the same region (Dahl and Nesje, 1992; Lie *et al.*, 2003a, b). In other words, the exact nature of a glacier response (e.g. growth or retreat rates) to any change in climate (e.g. temperature, and/or precipitation, and/or etc.) will depend on its unique geographic characteristics (e.g. Matthews, 2005; Mark and Seltzer, 2005). Nonetheless, the temporal variations of mass balance within a glaciated area or region are typically much larger than its associated spatial variability (Reynaud *et al.*, 1984; Haeberli *et al.*, 1989; Greene *et al.*, 1999), reflecting a systematic response of glaciers to a 'homogenous' or 'dominant' regional climate signal (cf. Lowell, 2000; Vincent *et al.*, 2004; Oerlemans, 2005).

The linkages and interactions between external forcing, internal modulation, and glacier response (= result) are schematically illustrated in Figure 2.10. Reconstructions and models of conditions on the right can be developed based on data from the left, and vice-versa (Furbish and Andrews, 1984; Whalley *et al.*, 1989; Kerr, 1993; Boulton *et al.*, 1995; Hubbard, 1999; Kleman *et al.*, 2002; Golledge and Hubbard, 2005). Most ice sheets models are, in fact, validated against the available geological evidence, which immediately raises concerns about circular reasoning when these models are used later on to explain the geologic evidence (van der Veen, 1999a, b; Fredin, 2002). The relationships between climate, glaciers, and topography are, however, not only those of simple cause-and-effect, but are also characterized by mutual interdependence (Sutherland, 1984; Glasser, 1995; Brocklehurst and Whipple, 2004), considerable complexity (Andrews *et al.*, 1970; Furbish and Andrews, 1984; Casely and Dugmore, 2004; Kovanen and Slaymaker, 2005), and non-linearity (e.g. Small, 1995; Hubbard, 1997; Evans *et al.*, 2002; Golledge and Hubbard, 2005). They are also scale - and time-dependent. In other words: as a glacier grows, it is increasingly able to modify its own surrounding climate and topography (Sutherland, 1984; Payne and Sugden, 1990; Kerr, 1993; Fredin, 2002; Golledge and Hubbard, 2005), even though climatic (e.g. Bradley and England, 1978) and topographic (e.g. Hubbard, 1997) constrains can also limit its growth:

> "The fundamental effect of topography is to decouple the response of a glacier or an ice sheet from the climate." (Kerr, 1993)

Figure 2.11 is an attempt to illustrate this interdependence by depicting schematically three successive stages of glacierization. In marginally glacierized areas (e.g. Hazen Plateau or North Coast,

Ellesmere Island), climate interacts with the available topography to sustain only small glaciers and snow fields at particularly favorable sites (cf. Oerlemans, 1991/1992; Kuhn, 1995). These ice bodies are in-turn almost entirely dependent on climate and available topography and have only a minimal localized effect on their surrounding climate and topography. In areas of more substantial glaciation (e.g. Swiss Alps, Canadian High Arctic), the larger glaciers and ice caps have a greater influence on climate and topography, for example by exerting strong local cooling effects. Finally, very large ice caps or ice sheets (e.g. the Greenland Ice Sheet, the Antarctic Ice Sheet, or the Laurentide Ice Sheet) completely dominate(d) the underlying topography and act(ed) as major and independent factors in regional or global climate – short-term climatic fluctuations have (had) only a minor impact on their existence.

2.4.3 Local vs. General Climate

In the context of climate change, and its effect on the initiation, existence, and disappearance of glaciers, it is also useful to distinguish between 'local' and 'general' climate (e.g. Whalley *et al.*, 1989; Kovanen and Slaymaker, 2005):

- Local Climate: Climate on the glacier and its immediate surroundings, modified to some extent by the presence of the glacier itself (cf. Fig. 2.11).
- General Climate: Average climatic conditions for a region or area, as a function of global or regional-scale atmospheric circulation patterns (Lowell, 2000; Vincent *et al.*, 2004; Oerlemans, 2005).

For example, in the Swiss Alps, there is a marked contrast between the marginal zones (e.g. Mt. Blanc area) with heavy precipitation and relatively low snow lines (= more active, temperate glaciers) and the more interior regions (e.g. Wallis, Engadin) with reduced precipitation and elevated snow lines (= less active, partially cold-based glaciers) (Haeberli *et al.*, 1989). Similar spatial patterns of climate and glaciation also exists in the Canadian High Arctic (Miller *et al.*, 1975; Koerner, 1979) (cf. Section 2.4.4.3). These spatial climate patterns have to be understood when developing an integrated mass balance history for a larger area or region based on several/many different glaciers (Fountain *et al.*, 1999).

2.4.4 Sensitivity of Glaciers: Climatic Considerations

The climatic sensitivity of the mass balance of a given glacier to changes in air temperature (C_T) or precipitation (C_P) is usually expressed as (e.g. Oerlemans, 2001):

- $C_T = \Delta B / \Delta T$ ($\Delta T = \pm 1°C$; either uniform throughout year or limited to summer months) (ΔB = change in mass balance).
- $C_P = \Delta B / \Delta P$ ($\Delta P = \pm 10$ percent annual precipitation) (ΔB = change in mass balance).

The choice of $\pm 1°C$ air temperature change (either prescribed as a uniform change throughout the year or limited to the summer months) or ± 10 percent annual precipitation change is more-or-less arbitrary, but represents a useful standard reference for comparison of different glaciers around the world (e.g. Oerlemans and Fourtin, 1992; Oerlemans, 1993, 2001; Braithwaite and Zhang, 1999, 2000) (cf. Chapter 6).

Oerlemans and Fourtin (1992) and Oerlemans (1993, 2001) argued that the climatic sensitivity of glaciers is primarily determined by their precipitation regime (Fig. 2.12): Glaciers in wetter climates are very sensitive to climatic variations. In contrast, polar glaciers exhibit a very low climatic sensitivity because they receive only small amounts of annual precipitation (cf. Laumann and Reeh, 1993; Dowdeswell, 1995; Savoskul, 1997; Hoelzle *et al.*, 2003). This generally-accepted notion seems, at least initially, somewhat counter-intuitive – why should glaciers in wetter climates be more sensitive to climate change than glaciers in dry climates? According to Oerlemans and Fourtin (1992), glaciers in wetter climates tend to have higher mass turnover rates (e.g. Munro, 1991; Braithwaite and Zhang, 1999) and thus are able to extend their ablation areas (i.e. termini) down to much lower elevations relative to their ELA. Consequently, the air temperature over much of these glaciers is higher, the melt season lasts much longer (up to the entire mass balance year), and a significant fraction of the annual precipitation (already) falls as rain on the glacier (Ohmura *et al.*, 1992; Oerlemans and Hoogendoorn, 1989; Chinn *et al.*, 2005). In addition, wetter (i.e. maritime or tropical) climates tend to produce steeper elevational gradients of net mass balance (i.e. a higher activity index; Meier, 1962) than those created under dry (i.e. Arctic)

conditions (Munro, 1991; Kerr, 1993; his Fig. 2). In other words: Small changes in air temperature have an effect on melting and mass loss throughout the entire year, if the glacier already exists in a wetter (and therefore warmer) environment to begin with (Gregory and Oerlemans, 1998; Oerlemans, 1998; Braithwaite and Zhang, 1999).

Figure 2.12 shows schematically the dependence of glacier mass balance sensitivity on annual precipitation (after Oerlemans, 1993; 2001). For (dry) polar glaciers, it does not make much difference whether a +1°C climate warming is distributed uniformly throughout the year (black solid line) or limited only to the summer month (black dotted line). It is simply too cold during the fall, winter, and spring season to cause significant amounts of additional melting during those seasons (Gregory and Oerlemans, 1998; Braithwaite *et al.*, 2002; Mackintosh *et al.*, 2002; Weber and Oerlemans, 2003; Oerlemans *et al.*, in press). For glaciers in wetter environments (e.g. Sub-Arctic, tropical, or alpine environments), a uniform increase in temperature over the entire year has a much greater effect on their mass balance, since melting and ablation are not limited to only the summer season, but also may occur during the fall, (winter), and spring (Gregory and Oerlemans, 1998; Braithwaite *et al.*, 2002; Weber and Oerlemans, 2003). This is elegantly illustrated by the fact that when warming is limited to only the summer months (Fig. 2.12; dotted line), the climatic sensitivity does not further increase for annual precipitation greater than about 1 m/year (Oerlemans, 1993; 1998).

Braithwaite and Zhang (1999) and Braithwaite *et al.* (2002) showed an almost identical graph, but instead decided to plot glacier sensitivity as a function of mass balance amplitude or mass turnover (i.e. the difference between mass accumulation and ablation), rather than annual precipitation (cf. Munro, 1991; Raper *et al.*, 2000; Klingbjer *et al.*, 2005). Koerner (2002) also argued that glaciers in the High Arctic are relatively insensitive to climate change because of their low activity index or annual mass turnover rates. On the other hand, Fountain *et al.* (1999) argued that the relative importance of even a small mass balance perturbation is larger for polar glaciers with smaller absolute values of annual mass accumulation and ablation.

2.4.4.1 Climatic Sensitivity: Temperature and/or Precipitation

The climatic sensitivity of glaciers is often discussed (and simplified in models) in terms of their specific response (e.g. advance or retreat) to changes in air temperature and/or precipitation (e.g. Oerlemans and Fourtin, 1992; Van de Wal and Wild, 2001; Bromwich *et al.*, 2002; Cia *et al.*, 2005; Kovanen and Slaymaker, 2005). A typical question to ask in this context might be: Are changes in air temperature more important for glaciation than changes in precipitation?

It is often stated (e.g. Walters and Meier, 1989; Koerner and Fisher, 2002; Shahgedanova *et al.*, 2005) that the mass balance of continental glaciers is primarily influenced by changes in ablation season temperature, whereas the mass balance of more maritime glaciers is dominated by accumulation season precipitation (e.g. Grove, 1988, Karlen, 1988; Pelto *et al.*, 1990; Kerr, 1993; Brugger, 2005; Chinn *et al.*, 2005; Lehmkuhl and Owen, 2005). This question is significant in the context of glacier response to past and future climatic change, as presumably increases/decreases in temperature will be accompanied to some extent by corresponding increases/decreases in precipitation. It follows that both changes in temperature and precipitation (and possibly other climatic variables) need to be considered when linking changes in climate to changes in glacier mass balance (e.g. Brooks, 1924; Dahl and Nesje, 1992; Raper *et al.*, 1996; Lie *et al.*, 2003b; Mölg *et al.*, 2003; Kaser *et al.*, 2004a). Unfortunately,

> "...the specific mix of temperature and precipitation inputs that result in mass balance changes is not easily deciphered." (Luckman, 2000) (cf. Ahlman, 1936)

For example, Dyurgerov (2002) and Arnold (2005) argued that snow accumulation is the dominant glacier mass balance control at high elevations, whereas temperature is more important at lower elevations. It is also reasonable to assume that the net effect of any change in temperature on glacier mass balance may be (at least in part) offset by corresponding changes in precipitation (= negative feedback process) (e.g. Weber and Oerlemans, 2003; Morris and Mulvaney, 2004; de Woul and Hock, 2004). The question above can be therefore re-worded from a more glaciological point-of-view to ask: What is the most important factor controlling the net mass balance of a given glacier: (Summer) temperature or (winter) precipitation?

2.4.4.2 General Considerations

Miller *et al.* (1975) and Porter (1977) argued that (accumulation season) precipitation and (ablation season) temperatures together are the two most relevant climatic factors determining the location of a glacier and its annual mass balance (cf. Sugden *et al.*, 2002). Kuhn (1984) considered the sensitivity of glaciers in response to climatic variations first theoretically and subsequently applied his model to seven glaciers, representing a variety of climatic regimes around the world. He concluded that the length and intensity of the melt season (cf. Hooke *et al.*, 1987) is of greatest importance in determining the annual mass balance of polar glaciers. Ahlman (1936) commented with respect to the mass balance of a glacier on Svalbard:

> "The economy of the glacier [14th of July Glacier, Svalbard] is considerably more sensitive to changes in the ablation than in the accumulation, or in other words: a given change in the economy [i.e. mass balance] of a glacier requires smaller as well as more commonly occurring changes in the dominant meteorological factors affecting ablation than in those affecting accumulation." (Ahlman, 1936)

In contrast, precipitation and accumulation, especially during the melt season, were very important for glaciers in wetter climates, with a much stronger maritime influence. Karlen (1973, 1988) noted that mean summer temperature was the primary control on glacier variations throughout the Holocene in northern Sweden. According to Sugden *et al.* (2002), "the mean temperature of the ablation season is the most important climatic factor influencing glacier survival". It is therefore not surprising that the height of the July atmospheric freezing level or the location of the July 0°C isotherm are commonly used as indices for glaciation and glacier mass balance in polar (e.g. Bradley, 1973, 1975; Miller *et al.*, 1975; Vaughn and Doake, 1996; Dahl *et al.*, 1997) and even alpine or tropical environments (Greene *et al.*, 1999; Hostetler and Clark, 2000; Porter, 2001).

On the other hand, Porter (1977) and Shea *et al.* (2004) showed beautifully that regional glaciation patterns in the Cascade Range of Washington State and in the Canadian Rockies are much more a function of winter/spring snowfall than summer temperature. A similar situation exists today in the Canadian High Arctic (see below), German Alps (Escher-Vetter and Rentsch, 1995), Swiss Alps (Haeberli *et al.*, 1989), southern Norway (Lie *et al.*, 2003b; Matthews, 2005), and the Himalayas (Owen *et al.*, 2005). Holmlund and Schneider (1997) also linked changes in climatic continentality to glacier

mass balance variations across northern Scandinavia: the (very maritime) glaciers along the Norwegian coast have been gaining mass in recent years in response to increased precipitation, whereas the (more continental) glaciers in northern Sweden continue to loose mass due to increased summer melting (cf. Chinn *et al.*, 2005). According to Sugden *et al.* (2002), precipitation "magnitude determines whether or not there is any surplus ice left over after the ablation season".

Braithwaite and Zhang (2000), Raper *et al.* (2000), Braithwaite *et al.* (2002), and Oerlemans (2001, 2005) have shown, using mass balance modeling for a large number of glaciers around the world, that a 25 to 40 percent increase in annual precipitation is typically required to compensate for the mass loss resulting from a uniform +1°C warming in temperature. A more specific example is provided by Hagen and Liestol (1990) for glaciers on Svalbard, where a winter precipitation increase of about 50 percent would be required to compensate for a summer temperature increase of 1°C (cf. de Woul and Hock, 2004). Oerlemans (1991) determined a similar value for the Greenland Ice Sheet. Such a large increase in precipitation may be possible to achieve under suitable conditions at the local or regional scale (e.g. Kattsov and Källen, 2005). For example, the recent advances of glaciers (between 1980 and 2000) in southwestern Norway and New Zealand have been linked to a strong increase in precipitation (Holmlund and Schneider, 1997; Oerlemans, 2001; Chinn *et al.*, 2005). In fact, Chinn *et al.* (2005) argued that Norway might be considered as an example how 'Global Warming' can lead (locally) to glacier advances (provided that air temperatures do not exceed a critical threshold, cf. Miller and de Vernal, 1992).

On a global scale, however, it is highly unlikely that any future 'greenhouse warming' will be accompanied by such a large increase in precipitation. For example, the modeled annual precipitation increases over the next 100 years using the IPCC B2 emissions scenario for the Arctic Ocean and surrounding five major watersheds are only 5 to 10 percent (Walsh, 2005). Other values in the literature typically range from 3 to 9 percent increases in annual precipitation per 1°C increase in annual mean temperature (Oerlemans, 1991; Morris and Mulvaney, 2004). Either way, this implies that the net effect of rising temperatures will still be detrimental to the existence of glaciers around the world (Miller and de Vernal, 1992; Oerlemans, 2001; Braithwaite *et al.*, 2002). Van de Wal and Wild (2001) concluded that precipitation changes can be neglected relative to temperature changes with respect to future sea level change. On the other hand, climatic cooling impacts glacier mass balance in two complementary ways

(Marshall, 2002): Summer melting (i.e. its intensity and duration) is reduced, and spring, summer, and fall precipitation is more likely to fall as snow rather than rain (cf. Ohmura *et al.*, 1999). Gregory and Oerlemans (1998) and Raper and Braithwaite (2006, and references therein), for example, predicted the contributions to global sea level rise for the 21st century associated with the melting of small mountain glaciers and ice caps solely on the basis of temperature forcing, based on the argument:

> "The main climate variable controlling past and future global changes in mountain glaciers and icecaps is temperature change, with precipitation being of secondary importance."

Marshall (2002) also argued that air temperature exerted the dominant control on ice sheet formation some 115 kyr ago. Ice sheet expansion was also much more sensitively linked to decreasing air temperature (i.e. nonlinear relationship) than increased precipitation rate (linear relationship). Marshall (2002) suggested that a temperature reduction of 5°C to 6°C represents a 'key threshold', beyond which large areas of North America and Eurasia suddenly become capable of supporting sufficient ice to cause a significant sea-level impact. In fact, Marshall (2002) compares this threshold situation to Ives *et al.* (1975) theory of 'Instantaneous Glacierization'. A colder and wetter climate, obviously, would facilitate rapid glacier inception with less severe cooling (Marshall, 2002).

2.4.4.3 The Situation in the Canadian High Arctic

The annual net mass balance of glaciers in the Canadian High Arctic is primarily controlled by variations in summer melting rather than by winter snow accumulation, which is relatively low and fairly constant on an inter-annual basis (Table 2.2) (Adams *et al.*, 1998; Koerner, 2002; Koerner and Fisher, 2002). The same statements holds true for Arctic glaciers in general (Fristrup, 1951; Sharp, 1956; Dowdeswell *et al.*, 1997). On the other hand, regional spatial patterns of glaciation in the Canadian High Arctic are also strongly influenced by regional precipitation and snow accumulation gradients (Miller *et al.*, 1975; Koerner, 1979). Maps of precipitation and winter mass balance in the Queen Elizabeth Islands (e.g. Koerner, 1979) show a pronounced decreasing gradient from the southeast (Baffin Bay) to the north/northwest (Hazen Plateau) across the Canadian Arctic island archipelago. This spatial pattern of precipitation and accumulation is associated with the growth of more dynamic, low-elevation glaciers in

the southeast and less dynamic, high-elevation glaciers in the north/northwest of the Queen Elizabeth Islands (Koerner, 2002). A secondary maximum in precipitation, snow accumulation, and associated glaciation occurs along the northern coast of Ellesmere Island, which is directly influenced by moisture advection from the Arctic Ocean (Koerner, 1979).

Bradley and England (1978) noted an interesting asymmetry of glacier mass balance in the Canadian High Arctic with respect to climatic change. Annual mass gains of a typical High Arctic glacier are fundamentally limited by the very low amounts of annual precipitation, whereas annual mass losses are (at least theoretically) unlimited. In other words: Glaciers and ice caps in the Canadian High Arctic can loose substantial amounts of mass in exceptionally warm summers (e.g. 1962, 1998, or 2003), but cannot gain more mass than they accumulate in any given mass balance year (Koerner, 1977a; Adams *et al.*, 1998). However, annual snowfall amounts are today, on average, so low that even a few 'good' years of net accumulation can be easily obliterated by a single 'normal' negative mass balance year (Koerner, 1980a; Bromwich *et al.*, 2002) (Table 2.2).

The overall climatic sensitivity of glaciers in the Canadian High Arctic can be therefore simplified, generalized, and summarized as follows:

1. Glacier mass gains are realistically only possible if summer temperatures decrease substantially (e.g. Hattersley-Smith, 1960a; Arnold, 1965; Bromwich *et al.*, 2002), as annual snow accumulation would need to increase between 56 and 489 percent for the glaciers to achieve a balanced state with unchanged summer temperatures (Table 2.2).
2. Significant and rapid glacier expansion, on the other hand, is realistically only possible with concurrent substantial increases in precipitation (Andrews *et al.*, 1972; Andrews and Mahaffy, 1976; Bradley and England, 1978; England and Bradley, 1978; Abe-Ouchi and Blatter, 1993; England, 1986a; Fredin, 2002; Marshall, 2002; Lie *et al.*, 2003b).

In conclusion, it is perhaps most appropriate to regard precipitation or snow accumulation (= mass additions) in the Canadian High Arctic as a more-or-less constant 'boundary condition' (cf. Bradley and England, 1978; England, 1986a; Hooke *et al.*, 1987; Oerlemans and Reichert, 2000, Sugden *et al.*, 2002; Raper and Braithwaite, 2006), which partly controls the spatial patterns of glaciation across the islands. Summer temperature and melting (= mass losses), in contrast, are much more variable from year-to-year and therefore exert the primary climatic forcing on glacier mass balance variations, at least since the end of the 'Little Ice Age' (Koerner, 1977a). Koerner and Fisher (2002) summarized the relationship between glacier mass balance and climate in the Canadian High Arctic very succinctly:

> "Summer conditions dominate the mass balance whereas winter snow accumulation bears very little relationship to that balance. In this case, ice-cap/ice-sheet attrition is driven by warmer summers, while growth is driven by cooler summers."

Yet, at longer time scales, precipitation changes may become more and more important (Andrews *et al.*, 1972):

> "In our view, the glaciation of arctic areas must rely primarily on an increase in solid precipitation."

Schneider (1999) and Greene *et al.* (1999) came to the same conclusion with respect to the modern glaciers on the Antarctic Peninsula and in the Swiss Alps. The climate of the High Arctic is dry (i.e. low annual/winter snowfall) and cold (i.e. short ablation season). The mass balance of the Hazen Plateau ice caps is therefore very sensitive to anything that influences the length and/or intensity of the ablation season, such as atmospheric freezing-levels (Bradley, 1975) or summer melting degree-day totals (Bradley and England, 1978). This dominant summer temperature sensitivity, however, is perhaps somewhat reduced for glaciers that experience more annual or winter snowfall (Bradley, 1975), such as the Ward Hunt Ice Rise and Ice Shelf.

2.4.4.4 Climatic Sensitivity of the Hazen Plateau Ice Caps

It is obvious that the climatic sensitivity should be regarded as one of the basic quantities that characterize a given glacier. To this end, Oerlemans (2001) introduced two simple empirical equations,

based on an assessment of 13 well-studied glaciers around the world (cf. Oerlemans and Fourtin, 1992). These two equations allow an estimation of the climatic sensitivity of unmeasured glaciers (Fig. 2.13) based exclusively on the amount of annual precipitation they receive:

- $C_T = -0.271 * (\text{annual precipitation})^{0.597}$

  (for a +1°C uniform warming throughout the entire year)
- $C_P = 0.0125 * (\text{annual precipitation})^{0.797}$

  (for a +10 percent increase in annual precipitation)

These two equations can provide simple first-order estimates of the climatic sensitivity of a particular glacier of interest (Dowdeswell, 1995; Oerlemans, 2001), based exclusively on their annual precipitation (i.e. its annual mass accumulation). Again, the choice of a +1°C uniform warming throughout the year or a +10 percent increase in annual precipitation is somewhat arbitrary, but provides a useful reference frame to compare the climatic sensitivity of different glaciers worldwide (Braithwaite and Zhang, 1999). The two equations and the associated graph (Fig. 2.13) highlight three basic (and obvious) features of the climatic sensitivity of glaciers:

1. The climatic sensitivity for a +1°C uniform warming is negative, i.e. annual glacier mass balance will become less positive/more negative with higher air temperatures.
2. The climatic sensitivity for a +10 percent increase in annual precipitation is positive, i.e. annual glacier mass balance will become more positive/less negative with increased precipitation.
3. $C_T >> C_P$ meaning that a +1°C uniform warming will have a much greater effect on annual glacier mass balance than a +10 percent increase in annual precipitation (cf. Oerlemans, 1993; Marshall, 2002).

The calculated temperature sensitivity (C_T) for the White and Baby Glacier (cf. Section 2.2.1.5), using the two Oerlemans (2001) equations, is –0.073 m weq/°C, assuming that both glaciers receive the same amounts of annual precipitation (i.e. 110 mm weq) (Fig. 2.13). However, the temperature sensitivity (C_T) for the White and Baby Glacier has also been determined independently from long-term on-site mass balance measurements:

- C_T (White Glacier) = –0.074 m weq/°C (Cogley *et al.*, 1996)
- C_T (Baby Glacier) = –0.3 m weq/°C (Adams *et al.*, 1998)

The close match between measured and estimated C_T for the White Glacier is quite remarkable, although it should be noted that the White Glacier was one of the 13 glaciers used by Oerlemans (2001) to define his two empirical equations. In contrast, the available mass balance measurements suggest that the Baby Glacier is about four times more climatically-sensitive than the neighboring White Glacier (Fig. 2.13). This result is entirely reasonable, given the specific geographic and topographic characteristics of the Baby Glacier, and its precarious situation with respect to the regional ELA (Adams *et al.*, 1998). But this simple comparison also demonstrates that the two Oerlemans (2001) equations cannot be used without caution to estimate the climatic sensitivity of small glaciers in what may be considered 'unusual' geographic situations, such as the Baby Glacier. The equations appear to work quite well for larger 'normal' glaciers, such as the White Glacier. This is not necessarily a surprising result. These two empirical equations are defined using glacier mass balance data from 13 fairly large ice bodies around the world – including the White Glacier and Devon Ice Cap as the two only representatives of High Arctic glaciers (Oerlemans and Fourtin, 1992; Oerlemans, 2001). It is therefore entirely reasonable that these equations are not able to estimate the climatic sensitivity of glaciers with characteristics not captured by the 13 glaciers used in their definition.

The predicted air temperature sensitivity for the Hazen Plateau ice caps (annual precipitation ~125 mm weq, cf. Chapter 5), calculated using the two Oerlemans (2001) equations, is about –0.078 m weq/°C (Fig. 2.13), which is consistent with the general notion that glaciers in dry environments are very insensitive to climatic fluctuations. However, given their strong geographic similarities to the Baby

Glacier, one might also expect the 'true' climatic sensitivity of the Hazen Plateau ice caps to be much greater. In fact, one could argue that the stagnant Hazen Plateau ice caps should respond extremely fast (i.e. immediately) to climatic change, because of their lack of appreciable ice flow (Paterson, 1969; see below).

Small, stagnant ice caps are fairly common in the Canadian High Arctic, either at high elevations (e.g. Hazen Plateau) or in close vicinity to the Arctic Ocean (e.g. Ward Hunt Ice Rise). They are also frequently located in vicinity of much larger, dynamic ice caps (Koerner, 2002), perhaps suggesting recent recession of those larger ice caps. Small, stagnant ice caps in the High Arctic (and elsewhere) are able to respond immediately to climatic change (Paterson, 1969; Haeberli *et al.*, 1989), because changes along their margins (i.e. advance or retreat) are not first modulated by internal ice flow (Jacobs *et al.*, 1993). Yet, a retreat of the ice margins does not necessarily imply that the entire ice cap experiences a net negative annual mass balance (Koerner and Lundgaard, 1995). The margins of a stagnant ice cap will continue to retreat as long as the ELA is inside/higher than its margins, even though the central parts of the ice cap may be located well above the ELA. Conversely, a stagnant ice cap can only advance if the ELA lies entirely beyond/below its margin (Paterson, 1969; Koerner, 2002). The retreat or advance of the ice margin is therefore not a linear or symmetric response to climate change in the case of a stagnant glacier or ice cap.

2.4.5 Sensitivity of Glaciers: Internal Characteristics of the Glacier

It is well-established that the temperature response of the high latitudes to increased greenhouse gases (i.e. 'Global Warming') will be stronger than the response of the mid- and low latitudes (e.g. Bigelow *et al.*, 2003; Meehl *et al.*, 2005). On the other hand, it is also well-established that High Arctic glaciers do not respond particularly rapidly or sensitively to changes in climate, because of the very dry climatic conditions (Weidick, 1984; Oerlemans and Fourtin, 1992; Koerner and Lundgaard, 1995) and resultant low mass turnover rates (ratio between total accumulation and total ablation) (Braithwaite and Zhang, 2000; Koerner, 2002). One could therefore ask: Are we looking at the correct (i.e. sensitive) region (i.e. the High Arctic), but perhaps using the wrong (i.e. insensitive) tool or indicator (i.e. High Arctic glacier mass balance) in terms of climate change detection?

Paterson (1981, 1994) provided one possible answer to this question in his benchmark textbook on the physics of glaciers (cf. Fig. 2.10; Furbish and Andrews, 1984) by emphasizing localized variability:

> "While advances and retreats of different glaciers appear to be broadly synchronous [globally], the picture becomes more confused on closer examination of the records. Some glaciers in an area may be advancing while others are retreating. This is the case at present [i.e. 1981] in the north-western U.S.A. Some variations can be explained by differences between the local climates of different glaciers. On the other hand, glaciers differ one from another in such features as size, steepness, and velocity. Hence different glaciers might be expected to react differently, or at least with different speeds, to a change in climate."

However, glacier response and glacier sensitivity to climate change may not always be the same. For example, a glacier with a small surface slope (and thus slower ice flow) responds relatively slowly to a given climatic/mass balance perturbation (see below), yet it may be very sensitive since a small change in the ELA, for example, affects a relatively larger surface area (Kerr, 1993). The four most important internal characteristics that modulate the specific response of a glacier or ice cap to an (external) change in climate are schematically illustrated in Figure 2.14 (cf. Fig. 2.10).

2.4.5.1 Internal Characteristics: Size of a Glacier or Ice Cap

Typically, smaller glaciers or ice caps tend to be much more sensitive to even small and/or rapid climatic fluctuations than larger glaciers, ice caps, or ice sheets (e.g. Nye, 1965; Paterson, 1981; Weidick, 1984; Ballantyne, 1990; Grudd, 1990; Hubbard, 1997; Cogley and Adams, 1998; Adams *et al.*, 1998; Chinn, 1999; Casely and Dugmore, 2004; Chinn *et al.*, 2005; Cia *et al.*, 2005), although theoretical considerations (Bahr *et al.*, 1998; Hoelzle *et al.* 2003) and numerical modeling experiments (Pfeffer *et al.*, 1998) have revealed that the relationship between glacier size and response is perhaps not as straightforward as conventionally understood (cf. Klingbjer *et al.*, 2005):

> "In reality, small glaciers in general may respond faster but not because of their intrinsic glacier dynamics. They do so because of their characteristic shape (slope and area-elevation distribution), which for small glaciers is typically dictated more by the bedrock topography on which the glacier sits than by dynamics or variations in ice thickness." (Pfeffer *et al.*, 1998)

It is interesting to note in this context that Koerner (1989a; 2002) mentioned a fairly robust relationship between the size and thickness of an ice cap in the Canadian High Arctic and its approximate age (cf. Andrews *et al.*, 1970). Many of the smallest stagnant ice caps such as the Hazen Plateau ice caps (diameter less than 5 km; thickness less than 30 m) probably began their existence only during the so-called 'Little Ice Age' some 200 to 300 years ago (Koerner, 1989a; 2002). In contrast, the larger stagnant ice caps (e.g. Meighen Ice Cap; cf. Section 2.2.1.6) probably began to grow and expand during the climatic deterioration following the Holocene Climatic Optimum some 4000 years ago (Koerner, 1989a; 2002). Kuhn (1995) distinguished between two different types of small glaciers in the context of their sensitivity to climate change (cf. Williams, 1978a; Allen, 1997; Dahl and Nesje, 1992; Porter, 2001):

1. Small glaciers that exist at the highest elevations of mountain ranges and plateau areas, just barely above the regional ELA. Such glaciers are very sensitive to climatic fluctuations and may rapidly and frequently disappear and reform over time.
2. Small glaciers that exist in topographically-sheltered locations, often well-below the regional ELA, due to abnormally high snow accumulation (through wind drift and snow avalanches). Such glaciers are very insensitive to climatic fluctuations, "as their survival is ensured more by topography than by climatic conditions" (cf. Kerr, 1993; Laumann and Reeh, 1993; Chinn, 1999; Lie *et al.*, 2003a, b).

2.4.5.2 Internal Characteristics: Slope of a Glacier or Ice Cap

It is also obvious that a steeper glacier or ice cap (with faster ice flow) should respond more sensitively to a given mass balance perturbation (in response to a climatic fluctuation) than a glacier with a small surface slope and slower ice flow (e.g. Hubbard, 1997; Bahr *et al.*, 1998; Hoelze *et al.*, 2003; Kovanen and Slaymaker, 2005; Chinn *et al.*, 2005). For example, Oerlemans (2005) calculated glacier response times ranging from as little as 20 years for the steepest glaciers (e.g. Franz-Joseph Glacier, New Zealand) to a couple of centuries for the largest and flattest glaciers and ice caps on Svalbard. Part of this

difference in the climatic sensitivity, however, must also be due to the very different precipitation regimes of Svalbard (very dry) and the west coast of New Zealands South Island (extremely wet). Glacier slope and precipitation regime may, in fact, be linked, as wetter (i.e. maritime or tropical) climates tend to produce steeper elevational gradients of net mass balance than those created under dry (i.e. Arctic) conditions (Munro, 1991; Kerr, 1993; Raper and Braithwaite, 2006).

2.4.5.3 Internal Characteristics: Ice flow/Mass Turnover Rates

Glaciers with faster ice flow (= higher mass turnover rates) will obviously respond faster than glaciers with slower ice flow and smaller mass turnover rates to a given mass balance perturbation (in response to a climatic fluctuation) (Munro, 1991; Hubbard, 1997; Bahr *et al.*, 1998; Raper *et al.*, 2000; Chinn *et al.*, 2005; Oerlemans, 2005) (Table 2.3). Chinn *et al.* (2005) argued that ice flow or mass turnover rates effectively modulate the effects of climatic variations: the higher the mass turnover, the greater the effect that variations of climatic variables (e.g. summer temperature and/or winter precipitation) will have on the glacier mass balance. Stagnant glaciers or ice caps essentially respond immediately to climate change, as their response is not first modulated by internal ice dynamics (Paterson, 1969). This means that interannual fluctuations in glacier length/area directly reflect changes in climate and glacier mass balance (Haeberli, 1998; 2004).

On the other hand, one could also argue that climatically and dynamically 'dead' ice masses (e.g. Messel, 1971) are in fact not sensitive at all to climatic variability, since they are completely out-of-equilibrium with contemporary climate and thus merely respond passively to external climatic variations (Bradley and Serreze, 1987a; Whalley *et al.*, 1995). For example, Bradley and Serreze (1987a) noted:

> "Overall, the [Hazen Plateau] ice caps today are wasting away and will eventually disappear if contemporary conditions are any guide to the climate of the next century or two. In the sense that they provide no long-term record of climate, they do not really provide any better indication of climatic variability than the Alert instrumental record."

2.4.5.4 Internal Characteristics: Area-Elevation Distribution

Ice masses with a highly non-linear (i.e. plateau-like) area-elevation distribution (= hypsography) are potentially very sensitive to climatic variations (Andrews *et al.*, 1976; Koerner, 1979;

1980a), but only if annual or inter-annual ELA fluctuations cover that particular sensitive altitudinal range, so that small changes in the ELA have a large effect on the amount of area contained, respectively, in the ablation and accumulation area (Ahlman, 1936; Furbish and Andrews, 1984; Haeberli *et al.*, 1989; Kerr, 1993; Laumann and Reeh, 1993; Hulton *et al.*, 1994; Small, 1995; Whalley *et al.*, 1995; Hagen *et al.*, 2003; Hoelzle *et al.*, 2003; Brocklehurst and Whipple, 2004; Carrivick and Brewer, 2004).

For example, the East Antarctic Ice Sheet has a plateau-like area-elevation distribution, but the main plateau surface is currently located today too far above the ELA for annual or inter-annual ELA changes to have a significant effect on the relative size of the ablation and accumulation area (Ohmura *et al.*, 1996a, b; Wild *et al.*, 2003; Pollard and DeConto, 2005). Likewise, a valley or cirque glacier is less sensitive to ELA changes than a plateau ice cap (Kuhn, 1995), for which even a small change in the ELA can significantly alter the ablation and accumulation area ratio (Laumann and Reeh, 1993; Dahl *et al.*, 1997). Mark and Seltzer (2005), for example, showed that glacier recession in the Cordillera Blanca of Peru between 1962 and 1999 was caused primarily by increasing temperatures, yet the associated spatial patterns of glacier recession were modulated significantly by the specific hypsometry of each glacier.

Figure 2.14 is an attempt to illustrate how the aforementioned four internal characteristics, combined with one external factor (precipitation), can be used to assess the overall climatic sensitivity of a glacier. This qualitative model is obviously incomplete and does not include all potentially relevant internal characteristics of a glacier (cf. Fig. 2.10). It is also not universally-applicable, as it is highly probable that one may find an individual glacier where in fact the opposite behavior is occurring today (e.g. Furbish and Andrews, 1984; Lie *et al.*, 2003a, b). For example, ablation on the very maritime Shokal'ski Glacier on Novaya Zemlya is almost exclusively a function of summer temperature (Zeeberg and Forman, 2001). This qualitative model is also perhaps less satisfying than the two simple equations presented by Oerlemans (2001) in the sense that it does not provide an absolute value for quantitative comparisons of different glaciers around the world. However, it incorporates at least some of the relevant internal characteristics of glaciers, which can be easily determined from topographic maps, aerial photographs, or satellite imagery (cf. Furbish and Andrews, 1984; Haeberli and Hoelzle, 1995). In that sense, the two models complement each other. Ultimately, the climatic sensitivity of a glacier can only be assessed through in-situ observations and at least basic mass balance/climate measurements.

2.4.6 Synopsis

When we discuss High Arctic glaciers and their apparent low climatic sensitivity (Oerlemans and Fourtin, 1992), we typically refer to the large High Arctic ice caps (e.g. Agassiz Ice Cap or Devon Ice Cap) or valley glaciers (e.g. White Glacier or Gilman Glacier). The fact that there are some highly-sensitive High Arctic glaciers or ice caps (e.g. Paterson, 1969; Adams *et al.*, 1998; Braun *et al.*, 2004a) does not fundamentally contradict this useful generalization, but rather serves to highlight the considerable heterogeneity of the High Arctic cyrosphere today. It is also somewhat unreasonable to expect one to comprehensively quantify every single nuance of the climatic sensitivity of a given glacier. After all, glaciers incorporate various aspects of the local and regional climate (which they also influence to some extent) into their mass balance, and then adjust their area and/or geometry to match (with some variable time lag) whatever climatic conditions they experience(d) today or at some point in the past. De-convoluting this variable process-, time-, and space-integration seems to be a-priori impossible for a natural system like a glacier (cf. van der Veen, 1999a).

Nevertheless, the question 'Are glaciers in wet environments more sensitive to climate change than glaciers in dry environments?' cannot be answered as simply as proposed originally by Oerlemans and Fourtin (1992) (e.g. Fountain *et al.*, 1999; Fujita and Ageta, 2000; Braithwaite and Raper, 2002):

1. Glaciers in dry environments (= low annual mass accumulation) are much more sensitive to mass losses than mass gains (Bradley and England, 1978; Koerner, 1980a; Adams *et al.*, 1998).
2. Glaciers in wet environments do respond faster to climatic fluctuations than glaciers in dry environments, but in this case precipitation regime is really used as a surrogate for high mass turnover rates and fast ice flow (Braithwaite and Zhang, 1999; Raper *et al.*, 2000; Klingbjer *et al.*, 2005), both of which are only in part related to precipitation.
3. The static sensitivity of glaciers in dry climates may be smaller than that of 'wet' glaciers, but the dynamic volume and area changes in response to a given climatic perturbation (i.e. the committed change) is presumably greater for

Arctic glaciers due to their much greater mass and volume (Haeberli and Hoelzle, 1995; Ohmura *et al.*, 1996a; Braithwaite and Raper, 2002).

4. A variety of secondary positive and negative feedback processes (e.g. snow/ice-albedo-temperature and height-mass balance) may lead to pronounced hysteresis effects during glacier expansion and recession cycles (North, 1984; Pollard and DeConto, 2005).

Again, this does not fundamentally contradict the useful generalization as originally proposed by Oerlemans and Fourtin (1992) that the precipitation regime of a glacier is intimately linked to its climatic sensitivity, but rather extends the discussion to also include the internal characteristics of the glacier (Fig. 2.14). This is obviously not a new idea (e.g. Furbish and Andrews, 1984):

> "Disparate responses [of glaciers to climate change] confuse any attempt to generalize in a simple way how glaciers of a region should, or have, responded to climatic events. Some variation can be explained by differences in local climate surrounding individual glaciers, but much variation must be explained by the many morphologic and glaciological features that distinguish individual glaciers, including differences in size, steepness, elevation, mass turnover, areal distribution of accumulation and ablation etc. (Andrews *et al.*, 1970; Paterson, 1981). (Many of these features, in fact, are linked with local climate)."

However, the climatic sensitivity of a glacier or glaciated area may also change gradually (or even abruptly) as the glacier adjusts its geometry in response to external climate change (Dugdale, 1972; Pelto *et al.*, 1990; Kerr, 1993; Klok and Oerlemans, 2003; Arnold, 2005). Globally, glacier mass turnover rates (and thus their climatic sensitivity) have been increasing in recent years due to overall more negative summer balances (i.e. enhanced melting) and more positive winter balances (i.e. enhanced precipitation and accumulation) (Dyurgerov, 2003).

Table 2.1 Mass balance data for the Gilman Glacier (1957 to 1959; measured at ~1050 m asl) (Hattersley-Smith *et al.*, 1961)

Year	Snow Depth (cm)	Snow Density	SWE (mm weq)	Ice Melt (cm)	Ice Melt (mm weq)	Net Melt (mm weq)	ELA (m asl)	Snowmelt Period (days)
1957	23.0	0.283	65	78.2	704	–770	1240	14
1958	22.5	0.289	65	54.9	494	–560	1200	18
1959	21.5	0.340[1]	73	NA	NA	NA	NA	NA

Notes

- The winter snowpack in 1959 included an exceptionally hard, wind-packed snow layer at the base, which appears to be a useful analogue to the 'Dole-Layer' (unofficial name) discovered on Murray Ice Cap in 2000.

Table 2.2 Long-term means and standard deviations of winter, summer, and annual mass balance (mm weq) of the six monitored glaciers in the Canadian High Arctic (Cogley *et al.*, 1996; Adams *et al.*, 1998; Koerner, pers. comm.). Note: The reported data for the White and Baby Glacier only include annual net balance, not winter/summer balances separately.

Glacier	Winter Balance	Summer Balance	Annual Balance	Ratio (Summer/Winter)
Meighen Ice Cap	174±58	–272±249	–97±266	1.56
Melville South Ice Cap	182±40	–369±259	–186±270	2.03
Devon Ice Cap	113±21	–192±144	–82±149	1.70
Drambuie Glacier	90±20	–530±190	–450±200	5.89
White Glacier	NA	NA	–144±239	NA
Baby Glacier	NA	NA	–160±379	NA

Notes

- Meighen Ice Cap: 1960 to 2001
- Melville South Ice Cap: 1963 to 2001
- Devon Ice Cap: 1961 to 2001
- Drambuie Glacier: 1977 to 2001
- White Glacier 1960 to 2001
- Baby Glacier 1960 to 2001 (data for 1978 to 1989 are missing)

Table 2.3 Glacier sensitivity to climate change in relationship to ice flow or mass turnover rates (cf. Section 2.4.5.3).

Ice Flow/Mass Turnover Rates	Glacier Sensitivity
Fast/High	High
Slow/Low	Low
None/None (= stagnant)	Very High (or none)

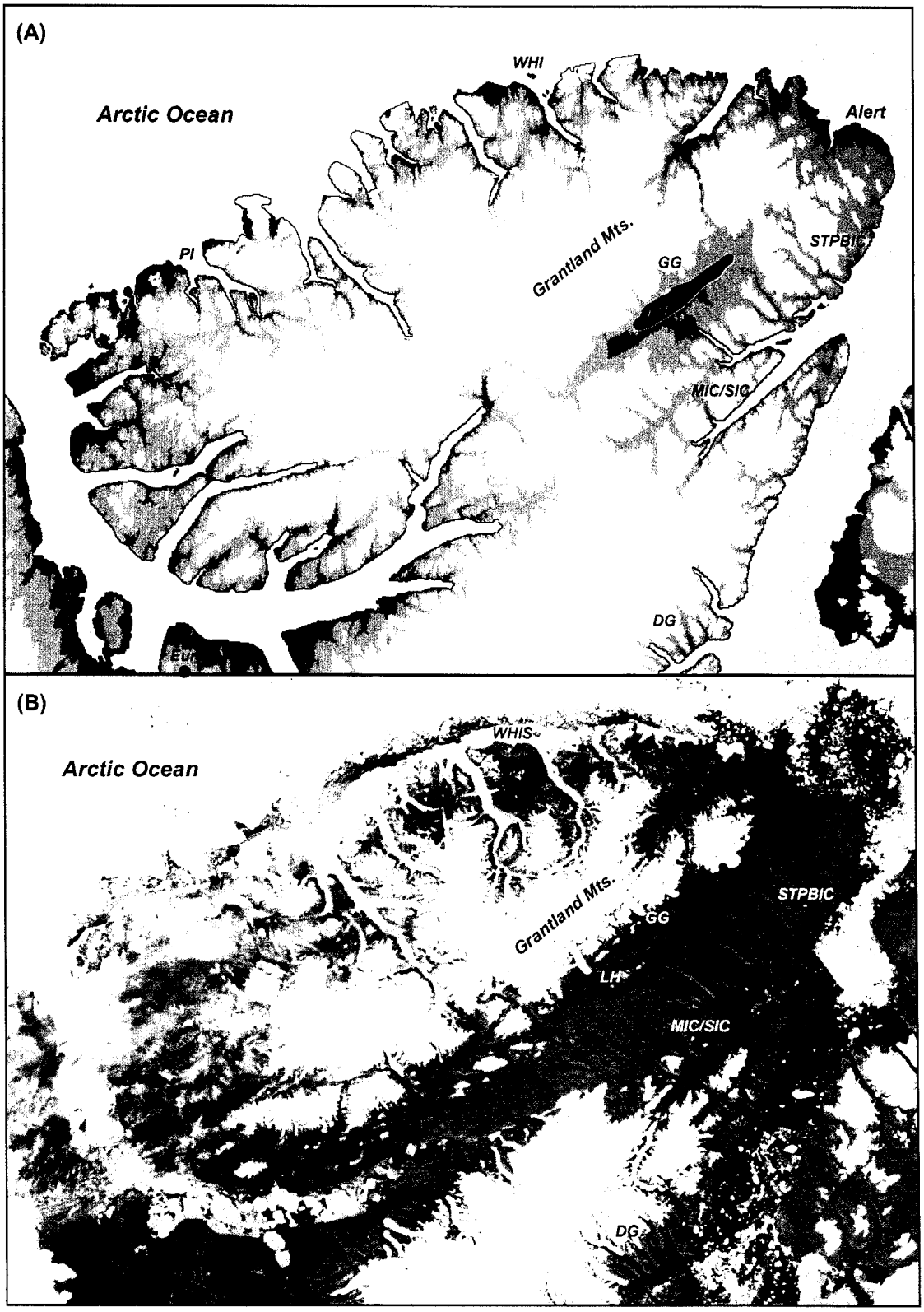
(A)
Arctic Ocean
WHI
Alert
PI
Grantland Mts.
GG
STPBIC
MIC/SIC
DG
(B)
Arctic Ocean
WHIS
Grantland Mts.
GG
STPBIC
LH
MIC/SIC
DG

Figure 2.1

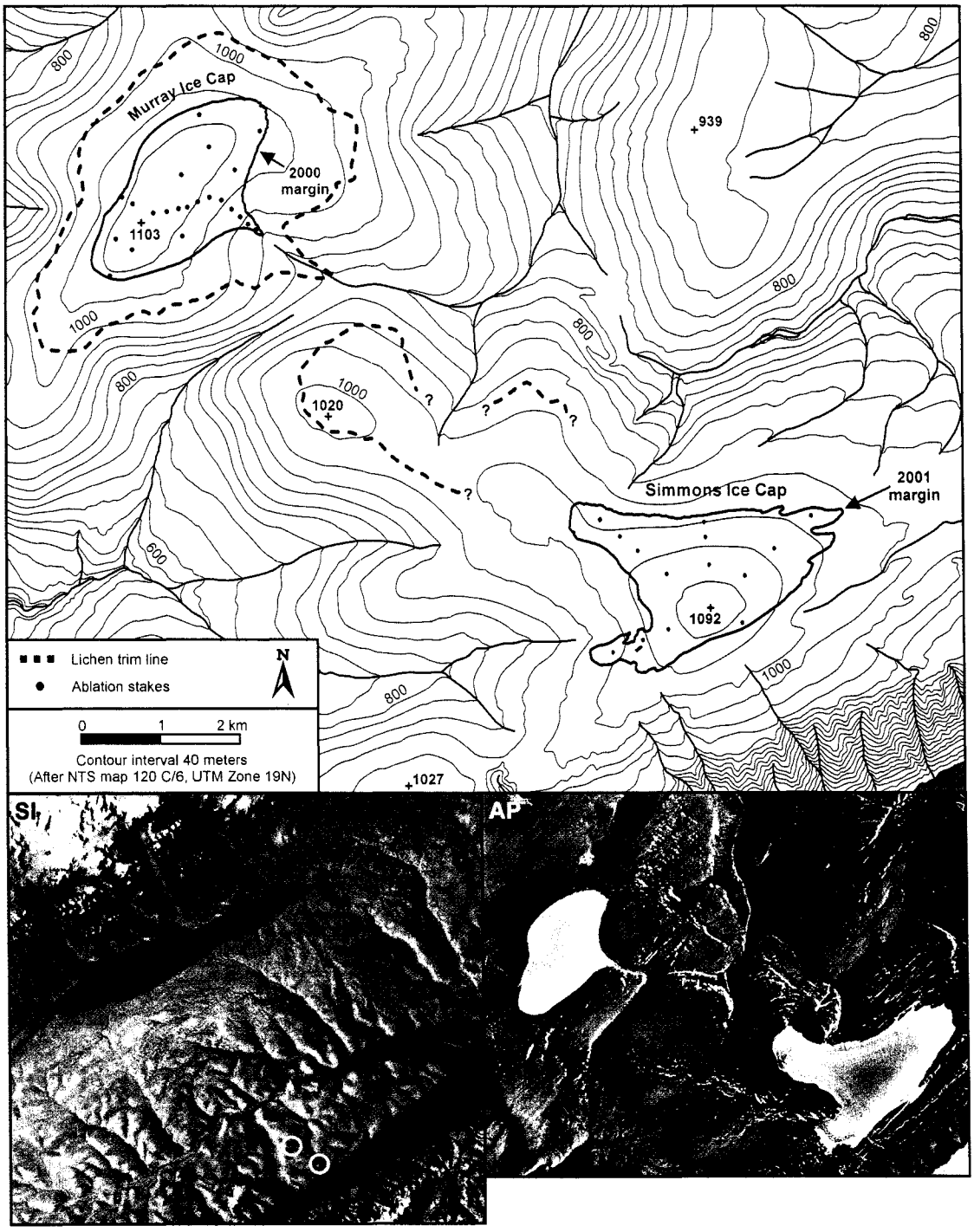

Figure 2.2 Topographic map, aerial photograph (AP), and late summer 1999 LANDSAT satellite image (SI) of the Hazen Plateau ice caps (unofficial name), Ellesmere Island, Nunavut, Canada: Murray and Simmons Ice Cap.

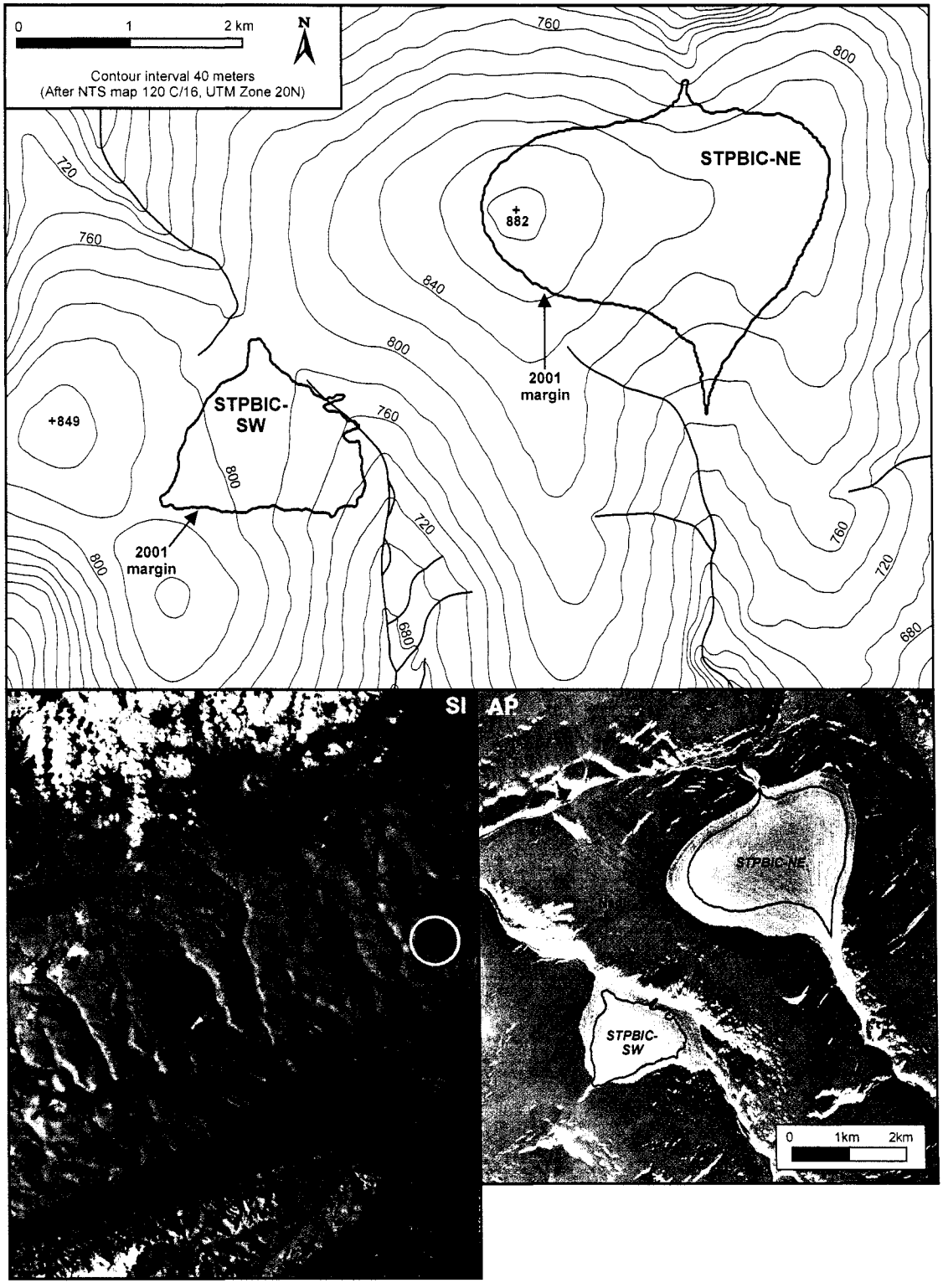

Figure 2.3 Topographic map, aerial photograph (AP), and late summer 1999 LANDSAT satellite image (SI) of the Hazen Plateau ice caps (unofficial name), Ellesmere Island, Nunavut, Canada: St. Patrick Bay ice caps (unofficial name).

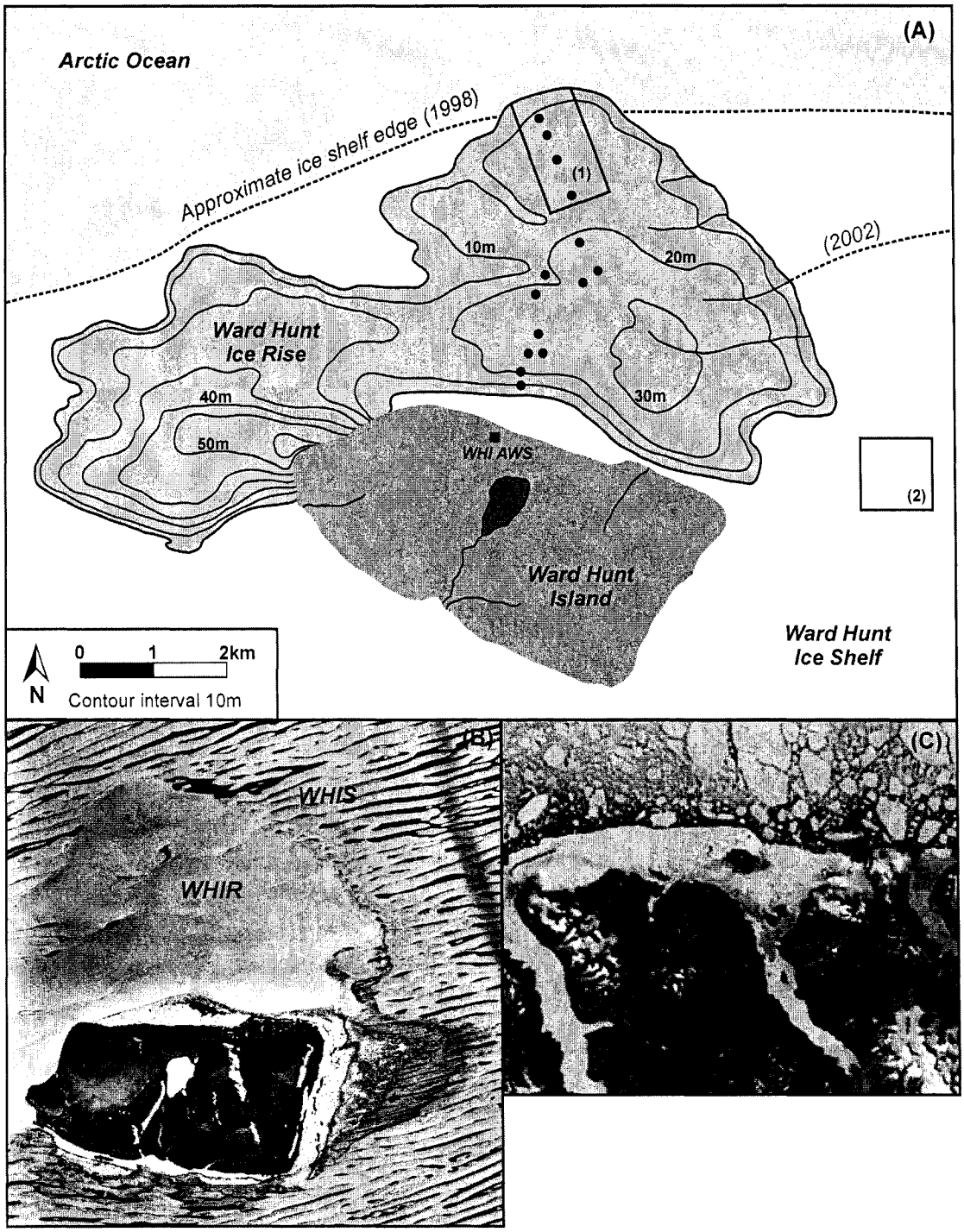

Figure 2.4 (A) Topographic map, (B) aerial photograph, and (C) late summer MODIS satellite image (17 August 2002) of the North Coast of Ellesmere Island, Nunavut, Canada. The Ward Hunt Ice Rise and Ice Shelf are marked. Black circles mark the ablation stake transect installed on the ice rise in 2002. The approximate locations and extents of the original 1959/1966 stake networks on the WHIR (1) and the WHIS (2) are indicated by the two solid rectangles (Serson, 1979). The Ward Hunt Island weather station (WHI AWS, black square) is located at ~81°05'N and 74°09'W.

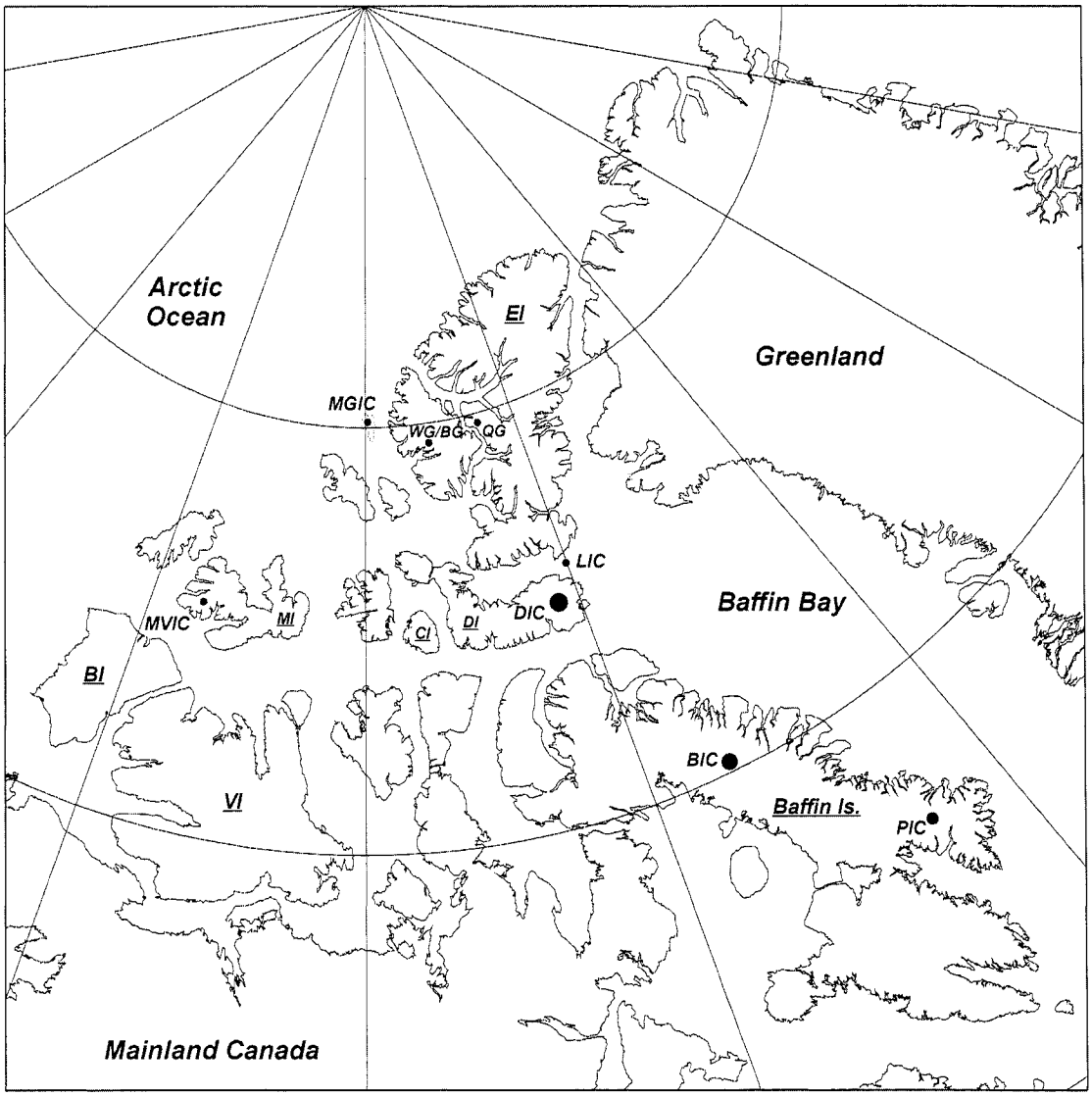

Figure 2.5 Location map of the Canadian High Arctic showing the locations of some of the geographic analogues discussed in Section 2.2. MGIC = Meighen Ice Cap; WG/BG = White and Baby Glacier; QG = Quviagivaa Glacier; LIC = Laika Ice Cap; DIC = Devon Ice Cap; MVIC = Melville South Ice Cap; BIC = Barnes Ice Cap; PIC = Penny Ice Cap; EI = Ellesmere Island; DI = Devon Island; CI = Cornwallis Island; MI = Melville Island; BI = Banks Island; VI = Victoria Island. The Tiger Ice Cap is adjacent to the Barnes Ice Cap. Locations are only approximate.

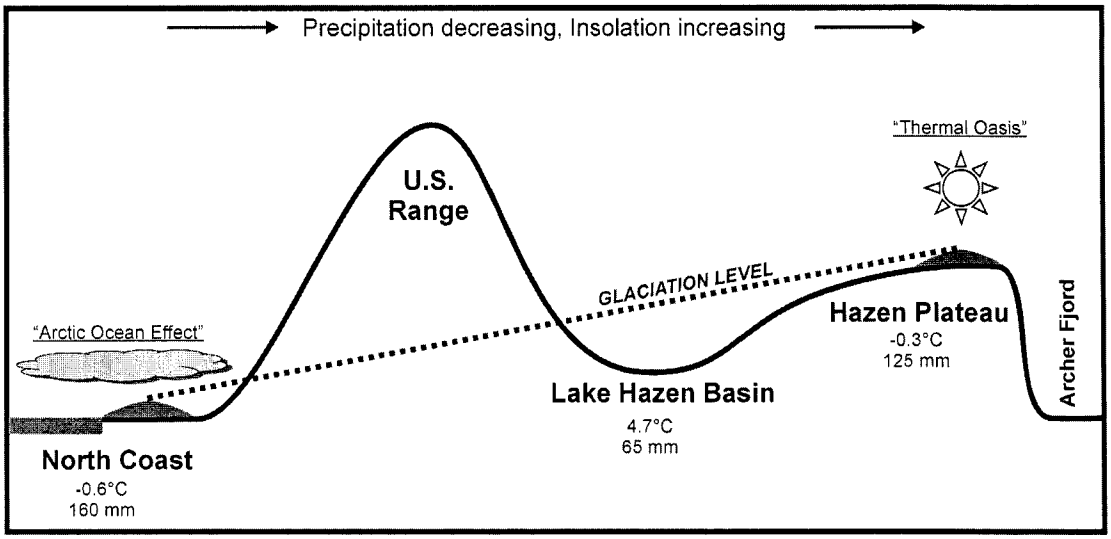

Figure 2.6 Schematic cross-section of northern Ellesmere Island (horizontal distance ~220 km; maximum elevation ~2300 m asl). The dotted line depicts the generalized glaciation-level gradient (after Miller *et al.*, 1975; their data based on topographic maps from 1959 aerial photographs). The 'Arctic Ocean Effect' (i.e. frequent low stratus/fog conditions), leading to reduced ablation and increased accumulation, is limited only to the immediate coastal fringe. In contrast, the interior highlands (e.g. the Hazen Plateau) experience a much more continental summer climate ('Thermal Oasis'). See Figure 2.7 or Chapter 5 for the Hazen Plateau and North Coast climate data. Lake Hazen summer temperature data from Parks Canada (1989 to 1996 mean); annual precipitation value after Jackson (1959).

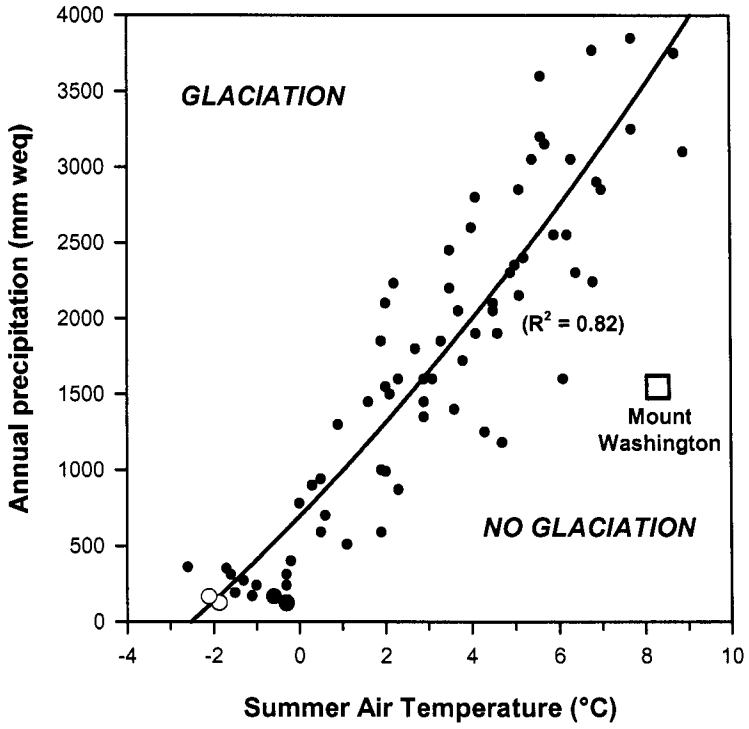

Figure 2.7 Mean summer air temperature and annual precipitation at the ELA of 69 glaciers around the world (modified from Humlum, 1997; data from Ohmura *et al.* 1992). Modern ranges for summer temperature and annual precipitation for the Hazen Plateau are indicated by the red solid circle (AWS T3*, 1951 to 2000): (–0.32±1.32°C) and (125±31 mm weq). Modern ranges for summer temperature and annual precipitation on the North Coast are indicated by the blue solid circle (WHI AWS*, 1951 to 2000): (–0.55±0.57°C) and (160±40 mm weq). See Chapter 5 for a comprehensive discussion of the climatology of the Hazen Plateau and North Coast. The respective red and blue open circles indicate approximate 'Little Ice Age' climatic conditions on northern Ellesmere Island (cf. Hattersley-Smith, 1963; Koerner, 1989a) with reduced summer temperatures of about 1.5°C. The black square marks the current climatic conditions at the summit of Mt. Washington, New Hampshire (1970 to 2000 means).

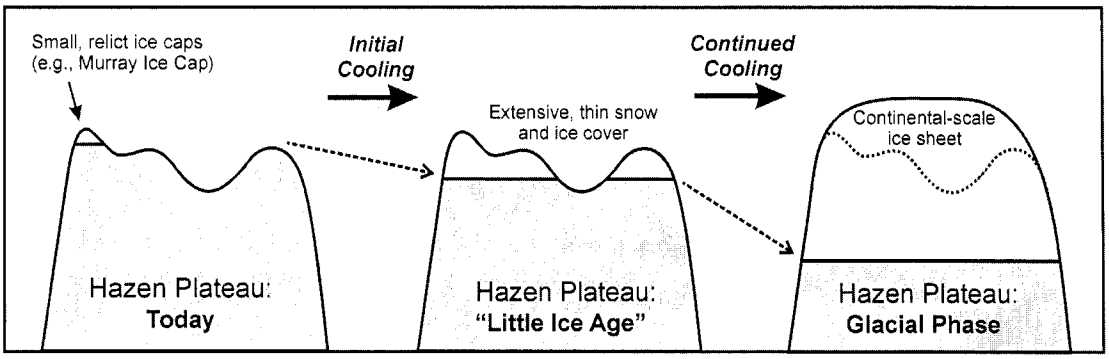

Figure 2.8 Schematic illustration of the Hazen Plateau today, during the so-called 'Little Ice Age', and during a full glacial phase (following the Ives *et al.*, 1975 model). The Hazen Plateau today is essentially unglacierized, except for several small, relict ice caps located at its highest elevation. Cooling, perhaps supplemented by increased precipitation, leads to an overall lowering of the regional snowline and glaciation level relative to the plateau surface. This leads to the initiation and rapid expansion of snow and ice across the plateau ('Little Ice Age' conditions) (Ives, 1962). Continued cooling, aided by secondary positive feedback processes (e.g. snow/ice-albedo-temperature feedback) eventually leads to an 'instantaneous glacierization' of the entire plateau surface and subsequent regional ice sheet formation (Ives *et al.*, 1975). Relatively small changes in climate can thus put large areas of the plateau either above or below the glaciation level and lead to significant changes in the extent of snow and ice cover on the Hazen Plateau. Figure design and layout inspired by Dahl and Nesje (1992; their Fig. 2). Kovanen and Slaymaker (2005) show a similar graphic (their Fig. 8) depicting the extent of ice on Mt. Baker, Washington State.

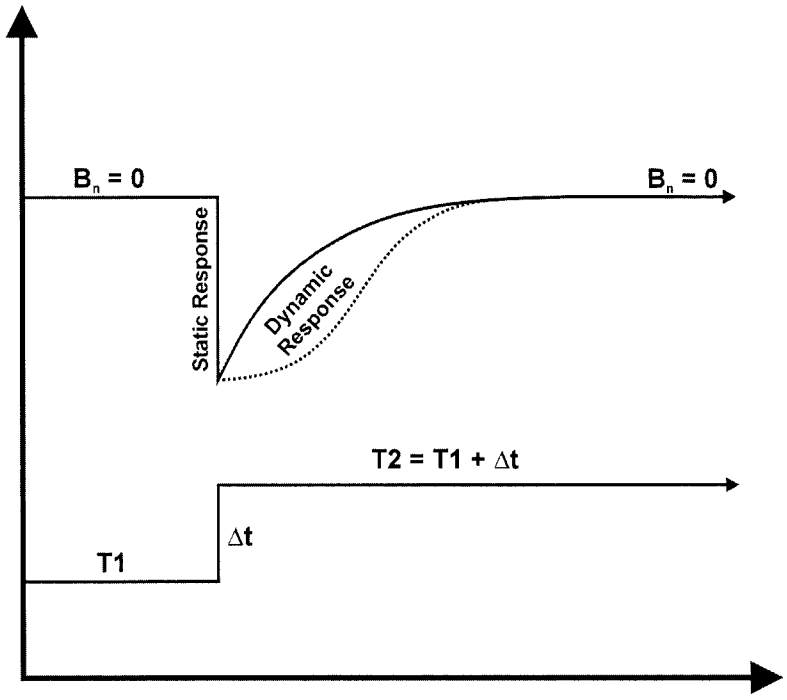

Figure 2.9 Static and dynamic sensitivity or response of a glacier to an abrupt (external) change in climate (e.g. increase in air temperature T1) (after Braithwaite and Zhang, 1999; cf. Section 2.4.1).

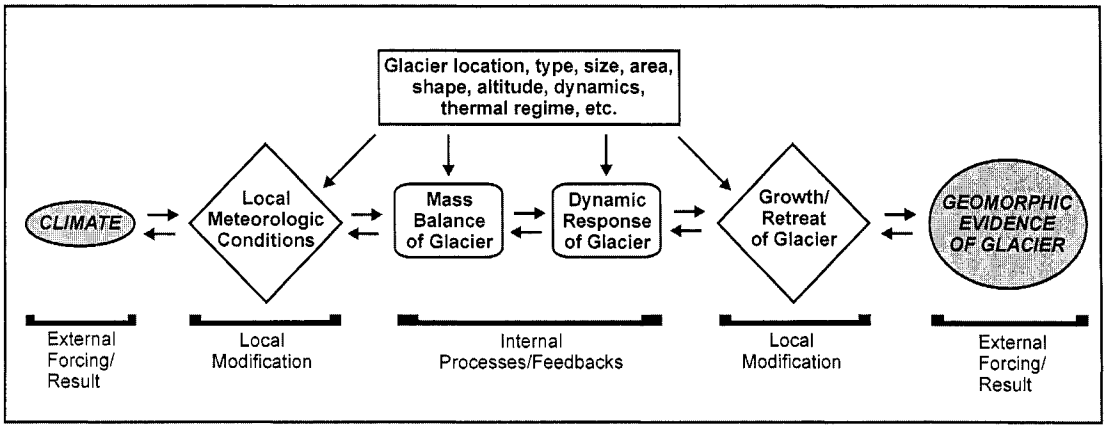

Figure 2.10 Schematic illustration of the relationships and interactions between climate and glaciers (modified from Whalley *et al.*, 1989). 'Left-to-right' modeling attempts to predict the effect(s) of climate change on glaciers, whereas 'Right-to-left' modeling attempts to reconstruct past climatic conditions based on evidence of former glaciation (e.g. Boulton *et al.*, 1995). Furbish and Andrews (1984) included a similar graph (their Fig. 1), as did Warren (1990, his Fig. 1).

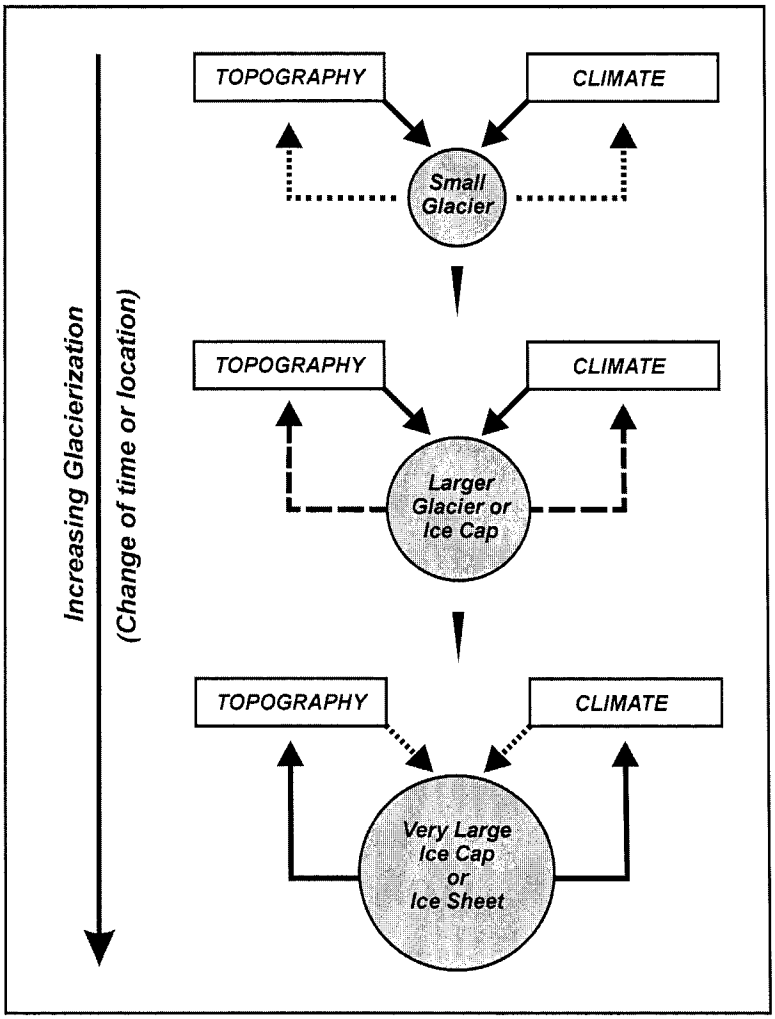

Figure 2.11 Schematic illustration of the interactions between climate, topography, and (changing) ice cover (modified from Sutherland, 1984). The solid arrows represent strong controls or feedbacks, the dashed arrows medium, and the dotted arrows weak controls or feedbacks.

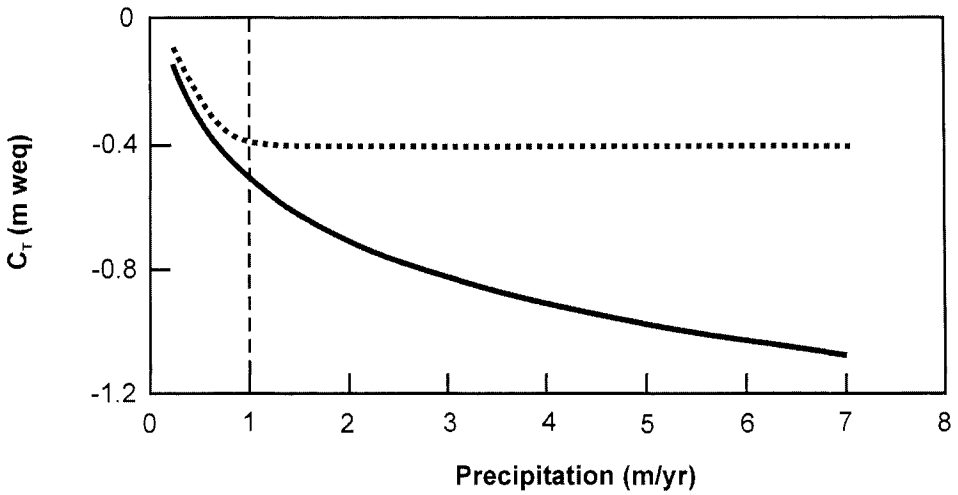

Figure 2.12 Sensitivity of glacier mass balance to climate change as a function of annual precipitation on the glacier (modified from Oerlemans, 1993). Black line: sensitivity for a +1°C uniform warming throughout the entire year; dotted line: sensitivity for a +1°C warming limited to only the summer months. The start of both curves is effectively defined by the White Glacier and Devon Ice Cap in the Canadian High Arctic.

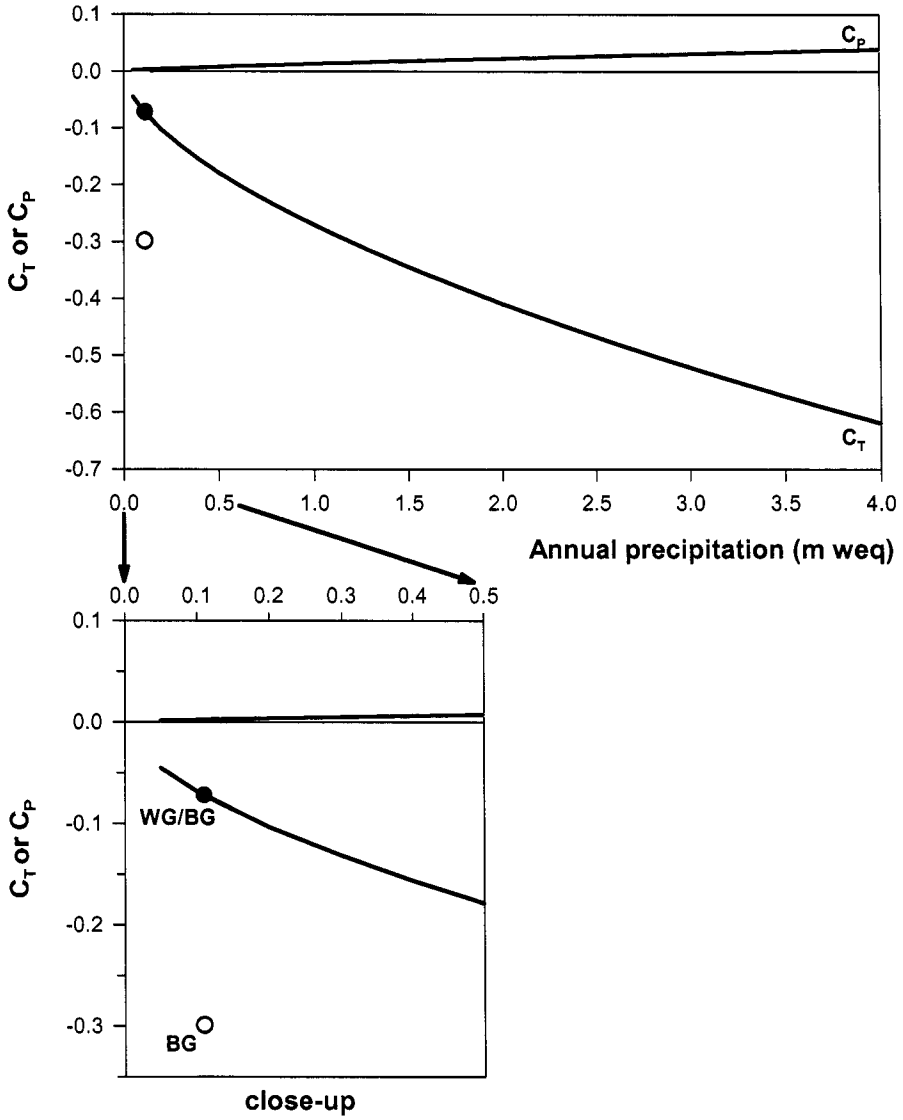

Figure 2.13 C_T and C_P plotted as function of annual precipitation (using the two equations presented by Oerlemans, 2001). C_T = climatic sensitivity for a +1°C uniform warming throughout the year; C_P = climatic sensitivity for a +10 percent increase in annual precipitation. Black circle: C_T estimated for White and Baby Glacier, assuming an annual precipitation of 110 mm weq (Eureka, 1951 to 2001 mean). White and Baby Glacier probably receive in reality somewhat more annual precipitation than Eureka (Cogley *et al.*, 1996), although Glenday (1989) was able to successfully model the mass balance of White Glacier using climatological data (including annual precipitation) from Eureka. White Circle: 'Measured' C_T value for the Baby Glacier as reported in Adams *et al.* (1998). The measured C_T value for the White Glacier (–0.74) is almost identical to the C_T for White Glacier estimated using the Oerlemans (2001) equation (–0.73). Grey shading: 100 to 150 mm weq annual precipitation range, which represents a reasonable envelope for current precipitation amounts on the Hazen Plateau (cf. Chapter 5).

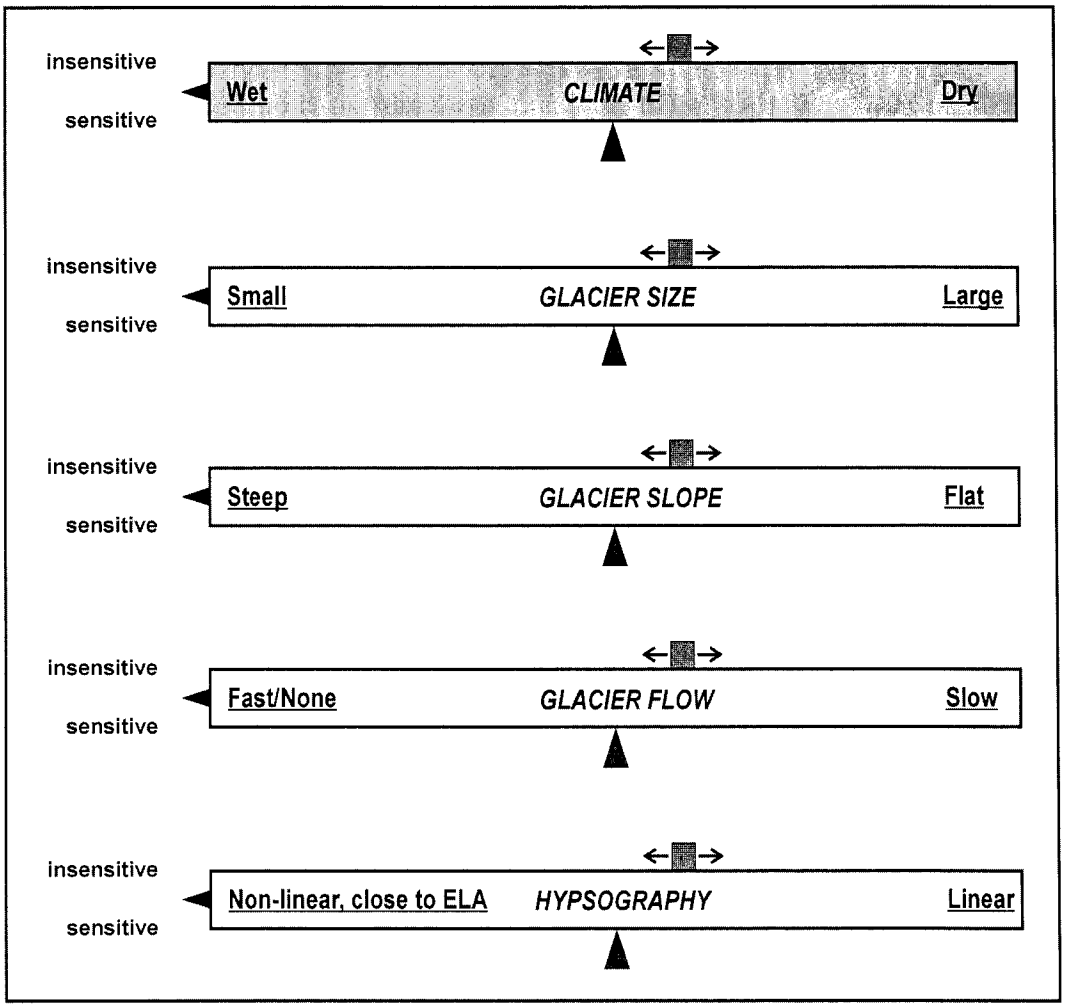

Figure 2.14 A qualitative glacier sensitivity model as discussed in Section 2.4.5.4. Haeberli (1995) and Chinn (1999) have used different systems to group or classify different glaciers with similar response times.

CHAPTER 3

MASS BALANCE AND AREA CHANGES OF FOUR HIGH ARCTIC PLATEAU ICE CAPS, 1959-2002

3.1 Abstract

Small, stagnating ice caps at high latitudes are particularly sensitive to climatic fluctuations, especially with regard to changes in ablation season temperature. We conducted mass balance measurements and GPS area surveys on four small High Arctic plateau ice caps from 1999 to 2002. We compared these measurements with topographic maps and aerial photography from 1959, and with previously published data. Net mass balance (b_n) of Murray Ice Cap was –0.49 (1999), –0.29 (2000), –0.47 (2001), and –0.29 (2002), all in meters of water equivalent (weq). The mass balance of nearby Simmons Ice Cap was also negative in 2000 (b_n = –0.40 m weq) and in 2001 (b_n = –0.52 m weq). All four ice caps experienced substantial marginal recession and area reductions of between 30 and 47 percent since 1959. Overall, these ice caps lost considerable mass since at least 1959, except for a period between the mid-1960s and mid-1970s characterized regionally by reduced summer melt, positive mass balance, and ice cap advance. The regional ELA is located, on average, above the summits of the ice caps, indicating that they are remnants of past climatic conditions and out-of-equilibrium with present climate. The ice caps reached a Holocene maximum and were several times larger during the 'Little Ice Age' (LIA) and their current recession reflects an adjustment to post-LIA climatic conditions. At current downwasting rates the ice masses on the Hazen Plateau will completely disappear by, or soon after, the mid-21st century.

3.2 Introduction

Small, stagnant ice caps at high latitudes without appreciable iceflow are particularly sensitive to climatic fluctuations, especially with regard to variations in ablation-season temperature (Paterson, 1969; Hattersley-Smith and Serson, 1973; Rosqvist and Østrem, 1989; Grudd, 1990). In a general sense, the position of the ice margin and the areal extent of a stagnant ice cap are strongly related to its annual mass

balance (Paterson, 1969). Here we report the results of recent mass balance and GPS area measurements on four small, stagnant plateau ice caps located on the Hazen Plateau of Ellesmere Island, Nunavut, Canada (Fig. 3.1). Most of the plateau is currently unglacierized and the ice caps persist today at about the same elevation as adjacent ice-free areas, indicating that the plateau surface is close to the regional equilibrium-line altitude (ELA) or glaciation level (Miller *et al.*, 1975). Therefore, relatively small changes in climate could lead to profound changes in the extent of snow and ice cover on the Hazen Plateau. Aerial photographs and topographic maps from 1959 and two earlier studies of Hazen Plateau ice caps (Hattersley-Smith and Serson, 1973; Bradley and Serreze, 1987a) provide a temporal context for the current data. We are specifically interested in assessing how snow and ice conditions on the ice caps and the surrounding plateau have changed since they were last visited some 20 years ago.

3.3 Background - Previous Studies

The Hazen Plateau forms a large upland region, gently rising from about 300 m above sea level (asl) near Lake Hazen to over 1000 m asl along the northeast coast of Ellesmere Island (Fig. 3.1). This part of Ellesmere Island is characterized by some of the lowest accumulation rates (<0.15 m; Koerner, 1979) and highest glaciation levels or ELA's (~800 to 1000 m asl, Miller *et al.*, 1975) in the Canadian High Arctic. The plateau is largely unglacierized today, except for two pairs of thin, stagnant ice bodies along its northeastern margin (Fig. 3.1, 3.2, 3.3) which we unofficially term the 'Hazen Plateau ice caps'. Murray and Simmons Ice Cap together range in elevation between 960 and 1100 m asl and are surrounded by ice-free plateau areas up to 1030 m asl (Fig. 3.2). The 'St. Patrick Bay' ice caps (Fig. 3.3; unofficial name) are located about 110 km to the northeast at lower elevation (~750 to 900 m asl), possibly related to local moisture sources (Hattersley-Smith and Serson, 1973). Our studies (1999 to 2001) focused on Murray Ice Cap (e.g. Braun *et al.*, 2001) and also included mass balance measurements on Simmons Ice Cap in 2000 and 2001. We visited the St. Patrick Bay ice caps in a reconnaissance survey on 15 July 2001. We re-measured the main ablation stake transect on Murray Ice Cap on 28 July 2002. Aerial photographs from 6 July 1959 show all four ice caps fully in the ablation zone and the Hazen Plateau entirely free of seasonal snow.

3.3.1 Previous Studies: Murray and Simmons Ice Cap

Prior to this study, no specific glaciologic studies had been conducted on Murray Ice Cap. An ablation stake network was established on nearby Simmons Ice Cap (Fig. 3.2) in early June 1976 (Bradley and England, 1977) when winter snow accumulation across the ice cap ranged between 0.1 and 0.18 m weq. The authors inferred that Simmons (and Murray) Ice Cap had probably gained mass over the 1975/76 balance year (Table 3.1) and experienced overall positive mass balance and lateral ice margin advance for some time before 1976. Only six of the original 18 ablation stakes were located during a return visit on 11 July 1983 (Bradley and Serreze, 1987a). They assumed that the other 12 stakes had melted out and estimated a minimum net mass loss of about 0.49 m weq between 1976 and 1983 (Table 3.1). Field observations also indicated a recession of the 1983 Simmons Ice Cap margin relative to its 1959 position (Table 3.2) (Bradley and Serreze, 1987a).

3.3.2 Previous Studies: St. Patrick Bay ice caps

G. Hattersley-Smith and others visited the St. Patrick Bay ice caps (Fig. 3.3) in July/August 1972 (Hattersley-Smith and Serson, 1973). They estimated net accumulation on the larger (NE) ice cap for the 1971/72 balance year of about 0.14 m weq (Table 3.1). The seasonal snowpack overlaid icy firn and superimposed ice (~0.39 m weq), which in turn rested on a distinct older ablation surface. This stratigraphy was interpreted as evidence that the ice cap experienced net ablation for an extended period until at least 1959 and more likely until the unusually warm summer of 1962. In contrast, 1963 to 1972 represented a phase of net accumulation on this ice cap, possibly interrupted by some years with net ablation. They reported that the ice cap in 1972 "appears to be in a healthy state and is spreading laterally as well as thickening." (Table 3.2). This positive regime however did not persist, as net annual mass balance was again negative for the 1974/75 and 1975/76 balance years (Table 3.1). The original 1972 stake network was re-surveyed in 1982 by a research group from the University of Massachusetts (Bradley and Serreze, 1987a) as part of a 2-year topoclimatic study of the St. Patrick Bay ice caps and surrounding Hazen Plateau (Bradley and Serreze, 1987b; Serreze and Bradley, 1987). Net mass balance between 1972 and 1982 was –1.3 m weq (Table 3.1); this mass loss led to a reduction in area of both ice caps (Table 3.2). Mass balance conditions and summer climate differed markedly between 1982 and

1983, with 1983 being notably colder and having more summer snowfall, resulting in a positive annual mass balance for the 1982/83 balance year on both ice caps (Table 3.1).

3.4 Methods

3.4.1 Ice Cap Mass Balance

We measured ice cap mass balance using conventional glaciological techniques as described by Østrem and Brugman (1991). We established a network of 11 ablation stakes on Murray Ice Cap in 1999 and expanded the network in 2000 to 29 stakes (Fig. 3.2). We established a network of 15 stakes on Simmons Ice Cap in 2000 (Fig. 3.2). Winter snow accumulation was measured each year in late May (1999 to 2001) and summer ablation was measured in late July / early August (1999 to 2002) and confirmed the following May (2000 and 2001 only). Individual stake measurements for each ice cap were grouped into 20 m elevation bands to determine a linear ablation gradient for each year (cf. Rosqvist and Østrem, 1989). This ablation gradient was used to integrate the net specific ablation measurements over the entire ice cap surface, based on a 10 m digital elevation model constructed from a 1:50,000 topographic map (Fig. 3.2) (cf. Jansson, 1999). We consider ±0.2 m weq as a conservative uncertainty estimate for the annual net mass balance values following Cogley and Adams (1998). We calculated minimum mass balance estimates for Simmons Ice Cap (1984 to 1998) and the St. Patrick Bay ice caps (1984 to 2000) using the mean remaining depth of stake insertion into the ice in 1983 (M. Serreze, pers. comm.) and assuming a relative ice density of 0.9 (Table 3.1).

3.4.2 Ice Cap Area

We digitized the 1959 ice margins of the four Hazen Plateau ice caps directly from available 1:50,000 topographic maps (Fig. 3.2, 3.3), scanned at 600 dpi and registered to UTM zone 19N (20N for the St. Patrick Bay ice caps). The topographic maps used are based on aerial photography from 6 July 1959. We visually confirmed the accuracy of the ice-cap outlines depicted on the topographic maps by detailed comparison with the original aerial photographs (see below).

We surveyed the 1999 to 2001 ice-cap margins and lichen trim lines on foot (or snowmobile) using a portable GPS receiver, logging discreet positions every 3 to 10 seconds (10 to 15 m). The points along each ice-cap 'trace' were imported into a Geographical Information System (GIS) software package and connected as polygons for area calculations. The 1999 and 2000 GPS positions collected for Murray Ice Cap were differentially corrected using data from the nearest available GPS base station (Thule AFB, Greenland, 76°20'N, 68°48'W). This 'low-tech' technique eliminates the need to operate a dedicated GPS base station on-site, a significant advantage in remote environments. The main disadvantages are (1) greater uncertainties associated with the differentially-corrected GPS positions compared to more sophisticated techniques and (2) the dependence on consistent base station data availability. The latter problem was illustrated in 2001, when we were not able to correct the four collected ice-cap traces because of partially missing base station data.

3.4.3 Ice Cap Area – Uncertainties

We assessed the uncertainties associated with our ice-cap area measurements (Table 3.2) by first quantifying each individual contributing error source (Table 3.3) and then calculating the resultant uncertainty for the position of the ice margin (Table 3.4). It is important to note that some of the absolute values assigned to individual uncertainties listed in Table 3.3 are estimates in-of-themselves. Furthermore, possible human errors and subjectivity associated with the creation of the topographic maps from aerial photographs cannot be rigorously quantified.

Uncertainties for the 1959 ice-cap area measurements were a combination of (1) registration errors of the scanned topographic maps relative to their respective coordinate system, and (2) generalization of the ice-cap margins during the digitization process. Inherent in this type of study are errors and uncertainties associated with the delineation of the ice-cap margin, whether it is on the original aerial photograph, the topographic map, or directly in the field. A certain amount of subjective generalization and human error is inevitable in this process and we estimated this uncertainty at ±2 pixel or about 5 m (Table 3.3), based on careful comparisons of the original aerial photographs, the topographic maps, and the actual ice margin in the field. Wind-drifted snow accumulations along the northeast margin of STPBIC-SW and along the terminus of STPBIC-NE, both on the 1959 aerial photographs and in 2001,

made it difficult to determine the precise positions of the ice margins at these locations. For consistency, we mapped 'maximum area' solutions in both cases in 2001. The uncertainty for each differentially-corrected GPS position collected in 1999 and 2000 was about 5 m (Table 3.3), which represents the maximum 99% confidence interval for the corrected GPS positions (generated by the differential-correction software). The horizontal error associated with the 2001 uncorrected GPS positions was estimated to be about 9.4 m (99% confidence limit of 22,739 positions collected over five days at a fixed point). It is interesting to note in this context that the difference in Murray Ice Cap area between the differentially-corrected and the uncorrected 2000 trace was less than 100 m^2 (<0.1‰). We determined the resulting uncertainty for ice-cap area by applying an area-buffer around the digitized ice-cap margins using a GIS software package, calculated as the quadratic sum of the individual contributing uncertainties (Table 3.4). The final values for the ice-cap area uncertainty estimates (Table 3.2) are a function of the applied area-buffer, but are also affected by ice-cap area and the length/irregularity of each ice-cap margin. They clearly represent worst-case estimates, as the area-buffer assumes that all points defining the ice margin are systematically displaced to induce maximum area change. In reality, we can expect a certain amount of error cancellation in terms of total ice-cap area.

3.5 Results

3.5.1 Ice Cap Mass Balance

Murray and Simmons Ice Cap experienced highly negative annual mass balances (–0.29 to –0.49 m weq) for at least the past four years (Table 3.1). Winter snow accumulation on both ice caps was relatively constant each year (0.06 to 0.1 m weq, 1999 to 2001), and variations in annual net mass balance were mainly a function of summer conditions. Summer climatic conditions in 2000 and 2002 were generally colder and snowier than in 1999 or 2001, leading to less negative annual mass balance on the ice caps (Table 3.1). We were not able to recover the six ablation stakes remaining on Simmons Ice Cap in 1983 (from the original 1976 network), but one was found melted 10 to 20 cm horizontally into the glacier surface. We were also unable to locate any of the ablation stakes from the 1972 and 1982 networks on the St. Patrick Bay ice caps during our visit 15 July 2001 and assume that they had melted

out as well. These observations suggest an overall negative mass balance for these three ice caps since at least 1984 (Table 3.1). The Hazen Plateau ice caps presently do not retain any accumulation of snow, firn, or superimposed ice, even on their highest or most-sheltered parts. The entire surface of Murray and Simmons Ice Cap at the end of each summer (1999 to 2002) and of the St. Patrick Bay ice caps (observed only 2001) was dirty, bare glacier ice characterized by accumulations of wind-blown dust in well-developed cryoconite holes – all suggesting net ablation over an extended period of time.

3.5.2 Ice Cap Area Changes

All four Hazen Plateau ice caps experienced considerable marginal recession since at least 1959 (Fig. 3.2, 3.3). Marginal recession was greatest (up to ~700 m) for the flat, low-lying parts of the ice caps and less along the steeper and sheltered sections of the ice margins. This presumably was due to local increases in snow accumulation related to wind drifting. This retreat of the ice margins led to decreases in overall ice-cap area amounting to between 30 and 47 percent since 1959 (Table 3.2). The margin of Murray Ice Cap retreated 10 to 30 m each year in 1999 to 2001, resulting in an annual area reduction of about 2.5 percent (Table 3.2). The margins of all four ice caps were visually thinning and rapidly disintegrating over the course of each summer. This was visibly illustrated by one section of the Simmons Ice Cap margin which retreated about 10 m over 15 days in late July 2001. In addition, two small holes (~200 m^2) developed in the SW-lobe of Simmons Ice Cap at about 1030 m asl during July/August 2001 (i.e. ice-free area), which are likely to accelerate ice margin disintegration and retreat in the coming years. We were unable to conduct quantitative area measurements in 2002, but field observations indicated a continued recession of Murray Ice Cap of about 40 m at its terminus in this year. The SW-lobe of Simmons Ice Cap in 2002 was almost completely separated from the main ice cap at an elevation of about 1030 m asl (Fig. 3.2, see also www.geo.umass.edu/climate/hazen/sic_99_02.html).

3.6 Discussion

Our new data, in combination with previously published work (Table 3.1, 3.2) allow a generalized reconstruction of the Hazen Plateau ice caps mass balance history for the last four decades (Fig. 3.4a). The ice caps experienced net ablation and shrinkage for an extended period of time until some

time in the early- to mid-1960s (Hattersley-Smith and Serson, 1973). This was followed by a phase of net accumulation and ice cap growth until the early- to mid-1970s (Hattersley-Smith and Serson, 1973; Bradley and England, 1977). Since that time, the ice caps have again experienced overall net mass loss and marginal recession. There is evidence for some inter-annual variations in mass balance superimposed on the general trend (e.g. 1982/83), as well as for spatial variability across the Hazen Plateau (e.g. 1976) (Table 3.2).

This general temporal pattern was also exhibited by other glaciers studied in the Canadian High Arctic, with generally positive mass balances from the mid-1960s to the mid-1970s, followed by generally negative mass balances thereafter (e.g. Fig. 3.4b). This documented increase in glacierization across much of the High Arctic coincided with a period of reduced summer melt conditions and increased annual precipitation (Bradley and Miller, 1972; Bradley, 1973; Bradley and England, 1978; Alt, 1987). Corroborating this are upper air sounding data (Fig. 3.4c) from the closest official Canadian weather station at Alert (Fig. 3.1), which show a decrease in July freezing level height of ~100 m between 1964 and 1976 relative to the long-term (1951 to 2001) mean of 1150 m asl July freezing level heights have also been shown to be highly correlated with glacier ELA's and mass balance (Bradley, 1975; Bradley and England, 1978) in the Canadian High Arctic. This comparatively small shift in climate and lowering of the ELA was evidently sufficient for the Hazen Plateau ice caps to experience predominantly positive mass balance years and expansion during this period from the mid-1960s to the mid-1970s (cf. Bradley, 1975). However, the regional ELA appears to be located, on average, above the summits of the ice caps for at least the last 50 years (Fig. 3.4c). This suggests that the contemporary climatic conditions on the Hazen Plateau are not severe enough to sustain permanent ice cover on the plateau (cf. Ohmura *et al.*, 1992). These findings support the interpretation by Bradley and Serreze (1987a) that the Hazen Plateau ice caps are out-of-equilibrium with current climate.

The overall cumulative mass balance of the Hazen Plateau ice caps and other Canadian High Arctic glaciers (Koerner, 1996; Dowdeswell *et al.*, 1997; Serreze *et al.*, 2000) has been negative for the last 40 years, with a turn towards even more negative values during the 1990s. This mass loss has led to a retreat of the ice margins and resulted in shrinkage of the Hazen Plateau ice caps since at least 1959 (Fig. 3.5). There is additional evidence from snow-pit and firn-core studies (Hattersley-Smith, 1963) for

elevated summer temperatures and increased melting in the period from ~1925 to 1961, suggesting overall more negative glacier mass balances in the Canadian High Arctic during the first part of the 20th century, compared to the last 40 years of direct measurements (Koerner, 1996).

The Hazen Plateau ice caps are to some extent end-members of the full glacier-climate response spectrum in the sense that their response to a given climatic perturbation is relatively more extensive and rapid than in the case of larger, more dynamic High Arctic ice caps or glaciers. These ice caps appear to have formed relatively recently (Koerner, 1989a) during the so-called 'Little Ice Age' (LIA, ~1600 to 1850). They probably maintained their maximum Neoglacial extents as late as 1925, similar to other small glaciers and ice caps on northern Ellesmere Island (Hattersley-Smith, 1969). Evidence for an increased extent of ice and/or perennial snow on the Hazen Plateau at some point in the recent past, probably the LIA, is also provided by a well-defined lichen trim line around Murray Ice Cap (~9.6 km^2) and on the plateau between Murray and Simmons Ice Cap (Fig. 3.2). A similar lichen trim line is evident around Simmons Ice Cap and the St. Patrick Bay ice caps, but has not yet been mapped in detail. Additional plateau surfaces of comparable elevation in this region probably also supported small ice caps or perennial snowfields at that time. In this context the period of overall positive glacier mass balances from the mid-1960s to mid-1970s may provide a useful analogue for the reduced summer melt conditions in the High Arctic during the LIA (cf. Alt, 1987).

3.7 Conclusions

The Hazen Plateau ice caps have experienced considerable marginal recession and significant overall mass loss since at least 1959. The sensitivity of these ice caps to changes in climate is enhanced by (1) the low amounts of winter snow accumulation, (2) the absence of iceflow, and (3) the small vertical relief. They are out-of-equilibrium with modern climate and considered to be relicts of past climatic conditions with reduced summer melt and/or increased snowfall although winter snowfall variations appear to be largely inconsequential in terms of annual mass balance today. The ice caps probably formed during the LIA and will continue to loose mass and retreat under current climatic conditions. They are likely to disappear over the next few decades, unless climatic conditions deteriorate as they did in the mid-1960s. The decay of these ice caps is likely to accelerate in the near future due to

feedback processes such as ice margin disintegration. This study demonstrates that even infrequent mass balance and ice area measurements can be useful in assessing the general mass balance regime of High Arctic glaciers, especially if some additional historical information is available.

3.8 Acknowledgements

Research was supported by a U.S. National Science Foundation Grant (OPP-9819362) to the University of Massachusetts. The Polar Continental Shelf Project (Energy, Mines, and Resources Canada) provided superb logistical and generous equipment support. We also thank Parks Canada (Nunavut Field Unit) for continuous support. M. Serreze generously shared his original field data and F. Keimig provided invaluable help with the data analysis. The thoughtful and detailed comments and suggestions of two reviewers greatly improved an earlier version of this manuscript.

Table 3.1 Net mass balances (m weq) of the Hazen Plateau ice caps. Where a value represents a multiyear period, the average annual value is shown in parentheses. * denotes a minimum estimate. Qualitative field observations are indicated by italics.

Balance year or period	Murray Ice Cap	Simmons Ice Cap	STPBIC-NE	STPBIC-SW
1963 to 1971			0.39 (0.04)[1]	
1972			0.14[1]	
1973			0.14[2]	
1974			0.14[2]	
1975			–0.08[2]	
1976	*positive*[3]	*positive*[3]	–0.07[2]	
1972 to 1982			–1.3 (–0.14)[4]	
1976 to 1983		*–0.49 (–0.08)[4]		
1982			–0.14[4]	
1983		*positive*[4]	0.14[4]	0.17[4]
1984 to 1998		*–0.49 (–0.03)		
1984 to 2000			*–1.01 (–0.06)	*–1.26 (–0.07)
1999	–0.49	*negative*		
2000	–0.29	–0.40		
2001	–0.47	–0.52	*negative*	*negative*
2002	–0.29	*negative*		

Notes
Sources: [1] Hattersley-Smith and Serson (1973), [2] Ommanney (1977), [3] Bradley and England (1977), [4] Bradley and Serreze (1987a). Data for STPBIC-NE are available at ftp://ftp.trentu.ca/pub/gghydro (Cogley and Adams, 1998).

Table 3.2 Ice cap area (km^2) of the Hazen Plateau ice caps and uncertainty estimates, 1959 to 2002. Qualitative field observations are indicated by italics.

AREA

Year	Murray Ice Cap	Simmons Ice Cap	STPBIC-NE	STPBIC-SW
1959	4.37[1]	7.45[1]	7.48[1]	2.93[1]
1972			*advance*[2]	
1976	*advance*[3]	*advance*[3]		
1978			6.69 (89%)[4]	2.74 (93%)[4]
1983		*recession*[5]		
1999	3.28 (75%)			
2000	3.15 (72%)			
2001	3.05 (70%)	3.94 (53%)	4.61 (62%)	1.72 (59%)
2002	*recession*	*recession*		

UNCERTAINTY ESTIMATE

Year	Murray Ice Cap	Simmons Ice Cap	STPBIC-NE	STPBIC-SW
1959	±1.3%	±1.3%	±1.1%	±1.7%
1978			NA	NA
1999	±1.7%			
2000	±1.8%			
2001	±2.7%	±3.2%	±2.2%	±3.8%

Notes

Sources: [1] Topographic map, [2] Hattersley-Smith and Serson (1973), [3] Bradley and England (1977), [4] Bradley and Serreze (1987a).

Table 3.3 Types and magnitudes of individual uncertainties associated with ice-cap area measurements.

Source of uncertainty	Type of uncertainty	Magnitude of uncertainty
Coordinate system registration	Registration error	±2 pixel[1] (generated by GIS software)
Ice margin delineation	Generalization/ Subjectivity	±2 pixel[1] (map), ±5 m (field) (both estimated)
Differential GPS	Individual position	±5 m (1999), ±5.2 m (2000) (generated by DGPS software)
Uncorrected GPS	Individual position	±9.4 m (2001) (estimated)

Notes
[1] Pixel size: 2.1 m

Table 3.4 Individual contributions of the uncertainties and resultant ice margin buffer.

Year	Ice Cap	Registration	Generalization	DGPS	GPS	Buffer
1959	All	±4.2 m	±4.2 m			±6 m
1999	MIC		±5 m	±5 m		±7.1 m
2000	MIC		±5 m	±5.2 m		±7.2 m
2001	All		±5 m		±9.4 m	±10.6 m

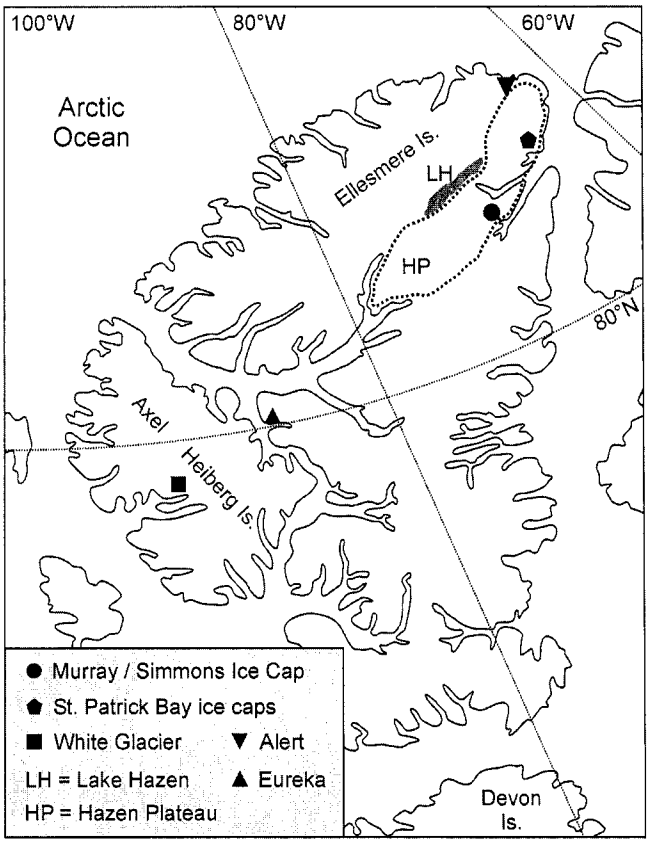

Figure 3.1 Ellesmere Island, Nunavut, Canada. For reference, the distance from Murray/Simmons Ice Cap to the St. Patrick Bay ice caps is about 110 km, to Alert about 160 km.

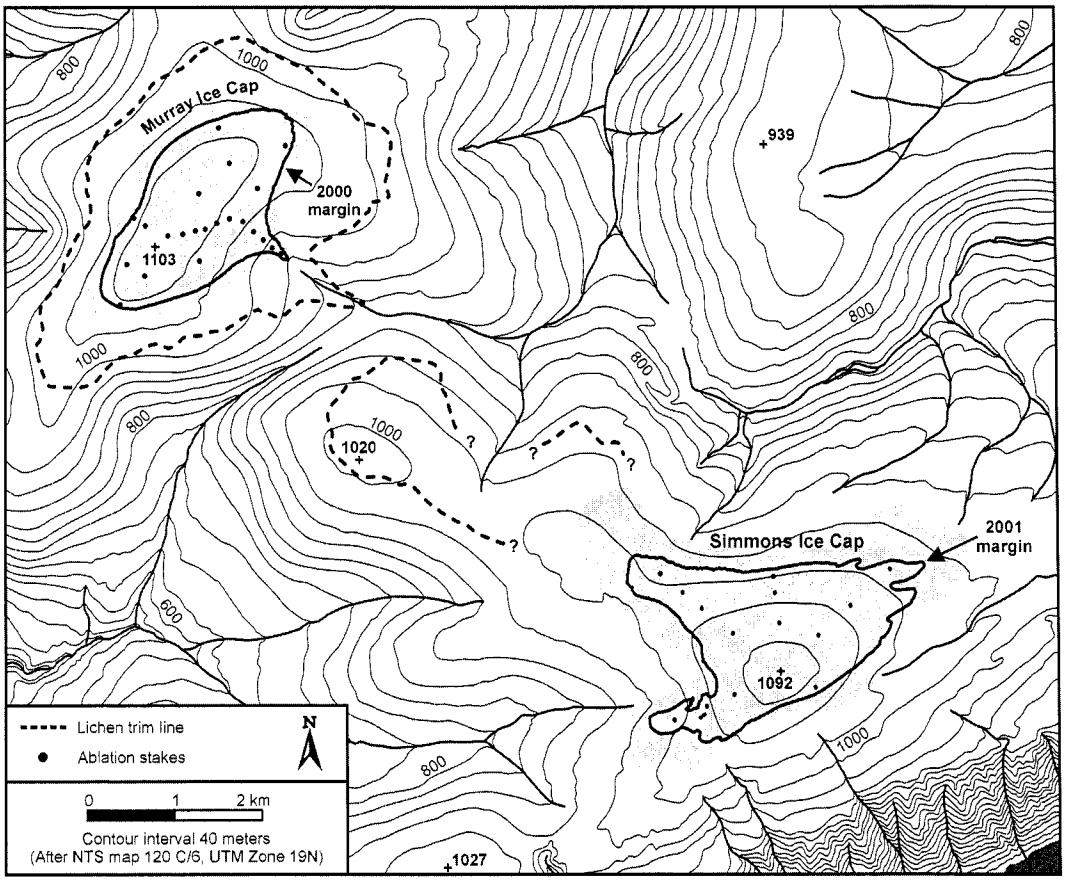

Figure 3.2 Murray and Simmons Ice Cap, Ellesmere Island, Nunavut, Canada. The summits are at 81°21'N, 69°15'W and 81°21'N, 68°50'W respectively. Ice extent on Canada National Topographic System (NTS) map sheet 120 C/6 (gray shading) is based on aerial photographs from 6 July 1959. The lichen trim line (dashed line) was mapped by field observations using GPS.

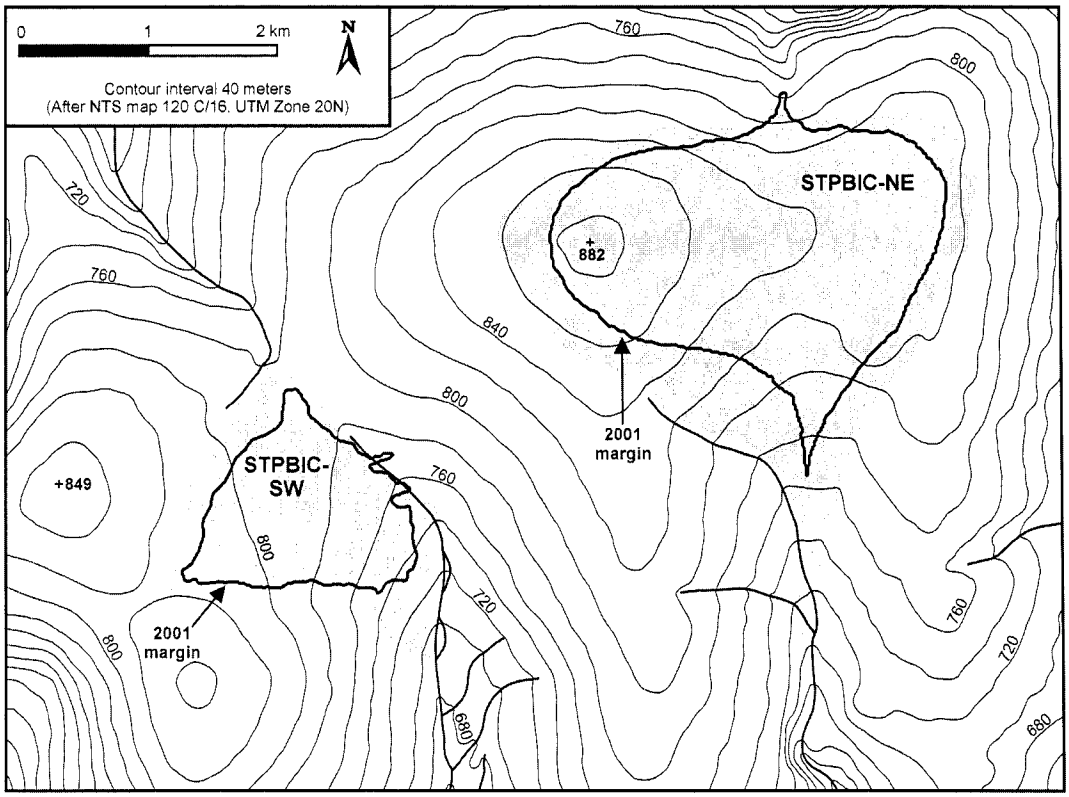

Figure 3.3 St. Patrick Bay Ice Caps, Ellesmere Island, Nunavut, Canada. The summit of the larger (NE) St. Patrick Bay ice cap (STPBIC-NE) is at 81°57'N, 64°10'W; the summit of the smaller (SW) St. Patrick Bay ice cap (STPBIC-SW) is at 81°54'N, 64°25'W. Ice extent on Canada National Topographic System (NTS) map sheet 120 C/16 (gray shading) is based on aerial photographs from 6 July 1959.

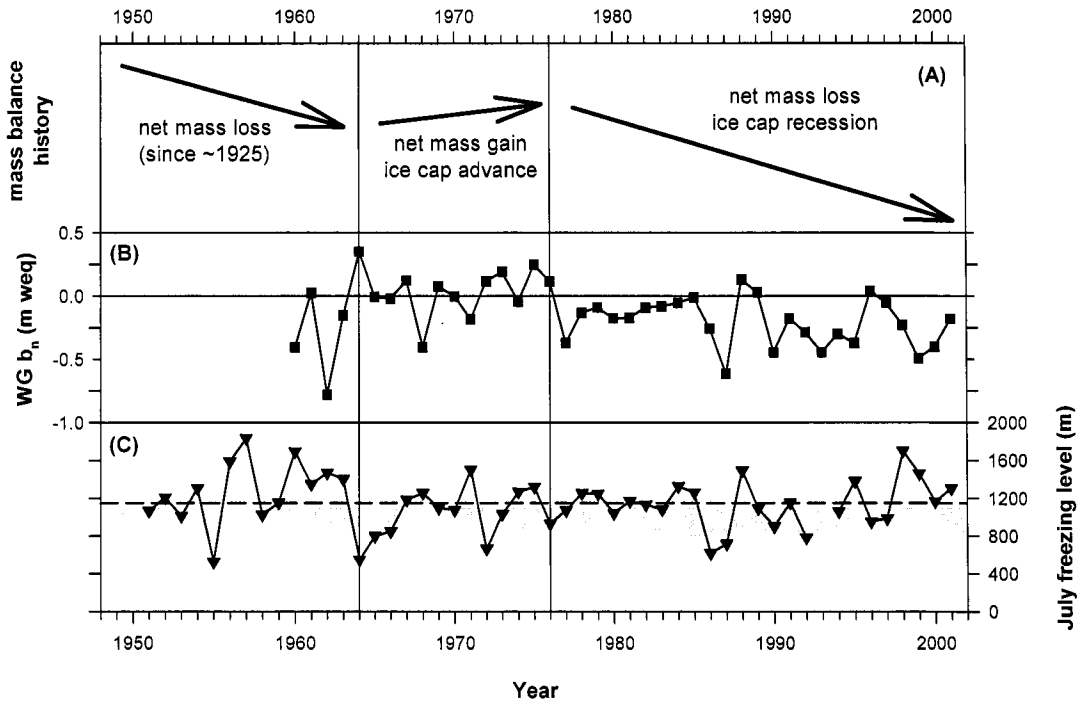

Figure 3.4 (A) Generalized mass balance history of the Hazen Plateau ice caps; (B) Annual net mass balance of the White Glacier (WG) (cf. Fig. 3.1); (C) July freezing level heights at Alert (1951 to 2001), with mean of 1150 m asl shown as a dashed line (1993 data missing). Grey shading indicates the elevation range of the Hazen Plateau ice caps (~800 to 1100 m asl). Mass balance data for White Glacier are from www.trentu.ca/geography/glaxmbal.htm; White Glacier is considered a representative example of Canadian High Arctic glaciers (Cogley *et al.*, 1996). Vertical lines through all three plots represent the period of reduced summer melt and increased glacierization in the High Arctic from around 1964 to 1976.

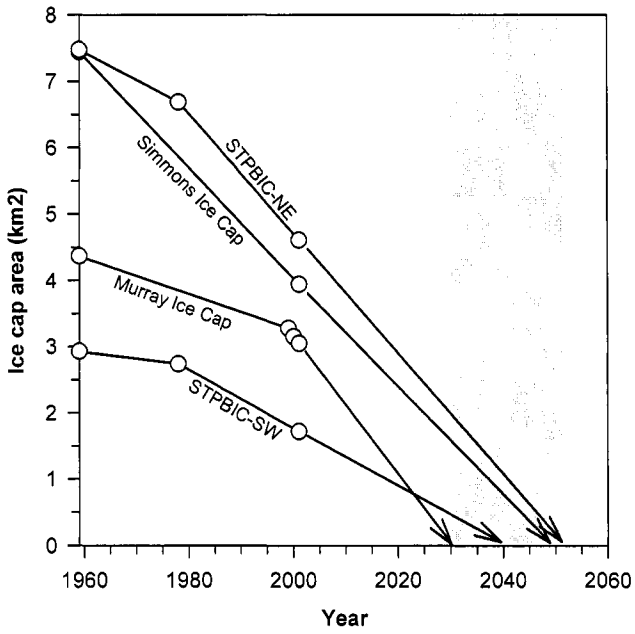

Figure 3.5 Area reduction of the Hazen Plateau ice caps 1959 to 2001, with a generalized linear projection suggesting complete disappearance of the ice caps by mid-21st century or soon thereafter.

CHAPTER 4

SURFACE MASS BALANCE OF THE WARD HUNT ICE RISE AND ICE SHELF, ELLESMERE ISLAND, NUNAVUT, CANADA

4.1 Abstract

The Ward Hunt Ice Rise and Ward Hunt Ice Shelf, located on Ellesmere Island, Canada, are two of the northernmost land ice masses on the North American continent. Surface mass balance measurements (excluding calving and sub-ice processes) began in 1959 on the ice rise, and in 1966 on the ice shelf, but were frequently interrupted, most recently between 1986 and 2002. The surface balance of the ice rise and ice shelf follows the temporal pattern seen on other measured High Arctic glaciers. The overall surface mass losses over the last 45 years have been comparatively low (1.68 m weq for the ice rise; 3.1 m weq for the ice shelf), which reflects their proximity to the Arctic Ocean. Nevertheless, the ice shelf appears to have weakened sufficiently in recent years to raise concerns about its possible disintegration in the near future. The 2002/2003 balance year was the most negative year on record (–0.33 m weq for the ice rise; –0.54 m weq for the ice shelf). Dynamical stresses related to wind, wave, and tidal action may further accelerate this process, as open water conditions on the Arctic Ocean become more prevalent. The Ward Hunt Ice Rise has so far remained in a reasonably healthy state in terms of its overall surface mass balance, although its long-term survival is also threatened by current and predicted future climatic conditions.

4.2 Introduction

The Ward Hunt Ice Rise (WHIR) and Ward Hunt Ice Shelf (WHIS) are two of the northernmost land ice masses on the North American continent (Fig. 4.1, 4.2). Scientific studies of the ice shelves and ice rises fringing the northern coast of Ellesmere Island started some 50 years ago (Hattersley-Smith *et al.*, 1955), with detailed surface mass balance measurements beginning in 1959 on the ice rise, and 1966 on the ice shelf (Hattersley-Smith and Serson, 1970). Those measurements continued more-or-less annually until the mid-1970s and more intermittently until the spring of 1989. The University of

Massachusetts (UMass) and Parks Canada re-initiated the surface balance measurement program on the WHIR in July 2002. Remarkably, some of the original ablation stakes from the 1959/1966 observation networks had not melted out since they were last surveyed in 1989 and we re-measured those in 2002 and 2003.

Much of the previously collected glaciologic data have been published as governmental or organizational reports (e.g. Ommanney, 1977; Serson, 1979; Jeffries, 1994; Koerner, 1996), not readily accessible to the international scientific community. In this paper we present updated surface balance records for the WHIR and WHIS, and compare them to other available glacier mass balance data from the Canadian High Arctic. These records are of particular relevance today in light of current public and scientific interest in the Arctic Ocean and its role in the ongoing environmental changes affecting the Arctic region as a whole (e.g. Serreze *et al.*, 2000; Comiso, 2003; Wang and Key, 2003) – and the glaciers of northern Ellesmere Island in particular (e.g. Vincent *et al.*, 2001; Mueller *et al.*, 2003; Braun *et al.*, 2004a).

4.3 Glaciation and Climate of Northern Ellesmere Island

Ice shelves in the Canadian High Arctic are typically formed from in-situ accumulations of multiyear landfast sea ice, surface snow accumulations, and basal freezing of seawater, with only minor direct mass input from associated upstream land glaciers (as opposed to the 'typical' Antarctic-type ice shelf) (Hattersley-Smith *et al.*, 1955; Vincent *et al.*, 2001). The ice shelves along Ellesmere Island's north coast formed initially some 3000 to 4000 years ago (Evans and England, 1992; Jeffries, 1994) as climatic conditions in the High Arctic deteriorated from the early/mid Holocene warm phase (Bradley, 1990). The entire northern coastline of the island appears to have been fringed by a continuous ice shelf ~500 km in length as late as the turn of the century (Vincent *et al.*, 2001). This large Ellesmere Ice Shelf progressively disintegrated over the course of the 20th century and today only about 10 percent remains (Vincent *et al.*, 2001), the largest remnant being the Ward Hunt Ice Shelf (Fig. 4.2). The ice shelf fractured into two distinct pieces south of Ward Hunt Island between 2000 and 2002, after experiencing some 20 years of relative stability (Mueller *et al.*, 2003). The causes behind the disintegration of the Ellesmere and Ward Hunt ice shelves over the last 100 years are still a subject of debate, but are likely a

combination of several mechanisms, including wind/wave/tidal action, pressure by Arctic Ocean pack ice, and recent climate change (Vincent *et al.*, 2001; Mueller *et al.*, 2003). The Ward Hunt Ice Rise (Fig. 4.2) is between 40 and 100 m thick and formed within the last 1500 years when the ice shelf thickened and grounded on the isostatically-uplifted seafloor north of Ward Hunt Island (Lyons *et al.*, 1972).

The lowest glaciation levels and equilibrium line altitudes (ELAs) in the Northern Hemisphere are found today along the northern coast of Ellesmere Island (Miller *et al.,* 1975), as manifested by coastal ice caps and marine ice shelves (such as the WHIR and WHIS). Frequent fog and low stratus clouds, associated with airflow from the Arctic Ocean, lead to reduced summer ablation in its immediate vicinity (Paterson, 1969; Hattersley-Smith and Serson, 1970; Koerner, 1979). At the same time, the Arctic Ocean represents a local moisture source (Bradley and Eischeid, 1985; Jeffries and Krouse, 1987), leading to increased precipitation along the coast relative to the interior parts of Ellesmere Island (Koerner, 1979; Edlund and Alt, 1989). However, this 'Arctic Ocean Effect' is limited to a narrow zone right along the coast line. By contrast, the highest ice margins and ELAs in the Canadian High Arctic (800 to 1000 m asl) occur on the other side of the British Empire / U.S. Range, on the dry plateau highlands of northeastern Ellesmere Island (Miller *et al.*, 1975; Koerner, 1979; Braun *et al.*, 2004a).

4.4 History of the Surface Mass Balance Measurements

Surface balance measurements on the Ward Hunt Ice Shelf began indirectly with R.E. Peary's quest for the North Pole at the turn of the 20th century (Peary, 1907). G. Hattersley-Smith and companions discovered one of Peary's old camp sites from 1906, during the first scientific exploration of Ellesmere Island's north coast in 1953 (Hattersley-Smith *et al.*, 1955). Their finding implies that there was no net accumulation of mass on the ice rise and ice shelf for the first half of the 20th century (Hattersley-Smith and Serson, 1970). Comprehensive surface balance measurements began in 1959 on the WHIR and in 1966 on the WHIS, with earlier estimates based on limited observations available from 1954 to 1958 (Sagar, 1962; Hattersley-Smith and Serson, 1970). The 1959 to 1968 ice rise and 1966 to 1968 ice shelf data were published by Hattersley-Smith and Serson (1970), and the records up until 1976 further assessed by Serson (1979). In addition, Ommanney (1977) and Koerner (1996) compiled parts of both records. The late Harold Serson also meticulously brought together annual summaries of all surface

balance measurements on the ice rise and ice shelf up until 25 May 1986 as a comprehensive, hand-written table (dated 1 May 1989). Those data have been discussed by Jeffries (1994). The ablation stake networks were re-measured by R. Fiennes and companions on 9 March1989, allowing H. Serson to calculate the cumulative surface balance of the WHIR and WHIS between 1986 and 1989 (Jeffries, pers. comm.). In 2002, UMass and Parks Canada personnel installed a new stake transect across the ice rise (Fig. 4.2); remaining useable ablation stakes from the original 1959/1966 networks were measured in 2002 and 2003.

4.5 Details of the Surface Mass Balance Measurements

The ablation stake networks on the Ward Hunt Ice Rise and Ice Shelf (Fig. 4.2) were designed to measure surface balance changes (excluding calving losses or sub-ice processes) within a relatively restricted area of about 1 km^2 (Serson, 1979). The surface balance records of the WHIR and WHIS do not, therefore, represent glacier-wide integrated values. Ice rise measurements began in 1959 at 45 ablation stakes (Sagar, 1962), installed in a grid pattern at its northern margin. The interior and higher elevation areas were not included in the original measurements. On the ice shelf, 100 ablation stakes were installed in 1966 in a 10 by 10 grid pattern (Fig. 4.2), thought to be representative of about 10 km^2 of the larger ice shelf surface (Ommanney, 1977). The number of ablation stakes measured each year decreased over time, as stakes melted out of the ice or were otherwise lost (Serson, 1979). This reduced stake density/coverage, but the accurate number or location of stakes used to determine each yearly value is largely unknown. We consider ±50 percent as a conservative uncertainty estimate for the presented surface balance data (Hattersley-Smith and Serson, 1970). Field measurements were conducted annually as early as 9 March (1989) and as late as 24 June (1967). Measurements of winter snow accumulation (snow depth and density) thus represent an 8 to 10 month long window of snow accumulation since the end of the previous summer's ablation season (Jeffries, 1994). The winter balance (b_w) for each site was determined as the average of all available individual stake measurements (Serson, 1979). The average change in ice-surface height from the previous year's measurement yielded the summer balance (b_s) for each site. Superimposed ice formation and summer snowfall were not explicitly measured. The annual net surface balance was then calculated as:

Equation 4.1 $b_n = b_w - b_s$

On the ice rise, we discovered 19 original ablation stakes in 2002, still in excellent condition, and were able to compare 16 of them with their last measurement on 9 March 1989. We were unable to find seven stakes measured in 1989, and assume that they melted out at some point between 1989 and 2002. We did find three additional stakes on the ice rise, which had not been measured in 1989, presumably missed due to darkness and otherwise difficult circumstances in early March. In 2003, we re-measured the original ablation stake network and the stake transect across the WHIR installed in 2002.

On the ice shelf, logistic constraints in 2002 prevented a comprehensive survey of the 1966 stake network, but two original ablation stakes in useable condition were located. We discovered four additional useable stakes during a detailed survey of the ice shelf on 10 August 2003. We were able to match all six recovered stakes with their 1989 measurements, and assume that the other nine found by Fiennes *et al.* melted out sometimes between 1989 and 2003. We averaged ice surface height change values from the 16 ice rise and six ice shelf stakes, and multiplied the average values by 0.9 (cf. Hattersley-Smith and Serson, 1970) to express net surface balance changes in water equivalent (weq) for 1989 to 2002 (WHIR) and 1989 to 2003 (WHIS).

4.6 Surface Mass Balance of the Ward Hunt Ice Rise and Ice Shelf

Figure 4.3 presents the surface balance records of the Ward Hunt Ice Rise and Ward Hunt Ice Shelf (1954 to 2003). The annual surface balance records are continuous, but measurements after 1976 occurred more intermittently (except for several years in the early 1980s), resulting in many multi-year balances. The absence of interannual variability between 1986 and 2002 reflects the aforementioned gap in the observations. Separately measured winter and summer balances are available for about half of all years on record. The 1954 to 1958 values are estimates based on limited measurements on the ice rise and ice shelf (Sagar, 1962; Hattersley-Smith and Serson, 1970).

Winter snow accumulation has remained relatively constant from year-to-year on the ice rise and ice shelf (Fig. 4.3) and compares well with values reported by Jeffries and Krouse (1987) for larger-scale snow surveys along the north coast of Ellesmere Island between 1982 and 1985 (Jeffries, 1994). In

contrast, summer ablation has been considerably more variable from year-to-year and largely controls annual surface balance variations. Both records show infrequent positive surface balance years (e.g. 1963 to 1965, 1972/73), but overall negative years dominate (Jeffries, 1994). Summer and annual surface balances have been consistently more negative on the ice shelf compared to those on the ice rise. These differences are consistent with the observations by Lister (1962), Sagar (1962), Hattersley-Smith and Serson (1970), Serson (1979), and Jeffries (1994) and appear to be related to the characteristic ridge/trough topography (Koenig *et al.*, 1952) and associated formation of elongated meltwater lakes on the ice shelf surface (Fig. 4.2). Ablation within these meltwater lakes is enhanced relative to the ice shelf ridges (or the ice rise) by the continuous presence and flow of liquid water (Hattersley-Smith, 1957; Lister, 1962).

Annual and summer balances for individually-measured years (i.e. excluding those annual values calculated as averages of multi-year balances) are highly correlated between the WHIR and WHIS, whereas the correlation for the respective winter balances is much lower (Table 4.1). We used this high degree of statistical association to extend the ice shelf record back to 1959 (using a simple linear regression), which allows a better comparison of the respective cumulative surface balances. Since 1959, there has been an overall surface mass loss of 1.68 m weq on the WHIR (0.04 m weq/year) and of 3.1 m weq on the WHIS (0.07 m weq/year) (Fig. 4.3c). Between 1989 and 2002, the ice rise lost 0.44 m weq ice (0.03 m weq/year), whereas the ice shelf experienced an overall surface mass loss of 1.03 m weq between 1989 and 2003 (0.07 m weq/year). Measurements of two WHIS stakes indicate that about 50 percent of this mass (0.54 m weq) was lost during the 2003 balance year. 2003 was also the most negative individually-measured year on record for the WHIR, with an annual surface mass loss of 0.33 m weq Measurements along the new stake transect showed that the WHIR was entirely in the ablation zone in 2003. Ice surface lowering was greatest (60 to 70 cm) at lower elevations near the ice margin (i.e. area of original stake network), and much less (~20 cm) at higher-elevation stakes towards the center of the ice rise.

It is important to note that the 1989 to 2003 surface balance (–1.03 m weq) of the WHIS is based on measurements at only six ablation stakes. Lister (1962), Sagar (1962), Hattersley-Smith and Serson (1970), and Serson (1979) have commented on the high degree of local variability in accumulation and

ablation; thus the 1989 to 2003 ice shelf value needs to be viewed with caution. We consider the 1989 to 2002 net surface balance of the WHIR (–0.44 m weq) as more reliable, because it represents an average of 16 individual stake measurements. However, the latter parts of both records may progressively underestimate actual surface mass losses, as the total number of stakes contributing to each annual average decreased, with those at (locally) high melt locations (e.g. stakes inside ice shelf meltwater lakes) likely to have been lost earlier. One must also keep in mind that these records represent a relatively small area at both sites (Fig. 4.2). Lastly, the ice shelf stakes are only useful to gauge mass changes at its upper surface, providing no information about mass gains or losses occurring at the bottom of the floating ice shelf through melting and accretion of sea water (cf. Hattersley-Smith and Serson, 1970). Past ice thickness estimates for the WHIS range between 40 and 60 m (Crary, 1958; Jeffries and Krouse, 1984; Jeffries, 1994), although Mueller *et al.* (2003) have shown evidence for a substantial thinning of the ice shelf (down to ~25 m) since 1980, at least in one area south of Ward Hunt Island.

4.7 Comparisons with other High Arctic Glaciers

The mass balance of all monitored glaciers in the Canadian High Arctic has been predominantly negative over the last four decades (Koerner, 1996; Dowdeswell *et al.*, 1997; Serreze *et al.*, 2000), with a consistent turn towards increasingly negative values during the 1990s (Fig. 4.4; Table 4.2). The surface balance of the WHIR and WHIS track this general temporal pattern, but the magnitude of their surface mass losses has been comparatively low, especially for the most recent decade (1991 to 2000). This difference, and, more fundamentally, their existence and survival, reflects the localized influence of the Arctic Ocean on the prevailing climatic conditions along the northern coast of Ellesmere Island (Paterson, 1969; Koerner, 1979). The glacier-wide integrated mass balance of the WHIR has probably been much less negative than the data from the restricted original observation network would suggest, as the ice rise supported an interior accumulation area for much of the last 45 years. Within the original stake network (Fig. 4.2), ablation stakes at lower elevations and closer to the ice margin experienced considerable surface lowering since 1989, whereas the more interior stakes (above ~15 m asl) actually showed net mass gains. The stake evidence is corroborated by the nature of the ice surface observed in 2002 and 2003. Considerable accumulations of wind-blown dust, together with well-developed cryoconite holes,

are characteristic at lower elevations near the ice margin, whereas the ice surface towards the center and higher elevations of the ice rise is very clean, white ice.

The closest glaciological analogue to the WHIR and WHIS in the Canadian High Arctic is the Meighen Ice Cap, a low-elevation, coastal ice cap located about 500 km to the southwest on Meighen Island (Fig. 4.1). The existence and survival of this ice cap and its continued survival have also been explained by locally increased snow accumulation and reduced summer ablation, because of its close proximity to the Arctic Ocean (Paterson, 1969; Alt, 1979; Koerner, 1979). However, the 1990s have been by far the most negative mass balance decade for the Meighen Ice Cap (Table 4.2), and follow three decades with a weak trend towards less negative mass balance values (Dowdeswell *et al.*, 1997).

4.8 Surface Mass Balance and Climate Change

Parks Canada has operated an automated weather station on Ward Hunt Island (WHI AWS; Fig. 4.2) since June 1995. Mean monthly air temperatures at Alert (Fig. 4.1) and Ward Hunt Island are highly correlated, and we used a 3rd order polynomial regression to reconstruct a monthly climatology for Ward Hunt Island (R^2=0.994; p=0.09; RMSE=0.94°C; n=5 years). July is the only month of the year at Ward Hunt Island with a mean air temperature above freezing (Fig. 4.5), making it a useful index for the surface balance of the ice rise and ice shelf (Serson, 1979; Vaughan and Doake, 1996). There is no statistically significant trend in the data over the entire 54 year long record, although there have been increases in local, as well as Arctic-wide, summer temperature, if one only looks at the last 20 to 30 years (cf. Vincent *et al.*, 2001; Mueller *et al.*, 2003; Comiso, 2003) or changes since the end of the 'Little Ice Age' (LIA) some 100 to 150 years ago. Decadal mean July air temperature has increased at Ward Hunt Island over the last few decades (Table 4.2), broadly matching the observed surface balance changes of the WHIR and WHIS (Fig. 4.4) as well as decreases in Arctic Ocean sea ice extent and thickness (Rothrock *et al.*, 1999; Comiso, 2002b). However, reduced Arctic Ocean sea ice could actually, at least to some extent, favor more positive surface balances of the WHIR and WHIS by locally increasing accumulation and reducing ablation via an enhanced 'Arctic Ocean Effect' (cf. Hattersley-Smith, 1960a). Increased summer snowfall may contribute only little additional mass to the ice rise and ice shelf, but indirectly reduces ablation by raising the albedo of the ice and surrounding land surface (Hattersley-Smith

and Serson, 1970; Alt, 1979). But it seems doubtful that such localized mechanism can sustain the WHIR and WHIS for much longer, as the direct effects of higher summer temperatures (i.e. increased surface melting) should at some point outweigh the localized secondary processes suppressing melt. This situation appears to have been reached on the Meighen Ice Cap further to the south already during the 1990s (Table 4.2). It is interesting to note that the four warmest Julys of the last 35 years (1993, 1998, 2002, and 2003; Fig. 4.5) all coincided with pronounced minima in Arctic Ocean sea ice cover (Serreze *et al.*, 2003; NASA online document at www.gsfc.nasa.gov/topstory/2003/1023esuice.html).

Hattersley-Smith *et al.* (1955) predicted the disappearance of the WHIS by the year 2035 if summer conditions similar to those of 1954 (mean July air temperature at Alert 5.6°C; ~2.2°C at Ward Hunt Island) were to become common. Such warm summers had not recurred at Alert over the last ~40 years (Fig. 4.5), until July 2003, which was the warmest July on record at Alert (6.8°C) and Ward Hunt Island (2.9°C). Consequently, the WHIR and WHIS experienced probably their most negative surface balance year (Fig. 4.3). The last several years have also seen considerable physical changes of the WHIS (such as enhanced calving from its northern margin, development of substantial cracks through the ice shelf, and ice shelf thinning), after two decades of relative stability (Vincent *et al.*, 2001; Mueller *et al.*, 2003).

We hypothesize that the gradual mass losses over the last 100 years may have weakened the ice shelf sufficiently to induce an irreversible disintegration in the near future. It seems likely that dynamic stresses on the ice shelf related to wave, wind, and tidal action have also increased in recent years, as open water conditions on the Arctic Ocean have become more prevalent (cf. Koenig *et al.*, 1952; Mueller *et al.*, 2003). The refreezing of surface meltwater inside existing ice shelf cracks and fractures may act as an additional positive feedback mechanism (Scambos *et al.*, 2000). Once the ice shelf has disintegrated, it is unlikely to reform again unless climatic conditions deteriorate dramatically (Hattersley-Smith *et al.*, 1955; Vaughan and Doake, 1996).

On the other hand, it is possible that we are witnessing merely an unusual phase of variability, as recorded before in terms of glacier mass balance during the comparatively warm 1950s and early 1960s. Those conditions however did not persist, and in fact much of the Canadian High Arctic experienced overall colder summers and positive glacier mass balance from the mid-1960s to the mid-1970s (Bradley

and Miller, 1972; Alt, 1987; Braun *et al.*, 2004a). The probability of either interpretation must be assessed against the considerable environmental changes already underway in the Arctic (cf. Serreze *et al.*, 2000; Comiso, 2003; Serreze *et al.*, 2003; Wang and Key, 2003) and the consistency of climate model predictions for a continued, and perhaps accelerated, warming at high latitudes (e.g. Houghton *et al.*, 2001; Walsh and Timlin, 2003; Johannessen *et al.*, 2004) in the foreseeable future. Under such conditions, the complete break-up of the WHIS may occur earlier than predicted by G. Hattersley-Smith 50 years ago.

4.9 Summary and Conclusions

We have compiled all surface mass balance data for the Ward Hunt Ice Rise and Ward Hunt Ice Shelf and updated both records through 2003. The surface balance of the ice rise and ice shelf track the mass balance changes of the other monitored High Arctic glaciers, but their surface mass losses over the last 45 years have been comparatively low. This difference reflects the localized influence of the Arctic Ocean on the climatic conditions along the north coast of Ellesmere Island. Nevertheless, overall ice shelf mass losses (including surface melting, reduction in ice thickness, and calving) since the end of the LIA appear to have reached a critical level in recent years, as evidenced by its recent fracturing (Mueller *et al.*, 2003). The floating ice shelf is particularly sensitive to short-term climatic variability, as its mass balance is not 'buffered' by input from upstream land glaciers. Dynamical stresses related to wind, wave, and tidal action may also promote the break-up of the Ward Hunt Ice Shelf as open water conditions on the Arctic Ocean become more prevalent. If the ice shelf disintegrates, it cannot readily reform, unless climatic conditions deteriorate dramatically (hysteresis-effect; cf. Hattersley-Smith *et al.*, 1955). This could leave the Ward Hunt Ice Rise as one of the last remnants of the once extensive ice shelves along the northern coast of Ellesmere Island. The ice rise has remained in a reasonably healthy state in terms of its overall mass balance for much of the last 45 years, although its long-term survival is also threatened by current and predicted future climatic conditions. A collapse of the WHIS would mean the disappearance of an important physical component of the High Arctic landscape, and lead to the destruction of a unique habitat for microbial-based ecosystems (Vincent *et al.*, 2001).

4.10 Acknowledgements

Research was supported by a U.S. National Science Foundation Grant (OPP-9819362) to the University of Massachusetts, and by Parks Canada (Nunavut Field Unit). The Polar Continental Shelf Project (Natural Resources Canada) provided superb logistical support. We thank Martin Jeffries (University of Alaska) for sharing H. Serson's original notes and tables, R.M. Koerner (Geological Survey of Canada) for the mass balance data used in Figure 4.4 and Table 4.2, Derek Mueller (Université Laval) for his help with the 2002 Ward Hunt Ice Shelf measurements, Warwick Vincent (Université Laval) for sharing the RADARSAT image used in Figure 4.2, and three anonymous reviewers for their helpful comments.

Table 4.1 Summary of surface mass balance measurements (1959 to 2003[a]) on the Ward Hunt Ice Rise (WHIR) and Ward Hunt Ice Shelf (WHIS). Values in parentheses refer to years with measurements at both sites.

Winter Balance	WHIR	WHIS
Mean snow depth (m)	0.52 (0.48)	0.50
Mean snow bulk density	0.35 (0.36)	0.31
Mean snow accumulation (m weq)	0.18 (0.17)	0.15
Number of years measured	21	16
Coefficient of determination (R^2; 16 years)	0.41 ($p=0.008$)	
Summer Balance		
Mean ablation (m weq)	–0.17 (–0.18)	–0.20
Number of years measured	16	11
Coefficient of determination (R^2; 11 years)	0.84 ($p<0.0001$)	
Annual Balance		
Mean annual balance (m weq)	–0.04	–0.07
Cumulative annual balance (m weq)	–1.68	–3.1
Number of years measured [a]	45	45[a]
Coefficient of determination (R^2; 12 years) [b]	0.89 ($p<0.0001$)	

Notes

- [a] WHIS measurements began in 1966; 1959 to 1965 values were estimated from WHIR measurements.
- [b] Using only individually measured years (i.e. excluding annual values based on averages of multi-year surface balances).

Table 4.2 Summary of glacier mass balance records from the Canadian High Arctic (decadal mean annual balance in m weq) and decadal mean July air temperature at Ward Hunt Island.

Glacier Name	1951-60 mean	1961-70 mean	1971-80 mean	1981-90 mean	1991-00 mean	1961-00 mean/cum.
Ward Hunt Ice Rise	–0.310[a]	–0.05	+0.01	–0.03	–0.03	–0.03/–1.11
Ward Hunt Ice Shelf	–0.34[a]	–0.12[b]	–0.03	–0.04	–0.04	–0.06/–2.2
Drambuie Glacier [c]	NA	NA	NA	–0.40	–0.51	NA
Melville S Ice Cap [d]	NA	+0.01[d]	–0.20	–0.15	–0.38	–0.18/–7.01
Meighen Ice Cap	NA	–0.08	–0.06	–0.02	–0.18	–0.08/–3.35
Devon Ice Cap NW	NA	–0.08	–0.01	–0.05	–0.14	–0.070/–2.82
Baby Glacier [e]	NA	–0.06	–0.01[e]	NA	–0.29	NA
White Glacier	NA	–0.08	–0.03	–0.16	–0.27	–0.14/–5.46
July air temperature [f]	1.22°C	1.04°C	0.80°C	0.93°C	0.99°C	0.94°C

Notes

White/Baby Glacier data are from www.trentu.ca/geography/glaxmbal.htm; Drambuie Glacier, Melville S Ice Cap, Meighen Ice Cap, and Devon Ice Cap NW data were provided by R.M. Koerner (pers. comm.).

- [a] Limited measurements began in 1954. Detailed measurements started on the WHIR in 1959. The 1959/1960 WHIS values are estimated from WHIR measurements.
- [b] Measurements began in 1966; 1961 to 1965 values are estimated from WHIR measurements.
- [c] Drambuie Glacier measurements began in 1977 ('index' balance only; Koerner, pers. comm.).
- [d] Melville South Ice Cap measurements began in 1963.
- [e] Baby Glacier measurements were interrupted between 1978 and 1989 (Adams *et al.*, 1998).
- [f] Mean July temperature at Ward Hunt Island, reconstructed from Alert instrumental data.

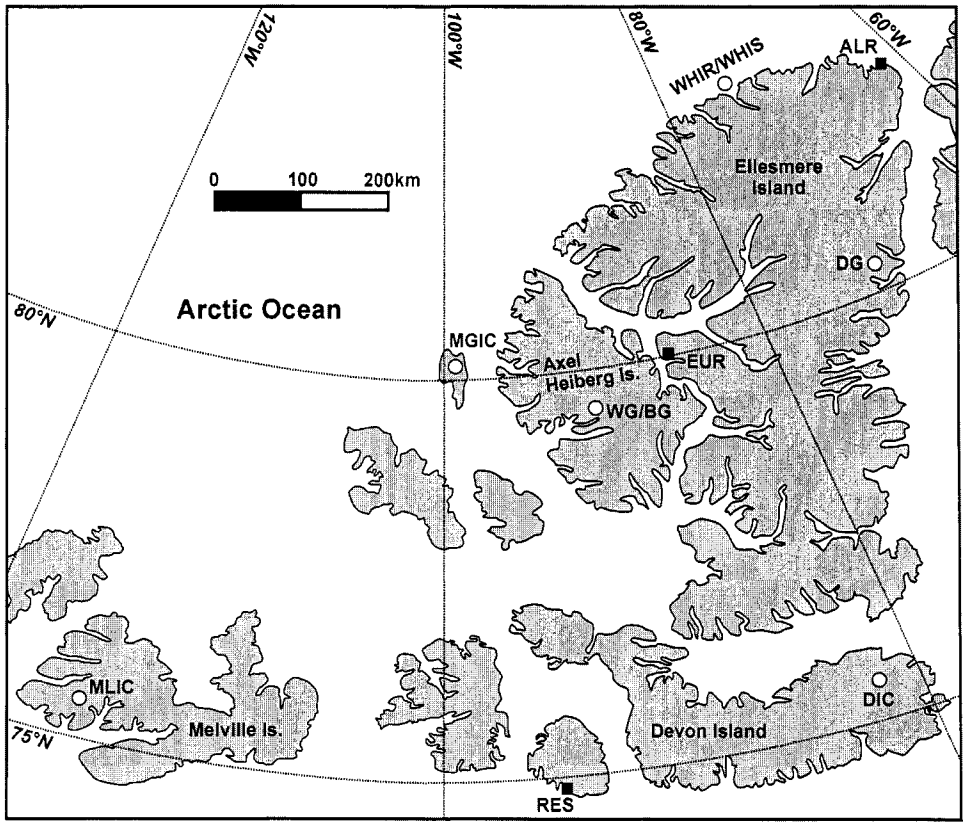

Figure 4.1 The Canadian High Arctic archipelago. Glaciers with long-term mass balance data are indicated by white circles (WHIR/WHIS: Ward Hunt Ice Rise/Ward Hunt Ice Shelf; DG: Drambuie Glacier; MGIC: Meighen Ice Cap; WG/BG: White and Baby Glacier; DIC: Devon Ice Cap NW; MLIC: Melville S Ice Cap). The operational long-term weather stations (RES: Resolute Bay; EUR: Eureka; ALR: Alert) are indicated with black squares.

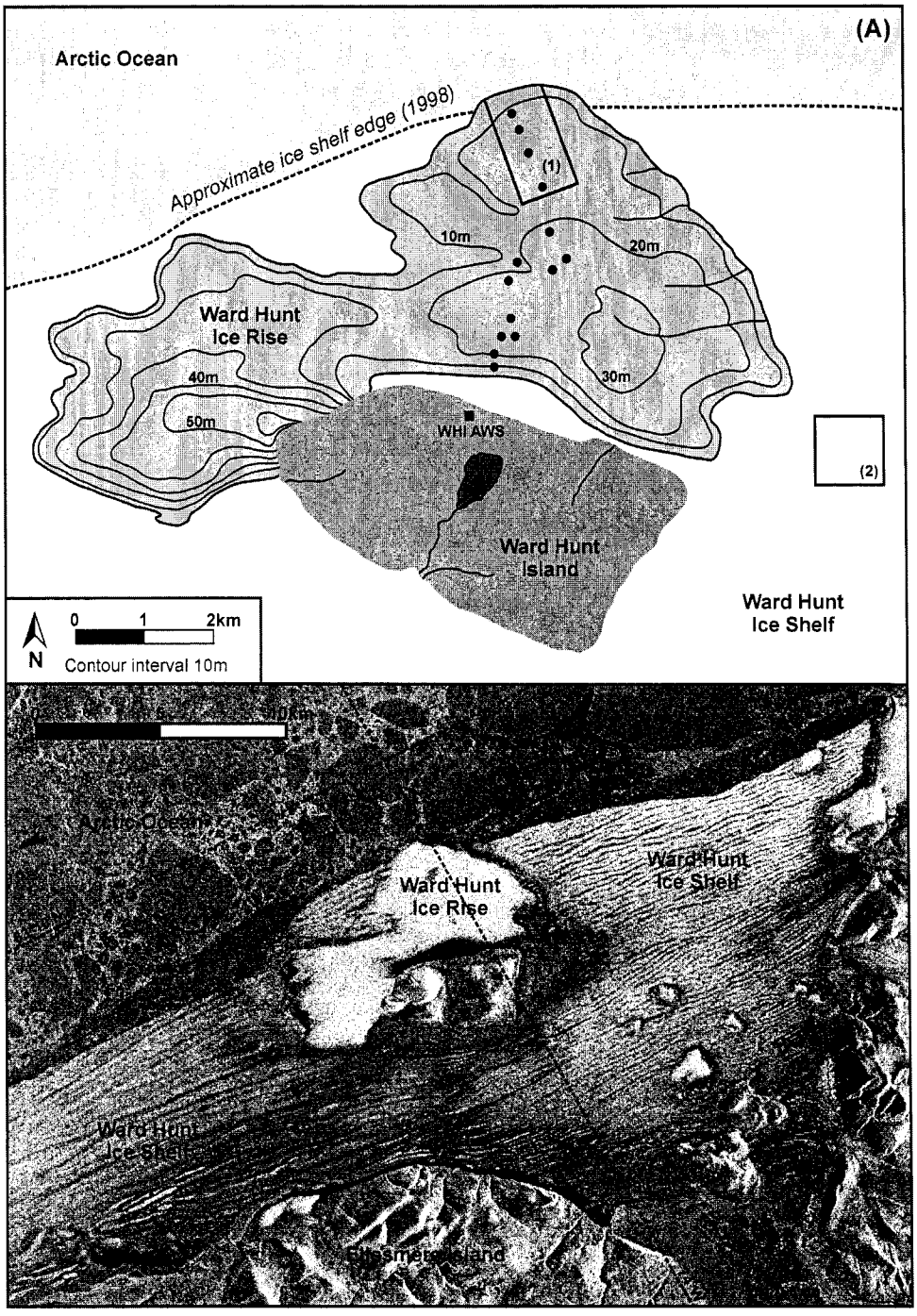

Figure 4.2 (A) Ward Hunt Ice Rise and surrounding Ward Hunt Ice Shelf. Black circles mark the ablation stakes installed on the ice rise in 2002. The approximate locations and extents of the original 1959/1966 stake networks on the WHIR (1) and the WHIS (2) are indicated by solid rectangles (Serson, 1979). The Ward Hunt Island weather station (WHI AWS, black square) is located at 81°05'N and 74°09'W. (B) RADARSAT 1 image of the Ward Hunt Ice Rise and surrounding Ward Hunt Ice Shelf, 30 August 1998. The ice shelf surface shows the characteristic series of long, parallel ridges and troughs, which form elongated meltwater lakes each summer. Recent calving events have altered the northern margin of the ice shelf (Mueller *et al.*, 2003). (Modified from Vincent *et al.*, 2001; their Fig. 2; reproduced with permission of the authors)

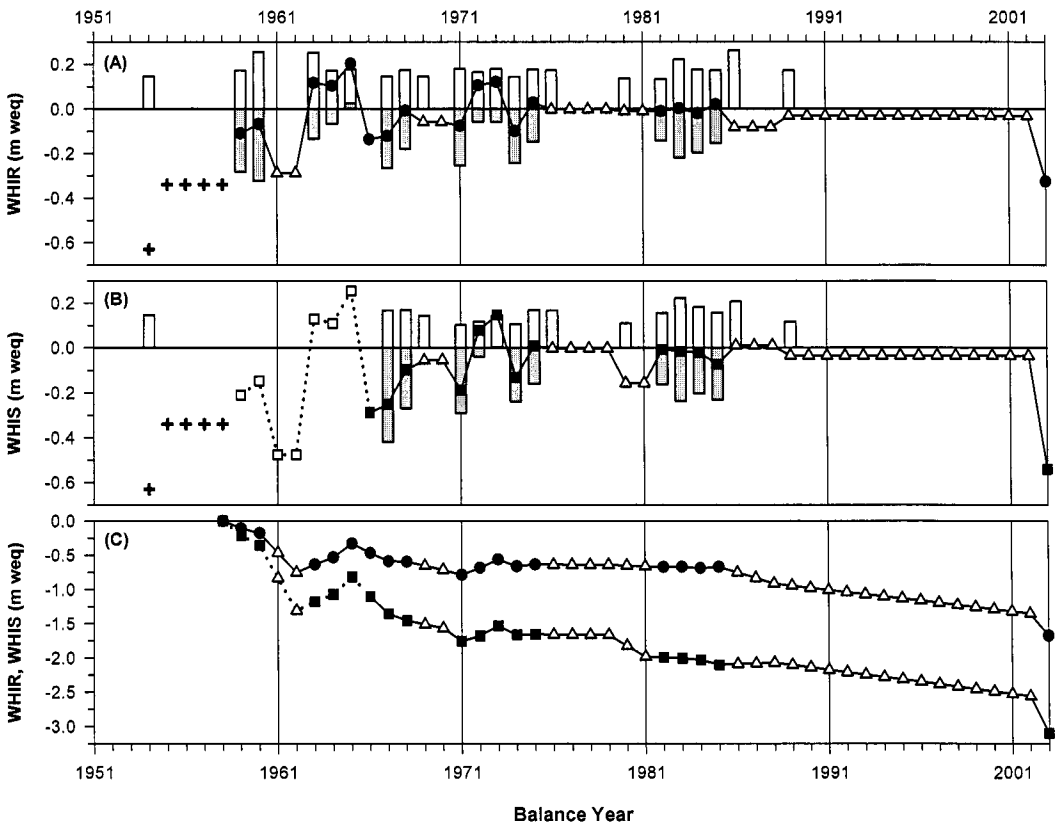

Figure 4.3 Surface mass balance of the Ward Hunt Ice Rise and Ward Hunt Ice Shelf (1954 to 2003). (A) WHIR: winter (white bar), summer (gray bar), and annual (black circle) surface balance. (B) WHIS: winter (white bar), summer (gray bar), and annual (black square) surface balance. (C) WHIR (circle) and WHIS (square) cumulative surface balance (1959 to 2003). Annual balance values from 1955 to 1958 (plus symbols) are a multi-year balance estimate based on limited measurements (Hattersley-Smith and Serson, 1970). The 1954 winter and annual balance estimates are from Sagar (1962) and Hattersley-Smith and Serson (1970). Annual values calculated as averages of multi-year balances are indicated with open triangles. The 1959 to 1965 values for the WHIS (open squares and dotted line) are calculated using a linear regression.

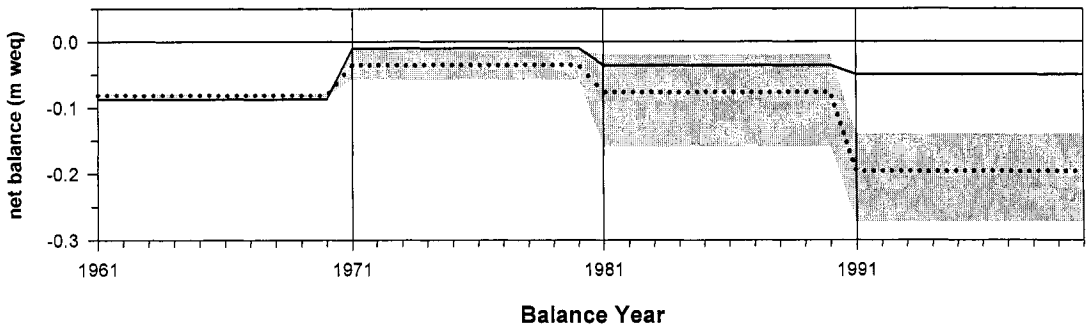

Figure 4.4 Decadal mass balance means for selected Canadian High Arctic Glaciers (1961 to 2000). Shown in grey is the composite range in decadal values for the White Glacier, Devon Ice Cap, and Meighen Ice Cap, with the decadal mean for this group of glaciers shown as a dashed line. The decadal mean combined surface mass balance for the WHIR and WHIS is shown by a solid black line.

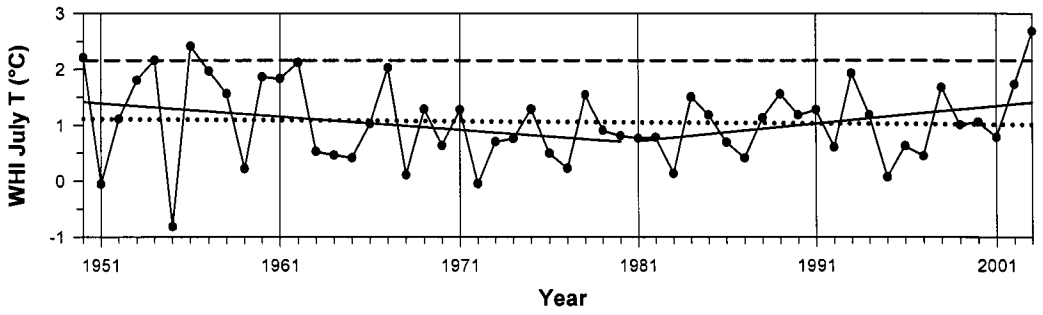

Figure 4.5 Reconstructed mean July air temperature at Ward Hunt Island (1950 to 2003), based on a transformation of corresponding Alert monthly temperature. The dotted line indicates the long-term trend between 1950 and 2003 (–0.002°C, p=0.76). The two solid lines show the 1950 to 1980 (–0.02°C, p=0.15) and the 1981 to 2003 trend (+0.03°C, p=0.1), corresponding to the 'pre-satellite' and 'satellite' era of environmental observations in the Arctic (cf. Comiso, 2003). The mean July air temperature in 1954 at Ward Hunt Island (2.2°C) is indicated by a dashed line.

CHAPTER 5

CLIMATOLOGY OF THE HAZEN PLATEAU AND NORTH COAST, ELLESMERE ISLAND, NUNAVUT, CANADA

In the Canadian High Arctic, virtually all available long-term climate data come from a very sparse network of low-elevation, coastal climate observing stations (such as Eureka and Alert; Fig. 5.1) – the weather and climate of the interior and high-elevation parts of the High Arctic Islands (such as the Hazen Plateau of Ellesmere Island) remains essentially unmonitored, even today. It is therefore necessary to develop a basic climatology (i.e. temperature and precipitation) for the Hazen Plateau, by placing the three years of data collected between 1999 and 2001 into a longer temporal and larger spatial context. This requires a detailed data comparison with the available surface and upper-air data from Eureka and Alert, weather station data collected by Parks Canada, and other available indirect climate data (such as glacier mass balance measurements, snow/firn pit/core data, etc.) (Fig. 5.1). The climatology developed here in Chapter 5 will provide some of the necessary climate input for the snow and ice cover modeling experiments in Chapter 6.

The situation is similar for the remote northern coast of Ellesmere Island (Fig. 5.1), although the long climate record from Alert is generally considered to be reasonably representative for the climatic conditions along the entire coast line (Sagar, 1962; Hattersley-Smith and Serson, 1970; Hardy *et al.*, 1996; Braun *et al.*, 2004b). In addition, the long mass balance records from the Ward Hunt Ice Rise and Ice Shelf (Braun *et al.*, 2004b) and the fairly detailed meteorological measurements on Ward Hunt Island by Parks Canada since June 1995 provide an additional useful local reference.

It is however appropriate here to include a word of caution regarding the usability of distant climate station data to assess specific local and regional climatic conditions (Lotz, 1961b):

> "The short length of the observational period, the variability of the climate, and the great distance separating the Ice Shelf and the two Joint Weather Stations [i.e. Alert and Eureka] all mean that great caution must be used in taking data from Alert and Eureka, and using them in a study of the Ice Shelf region."

This cautionary statement by Lotz (1961b) specifically concerned the situation along the North Coast of Ellesmere Island, but clearly also applies to the Hazen Plateau (as well as anywhere else around the world, cf. Mair *et al.*, 2005). G. Hattersley-Smith (1968) picked up on this issue several years later during a discussion of a paper presented by O.H. Løken and R.B. Sagar (1968):

> "The divergence between accumulation on the [Barnes] ice cap and precipitation measurements at the nearest weather station (all near sea level) make a strong case for automatic weather stations actually on the ice cap, in order to obtain weather data relevant to the regime of the ice cap."

5.1 The Climate of Northern Ellesmere Island: A Selective Literature Review

Much of our current knowledge and understanding of the modern climate of northern Ellesmere Island comes from only a handful empirical meteorological studies conducted during the 1950s and 1960s (e.g. Jackson, 1959; Lotz, 1961a, b; Sagar, 1962; Lister, 1962; Jackson, 1965; Barry and Jackson, 1969) and only a few regional synthesis studies (e.g. Maxwell, 1981; Edlund and Alt, 1989; Atkinson and Gajewski, 2002). This paucity of scientific literature is perhaps an expression of the paucity of available data and the insufficient spatial density of permanent, long-term climate stations (Fig. 5.1), which is completely inadequate to capture local, and even regional-scale, climatic patterns across the Canadian High Arctic islands (Maxwell, 1980; Kattsov and Källen, 2005).

On the other hand, it is also possible to argue the other way around: Given the paucity of climate data, any regional-scale synthesis based on those limited data will be very much influenced by the specific local conditions measured at those few stations. The spatial representativeness of the long-term climate station data is especially problematic due to their inherent coastal bias (Gajewski and Atkinson, 2003; Abdalati *et al.*, 2004) – yet the interior of Ellesmere Island is known to experience a very continental climate (Lotz, 1961b; Edlund and Alt, 1989; Ohmura, 2000). For example, Ohmura (2000) argued that a marked transition between maritime (coastal) and interior (continental) climate occurs within only a few km of the coastline in the Canadian High Arctic, yet this transition is not captured at all by any of the official long-term climate observing stations. The following represents by no means a comprehensive review of all the available scientific literature regarding the climate of the High Arctic, but rather an attempt to highlight a few of the unique and relevant characteristics of the climate of

northern Ellesmere Island, especially concerning the stark climatic contrast between the continental Hazen Plateau and maritime North Coast.

5.1.1 Empirical Studies: The Hazen Plateau of Ellesmere Island

5.1.1.1 Jackson (1959)

Jackson (1959) summarized the meteorological measurements and observations conducted at Lake Hazen (Fig. 5.1) between September 1957 and July 1958 (11 full months of data; cf. Jackson, 2002) in the context of the regional climate of northern Ellesmere Island, as defined by the official climate recording stations at Eureka and Alert. Jackson (1959) was the first to describe and quantify some of the unique local climatic characteristics of the Lake Hazen basin/trough, especially during the (dark) winter season:

> "One reason is the frost-hollow site of the Lake Hazen station: cool air drains down the mountains and tends to collect over the lake. In this respect, therefore, Lake Hazen is perhaps not representative of the more exposed situations inland [e.g. Hazen Plateau]."

Summer temperatures measured at Eureka and Lake Hazen were very similar in terms of their monthly and seasonal means, whereas Alert experienced considerably colder temperatures during the summer months. Jackson (1959) offered the following reasonable explanation for this phenomenon:

> "When the snow has gone from the land surface, contrasts between coastal and inland sites tend to increase in relative importance. Eureka, although on tidewater, is relatively landlocked compared to Alert and therefore shares part of the Lake Hazen [climatic] regime."

Jackson's (1959) description of the winter and summer climate of interior Ellesmere Island immediately raises some concerns about the validity of a direct comparison between the high-elevation Hazen Plateau and surface-based Eureka and Alert climate data (cf. Hardy, 1996; Mair *et al.*, 2005). Alert is located much closer to the Hazen Plateau than Eureka (~110 miles vs. ~200 miles), but may actually be less representative climatically because of its stronger local maritime influences. Indeed, Ohmura (2000)

argued that Eureka is the "most representative" of all three currently operational High Arctic climate stations for the climatic conditions in the interior of the High Arctic Islands.

5.1.1.2 Jackson (1965)

Jackson (1965) discussed vertical wind profile measurements conducted at Lake Hazen (Fig. 5.1) during the summer of 1961, but also incorporated some of his previous work during the 1957/58 winter season (Jackson, 1959; 2002). He noted (again) that Lake Hazen experiences much colder surface temperatures and much less surface wind than either Eureka or Alert, especially during the long (dark) winter months. These abnormally low winter air temperatures appear to be linked, in his opinion, to the absence of appreciable surface winds near Lake Hazen. The explanation of the light surface winds, in turn, is provided by the sheltering effect of the mountains to the northwest and the general thermal stability of the atmosphere inside the Lake Hazen basin/trough, both during the winter and summer. Jackson (1965) thus concluded that:

> "...there must exist throughout virtually the whole winter a strong temperature inversion, with surface temperatures frequently below –40°C, while those in the troposphere a few thousand feet above are often 20°C or so warmer."

These relatively calm surface wind conditions are thought to favor the formation of still more intense temperature inversions and thus "a self-sustaining system is established" (Jackson, 1965; Page 31). These strong inversions are only infrequently broken down, either by a warming of the surface/lower troposphere by long-wave radiation (associated with cloud cover and/or precipitation) or by the occurrence of high winds above (inversion roll-up) associated with the passing of especially strong synoptic disturbances. During the summer months, the ice cover on Lake Hazen may also help to maintain a very shallow local thermal temperature inversion, favoring light surface winds over the lake and surrounding terrain. The wind speed contrast between Lake Hazen and Eureka/Alert diminished above about 7000 ft asl (= elevation of the highest parts of the U.S. Range), indicating that above this altitude the local topographic effects around Lake Hazen become more-or-less insignificant (Fig. 5.2).

Jackson (1965) was not able to fully answer the underlying 'chicken-and-egg' question: Are the persistent air temperature inversions in the Lake Hazen basin caused by the frequent light winds, or vice-

versa. He thus (carefully) concluded that the frequent air temperature inversions at Lake Hazen are a result of "...the sheltering effect of the mountains to the northwest and the great thermal stability of the air in the Lake Hazen trough, both winter and summer".

How relevant are these findings for the climate of the Hazen Plateau? The main part of the Hazen Plateau is about 2500 ft higher in elevation than Lake Hazen (Fig. 5.2), but well-below the 7000 ft asl threshold elevation suggested by Jackson (1965). This would suggest that (a) temperature inversions during the winter should also be quite common on the Hazen Plateau, and (b) those inversions are probably more frequently broken-down than at Lake Hazen, since the plateau is higher in elevation and less sheltered (i.e. more exposed – higher wind speeds) than the lake.

5.1.1.3 Barry and Jackson (1969)

Barry and Jackson (1969) discussed the summer weather conditions at Tanquary Fjord (Fig. 5.1) as measured between 1963 and 1967. Tanquary Fjord was consistently warmer than Eureka in the summer on average by 1 to 1.5°C. This was explained by (1) the greater continentality of Tanquary Fjord and (2) the frequent occurrence of localized Föhn conditions during the summer at Tanquary Fjord. Barry and Jackson (1969) found no valid statistical relationships between the occurrence of precipitation at Eureka and Tanquary Fjord, highlighting the great spatial variability of precipitation in the Canadian High Arctic. They therefore concluded that synoptic-scale disturbances do not (necessarily) lead to associated, well-defined belts or regions of precipitation (cf. Braun, 1997; Lewis *et al.*, 2005). Eureka and Tanquary Fjord appeared to receive approximately the same amounts of total summer precipitation (20 to 25 mm weq; 1963 to 1967 mean), but Tanquary Fjord received about 90 percent of this precipitation as rain, whereas the percentage at Eureka is only about 70 percent. Barry and Jackson's (1969) finding of no statistical relationship for precipitation is relevant for the climatology of the Hazen Plateau and North Coast. It implies that it is probably unreasonable to expect to define a simple 'regression-type' transfer function between precipitation on the Hazen Plateau or North Coast and at Eureka or Alert (cf. Mair *et al.*, 2005) – which raises the question of how we can develop an appropriate precipitation climatology for the Hazen Plateau (Section 5.3.1) or North Coast (Section 5.3.2) in the context of this study.

5.1.2 Empirical Studies: The North Coast of Ellesmere Island

5.1.2.1 Lotz (1961a, 1961b)

Lotz (1961a, b) presented a very detailed compilation and discussion of the meteorological measurements conducted over the summer of 1959 (June to September) at two different sites on the Ward Hunt Ice Rise and adjacent Ice Shelf. Despite their close proximity, Lotz (1961b) noted that the meteorological station located on the ice rise "experienced much local weather, especially fog" compared to the ice shelf station, only a short horizontal distance (~1 to 2 km) away:

> "The survey line on the Shelf, and the island and the moat were on occasion, clear of fog when the Ice Rise station was 'socked in'. The presence of pack ice, with leads of open water opening and closing before and after the melt season, and with water on its surface during the melt, meant that there was always a source of moisture near the station. Air with a small saturation deficit would tend to produce fog when lifted only a few feet. The Ice Rise station overlooked the Shelf, and was some thirty to forty feet above the general level of the roll summit of the Shelf. This minor orographic feature probably accounts for the amount of fog experienced at the main station when compared to other places in the area. Otherwise it would appear that weather conditions at the Ice Rise station were typical of those experienced over the Shelf and the Rise."

Lotz (1961b) also noted the strong climatic contrast between the interior (continental) parts of Ellesmere Island (e.g. Hazen Plateau) and the more maritime North Coast, especially with respect to the occurrence of fog and the associated duration of sunshine:

> "During the period on record, fog was noted at 46.2% of all observations [on the ice rise]. Dense fog, cutting down visibility to half a mile or less, was rare in June, but occurred at 24.2% of the observations [12 times/day at 2-hour intervals] during July, and at 26.6% in August [1959]. On Gilman Glacier, in 1957, June and July recorded dense fog only 0.4% and 5.6% of the time."

> And:

> "For the period on record [summer 1959], the total possible hours of sunshine that could be recorded [on the ice rise] was 2394.0. Hours recorded were 847.5, a 27.2% occurrence. This is a very low sunshine figure, especially when compared to that of the Gilman Glacier for previous summers. In 1957, between May 18 and August 8, the Gilman Glacier station recorded 64.5% of possible sunshine; for the same period in 1958, the percentage was 56.1."

5.1.2.2 Sagar (1962)

Sagar (1962) summarized the glaciological and meteorological studies conducted on the Ward Hunt Ice Rise (Fig. 5.1) between May and September 1959. Spring and early summer (April and May) are typically characterized by "...high sunshine totals, a preponderance of middle- and high-cloud forms, and lights winds". June, July, and August, in contrast, are commonly characterized by "...relatively low sunshine totals, high mean cloudiness (usually of the stratiform type), moderate winds speeds, and moderate periods of precipitation".

Relative humidities during the summer melt season from June to September were always above 80 percent, and frequently over 90 percent for extended periods of time. At the same time, low cloud types (stratus, strato-cumulus, and fog) occurred at about 70 percent of all observations (12 times/day at 2-hour intervals). The main source of melt energy in 1959 was net radiation, whereas turbulent heat transfer was, in comparison, "negligible". Lister (1962) presented very similar results and measurements for the 1960 melt season. Sagar (1962) thus concluded:

> "It is concluded that relatively small changes in the amount of accumulation and in the radiative energy flux, or both, can have a marked effect on the mass balance of the Ward Hunt Ice Rise and Ice Shelf."

Hattersley-Smith and Serson (1970) also noted the lack of "close correlation" between summer ablation on the Ward Hunt Ice Rise/Ice Shelf and corresponding mean monthly temperatures at Alert, but also emphasized the importance of "...the correlation between more than average warm summers and more than average cold summers in the two areas", in terms of glacier mass balance.

5.1.3 Regional Synthesis Studies

There have been essentially only three regional synthesis studies which have attempted to define and quantify the dominant regional climatic patterns in the Canadian High Arctic. Maxwell (1981) defined climatic regions largely qualitatively, using only the 'officially' collected climate data from the long-term monitoring stations. Edlund and Alt (1989) extended that approach by incorporating regional vegetation patterns and additional short-term (summer) data sets collected by research parties conducting field work in the High Arctic. Atkinson and Gajewski (2002) presented a spatially-distributed,

quantitative model of summer temperatures for the Canadian High Arctic, based on a digital elevation model and a comprehensive data base containing all available long-term and short-term climate data (Atkinson *et al.*, 2000).

5.1.3.1 Maxell (1981)

Maxell (1981) assessed the climate of the entire Canadian Arctic Archipelago and was the first to define its now well-established broad regional and sub-regional climatic characteristics or regions. He noted that all official climate observing sites are located on the coasts of the High Arctic islands. Therefore, the weather and climate over the inland areas (e.g. Hazen Plateau) has/had to be empirically or subjectively assumed (cf. Ohmura, 2000) relative to the sparse climate data available from the coastal stations (Fig. 5.1).

North-central Ellesmere Island (Maxwell's region Vb and Vc) is more-or-less entirely surrounded by high mountain ranges, which result in a rain shadow effect and thus the least total annual precipitation recorded anywhere in Canada. These mountain chains also protect this inter-montane region (Edlund and Alt, 1989) from traveling cyclonic disturbances, promoting a very continental climate with only few outside synoptic influences. Lake Hazen, and other interior locations, experience an even more continental climate than Eureka, as the influence of nearby Eureka Sound moderates the summer temperatures at Eureka to some extent (Jackson, 1959). Also relevant in this context is Maxwell's assessment of the annual precipitation amounts in the interior, high-elevation parts of northern Ellesmere Island of about 200 mm weq (or about 150 mm weq annual snowfall, his Table 6).

In contrast, the climate along the northern coastline of Ellesmere Island (Maxwell's region Ib) is directly and intimately linked to the changing sea ice conditions on the Arctic Ocean:

> "The feature that distinguishes this area, which extends along the northwestern islands from M'Clure Strait to Lincoln Sea, ... is the generally poor flying conditions that exist here. In summer, the Arctic Ocean pack-ice cover is not complete and is extensively puddled. The resulting moisture source maintains a constant layer of stratus and stratocumulus. These cloud and fog features are frequently advected over the islands and waterways of this sub-region."

5.1.3.2 Edlund and Alt (1989)

Edlund and Alt (1989) defined regional spatial climate patterns by combining distinct vegetation patterns and a variety of summer climate measurements in the Canadian High Arctic (Fig. 5.1). They argued that the high mountains of Axel Heiberg and Ellesmere Island create a significant topographic barrier that effectively shelters a large intermontane region (Lake Hazen Basin / Hazen Plateau) from both persistent Arctic Ocean climate and traveling cyclonic systems:

> "The highest summer temperatures occur in the protected Eureka Sound intermontane region, where the lowest cloud amounts and least precipitation occur. This area [which includes the Hazen Plateau] has also the longest snow-free period and the longest period with temperatures above 0°C."

In contrast, the lowest summer temperatures in the Canadian High Arctic occur along the northern coast of Ellesmere Island, which is unprotected from the direct climatic influence of the Arctic Ocean (cf. Walsh *et al.*, 2002), thus "...persistent low cloud cover, fog, low temperatures, and shortest snow-free season make this the harshest regional summer climate in North America."

5.1.3.3 Atkinson and Gajewski (2002)

Atkinson and Gajewski (2002) presented the latest attempt at quantitative regional climate integration in the form of a spatially-distributed summer air temperature model for the entire Canadian High Arctic. Their 'topoclimatic' model was designed with the goal to account for the effects of elevation and proximity to oceans on the basis of a digital elevation model (Atkinson, 2002). The model was in fact (reasonably) able to reproduce the (already) well-known larger-scale spatial climate patters across the islands, but had considerable problems in some of the interior locations, such as north-eastern Ellesmere Island.

For example, their model considerably underestimated summer temperatures on the Hazen Plateau. Atkinson and Gajewski (2002) argued that the climate of this particular region is especially difficult to reproduce within a comprehensive regional model, since none of the existing upper-air sounding stations (e.g. Eureka or Alert) are very characteristic for this particular region (cf. Section 5.2.2.2). Nevertheless, their model incorporated upper-air sounding data from Alert as the main estimator for the climate of the interior Hazen Plateau and Lake Hazen basin, although Alert is locally cooled at the

surface by cold air advection from the Arctic Ocean and the blocking of insolation by associated low-level clouds. Atkinson and Gajewski's (2002) model was reasonably successful in reproducing the well-known coastal cooling effect along the northern coast of Ellesmere Island ('Arctic Ocean Effect', Braun *et al.*, 2004b), but was not able to reproduce the important climatic transition (Ohmura, 2000) to the more continental interior parts of Ellesmere Island (e.g. Hazen Plateau).

5.1.4 Synopsis

It has been suggested (e.g. Sellers and Liu, 1988) that the climatic signal associated with increased greenhouse gases should be greater (i.e. more noticeable) at higher elevations in the troposphere than at the surface (cf. Chapter 1). Kahl *et al.* (1993) tested this notion using an extensive historical data base of Arctic rawinsonde soundings. They concluded that an Arctic-wide 'greenhouse warming' signal was not (yet?) present during the 1958 to 1986 time period. In fact, the only statistically-significant 30-year trends at Alert, Eureka, Resolute Bay, and Thule (Greenland) were summer and fall season cooling trends of about 0.5 to 1.5°C. Their study does not, however, confirm the absence of a greenhouse signal – the 'greenhouse warming' signal may not (yet?) be detectable above 'noise' of natural climate variability (cf. Cogley *et al.*, 1996; Cogley and Adams, 1998; Cogley, 2004). The basic conclusions of Kahl *et al.* (1993) are (still) valid today for Alert and Eureka (cf. Section 5.7.1.2), even with two additional decades of data, although there is considerable mounting evidence (e.g. Serreze *et al.*, 2000; Mueller *et al.*, 2003; ACIA, 2004, Hinzman *et al.*, 2005; Overpeck *et al.*, 2005) for significant and potentially irreversible environmental change in the Arctic.

Numerous studies have identified decreases in both Arctic Ocean sea-ice extent and ice thickness over the last 40 years (e.g. Chapman and Walsh, 1993; Vinnikov *et al.*, 1999; Rothstock *et al.*, 1999; ACIA, 2004). More importantly in the context of regional precipitation, the reduction in sea-ice extent is most pronounced in late-summer and fall (Serreze *et al.*, 2000), which may have led to increased precipitation and accumulation rates along the northern coast of Ellesmere Island – areas directly affected by airflow from the Arctic Ocean. Solid precipitation in the Canadian Arctic has indeed increased over the last ~50 years, with the greatest increases in the fall, winter, and spring seasons (Przyblak, 2002). While some of the increase seen at coastal stations (e.g. Alert) is likely due to changes in sea-ice extent,

large-scale atmospheric circulation patterns such as the Arctic Oscillation (AO) may also account for some of the trend, and associated year-to-year variability (SEARCH, 2001; Przyblak, 2002; ACIA, 2004). Over longer timescales and into the future, climate models consistently predict further decreases in sea-ice extent and thickness, and continued increases in the duration of open water each summer and fall (Johannessen *et al.*, 2004; ACIA, 2004).

The lowest glaciation levels in the Northern Hemisphere are found today along the northern coast of Ellesmere Island (Fig. 5.2), as defined by low elevation, coastal ice caps/ice rises and marine ice shelves (Miller *et al.* 1975). Higher levels of precipitation, and reduced ablation due to frequent low stratus/fog conditions associated with orographically-uplifted Arctic Ocean moisture, help to maintain the very low glacier ELAs in this region (Koerner, 1979; Maxwell, 1981; Hardy, 1996). High frequency of low stratus and fog associated with Arctic Ocean proximity is also thought to result in reduced summer ablation, allowing these ice masses to persist near sea level (Paterson, 1969; Hattersley-Smith and Serson, 1970; Koerner, 1979). At the same time, the Arctic Ocean represents the most important moisture source along the north coast of Ellesmere Island (Bradley and Eischeid, 1985; Jeffries and Krouse, 1987), leading to increased snow accumulation there relative to interior, continental areas such as the Hazen Plateau (Koerner, 1979). This 'Arctic Ocean Effect' (Braun *et al.*, 2004b) is however limited to a narrow zone along the coast (Koerner, 1979).

By contrast, the highest ice margins in the region occur just on the other side of the U.S. Range (Fig. 5.2), on the dry continental plateau highlands (Hazen Plateau) of northeastern Ellesmere Island (Miller *et al.*, 1975; Koerner, 1979). There, accumulation is much lower and summer ablation plays a dominant role in glacier mass balance (Braun *et al.*, 2004a). This sharp regional glaciation-level gradient presumably represents a correspondingly sharp climatic gradient, specifically in terms of (winter) snow accumulation and summer melt. Accumulation (ablation) appears to decrease (increase) with horizontal distance from the Arctic Ocean, as the frequency of stratus/fog conditions decreases towards the interior and high-elevation parts of the island. It is important to note that the existence of these gradients is largely inferential; detailed, comprehensive measurements of glacier mass balance, modern climate, and paleoclimate do not (yet) exist across these (inferred) gradients and transitions.

5.2 Temperature Climatology

The two main automated weather stations (AWS) employed in this study (AWS G3 and AWS T3, for glacier and tundra at 3 m) operated year-around on the Hazen Plateau from June 1999 to August 2001 (Table 5.1). AWS G3 (located on the broad summit plateau of Murray Ice Cap) was deployed on 3 June 1999 and operated without a flaw until 1 December 2000, when hungry foxes damaged (i.e. ate) most of the exposed instrument and battery cables, disabling the station. The station was repaired and re-started 26 May 2001 and finally dismantled 6 August 2001 upon completion of the project. AWS T3 (located on the nearby ice-free tundra) was installed 7 June 1999 and dismantled 4 August 2001. This weather station was not operational from 24 June to 12 July 1999 due to a datalogger malfunction. Data were recorded at both AWS in 30-minute (half-hourly) intervals. It is worth noting that the collected winter data represent the first continuous winter meteorological observations from the high-elevation continental Hazen Plateau. The local climatic reference for the North Coast (Section 5.2.3) is provided by a simple AWS operated on Ward Hunt Island by Parks Canada since June 1995. The meteorological record from that station is unfortunately quite patchy due to frequent instrument/battery failures and lack of adequate station maintenance and service.

5.2.1 Temperature Variability on the Hazen Plateau

Air temperature is arguably the single most important meteorological variable for glaciology, as it is a function of/integrates many different meteorological factors, such as insolation, wind speed, and humidity (Orvig, 1951). It is also arguably the most robust meteorological variable to measure in the field (i.e. it poses the least difficulties regarding data quality-control).

5.2.1.1 Half-Hourly Variability

Figure 5.3 shows the raw half-hourly air temperature measurements at AWS G3 and AWS T3 between 1999 and 2001. The two most noticeable features of these two time series are (1) the long 2000/2001 data gap in the AWS G3 data (due to fox damage) and (2) the shorter 1999 data gap in the AWS T3 data (due to datalogger malfunction). Air temperatures during the winter were surprisingly variable on the Hazen Plateau, with up to 20°C fluctuations occurring frequently over periods of just a

few days. Air temperatures during the (short) summer season on the Hazen Plateau can reach over 10°C. The highest half-hourly air temperature value measured at AWS G3 (T3) was 10.71°C (11.62°C) on 21 July 2001 (22 July 2001). The lowest half-hourly air temperature value measured at AWS G3 (AWS T3) was –36.15°C (–39.05°C) on 7 February 2000 (6 April 2001) – but AWS G3 was unfortunately not operational in April of 2001 due to fox damage.

Figure 5.4 shows two simple scatter plots of all AWS G3 half-hourly air temperature measurements plotted against all AWS T3 half-hourly air temperature measurements. As expected, the slope of the linear regression line is almost 1 (0.961) and AWS T3 was overall warmer than AWS G3 by about 1°C (cf. Section 5.5). The overall R^2 (0.994) is extremely high and the associated RMS error (0.85°C) quite low. However, there is considerable scatter evident in the relationship, especially at higher temperatures, as well as some suggestion of non-linearity, especially for air temperatures above about 5°C (Fig. 5.4b). This suggests that, even though a simple linear regression line overall fits the data very well, the good statistical fit is largely a function of the dominant annual temperature cycle common to both time series, and the large number of available data points.

5.2.1.2 Daily Variability

Figure 5.5 shows exactly the same data as Figure 5.3, but the half-hourly values were first averaged over 24 hours to produce daily means (Table 5.2). The multi-day air-temperature variability during the winter on the Hazen Plateau is again very noticeable, with fluctuations of up to 20°C occurring within only a few days (e.g. AWS T3 in early April of 2001). This type of variability is difficult to explain by changes in synoptic circulation patterns alone. More likely, they reflect the effects of air temperature inversions and their (frequent) break-up and subsequent reestablishment (Jackson, 1965). The lowest mean daily air temperature value recorded at AWS G3 (AWS T3) was –34.79°C (–37.71°C) on 7 February 2000 (6 April 2001) – but AWS G3 was unfortunately not operational in April of 2001 due to fox damage. The highest mean daily air temperature value measured at AWS G3 (T3) was 8.66°C (9.80°C) and occurred on 21 July 2001 (21 July 2001).

Figure 5.6 shows again (cf. Fig. 5.4) two simple scatter plots of AWS G3 against AWS T3 measurements (mean daily air temperature; all values). The coefficients of the linear regression equation

are very similar to those of the respective half-hourly regression (Fig. 5.4). Figure 5.6b shows the identical scatter plot, but only for air temperatures above freezing (i.e. melting conditions). Again, the overall R^2 (0.997) is extremely high and the associated RMS error (0.60°C) is quite low, but much of this strong statistical association can be explained by the dominant annual cycle common to both data sets.

5.2.1.3 Monthly Variability

Table 5.3 compiles the mean monthly air temperatures measured at AWS G3 and AWS T3 from 1999 to 2001 (and the corresponding Eureka and Alert surface temperature measurements). AWS G3 was started 3 June 1999 (first full day of measurements was 4 June 1999), so June 1999 is in reality not a 100 percent complete month. AWS G3 also misses data entirely from December 2001 to May 2001 due to fox damage. AWS T3 was not started until 7 June 1999 (first full day of measurements was 8 June 1999) and was defective from 26 June to 12 July 1999, which means that there are no directly measured mean monthly air temperature values for June and July 1999 from AWS T3 (see below).

Figure 5.7a shows the mean monthly air temperatures measured at AWS G3 and AWS T3 from 1999 to 2001. It is somewhat sobering to realize that over the course of a three year project, it was only possible to collect 20 months (AWS G3) and 24 month (AWS T3) of in-situ meteorological data. The missing six winter month at AWS G3 are not a too great concern in the context of snowmelt and glacier mass balance modeling. However, it is unfortunately necessary to 'patch' the AWS T3 record to at least estimate air temperatures for June and July 1999 (see below).

Figure 5.7b shows the mean monthly air temperature difference between AWS T3 and AWS G3 (i.e. AWS T3 minus AWS G3) (cf. Table 5.3), which was between 1.0 and 1.4°C for the summer months (June, July, and August) and much lower during the winter months. Figure 5.8 shows two scatter plots of mean monthly air temperatures measured at both stations (AWS G3 plotted against AWS T3). The y-intercept of the linear regression line is about –1.1°C, meaning that AWS G3 is colder than AWS T3 by ~1.1°C (on average). Part of this difference is due to the elevation difference between the two stations (AWS T3 was about 75 m lower in elevation than AWS G3). In addition, if one assumes no measurement error, AWS T3 should record higher air temperatures during the snow-free parts of the summer, when more radiative energy is absorbed by the snow-free tundra, and AWS G3 experiences a relative cooling

the last two days of 2001). These two offsets were applied to the AWS G3 data (mean daily air temperature) to produce a continuous mean daily air temperature time series for AWS T3.

5.2.1.5 Seasonal Variability

Table 5.4 compares the monthly and seasonal (i.e. summer) climatic means and totals measured between 1999 and 2001 at AWS G3 and T3. Overall, AWS T3 was about 1°C warmer than AWS G3 and experienced 30 percent more melting degree-days over the two summer melt seasons (1999 and 2000). These values compare well with those previously published by Bradley and Serreze (1987b) for the very similar St. Patrick Bay ice caps on the Hazen Plateau (Fig. 5.1). The climatic differences between ice-covered and ice-free parts of the Hazen Plateau are further explored in Section 5.5.

5.2.2 Comparison: Hazen Plateau and Eureka/Alert

In order to develop a basic (air temperature) climatology for the Hazen Plateau, it is necessary to 'tie' the short-term in-situ meteorological data collected between 1999 and 2001 at AWS G3 and T3 into the available long-term climate records from Eureka and Alert by developing some type of appropriate transfer function:

Equation 5.1 $\quad \text{Climate}_{\text{Hazen Plateau}} = f(\text{Climate}_{\text{Eureka; Alert}})$

This is a fairly common situation and approach in glaciology, as on-site measurements are typically available for only relatively short time periods during dedicated field measurement campaigns. Those in-situ data are therefore only useful in relation to current glacier mass balance conditions. However, if one wants to assess changes in past (or future) conditions, a longer data set or temporal perspective is obviously required. The following example briefly illustrates the typical approach used in this context to create a longer temporal reference frame.

Braithwaite and Olesen (1993) compared mean monthly air temperatures measured at coastal Nuuk, Greenland (48 m asl) for the last 100 years and on the interior glacier Qamanarssup sermia glacier, Greenland (QS; 790 m asl) for about seven years (107 months) between 1980 and 1990 (horizontal

distance ~115 km). Their transfer function, using the available mean monthly air temperatures, had an R^2 of 0.98 and an associated root mean square (RMS) error of ±1.2°C (which represents a measure of the accuracy of the monthly air temperature estimates determined using the transfer function, i.e. estimations of mean monthly air temperatures on QS have an uncertainty of ±1.2°C using the long-term record from Nuuk). The RMS error (and hence accuracy) for the summer months (June, July, and August) was slightly better, with a maximum RMS error of 0.93°C (Taurisano *et al.*, 2004). They subsequently used this equation, combined with Braithwaite's probability model (Braithwaite, 1984), to determine monthly melting degree-day totals and estimate monthly ablation rates on QS. This approach is obviously based on the implicit assumption that the climatic relationship between Nuuk and QS did not change significantly over the last 100 years or so – a problematic assumption that cannot be directly tested (Taurisano *et al.*, 2004).

The situation is quite similar to that facing this project. Unfortunately, the long-term climate record from Eureka and Alert spans only the last 50 years, and the in-situ data collected on the Hazen Plateau only spans about 20 to 24 months over three years (1999 to 2001). This means that there are considerable less data available to define an appropriate transfer function than Braithwaite and Olesen (1993). The ultimate goal would be to develop a robust daily climatology for the Hazen Plateau (with a sufficiently low uncertainty) to allow a determination of annual melting degree-day totals directly through a daily time summation (cf. Arnold and MacKay, 1964; Bradley and England, 1978). However, it is more appropriate and realistic to instead use monthly mean air temperature data and one of the available probabilistic melting degree-day models (e.g. Braithwaite, 1984; Reeh, 1991) to calculate annual melting degree-day totals indirectly from the monthly air temperature climatology (cf. Section 5.6).

5.2.2.1 Hazen Plateau and Eureka/Alert: Surface Temperature Comparison

Figures 5.10 and 5.11 show the daily air temperature data recorded at AWS T3 and AWS G3 plotted as a function of the corresponding daily surface measurements at Eureka and Alert. In all four cases, the overall R^2 is quite high (~0.89). The statistical fit parameters and scatter are almost identical for AWS T3 and AWS G3, which is expected given that daily air temperatures at AWS T3 and AWS G3 are highly correlated themselves (Fig. 5.6). The data scatter appears to be somewhat greater at lower

temperatures, and it appears as though the relationships are perhaps quite non-linear, or at least different, for air temperatures above freezing. This is especially obvious in the AWS T3/G3 comparison with the Eureka data. Table 5.5 summarizes the results of the statistical comparisons shown in Figures 5.10 and 5.11.

Figure 5.12 and 5.13 show the mean monthly air temperature data from AWS T3 and AWS G3 plotted as a function of the corresponding surface measurements at Eureka and Alert (Table 5.3). The 2nd-order polynomial regression equation clearly describes the data very well in all four cases, and is also 'well-behaved' even up to mean monthly air temperatures of 20°C (i.e. considerably beyond the range of values used for its definition). In contrast, the simple linear regression equation does not capture the relationship very well, although the values for explained variance are also very high. The values for R^2 and RMS error (Table 5.6) for all four comparisons are very similar to those presented by Braithwaite and Olesen (1993).

Figure 5.14 shows a summary graph of the monthly air temperature comparison between AWS T3/G3 and Eureka/Alert (using the available surface data). The top graph shows the four monthly time series (1999 to 2001; Table 5.3) and the bottom graphs are the two 'best' scatter plots: AWS T3 vs. Eureka and AWS G3 vs. Eureka, with the appropriate 2nd-order polynomial regression line. It is clear that the regression equations are able to describe the relationships very well, across the full range of measured values. The 2nd-order polynomial also appears to behave reasonably for mean monthly temperatures at Eureka and Alert up to 20°C, which may be important under a 'global warming' scenario (e.g. Ridley *et al.*, 2005).

5.2.2.2 Hazen Plateau and Eureka/Alert: Sounding Temperature Comparison

Upper air sounding data from rawinsonde ascents can often provide more reliable estimates of high-elevation climatic conditions than measurements from low-elevation weather stations (Conway *et al.*, 1995; Hardy, 1996; Tjernström *et al.*, 2004), as air temperature inversions and frequent fog/low stratus cloud conditions often 'cold-bias' surface-based measurements at low-elevation stations (Green and Harding, 1980). Conway *et al.* (1995), for example, found that air temperature data from a nearby low-altitude weather station gave only poor estimates of air temperatures on the Blue Glacier in

Washington State ($R^2 = 0.19$). In contrast, rawinsonde data provided much better estimates ($R^2 = 0.78$). The measurements at the low-lying station were frequently influenced by low-level stratus clouds and associated temperature inversions (Conway *et al.*, 1995). This presumably caused the large underestimation of air temperatures on the Devon Ice Cap as reported recently by Mair *et al.* (2005) in the context of a mass balance modeling study (cf. Bradley, 1975; Bradley and England, 1978). Rawinsondes are launched twice daily at Eureka and Alert (00:00 and 12:00 UTC) since about 1950. Therefore, the available rawinsonde data cannot capture the details of the diurnal air temperature cycle. Measurements are typically available from several standard pressure levels and thus have to be interpolated (linearly) to the specific elevation of interest (e.g. 1100 m asl for the Hazen Plateau) (Conway *et al.*, 1995).

Figure 5.15 shows the four time series of mean monthly air temperature at AWS G3 (1100 m asl) and AWS T3 (1025 m asl), together with the corresponding mean monthly air temperatures at 1100 m asl above Eureka and Alert based on rawinsonde ascents (Table 5.7). It is immediately obvious that the sounding data from Eureka and Alert match very well the data from AWS G3 and AWS T3, even during the winter months. This visual impression is reinforced by the four associated scatter plots (Fig. 5.16 and 5.17) – the linear regression equations are able to describe the data extremely well (Table 5.8). Figure 5.18 shows a summary graph of the four monthly time series and the two associated 'best-fit' scatter plots.

5.2.2.3 Synopsis: Temperature Climatology for the Hazen Plateau

The temperature climatology for the Hazen Plateau is defined by the following two equations with respect to the surface air temperature data from Alert and Eureka:

Equation 5.2 $$\text{AWS T3}_{(\text{predicted})} = -3.2815 + (0.8459 * \text{Eur\_surface}) + 0.0055 * (\text{Eur\_surface})^2$$

Equation 5.3 $$\text{AWS G3}_{(\text{predicted})} = -4.4455 + (0.8530 * \text{Alr\_surface}) + 0.0072 * (\text{Alr\_surface})^2$$

The temperature climatology for the Hazen Plateau is defined by the following two equations with respect to the sounding air temperature data from Alert and Eureka:

Equation 5.4 $\text{AWS T3}_{(\text{predicted})} = 1.6624 + (1.1893 * \text{Alert\_1100m\_monthlymean})$

Equation 5.5 $\text{AWS G3}_{(\text{predicted})} = 0.6434 + (1.1589 * \text{Alert\_1100m\_monthlymean})$

The relationships with the upper air sounding data, especially from Alert, are both better and simpler (i.e. it avoids possible issues with the behavior or extrapolation of a 2nd-order polynomial) than the relationships with the surface data. The statistical fit parameters (e.g. R^2 and RMS error) are similar, or slightly better, than those reported by Braithwaite and Olesen (1993) and Taurisano *et al.* (2004). Equations 5.4 and 5.5 will therefore be used to convert the 1100 m asl sounding temperature record from Alert into a monthly air temperature climatology for the Hazen Plateau (Section 5.7).

5.2.3 Temperature Variability along the North Coast

Parks Canada has operated a simple automated weather station on Ward Hunt Island, about 1.5 km south of the Ward Hunt Ice Rise, since June 1995 (Table 5.9) (Braun *et al.*, 2004b). Mean monthly air temperatures on Ward Hunt Island and at Alert are highly correlated (Fig. 5.19). The 3rd-order polynomial equation clearly fits the available data better than the simple linear regression equation. Therefore, the following equation was used to construct a monthly air temperature climatology for Ward Hunt Island based on the available surface measurements from Alert (Braun *et al.*, 2004b):

Equation 5.6 $\text{WHI AWS}^* = -1.3235 + (0.7494 * \text{Alert}) + (-0.0207) * \text{Alert})^2 + (-0.0004) * (\text{Alert})^3$

(WHI AWS* = Predicted mean monthly air temperature on Ward Hunt Island;
Alert = mean monthly surface air temperature at Alert).

It is important to remember that this transfer function is valid only for the unglaciated Ward Hunt Island and the North Coast (cf. Section 5.7). Air temperatures on the nearby Ward Hunt Ice Rise and Ward Hunt Ice Shelf are presumably somewhat lower due to the 'ice cap cooling effect' (cf. Section 5.5).

5.3 Precipitation Climatology

Even today, the amount of annual (or winter) snowfall or snow accumulation on northern Ellesmere Island (or the rest of the Canadian High Arctic) is still essentially unknown. The three years of detailed measurements and observations on the Hazen Plateau between 1999 and 2001 give only a very limited 'snapshot' of snow accumulation, both in time and space. In an ideal world, there would be a long and consistent record of snow accumulation directly from the Hazen Plateau (and North Coast) for perhaps the last 300 years or so (to include precipitation variability and changes during and since the so-called 'Little Ice Age'). In reality, the available data are today limited to the about 50-year long instrumental precipitation records from coastal Eureka and Alert, several long-term records of mass (i.e. snow) accumulation from high-elevation snow/firn cores and pits, a series of scattered short-term glacier mass balance records, and several generalized estimates of regional precipitation and snow accumulation in the Canadian High Arctic (Fig. 5.1). What are lacking (even today) are consistent long-term observations that capture the temporal variability of precipitation (at appropriate time scales), as well as its associated spatial variability. It is also important to note that snowfall measurements in the High Arctic are notoriously difficult and fraught with substantial error (e.g. Church, 1924; Moss, 1938; Fristrup, 1951; Jackson, 1959; Mekis and Hogg, 1999; Ohmura *et al.*, 1999). In addition, measured snowfall at a single point (for example at a climate observing station) is not directly comparable to actual spatial snow accumulation on the ground (Church, 1924; Moss, 1938; Dorsey, 1945; Arnold, 1965; Løken and Sagar, 1968; Ohmura *et al.*, 1996a, 1999, Jacobs *et al.*, 1997; Yang and Woo, 1999) due to post-depositional processes such as snow drifting and snow compaction.

Precipitation in the Canadian High Arctic generally increases with increasing elevation, but also generally decreases with increasing distance from the coast (Miller *et al.*, 1975; Koerner, 1979). Jackson (1959) published the only available precipitation data set from interior Ellesmere Island and compared the 11 month of measurements at Lake Hazen (from September 1957 to July 1958) with the corresponding measurements at Eureka and Alert. Jackson (1959) came to the following two conclusions with respect to precipitation on northern Ellesmere Island:

1. Alert received more than twice the amount of precipitation as Eureka (on average).
2. Eureka received about twice the amount of precipitation as Lake Hazen (on average) (his Table 13).

Jackson (1959) and Hattersley-Smith (1960b) therefore concluded that annual precipitation amounts at Lake Hazen are, on average, only about 65 mm weq, the majority of which (~80 percent) represents winter snowfall. In contrast, annual snow accumulation on the nearby Gilman Glacier at about 1660 m asl in 1961 was about 185 mm weq, 80 percent of which (~150 mm weq) represented winter snowfall/accumulation (Sagar, 1964).

Barry and Jackson (1969) found no statistical relationship between measurable precipitation at Tanquary Fjord and Eureka (1963 to 1967), highlighting once again the high-degree of spatial variability of precipitation on Ellesmere Island (cf. Section 5.1.1). Braun (1997) and Lewis *et al.* (2005) described similar findings for high-intensity summer precipitation events on Cornwallis Island and Ellesmere Island. The precipitation records from the official long-term weather stations such as Alert and Eureka also generally bear no relationship with actual spatial snow accumulation on glaciers and in watersheds (e.g. Arnold, 1965; Hooke *et al.*, 1987, Jacobs *et al.*, 1997; Yang and Woo, 1999). These studies make it unlikely that one will be able to develop a simple transfer function between, for example, annual, seasonal, or daily precipitation at Eureka or Alert and corresponding precipitation on the Hazen Plateau and North Coast (cf. Mair *et al.*, 2005), except perhaps for the most generalized of cases (Hattersley-Smith and Serson, 1970).

Four different types of data are available today to develop a simple precipitation climatology for the Hazen Plateau and North Coast of Ellesmere Island (Fig. 5.1; Table 5.10):

1. Actual (instrumental) precipitation measurements at the two long-term climate observing stations Eureka and Alert. Problems: Measurement quality/accuracy, spatial variability (point measurements), measured precipitation is not equal to

actual spatial snow accumulation, low-elevation, coastal bias of both long-term climate stations.

2. Long-term annual mass (i.e. snow) accumulation records from several high-elevation snow/firn cores and pits. Problems: Spatial variability (point measurements), high-elevation bias of the available records.
3. Short-term winter mass balance/snow accumulation measurements on selected glaciers, ice caps, and on Lake Hazen. Problems: Spatial variability, very limited number of available measurements.
4. Semi-qualitative, generalized assessments or estimates of regional precipitation, snowfall, and snow accumulation. Problems: Spatial variability, temporal variability, subjectivity of analysis.

Therefore, the most appropriate approach seems to be to assess whatever are available in terms of (limited) measurements or data, and then attempt to make reasonable inferences based on that (cf. Maxwell, 1981; Ohmura, 2000). This is more-or-less impossible to do in a rigorous, quantitative manner, since the data are very different (e.g. types of data, length of record, etc.). Therefore, such an assessment has to be conducted in a more subjective manner, guided by an understanding of the general climate and topography on northern Ellesmere Island. It is also important to keep in mind that the available data as compiled in Table 5.10 represent different types of measurements (e.g. point measurements vs. spatial averages, annual vs. winter snow/mass accumulation, snowfall vs. snow accumulation).

Nevertheless, in terms of snowfall and snow accumulation on the Hazen Plateau and North Coast of Ellesmere Island, it is important to address the following three questions:

1. What are the 'normal' conditions in terms of snowfall and snow accumulation today?
2. What is the associated spatial and temporal variability?
3. How do 1999, 2000, and 2001 compare to the available long-term record (both in time and space)?

This arguably sounds like a hopeless task to try to accomplish (given the nature of the available data, cf. Table 5.10) – but in terms of glacier mass balance modeling the situation is somewhat fortunate. In the Canadian High Arctic, annual glacier mass balance is largely a function of summer melt conditions (e.g. Koerner and Lundgaard, 1995; Koerner and Fisher, 2002; cf. Chapter 2). For example, Bradley and England (1978) and Hooke *et al.* (1987) were able to show that the annual mass balance of the Devon and Barnes Ice Caps was almost exclusively a function of summer temperatures, regardless of changes in winter snow accumulation. Their findings also match the results presented by Oerlemans and Reichert (2000) for the White Glacier on Axel Heiberg Island. It thus seems reasonable to follow the approach of Hooke *et al.* (1987) and treat winter snow accumulation initially as a constant and investigate the response of glacier mass balance to prescribed precipitation changes (i.e. sensitivity analysis, cf. Oerlemans, 2001). Alternatively, Mair *et al.* (2005) defined two different snow accumulation gradients (or accumulation lapse rates) for the Devon Ice Cap relative to adjusted values based on daily snowfall measurements at Resolute Bay. This approach seems inappropriate, given the nature of the used/available data. On the other hand, Marshall (2002) simply assumed that precipitation remains constant up to an elevation of 1000 m asl and then decreases as a simple function of decreasing absolute humidity with elevation. In this case it is obviously necessary to determine an appropriate value for this constant and an associated reasonable range for its temporal variability. In addition, it would be helpful to identify which of the available annual precipitation records (Table 5.10) is the 'most representative' for the Hazen Plateau and North Coast (cf. Chapter 6).

The situation for the even more remote northern coast of Ellesmere Island is actually somewhat better in terms of available precipitation measurements, since there is a long snow accumulation record directly from the Ward Hunt Ice Rise and Ice Shelf (Braun *et al.*, 2004b). In addition, the spatial variability along the coast line appears to be adequately captured (Hattersley-Smith and Serson, 1970; Jeffries and Krouse, 1987) by the long mass balance record from the Meighen Ice Cap to the west and the long instrumental precipitation record from Alert to the east of Ward Hunt Island (Fig. 5.1).

5.3.1 Snowfall and Snow Accumulation on the Hazen Plateau

5.3.1.1 Normal Conditions and Spatial Variability

Table 5.10 represents a comprehensive compilation of all available precipitation and snow accumulation data from northern Ellesmere Island (Fig. 5.1) and also includes the long winter balance record from the Meighen Ice Cap. This table gives a fairly detailed picture of regional snowfall and snow accumulation on northern Ellesmere Island, and its associated spatial variability. But a direct comparison the 27 records listed in Table 5.10 is difficult, and cannot be done in a fully rigorous and quantitative manner, since the different records do not represent exactly the same thing.

For example, the data from the high-elevation snow/firn pits and cores represent net annual mass (i.e. snow) accumulation at a single point, whereas the available glacier mass balance data represent spatially-integrated winter snow accumulation measurements at specific, albeit arbitrary, dates. Most data sets are in-fact simple point measurements (e.g. Alert, Eureka, Lake Hazen, or the snow/firn cores and pits), whereas some of the other records are spatially-integrated across a glacier or ice cap (e.g. Gilman Glacier, Drambuie Glacier, Hazen Plateau ice caps, or Meighen Ice Cap). Some of the available records span a relatively long time period, whereas others represent only a few years of measurements, with varying degree of temporal overlap. Some values are subjective regional estimates, rather than actual in-situ measurements. Finally, the instrumental data for Eureka and Alert are direct (daily) point measurements of snowfall, which is typically not the same as spatially-integrated snow accumulation within a watershed or on a glacier (Arnold, 1965; Ohmura *et al.*, 1996a, 1999; Yang and Woo, 1999). Table 5.10 is therefore very difficult to interpret (and graph) – which makes the associated Figure 5.20 also somewhat difficult to interpret.

Nevertheless, the data from Table 5.10 (means only) are graphed in Figure 5.20, with the two long dashed lines representing the ±1 standard deviation envelope (±57 mm weq) for the long Agassiz Ice Cap pit/core record from 1989 (record #9 in Table 5.10). The following conclusions can be reached after a visual inspection of the graph and associated table:

1. The highest snow accumulation values (~150 to 200 mm weq) occur at the highest elevations of northern Ellesmere Island (e.g. on the Agassiz Ice Cap or near Mt. Oxford).
2. The lowest snow accumulation values (~50 to 100 mm weq) occur at the inland, continental sites of northern Ellesmere Island (e.g. Lake Hazen, Gilman Glacier, Drambuie Glacier, or Hazen Plateau ice caps).
3. The coastal sites (e.g. Alert, Meighen Ice Cap, or Ward Hunt Ice Rise/Shelf) receive considerably more snowfall than the more interior, continental sites of northern Ellesmere Island (e.g. Lake Hazen, Eureka, or Hazen Plateau ice caps).
4. The difference between winter and annual snowfall at Alert (27 percent) is considerably greater than at Eureka (14 percent), which experiences a considerably more continental climate (Ohmura, 2000). (Note: This difference was about 20 percent at Lake Hazen and on the Gilman Glacier (Jackson, 1959; Hattersley-Smith, 1960b; Sagar, 1964)

Elevation and distance-from-coastline, therefore, can explain much of the observed spatial variability of precipitation across northern Ellesmere Island (Miller *et al.*, 1975; Koerner, 1979), but not in a rigorous, quantitative manner (Atkinson and Gajewski, 2002; cf. Section 5.7.2). Actual, in-situ, snow fall or snow accumulation data from the higher-elevation parts of the Hazen Plateau are unfortunately very sparse. In addition to the snow accumulation measurements on Murray and Simmons Ice Cap (records #26, 27; Braun *et al.*, 2004a), seven years of winter snow accumulation measurements are available from the larger (NE) St. Patrick Bay ice cap (mean = 115 mm weq) and one year from the smaller (SW) St. Patrick Bay ice cap (183 mm weq), which occupies a localized topographic depression (Bradley and Serreze, 1987a). Combining all data complied in Table 5.10 and shown in Figure 5.20, it seems reasonable to conclude that the higher elevation parts of the Hazen Plateau probably receive (on average) about 100 to 125 (125 to 150) mm weq winter (annual) snowfall or snow accumulation. This makes the Alert winter snowfall or snow accumulation records (records #2 and #3) the two most

representative long-term records in terms of their overall magnitude for the Hazen Plateau. The situation along the North Coast of Ellesmere Island is further discussed in Section 5.3.2.

5.3.1.2 Trends and Temporal Variability

Appropriate values for winter or annual snow accumulation on the Hazen Plateau (e.g. 100 or 125 mm weq) can only be interpreted in the context of associated temporal trends and its (inter-annual) variability. The question of trends and variability, and especially their significance in the context of climatic change, is of course very much dependent on the time interval used to define them in the first place:

- The last 50 years or so are frequently used for climatic trend analysis in the Canadian High Arctic for no other scientific reason than that the instrumental records collected at Eureka and Alert started around 1950 (e.g. Przybylak, 2002).
- The last 20 to 30 years are also a popular time period to use to assess climatic trends, for no other apparent reason than that this time period is covered by sophisticated (i.e. expensive) satellite observations (e.g. Comiso *et al.*, 2003; Comiso and Parkinson, 2004).
- Precipitation changes since the end of the so-called 'Little Ice Age' (~1850) are perhaps the most interesting in the context of 'real' climatic and cryospheric variability, since the 'Little Ice Age' had a profound effect on glacier mass balance and extent all across the Canadian High Arctic (e.g. Hattersley-Smith, 1969; Andrews *et al.*, 1976; Miller, 1976; Braun *et al.*, 2004a).

Finally, the detection of any trend in High Arctic snowfall or snow accumulation is complicated by the large inter-annual variability (see below), large spatial variability (e.g. Yang and Woo, 1999), and the large error associated with the actual measurements (Kahl *et al.*, 1993; Cogley *et al.*, 1996; Cogley and Adams, 1998; Cogley, 2004).

5.3.1.2.1 The Last 100 years: Trends and Temporal Variability

The long record from the 1989 Agassiz Ice Cap snow pit/firn core (record #9 in Table 5.10) provides an annual, un-scoured record of net annual (snow = mass) accumulation between 1883 and 1988 (Fisher and Koerner, 1994) at this particular point on northern Ellesmere Island. Figure 5.21 shows that snow accumulation was considerably above the long-term mean of 170 mm weq during the 1920s and 1930s, but below-average for much of the 1940s, 1950s, and 1960s (cf. Fisher and Koerner, 1994). This general temporal pattern is also evident in the long snow accumulation record from Mt. Oxford (Hattersley-Smith, 1963) and also broadly matches (with some lags) the air temperature record from Upernivik, Greenland starting in 1874 (Hattersley-Smith, 1963), the air temperature record from Nuuk, Greenland starting in 1870 (Warren, 1990), and from the Arctic region as a whole (Bengtsson *et al.*, 2004, their Fig. 1).

There is no statistically significant trend in the data (Fig. 5.21a; blue line) when considering the entire 100 year record (Table 5.11), which matches the conclusion reached by Koerner and Lundgaard (1995) and Koerner (2001) that snow accumulation rates in the Canadian High Arctic have remained more-or-less constant for much of the 20th century (cf. Kahl *et al.*, 1993). However, if one restricts the temporal domain of the trend analysis only to changes after 1950 (which happens to coincide with the start of the instrumental measurements at Alert and Eureka after World War II), one does find a statistically significant increasing trend in annual snow accumulation at this particular site (Fig. 5.21a; red line; Table 5.11), elsewhere in the Canadian High Arctic (Przybylak, 2002), and in the Arctic region in general (e.g. Serreze *et al.*, 2000; Hinzman *et al.*, 2005). Figure 5.21b shows that there is considerable inter-annual variability in the snow accumulation data from this particular point on the Agassiz Ice Cap. The long-term mean is 170 mm weq, with a standard deviation of 57 mm weq (about 34 percent of the mean) (Table 5.12).

5.3.1.2.2 The Last 50 years: Trends and Temporal Variability

For the last 50 years, most of the available long-term and more continuous precipitation records (except for Drambuie Glacier (record #13) and Eureka max SWE (record #7)) show minor increases in snowfall or snow accumulation (Table 5.11; Fig. 5.22), although some with rather low statistical

significance. This again matches the overall conclusions reached by Koerner and Lundgaard (1995) and Koerner (2001), who found no significant trends in winter mass/snow accumulation on the monitored glaciers in the Canadian High Arctic over the last 40 years (cf. Kahl *et al.*, 1993). However, this does not necessarily imply that precipitation has not been increasing in recent decades (cf. Kahl *et al.*, 1993; Zhang *et al.*, 2000; Przybylak, 2002). Cogley *et al.* (1996) have argued that excessive measurement error alone can explain the absence of climatically-plausible trends in the available glacier mass balance data from the Canadian High Arctic (cf. Cogley and Adams, 1998; Cogley, 2004):

> "However, present methods of [glacier mass] balance measurements are inadequate for detecting trends of the magnitude to be expected from generalized climatological reasoning...Research on more accurate ways of estimating mass balance deserves high priority."

Another issue that complicates the detection of temporal trends in addition to measurement error, is the high-degree of natural (i.e. inter-annual) variability (Kahl *et al.*, 1993; Cogley *et al.*, 1996; Cogley and Adams, 1998; Przybylak, 2002; Cogley, 2004). Table 5.12 presents the mean and standard deviations for the long-term and more continuous precipitation records listed in Table 5.10. For better comparison, the standard deviations are also expressed as percentages of the corresponding means and plotted as a simple bar graph in Figure 5.23. Snowfall and snow accumulation typically varied between 15 and 35 percent from year-to-year, with an average of 25 percent, assuming that the simple standard deviation represents a reasonable estimate for 'normal' levels of inter-annual variability.

Finally, it is necessary to assess whether 1999, 2000, and 2001 were 'normal' or 'exceptional' years in terms of precipitation on northern Ellesmere Island in the context of the available long-term records (Table 5.13). Overall, as expected, there is little consistency between the different available precipitation records. Snowfall and snow accumulation have increased at Alert and on the Meighen Ice Cap during the 1990s (together with their associated inter-annual variability), whereas they remained more-or-less constant at Eureka and on the Drambuie Glacier (Fig. 5.24). 2001 was an above-average precipitation year at Eureka and on the Meighen Ice Cap, but below average at Alert and on the Drambuie Glacier. The reverse statement applies to 1999 and 2000.

5.3.1.3 Synopsis

Snowfall and snow accumulation on northern Ellesmere Island are characterized by high levels of spatial and temporal variability. Quantitative regional or long-term assessments (i.e. precipitation climatologies) are further complicated by systematic differences in measurement type, large measurement uncertainty (Cogley *et al.*, 1996; Cogley and Adams, 1998; Cogley, 2004), and the overall paucity of data, especially from inland and high-elevation sites (cf. Ohmura *et al.*, 1999; Ohmura, 2000).

Snowfall and snow accumulation appears to have increased somewhat on northern Ellesmere Island over the last 50 years (Zhang *et al.*, 2000; Przybylak, 2002), the start of instrumental observations at Eureka and Alert, or last 20 to 30 years (Comiso and Parkinson, 2004), the start of global satellite-based observations. However, this increase only represents a recovery from the drier conditions during the 1940s and 1950s, when viewed in the context of the last 100 years (Fig. 5.21). Precipitation (and temperature) trends in the High Arctic are thus very much dependant on the specific time period considered (cf. Comiso, 2003).

Nevertheless, it seems reasonable to conclude that the higher elevation parts of Ellesmere Islands Hazen Plateau receive (on average) about 125 (100) mm weq annual (winter) snowfall and snow accumulation, with a typical inter-annual variability of about ±25 percent. This range and variability matches very well the frequently-cited value of 128 mm weq for interior northern Ellesmere Island (Hattersley-Smith, 1960c, 1963) and northern Greenland (Fristrup, 1951). More recently, Ohmura *et al.* (1999) presented large-scale precipitation and accumulation maps for the Greenland Ice Sheet and northern Ellesmere Island, indicating about 150 mm weq annual precipitation and snow accumulation on northern Ellesmere Island for the last 50 years or so. About 80 percent of the annual snowfall (~100 mm weq) typically occurs during the fall, winter, and spring (i.e. winter snow accumulation); the remaining 20 percent represent summer snowfall (~25 mm weq).

5.3.2 Snowfall and Snow Accumulation on the North Coast

As noted before, the situation for the more remote northern coast of Ellesmere Island (Fig. 5.1) is actually somewhat better in terms of precipitation data availability, because of the relatively long snow accumulation record directly from the Ward Hunt Ice Rise and Ice Shelf (Braun *et al.*, 2004b). In

addition, the spatial variability of precipitation along Ellesmere Island's Arctic Ocean coast line is adequately captured by the long mass balance record from the Meighen Ice Cap to the west, and the long instrumental precipitation record from Alert (Lotz, 1961b; Sagar, 1962; Hattersley-Smith and Serson, 1970; Jeffries and Krouse, 1987) to the east of Ward Hunt Island (Fig. 5.1).

5.3.2.1 Normal Conditions and Spatial Variability

Figure 5.25 represents a simple 'precipitation' transect along Ellesmere Islands Arctic Ocean coast (cf. Fig. 5.1), extending westward to include the climatically-similar Meighen Ice Cap (Paterson, 1969), using the four available long-term snowfall and snow accumulation records. The means and standard deviations of all four long records are fairly consistent (Table 5.14) and compare well with those reported previously by Jeffries and Krouse (1987) for larger-scale spatial snow surveys along parts of the northern coast of Ellesmere Island between 1982 and 1985 (mean snow depth = 540 mm; bulk density range 0.3 to 0.4).

5.3.2.2 Trends and Temporal Variability

For the last 40 to 50 years, three of the four records (Meighen Ice Cap, Ward Hunt Ice Shelf, and Alert winter snowfall) show slight increases in winter snowfall or snow accumulation (Fig. 5.26), although overall with rather low statistical significance (Table 5.14). The record from the Ward Hunt Ice Rise shows a very slight decreasing trend. This again matches the general conclusion reached by Koerner and Lundgaard (1995) and Koerner (2001) who found no significant trends in winter snow accumulation on the monitored glaciers in the Canadian High Arctic over the last 40 years or so. Nevertheless, a visual inspection of the time series from the Meighen Ice Cap and Alert suggests that snow accumulation (and its associated variability) appears to have increased somewhat since the mid- to late-1990s (Przybylak, 2002). Again, possible 'trends' in the precipitation/snow accumulation data may be masked by the considerable measurement error (Cogley *et al.*, 1996; Cogley and Adams, 1998; Cogley, 2004) and the high-degree of inter-annual variability within the time series (Kahl *et al.*, 1993). The standard deviation of the four time series, expressed as percentage of the corresponding mean, ranges between 21 and 33 percent, with an average of 26 percent (Table 5.14). 2001 was an above-average winter balance (= snow

accumulation) year on the Meighen Ice Cap, whereas 1999 and 200 were below average (Fig. 5.24). The reverse statement applies to winter snowfall measured at Alert in those three years. There are unfortunately no current winter mass balance measurements conducted on the Ward Hunt Ice Rise or Ice Shelf (Braun *et al.*, 2004b).

5.3.2.3 Synopsis

In terms of data input for a simple glacier mass balance model (cf. Chapter 6), the situation is fairly straightforward for the Ward Hunt Ice Rise and Ice Shelf since it is obviously possible (and quite reasonable) to use the in-situ data collected at those two specific sites (Braun *et al.*, 2004b). Unfortunately, winter mass balance measurements ended in 1989. This analysis shows that snow accumulation along the northern coast of Ellesmere Island has remained reasonably constant over the last 40 years, both in time and in space, around a mean of about 160 mm weq, with a typical inter-annual variability of about 25 percent, although there is some evidence to suggest increases in magnitude and variability during the 1990s. This value compares well with the mean annual corrected precipitation of 169 mm for the central Arctic Ocean as proposed recently by Bogdanova *et al.* (2002) and the mean annual precipitation along the northern coast of Greenland of about 154 mm weq as reported by Davies and Krinsley (1962).

5.4 Air Temperature Lapse Rates

One of the first steps in any snowmelt or glacier mass balance modeling exercise is to extrapolate the available meteorological, hydrological, or glaciological point measurements to all other parts of the area of interest (e.g. watershed or glacier). A simple (i.e. constant) air temperature lapse rate is typically used to extrapolate measured air temperatures at a weather station to other elevations on the glacier, which may be located above or below the elevation of the weather station. Under neutral atmospheric conditions, unsaturated air cools at the dry adiabatic lapse rate (9.8°C/1000 m), but the saturated lapse rate is lower, more so at higher temperatures (Ferguson, 1999).

Measured air temperature lapse rates in mountainous terrain show great local, diurnal, synoptic, and seasonal variations (e.g. Greuell *et al.*, 1997; Bøggild *et al.*, 1999; Marshall, 2002; Shea *et al.*, 2004;

Owen *et al.*, 2005) around a mean of about 6 to 6.5°C/1000 m (Young, 1982; Martinec and Rango, 1986; Braithwaite and Olesen, 1990a; Barry, 1992). The lapse rate, however, can also be negative (= temperature inversion) through radiative cooling of still air over a (cold) snowpack, adiabatic warming of descending air masses, or lifting of warm above cold air (Jackson, 1965; Ferguson, 1999). It is therefore not surprising that snowmelt and glacier mass balance models are often quite sensitive to the lapse rates used in the spatial air temperature interpolation and extrapolation (Martinec and Rango, 1986; Marshall, 2002; Braun and Hock, 2004; Hubbard *et al.*, 2005; Kovanen and Slaymaker, 2005; Mair *et al.*, 2005; Ridley *et al.*, 2005). For example, uncertainties related to the air temperature lapse rates (precipitation lapse rates) contributed uncertainties in the calculated temperature sensitivities (precipitation sensitivities) of about ±0.5°C (±30 percent) (Laabs *et al.*, 2005).

Despite these complications, most operational snowmelt and glacier mass balance models typically assume a single constant (in time and space) air temperature lapse rate, which is usually fixed during model calibration or sometimes used as a tuning parameter (Martinec and Rango, 1986; Oerlemans and Hoogendoorn, 1989; Reasoner *et al.*, 2001; Bintanja and Oerlemans, 1995; Glasser, 1995; Greuell *et al.*, 1997; Pollard and Thompson, 1997; Ferguson, 1999; Porter, 2001; Braithwaite *et al.*, 2002; Kleman *et al.*, 2002; Marshall, 2002; Oerlemans, 2002; Arnold, 2005; Kovanen and Slaymaker, 2005; Laabs *et al.*, 2005; Mair *et al.*, 2005; Raper and Braithwaite, 2006). For example, Glasser (1995) simply picked a lapse rate (7°C/1000 m) determined for the Greenland Ice Sheet by Diamond (1960) for a modeling study of the basal temperatures of the former Scottish ice sheet. Blöschl (1991) provided a useful discussion about the problems and issues surrounding air temperature inter- and extrapolation based on constant vertical lapse rates. He argued that the use of a constant lapse rate becomes more problematic with increasing distance (horizontally and vertically) from the applicable reference station(s) (cf. Green and Harding, 1980). Fortunately, Blöschl (1991) was also able to show that the random errors introduced by such an approach tend to cancel when estimating seasonal snowmelt or annual glacier mass balance. Marshall (2002) showed that modeled ice volume in the Northern Hemisphere was not very sensitive to air temperature lapse rate changes between 5 and 8°C/1000 m.

This section now tries to answer a seemingly simple question: How does air temperature vary with changing elevation across the Hazen Plateau? This question should be answered ideally using a

series of on-site air temperature measurements along an elevational transect across the Hazen Plateau (e.g. at 0, 200, 400, 600, 800, and 1000 m asl). Unfortunately, such a data set is not available. Therefore, the challenge is to find an appropriate value for the air temperature lapse rate on the Hazen Plateau, based on a few different available data sources:

1. Lapse rates previously measured elsewhere in the Canadian High Arctic (from the scientific literature) – 'General' lapse rates (Fig. 5.1)
2. Lapse rates determined using in-situ measured data on the Hazen Plateau and available Parks Canada AWS data from Lake Hazen – 'Regional' lapse rates (Fig. 5.1).
3. Lapse rates determined from the HOBO network operated on the Hazen Plateau in the vicinity of Murray and Simmons Ice Cap – 'Local' lapse rates (Fig. 5.28).

5.4.1 General Lapse Rates

It is perhaps debatable whether or not air temperature lapse rates from other, albeit similar, High Arctic locations are really applicable for the Hazen Plateau, but this represents presumably a more robust scientific approach (Porter, 2001) than simply assuming a value of 6.5°C/1000 m (or any other value), which is frequently done in the scientific literature (Martinec and Rango, 1986; Ferguson, 1999). Table 5.15 compiles all available summer air temperature lapse rates determined by other scientific studies in the Canadian High Arctic, or calculated directly from published data therein and publicly available climate data (Fig. 5.1). Measured lapse rates ranged from about 4.4°C to 6.0°C/1000 m, with a simple mean of 5.3±0.6°C/1000 m. The air temperature lapse rates calculated between the St. Patrick Bay ice caps and Alert (records #10 and #11) are both anomalously low, presumably since summer-time surface air temperatures at Alert are often (locally) reduced due to frequent fog and low stratus cloud conditions at Alert (e.g. Edlund and Alt, 1989; Hardy, 1996; Braun *et al.*, 2004b) ('coastal effect', cf. Green and Harding, 1980).

The lapse rates from Table 5.15 are plotted as relative air temperature changes with elevation in Figure 5.27, which highlights (1) the clear differences of the Alert/St. Patrick Bay ice caps data, and (2)

the surprising similarity of all other measured air temperature apse rates. Thus, using the mean of 5.3±0.6°C/1000 m as an 'appropriate value' for the larger Hazen Plateau seems to be a more robust approach than merely assuming some arbitrary or standard value (e.g. 6.5°C/1000 m)as is done frequently in the scientific literature (Ferguson, 1999; Porter, 2001). It is interesting to note that the range of lapse rates compiled in Table 5.15 (4.4 to 6°C/1000 m) and their associated mean (5.3°C/1000 m) correspond almost exactly to the air temperature lapse rates determined in the Canadian Rockies (monthly range = 4.6 to 6°C, mean for summer months = 5.3°C/1000 m) (Shea *et al.*, 2004). For the Peyto Glacier in the Canadian Rockies, Munro (1991) determined a mean air temperature lapse rate of 5.7°C/1000 m. These values compare well to the lapse rates determined for the Washington Cascades by Porter (1977) and Kovanen and Slaymaker (2005) (e.g. 6.2°C/1000 m for the summer ablation season).

Podlech *et al.* (2004) reported a mean summer air temperature lapse rate of 6.1°C/1000 m between 270 and 1150 m asl on a glacier located in southern Greenland, which is very similar to the 6°C/1000 m measured by Bøggild *et al.* (1999) in western Greenland. Oerlemans and Vugts (1993) calculated an air temperature lapse rate of 5.1°C/1000 m between 519 and 1028 m asl on the Greenland Ice Sheet margin, whereas Braithwaite and Olesen (1990a) used (i.e. assumed) a lapse rate of 6.5°C/1000 m for a glacier mass balance modeling study along the Greenland Ice Sheet margin. Most recently, Hanna *et al.* (2005) determined air temperature lapse rates between 4 and 6°C/1000 m for the Greenland Ice Sheet below 1000 m asl, and around 8°C/1000 m for elevations above 1000 m asl. These values are consistent with the lapse rates reported by Steffen and Box (2001) of about 7°C/1000 m, determined using a network of 18 climate stations scattered across the ice sheet and the lapse rates reported over 40 years ago by Diamond (1960). Oerlemans (1991) determined air temperature lapse rates between 6.5 and 7.8°C/1000 m for four different climatic regions of the Greenland Ice Sheet. Despite these variations, Ridley *et al.* (2005) simply used a fixed lapse rate of 8°C/1000 m when modeling the complete disappearance of the Greenland Ice Sheet under a future high CO_2 climate. For southern and western Norway, a mean summer lapse rate between 6 and 6.5°C/1000 m was determined by Green and Harding (1980) and used for Holocene ELA modeling by Dahl and Nesje (1992), Dahl *et al.* (1997), and Lie *et al.* (2003a, b), similar to the air temperature lapse rate used by Ballantyne (1990) for northern Norway (5.0°C/1000 m). Williams (1979, and references therein) determined an air temperature lapse rate of

6.0°C/1000 m for Baffin Island, based on a variety of (unspecified) surface meteorological measurements conducted at different elevations across the island. Finally, Morris (1999) and Braun and Hock (2004) noted air temperature lapse rates between 5.7 and 6.2°C/1000 m at various locations on the Antarctic Peninsula (cf. Reynolds, 1981).

5.4.2 Regional Lapse Rates

It was also possible to determine a more 'regional' air temperature lapse by comparing the meteorological measurements at the tundra AWS T3 (~1025 m asl) with the corresponding measurements at the Lake Hazen AWS (~175 m asl), operated by Parks Canada (Fig. 5.1). Data from the Lake Hazen station and AWS T3 overlapped for two time periods between 1999 and 2001: 4 June to 31 August 1999 and 30 June to 5 August 2001 (total number of days = 126; cf. Table 5.16). No data are available for Lake Hazen station in 2000 due to a technical malfunction of the AWS.

Mean daily air temperatures during the three summer months (June, July, and August) at these two sites were highly correlated ($R^2 = 0.78$), which is not surprising given their very similar (i.e. identical) overall climatic situation and environment (Edlund and Alt, 1989). The mean daily temperature difference was 4.68°C, which, combined with the elevation difference of 850 m, gives a mean air temperature lapse rate of 5.51°C/1000 m (Table 5.16) – very similar to the mean of other High Arctic locations shown in Table 5.15 of 5.3°C/1000 m.

5.4.3 Local Lapse Rates

The local-scale spatial variability of air temperature across the Hazen Plateau in the immediate vicinity of Murray and Simmons Ice Cap was investigated between 1999 and 2001 using a small network of simple air temperature loggers (Onset HOBO) (Fig. 5.28). The overarching goal was to quantify:

1. The local air temperature lapse rate (i.e. changes of air temperature across a narrow elevation band in the immediate vicinity of Murray and Simmons Ice Cap).

2. Possible local spatial temperature gradients across the Hazen Plateau (e.g. as a function of distance from Archer Fjord).
3. Differences in topographic climate as a function different slope aspects (2000 and 2001 only).
4. Localized ice-cap cooling effects (cf. Section 5.5).

Unfortunately, the inferior quality of the Onset HOBO temperature loggers (cf. Shiklomanov and Nelson, 2003) meant that it was necessary to perform extensive data quality control and adjustments on the measured raw data as detailed below. Furthermore, overall data recovery was only about 50 to 60 percent due to frequent technical malfunctions of the Onset HOBO temperature loggers.

5.4.3.1 1999 and 2001: Data Quality Control

The 1999 air temperature data from the HOBO network were not useable at all, since all HOBO stations fell over once the snow pack on the Hazen Plateau melted in June 1999. In 2001, there was insufficient temporal overlap between the recovered HOBO data (due to technical malfunctions) to allow any reasonable inter-comparison in this context. 2001 data from selected HOBO stations (e.g. H5, G2, and C2), however, might be useable to assess the local ice-cap cooling effect exerted by Murray and Simmons Ice Cap (cf. Section 5.5).

5.4.3.2 2000: Data Quality Control

It was unfortunately necessary to extensively quality-control and adjust the raw 2000 HOBO data, as the recorded hourly data showed frequent clear 'outliers' or anomalous values (see below). The raw data were therefore compared with the corresponding hourly data from AWS G3 and AWS T3, outliers identified and deleted, and missing values 'patched' to yield complete hourly time series (Table 5.17). Outliers were identified by calculating the absolute air temperature differences between each HOBO station and AWS G3/T3 (AWS G3 for ice cap HOBO stations, AWS T3 for tundra HOBO stations). All raw values with an absolute hourly difference greater than the (mean ± 3 standard

deviations) were deleted from the HOBO station record and the resultant data gaps patched, using the following two techniques:

- Gaps of one or two hours were patched using a simple linear interpolation of the individual HOBO station time series.
- Gaps of three hours or more (very rare) were patched using a simple linear regression with the corresponding AWS T3 and AWS G3 air temperature measurements.

HOBO station H6 (Fig. 5.28) was excluded entirely from any further analysis, since about 23 percent of all recorded raw hourly values were considered suspicious (Table 5.17). It is also worth mentioning that the HOBO stations only sample air temperature once every hour, whereas AWS T3 and AWS G3 measure air temperature every 60 s and then calculate averages over 30 minutes. Hence, the raw data from the HOBO stations is inherently much more noisy (cf. Shiklomanov and Nelson, 2003). Furthermore, the Onset HOBO temperature loggers are about one order of magnitude less expensive than the high-quality air temperature and humidity sensors used on AWS T3 and AWS G3. It is therefore reasonable to assume and expect that their electronic stability and quality is inferior, hence some anomalous raw values are very much expected (Shiklomanov and Nelson, 2003). Therefore, it seems more robust to restrict any further analysis to mean daily data (Table 5.18), which 'smooth' out some of the inherently noisy raw hourly data recorded by the HOBO stations.

5.4.3.3 2000: Air Temperature Lapse Rates

A direct inter-comparison of the HOBO station data collected in 2000 is additionally complicated by two issues: (1) The data availability for the HOBO stations is not the same (i.e. different HOBO stations recorded data for different time periods in 2000) and (2) the HOBO stations were located (on purpose) in different topographic and climatic situations (Fig. 5.28; Table 5.18)

- HOBO stations T2, H1, H2, H3, H4, H6, and H7 were all located on broad, exposed, ice-free plateau summits (Note: H6 was excluded from the subsequent analysis).
- HOBO station C2 was located within ~50 m of Murray Ice Cap on a south-west facing valley slope near the main camp.
- HOBO stations G2, H5, and H9 were located on broad, exposed ice cap summits (Murray, Simmons, and the larger Roberts Ice Cap (unofficial name)).
- HOBO stations H-N, H-E, H-S, and H-W were installed on accessible slopes of different aspects (North, East, South, and West) at lower elevations (~800 m asl).

Six HOBO stations (T2, H1, H2, H3, H4, H7; 1 June to 19 August; n = 80 days) were all located on very similar broad, exposed, ice-free plateau summits, with slightly different elevations. Table 5.19 lists the mean air temperature and elevation of these stations, and Figure 5.29a shows the associated scatter plot. It is clear that elevation differences alone can explain the differences in air temperature measured between these HOBO six stations. The slope of the linear regression line (= air temperature lapse rate) is about 6.8°C/1000 m (Table 5.19). Note that the elevation range covered by these six HOBO stations is only about 100 m (~935 to 1035 m asl).

The time period of overlap is reduced by six days (7 June to 19 August; n = 74 days) when adding three additional HOBO stations (C2, H5, H-S) into the analysis (Fig. 5.29b): HOBO station C2 (located in close proximity to Murray Ice Cap), HOBO station H5 (located on the exposed summit plateau of Simmons Ice Cap), and HOBO station H-S (located on a south-facing slope at ~800 m asl) (Fig. 5.28). As expected, HOBO station H5 plots below the linear regression line as defined by the six plateau HOBO stations, which means that HOBO station H5 was 'too cold' given the air temperature lapse rate, presumably due to the (relative) ice-cap cooling effect exerted by Simmons Ice Cap (cf. Section 5.5). HOBO station C2 appears to be also somewhat 'too cold' for its elevation, presumably due to its close proximity to Murray Ice Cap. HOBO station H-S, on the other hand, plots above the linear regression line, implying that it was somewhat 'too warm' for its elevation. This was presumably due to

greater solar radiation receipts (on the south-facing slope) and/or its more sheltered location at a lower elevation (~800 m asl). The air temperature lapse rate for the six plateau HOBO stations was 7.0°C/1000 m (Table 5.19) over this particular time interval, very similar to the 6.8°C/1000 m determined for the slightly longer time interval (Fig. 5.29a).

Adding one additional HOBO station (H9), located at about 1300 m asl on the much larger Roberts Ice Cap (Fig. 5.28), reduces the overlap time period for the analysis to only 53 days (28 June to 19 August) (Table 5.19). As expected, HOBO station H9 was also colder than it should have been based on its elevation alone (Fig. 5.29c), which can presumably be explained again by the ice-cap cooling effect exerted by the Roberts Ice Cap (cf. Section 5.5).

5.4.4 Possible Problems Using a Constant Lapse Rate

Most operational snowmelt and glacier mass balance models typically assume a single constant air temperature lapse rate, which is usually fixed during model calibration (e.g. Martinec and Rango, 1986; Greuell *et al.*, 1997; Ferguson, 1999). This assumption is, in reality, incorrect (e.g. Bøggild *et al.*, 1999; Shea *et al.*, 2004) as air temperature changes with elevation can be expected to vary across a wide range of temporal and spatial (horizontal and vertical) scales (Green and Harding, 1980; Blöschl, 1991; Kovanen and Slaymaker, 2005;). Assuming a constant lapse rate therefore represents an unfortunate, but frequently necessary and unavoidable, simplification of reality (Martinec and Rango, 1986).

5.4.4.1 Temperature Inversions on the Hazen Plateau

The possible presence of air temperature inversions on the Hazen Plateau could pose a significant problem when using a fixed lapse rate to extrapolate point air temperature measurements at AWS G3 and AWS T3 across the larger plateau surface as a function of its elevation. It is very likely that air temperature inversions on the Hazen Plateau are a common and persistent occurrence during the winter months (cf. Jackson, 1959). However, this would not present a great concern in the context of this study, which is focused on (summer) climatic conditions relevant for snowmelt and glacier mass balance. Figure 5.30 shows the mean monthly air temperatures measured between 1999 and 2001 at the Lake Hazen AWS (175 m asl) and AWS T3 (1025 m asl). As expected, Lake Hazen was warmer than AWS T3

during the important summer months (June, July, and August; cf. Section 5.4.2), but also much colder during the winter months, which presumably reflects the effects of air temperature inversions on the Hazen Plateau and over Lake Hazen basin. Air temperature inversions between Lake Hazen and AWS T3 during the summer months, for which corresponding daily data are available, occurred only on five days of a total of 126 days (cf. Section 5.4.2). Excluding those five days would increase the mean air temperature lapse rate between Lake Hazen and AWS T3 from 5.51°C to 5.79°C/1000 m. In conclusion, air temperature inversions during the important summer months on the Hazen Plateau appear to be very rare. This matches the overall subjective impressions gathered while spending about 11 summer months on the Hazen Plateau and northern Ellesmere Island between 1999 and 2003.

5.4.4.2 Seasonality of Lapse Rates

Shea *et al.* (2004) showed that the air temperature lapse rate in the Canadian Rockies varied seasonally, from 4.6°C/1000 m in the fall to 6.0°C/1000 m in the spring. The summer lapse rate (5.3°C/1000 m) was very close to the annual mean lapse rate of 5.2°C/1000 m. The lowest correlation between air temperature and elevation occurred during the winter months (lapse rate 4.9°C/1000 m) because of the effects of low-level temperature inversions. Blöschl (1991) presented station data from the Austrian Alps for five months (March to July) collected in 1988 and 1989, which showed that (1) the mean monthly air temperature lapse rate was 6.5°C/1000 m, and (2) that the mean monthly lapse rate for the 10 months was remarkably similar (±0.5°C/1000 m, estimated from his Fig. 3). Another useful example of air temperature lapse rate seasonality in the Canadian Arctic comes from Blatter and Kappenberger (1988), using measurements between July 1972 and September 1976 on Coburg Island. The mean summer lapse rate on the island was 5.0°C/1000 m (Table 5.15). However, the mean air temperature lapse rate during the winter months was close to zero, which resulted in a mean annual air temperature lapse rate of only about 3°C/1000 m. Coburg Island is characterized by a very maritime arctic climate, and presumably experiences strong and persistent temperatures inversions, especially during the winter months, because of frequent low stratus and fog conditions (Blatter and Kappenberger, 1988). In conclusion, seasonal changes in air temperature lapse rate on the Hazen Plateau seem to be primarily related to the presence of air temperature inversions during the winter months (cf. Section

5.4.4.1). It is therefore prudent to limit the spatial extrapolation of the available point measurements at AWS G3 and AWS T3 only to the summer months relevant for snowmelt and glacier mass balance (i.e. June, July, and August).

5.4.4.3 Changing Surface Conditions on the Hazen Plateau

It has been previously suggested (e.g. Williams, 1979) that the air temperature lapse rate should be lower at times of more extensive snow cover. For example, Lotz and Sagar (1962) found essentially no air temperature difference between Lake Hazen (–12°C; 175 m asl) and their research camp on the Gilman Glacier (–12.5°C; 1000 m asl) between 5 May and 31 May 1958. In contrast, the air temperature lapse rate for July 1958 was 4.6°C/1000 m between those two sites (Table 5.15). This difference may be due to changes in surface conditions (i.e. snow cover), but more likely is also a reflection of less persistent and less intense air temperature inversions in July (Jackson, 1959) as opposed to May. The only data set available to test whether or not the air temperature lapse rate on the Hazen Plateau changes once the snow cover disappears is the 2000 data from the HOBO network (Fig. 5.29). The mean lapse rate between 1 and 19 June 2000 (= 100 percent snow cover) was only 3.3°C/1000 m. In contrast, the mean lapse rate between 23 June and 8 July was 10.3°C/1000 m, close to the dry adiabatic lapse rate. For reference, the monthly mean lapse rates for June (July) 2000, ignoring changes in snow cover, were 5.3°C/1000 m (7.9°C/1000 m). It is also interesting to note that the mean air temperature difference between AWS T3 (ice-free tundra) and AWS G3 (ice cap) for the winter month was 0.24°C (cf. Table 5.23). This difference, together with the elevation difference of 75 m, gives a mean winter lapse rate of 3.2°C/1000 m, very close to the value for 100 percent snow cover from the HOBO network. The above considerations suggest that there is indeed some connection between the air temperature lapse rate and the presence or absence of seasonal snow cover on the Hazen Plateau. Unfortunately, no additional data are available to further investigate this aspect of the climatology. Furthermore, the air temperature climatology the Hazen Plateau is defined by mean monthly values (cf. Section 5.2) and it is therefore not possible to incorporate any air temperature lapse rate changes during, before, and after snowmelt (cf. Martinec and Rango, 1986).

5.4.5 Synopsis: Air Temperature Lapse Rates

Table 5.20 and Figure 5.31 summarize the general, regional, and local air temperature lapse rates determined in Section 5.4. The mean lapse rate based on the applicable scientific literature is 5.3±0.6°C/1000 m (cf. Porter, 2001) and is based on a variety of different glacial environments in the Canadian High Arctic and covers an extremely large elevation range (0 to ~2000 m asl). The regional lapse rate on the Hazen Plateau in 1999 and 2001 was about 5.5°C/1000 m, remarkably similar to the mean of the scientific literature. The local lapse rate (available for 2000 only), determined using data from the HOBO station network, was 6.8°C/1000 m, which is somewhat higher than either the general or regional lapse rate (Fig. 5.31), but well within the range of lapse rates found in other studies (e.g. Steffen and Box, 2001).

It is important to note that the general and regional lapse rates integrate air temperature changes over a large elevation range of between 1000 and 2000 m, whereas the local lapse rate only covers a thin, but important, elevation slice of about 100 m (~935 to 1035 m asl) in one small area of the Hazen Plateau. Therefore, the fact that the local lapse rate, measured for 2000 only, was somewhat larger than the general or regional lapse rate may not be all that climatically significant at larger spatial and longer temporal scales. Approximating air temperature variability across an elevation range of about 2000 m, and a much larger area, using a single, linear value obviously smoothes out any localized variations of air temperature with elevation (cf. Oerlemans and Vugts, 1993). Assuming a constant air temperature lapse rate (e.g. 5.5°C/1000 m as the preferred value for this study) for the relevant summer months (i.e. June, July, and August) on the Hazen Plateau is clearly a simplification of reality (cf. Braun and Hock, 2004), but seems to be a reasonable approximation given the above considerations, circumstances, and overall objective of this study (cf. Martinec and Rango, 1986; Porter, 2001).

5.5 Ice-cap Cooling Effect

Prior to the onset of melt, the localized climatic differences in the Canadian High Arctic are relatively small because of the overall homogeneity of the land surface – the vast majority of the land is covered by (dry) snow, regardless of whether the underlying surface is glacier ice, sea ice, lake ice, or frozen tundra. This spatial homogeneity gradually disappears during the spring and summer melt season,

as different surface types with very different radiative and thermal characteristics are exposed during snowmelt (Oerlemans and Vugts, 1993; Marsh, 1999; Ohmura, 2000; Ogura and Abe-Ouchi, 2001). This resultant spatial heterogeneity (Marsh, 1999) is expressed, for example, by higher air temperatures over the ice-free tundra than over sea ice or glacier ice once the seasonal snow cover has disappeared (Loewe, 1971; Wendler, 1974; Ohmura, 2000, Braithwaite *et al.*, 2002). At one extreme end of the spectrum, Ridley *et al.* (2005) calculated that a disappearance of the Greenland Ice Sheet would lead to temperature increases between about 8°C (winter) and 13°C (summer) over an ice-free Greenland.

One of the objectives of this study was to assess how, and to what extent, a small glacier or ice cap (such as Murray Ice Cap) is able to modify its own surrounding climate, simply through its existence (cf. Chapter 6). Intuitively, air temperatures above a glacier or an ice cap should be (relatively) lower than air temperatures at the same elevation outside of the glacier (Greuell *et al.*, 1997; Greuell and Genthon, 2003). This 'ice-cap cooling effect' or 'glacier cooling effect' (cf. Braithwaite and Raper, 2002) can be experimentally tested by installing one weather station directly on an ice cap or glacier and a second weather station far enough away from the ice body to be beyond its local influence, yet close enough to experience the same overall climatic and meteorological conditions (i.e. no significant differences in elevation, exposure, shading, slope, etc.) (e.g. Bradley and Serreze, 1987b; Greuell and Oerlemans, 1989; Ohmura, 2000). Of course, just how far the local climatic effects of a small ice cap or glacier extend beyond their margin is not a-priori known when installing the paired weather stations. In addition, logistic constraints, such as accessibility and available topography, can also influence or limit site selection in the field.

5.5.1 Ice-Cap Cooling Effect: Some Background Information

The local advection of heat from bare to snow- or ice-covered ground is frequently described as an important snowmelt process on open, exposed landscapes (Neumann and Marsh, 1998; Marsh, 1999) or High Arctic glaciers (Hattersley-Smith *et al.*, 1961; Wolfe and English, 1995). On the other hand, Bradley and Serreze (1987b) documented that thermal influence of even a very small ice body can extend some distance beyond its actual margin. Conceptually, this 'ice-cap cooling' is a simple process. The surface temperature of an ice- or snow-covered surface (e.g. glacier or snow patch) cannot rise above the

melting point, which means (1) that the sensible heat flux over snow/ice is typically downward (if the overlying air is warmer than 0°C), and (2) that any 'surplus' energy will be used entirely for additional melting (rather than for surface heating). Therefore, any increases in air temperature will increase the temperature difference between ice- or snow-covered areas and the bare surroundings, causing an even larger advection of sensible heat to the ice- or snow-covered areas (Oerlemans, 1989; Marsh, 1999). However, the resulting temperature inversion can strongly limit turbulent heat transfer.

However, this process is exceedingly difficult to measure and quantify in the field (Neumann and Marsh, 1998). Modeling studies (e.g. Liston, 1995; Granger *et al.*, 2002) indicate that the effect of local heat advection decreases exponentially with distance from the snow/ice edge to quickly reach a near steady-state (Marsh, 1999). Marsh and Pomeroy (1996) and Neumann and Marsh (1998) attempted to include local advection into a surface energy balance model, but found it difficult to validate and verify their crude model parameterization (cf. van der Veen, 1999a). One of the few field studies (Wendler, 1974) attempted to measure this local heat advection on and around the McCall Glacier, Alaska, over 17 days during the summer melt season. Wendler (1974) noted:

> "The air above the rocks or moraine, which surround the glacier, is warmed in summer to a greater extent than the air above the ice. Advection of this warm air towards the glacier will cause differential ablation which is greatest near the rock-ice boundary."

In his study, this 'edge-effect' or 'local advection' (Marsh *et al.*, 1997) increased ablation by about 10 percent within 100 to 200 m of the ice margin (from ~45 to ~55 cm weq). Van de Wal *et al.* (1992) reported somewhat larger values for the Hintereisferner, Austria, in 1989 (ablation near margins ~2.64 m weq, ablation at center ~2.17 m weq). Male and Gray (1981) and Moore (1983) also concluded that local advection diminishes about 100 to 200 m from the edge of the glacier or snow field, but offered no quantitative data. Takahara and Higuichi (1985) noted a similar situation for a small snow patch (~70 m by 30 m) in Japan. Air temperatures dropped rapidly within 10 to 20 m from the edge of the snow patch, and reached more-or-less constant values after 40 to 50 m. As a result, measured snowmelt and turbulent heat fluxes were about 25 percent lower at about 50 m distance from the edge of the snow patch. Modeling studies reviewed by Neumann and Marsh (1998) suggest that the influence of local advection more-or-less diminishes about 100 to 300 m from the edge of the snow patch or glacier. One

could therefore argue that the ice margins effectively represent a 'buffer zone' of enhanced melt, thereby protecting the more interior parts of the glacier and ice cap from the influence of local heat advection. This could also be interpreted as a mechanism by which an ice cap or glacier attempts to promote its own survival (Serreze, 1985). However, this mechanism is probably not very efficient if the ice margins are continuously retreating from year-to-year, as is the case for the Hazen Plateau ice caps (Braun *et al.*, 2004a).

5.5.2 Ice-Cap Cooling Effect: Values from the Literature

Table 5.21 summarizes the ice-cap or glacier cooling effects reported either directly by other applicable studies in the scientific literature or calculated from published data therein. This is not necessarily a fully comprehensive literature review, but it is nevertheless apparent that not many studies have actually attempted to directly measure the thermal effect of a small glacier or ice cap. Nonetheless, there appears to be a measurable air temperature cooling effect of about 1 to 3°C associated with the presence of permanent ice cover (relative to the surrounding ice-free terrain). The slightly higher values for the White Glacier, Hintereisferner, Pasterze Glacier, and Haut Glacier d'Arolla may be additionally influenced by significant topographic relief and associated localized cold-air drainage and shading (Bradley and Serreze, 1987b; Strasser *et al.*, 2004). On the other hand, Orvig (1951, 1954) and Arnold (1965) concluded that the much larger Barnes and Meighen Ice Caps only exerted very little or no influence on the climate of the ice-free terrain in their immediate vicinity.

The data reported by Ohmura (2000) for the White Glacier are perhaps the most interesting in the context of this study (Fig. 5.32). The ice-cap cooling effect was non-existent in May (0°C), when there is 100 percent snow cover everywhere (cf. Bradley and Serreze, 1987b) and became the highest (1.7°C) in July, when the Arctic tundra surrounding the White Glacier is typically 100 percent snow-free. June and August are transition months with intermediate values. These monthly values can be directly compared to similar measurements on the Hazen Plateau and on the Ward Hunt Ice Rise and Ice Shelf (i.e. air temperature difference between AWS T3 and AWS G3; see below). The ice-cap cooling effect reported by Bradley and Serreze (1987b) for the St. Patrick Bay ice caps was only about 0.8 to 1°C (grey shading in Fig. 5.32), considerable less than most of the other examples listed in Table 5.21. The reasons

for this difference are not immediately obvious. The St. Patrick Bay ice caps (~2 to 4 km^2) are certainly much smaller than the other glaciers or ice caps listed in Table 5.21. In addition, Bradley and Serreze (1987b) were forced to install their tundra weather station much closer to the ice-cap (~1 to 2 km) than the other studies listed in Table 5.21, because of topographic and logistic constraints.

The ice-cap cooling values for the Ward Hunt Ice Rise were calculated from data reported by Sagar (1962) and the reconstructed monthly air temperature climatology for Ward Hunt Island (cf. Section 5.2). They compare well with the in-situ observations in 2002 by Derek Mueller (Mueller *et al.*, 2003; pers. comm.). They also compare well (Fig. 5.32) with those reported for the White Glacier (Ohmura, 2000) and measured directly on the Hazen Plateau between 1999 and 2001 (see below)

5.5.3 Ice-Cap Cooling Effect: Measurements on the Hazen Plateau

The ice-cap cooling effect associated with the existence of Murray Ice Cap on the Hazen Plateau was measured between 1999 and 2001 using a pair of (almost) identical automatic weather stations (AWS). AWS G3 was installed at about 1100 m asl on the summit of Murray Ice Cap, whereas AWS T3 was installed at about 1025 m asl on the nearby ice-free Hazen Plateau (cf. Table 5.1). The horizontal distance between the two weather stations was about 3.5 km. Site selection was a function of the available topography and accessibility.

5.5.3.1 Ice-Cap Cooling Effect: AWS G3 and AWS T3 (1999 to 2001)

Perhaps the simplest measure of the localized ice-cap cooling effect associated with the presence of Murray Ice Cap is the mean seasonal air temperature difference between AWS G3 and AWS T3, integrated over the entire summer melt season (June/July/August; 1999 and 2000 only; Table 5.22). This obviously ignores any changes in the surface conditions at both stations (i.e. snow-to-ice; snow-to-tundra), but provides average values most compatible with those summarized in Table 5.21. Air temperatures at AWS G3 were about 1°C colder and resulted in about 50 (~30%) less melting degree-day totals than at AWS T3 (Table 5.22). These values compare well with those previously reported by Bradley and Serreze (1987b) for the similar-sized St. Patrick Bay ice caps (Table 5.21). It is important to note that this 'ice-cap cooling effect' also includes an elevation difference of about 75 m between AWS

G3 and AWS T3 (i.e. the 'true' ice-cap cooling effect is presumably somewhat less than ~1°C), although other studies (e.g. Bradley and Serreze, 1987b; Greuell and Oerlemans, 1989; Ohmura, 2000) have simply ignored such small elevation differences in this context and attributed the entire temperature difference solely to the presence of ice.

It is reasonable to expect a strong annual cycle in the air temperature difference between AWS G3 and AWS T3. The difference should be minimal during the winter month (cf. Section 5.5.3), when the entire Hazen Plateau is completely snow-covered and the ice-cap cooling effect therefore not operational (Bradley and Serreze, 1987b; Oerlemans and Vugts, 1993; Ohmura, 2000; Braithwaite *et al.*, 2002). The only cause for an air temperature difference at that time should be the minor elevation difference of about 75 m between the two stations. The air temperature difference should in turn be much larger during the summer months, especially after the Hazen Plateau around AWS T3 becomes snow-free. Figure 5.33 shows the monthly air temperature difference between AWS G3 and AWS T3 (cf. Table 5.23). The mean difference for the three summer months (June/July/August) was 1.09°C, the respective difference for the winter months (September to May) was only 0.24°C. Assuming that 0.24°C is due to the difference in elevation (~75 m), the 'net' average summer ice-cap cooling effect is 0.85°C, which corresponds well to the values previously reported for the similar-sized St. Patrick Bay ice caps (Bradley and Serreze, 1987b) (Table 5.21).

5.5.3.2 Ice-Cap Cooling Effect: Temperature Climatology

Another simple approach to assess the air temperature difference between AWS G3 and AWS T3 (= ice-cap cooling effect) is to compare the two regression equations that define the temperature climatology for the Hazen Plateau (cf. Section 5.2.2.3). Figure 5.34 simply plots the mean monthly air temperature at AWS G3 and AWS T3 as a function of the Alert 1100 m asl sounding air temperature, using the two equations specified previously in Section 5.2.2.3. The AWS T3 equation plots, as expected, above the AWS G3 equation, which implies that AWS T3 is consistently warmer than AWS G3. The temperature difference increases slightly with increasing air temperature, since the slopes of the two equations are not 100 percent identical. Mean monthly air temperatures for the three summer months (June, July, August) from 1999 to 2001 measured at AWS G3 and AWS T3 ranged from about –4 to 4°C

(Table 5.23), corresponding to an air temperature difference or ice-cap cooling effect between about 0.9 and 1.1°C (Figure 5.34).

5.5.3.3 Ice-Cap Cooling Effect: Different Surface Conditions

Arguably, stratifying air temperature differences between permanently ice-covered and seasonally snow-covered sites based solely as a function of time (e.g. annual, seasonal, or monthly) is convenient, but perhaps not the most appropriate approach (cf. Martinec and Rango, 1986). It may be more appropriate to assess the changing 'ice-cap cooling effect' through time as a function of the changing surface conditions on the Hazen Plateau. In theory, it should be possible to distinguish between at least three different air temperature differences, depending on the (changing) surface conditions at AWS G3 and AWS T3 (and even that may be somewhat of a simplification of reality). This may seem like an obvious approach to take, however, there is no scientific literature available on this subject. Most studies (Table 5.21) have simply reported mean differences over a given time period (usually determined somewhat arbitrarily by the length of the field season). In fact, only Ohmura (2000) has directly reported specific monthly values, but even calendar month resolution can only partially account for surface type and surface conditions changes over time (Martinec and Rango, 1986). Bradley and Serreze (1987b) were able to show that the ice-cap cooling effect becomes negligible in years with extensive and persistent snow cover on the Hazen Plateau. The same is true, presumably, on an intra-annual time scale at times of 100 percent snow cover on the ice caps and surrounding ice-free terrain, for example before the onset of snowmelt (e.g. White Glacier, May 1969-1972 or Ward Hunt Ice Rise, June 1960, cf. Table 5.21) or for some time after large summer snowfall events (cf. Oerlemans and Klok, 2004).Unfortunately, the air temperature climatology for the Hazen Plateau and North Coast is defined by mean monthly values; thus it is not possible to account for changing surface conditions during and after the snowmelt season (cf. Section 5.4.4.3).

5.5.4 Synopsis: Ice-Cap Cooling Effect

The above considerations are consistent with the conclusions reached by Bradley and Serreze (1987b) that even small ice caps and glaciers are able to modify their own surrounding climate simply by

'consuming' some of the available energy through melting or other mass loss processes. However, precisely how far this 'ice cap cooling effect' extends beyond the ice margins is still not well-understood and presumably depends on its overall magnitude and the size of the ice mass. For example, Orvig (1951, 1954) and Arnold (1965) concluded that the Barnes and Meighen Ice Caps only exert very little (thermal) influence on the climate of the ice-free terrain in their immediate vicinity. This may explain why some researchers (e.g. Oerlemans and Hoogendoorn, 1989; Oerlemans and Fortuin, 1992; Johannesson *et al.*, 1995) choose not account for the 'ice cap cooling effect' in their glacier mass balance modeling (Greull and Böhm, 1998; Braithwaite *et al.*, 2002).

An appropriate value for the mean melt season 'ice cap cooling effect' on the Hazen Plateau and North Coast of Ellesmere Island is about 1.0±0.15°C (using the values listed in Table 5.21 and the values determined from the AWS G3 and AWS T3 measurements, but excluding the non-Arctic examples and the anomalously high 1962 value for the White Glacier). It is also possible to determine appropriate monthly mean values for the 'ice cap cooling effect' on the Hazen Plateau and North Coast of Ellesmere Island, by combining the AWS G3 and AWS T3 measurements with the White Glacier and Ward Hunt Ice Rise values shown in Table 5.21: 0°C (May), 0.74±0.42°C (June), 1.36±0.23°C (July), 0.78±0.44°C (August), and 0°C (September). These values can be used, together with appropriate air temperature lapse rates (Section 5.4), to spatially-distribute the point measurements at AWS G3 and AWS T3, or their monthly climatologies (Section 5.2), across the Hazen Plateau and North Coast (cf. Section 5.7).

Braithwaite *et al.* (2002), finally, presented and used two simple empirical equations, based on Braithwaite's own doctoral research on the Sverdrup Glacier (Devon Island) and White Glacier (Axel Heiberg Island) (Braithwaite, 1977), to parameterize the 'ice cap cooling effect' in a simple temperature-index melt model:

Equation 5.7 $T_{ice} = -0.7 + 0.85 * T_{tundra}$ $(T_{tundra} > -5°C)$

Equation 5.8 $T_{ice} = T_{tundra}$ $(T_{tundra} <= -5°C)$

Applying these two equations to the AWS T3 (i.e. tundra) air temperatures almost perfectly reproduces the temperatures measured at AWS G3 (i.e. ice) (cf. Chapter 6).

5.6 Melting Degree-Day Model

Section 5.2 presented two simple equations, which can be used as transfer functions to convert the upper-air sounding temperatures at 1100 m asl above Alert into mean monthly air temperatures at AWS G3 and AWS T3 on the Hazen Plateau. In addition, an equation was presented to construct a monthly climatology for Ward Hunt Island based on surface air temperature measurements at Alert (Braun *et al.*, 2004b). Sections 5.4 and 5.5 presented two simple approaches to spatially-distribute mean monthly air temperatures across the Hazen Plateau as functions of elevation and surface conditions. The next step is to develop a robust methodology to calculate annual melting degree-day totals from monthly mean air temperatures, which are needed in Chapter 6 as climate input for the temperature-index melt model. Obviously, monthly, seasonal, or annual melting degree-day totals are best calculated as the positive sum of a high-quality daily air temperature time series (Arnold and MacKay, 1964; Bradley and England, 1978; Braithwaite, 1984; 1996). In the absence of such data, two different approaches are commonly used today in the scientific literature to 'model' ablation or melting degree-day totals based on either mean monthly or mean annual air temperatures:

1. Regression-type degree-day models, which rely on the strong statistical association between mean summer (June, July, and August) air temperature and annual/summer melting degree-day totals (e.g. Ahlmann, 1924; Krenke, 1975; Wild *et al.*, 2003) (cf. Section 5.6.1).
2. Probabilistic degree-day models (e.g. Braithwaite, 1984; Reeh, 1991), which determine annual melting degree-day totals based on a monthly or annual air temperature climatology and an assumed probability function (cf. Section 5.6.2).

5.6.1 Regression Degree-Day Models

The basic idea behind regression-type degree-day models is to determine the most appropriate 'surrogate' air temperature metric to use as a proxy for total annual melting degree-days, using a simple regression equation (cf. Ahlmann, 1924; Krenke, 1975; Wild *et al.*, 2003). Such an approach is obviously entirely empirical and is therefore strictly speaking not applicable for climatic conditions drastically

different from those of the last 50 years (cf. Ridley *et al.*, 2005). In addition, it is somewhat questionable if it is appropriate to apply a regression equation, defined using the long-term climate data collected at Alert and Eureka, anywhere else in the Canadian High Arctic (e.g. Hazen Plateau or North Coast).

5.6.1.1 Comparison: Melting Degree-Day Totals and Mean Summer Air Temperature

A simple relationship between annual melting degree-day totals and mean summer temperature would be very appealing, since many paleoclimate proxy records (e.g. ice core percent melt, ice core isotopic composition, and lake sediment lamination thickness) are usually interpreted to represent mean summer air temperature variability (e.g. Fisher and Koerner, 1994; Bradley *et al.*, 1996; Smith *et al.*, 2004). Furthermore, future climate change scenarios are often formulated in terms of an increase of summer air temperature over some defined time interval (e.g. Oerlemans *et al.*, 1998). Table 5.24 lists the available surface air temperature data for Eureka and Alert: annual melting degree-day totals, summer (June, July, and August) melting degree-day totals, and mean summer (June, July, and August) air temperature from 1951 to 2003 (n = 53 years). The 1991 data for Eureka cannot be used, since the last nine days of July 1991 are entirely missing from the record. This data gap has only a minor effect on the mean summer temperature for 1991, but a much larger influence on the corresponding seasonal or annual melting degree-day totals. Therefore, the 'combined' record for Alert and Eureka includes only 105 years of data.

Figure 5.35 shows the associated two scatter plots, which reveal, as expected, a very strong statistical association between mean summer temperature and corresponding melting degree-day totals (cf. Braithwaite, 1984). The black lines in each scatter plot depict the simple linear regression lines for the combined Eureka/Alert data set (n = 105 years). Such a combination is reasonable, since a 'cold' summer at Eureka is equivalent to a 'warm' summer at Alert in this context (cf. Martinec and Rango, 1986) and simply defines the relationship between mean summer temperatures and resultant melting degree-days over a wider range of values. The scatter appears to be greater for lower temperatures (~0 to 2°C) and is considerably reduced for air temperatures above about 2°C. This was entirely expected, given the way melting degree-days are calculated from mean daily air temperatures (Braithwaite, 1984). The relationship for higher temperatures (above ~2°C) appears to be (almost) linear, which was also expected

given the way melting degree-days are calculated from mean daily air temperatures (cf. Braithwaite, 1984). However, the relationship between seasonal or monthly mean air temperatures and corresponding melting degree-day totals for temperatures below and around freezing is, in reality, not linear (Braithwaite, 1984), but instead trends asymptotically towards zero. A simple linear regression equation is therefore not capable to adequately describe the relationship across the full range of expected values (cf. Andrews *et al.*, 1970). The two different probability models developed by Braithwaite (1984) and Reeh (1991) are essentially attempts to better address this particular issue (see below).

5.6.2 Probabilistic Melting Degree-Day Models

It is obviously best to determine annual, seasonal, or monthly melting degree-day totals as the positive sum of a high-quality daily air temperature time series (Braithwaite, 1984; 1996), assuming that such data are available. Such a time summation is mathematically trivial today, although the use of mean daily air temperatures may not always provide the best estimate of an ablation season melting degree-day total (Arnold and MacKay, 1964; Bradley and England, 1978). In the absence of a daily air temperature time series, it is also possible (and common practice) to estimate seasonal or annual melting degree-day totals from an monthly (Braithwaite, 1984) or annual (Reeh, 1991) climatology and an assumed probability distribution.

The original probability model introduced by Braithwaite (1984) estimates monthly melting degree-day totals indirectly from mean monthly air temperatures by assuming that mean daily air temperatures (during any given month) are distributed randomly around their respective monthly mean temperature, with a Gaussian distribution describing the associated probability function (van der Veen, 1999b). Reeh (1991) proposed essentially a modification or simplification of the original Braithwaite (1984) model, aimed at estimating annual melting degree-day totals based on mean annual air temperature, mean July air temperature, and a cosine function combined with an assumed probability function (cf. Lundquist, 1982).

Both models are well-established today and highly-regarded in the scientific literature (e.g. Laumann and Reeh, 1993; Johannesson *et al.*, 1995; van der Veen, 1999b; Raper *et al.*, 2000; Marshall *et al.*, 2004; Podlech *et al.*, 2004). The Reeh (1991) model represents an elegant, albeit mathematically-

complex, solution (van der Veen, 1999b; Calov and Greve, 2005) to calculate annual totals with very little climate input data requirements. The Braithwaite (1984) model has the advantage of providing monthly resolution for the modeled melting degree-days, provided that a robust monthly air temperature climatology is available as input data (cf. Section 5.2).

5.6.2.1 Braithwaite (1984) Melting Degree-Day Model

The only model parameter used in the Braithwaite (1984) model is typically referred to as the 'monthly standard deviation of air temperature' (σ), which essentially describes the 'width' of the assumed Gaussian probability distribution around the corresponding monthly mean air temperature (or around the assumed and parameterized annual air temperature cycle in the case of the Reeh (1991) model). In essence, this parameter allows for days with melting to occur, even when the mean monthly air temperature is below freezing. Conversely, it also allows for days without melting, even if the mean monthly air temperature is positive. Such short-term air temperature variations can occur superimposed on the long-term (i.e. annual) temperature cycle because of:

1. The deterministic daily air temperature cycle (Arnold and MacKay, 1964).
2. Stochastic (i.e. random) weather fluctuations, with a typical periodicity of perhaps five to seven days (Lefebre *et al.*, 2002).

Both of these types of short-term temperature variations that can lead to positive/negative air temperatures even if the mean monthly air temperature (defined by the climatology or assumed annual temperature cycle) is negative/positive (Lefebre *et al.*, 2002). Braithwaite (1984) combined both types of short-term variability and assumed that the daily air temperature deviations from their respective monthly means are normally-distributed with a characteristic standard deviation σ (cf. Johannesson *et al.*, 1995). He bluntly admitted that his assumption is strictly speaking incorrect, since air temperature changes over many days also exhibit a distinct seasonal or annual trend. Braithwaite (1984) argued, however, that the violations of the mathematical assumptions underlying his model lead to only to negligible errors in the calculation of seasonal or annual melting degree-day totals (cf. Bøggild *et al.*, 1994).

Braithwaite (1984) tested his model with high-quality daily air temperature data from the Swiss Alps and West Greenland. Using a value for σ of 4°C, he was able to show that his model caused only a (negligible) error of one to two percent (cf. Wild *et al.*, 2003) in the modeled annual melting degree-day totals (as compared to the measured annual melting degree-day totals). Monthly melting degree-day totals, using the Braithwaite (1984) model, are thus defined as:

Equation 5.9 $$MDD = N \sum_{i=0}^{i=1} f(T_m)\, T_m$$

where N is the number of days for each month, T_m the monthly mean air temperature, and f (T_m) the assumed probability function (Gaussian normal distribution) used for generating a distribution of daily air temperatures around their respective mean monthly temperature with a standard deviation of σ. In practice, an implementation of the Braithwaite (1984) model requires the following four steps:

1. A monthly temperature climatology (i.e. time series of mean monthly air temperature) as input data.
2. An appropriate value for σ for each individual month, or an appropriate constant value applicable for all month of interest (see below).
3. A 'look-up' table (Table 5.25) to determine the amount of melting degree-days per day as a function of mean monthly air temperature and associated σ value (see below).
4. Multiplication by 28, 30, or 31 as needed for the individual month of interest.

It is intuitively obvious that a successful implementation of the Braithwaite (1984) model is somewhat dependant (cf. Ridley *et al.*, 2005) on the choice of an appropriate value for σ, which unfortunately is not constant for all month of the year (Lefebre *et al.*, 2002). For example, July typically shows the lowest air temperature fluctuations over glaciers due to the modulating effect of the melting snow and ice surface (Lefebre *et al.*, 2002). It would therefore make sense to evaluate σ by assessing

short-term air temperature variability for each month of the 'extended' melt season (May to September) separately (Johannesson *et al.*, 1995). Nevertheless, Braithwaite and Zhang (1999, 2000) used a constant value for σ of 4°C to successfully model the mass balance of five glaciers in the Swiss Alps and 37 glaciers around the world. Johannesson *et al.* (1993) and van de Wal (1996) also showed that annual melting degree-day totals, as determined by either the Braithwaite (1984) or Reeh (1991) model, are in fact not very sensitive to the exact value used for σ (cf. Zweck and Huybrechts, 2005). On the other hand, Ridley *et al.* (2005) noted that such a melting degree-day parameterization is (obviously) highly sensitive to its internal parameters (e.g. σ, DDF (snow), and DDF (ice) (cf. Chapter 6). It is therefore somewhat surprising that a comprehensive review of the available scientific literature (Table 5.26) revealed that the vast majority of studies have simply assumed a constant value for σ for all months of interest.

Table 5.27 lists monthly mean values for σ, calculated from the daily surface air temperature data from Alert and Eureka (1951 to 2003 means). As expected, σ is higher (~3 to 5°C) for the 'transition months' of May, June, August, and September, and lowest for the main summer melt month of July (2 to 3°C) (cf. Lefebre *et al.*, 2002). The 1999 to 2001 values for Alert and Eureka (Table 5.28) are overall consistent with their long-term averages (Table 5.27), but there is, as expected, considerable inter-annual variability. This is also highlighted by comparing the σ values for June 1999 (~2.5°C) and 2000 (~6.4°C) measured at AWS G3 and AWS T3 on the Hazen Plateau (Table 5.28). The values for Ward Hunt Island are overall lower than those for Eureka/Alert and the Hazen Plateau, presumably due to the moderating influence of the nearby Arctic Ocean. Nevertheless, the simple means for σ shown in Tables 5.26 and 5.27 (~3.6 to 3.9°C) are consistent with those previously used in the scientific literature (Table 5.26) and the original (and frequently used) value of σ = 4°C determined by Braithwaite (1984).

5.6.2.2 Testing the Braithwaite (1984) Melting Degree-Day Model

It is prudent to test the performance of the Braithwaite (1984) model under specific 'High Arctic' climatic conditions, even though it is by all accounts (cf. Table 5.26) an excellent and robust approach to estimate monthly melting degree-day totals (e.g. van der Veen, 1999b; Raper *et al.*, 2000; Marshall *et al.*, 2004; Podlech *et al.*, 2004) for many parts of the world. Such a test should be able to adequately address the following two questions:

1. How well does the Braithwaite (1984) model perform using the available in-situ data (short-term) from the Hazen Plateau and North Coast?
2. How well does the Braithwaite (1984) model perform using the available long-term (1951 to 2003) climate record from Alert and Eureka?

The main question to answer is whether or not it is appropriate to use a simple constant value for σ for all month (which is the common strategy; cf. Braithwaite, 1984) or if it is more appropriate and beneficial to use a specific value for σ for each month of interest (i.e. May to September) in the context of this study.

5.6.2.2.1 Test 1: AWS G3 and AWS T3 (1999 to 2001)

Table 5.29 summarizes the results of Test 1, using the measured data from AWS G3 and T3 (1999 to 2001). As expected, the Braithwaite (1984) model was able to accurately predict monthly and annual melting degree-day totals recorded at both weather stations. Differences between measured and modeled annual melting degree-day totals were between 0.1 and 3 percent, consistent with the expected errors (1 to 2 percent) as reported by Braithwaite (1984).

The largest discrepancies occurred for June 2000, which had an unusually high σ value of about 6.5°C. June 2000 was very cold for the first half of the month, and then very warm for the last two weeks. As a result, the mean monthly air temperature was quite low, the monthly melting-degree day totals were unusually high, and the distribution of daily air temperature bi-modal, rather than normal. Nevertheless, the Braithwaite (1984) model, using the associated high σ value, was able to account for this unusual type of air temperature variability and predicted reasonable monthly melting degree-day totals for June 2000 at AWS G3 and AWS T3.

5.6.2.2.2 Test 2: Ward Hunt Island AWS (1996 and 2001)

Table 5.30 summarizes the results of Test 2, using the measured data from the Ward Hunt Island (WHI) AWS for 1996 and 2001 (which are the only two years available with a complete air temperature record from May to September). Here, the differences between the measured and modeled annual melting

degree-day totals, especially for 1996, were considerably greater than those for AWS G3 and AWS T3 (cf. Test 1) or those previously reported by Braithwaite (1984). To some extent, these larger discrepancies for smaller absolute values of annual melting degree-day totals are to be expected, as slight differences for individual months have a greater impact on the respective annual totals. Braithwaite (1984) also noted that the presence of low-level air temperature inversions may favor oblique or skewed frequency distributions of the daily mean air temperatures, thus creating more 'difficult' circumstances for his model and reducing its predictive capabilities.

5.6.2.2.3 Test 3: 'Optimization' of σ for AWS G3, AWS T3, and WHI AWS

The basic goal of Test 3 was to determine an 'optimum' value for σ, that, when used for all month of interest (May to September) provided the best overall prediction of the annual melting degree-day totals (cf. Johannesson *et al.*, 1995). First, monthly melting degree-day totals were calculated for AWS G3, AWS T3, and WHI AWS, using actually measured mean monthly temperatures and a range of σ values between 2 and 6. These monthly values were then combined to yield modeled annual melting degree-day totals and compared with the actually measured annual melting degree-day totals. The 'skill' of the Braithwaite (1984) was then evaluated by comparing the respective absolute monthly and annual differences (measurements vs. model predictions) for each prescribed σ value.

The so-determined optimum σ value for WHI AWS was 2.2°C and resulted in a mean absolute monthly difference (model minus measurements) of 5.0 MDD. However, the optimization results were not, as expected, very sensitive for σ values between about 1.6 and 2.2°C (Braithwaite, 1984; Johannesson *et al.*, 1993; van de Wal, 1996; Zweck and Huybrechts, 2005). The optimum σ value for AWS G3 (AWS T3) was 3.7°C (4.0°C), with a mean absolute monthly difference (model minus measurements) of 7.6 MDD (9.2 MDD). Again, the optimization results were not, as expected, very sensitive for σ values between about 3 and 4.5°C (Braithwaite, 1984; Johannesson *et al.*, 1993; van de Wal, 1996; Zweck and Huybrechts, 2005).

The lower optimum σ value for the WHI AWS data was expected, since surface air temperatures are presumably less variable along the North Coast due to the moderating influence of the adjacent Arctic Ocean. A similar argument can explain the slightly lower optimum σ value for AWS G3, as opposed to

AWS T3. Figure 5.36 shows the measured melting degree-days per day, plotted as a function of their corresponding mean monthly temperatures (circles). The three lines represent the respective Braithwaite (1984) model predictions, using the three optimum σ values discussed above.

5.6.2.2.4 Test 4: Long-term Means at Alert and Eureka (1951 to 2003)

Table 5.31 summarizes the results of Test 4, in which the Braithwaite (1984) model was used to predict the 1951 to 2003 mean annual melting degree-day totals at Alert and Eureka. The differences (modeled minus measured) of the monthly and annual totals were remarkably small and consistent with the expected errors as reported by Braithwaite (1984). This test used both a specific mean measured σ value for each month of interest (May to September), as well as an constant σ value for all month (cf. Table 5.27).

5.6.2.2.5 Test 5: Monthly Totals at Alert and Eureka (1951 to 2003): Specific σ Values

Table 5.32 summarizes the results of Test 5, in which the Braithwaite (1984) model was used to calculate monthly melting degree-day totals at Alert and Eureka using specific σ values (Table 5.27, 4^{th} column) for each month of interest (May to September) from 1951 to 2003. These monthly totals were then summed to yield annual totals for each year, and compared to the actually measured annual melting degree-day totals, as determined by a summation of positive daily temperatures.

The mean monthly absolute difference (measured minus modeled) for both Alert and Eureka was 13.2 MDD (Table 5.32). The relative difference (in percent) is obviously larger for Alert (i.e. colder conditions = lower annual melting degree-day totals). In addition, it is 'more difficult' for the Braithwaite (1984) model to perform as expected during colder months, since it is more likely that daily air temperatures fluctuate around freezing (Braithwaite, 1984). Figure 5.37 shows a scatter plot of modeled annual melting degree-day totals plotted as a function of the corresponding measured totals. It is clear that the model was able to accurately predict the annual melting degree-day totals, without any apparent systematic bias as a function of the absolute values (note: the slope of relationship is 1.0096).

5.6.2.2.6 Test 6: Monthly Totals at Alert and Eureka (1951 to 2003): Constant σ Value

Test 6 was essentially identical to Test 5, except a constant value for σ (3.7°C) was used to calculate the monthly melting degree-day totals at Alert and Eureka. The mean absolute difference between measured and modeled annual melting degree-day totals at Alert was 22.2 MDD (or 13.3 percent). At Eureka, the mean absolute difference between measured and modeled annual melting degree-day totals was 16.7 MDD (or 5.0 percent). These results and respective differences are again consistent with the well-established model capabilities and limitations (Braithwaite, 1984). Figure 5.38 shows a scatter plot of modeled annual melting degree-day totals plotted as a function of the corresponding measured totals, which shows that the Braithwaite (1984) model tends to slightly overestimate annual melting degree-day totals, in this case, especially for smaller absolute values.

5.6.3 Synopsis: Melting Degree-Day Models

The probabilistic melting degree-day model introduced by Braithwaite (1984) is well-established today in the field of glaciology (Paterson, 1994; van der Veen, 1999b), both for short-term, process-based glacier mass balance investigations (e.g. Raper *et al.*, 2000; Podlech *et al.*, 2004) and large-scale modeling investigations (e.g. Hostetler and Clark, 2000; Marshall *et al.*, 2004). However, based on the above considerations, the model uncertainties as originally reported by Braithwaite (1984) of only one to two percent appear to be somewhat too optimistic, at least in the context of this study. Two additional conclusions have also emerged from the above considerations:

1. Model performance was better when using specific σ values for each month of interest.
2. Model performance was better on the continental Hazen Plateau than on the maritime North Coast.

Both conclusions are consistent with the model expectations and limitations as discussed by Braithwaite (1984). Unfortunately, the limited data availability for the Hazen Plateau (1999 to 2001) and North Coast (1996 and 2001) makes it impossible to determine appropriate σ values for each month of

interest directly from the in-situ collected weather station data. It seems therefore most appropriate (cf. Johannesson *et al.*, 1995) to use the optimized σ values determined during Test 3 (3.7°C for AWS G3, 4.0°C for AWS T3, and 2.2°C for WHI AWS) for the annual melting degree-day calculation . The other option would be to use the long-term mean σ values for Eureka (Alert) for the Hazen Plateau (North Coast) (Table 5.27). Fortunately, annual melting degree-day totals, as determined by either the Braithwaite (1984) or Reeh (1991) model, are not very sensitive to the exact value used for σ (Braithwaite, 1984; Johannesson *et al.*, 1993; van de Wal, 1996; Zweck and Huybrechts, 2005), although the recent studies by Lefebre *et al.* (2002) and Ridley *et al.* (2005) challenge that notion. It is also worth noting that this issue (melting degree-day model performance and associated uncertainty) has no direct effect on the mass balance sensitivity tests conducted in Chapter 6, but reinforces the concerns expressed by Oerlemans (2001) regarding the ability of glacier mass balance models in general to quantitatively assess the absolute mass balance of a given glacier through time (cf. Chapter 6).

5.7 A Climatology for Northern Ellesmere island: Spatial and Temporal Variability

The previous sections of this chapter have developed all the necessary 'pieces-of-the-puzzle', which together enable the formulation of a basic air temperature and precipitation climatology for the Hazen Plateau and North Coast of Ellesmere Island. This climatology will provide some of the necessary climate input for the temperature-index melt modeling experiments conducted in the Chapter 6. The objective of this section is to provide a basic discussion of the climatology of northern Ellesmere Island (cf. Section 5.1), specifically regarding the temperature contrasts between high-elevation, interior locations (i.e. the Hazen Plateau) and low-elevation, coastal locations (i.e. the North Coast).

5.7.1 Temperature Climatology

The air temperature climatology for the Hazen Plateau and North Coast of Ellesmere Island consists of the following three successive steps or procedures:

1. Transfer Functions (Section 5.2 – to convert the monthly air temperature data from Alert (surface or upper air) to the Hazen Plateau and North Coast).

2. Spatial Distribution (based on elevation and surface conditions (Sections 5.4 and 5.5)), using a digital elevation model (Hazen Plateau only).
3. Melting Degree-Day Model (Section 5.6 – to calculate annual melting degree-day totals from the monthly air temperature climatology).

5.7.1.1 Transfer Functions and Data Availability

Section 5.2 provided a comprehensive assessment of the short-term, in-situ temperature data collected on the Hazen Plateau and North Coast in the context of the available long-term records from Alert and Eureka (Fig. 5.1). This resulted in the formulation of the following three equations or transfer functions:

- AWS T3* = 1.6624 + (1.1893 * Alert_1100m_monthlymeantemperature) (Equation 5.4)
- AWS G3* = 0.6434 + (1.1589 * Alert_1100m_monthlymeantemperature) (Equation 5.5)
- WHI AWS* = –1.3235 + (0.7494*Alert_surf) + (–0.0207) * $(Alert\_surf)^2$ + (–0.0004) * $(Alert\_surf)^3$ (Equation 5.6)

The upper-air sounding data used in this study is a sub-set of the CARDS data set (available from the National Climatic Data Center), and spans the time interval from 1 January 1951 to 31 July 2001. It is unfortunate, but unavoidable, that the CARDS data set does not include (at least) August 2001. It is also necessary to recognize that whole months, or entire multi-day sections of months, are occasionally missing from the CARDS data set for Alert.

- Total months available (in 'Theory'): n = 607 (January 1951 to July 2001)
- Total months available (in 'Reality'): n = 590 (i.e. 17 monthly means missing due to missing daily sounding data)

For this study, missing monthly air temperature data are only problematic for the melt modeling experiments on the Hazen Plateau in Chapter 6 if they occur during the important summer months (n = 3 or n = 4, if including August 2001). Missing data are much less an issue for the climatology of the North Coast, which is based on the (less-patchy) surface air temperature record from Alert.

5.7.1.2 Time Series of Summer Temperatures

Figure 5.39 presents the reconstructed three time series of mean summer (A) and mean July (B) air temperature for the Hazen Plateau and North Coast of northern Ellesmere Island. Mean summer air temperatures are commonly used as generalized (e.g. Paterson, 1994) and sometimes even quantitative (e.g. Ahlmann, 1924; Krenke, 1975; Wild *et al.*, 2003) proxies for glacier mass balance. July air temperatures are another popular climatic parameter in the context of glaciation and glacier mass balance, since (a) July is the warmest month of the year in the Canadian High Arctic, and (b) the position of the July 0°C isotherm or elevation of the July atmospheric freezing level are frequently used as generalized indices for glaciation potential and glacier ELA (e.g. Flint, 1971; Bradley, 1973, 1975; Vaughn and Doake, 1996; Hostetler and Clark, 2000; Porter, 2001).

The temporal variability of the six presented time series (Fig. 5.39) is characterized by relatively warm summer conditions during the mid-1950s to early-1960s, colder conditions until the mid-1970s, and overall increases in summer temperature since the mid-1980s to early-1990s (cf. Braun *et al.*, 2004a, b). Superimposed on this general temporal pattern is obviously a high-degree of interannual variability. These long-term 'trends' (or lack thereof) of the data (Table 5.33) are obviously strongly influenced by the comparatively warm conditions during the mid-1950s to early-1960s (cf. Hattersley-Smith *et al.*, 1955). Choosing a different (i.e. shorter) reference period, for example starting only in the mid-1970s or mid-1980s, obviously results in highly statistically-significant warming trends (e.g. Vincent *et al.*, 2001; Comiso, 2003; Mueller *et al.*, 2003).

In the context of the last 100 years (i.e. 1900 to 2000), even the comparatively warm mid-1950s to early-1960s pale in comparison with the much warmer 1920s, 1930s, and 1940s (Davies and Krinsley, 1962; Hattersley-Smith, 1963; Holdsworth, 1984; Bengtsson *et al.*, 2004; Johannesson *et al.*, 2004). In fact, the apparent warming trend that began in the mid-1970s appears to have just now reached the peak

values of the 1940s (Davies and Krinsley, 1962; Warren, 1990; Bengtsson *et al.*, 2004), at least when considering the 'entire' Arctic domain (i.e. 60 to 90°N). By the end of the 21st century (cf. Chapter 6), surface air temperatures over the Arctic as a whole (again, 60 to 90°N) are projected to increase by about 3.5°C relative to the 1981 to 2000 reference period (Kattsov and Källen, 2005), with the strongest warming in the fall and winter. By contrast, summer temperature increases over the Arctic Ocean are projected to remain less than 1°C throughout much of the 21st century (Kattsov and Källen, 2005) (i.e. 'cold ocean-warm land' pattern, cf. Wallace *et al.*, 1996; Serreze *et al.*, 2000).

5.7.1.3 The Ice-Cap Cooling Effect

It is interesting at this point to compare the long-term reconstructed monthly mean air temperatures (from 1951 to 2000) at AWS G3 and AWS T3 in the context of the 'ice-cap cooling effect' associated with the presence of Murray Ice Cap, as determined previously in Section 5.5 for the 1999 to 2001 short-term, in-situ weather station measurements.

The mean air temperature difference between AWS G3* and AWS T3* for the important summer melting months (June, July, and August) was 0.97°C (Table 5.34), whereas the mean air temperature difference for the main (dark) winter months (December, January, and February) was only 0.26°C. Assuming once again (cf. Section 5.5.2.1) that this temperature difference can be (to a large degree at least) explained by the elevation difference of 75 m between the two weather stations, the 'average' net summer ice-cap cooling effect associated with the presence of Murray Ice Cap is 0.97°C minus 0.26°C = 0.71°C (Fig. 5.40). These long-term values compare well with those actually measured between 1999 and 2001 on the Hazen Plateau (cf. Fig. 5.32, 5.33). It should be mentioned, however, that other authors (e.g. Bradley and Serreze, 1987b; Greuell and Oerlemans, 1989; Ohmura, 2000) have simply ignored such small elevation differences in similar studies, and attributed the full air temperature difference (i.e. 0.97°C) entirely to the influence of the ice-cap cooling effect.

5.7.1.4 The Arctic Ocean Effect

It is also interesting to compare the climatology of the high-elevation, continental Hazen Plateau with the climatology of the low-elevation, maritime North Coast to assess the influence of the 'Arctic

Ocean Effect' (cf. Braun *et al.*, 2004b) (Table 5.34). Given a 'normal' air temperature lapse rates (i.e. 5.5°C/1000 m, cf. Section 5.4), one would expect the unglaciated Hazen Plateau (= AWS T3* at 1025 m asl) to be about 5.6°C colder than the North Coast, on average, during the summer months.

Figure 5.41 shows that the reconstructed air temperature difference (and its annual cycle) between the Hazen Plateau and North Coast cannot be explained by assuming a 'normal' temperature lapse rate. The North Coast of Ellesmere Island is much colder than the Hazen Plateau during the fall, winter, and spring – presumably due to the influence of frequent and persistent surface-based air temperature inversions. During the summer months, the North Coast is still slightly on average colder than the Hazen Plateau, especially in July (Table 5.34), when the air temperatures along the North Coast (at ~0 m asl) are essentially the same as on the summit of Murray Ice Cap at 1100 m asl. This presumably reflects the influence of the 'Arctic Ocean Effect', suppressing surface air temperatures along the North Coast during the summer due to frequent fog and low stratus cloud conditions (Braun *et al.*, 2004b). Tjernström *et al.* (2004) also noted the presence and persistence of strong air temperature inversions during the summer season over the central Arctic Ocean, with the highest tropospheric air temperatures occurring well-above the surface, typically at around 1000 m asl (cf. Hardy *et al.*, 1996).

5.7.1.5 Atmospheric Freezing Levels on the Hazen Plateau

Finally, it is also interesting to evaluate changes in the atmospheric freezing level over the last 50 years (Fig. 5.42), since freezing levels, especially in July, frequently constitute a critical climatic control for glaciation and glacier mass balance in the Canadian High Arctic and elsewhere around the world (e.g. Flint, 1971; Bradley, 1973, 1975; Miller *et al.*, 1975; Vaughn and Doake, 1996; Dahl *et al.*, 1997; Hostetler and Clark, 2000; Porter, 2001). The elevation of the atmospheric freezing level has obviously a direct effect on the amount of melt, but it is also indirectly related to melt and accumulation via its influence on the partitioning of precipitation into rain or snow (cf. Miller *et al.*, 1975).

July freezing levels (red) shown in Figure 5.42 were be calculated using the AWS T3* climatology, which represent an index for the glaciation potential of the currently un-glaciated Hazen Plateau. Calculating freezing levels based on the AWS G3* climatology (blue), on the other hand, provides an index for the mass balance or ELA of a large (hypothetical) 'Hazen Plateau Ice Sheet'. It is

clear that both long-term means for the July freezing level (1423 and 1236 m asl respectively) are considerably above the elevation range of the modern Hazen Plateau and its ice caps, which implies (1) that the Hazen Plateau is about 300 m too low in elevation for glaciation today, (2) that the ELA is located today, on average, well-above (>100 m) the summits of the Hazen Plateau ice caps, and (3) that the mass balance of the Hazen Plateau ice caps is therefore, on average, highly negative today (cf. Braun *et al.*, 2004a). It is interesting to note that the ELA of the Gilman Glacier (cf. Chapter 2) and other glaciers on northern Ellesmere Island in the late-1950s and early 1960s was located at about 1200 m asl (Hattersley-Smith, 1960c; 1969). On the other hand, Miller *et al.* (1975) noted that the mean July freezing level in the Canadian High Arctic is located, on average, a few hundred meters above the ELA of a glacier (cf. Bradley, 1975). This would imply that the ELA of a (hypothetical) 'Hazen Plateau Ice Sheet' could be as low as about 900 m asl (cf. Chapter 6).

Nevertheless, positive mass balance years and snow cover expansion may have occurred on the Hazen Plateau and its ice caps, especially during the mid-1960s to mid-1970s (Braun *et al.*, 2004a, and references therein). It is also worth noting that the relatively warm conditions of the last several years, which have been the focus of much recent scientific and public interest (e.g. Brown and Alt, 2001; Serreze *et al.*, 2000; Mueller *et al.* 2003; Serreze *et al.*, 2003; Hinzman *et al.*, 2005; Overpeck *et al.*, 2005), are still not as 'extreme' as the warm phase of the mid-1950s and early 1960s documented by instrumental measurements. There is additional evidence from snow-pit and firn-core studies (Hattersley-Smith, 1963; Holdsworth, 1984) for even higher summer temperatures (cf. Davies and Krinsley, 1962; Warren, 1990; Bengtsson *et al.*, 2004; Johannessen *et al.*, 2004) and considerably increased melting in the period from about 1925 to 1961, suggesting overall more negative glacier mass balances in the Canadian High Arctic during the first part of the 20th century, compared to the last 40 years of direct glaciologic measurements (Koerner, 1996). This once again emphasizes that the climatic significance of so-called statistically-significant 'trends' or 'extremes' depends considerably on the associated temporal reference frame.

5.7.1.6 North Coast Climate: Ice-free vs. ice-covered areas

The reconstructed climatology for the North Coast of Ellesmere Island (WHI AWS*) is only useable for ice-free areas in the vicinity of Ward Hunt Island (Braun *et al.*, 2004b). More interesting, at least in the context of this study, would be a climatology for the nearby ice-covered areas, such as the Ward Hunt Ice Rise and Ward Hunt Ice Shelf. Temperatures there are, presumably, somewhat lower than on the adjacent ice-free island due to the presence of the 'ice-cap cooling effect' (cf. Section 5.5). Unfortunately, there are no 'paired' measurements sets available from the North Coast. Lotz (1961a, b), Lister (1962), and Sagar (1962) conducted comprehensive meteorological measurements on the Ward Hunt Ice Rise and Ice Shelf, but not on the adjacent ice-free land. The automated weather station operated on Ward Hunt Island by Parks Canada is located about 1.5 km south of the Ward Hunt Ice Rise (Braun *et al.*, 2004b). Therefore, it was necessary to construct an air temperature climatology for the Ward Hunt Ice Rise and Ward Hunt Ice Shelf (WHIRWHIS*) by subtracting the ice-cap cooling effect (cf. Section 5.5.4) from the WHI AWS* record (Fig. 5.43).

The inter-annual variability of mean summer and mean July air temperatures on the Ward Hunt Ice Rise and Ward Hunt Ice Shelf is much smaller than on Murray Ice Cap (Fig. 5.43), presumably due to the modulating influence of the adjacent Arctic Ocean. More remarkably, however, is that the ice rise and ice shelf experience considerably colder summers than Murray Ice Cap (Table 5.33, 5.34), even though they are located more than 1000 m lower in elevation. This presumably reflects again the influence of the 'Arctic Ocean Effect', suppressing surface air temperatures along the North Coast during the summer due to frequent fog and low stratus cloud conditions (Braun *et al.*, 2004b). The severity of the North Coast climate has already been noted by Edlund and Alt (1989) (cf. Sections 5.1.2 and 5.1.3):

> "Persistent low cloud cover, fog, low temperatures, and shortest snow-free season make this the harshest regional summer climate in North America."

Figure 5.43 also helps to explain why the surface mass balance of the Ward Hunt Ice Rise and Ward Hunt Ice Shelf has been much less negative than the mass balance of the Hazen Plateau ice caps over the 40 to 50 years (Braun *et al.*, 2004a, b).

5.7.1.7 Melting Degree-Day Totals on the Hazen Plateau and North Coast

The four monthly air temperature climatologies (AWS G3*, AWS T3*, WHI AWS*, and WHIRWHIS*; cf. Section 5.7.1.2 and 5.7.1.6), together with their optimized σ values specified in Section 5.6.3, finally enable the calculation of a melting degree-day climatology for the Hazen Plateau and North Coast (Fig. 5.44, Table 5.35). The main temporal feature of the four time series is again the distinct warm phase during the mid-1950s to early/mid-1960s, which dominates the long-term trends (Table 5.35). Choosing a different (i.e. shorter) reference period, for example starting only in the mid-1970s or mid-1980s, obviously results in highly statistically-significant warming trends (e.g. Comiso, 2003; Vincent *et al.*, 2001; Mueller *et al.*, 2003).

Table 5.36 provides an uncertainty assessment of this melting degree-day reconstruction, by comparing the in-situ measured annual melting degree-day totals with those determined based on the monthly climatologies and the Braithwaite (1984) melting degree-day model. The mean absolute difference was about 9 percent, which again reinforces the concerns expressed by Oerlemans (2001) regarding the ability of glacier mass balance models in general to quantitatively assess the absolute mass balance of a given glacier through time (cf. Chapter 6). Nevertheless, these melting degree-day climatologies can provide appropriate initial conditions for the temperature-index melt model experiments in Chapter 6.

Table 5.1 Operation of the two year-around automated weather stations (AWS G3 and AWS T3) on the Hazen Plateau (1999 to 2001). AWS G3 was located on the summit plateau of Murray Ice Cap (~1100 m asl); AWS T3 was located on the nearby ice-free tundra (~1025 m asl).

AWS	Start	End	Break in Measurements
G3	3 June 1999/09:00	6 August 2001/09:00	1 December 2000/08:30 to 26 May 2001/13:30 (due to fox damage)
T3	7 June 1999/18:00	4 August 2001/09:30	24 June 1999/19:30 to 12 July 1999/14:30 (due to datalogger malfunction)

Table 5.2 Data collection at AWS G3 and AWS T3 (1999 to 2001): Number of measured daily mean values for each year (i.e. calculated from the 30-minute measurements). In parentheses: Number of days available from AWS T3 after the 'record patching' procedure (cf. Section 5.2.1). This increased the data overlap from 592 to 617 days. 'Record patching' added 23 days in 1999 (June 4 to 7; June 24 to July 12) and two days for August 2001 (August 4 and 5). Note that 2000 was a leap year.

AWS	1999	2000	2001	1999 to 2001
G3	211	335	71	617
T3	188 (211)	366	215 (217)	769 (794)
Overlap	188 (211)	335	71	592 (617)

LIST OF TABLES

Table 5.3 Mean monthly air temperatures (°C) at AWS G3, AWS T3, Eureka, and Alert (1999 to 2001). AWS G3 was started 3 June 1999, i.e. first full daily mean was recorded 4 June 1999. AWS T3 was defective 26 June to 12 July 1999. AWS G3 was not operational from December 2000 to May 2001 (due to fox damage, cf. Section 5.2.1).

Month	Year	AWS G3	AWS T3	AWS T3 – AWS G3	Eureka (surface)	Alert (surface)
JAN	1999	NA	NA	NA	–38.75	–33.43
FEB	1999	NA	NA	NA	–37.11	–32.04
MAR	1999	NA	NA	NA	–36.35	–29.90
APR	1999	NA	NA	NA	–26.60	–22.71
MAY	1999	NA	NA	NA	–11.85	–12.51
JUNE	1999	–4.05	–3.44*	0.61*	1.01	–1.84
JULY	1999	2.91	4.07*	1.16*	6.95	3.46
AUG	1999	–1.87	–0.82	1.05	4.76	–1.83
SEP	1999	–9.75	–9.55	0.20	–5.75	–9.05
OCT	1999	–20.88	–20.19	0.69	–22.22	–18.94
NOV	1999	–22.59	–22.38	0.21	–28.79	–23.00
DEC	1999	–26.94	–27.09	–0.15	–41.37	–33.49
JAN	2000	–28.09	–28.04	0.05	–39.82	–34.18
FEB	2000	–25.52	–25.86	–0.34	–37.01	–34.28
MAR	2000	–26.05	–25.96	0.09	–33.11	–31.61
APR	2000	–19.43	–19.17	0.27	–26.04	–25.52
MAY	2000	–13.94	–13.34	0.61	–11.91	–12.75
JUNE	2000	–0.22	0.80	1.02	3.85	2.38
JULY	2000	0.20	1.35	1.15	6.21	3.55
AUG	2000	–4.15	–3.09	1.06	0.38	0.48
SEP	2000	–12.03	–11.56	0.46	–10.18	–10.93
OCT	2000	–19.39	–19.04	0.35	–20.34	–18.28
NOV	2000	–22.58	–22.15	0.43	–29.44	–26.19
DEC	2000	NA	–25.09	NA	–30.52	–28.03
JAN	2001	NA	–27.13	NA	–35.81	–30.20
FEB	2001	NA	–30.13	NA	–37.11	–33.73
MAR	2001	NA	–27.29	NA	–34.65	–33.64
APR	2001	NA	–21.05	NA	–26.10	–24.03
MAY	2001	NA	–11.28	NA	–13.86	–13.04
JUNE	2001	–1.60	–0.37	1.23	2.62	0.22
JULY	2001	1.39	2.82	1.43	5.52	3.09
AUG	2001	NA	NA	NA	3.17	1.57
SEP	2001	NA	NA	NA	–6.98	–8.21
OCT	2001	NA	NA	NA	–22.09	–17.80
NOV	2001	NA	NA	NA	–27.50	–25.05
DEC	2001	NA	NA	NA	–31.71	–24.00
Total		20	24(26*)	18(20*)	36	36

* Note: The June/July 1999 AWS T3 data is patched (cf. Section 5.2.1).

Table 5.4 Monthly and seasonal air temperatures and their respective differences measured between 1999 and 2001 at AWS G3 and AWS T3 on the Hazen Plateau.

Year	Parameter	AWS G3	AWS T3	Difference
1999	June Mean	–4.05°C	–3.44°C	0.61°C
	July Mean	2.91°C	4.07°C	1.16°C
	August Mean	–1.87°C	–0.82°C	1.05°C
	JJA Mean	–0.87°C	0.09°C	0.96°C
	Annual MDD	121	174	53 (30%)
	# of melt days	42	45	3
2000	June Mean	–0.22°C	0.80°C	1.02°C
	July Mean	0.20°C	1.35°C	1.15°C
	August Mean	–4.15°C	–3.09°C	1.06°C
	JJA Mean	–1.40°C	–0.32°C	1.08°C
	Annual. MDD	119	170	51 (30%)
	# of melt days	36	44	8
2001	June Mean	–1.60°C	–0.37°C	1.23°C
	July Mean	1.39°C	2.82°C	1.43°C
	August Mean	NA	NA	NA
	JJ Mean	–0.08°C	1.25°C	1.33°C
	June/July MDD	106	156	50 (32%)
	# of melt days	31	40	9

Notes

- June and July 1999 for AWS T3 are patched (cf. Section 5.2.1).
- For 2001, only June and July are available (i.e. the field season ended 8 August 2001).
- 2001 melt day totals assume none after 3 or 5 August (AWS T3, G3, respectively).
- JJA = June, July, and August.
- MDD = Melting degree-days.

Table 5.7 Mean monthly air temperatures at AWS G3 and AWS T3 and 1100 m asl sounding air temperature above Eureka and Alert (1999 to 2001). AWS G3 started 3 June 1999, i.e. first full daily mean recorded was 4 June 1999. AWS T3 was defective 26 June to 12 July 1999. AWS G3 was not operational from December 2000 to May 2001 (due to fox damage).

Month	Year	AWS G3	AWS T3	AWS T3 – AWS G3	Eureka (1100 m)	Alert (1100 m)
JAN	1999	NA	NA	NA	–26.54	–26.07
FEB	1999	NA	NA	NA	–24.15	–26.33
MAR	1999	NA	NA	NA	–21.69	–21.27
APR	1999	NA	NA	NA	–19.54	–18.76
MAY	1999	NA	NA	NA	–15.24	–14.77
JUNE	1999	–4.05	–3.44*	0.61*	–4.78	–6.26
JULY	1999	2.91	4.07*	1.16*	2.95	2.33
AUG	1999	–1.87	–0.82	1.05	0.10	–2.13
SEP	1999	–9.75	–9.55	0.20	–8.50	–8.22
OCT	1999	–20.88	–20.19	0.69	–18.29	–19.16
NOV	1999	–22.59	–22.38	0.21	–19.44	–20.26
DEC	1999	–26.94	–27.09	–0.15	–24.11	–23.66
JAN	2000	–28.09	–28.04	0.05	–26.48	–24.68
FEB	2000	–25.52	–25.86	–0.34	–22.49	–21.21
MAR	2000	–26.05	–25.96	0.09	–22.24	–22.84
APR	2000	–19.43	–19.17	0.27	–17.58	–18.57
MAY	2000	–13.94	–13.34	0.61	–14.48	–13.39
JUNE	2000	–0.22	0.80	1.02	–0.13	–1.05
JULY	2000	0.20	1.35	1.15	0.64	0.31
AUG	2000	–4.15	–3.09	1.06	–3.63	–3.97
SEP	2000	–12.03	–11.56	0.46	–9.67	–10.76
OCT	2000	–19.39	–19.04	0.35	–15.97	–17.24
NOV	2000	–22.58	–22.15	0.43	–20.95	–19.23
DEC	2000	NA	–25.09	NA	–23.40	–22.42
JAN	2001	NA	–27.13	NA	–24.64	–24.01
FEB	2001	NA	–30.13	NA	–28.67	–27.03
MAR	2001	NA	–27.29	NA	–25.92	–25.94
APR	2001	NA	–21.05	NA	–20.02	–19.08
MAY	2001	NA	–11.28	NA	–11.56	–10.80
JUNE	2001	–1.60	–0.37	1.23	–2.10	–1.73
JULY	2001	1.39	2.82	1.43	1.15	0.95
AUG	2001	NA	NA	NA	NA	NA
SEP	2001	NA	NA	NA	NA	NA
OCT	2001	NA	NA	NA	NA	NA
NOV	2001	NA	NA	NA	NA	NA
DEC	2001	NA	NA	NA	NA	NA
Total		20	24(26*)	18(20*)	31	31

* Note: The June/July 1999 AWS T3 data is patched (cf. Section 5.2.1).

Table 5.8 Summary of the statistical comparison between AWS G3/T3 and Eureka/Alert (using the 1100 m asl sounding air temperature) (cf. Fig. 5.16 and 5.17), using mean monthly data (cf. Section 5.2.1). This comparison uses the patched AWS T3 record, i.e. with June/July 1999 and 4/5 August 2001 patched using an appropriate offset with AWS G3.

MONTHLY – 1100 m asl sounding data

ind_var	dep_var	Time step	Range	n	R^2	RMS	y-intercept	Slope
Eureka	AWS T3	Monthly	All	26	0.991	1.13	0.7544	1.1231
Alert	AWS T3	Monthly	All	26	0.993	0.97	1.6624	1.1893
Eureka	AWS G3	Monthly	All	20	0.991	1.07	–0.2595	1.1034
Alert	AWS G3	Monthly	All	20	0.993	0.93	0.6434	1.1589

Notes

- Equation: $y = y_o + ax$ (linear regression)
- RMS = Root Mean Square Error (same as standard error of the estimate): A measure of the accuracy of the prediction using the regression equation (cf. Taurasino *et al.*, 2004).

Table 5.9 Mean monthly air temperatures measured on Ward Hunt Island (Parks Canada AWS) and at Alert (surface) (1995 to 2003). NA: No data available for Ward Hunt Island due to weather station malfunction.

Ward Hunt Island AWS

Month	1995	1996	1997	1998	1999	2000	2001	2002	2003
Jan	NA	–34.57	–34.23	NA	–35.99	NA	–32.61	NA	–30.07
Feb	NA	–33.31	–35.37	NA	–33.60	NA	–36.51	NA	–35.21
Mar	NA	–32.82	–29.63	NA	–32.05	NA	–36.13	NA	–35.48
Apr	NA	–23.23	–22.96	NA	–24.30	NA	–25.63	NA	–25.01
May	NA	–9.65	–11.40	NA	–11.54	NA	–13.41	NA	–10.77
Jun	NA	–1.69	–2.57	NA	–1.59	NA	–0.60	NA	–1.56
Jul	NA	0.72	1.10	NA	1.50	NA	1.26	NA	2.92
Aug	–1.20	–2.70	NA	NA	NA	NA	–0.76	0.56	NA
Sept	–7.17	–12.13	NA	NA	NA	–12.61	–9.76	–6.84	NA
Oct	–21.38	–22.09	NA	–21.02	NA	–18.21	–17.56	–14.56	NA
Nov	–29.09	–20.14	NA	–22.99	NA	–29.09	–25.82	–26.98	NA
Dec	–33.61	–30.49	NA	–31.54	NA	–30.54	NA	–28.34	NA

Alert surface data

Month	1995	1996	1997	1998	1999	2000	2001	2002	2003
Jan	–33.63	–32.14	–33.46	–31.36	–33.43	–34.18	–30.20	–32.18	–28.15
Feb	–33.68	–29.79	–33.95	–33.43	–32.04	–34.28	–33.73	–37.33	–33.60
Mar	–33.99	–30.78	–27.72	–28.43	–29.90	–31.61	–33.64	–26.28	–34.65
Apr	–15.35	–21.94	–22.10	–21.97	–22.71	–25.52	–24.03	–26.01	–24.62
May	–9.84	–9.29	–12.20	–11.86	–12.51	–12.75	–13.04	–11.22	–10.68
Jun	–0.47	–0.61	–2.10	1.11	–1.84	2.38	0.22	0.65	–0.59
Jul	1.96	2.83	2.55	4.65	3.46	3.55	3.09	4.76	6.77
Aug	1.68	–0.21	–1.09	1.45	–1.83	0.48	1.57	3.98	NA
Sept	–5.72	–10.22	–9.81	–6.89	–9.05	–10.93	–8.21	–6.84	NA
Oct	–19.08	–19.66	–19.37	–17.64	–18.94	–18.28	–17.80	–12.78	NA
Nov	–25.08	–20.11	–23.27	–21.21	–23.00	–26.19	–25.05	–24.76	NA
Dec	–32.50	–26.73	–29.80	–29.09	–33.49	–28.03	–24.00	–25.45	NA

Table 5.10 Compilation of all available snowfall, snow accumulation, and precipitation records (mm weq) from northern Ellesmere Island (cf. Fig. 5.20). Also included is the Meighen Ice Cap to the west (Fig. 5.1).

#	Location	Description	Period	Years	Mean	SD	Range
1	Alert	Ann_snowfall	1952-2001	50	194	51	103-341
2	Alert	Win_snowfall	1952-2001	50	142	38	80-292
3	Alert	Max_snow_accu	1967-1999	33	139	45	47-232
4	Alert	Sum_snowfall	1952-2001	50	52	24	9-120
5	Eureka	Ann_snowfall	1952-2001	49	78	23	22-131
6	Eureka	Win_snowfall	1952-2001	49	67	20	20-117
7	Eureka	Max_snow_accu	1967-1999	32	81	17	53-117
8	Eureka	Sum_snowfall	1952-2001	49	11	9	0-40
9	AIC pit/core (1989)	Ann_mass_accu	1883-1988	106	170	57	60-330
10	AIC pit (1977)	Ann_mass_accu	1951-1977	27	177	48	90-315
11	Mt.Ox pit/core (1961)	Ann_mass_accu	1915-1961	47	159	NA	110-200
12	AIC summit (Nipple)	Win_snow_accu	1983-2002	18	158	24	120-207
13	Drambuie Glacier	Win_snow_accu	1977-2002	26	87	20	50-120
14	Meighen Ice Cap	Win_snow_accu	1960-2002	43	174	58	100-410
15	WH Ice Rise	Win_snow_accu	1959-1989	21	180	37	134-261
16	WH Ice Shelf	Win_snow_accu	1967-1989	16	152	36	102-222
17	Lake Hazen	Win_snow_accu	1882, 1956-59	5	67	10	51-77
18	Gilman Glacier	Win_snow_accu	1957-1959	3	68	5	65-73
19	Mt. Ox/GG/Disraeli	Win_snow_accu	1958, 1961	2	141	13	131-150
20	STPBIC-NE	Win_snow_accu	1972-76, 1982/83	7	115	27	82-159
21	STPBIC-SW	Win_snow_accu	1983	1	183	NA	NA
22	Hazen Plateau	Ann_snow_accu	1962-1974	13	150	NA	NA
23	Hazen Plateau	Ann_snow_accu	1951-1980	30	125	NA	100-150
24	NE Ellesmere Is.	Ann_snowfall	1953-1976	24	150	NA	NA
25	Lake Hazen	Ann_precip	1882-1960	79	65	NA	NA
26	Simmons Ice Cap	Win_snow_accu	1976, 2000/01	3	104	3	102-108
27	Murray Ice Cap	Win_snow_accu	1999-2001	3	84	17	65-96

Continued next page

Table 5.10 continued: Notes and description of the records.

1. Alert (62 m asl) annual snowfall (mm weq; 9/1 to 8/31). Data available at http://www.cccma.bc.ec.gc.ca/hccd/ (cf. Mekis and Hogg, 1999).
2. Alert (62 m asl) winter snowfall (mm weq; 9/1 to 5/31). Data available at http://www.cccma.bc.ec.gc.ca/hccd/ (cf. Mekis and Hogg, 1999).
3. Alert (62 m asl) maximum measured snow accumulation (mm weq) in May/June each year from bi-weekly snow courses. Data available at http://www.ccin.ca/.
4. Alert (62 m asl) summer snowfall (mm weq; June/July/August). Data available at http://www.cccma.bc.ec.gc.ca/hccd/ (cf. Mekis and Hogg, 1999).
5. Eureka (10 m asl) annual snowfall (mm weq; 9/1 to 8/31). Data available at http://www.cccma.bc.ec.gc.ca/hccd/ (cf. Mekis and Hogg, 1999); data for 1991 are missing.
6. Eureka (10 m asl) winter snowfall (mm weq; 9/1 to 5/31). Data available at http://www.cccma.bc.ec.gc.ca/hccd/ (cf. Mekis and Hogg, 1999); data for 1991 are missing.
7. Eureka (10 m asl) maximum measured snow accumulation (mm weq) in May/June each year from bi-weekly snow courses. Data available at http://www.ccin.ca/; data for 1983 are missing.
8. Eureka (10 m asl) summer snowfall (mm weq; 9/1 to 5/31). Data available at http://www.cccma.bc.ec.gc.ca/hccd/ (cf. Mekis and Hogg, 1999); data for 1991 are missing.
9. Agassiz Ice Cap (~1600 m asl) snow pit / core from 1989 (Fisher and Koerner, 1994). This record is un-scoured, i.e. represents total winter snow accumulation; data available online.
10. Agassiz Ice Cap snow pit from 1977 (~1670 m asl) (Fisher and Koerner, 1994). This record is un-scoured, i.e. presents total winter snow accumulation; data available online.
11. Mt. Oxford snow pit and core from 1961 (Hattersley-Smith; 1963), only mean and range of values are given – annual values are not available (~1660 m asl).
12. AIC summit ('Nipple'; ~1800 m asl) measured winter snow accumulation (Koerner, pers. comm.). Data for 1985 and 1987 are missing.
13. Drambuie Glacier (~700 to 1400 m asl) measured winter snow accumulation (Koerner, pers. comm.).
14. Meighen Ice Cap (Meighen Island; cf. Fig. 5.1) measured winter snow accumulation (Koerner, pers. comm.) (~50 to 250 m asl).
15. Ward Hunt Ice Rise (~0 to 40 m asl) measured winter snow accumulation (Braun *et al.*, 2004b), with gaps.
16. Ward Hunt Ice Shelf (~0 to 10 m asl) measured winter snow accumulation (Braun *et al.*, 2004b), with gaps.
17. Winter snow accumulation on Lake Hazen (~175 m asl) (Jackson, 1959; Hattersley-Smith, 1963).
18. Winter snow accumulation on the Gilman Glacier (~1050 m asl) (Hattersley-Smith, 1960b).
19. Winter snow accumulation near Mt. Oxford, Gilman Glacier accumulation area, and Disraeli Glacier accumulation area (Hattersley-Smith, 1960b) (~1400 to 1800 m asl).
20. Winter snow accumulation on the St. Patrick Bay ice cap (NE; ~900 m asl) (Ommanney, 1977; Bradley and Serreze, 1987a).
21. Winter snow accumulation on the St. Patrick Bay ice cap (SW; ~800 m asl) (Bradley and Serreze, 1987a).
22. Generalized annual snow accumulation on the Hazen Plateau (Koerner, 1979; Fig. 2/3).
23. Generalized annual snow accumulation on the Hazen Plateau (Edlund and Alt, 1989; Fig. 15B). Valid for elevations >600 m asl.
24. Generalized annual snowfall on the higher elevations of north-eastern Ellesmere Island (Maxwell, 1981; Table 6)
25. Annual precipitation at Lake Hazen (~175 m asl) (Jackson, 1959; Hattersley-Smith, 1960b)
26. Winter snow accumulation on Simmons Ice Cap (~950 to 1100 m asl) (Bradley and England, 1977; this study). Simple mean of the (initial) winter snow accumulation measurements (2000 and 2001).
27. Winter snow accumulation on Murray Ice Cap (~950 to 1100 m asl) (this study). Simple mean of the initial winter snow accumulation measurements (1999 to 2001).

Table 5.11 Snow accumulation and snowfall records (mm weq) for northern Ellesmere Island: Trends (cf. Fig. 5.22) over the last ~50 years (or last ~100 years in case of the Agassiz Ice Cap snow pit/firn core from 1989. See Table 5.10 for record descriptions.

Record	Time Period	Mean	Trend	P-value
AIC pit/core (1989)	1883 to 1988	170 mm	–0.108 mm/yr	P=0.55
AIC pit/core (1989)	1950 to 1988	162 mm	1.652 mm/yr	P=0.02
Alert Ann_snowfall	1952 to 2001	194 mm	1.68 mm/yr	P=0.0004
Alert Win_snowfall	1952 to 2001	142 mm	1.176 mm/yr	P=0.001
Alert Max_snow_accu	1967 to 1999	139 mm	0.226 mm/yr	P=0.75
Alert Sum_snowfall	1952 to 2001	52 mm	0.504 mm/yr	P=0.03
Eureka Ann_snowfall	1952 to 2001	78 mm	0.93 mm/yr	P<0.0001
Eureka Win_snowfall	1952 to 2001	67 mm	0.66 mm/yr	P=0.0003
Eureka Max_snow_accu	1967 to 1999	81 mm	–0.66 mm/yr	P=0.03
Eureka Sum_snowfall	1952 to 2001	11 mm	0.27 mm/yr	P=0.002
AIC summit (Nipple)	1983 to 2002	158 mm	1.717 mm/yr	P=0.09
Drambuie Glacier	1977 to 2002	87 mm	–0.438 mm/yr	P=0.41
AIC pit (1977)	1951 to 1977	177 mm	3.248 mm/yr	P=0.004
Meighen Ice Cap	1960 to 2002	174 mm	0.651 mm/yr	P=0.36

Table 5.12 Mean and standard deviation for selected long-term snowfall or snow accumulation records from northern Ellesmere Island with annual resolution (mm weq). The standard deviation is also expressed as a percentage of the corresponding mean. See Table 5.10 for record descriptions.

Record	# of years	Mean (mm weq)	SD (mm weq)	SD (% of mean)
Alert Ann_snowfall	50	194	51	26
Alert Win_snowfall	50	142	38	27
Alert Max_snow_accu	33	139	45	32
Eureka Ann_snowfall	49	78	23	29
Eureka Win_snowfall	49	67	20	30
Eureka Max_snow_accu	32	81	17	21
AIC pit/core (1989)	106	170	57	34
AIC pit (1977)	27	177	48	27
AIC summit (Nipple)	18	158	24	15
Drambuie Glacier	26	87	20	23
Meighen Ice Cap	43	174	58	33
WH Ice Rise	21	180	37	21
WH Ice Shelf	16	152	36	24
Lake Hazen	5	67	10	15
STPBIC_NE	7	115	27	23
Mean		132	34	25

Table 5.13 Comparison of the 1999, 2000, and 2001 precipitation data with the long-term precipitation data at Alert/Eureka and available winter mass balance data (mm weq).

Parameter	Period (# of years)	Mean (SD) (full record)	Mean (SD) (1990s)	1999	2000	2001
Drambuie Glacier	1977-2002 (26)	87 (20)	83 (23)	100	80	70
AIC summit (Nipple)	1983-2002 (18)	158 (24)	165 (28)	180	162	142
Meighen Ice Cap	1960-2002 (43)	174 (58)	187 (89)	140	150	250
Alert Ann_snowfall	1952-2001 (50)	194 (51)	219 (60)	279	274	208
Alert Win_snowfall	1952-2001 (50)	142 (38)	163 (55)	213	189	143
Alert Max_snow_accu	1967-1999 (33)	139 (44)	146 (36)	124	NA	NA
Alert Sum_snowfall	1952-2001 (50)	52 (24)	56 (21)	65	84	66
Alert Sum_rainfall	1952-2001 (50)	23 (15)	24 (9)	29	24	23
Eureka Ann_snowfall	1952-2001 (49)	78 (23)	90 (23)	75	95	95
Eureka Win_snowfall	1952-2001 (49)	67 (20)	71 (17)	67	63	90
Eureka Max_snow_accu	1967-1999 (32)	81 (17)	74 (14)	64	NA	NA
Eureka Sum_snowfall	1952-2001 (49)	11 (9)	19 (12)	8	32	6
Eureka Sum_rainfall	1952-2001 (49)	32 (17)	35 (16)	14	27	41
Murray Ice Cap				92	65	96
Simmons Ice Cap				NA	108	103

Notes

- Annual snowfall was calculated based on the approximate 'glacier mass balance year' (1 September to 31 August, 1952 to 2001).
- 1991 precipitation data for Eureka are missing.
- 2000 and 2001 maximum snow accumulation data are not available for Eureka and Alert.
- Simmons Ice Cap: see notes for Table 5.10.
- Murray Ice Cap: see notes for Table 5.10.

Table 5.14 Winter snow accumulation (mm weq) along the northern (i.e. Arctic Ocean) coast of Ellesmere Island (cf. Fig. 5.1).

Location	Time Interval (# of years)	Mean	SD	SD(%)	Trend
Meighen Ice Cap	1960 to 2002 (43)	174	58	33	0.651 mm/yr (P = 0.36)
WH Ice Rise	1959 to 1989 (21)	180	37	21	–0.399 mm/yr (P = 0.68)
WH Ice Shelf	1967 to 1989 (16)	152	36	24	1.334 mm/yr (P = 0.32)
Alert Win_snowfall	1952 to 2001 (50)	142	38	27	1.176 mm/yr (P = 0.001)
Mean		162	42	26	

Notes

- The records from the Ward Hunt (WH) Ice Rise and Ward Hunt (WH) Ice Shelf have some temporal gaps (cf. Braun *et al.*, 2004b).
- Alert Win_snowfall = 1 September to 31 May snowfall totals (which corresponds approximately to the winter mass balance period in the Canadian High Arctic).

Table 5.15 Altitudinal variability of air temperature (i.e. lapse rates) in the Canadian High Arctic: Data from previous studies (Fig. 5.1). Note the different time intervals and elevation ranges (cf. Fig. 5.27). See Porter (2001) for a similar compilation focused on tropical sites.

Location	Time Interval	Elevation Range	ΔT	Lapse Rate
[1]Alert/Gilman Glacier	June, July 1961	62 to 1660 m asl	NA	5.4°C/1000 m
[2]Lake Tuborg area	61/1 to 7/19/1995	63 to 800 m asl	4.45°C	6.0°C/1000 m
[3]John Evans Glacier	6/21 to 7/21/1996	824 to 1183 m asl	NA	5.6°C/1000 m
[4]Barnes Ice Cap	June-August 1950	27 to 866 m asl	5°C	6.0°C/1000 m
[5]Penny Ice Cap	June-August 1953	396 to 2050 m asl	9.3°C	5.6°C/1000 m
[6]Coburg Island	July 1972 to Sept 1976	4 to 700 m asl	NA	5.0°C/1000 m
[7]Gilman Glacier	July 1958	175 to 1000 m asl	5.6°C	4.6°C/1000 m
[8]Eureka/STPBIC	6/18 to 7/25/1982	10 to 835 m asl	3.6°C	4.4°C/1000 m
[9]Eureka/STPBIC	6/18 to 7/25/1983	10 to 835 m asl	4.2°C	5.1°C/1000 m
[10]Alert/STPBIC	6/18 to 7/25/1982	63 to 835 m asl	1.1°C	1.5°C/1000 m
[11]Alert/STPBIC	6/18 to 7/25/1983	63 to 835 m asl	1.4°C	1.8°C/1000 m
Mean /wo Alert				(5.3±0.6)°C

Notes

1. Sagar (1964)
2. Braun (1997)
3. Arendt (1997)
4. Orvig (1951)
5. Orvig (1954)
6. Blatter and Kappenberger (1988), mean value for June, July, and August.
7. Lotz and Sagar (1962)
8. STPBIC (= St. Patrick Bay ice caps) data from Bradley and Serreze (1987b); compared with the corresponding Eureka and Alert data (also 9, 10, 11)

- After completion of this chapter, Mair *et al.* (2005) published an air temperature lapse rates for the Devon Ice Cap of 4.8°C/1000 m, which would not change the mean and standard deviation shown above.
- Wang *et al.* (2005) also published new air temperature lapse rates measured between 100 and 2000 m asl on the large Prince of Wales Ice Cap in southern Ellesmere Island. The lapse rate was 3.7°C/1000 m in 2001 and 5.1°C/1000 m in 2002, which they linked to different synoptic-scale atmospheric circulation pattern in these two years.
- The mean and standard deviation of 5.3±0.6°C/1000 m was calculated excluding records #10 and #11 (cf. Fig. 5.27).

Table 5.16 Altitudinal variability of air temperature (i.e. lapse rate) measured on the Hazen Plateau, Ellesmere Island in 1999 and 2001.

Location	Time Period	Elevation Range	ΔT	Lapse Rate
Lake Hazen AWS AWS T3	June 4 to August 31 1999 June 30 to August 5 2001 (n = 126 days)	175 to 1025 m asl (Δh = 850 m)	4.68°C	5.51°C/1000 m

Notes

- Lake Hazen AWS data provided by Parks Canada. No data available for 2000 from Lake Hazen due to a technical malfunction of the Lake Hazen AWS.

Table 5.17 HOBO station data set for 2000: Number of raw hourly measurements and number of outliers (cf. Section 5.4.3).

HOBO station	Start of record	End of record	Number of hourly measurements	Number of outliers[1]
H1	5/31/12:30	8/31/23:30	2220	25
H2	5/30/12:00	8/24/6:00	2059	20
H3	5/30/12:30	8/24/6:30	2059	25
H4	5/29/14:00	8/31/23:00	2266	22
H5	6/6/10:30	8/20/13:30	1288	21
[2]H6	5/29/12:30	8/31/23:30	2268	530
H7	5/29/13:30	8/20/7:30	1987	153
H9	6/28/00:00	8/20/15:00	1288	28
G2	8/3/15:30	8/20/9:30	403	6
C2	5/31/16:30	8/31/23:30	2216	40
T2	5/29/11:30	8/20/9:30	1991	19
HS	6/2/00:30	8/31/23:30	2184	10
HN	8/5/14:00	8/24/00:00	443	7
HW	8/3/11:30	8/31/23:30	685	0
HE	8/3/10:30	8/20/12:30	411	3

Notes

1. See text for definition and treatment of outliers.
2. HOBO station H6 was excluded from further analysis (see text).

Table 5.18 HOBO station data set for 2000: Mean daily air temperature (cf. Section 5.4.3).

HOBO station	Start of Record	End of Record	Number of days	Location (cf. Fig. 5.28)
T2	5/30/2000	8/19/2000	82	Plateau summit (near AWS T3)
H1	6/1/2000	8/31/2000	92	Plateau summit
H2	5/31/2000	8/23/2000	85	Plateau summit
H3	5/31/2000	8/23/2000	85	Plateau summit
H4	5/30/2000	8/31/2000	94	Plateau summit
H6				Not used in analysis
H7	5/30/2000	8/19/2000	82	Plateau summit
C2	6/1/2000	8/31/2000	92	~50 m from Murray Ice Cap
G2	8/4/2000	8/19/2000	16	On Murray Ice Cap (near AWS G3)
H5	6/7/2000	8/19/2000	74	On Simmons Ice Cap summit
H9	6/28/2000	8/19/2000	53	On Roberts Ice Cap (~1300 m asl)
H-E	8/4/2000	8/19/2000	16	On E-facing slope
H-W	8/4/2000	8/31/2000	28	On W-facing slope
H-N	8/6/2000	8/23/2000	18	On N-facing slope
H-S	6/2/2000	8/31/2000	91	On S-facing slope

Table 5.19 Air temperature lapse rates from daily data in the immediate vicinity of Murray and Simmons Ice Cap (2000), measured using the HOBO station network (Fig. 5.28).

HOBO station	Location	Elevation (m asl)	Mean T (°C) (6/1 to 8/19)	Mean T (°C) (6/7 to 8/19)	Mean T (°C) (6/28 to 8/19)
T2	Plateau	1025	0.81	1.59	0.99
H1	Plateau	955	1.29	2.06	1.48
H2	Plateau	1005	0.92	1.69	1.12
H3	Plateau	935	1.42	2.20	1.66
H4	Plateau	975	1.13	1.90	1.43
H7	Plateau	1035	0.74	1.48	0.83
C2	Near MIC	990		1.63	1.16
H5	SIC	1095		0.70	0.04
H-S	Slope	800		3.64	3.08
H9	RIC	1300			−1.47
	Lapse Rate		6.8°/1000 m	7°C/1000 m	7.9°C/1000 m

Notes

- The air temperature lapse rate was calculated using only the six plateau HOBO stations (T2, H1, H2, H3, H4, and H7) in each of the three cases.

Table 5.20 Summary table: Air temperature lapse rates. Note the drastically different elevation ranges.

Type	Source	Elevation Range	Lapse Rate
General Lapse Rate	Scientific literature	10 to 2050 m asl	5.3±0.6°C/1000 m
Regional Lapse Rate	Lake Hazen/AWS T3	175 to 1025 m asl	5.5°C/1000 m
Local Lapse Rate	HOBO network (2000)	935 to 1035 m asl	6.8°C/1000 m

Table 5.21 Glacier or ice-cap cooling effect: Values reported previously in the scientific literature or calculated from available published data.

Glacier/Ice Cap Cooling Effect	Location	Time Period	Note
1.1 to 2.4°C	Haut Glacier d'Arolla (Swiss Alps)	1 June to 31 August 2001	1
1 to 1.5°C	White Glacier (Canada)	Summer 1961	2
3°C	White Glacier (Canada)	Summer 1962	3
1.5°C	Langjökull Ice Cap (Iceland)	Ablation season 2001	4
2.1°C	Hintereisferner (Austria)	2 to 22 July 1986	5
0.8 to 1°C	St. Patrick Bay Ice Cap (NE) (Canada)	19 June to 26 July 1982	6
~2°C	Pasterze Glacier (Austria)	Summer 1994	7
~1.14°C	Greenland Ice Sheet margin	10 June to 31 July (1990/91)	10
1.7°C	'Mean'	'All sites' listed above	
0°C	May, White Glacier (Canada)	1969 to 1972	8
0.7°C	June, White Glacier (Canada)	1969 to 1972	8
1.7°C	July, White Glacier (Canada)	1969 to 1972	8
0.9°C	August, White Glacier (Canada)	1969 to 1972	8
0.12°C	June, Ward Hunt Ice Rise (Canada)	1960	9
1.36°C	July, Ward Hunt Ice Rise (Canada)	1960	9
0.89°C	August, Ward Hunt Ice Rise (Canada)	1960	9

Notes

1. Value determined using data presented by Strasser *et al.* (2004). Strasser *et al.* (2004) also determined a remarkably low air temperature lapse on the gently-sloped glacier of only about 2°C/1000 m.
2. The Müller and Roskin-Sharlin (1967) value is after Bradley and Serreze (1987b).
3. The Havens *et al.* (1965) value was used by Atkinson and Gajweski (2002) in their regional summer temperature model for the Canadian High Arctic.
4. Value determined from data reported by Gudmundsson *et al.* (2003).
5. Greuell and Oerlemans (1989; their Table 2), which also includes the differences of the other components of the surface energy balance measured at and near the snout of the Hintereisferner.
6. Bradley and Serreze (1987b). They also measured 35 to 40 percent less seasonal melting degree-day totals on the ice-cap compared to the ice-free surrounding terrain (cf. Table 5.22).
7. Approximated from Greuell *et al.* (1997, their Fig. 4).
8. Ohmura (2000); calculated using data from meteorological stations 'Base Camp' and 'Lower Ice' (both at about 200 m asl) near/on the White Glacier.
9. Calculated from mean monthly temperatures measured on the Ward Hunt Ice Rise (Sagar, 1962) and the monthly climatology for Ward Hunt Island developed in Section 5.2.
10. Value determined using data from two weather stations summarized by Oerlemans and Vugts (1993; their Table 1).

- D. Mueller (pers. comm.) measured a cooling effect associated with the Ward Hunt Ice Shelf of about 1.5 to 2°C relative to the ice-free Ward Hunt Island (cf. Mueller *et al.*, 2003).

Table 5.22 'Ice-cap cooling effect': Mean measured values from AWS G3 and AWS T3 for the summers of 1999 and 2000.

Parameter	Year	AWS G3	AWS T3	ΔT (AWS T3 – AWS G3)
JJA mean	1999	–0.87°C	0.09°C	0.96°C
JJA mean	2000	–1.40°C	–0.32°C	1.08°C
JJA MDD	1999	121	174	53 (70%)
JJA MDD	2000	119	170	51 (70%)

Notes

- JJA mean = June, July, and August mean air temperature.
- JJA MDD = June, July, and August melting degree-day total.

Table 5.23 'Ice-cap cooling effect': Mean monthly values from AWS G3 and AWS T3 (1999 to 2001).

Year	Month	AWS G3	AWS T3	ΔT
1999	June	–4.05	–3.44	0.61
1999	July	2.91	4.07	1.16
1999	August	–1.87	–0.82	1.05
1999	September	–9.75	–9.55	0.20
1999	October	–20.88	–20.19	0.69
1999	November	–22.59	–22.38	0.21
1999	December	–26.94	–27.09	–0.15
2000	January	–28.09	–28.04	0.05
2000	February	–25.52	–25.86	–0.34
2000	March	–26.05	–25.96	0.09
2000	April	–19.43	–19.17	0.27
2000	May	–13.94	–13.34	0.61
2000	June	–0.22	0.80	1.02
2000	July	0.20	1.35	1.15
2000	August	–4.15	–3.09	1.06
2000	September	–12.03	–11.56	0.46
2000	October	–19.39	–19.04	0.35
2000	November	–22.58	–22.15	0.43
2000	December	NA	–25.09	NA
2001	January	NA	–27.13	NA
2001	February	NA	–30.13	NA
2001	March	NA	–27.29	NA
2001	April	NA	–21.05	NA
2001	May	NA	–11.28	NA
2001	June	–1.60	–0.37	1.23
2001	July	1.39	2.82	1.43
Mean	'Winter'			0.24°C
Mean	'Summer'			1.09°C
Mean	June			0.95°C
Mean	July			1.25°C
Mean	August			1.06°C

Notes

- 'Winter' September to May
- 'Summer' June, July, and August

Table 5.24 Surface climate data from Eureka and Alert: Mean June, July, and August (JJA) air temperature, annual melting degree-day totals (ann MDD), and JJA MDD (1951 to 2003).

Year	Eureka (ann MDD)	Eureka (JJA MDD)	Eureka (JJA T)	Alert (ann MDD)	Alert (JJA MDD)	Alert (JJA T)
1951	371.2	366.8	3.80	157.1	157.1	0.70
1952	452.1	450.8	4.73	185.1	185.1	0.87
1953	234.3	230.0	2.30	238.4	237.0	1.87
1954	455.2	435.0	4.62	294.9	290.1	2.59
1955	284.2	283.9	2.95	103.2	103.2	0.50
1956	354.6	354.6	3.16	335.3	335.3	2.07
1957	453.2	452.4	4.78	287.7	287.7	2.23
1958	418.2	411.8	4.11	232.8	225.3	2.05
1959	418.2	418.2	4.26	135.6	135.6	0.58
1960	534.6	532.2	5.78	249.0	249.0	1.98
1961	269.5	269.5	2.29	183.1	183.1	0.33
1962	472.0	472.0	5.00	326.4	326.4	2.83
1963	319.8	319.8	3.04	195.5	195.5	0.71
1964	314.2	314.2	3.33	185.4	185.4	1.55
1965	339.0	334.8	3.42	125.7	125.7	0.00
1966	386.9	381.6	3.62	277.1	274.9	2.19
1967	329.6	321.7	3.32	267.1	260.3	1.74
1968	385.9	385.9	4.16	116.9	116.9	0.63
1969	340.3	339.5	3.25	235.2	235.2	1.51
1970	297.5	297.5	2.57	133.0	133.0	0.10
1971	420.8	420.8	4.51	229.1	229.1	1.58
1972	257.6	257.6	2.35	123.1	123.1	0.01
1973	345.5	335.7	3.53	171.6	164.5	1.16
1974	321.1	320.8	2.47	217.8	217.8	1.17
1975	350.7	350.7	3.53	227.3	227.3	1.02
1976	277.0	274.0	2.64	155.6	155.0	0.44
1977	443.4	443.4	4.67	113.9	113.9	0.13
1978	347.7	347.7	3.34	256.6	256.6	1.78
1979	228.6	228.5	1.48	139.1	139.1	–0.33
1980	280.3	276.8	2.29	184.0	180.6	0.88
1981	402.6	402.3	4.27	217.6	212.1	1.80
1982	328.0	327.8	3.40	205.6	205.6	1.23
1983	394.2	380.5	4.10	133.1	129.9	0.78
1984	349.4	349.4	3.67	210.4	209.7	1.49
1985	351.3	347.4	3.24	216.4	214.7	1.14
1986	272.5	272.5	2.28	223.4	222.1	1.46
1987	425.9	425.9	4.56	203.0	196.4	1.41
1988	423.8	422.3	4.39	207.1	207.1	1.37

Continued next page

Table 5.24 continued

1989	296.1	292.6	3.17	215.3	214.8	1.95
1990	439.4	438.9	4.67	207.2	207.2	1.39
1991	330.7*	328.9*	3.94*	243.6	243.6	2.20
1992	269.5	269.5	2.42	128.1	127.5	0.25
1993	405.7	404.3	4.21	216.0	216.0	1.27
1994	372.8	369.0	3.90	252.0	252.0	2.40
1995	454.4	436.7	4.72	149.7	135.6	1.07
1996	232.2	232.2	2.03	153.4	153.4	0.69
1997	344.0	344.0	3.09	124.3	124.3	–0.19
1998	491.6	481.3	5.23	245.8	244.3	2.42
1999	428.2	428.2	4.28	142.0	142.0	–0.05
2000	374.3	374.3	3.48	279.0	279.0	2.13
2001	365.4	365.4	3.79	209.4	209.1	1.64
2002	433.6	428.7	4.59	325.4	325.4	3.16
2003	435.0	427.8	4.53	361.4	361.1	3.15
Mean	365.3*	362.5*	3.64*	206.6	205.3	1.30

Notes

- The 1991 daily surface air temperature record from Eureka (indicated by *) misses the last nine days of July, hence 1991 is excluded the analysis (cf. Fig. 5.35)

Table 5.25 'Look-up' table used in the Braithwaite (1984) degree-day model (cf. his Table 1). 'Mean' is the mean monthly air temperature (°C); σ is the corresponding monthly standard deviation of air temperature (°C). Cell contents are monthly melting degree-days per day, which have to be multiplied by 28, 30, or 31 as needed for each month of interest to determine total monthly melting degree-days.

Mean	σ = 1	σ = 2	σ = 3	σ = 4	σ = 5
–10	0	0	0	0	0
–8	0	0	0	0	0.1
–6	0	0	0	0.1	0.3
–4	0	0	0.1	0.3	0.6
–2	0	0.2	0.5	0.8	1.1
0	0.4	0.8	1.2	1.6	2.0
2	2	2.2	2.5	2.8	3.1
4	4	4	4.1	4.3	4.6
6	6	6	6	6.1	6.3
8	8	8	8	8	8.1
10	10	10	10	10	10

Notes

- An expanded table with a resolution of 0.1°C was used for the testing of the Braithwaite (1984) model and for the melting degree-day calculations in Section 5.7.

Table 5.26 Values of the 'monthly standard deviation of air temperature' (σ, cf. Braithwaite, 1984) previously measured, modeled, or assumed in the scientific literature.

σ (°C)	Reference	Location/Comment
4	Braithwaite (1984)	Swiss Alps, West Greenland
4	Braithwaite and Zhang (1999)	Swiss Alps (5 glaciers)
4.5	Reeh (1991)	Greenland Ice Sheet
3.5	Johannesson *et al.* (1995)	West Greenland
3 to 5	Lefebre *et al.* (2002)	Southern GIS, May/June and Aug/Sept (modeled)
<3	Lefebre *et al.* (2002)	Southern GIS, July (modeled)
4	Podlech *et al.* (2004)	Southern Greenland
5	Huybrechts *et al.* (1991)	Greenland Ice Sheet
4.4	Laumann and Reeh (1993)	Southern Norway (measured)
4.6	Laumann and Reeh (1993)	Southern Norway (modeled)
3.32	Johannesson *et al.* (1995)	Iceland (optimized)
3.12	Johannesson *et al.* (1995)	Norway (optimized)
4	Braithwaite and Zhang (1999)	37 glaciers around the world
4.2 to 5.2	Lefebre *et al.* (2002)	Common values used in the scientific literature

Notes

- GIS = Greenland Ice Sheet

Table 5.27 1951 to 2003 Alert and Eureka monthly standard deviation of air temperature (σ; °C) for May to September, calculated from the measured mean daily temperatures (cf. Braithwaite, 1984).

Month	Alert σ	Eureka σ	Mean σ
May	4.54	5.30	4.9
June	3.36	3.09	3.2
July	2.79	1.99	2.4
August	3.32	2.57	3.0
September	4.95	5.27	5.1
Mean	3.79	3.65	3.7

Table 5.28 1995 to 2001 monthly standard deviation of air temperature (σ; °C) for Alert, Eureka, AWS G3, AWS T3, and WHI AWS (May to September).

Month	Year	Alert σ	Eureka σ	AWS G3 σ	AWS T3 σ	WHI AWS σ
May	1995	4.11	4.05	NA	NA	NA
June	1995	2.10	2.23	NA	NA	NA
July	1995	1.98	2.59	NA	NA	NA
August	1995	1.30	2.15	NA	NA	2.89
September	1995	5.24	3.68	NA	NA	4.08
May	1996	5.01	7.78	NA	NA	5.23
June	1996	3.61	3.46	NA	NA	3.05
July	1996	1.98	1.67	NA	NA	1.47
August	1996	3.24	2.44	NA	NA	3.37
September	1996	4.38	6.74	NA	NA	4.83
May	1997	3.52	4.67	NA	NA	3.78
June	1997	2.25	3.52	NA	NA	1.80
July	1997	3.29	2.07	NA	NA	2.00
August	1997	4.05	3.91	NA	NA	NA
September	1997	3.50	6.34	NA	NA	NA
May	1999	3.72	5.29	NA	NA	3.95
June	1999	3.74	2.87	2.55	2.52	3.29
July	1999	2.83	2.17	2.79	2.92	1.77
August	1999	3.30	4.39	4.00	4.28	NA
September	1999	2.71	2.76	3.03	2.67	NA
May	2000	4.25	5.24	3.82	3.86	NA
June	2000	4.99	4.70	6.33	6.58	NA
July	2000	3.09	3.05	2.49	2.80	NA
August	2000	4.18	3.31	3.47	3.52	NA
September	2000	4.89	4.97	3.95	4.19	7.28
May	2001	4.96	6.86	NA	3.85	4.25
June	2001	3.17	3.09	4.71	4.82	2.80
July	2001	2.22	2.17	3.75	3.89	1.49
August	2001	3.76	2.58	NA	NA	2.67
September	2001	4.92	5.50	NA	NA	4.89
May	2002	4.90	4.54	NA	NA	NA
June	2002	3.08	2.79	NA	NA	NA
July	2002	3.04	1.72	NA	NA	NA
August	2002	3.81	2.68	NA	NA	1.86
September	2002	5.18	3.91	NA	NA	5.46
May	2003	3.71	5.51	NA	NA	3.66
June	2003	4.14	3.34	NA	NA	2.81
July	2003	3.31	2.71	NA	NA	2.20
August	2003	3.25	1.72	NA	NA	NA
September	2003	3.64	3.98	NA	NA	NA
Mean		3.61	3.73	3.71	3.83	3.37

Table 5.29 Test of the Braithwaite (1984) degree-day model using data from AWS T3 and AWS G3 (1999 to 2001).

AWS T3

Year	Month	Mean T (°C)	σ	MDD per day	# of days	MDD/month modeled	MDD/month measured	Delta
1999	May	NA	NA	NA	31	NA	NA	
1999	June	–3.4	2.5	0.1	30	3	1.3	
1999	July	4.1	2.9	4.2	31	130.2	130	
1999	Aug	–0.8	4.3	1.3	31	40.3	42.4	
1999	Sept	–9.6	2.7	0	30	0	0	
					Totals	173.5	173.7	0.2 (0.1%)
2000	May	–13.3	3.9	0	31	0	0	
2000	June	0.8	6.6	3.1	30	93	102.3	
2000	July	1.4	2.8	2	31	62	59	
2000	Aug	–3.1	3.5	0.4	31	12.4	8.3	
2000	Sept	–11.6	4.2	0	30	0	0	
					Totals	167.4	169.6	2.2 (1.3%)
2001	May	–11.3	3.9	0	31	0	0	
2001	June	–0.4	4.8	1.7	30	51	57.7	
2001	July	2.8	3.9	3.3	31	102.3	97.9	
2001	Aug	NA	NA	NA	31	NA	NA	
2001	Sept	NA	NA	NA	30	NA	NA	
					Totals	153.3	155.6	2.3 (1.5%)

AWS G3

Year	Month	Mean T (°C)	σ	MDD per day	# of days	MDD/month modeled	MDD/month measured	Delta
1999	May	NA	NA	NA	31	NA	NA	
1999	June	–4.1	2.6	0.1	30	3	0.4	
1999	July	2.9	2.8	3.1	31	96.1	97.1	
1999	Aug	–1.9	4.0	0.8	31	24.8	23.5	
1999	Sept	–9.8	3.0	0	30	0	0	
					Totals	123.9	121	2.9 (2.4%)
2000	May	–13.9	3.8	0	31		0	
2000	June	–0.2	6.4	2.5	30	75	81.2	
2000	July	0.2	2.5	1.1	31	34.1	35.7	
2000	Aug	–4.2	3.5	0.2	31	6.2	1.9	
2000	Sept	–12.0	4.0	0	30	0	0	
					Totals	115.3	118.8	3.5 (3%)
2001	May	NA	NA	NA	31	NA	NA	
2001	June	–1.6	4.7	1.2	30	36	36	
2001	July	1.4	3.8	2.3	31	71.3	70.3	
2001	Aug	NA	NA	NA	31	NA	NA	
2001	Sept	NA	NA	NA	30	NA	NA	
					Totals	107.3	106.3	1.0 (0.9%)

Table 5.30 Test of the Braithwaite (1984) degree-day model using measured data from the Ward Hunt Island (WHI) AWS (1996 and 2001).

WHI AWS

Year	Month	Mean T (°C)	σ	MDD per day	# of days	MDD/month modeled	MDD/month measured	Delta
1996	May	–9.7	5.23	0.02	31	3.1	0.5	
1996	June	–1.7	3.05	0.31	30	15	9.2	
1996	July	0.7	1.47	1.01	31	31	31.4	
1996	Aug	–2.7	3.37	0.22	31	9.3	7	
1996	Sept	–12.1	4.81	0	30	0	0	
					Totals	58.4	48.1	10.3 (17.6%)
2001	May	–13.4	4.25	0	31	0	0	
2001	June	–0.6	2.8	0.83	30	24	24.8	
2001	July	1.26	1.49	1.33	31	46.5	41.3	
2001	Aug	–0.76	2.67	0.67	31	21.7	20.6	
2001	Sept	–9.76	4.89	0	30	0	0	
					Totals	92.2	86.8	5.4 (5.9%)

Table 5.31 Test of the Braithwaite (1984) degree-day model using the 1951 to 2003 measured data from Alert and Eureka. This test was performed using the σ values listed in Table 5.27.

ALERT

Month	Mean T (°C)	σ	MDD per day	# of days	MDD/month (model)	MDD/month (measured)	Delta
May	–11.55	4.54	0	31	0	0.3	
June	–0.65	3.36	1.0	30	30	34.4	
July	3.58	2.79	3.7	31	114.7	112.5	
Aug	0.92	3.32	1.8	31	55.8	58.5	
Sept	–9.36	4.95	0.1	30	3	1	
				Totals	203.5	206.6	3.1 (1.5%)
May	–11.55	3.79	0	31	0	0.3	
June	–0.65	3.79	1.2	30	36	34.4	
July	3.58	3.79	3.9	31	120.9	112.5	
Aug	0.92	3.79	2	31	62	58.5	
Sept	–9.36	3.79	0	30	0	1	
				Totals	218.9	206.6	12.3 (5.6%)

EUREKA

Month	Mean T (°C)	σ	MDD per day	# of days	MDD/month (model)	MDD/month (measured)	Delta
May	–10.61	5.30	0	31	0	0.65	
June	2.23	3.09	2.6	30	78	86.5	
July	5.63	1.99	5.6	31	173.6	173.3	
Aug	3.05	2.57	3.2	31	99.2	102	
Sept	–7.60	5.27	0.1	30	3	2.1	
				Totals	353.8	364.6	10.8 (3.1%)
May	–10.61	3.65	0	31	0	0.65	
June	2.23	3.65	2.8	30	84	86.5	
July	5.63	3.65	5.7	31	176.7	173.3	
Aug	3.05	3.65	3.5	31	108.5	102	
Sept	–7.60	3.65	0	30	0	2.1	
				Totals	369.2	364.6	4.6 (1.2%)

Table 5.32 Summary of Tests 5 and 6 (cf. Section 5.6.2.2) of the Braithwaite (1984) degree-day model.

Station	Time Period	Mean measured annual MDD totals	Mean modeled annual MDD totals	Mean difference (absolute, relative)
Test 5				
Alert	1951 to 2003	206.6	206.1	13.2 MDD, 6.7%
Eureka	1951 to 2003	364.6	372.2	13.2 MDD, 3.7%
Test 6				
Alert	1951 to 2003	206.6	224.7	22.2 MDD, 13.3%
Eureka	1951 to 2003	364.6	379.5	16.7 MDD, 5.0%

Table 5.33 Summer climate on the Hazen Plateau (AWS G3* and AWS T3*) and on the North Coast of Ellesmere Island (WHI AWS* and WHIRWHIS*), based on the long-term climatologies developed in Section 5.2 (cf. Fig. 5.39, 5.43).

Station	JJA T (°C) Mean	JJA T (°C) Trend (P-value)	July T (°C) Mean	July T (°C) Trend (P-value)
AWS G3*	–1.29	–0.02 (0.06)	1.15	–0.01 (0.55)
AWS T3*	–0.32	–0.02 (0.06)	2.18	–0.01 (0.55)
WHI AWS*	–0.55	0.004 (0.48)	1.00	–0.002 (0.76)
WHIRWHIS*	–1.51	0.004 (0.48)	–0.36	–0.002 (0.76)

Notes

AWS G3* and AWS T3* (1951 to 2001)

- Mean summer (JJA) air temperatures for 1972, 1974, 1993, and 2001 are missing due to missing or unavailable sounding data. Mean July air temperature missing for 1993 due to missing sounding data.

WHI AWS*

- 1951 to 2003 are available for mean summer (JJA) air temperature (climate observations at Alert began July 1950). 1950 to 2003 available for mean July air temperature.

WHIRWHIS*

- 1951 to 2003 available for mean summer (JJA) air temperature (climate observations at Alert began July 1950). 1950 to 2003 available for mean July air temperature. Calculated from WHI AWS* and the monthly ice-cap cooling effect offsets specified in Section 5.5.4: 0°C (May), 0.74±0.42°C (June), 1.36±0.23°C (July), 0.78±0.44°C (August), and 0°C (September).

Table 5.34 Monthly air temperature climatology for the Hazen Plateau (AWS G3* and AWS T3*) and the North Coast (WHI AWS*) (January 1951 to July 2000).

Time Period	AWS G3* (°C)	AWS T3* (°C)	WHI AWS* (°C)	'Ice-cap Cooling Effect' (°C)	'Arctic Ocean Effect' (°C)
January	–28.40	–28.14	–34.18	0.26	–6.04
February	–29.20	–28.96	–35.08	0.24	–6.12
March	–28.36	–28.10	–34.49	0.26	–6.39
April	–22.23	–21.81	–26.40	0.42	–4.59
May	–13.35	–12.70	–12.19	0.65	0.51
June	–3.69	–2.78	–1.89	0.91	0.89
July	1.15	2.18	1.00	1.03	–1.18
August	–1.51	–0.55	–0.77	0.96	–0.22
September	–10.00	–9.26	–10.03	0.74	–0.77
October	–18.59	–18.07	–20.91	0.51	–2.84
November	–23.67	–23.29	–28.33	0.38	–5.04
December	–27.16	–26.87	–32.00	0.29	–5.13
Winter (DJF)	–28.11	–27.85	–33.78	0.26	–5.93
Spring (MAM)	–21.31	–20.87	–24.36	0.44	–3.49
Summer (JJA)	–1.29	–0.32	–0.55	0.97	–0.23
Fall (SON)	–17.52	–16.86	–19.76	0.66	–2.90
Annual (MAT)	–17.00	–16.45	–19.61	0.55	–3.16

Notes

- Monthly means were calculated from 1951 to 2000 (i.e. using only the full years available, the 2001 Alert sounding data are only available until July 2001).
- Seasonal and annual means only calculated when complete monthly data for a given season or year were available.
- Notation AWS G3*, AWS T3*, WHI AWS* is used to indicate modeled air temperatures (as opposed to measured temperatures).
- WHI AWS* data include the period from July 1950 to August 2003, but here only data from January 1951 to July 2000 were used to facilitate comparison with the available AWS G3* and AWS T3* data.
- 'Ice-cap cooling effect' = AWS T3* minus AWS G3*.
- 'Arctic Ocean Effect' = WHI AWS* minus AWS T3*.

Table 5.35 Annual melting degree-day totals for AWS G3*, AWS T3*, WHI AWS*, and WHIRWHIS* (cf. Section 5.7.1.7).

Record	Mean (SD)	Trend (P-value)	Length
AWS G3*	115.5 (51.6)	–0.89 (0.08)	1951 to 2000
AWS T3*	165.3 (63.0)	–1.17 (0.06)	1951 to 2000
WHI AWS*	76.7 (23.1)	0.11 (0.61)	1951 to 2003
WHIRWHIS*	40.9 (15.4)	0.09 (0.50)	1951 to 2003

Notes

AWS G3* and AWS T3*

- Annual melting degree-day totals for 1972, 1974, 1993, and 2001 are missing due to missing or unavailable sounding data.

WHI AWS*

- Annual melting degree-day totals are available from 1951 to 2003.

WHIRWHIS*

- Annual melting degree-day totals are available from 1951 to 2003. Calculated from WHI AWS* and the monthly ice-cap cooling effect offsets specified in Section 5.5.4: 0°C (May), 0.74±0.42°C (June), 1.36±0.23°C (July), 0.78±0.44°C (August), and 0°C (September).

Table 5.36 Comparison between measured and modeled annual melting degree-day totals (cf. Section 5.7.1.7).

	Measured	Modeled	Difference
AWS G3* (σ = 3.7°C)			
Ann MDD total (1999)	121.0	139.4	+18.4 (+15%)
Ann MDD total (2000)	118.8	107.3	–11.5 (–10%)
June/July MDD total (2001)	106.3	104.5	–1.8 (–2%)
AWS T3* (σ = 4.0°C)			
Ann MDD total (1999)	173.7	185.9	+12.2 (+7%)
Ann MDD total (2000)	169.6	156.3	–13.3 (–8%
June/July MDD total (2001)	155.6	147.4	–8.2 (–5%)
WHI AWS* (σ = 2.2°C)			
Ann MDD total (1996)	48.1	55.5	+7.4 (+15%)
Ann MDD total (2001)	86.8	77.1	–9.7 (–11%)

Notes

- Measured annual melting degree-day totals were determined directly from the actual mean daily air temperature measurements at the automatic weather stations.
- Modeled annual melting degree-day totals were determined from mean monthly air temperatures calculated using transfer functions (Section 5.2) and the Braithwaite (1984) melting degree-day model (Section 5.6).

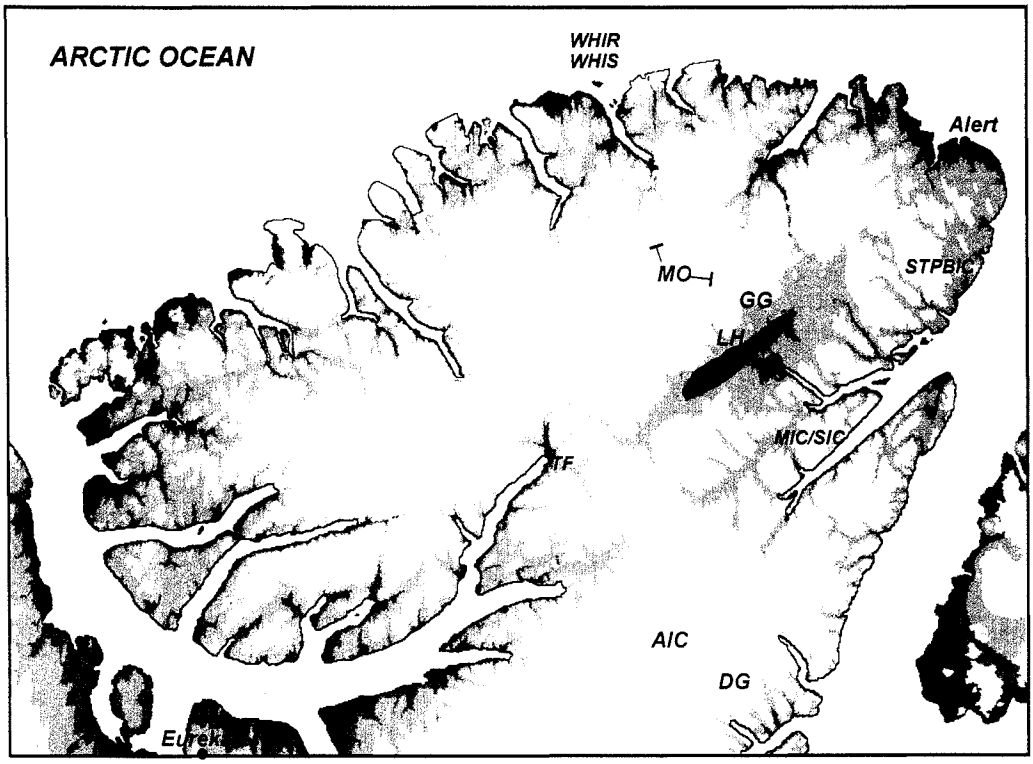

Figure 5.1 Generalized location map of northern Ellesmere Island, showing some of the locations mentioned in Chapter 5 and Table 5.10. TF = Tanquary Fjord; AIC = Agassiz Ice Cap (#9, 10, 12); DG = Drambuie Glacier; MIC/SIC = Murray and Simmons Ice Cap; STPBIC = St. Patrick Bay ice caps; LH = Lake Hazen; GG = Gilman Glacier; MO = Mt. Oxford area (#11, 19); WHIR, WHIS = Ward Hunt Ice Rise and Ice Shelf. Locations are only approximate. White colors delineate the generalized extent of glaciers and ice caps, the other colors denote generalized elevation zones.

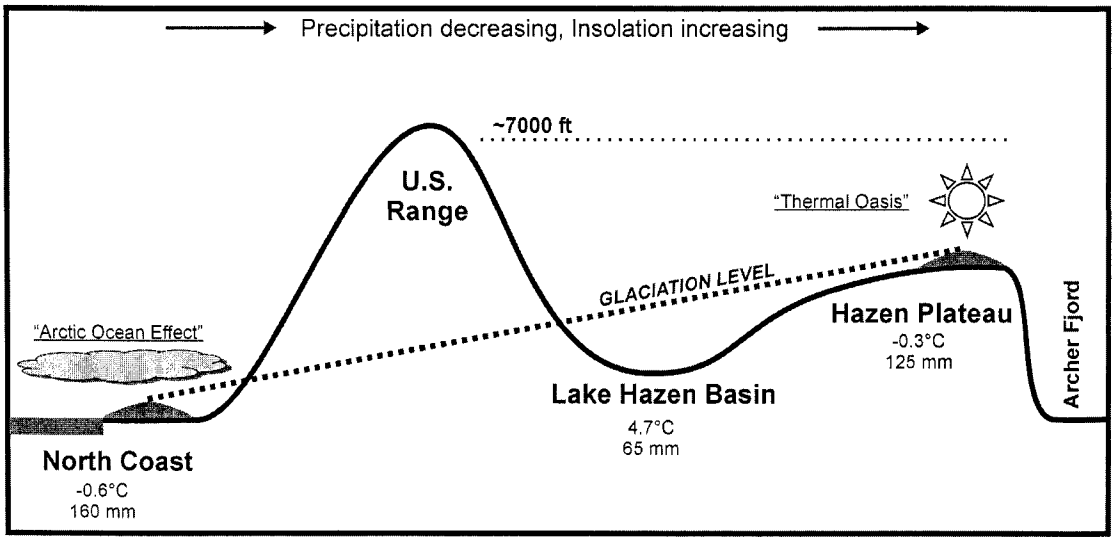

Figure 5.2 Schematic cross-section of northern Ellesmere Island (horizontal distance ~220 km; maximum elevation ~2300 m asl or 7500 ft). The thick dotted line depicts the generalized glaciation-level gradient (after Miller *et al.*, 1975; their data based on topographic maps constructed from 1959 aerial photographs). The 'Arctic Ocean Effect' (i.e. frequent low stratus/fog conditions), leading to reduced ablation and increased accumulation, is limited only to the immediate coastal fringe (Braun *et al.*, 2004b). In contrast, the interior highlands (e.g. the Hazen Plateau) experience a much more continental summer climate ('Thermal Oasis') (Braun *et al.*, 2004a). See Figure 2.6 or Chapter 5 for a description of the Hazen Plateau and North Coast climate data shown. Lake Hazen summer air temperature data from Parks Canada AWS (1989 to 1996 mean); annual precipitation value after Jackson (1959) and Hattersley-Smith (1960b). The thin dotted line depicts the 7000 ft 'threshold' elevation, above which with characteristic localized topographic-climatic effects around Lake Hazen diminish (Jackson, 1965).

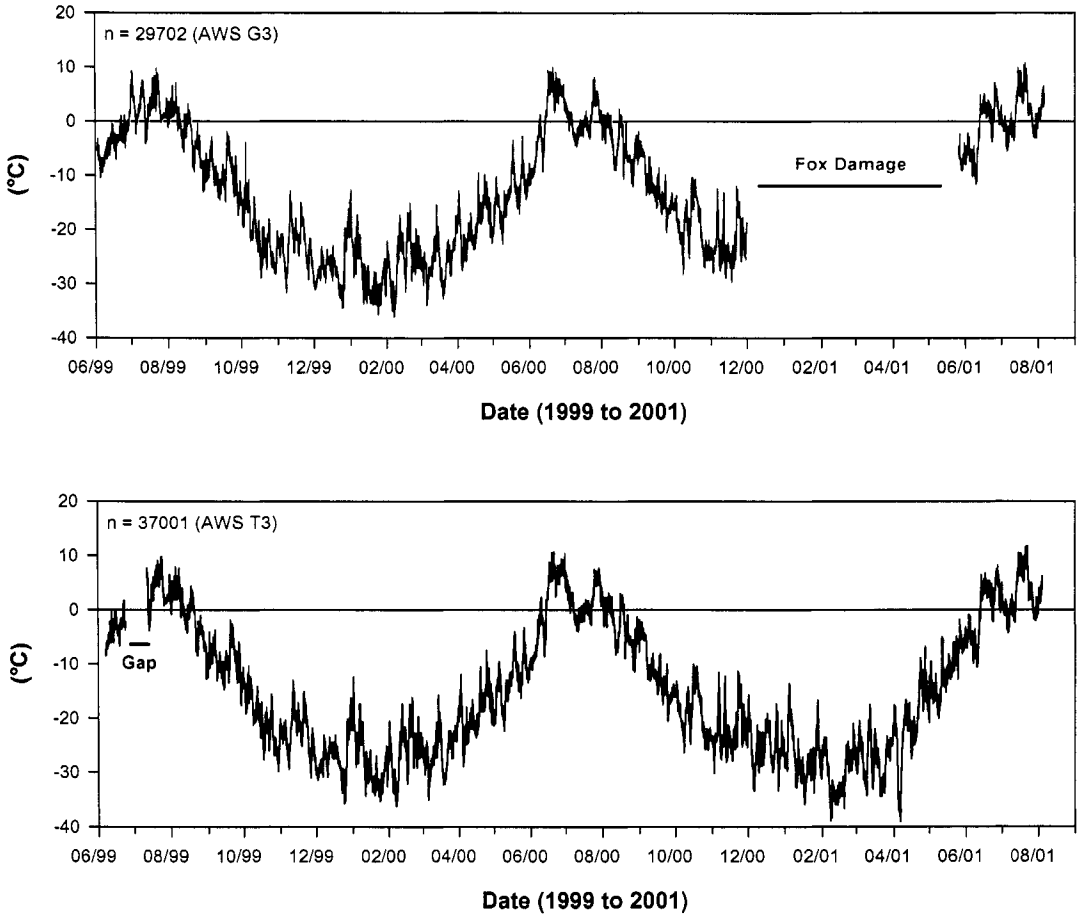

Figure 5.3 Time series of raw half-hourly air temperatures measured at AWS G3 (top) and AWS T3 (bottom) (1999 to 2001). Note the gaps in both time series (cf. Tables 5.1 and 5.2).

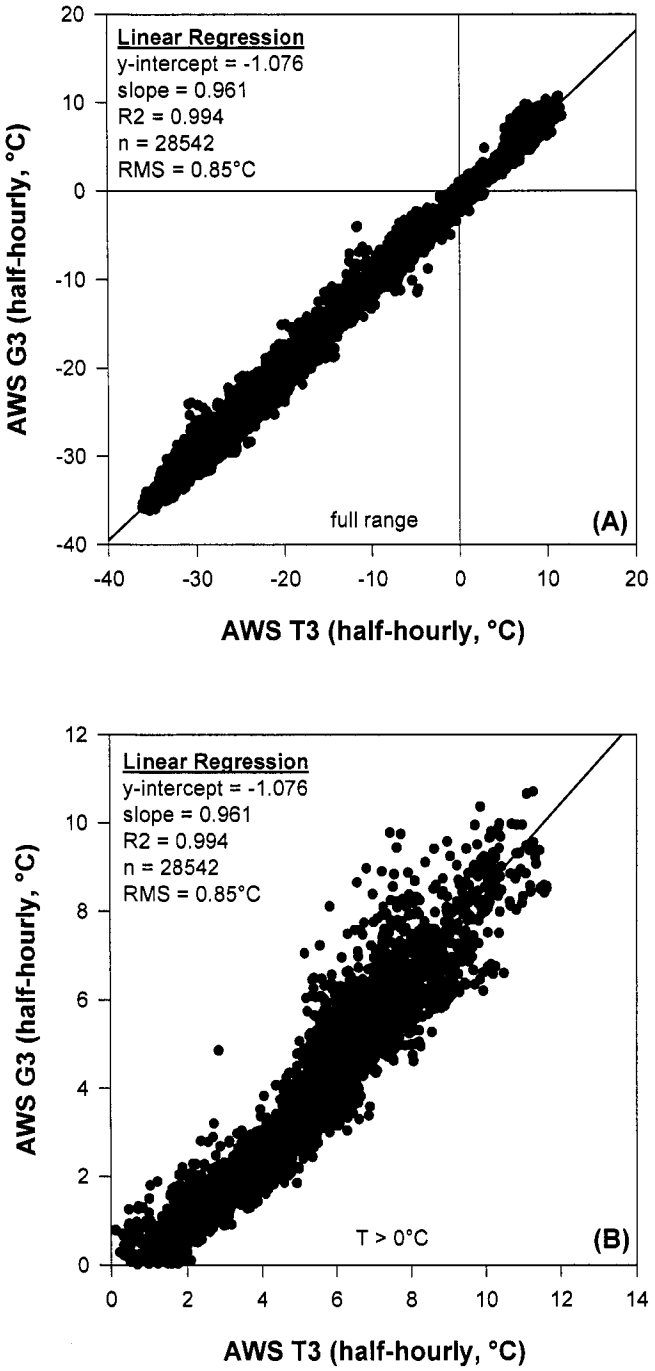

Figure 5.4 Scatter plots of all raw half-hourly air temperatures measured at AWS G3 plotted against the corresponding measurements at AWS T3 (1999 to 2001) with linear regression lines: (A) Full range of recorded values; (B) only showing half-hourly air temperatures above freezing. Note: this figure uses the un-patched AWS T3 record (cf. Section 5.2.1). The regression equation shown in (A) and (B) was calculated for the full range of recorded values.

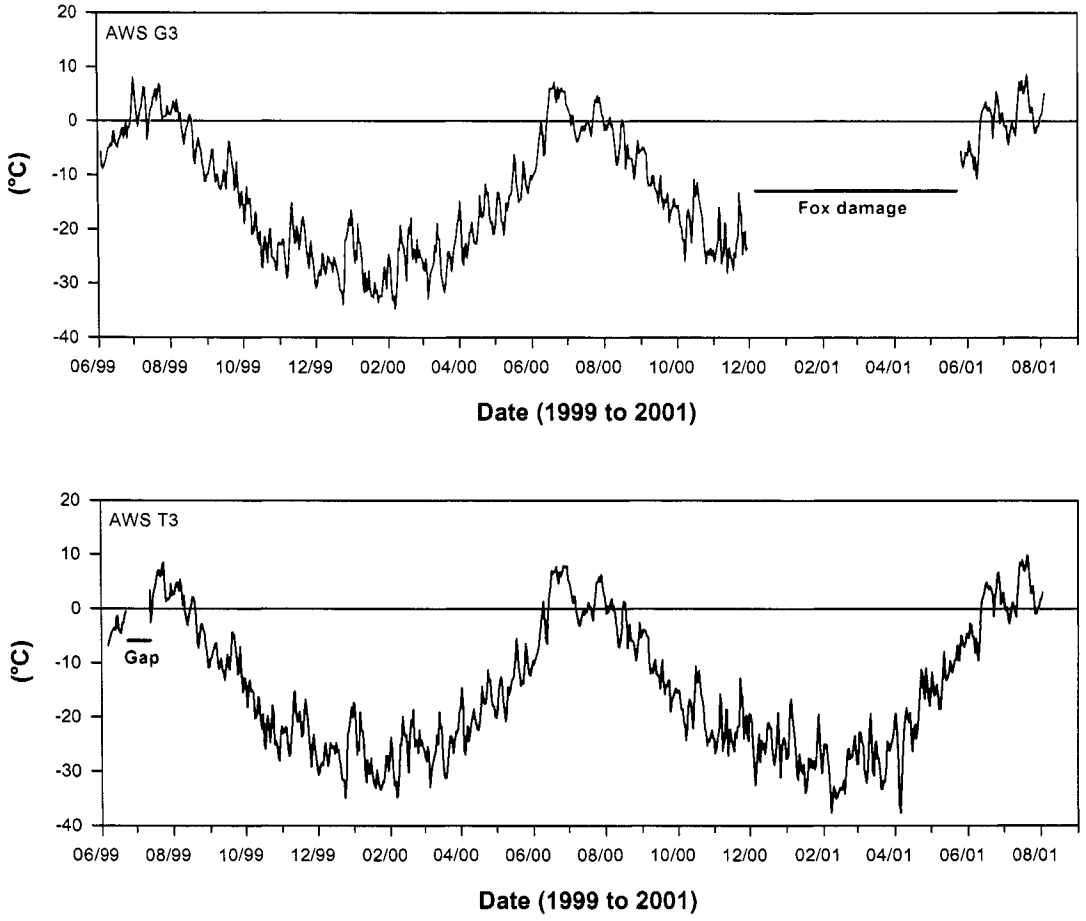

Figure 5.5 Time series of mean daily air temperatures measured at AWS G3 (top) and AWS T3 (bottom) (1999 to 2001). Note the gaps in both time series (cf. Tables 5.1 and 5.2).

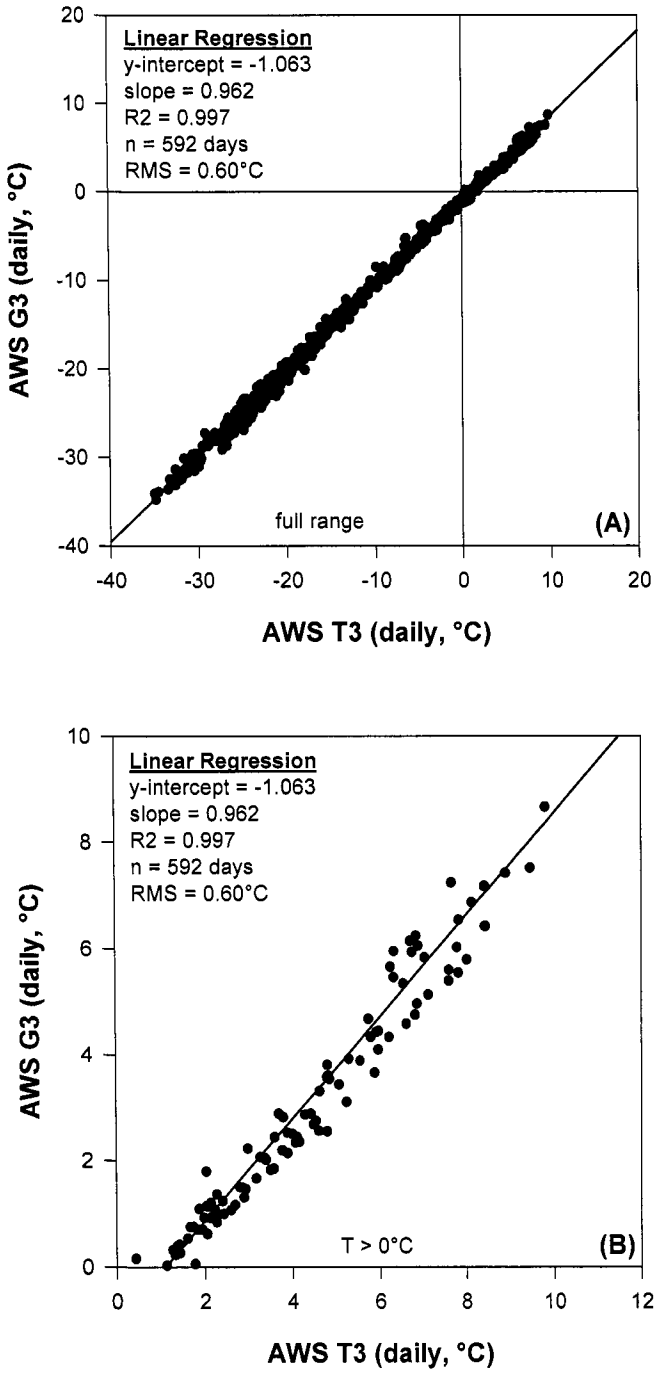

Figure 5.6 Scatter plots of mean daily air temperatures measured at AWS G3 plotted against the corresponding air temperature measurements at AWS T3 (1999 to 2001) with linear regression lines: (A) Full range of values; (B) only showing daily air temperatures above freezing. Note: this figure also uses the un-patched AWS T3 record (cf. Section 5.2.1). The regression equation shown in (A) and (B) was calculated for the full range of recorded values.

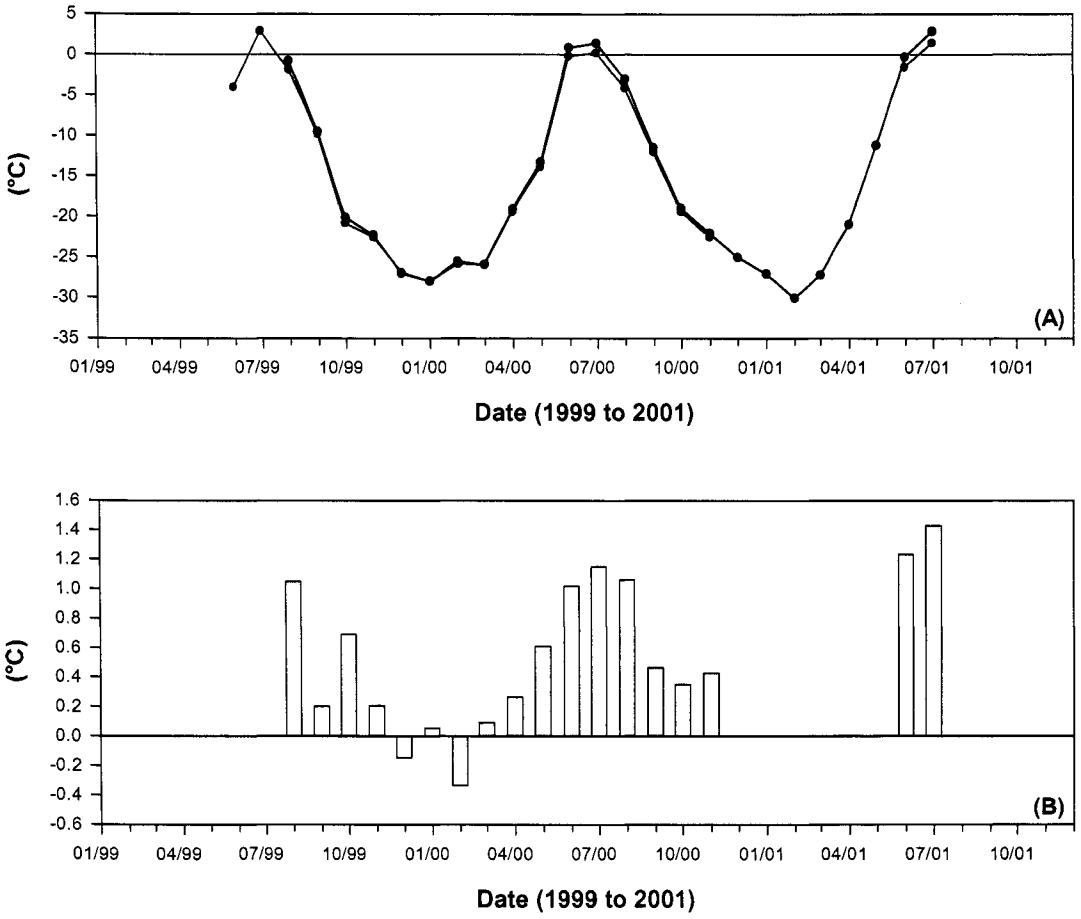

Figure 5.7 (A) Mean monthly air temperatures measured at AWS G3 (blue) and AWS T3 (red). (B) The (AWS T3 minus AWS G3) monthly air temperature difference (1999 to 2001).

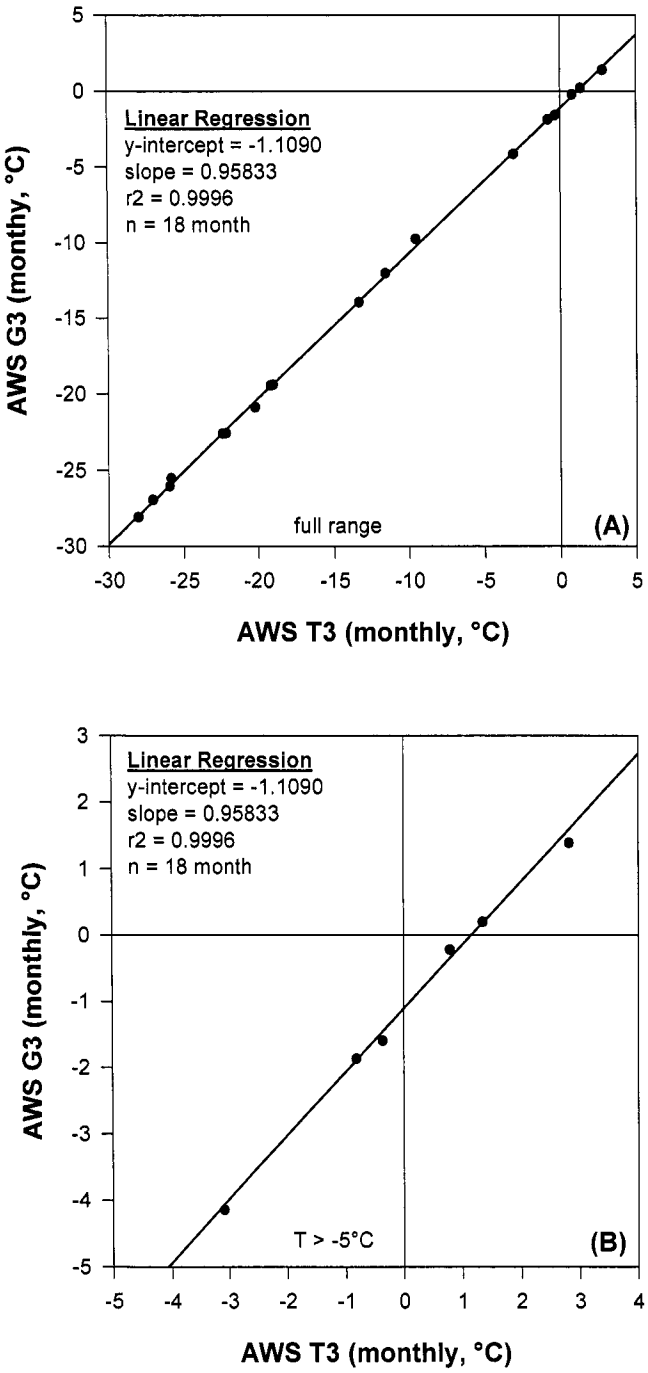

Figure 5.8 Scatter plots of corresponding mean monthly air temperatures measured at AWS G3 and AWS T3 (n = 18 months; AWS T3 record not patched, i.e. this figure does not include values for June and July 1999). (A) Full range of values; (B) only showing monthly air temperatures above –5°C (1999 to 2001). The regression equation shown in (A) and (B) was calculated for the full range of recorded values.

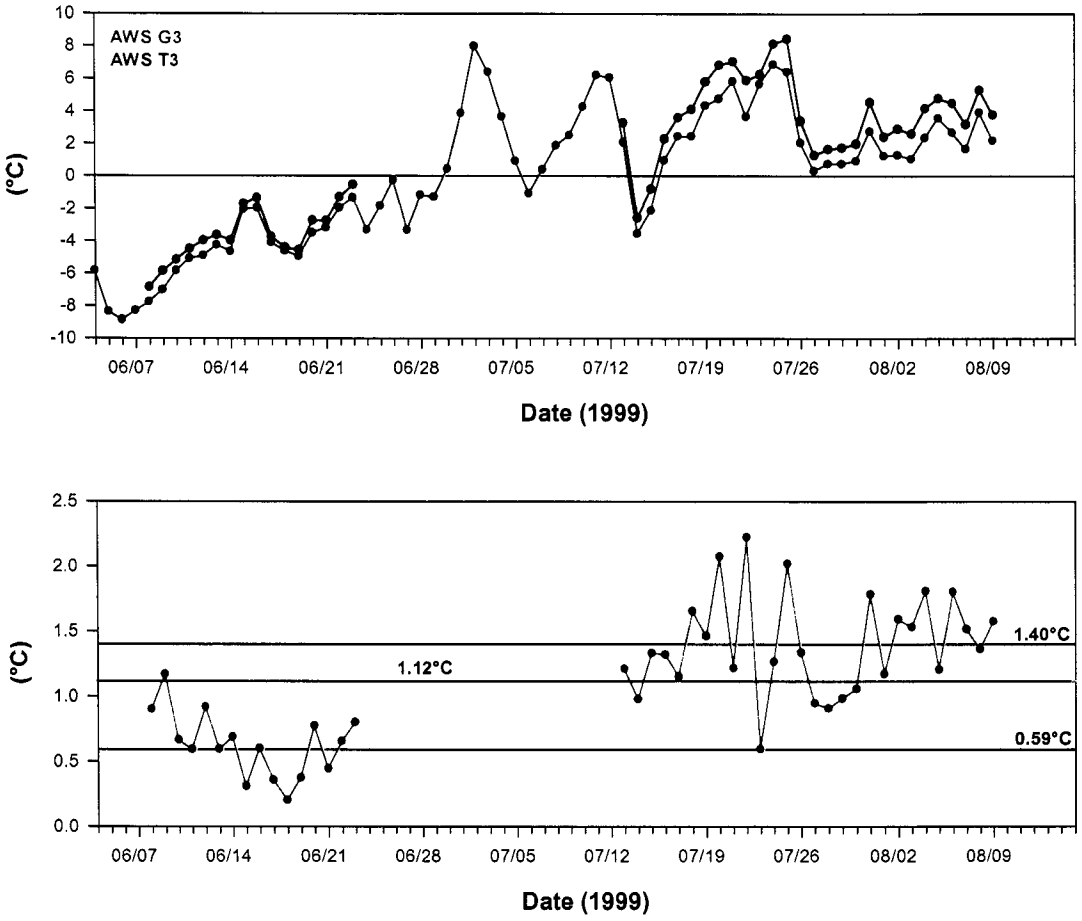

Figure 5.9 (A) Mean daily air temperatures measured at AWS G3 and AWS T3 from 4 June to 9 August 1999; (B) Air temperature difference between the two stations (i.e. AWS T3 minus AWS G3) (for 'patching' the AWS T3 record, cf. Section 5.2.1). The green horizontal line marks the mean air temperature difference (1.12°C, 4 June to 9 August), the two black horizontal lines denote the 'snow cover offset' (0.59°C) and the 'snow-free offset' (1.40°C) (cf. Section 5.2.1).

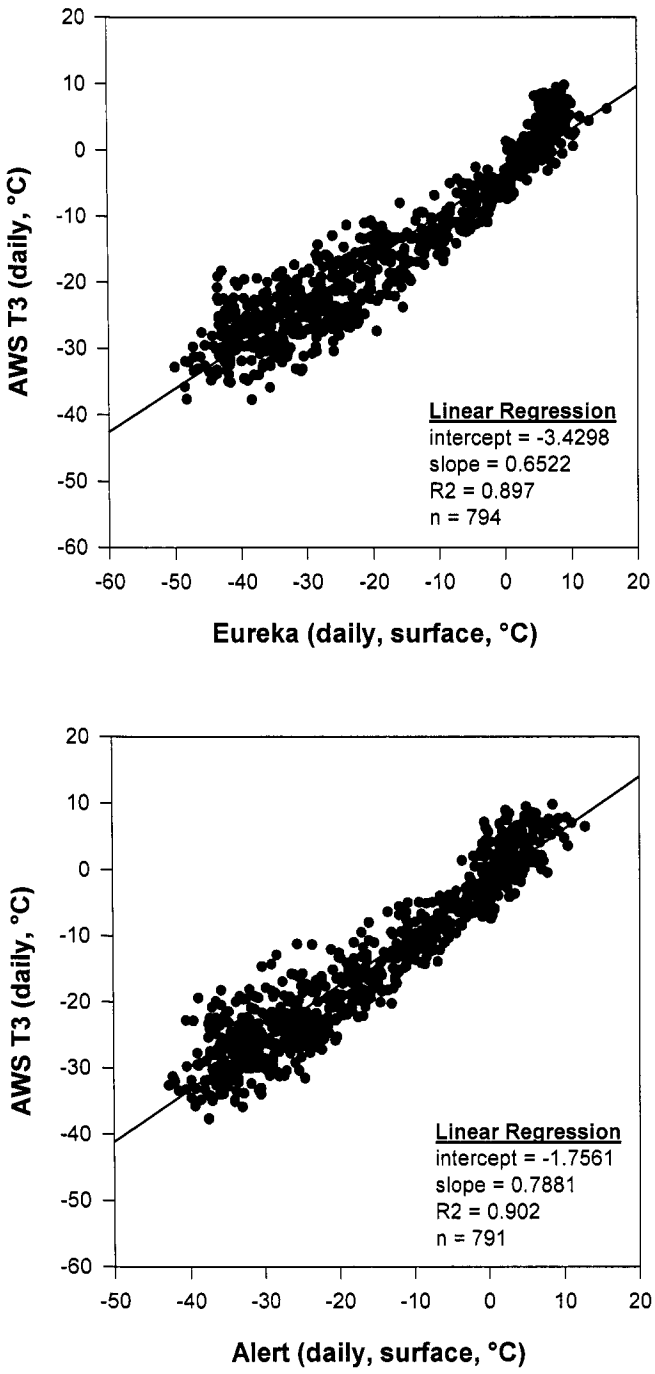

Figure 5.10 Scatter plots with linear regression line for AWS T3 vs. Eureka (top) and Alert (bottom) – using the mean daily surface temperatures from Eureka and Alert (using the patched AWS T3 record).

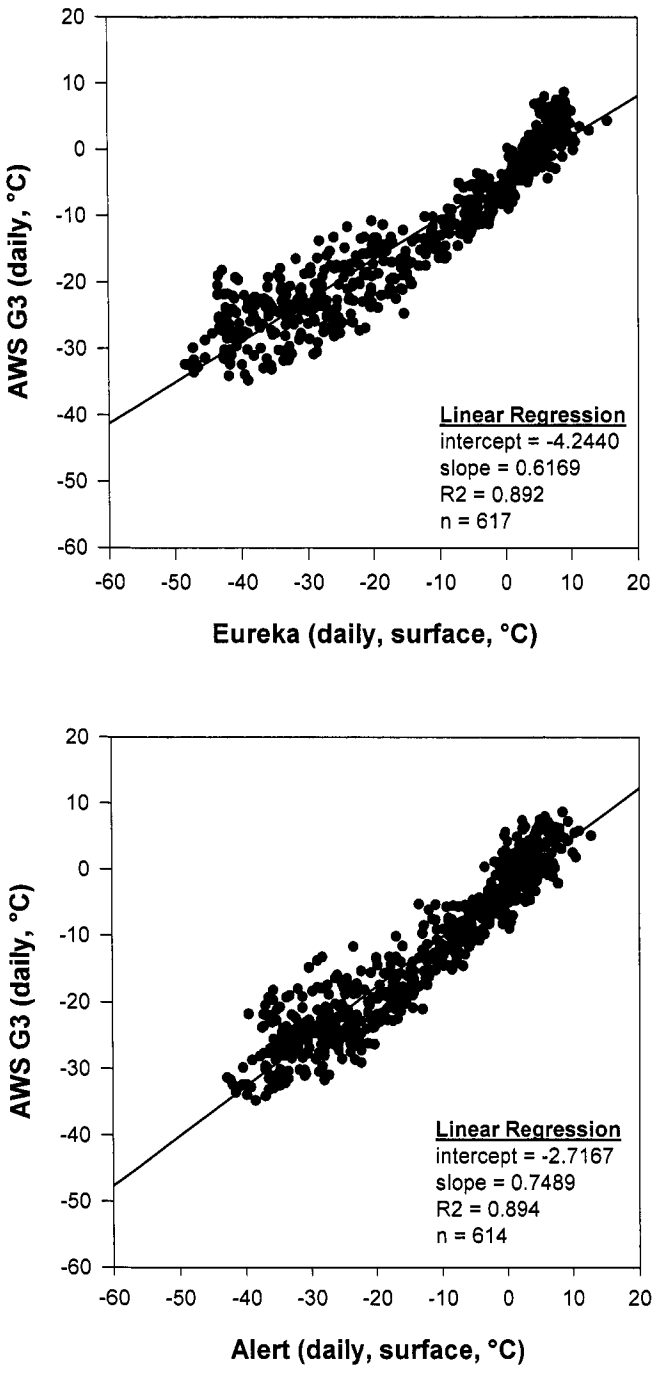

Figure 5.11 Scatter plots with linear regression line for AWS G3 vs. Eureka (top) and Alert (bottom) – using the mean daily surface temperatures from Eureka and Alert.

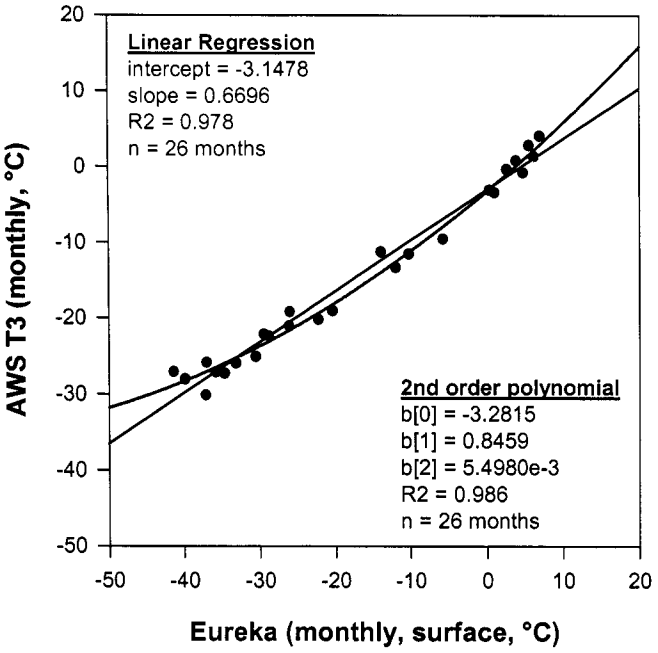

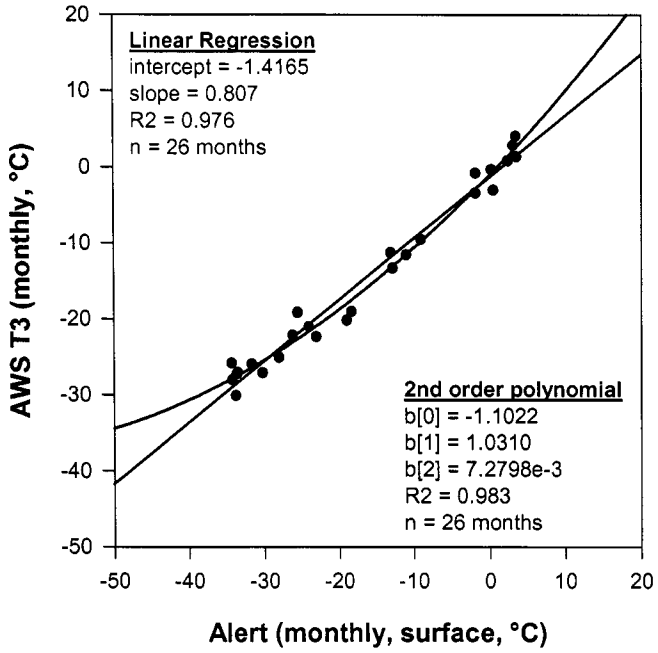

Figure 5.12 Scatter plots with linear regression line and 2nd order polynomial for AWS T3 vs. Eureka (top) and Alert (bottom) – using the mean monthly surface temperatures from Eureka and Alert (using the patched AWS T3 record).

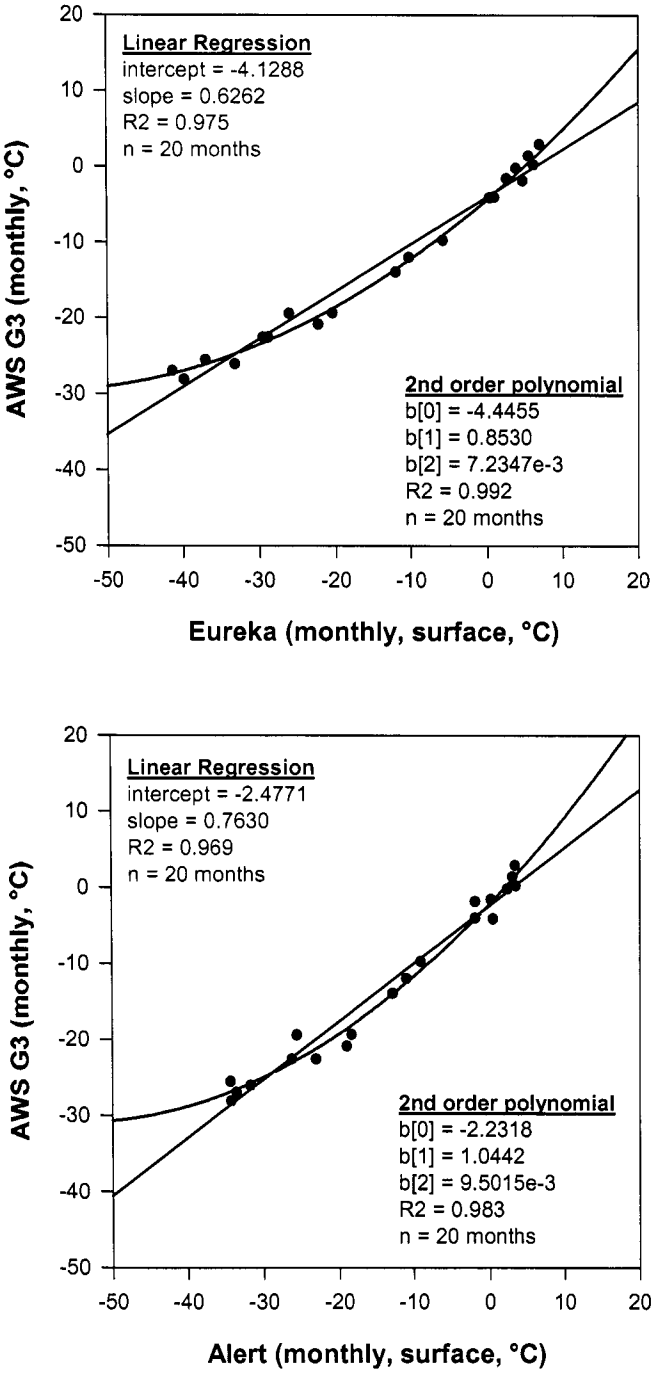

Figure 5.13 Scatter plots with linear regression line and 2nd order polynomial for AWS G3 vs. Eureka (top) and Alert (bottom) – using the mean monthly surface temperatures from Eureka and Alert.

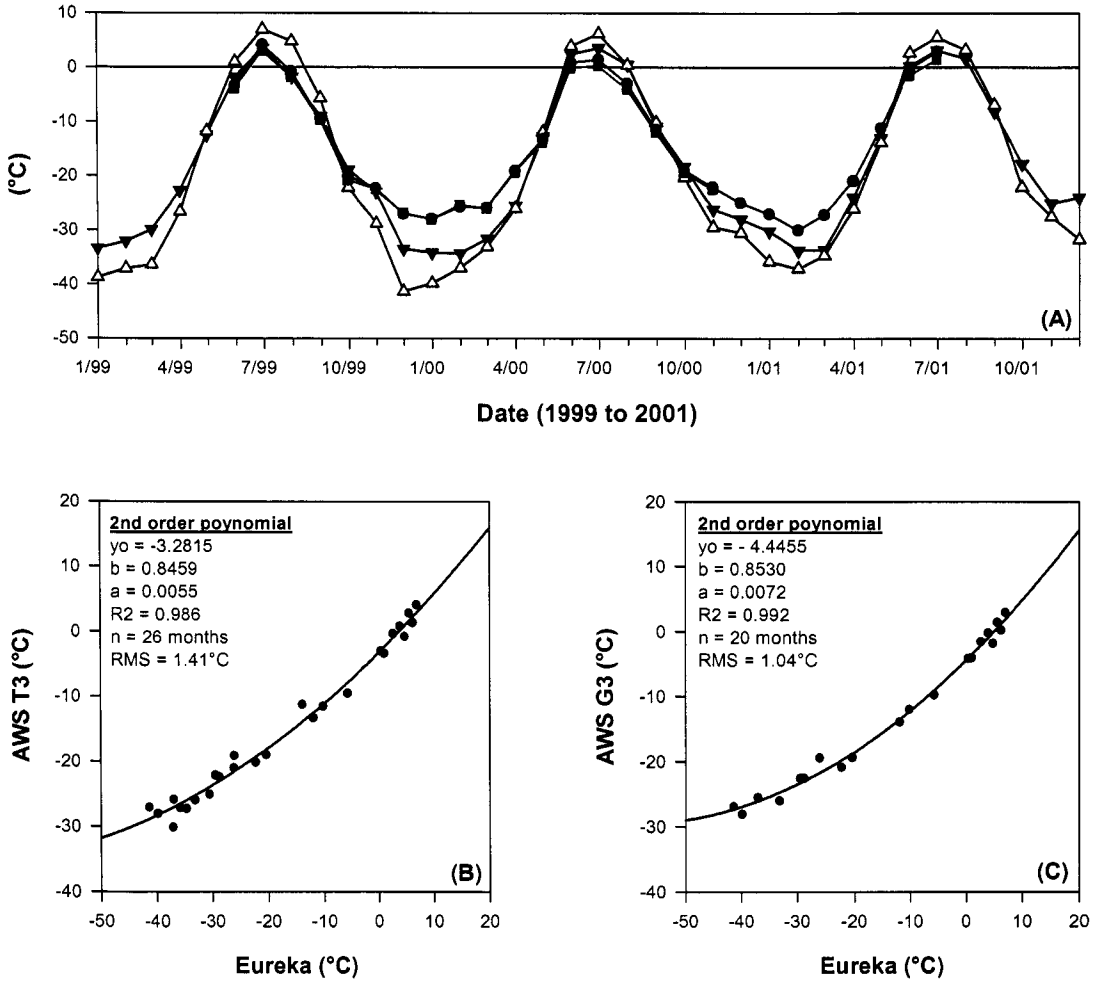

Figure 5.14 Summery graph of the mean monthly surface air temperature data comparison (cf. Section 5.2.2). (A) The four monthly time series (AWS T3, AWS G3, Eureka, and Alert); (B) AWS T3 vs. Eureka; (C) AWS G3 vs. Eureka. The two scatter plots show the 2nd-order polynomial regression line and associated statistical fit parameters (cf. Table 5.6). Legend: red: AWS T3; blue: AWS G3; solid triangle (down): Alert; open triangle (up): Eureka.

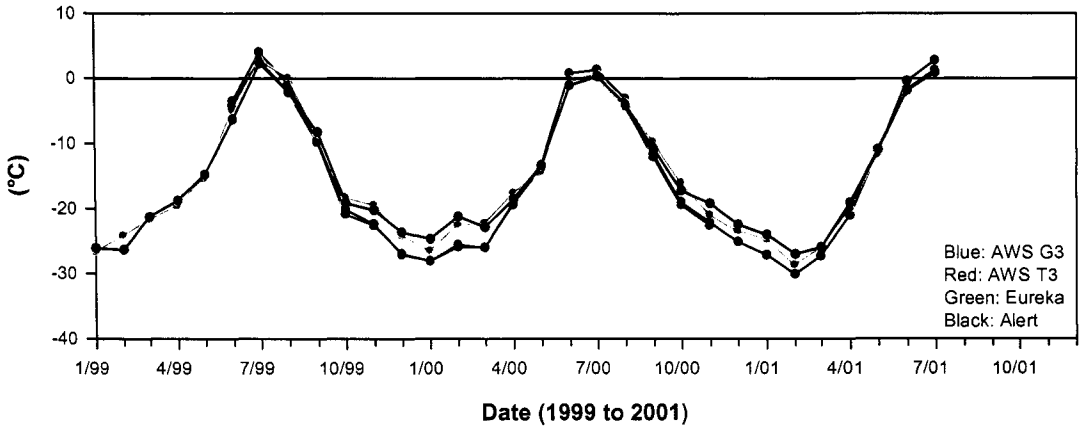

Figure 5.15 Time series of mean monthly air temperature (1999 to 2001) measured at AWS G3 (blue) and AWS T3 (red) and the mean monthly sounding air temperatures at 1100 m asl above Alert (black) and Eureka (green) (available from January 1951 to July 2001 using the CARDS data set).

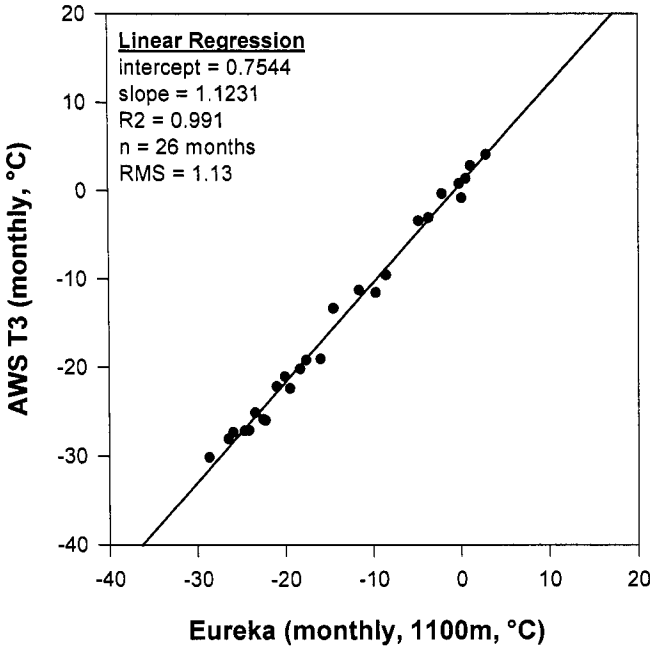

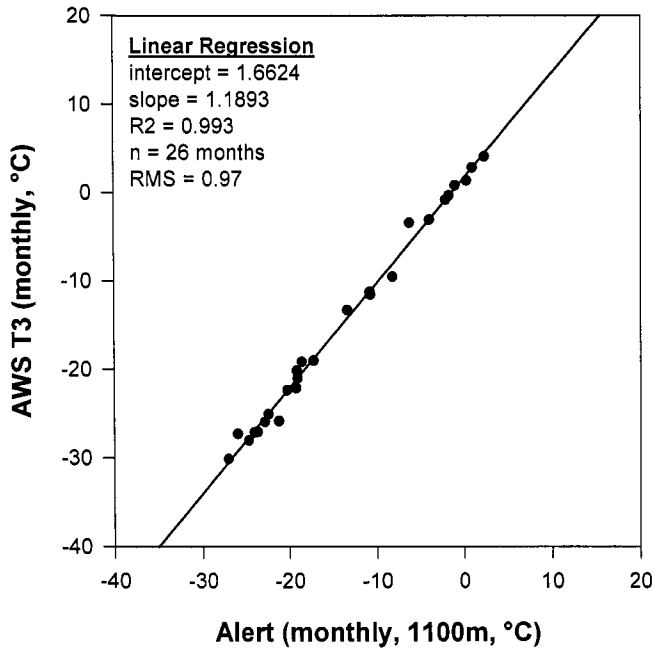

Figure 5.16 Scatter plots with linear regression lines for AWS T3 vs. Eureka (top) and Alert (bottom) – using the mean monthly 1100 m asl sounding temperatures from Eureka and Alert (using the patched AWS T3 record).

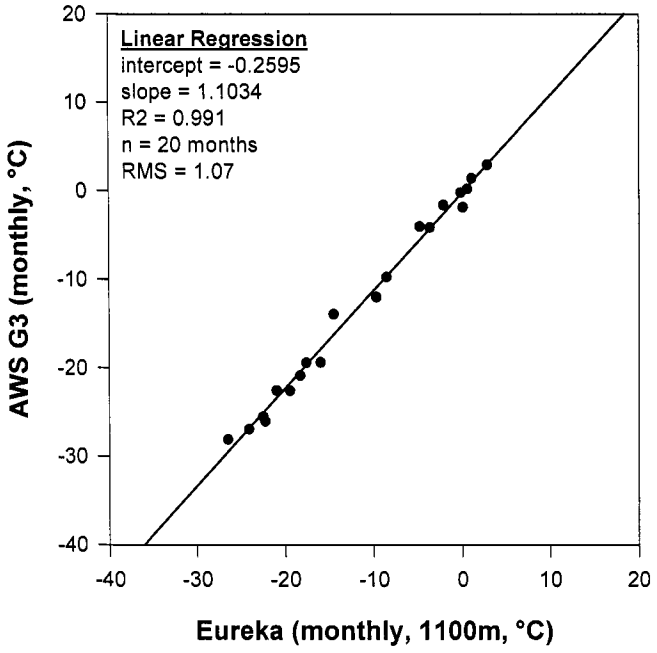

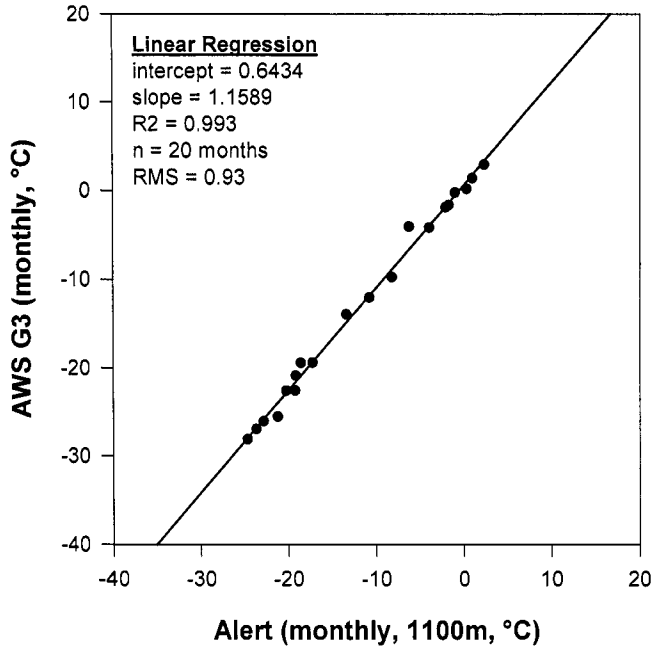

Figure 5.17 Scatter plots with linear regression lines for AWS G3 vs. Eureka (top) and Alert (bottom) – using the mean monthly 1100 m asl sounding temperatures from Eureka and Alert.

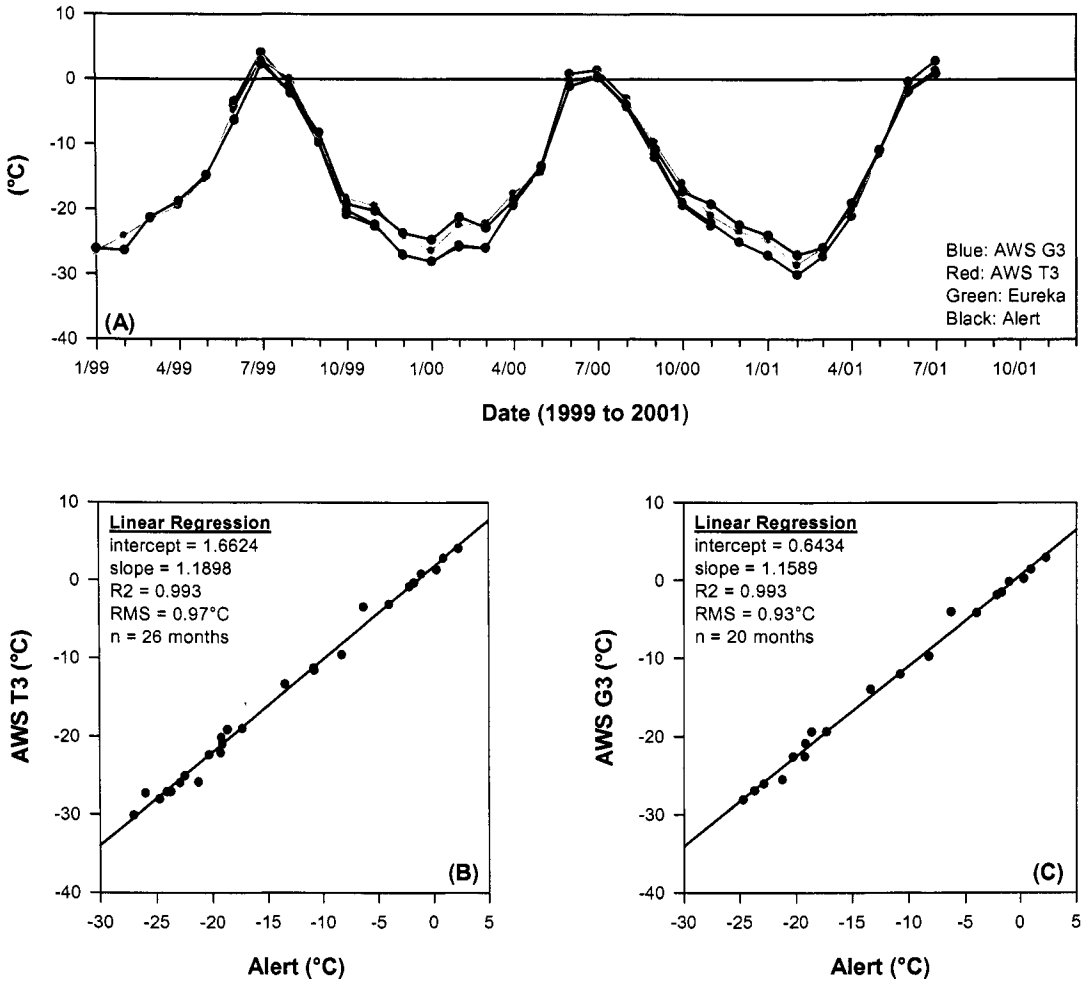

Figure 5.18 Summery graph of the mean monthly upper-air data (1100 m asl) comparison (cf. Section 5.2.2). (A) The four time series (AWS T3, AWS G3, Eureka, and Alert); (B) AWS T3 vs. Eureka; (C) AWS G3 vs. Eureka. The two scatter plots show the linear regression line and associated statistical fit parameters (cf. Table 5.8).

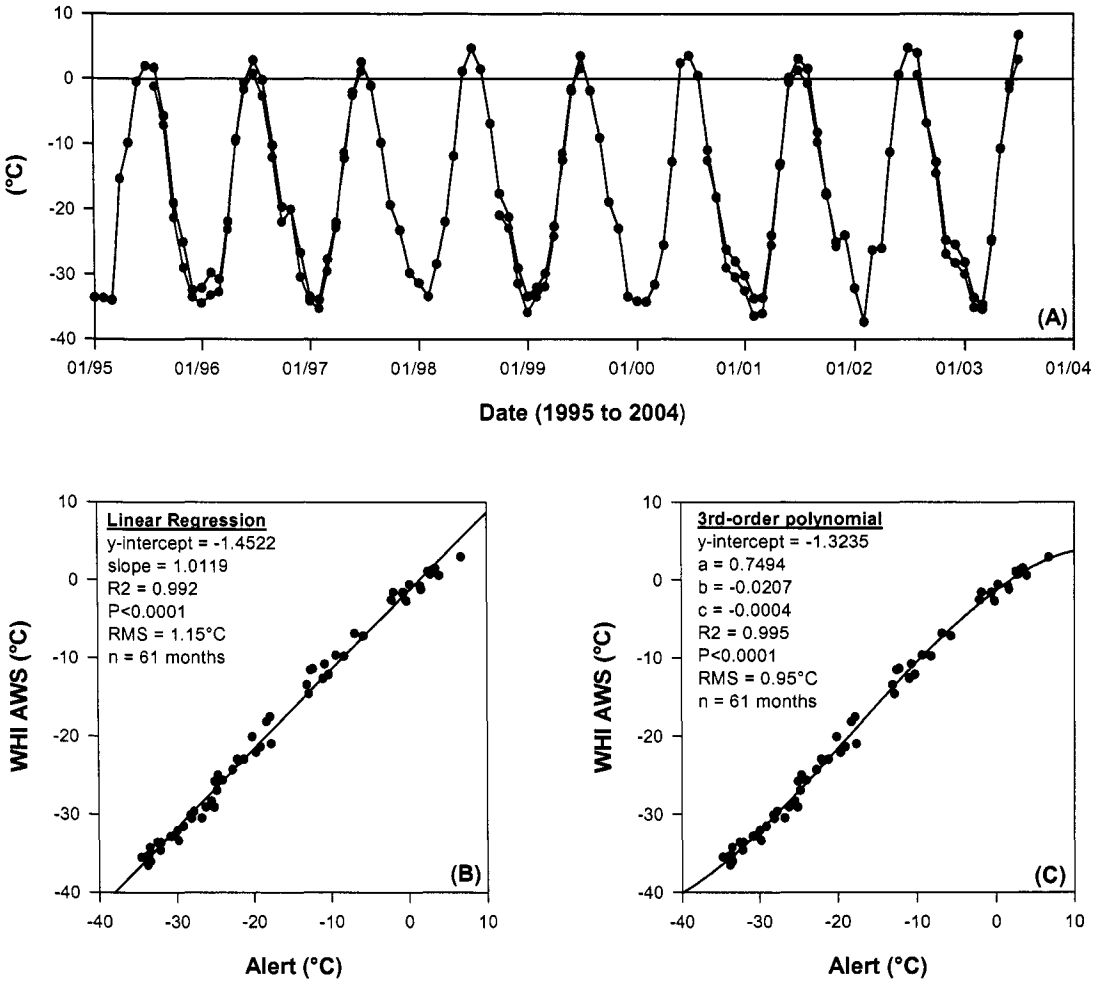

Figure 5.19 Summery graph for the North Coast of Ellesmere Island (cf. Section 5.2.3). (A) Mean monthly air temperature on Ward Hunt Island (red) and at Alert (black) from 1995 to 2003; (B) and (C) scatter plots of monthly air temperature on Ward Hunt Island vs. corresponding measurements at Alert, showing the two different regression equations.

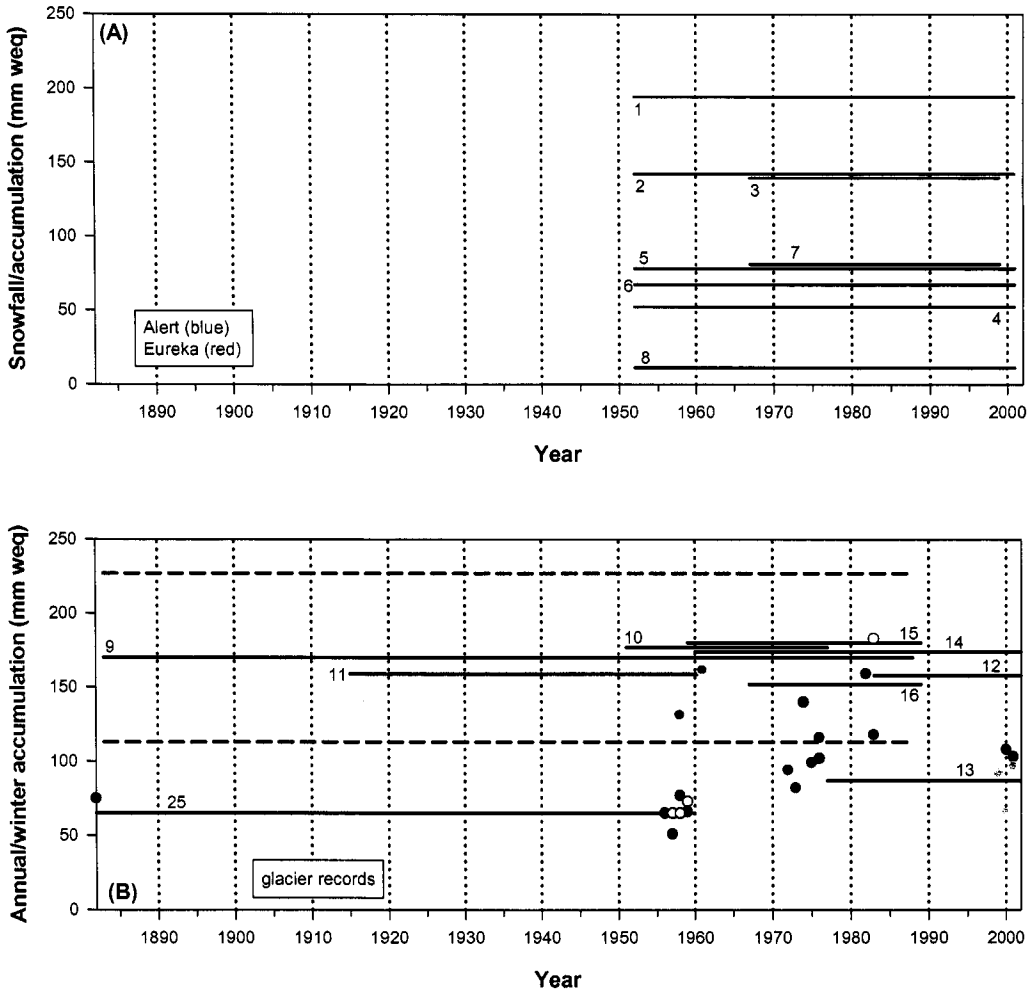

Figure 5.20 Snowfall and snow accumulation records from northern Ellesmere Island, Canada. Numbers on the graph refer to the records listed in Table 5.10. Shown are only the long-term means of the records (for clarity). (A) Instrumental data from Alert (blue) and Eureka (red). (B) Snow accumulation data from glaciers and ice caps on northern Ellesmere Island. Also shown (grey rectangle) are the subjective estimates of regional precipitation (records #22 to 24 in Table 5.10). Red circle: Lake Hazen; White Circle: Gilman Glacier; Green Circle: Mt. Oxford, Gilman, and Disraeli Glacier; Blue solid circle: St. Patrick Bay Ice Cap (NE); Blue open circle: St. Patrick Bay Ice Cap (SW); Pink circle: Simmons Ice Cap; Cyan circle: Murray Ice Cap. The two dashed lines denote the ±1 standard deviation envelope for record #9.

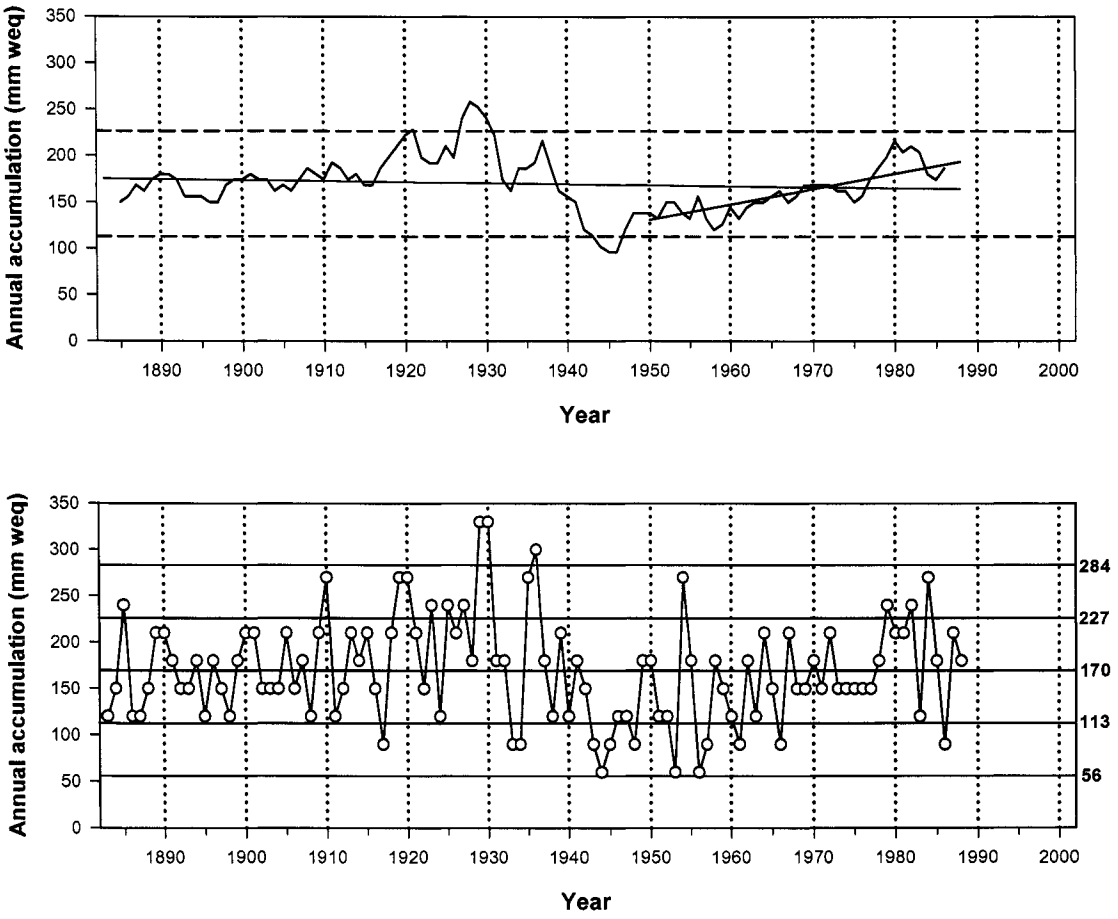

Figure 5.21 Snow accumulation on northern Ellesmere Island between 1883 and 1988 from the Agassiz Ice Cap snow pit/core from 1989 (Fisher and Koerner, 1994). (A): 5-year running mean in black; 1883 to 1988 linear trend in blue; and 1950 to 1988 linear trend in red. Dashed lines denote the ±1 standard deviation envelope. (B): Annual values plotted with the long-term mean (170 mm weq; black line) and ±1 standard envelope (113 to 227 mm weq; red line) and ±2 standard deviation envelope (56 to 284 mm weq; blue line).

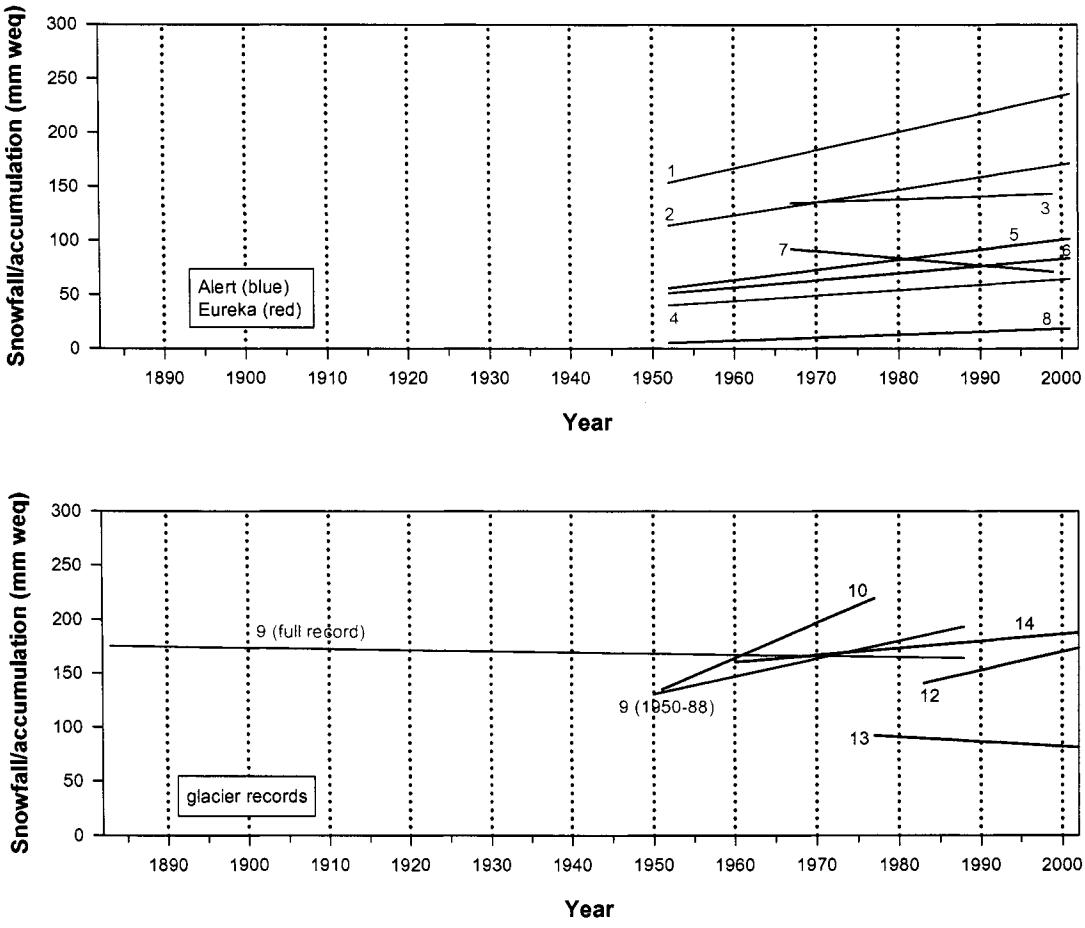

Figure 5.22 Snowfall and snow accumulation trends (Table 5.10) on northern Ellesmere Island for the last ~100 years. Numbers shown on the graph refer to the records listed Table 5.10. (A) Instrumental records from Alert (blue) and Eureka (red); (B) Selected long-term and more continuous snow accumulation records from glaciers.

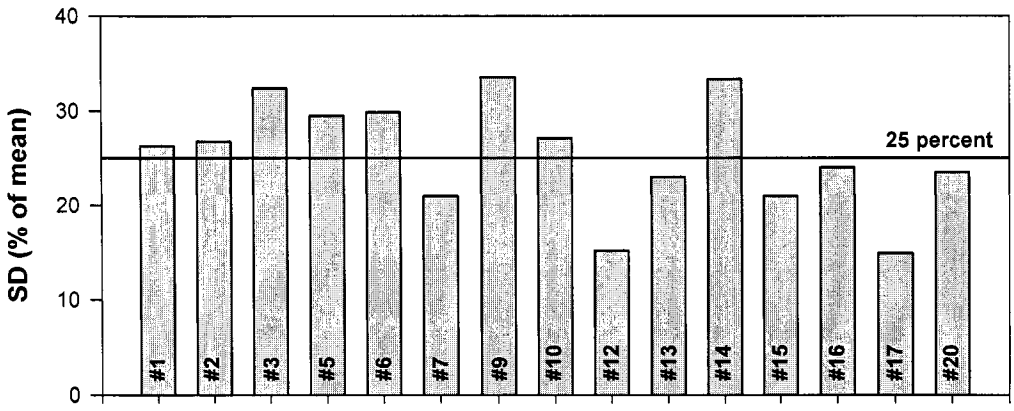

Figure 5.23 Standard deviation of the available long-term (annual) records, expressed as percentage of the corresponding mean (see Table 5.10 and 5.11 for a description of the records shown).

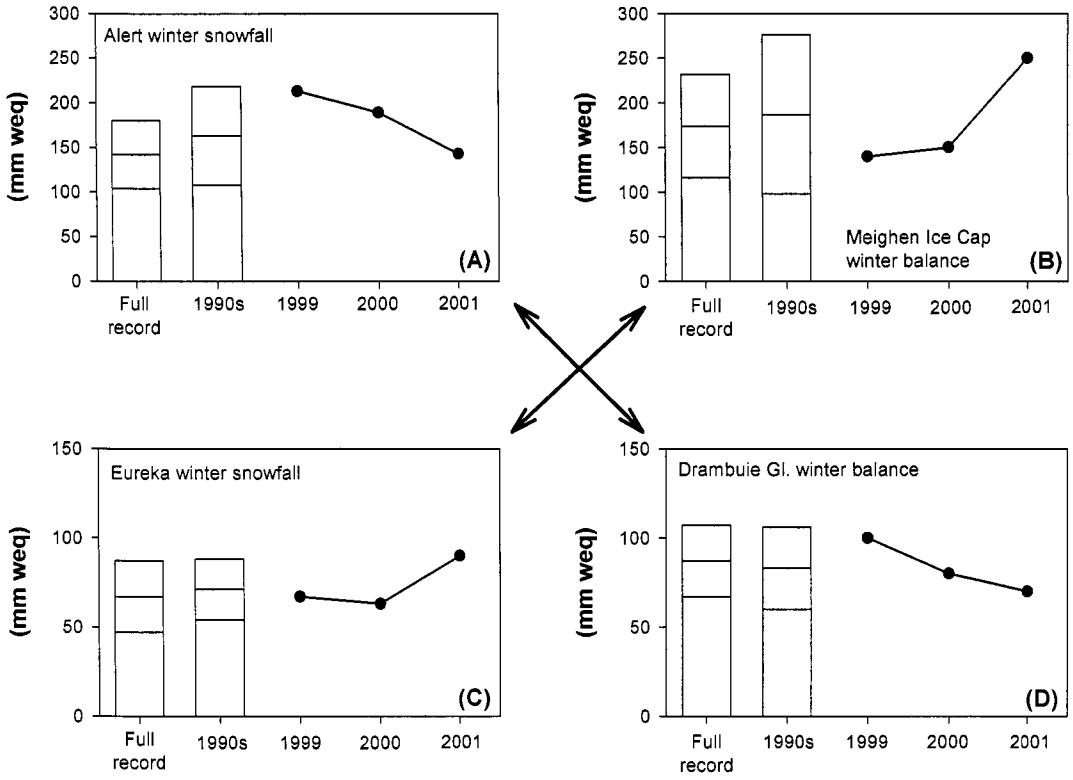

Figure 5.24 Snowfall and snow accumulation for 1999, 2000, and 2001 in the context of the last decade (1991 to 2000) and the full available record (cf. Table 5.10 and 5.12). (A) Alert winter snowfall, (B) Meighen Ice Cap winter mass balance, (C) Eureka winter snowfall, (D) Drambuie Glacier winter mass balance. The middle line in each vertical bar denotes the mean for the respective time period, the two lines above and below mark the ±1 standard deviation envelope.

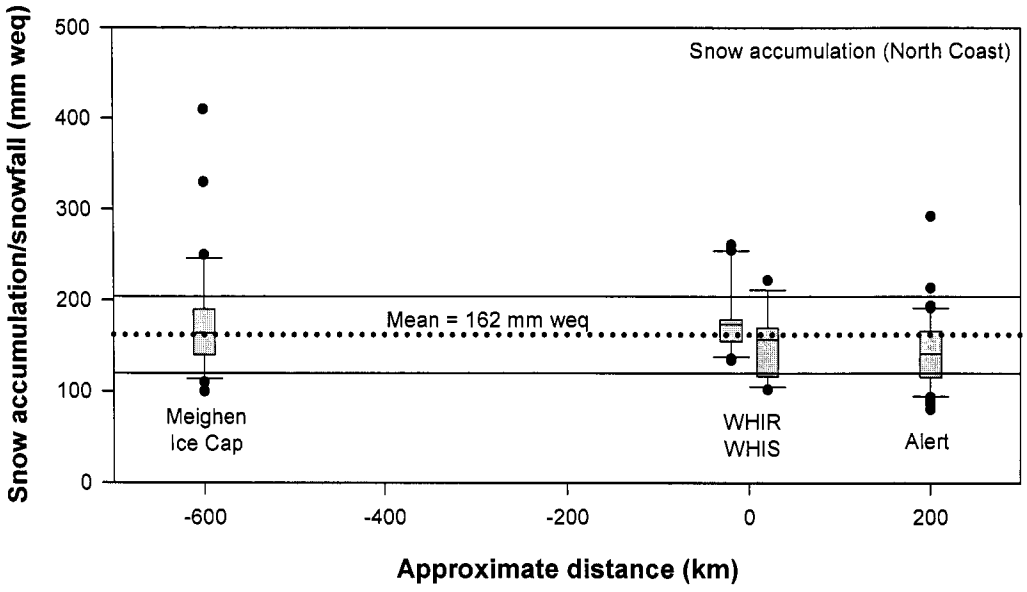

Figure 5.25 Box-Whisker plots of winter snow accumulation (Meighen Ice Cap, Ward Hunt Ice Rise, and Ward Hunt Ice Shelf) and 1 September to 31 May snowfall at Alert, representing a generalized west-to-east transect along the North Coast of Ellesmere Island. The distances between the sites are only approximate. The dotted and solid horizontal reference lines denote the mean (162 mm weq) and standard deviation (42 mm weq) shown in Table 5.14.

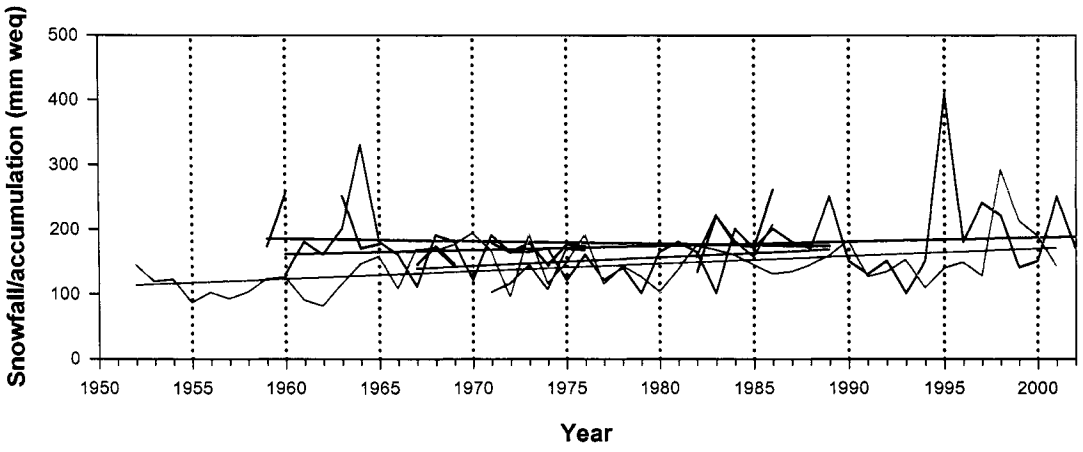

Figure 5.26 Time series of winter snow accumulation (Meighen Ice Cap (red), Ward Hunt Ice Rise (black), and Ward Hunt Ice Shelf (blue)) and 1 September to 31 May 'winter' snowfall at Alert (green). The thin solid lines represent simple linear trend lines.

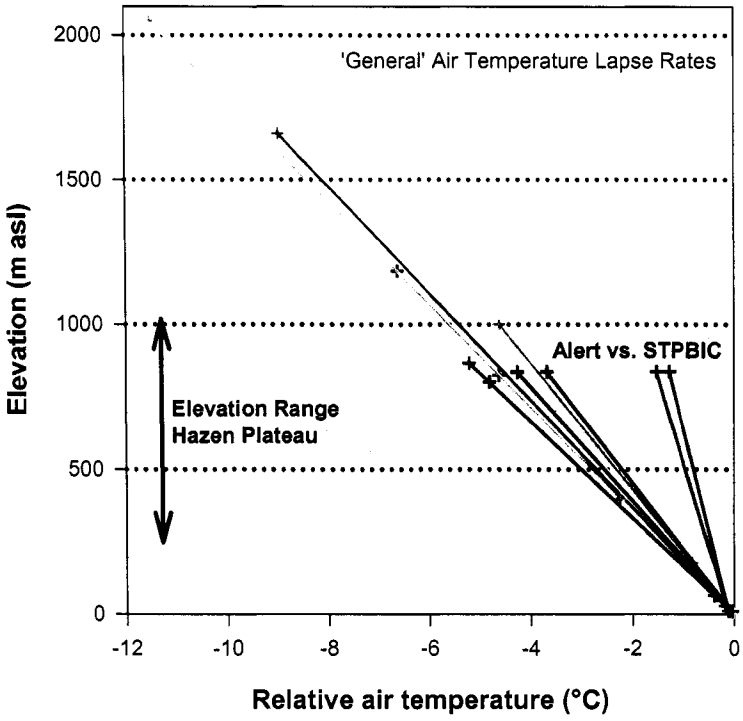

Figure 5.27 Air temperature lapse rates measured in the Canadian High Arctic (cf. Table 5.15) – values from the scientific literature plotted as relative changes (reference = 0°C). Note the large differences in the elevation ranges and the difference of the Alert/STPBIC (= St. Patrick bay ice caps) lapse rates (blue and pink) in the context of the other lapse rates. Grey shading indicates the approximate elevation range (175 to 1100 m asl) of the Hazen Plateau in the extended study area. Dark green: Alert vs. Gilman Glacier, Red: Lake Tuborg, Pink: John Evans Glacier, Blue: Barnes Ice Cap, Cyan: Penny Ice Cap, Yellow: Coburg Island, Dark red: Eureka vs. St. Patrick Bay ice caps (1982), Black: Eureka vs. St. Patrick Bay ice caps (1983).

Figure 5.28 Map of HOBO station network in vicinity of Murray and Simmons Ice Cap (cf. Section 5.4.3). The black line depict the outlines of Murray and Simmons Ice Cap in 2003.

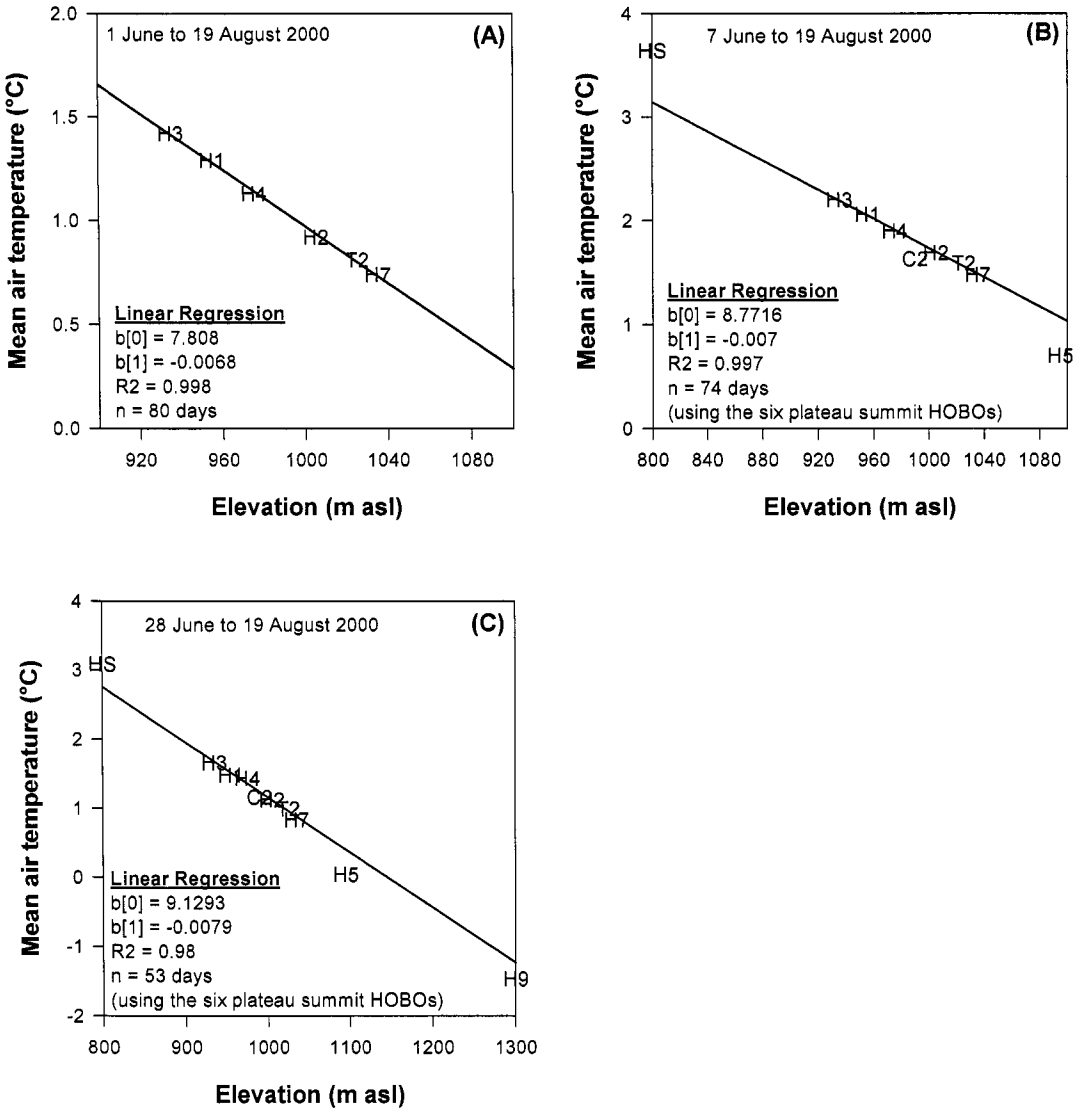

Figure 5.29 Air temperature lapse rates determined for 2000 from the HOBO station network in the immediate vicinity of Murray and Simmons Ice Cap (cf. Fig. 5.28). (A) Plateau summit HOBO stations only; (B) as (A), but including HOBO stations C2, H5, and H-S; (C) as (B), but also including HOBO stations H9. Note that the time periods of overlap, the axis scales, and the lapse rate change between (A), (B), and (C) (cf. Table 5.17 to 5.19).

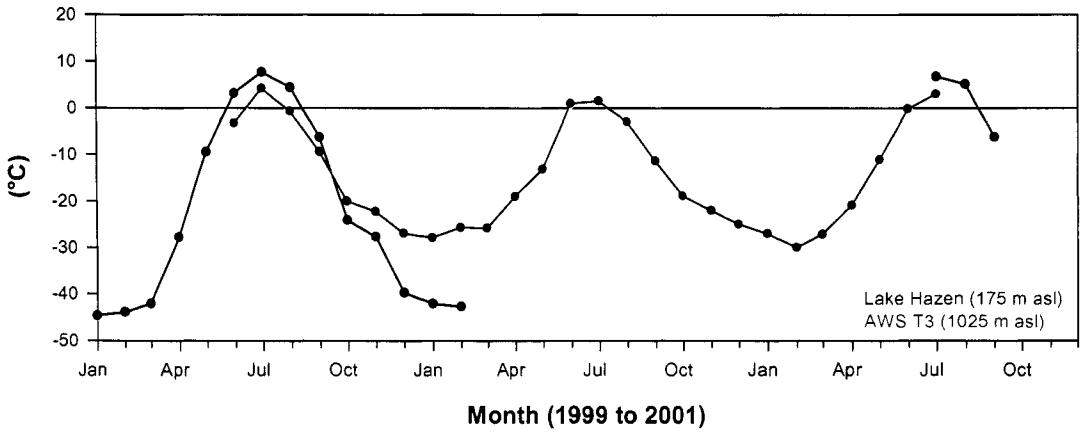

Figure 5.30 Mean monthly air temperature (1999 to 2001) on the Hazen Plateau, as measured at the Lake Hazen AWS (red; 175 m asl) and at AWS T3 (blue; 1025 m asl). The effect of the strong winter temperature inversions is clearly visible. During the summer months, Lake Hazen is considerably warmer than AWS T3. AWS T3 data starts 4 June 1999, i.e. June 1999 is not a 100 percent complete month (cf. Section 5.2).

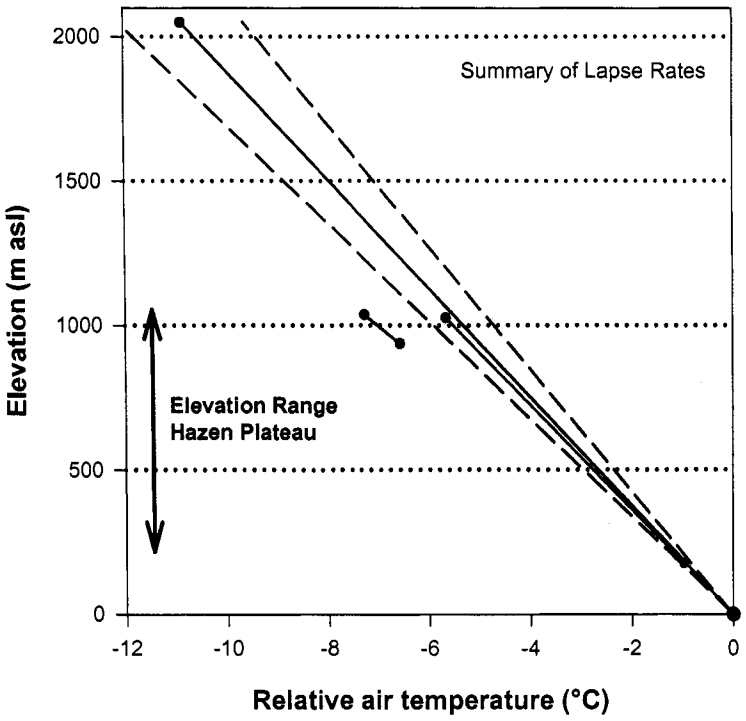

Figure 5.31 Summary graph (cf. Table 5.20) for the air temperature lapse rate section (i.e. Section 5.4) Shown in black is the 'general' lapse rate (based on the scientific literature), with the dotted lines representing the ±1 standard deviation envelope (±0.6°C) (cf. Table 5.15); in blue is the 'regional' lapse rate (Table 5.16); and in black the 'local' lapse rate (Table 5.19). Grey shading indicates the approximate elevation range (175 to 1100 m asl) of the Hazen Plateau in the extended study area.

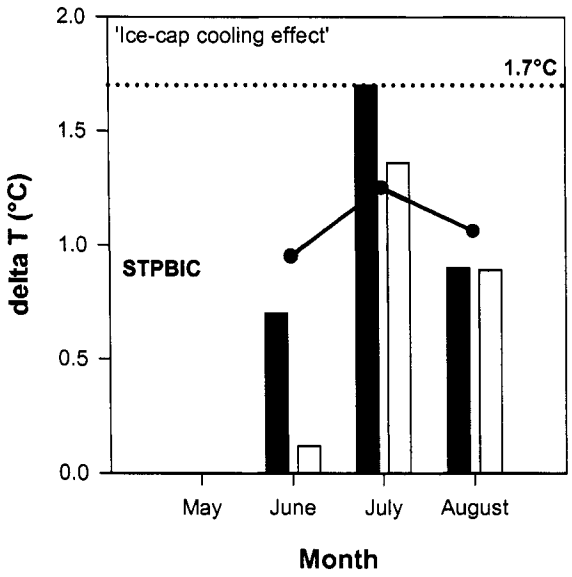

Figure 5.32 The ice-cap cooling effect. Shown as vertical bars are the data from Ohmura (2000) for the White Glacier (1969 to 1972; red) and for the Ward Hunt Ice Rise (yellow) (cf. Table 5.21). The dotted line (1.7°C) represents the mean of Table 5.21 (records #1-7; 10); the grey shading the range of values determined for the St. Patrick Bay ice caps (Bradley and Serreze, 1987b). The 1999 to 2001 means for June, July, August on the Hazen Plateau are shown in blue circles (cf. Table 5.23).

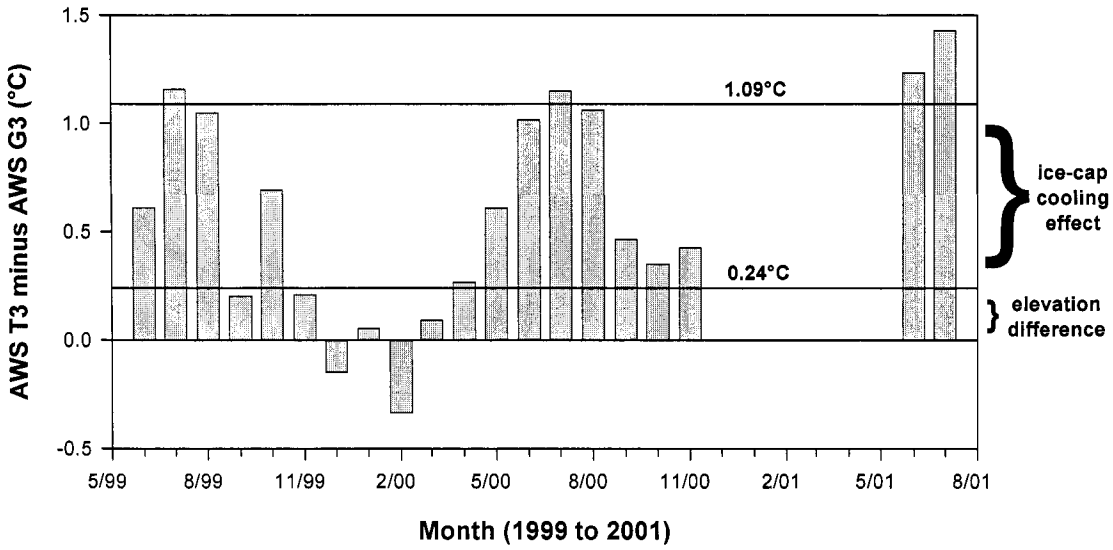

Figure 5.33 Monthly air temperature difference between AWS G3 and AWS T3 (1999 to 2001). The mean during the winter season (September to May) was 0.24°C; the mean during the summer season (June, July, August) was 1.09°C) (Table 5.23).

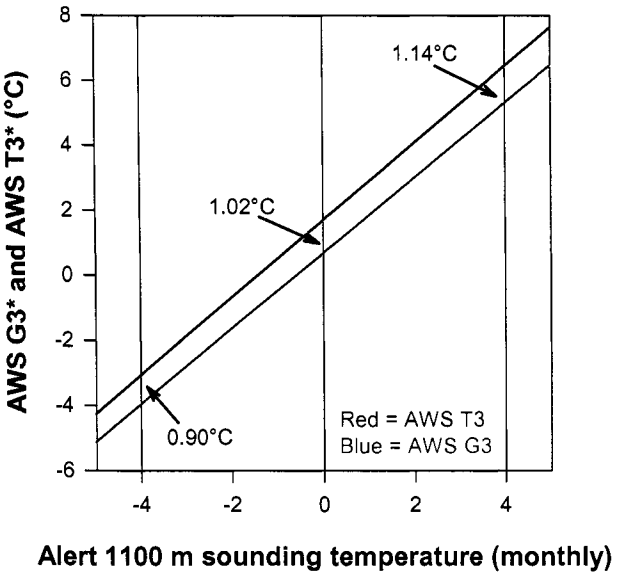

Figure 5.34 Ice-cap cooling effect based on the temperature climatology, using the two regression equations developed in Section 5.2.2.3 for AWS T3 (red) and AWS G3 (blue).

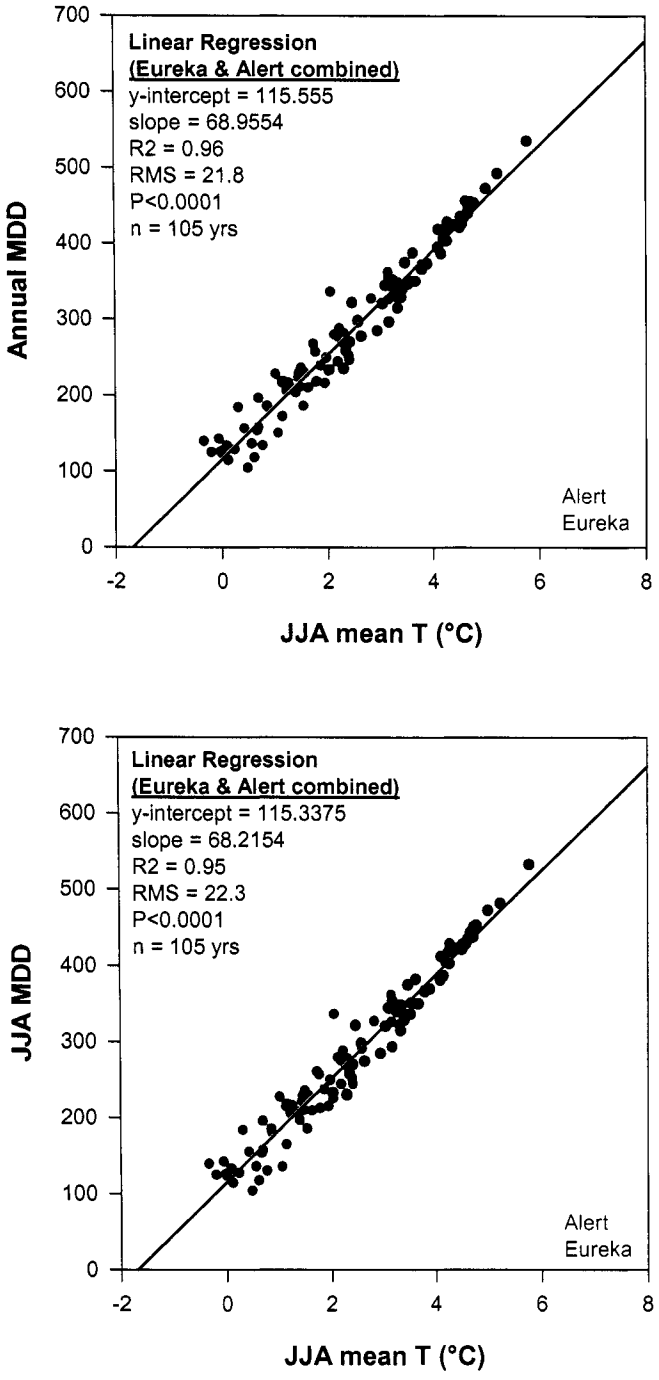

Figure 5.35 Annual (top) and summer (June, July, and August) (bottom) melting degree-day totals plotted as a function of mean summer (June, July, and August) air temperature at Eureka (red) and Alert (blue) (1951 to 2003). The Eureka data for 1991 are excluded, since part of July are missing, hence only n = 105 values used.

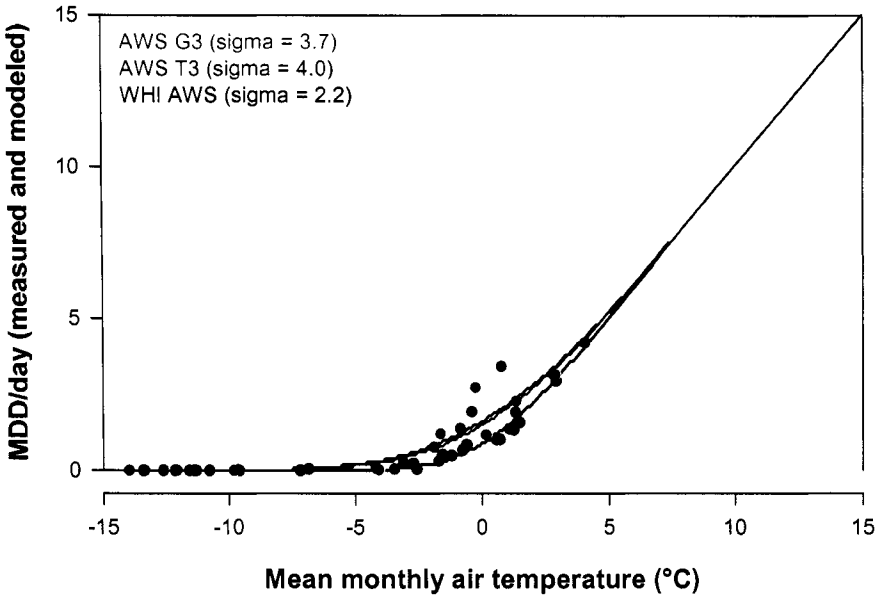

Figure 5.36 Measured and modeled melting degree-days per day. The measured values are based on the records from the Ward Hunt Island (WHI) AWS (1996 and 2001), AWS T3, and AWS G3 (1999 to 2001). The modeled values were determined using the optimum σ values for the Braithwaite (1984) model as detailed in Section 5.6.2.2 (Test 3).

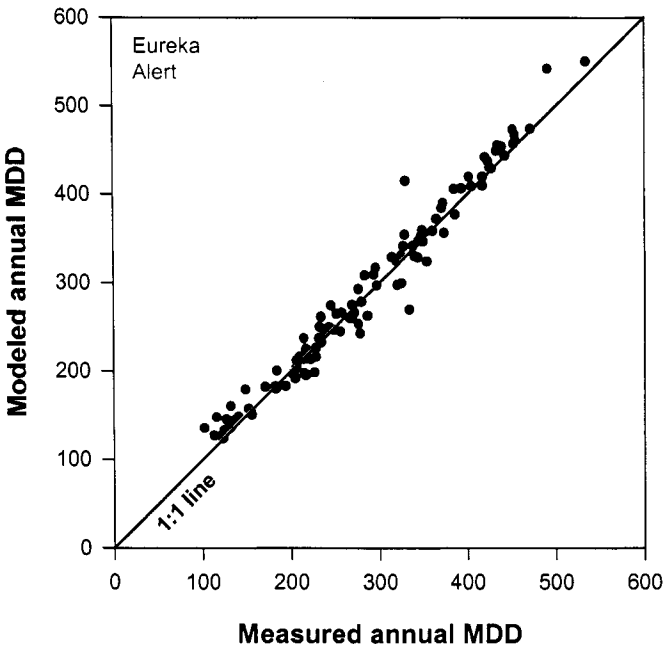

Figure 5.37 Measured and modeled annual melting degree-day totals, as determined during Test 5 (cf. Section 5.6.2.2) of the Braithwaite (1984) model. The black line is the 1:1 line. σ values used: May: 4.9°C; June: 3.2°C; July: 2.4°C; August: 3.0°C; September: 5.1°C (cf. Table 5.27).

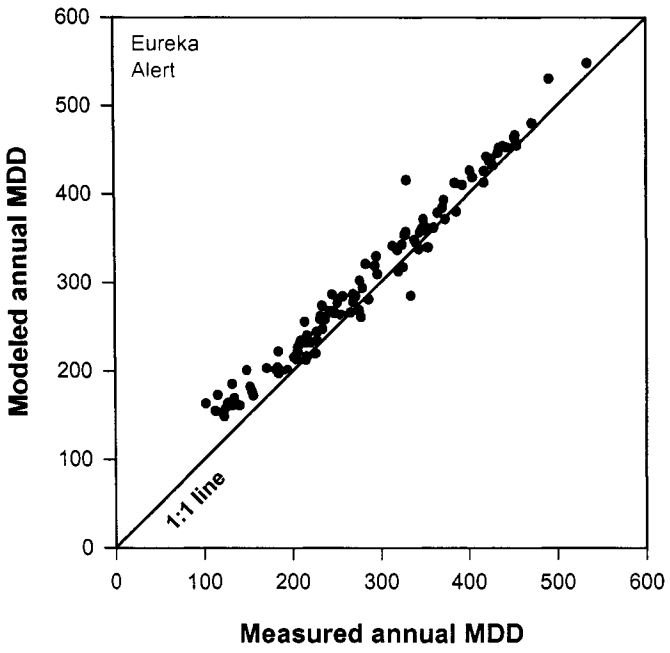

Figure 5.38 Measured and modeled annual melting degree-day totals, as determined during Test 6 (cf. Section 5.6.2.2) of the Braithwaite (1984) model. The black line is the 1:1 line. σ value used 3.7°C (cf. Table 5.27).

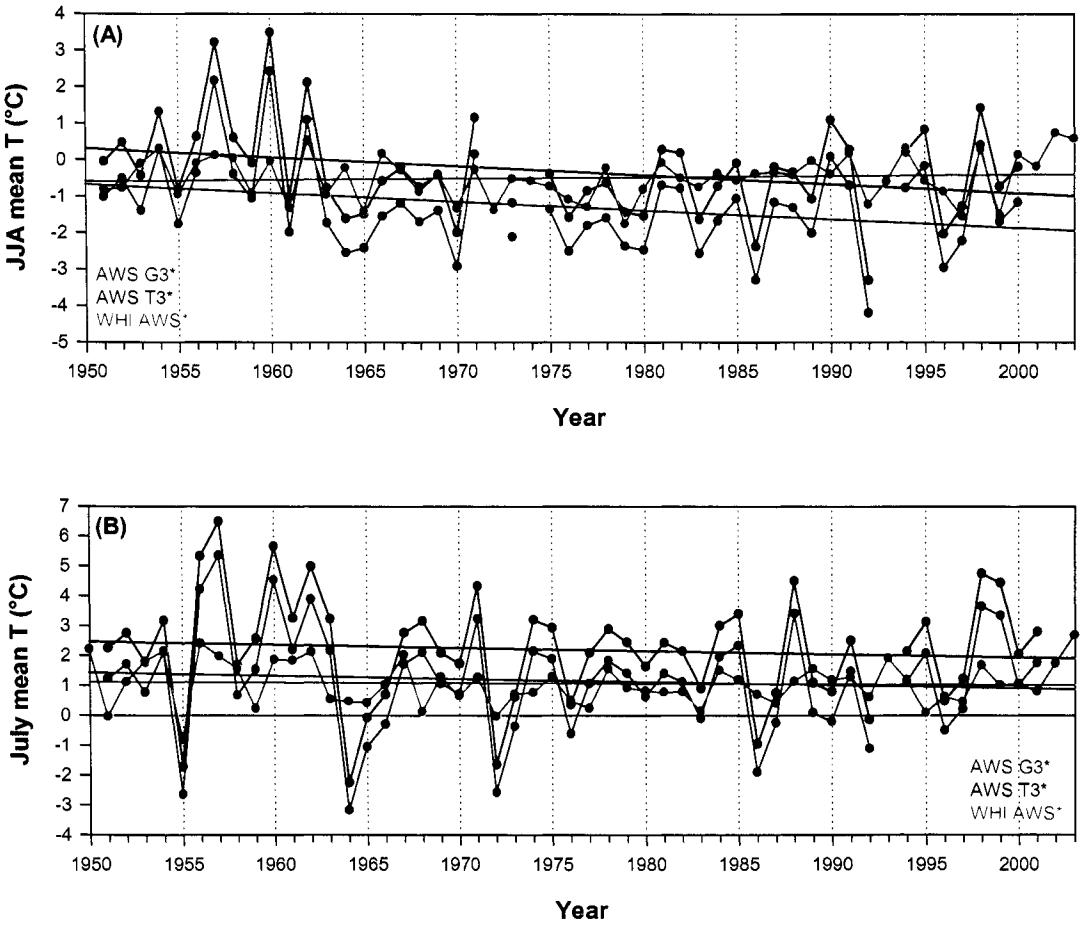

Figure 5.39 Mean summer (A) and mean July (B) air temperature on the Hazen Plateau and North Coast of Ellesmere Island, based on the transfer functions developed in Section 5.2. Note the missing data (cf. Table 5.33). The lines represent simple linear trends (cf. Table 5.33).

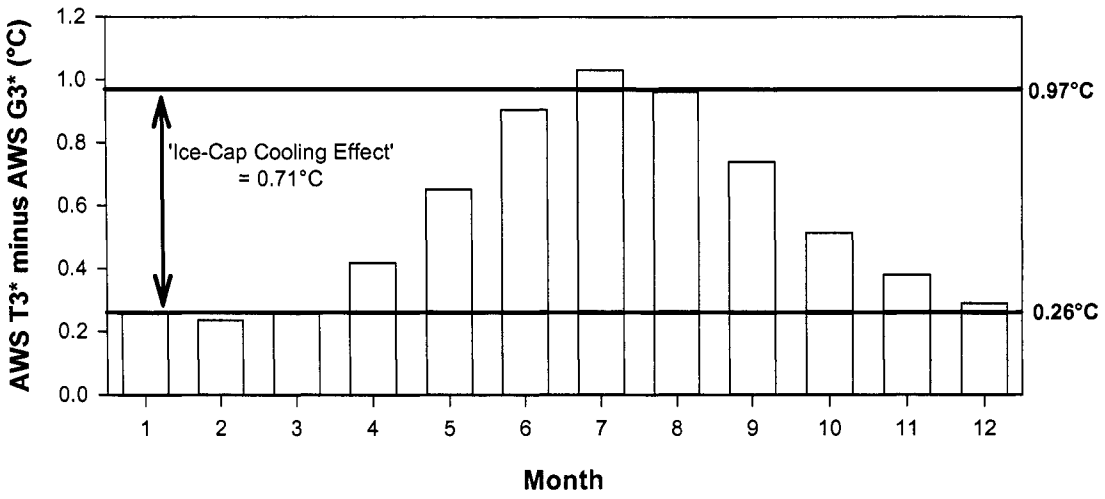

Figure 5.40 The 'ice-cap cooling effect': monthly air temperature difference between AWS G3*and AWS T3*(1951 to 2000). The mean difference during the main winter season (December, January, and February) was 0.26°C; the mean difference during the main summer season (June, July, and August) was 0.97°C (cf. Table 5.34).

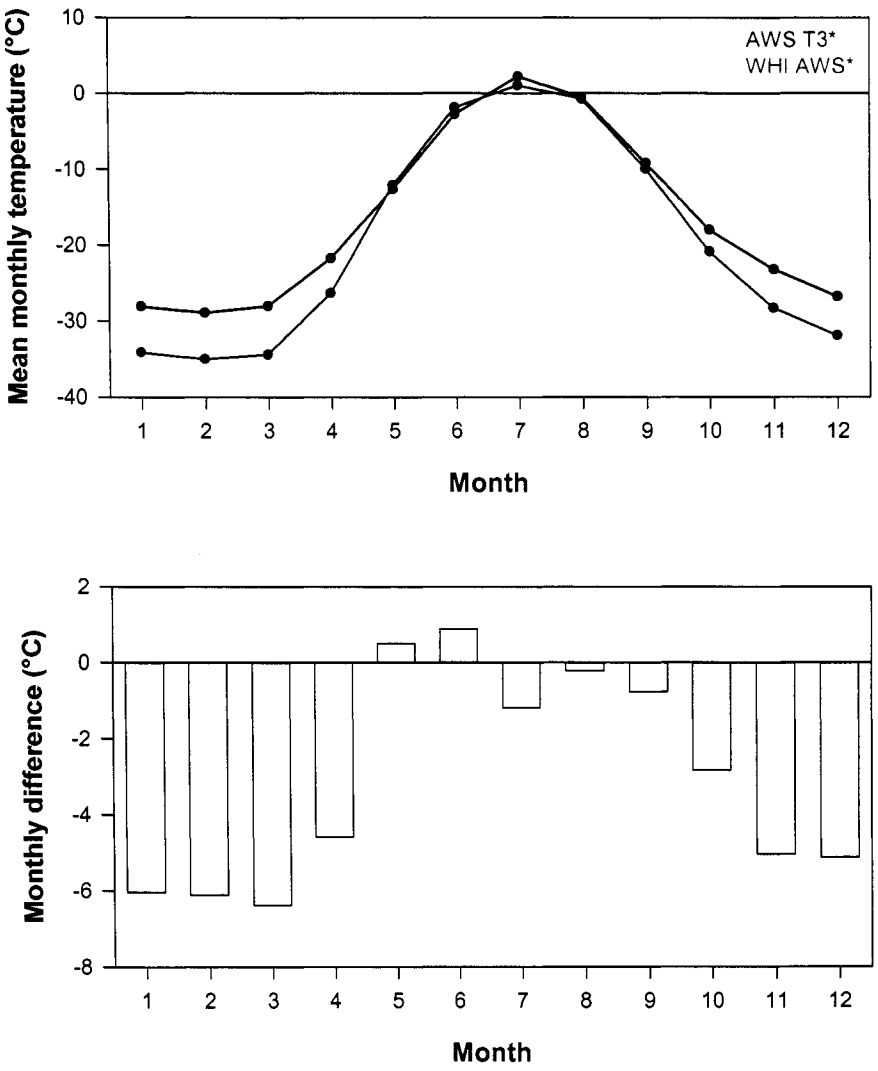

Figure 5.41 The 'Arctic Ocean Effect': monthly air temperatures at AWS T3* and WHI AWS* (1951 to 2000, top) and their respective differences (bottom) (cf. Table 5.34).

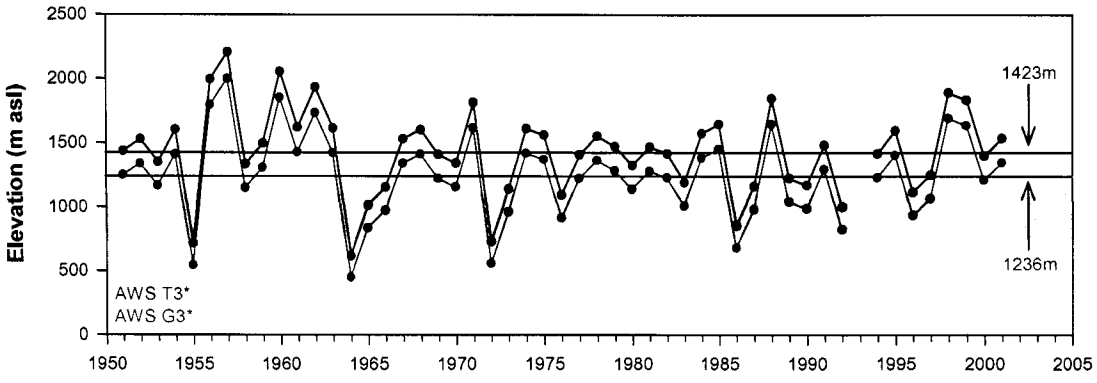

Figure 5.42 July atmospheric freezing levels (m asl) on the Hazen Plateau, calculated using the AWS G3* climatology (blue) and AWS T3* climatology (red) (cf. Section 5.2), assuming an air temperature lapse rate of 5.5°C/1000 m (cf. Section 5.5). The horizontal lines denote the 1950 to 2001 means, the grey shading approximates the elevation range of the Hazen Plateau ice caps (~950 to 1100 m asl for Murray and Simmons Ice Cap and ~750 to 900 m asl for the St. Patrick Bay ice caps). The July atmospheric freezing level for 1993 is missing due to missing sounding data.

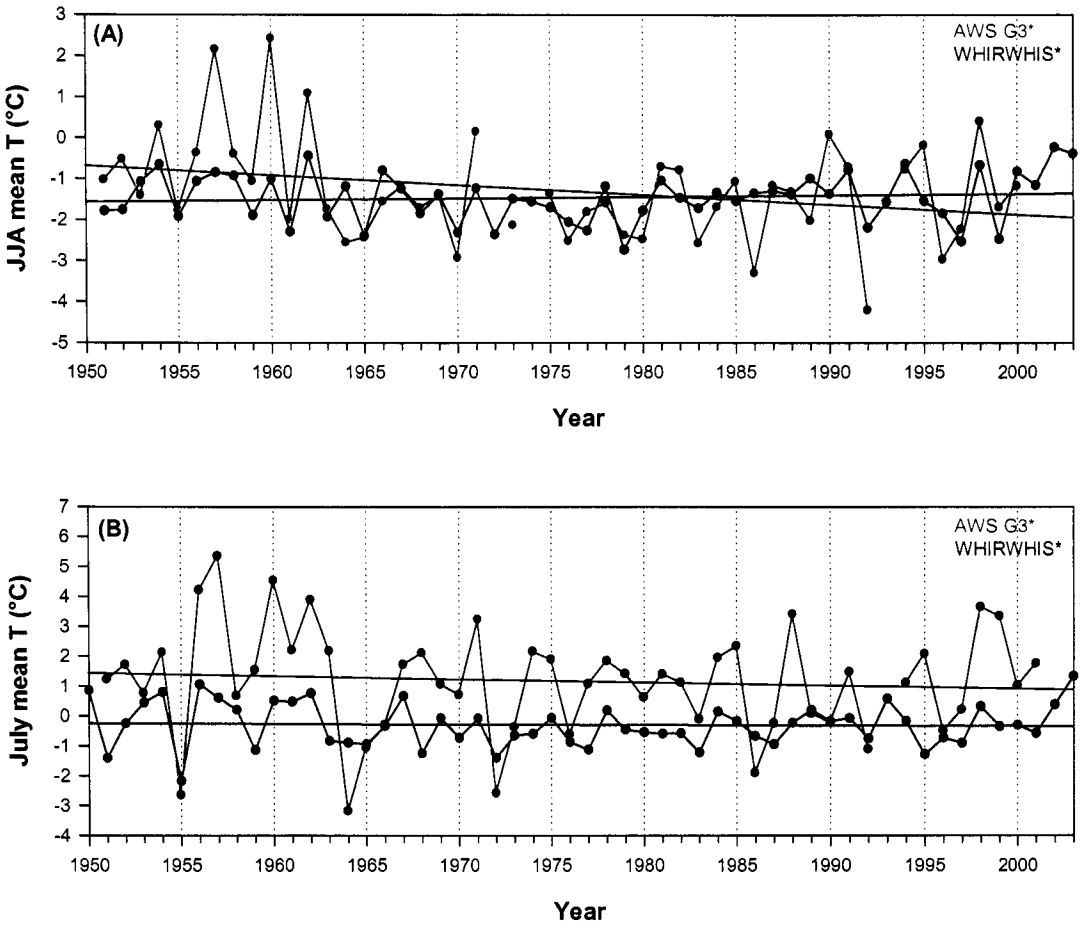

Figure 5.43 Mean summer (A) and mean July (B) air temperature on Murray Ice Cap (AWS G3*) and on the Ward Hunt Ice Rise/Ice Shelf (WHIRWHIS*), based on the transfer functions developed in Section 5.2. Note the missing data (cf. Table 5.33). The lines represent simple linear trend lines (cf. Table 5.33). The WHIRWHIS* record was calculated from the WHI AWS* record using the monthly ice-cap cooling effect offsets specified in Section 5.5.4: 0°C (May), 0.74±0.42°C (June), 1.36±0.23°C (July), 0.78±0.44°C (August), and 0°C (September) (cf. Table 5.35).

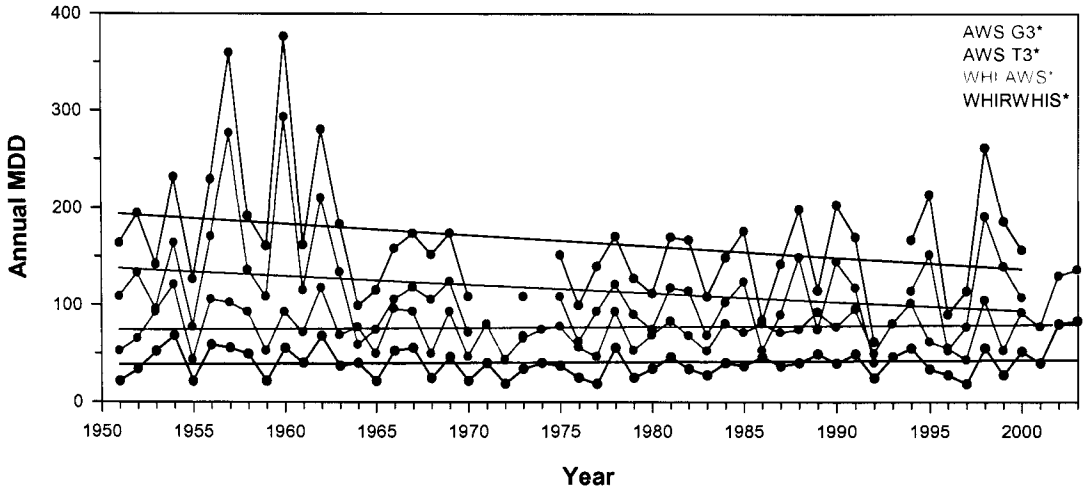

Figure 5.44 Annual melting degree-day totals for AWS G3* (blue), AWS T3* (red), WHI AWS* (green), and WHIRWHIS* (black). See Table 5.35 and 5.36 for a detailed description of the four records. The solid lines denote simple linear trend lines.

CHAPTER 6

SENSITIVITY OF THE HAZEN PLATEAU AND NORTH COAST TO CLIMATE CHANGE

6.1 Introduction – Hypothesis – Objectives

The basic objective of Chapter 6 is to assess the sensitivity of snow and ice cover on the Hazen Plateau and North Coast of Ellesmere Island to climate change. This rather broad objective can be simplified and generalized into one single question: What changes in temperature and/or precipitation are necessary to initiate and sustain glaciation of the Hazen Plateau and North Coast? It is helpful at this point to illustrate the overarching objective of this chapter (and thesis) with a few selected examples from the recent scientific literature. A comprehensive literature review can be found in Chapter 2.

6.1.1. Hagen and Liestol (1990): 'Long-term Glacier Mass Balance Investigations in Svalbard, 1950-1988'

Hagen and Liestol (1990) evaluated the climatic sensitivity of two glaciers on Svalbard by investigating simple statistical correlations between available climatological and long-term mass balance measurements (i.e. regression-type mass balance model, Greuell and Genthon, 2003). Hagen and Liestol (1990) showed that a reduction of mean summer temperature of about 1°C, or an increase of winter precipitation of about 50 percent, would result in a zero net mass balance for these two particular glaciers on Svalbard. This simple statistical modeling approach is obviously only feasible when long-term climate and corresponding glacier mass balance data are available for a given glacier or region.

6.1.2 Fleming *et al.* (1997): 'Modelling the mass balance of northwest Spitsbergen glaciers and responses to climate change'

Fleming *et al.* (1997) assessed the sensitivity of two glaciers in northwest Spitsbergen to climate change, using a highly-parameterized surface energy-balance model (cf. Section 6.2). Increases in summer air temperature had a considerable effect on glacier mass balance, whereas increases in winter temperature were of little significance (cf. Oerlemans and Fourtin, 1992). A decrease in mean annual

temperature of about 0.6°C, or an increase in annual precipitation of about 23 percent, was able to bring these two particular glaciers into a balanced mass balance state. For reference, the estimated climatic cooling during the so-called 'Little Ice Age' (LIA) for the Svalbard Archipelago was between –1.5 and –2.2°C (i.e. sufficient for glacier initiation and expansion).

6.1.3 Hock *et al.* (2002): 'Modeling Climate Conditions Required for Glacier Formation in Cirques of the Rassepautasjtakka Massif, Northern Sweden'

Hock *et al.* (2002) were interested in the climatic conditions (in terms of temperature and precipitation changes) that would lead to a re-glaciation of several abandoned high-elevation cirques in the mountains of northern Sweden. They calibrated a simple temperature-index melt model (Hock, 1999) with relatively scant meteorological and snow survey data collected in 1995 and 1999. Hock *et al.* (2002) then conducted an array of sensitivity experiments by varying winter snow accumulation, summer air temperature, or both, to determine what magnitude of changes in precipitation and summer melt are necessary to allow snow to survive a given summer melt season (= initiation of glaciation; cf. Bromwich *et al.*, 2002; Ruddiman *et al.*, 2005). These model experiments were 'time-less' in the sense that they simply referred to arbitrary temperature and precipitation changes relative to some predefined initial conditions (= sensitivity tests). Hock *et al.* (2002) then discussed their results in the context of reconstructed regional Holocene and predicted future climatic variability in northern Sweden. A similar approach has been presented recently by Kovanen and Slaymaker (2005) with respect to Holocene changes in glacier extent on Mt. Baker, Washington State.

Hock *et al.'s.* (2002) simple and elegant study is a good example of a pure 'sensitivity' experiment (cf. Section 6.1.1) using a simple melt model, calibrated with very limited in-situ data. The results of such experiments have to be evaluated relative to available independent paleoclimatic data and/or climate model predictions. The basic goal of this chapter is to formulate a similar modeling experiment for the Hazen Plateau and North Coast of Ellesmere Island. Sensitivity experiments are usually conducted by varying model input data (and/or model parameters) relative to some defined initial conditions. The resultant model results are then evaluated, compared with, and interpreted in the context

of other available independent data or a model control run. The required initial conditions for such sensitivity experiments can be defined in two ways:

- Using the in-situ measurements on the Hazen Plateau or on the North Coast (Braun *et al.* 2004a, b).
- Using the long-term means and variations of air temperature and precipitation determined from the two climatologies developed in Chapter 5.

Sensitivity experiments can then be conducted for single points on the North Coast and Hazen Plateau, along an elevational transect across northern Ellesmere Island, or spatially-distributed across the area of interest on the basis of a digital elevation model. Going to two or three dimensions assumes that the required model input data and model parameters do not change significantly across the spatial domain of interest, unless such variability can be adequately quantified or parameterized within the model.

6.1.4 A Note of Caution

Oerlemans (1991, 1998, 2000, 2001) emphasized that it is impossible/inappropriate to use a glacier mass balance model, in general, to quantify the absolute mean specific mass balance of a given glacier and its associated temporal variability. Oerlemans argued that the uncertainty associated with the climatological forcing data alone leads to unacceptably large error bars for the modeled glacier mass balance, even if the model itself was (almost) perfect (van de Wal and Oerlemans, 1994; Bintanja and Oerlemans, 1995; Bugnion, 1999; van der Veen, 1999a; Hubbard *et al.*, 2005). Oerlemans therefore suggested that the most appropriate modeling approach in this context consists of (1) the incorporation of all (relevant) physical melt processes, (2) calibration of the model against available in-situ data, (3) sensitivity tests, and (4) a comparison of the model results with (other) independent data (cf. van der Veen, 1999a; 2002b).

6.2 Snowmelt and Glacier Mass Balance Modeling: A Review of the Different Modeling Strategies

> "Any exercise in glacier modeling is by definition an exercise in simplifying reality, and the work presented here constitutes no exception." (Bingham *et al.*, 2003) (cf. Andrews and Mahaffy, 1976)

> "In climate modeling, nearly everybody cheats a little." (Kerr, 1994)

Van der Veen (2002b) provided this elegant elaboration on the fundamental limitations of natural systems models, based largely on the work of Oreskes *et al.* (1994):

> "Any geophysical model is an embodiment of scientific hypotheses and, as such, cannot be verified in the sense that it can never be proven that the model is an accurate representation of the physical reality (Konikov and Bredehoeft, 1992; Oreskes *et al.*, 1994; van der Veen, 1999a). At best, models can be confirmed by matching observational data that were not used to calibrate model parameters. The more such data agree with model predictions, greater confidence can be placed in the model (Strahler, 1987). It should be kept in mind, however, that if the model fails to reproduce observations it can be concluded that the model is faulty in some way, but the reverse is never the case (the 'fallacy of affirming the consequent'; Oreskes *et al.*, 1994). Moreover, even if the model turns out to be consistent with present or past observations, there is no guarantee that the model will perform equally well when used to predict the future (Oreskes *et al.*, 1994)."

Nevertheless, snowmelt and glacier mass balance modeling are two crucial elements in any attempt to predict cryospheric changes associated with past, current, or future climate change (cf. van der Veen, 1999a):

> "...models provide a framework for synthesizing field information and for testing ideas about how the system works. They can alert the modeler to phenomena not previously considered. They may identify areas where more field information is required." (Anderson and Woessner, 1992)

Melt models for snow and ice generally fall into two different categories, representing two very different modeling philosophies (Fig. 6.1):

1. Physically-based energy-balance models (EBM's), which determine snow and ice melt as the residual of the surface energy balance equation (cf. Section 6.2.1).
2. Empirical temperature-index models (TIM's), which instead assume a simple empirical relationship between air temperature and snow/ice melt (cf. Section 6.2.2).

The fundamental difference between these two types of models is that an empirical temperature-index model invokes a single parameterization to estimate snow/ice melt, whereas a physically-based energy-balance model calculates melt directly from the conservation of energy and mass at the melting snow or ice surface and at the bed. Temperature-index models thus have to rely on 'implicit' or 'indirect' information about the involved surface energy exchanges as captured by the associated air temperature variability (Willis *et al.*, 1991/1992). Intuitively, one could argue that energy-balance models represent a more sophisticated and superior modeling approach, as they 'explicitly' capture the physical processes and energy exchanges involved in snow and ice melt (Föhn, 1973; Oerlemans, 1998; Greuell and Genthon, 2003). Temperature-index models are in fact sometimes considered a 'crude' and 'inferior' method (Ohmura, 2001) and their usage is often 'justified' merely by the good availability of air temperature data, and the frequent non-availability of necessary surface energy-balance data.

> "Air temperature and precipitation in the summer months are the variables most commonly correlated with glacier behavior. This selection is not one of preference but rather one of convenience and necessity as other variables have not been recorded regularly for a long enough period of time." (Posamentier, 1977)

The predictive capabilities of temperature-index models are however "too good to be called crude and inferior" according to Ohmura (2001), and in fact often as good as, and sometimes even better than, those of more sophisticated energy-balance models (e.g. Plüss and Mazzoni, 1994; Bøggild *et al.*, 1999; Hock, 2003; Wild *et al.*, 2003; Essery and Etchevers, 2004). It is therefore not surprising that temperature-index models are today the most commonly used approach for snow and ice melt modeling due to four reasons (Martinec and Rango, 1986; Hook, 2003; 2005):

1. Good availability of air temperature data (from measurements, model output, and paleoclimate records).
2. Relatively robust interpolation and extrapolation possibilities of air temperature across time and space (see Blöschl (1991) for an interesting discussion regarding the validity of this commonly-held notion).
3. Generally good model performance (cf. Hock, 2003; 2005).
4. Computational simplicity (cf. Mineter and Hulton, 2001).

Most operational runoff models therefore rely on temperature-index methods to provide the melt modeling component (Martinec and Rango, 1986; Kustas *et al.*, 1994; Ferguson, 1999; Hock, 2003). Temperature-index models can also be used to determine the mass balance forcing for dynamic ice flow models (e.g. Oerlemans *et al.*, 1998; Greve, 2000; Tarasov and Peltier, 2005; Zweck and Huybrechts, 2005) and have been used extensively to quantify the response of glacier mass balance to climate change (e.g. Lauman and Reeh, 1993; Bøgghild *et al.*, 1994; Johannesson *et al.*, 1995; Braithwaite and Zhang, 1999; Marshall and Clarke, 1999; Raper *et al.*, 2000; Hostetler and Clark, 2000; Braithwaite and Raper, 2002; Braithwaite *et al.*, 2002; Marshall, 2002; DeConto and Pollard, 2003; Schneeberger *et al.*, 2003, Marshall *et al.*, 2004; Hanna *et al.*, 2005; Pollard and DeConto, 2005; Zweck and Huybrechts, 2005; Ridley *et al.*, 2005; Raper and Braithwaite, 2006). Temperature-index methods are probably less appropriate in low-latitude, tropical environments, where glacier mass balance is strongly influenced by sublimation and atmospheric moisture content (Kaser, 1999; Kaser *et al.*, 2004b). The following section gives a brief overview of energy-balance and temperature-index models, aimed at assessing their respective differences, advantages, and disadvantages in the context of this particular study. More comprehensive reviews and comparisons have been provided for example by Braithwaite (1981), Melloh (1999), van der Ween (1999b), Ohmura (2001), Hock (2003, 2005), and Greuell and Genthon (2003). Hindmarsh (1993) and Van der Veen (1999a; 2002b) provided excellent reviews about the validity, assumptions, and issues surrounding cryospheric modeling in general.

6.2.1 Energy-Balance Melt Models

Physically-based energy-balance models determine the mass of snow and ice loss directly by calculating all relevant components of the energy balance over a melting snow or ice surface – any 'residual' energy is then converted into snow or ice melt. The strength of such models lies in their unique ability to describe and quantify the processes and energy exchanges involved in snow and ice ablation (Greuell and Genthon, 2003; Konya *et al.*, 2004). Furthermore, energy-balance melt models are (at least in theory) not site- or time-specific, as they are based on physical principles – which means that an energy-balance model should be (at least in theory) universally applicable (i.e. 'portable' from site-to-site or back/forward in time without any significant model modifications).

6.2.1.1 The Energy Balance Equation

In snowmelt and glacier mass balance studies, the surface energy-balance equation of the (melting) snow/ice surface is usually written as:

Equation 6.1 $$R + SHF + LHF + GHF + PHF + M = 0$$

where R is net radiation, SHF is the sensible heat flux, LHF is the latent heat flux, GHF is the subsurface heat flux, PHF is heat supplied by precipitation, and M is the (residual) energy available for snow and ice melt. The signs of the individual components are usually taken as positive when the term represents an energy source for the melting surface. GHF and PHF are typically neglected in most studies due to their small magnitude compared to the other energy-balance components (e.g. Kuunisto, 1986; Wendler *et al.*, 1988; Braithwaite and Olesen, 1990a; Paterson, 1994; Favier *et al.*, 2004; Strasser *et al.*, 2004).

The fundamental problem with using the energy-balance approach in snow and ice melt modeling is that the components of the energy balance (except for radiation balance) cannot be measured directly in reality (e.g. Etchevers *et al.*, 2004). Instead, they have to be indirectly calculated using empirical/semi-empirical parameterizations from measured (or parameterized) meteorological/glaciological data and associated empirical model parameters. Oerlemans (2001), Greuell

and Genthon (2003), and Hock (2005) provided comprehensive reviews of current methods to calculate the energy-balance equation for a melting snow or ice surface and Etchevers *et al.* (2004) offered a comprehensive assessment and performance comparison of 23 currently-used snowmelt models with different complexities.

6.2.1.2 Theory and Reality of Energy-Balance Melt Models: Model Parameters and Model Parameterizations

In order to solve the energy-balance equation, energy-balance models rely on a variety of empirical and semi-empirical parameterizations and model parameters, which have to be determined from, or calibrated against, available in-situ meteorological and glaciological observations (e.g. Arnold *et al.*, 1996; Schneider, 1999; Favier *et al.*, 2004). Etchevers *et al.* (2004), for example, discussed the specific albedo parameterizations (and their respective limitations) included in 23 different snowmelt models of varying complexity. These internal albedo parameterizations are typically based either on air temperature, snow type and/or grain size, and/or snow age (i.e. time), which in essence represent 'proxy' or surrogate variables to account for the physically-controlled changes in the reflectance properties of the snow surface during melt (Robock, 1980; Brock *et al.*, 2000a; Brock, 2004; Hall, 2004). Some models combined two different albedo parameterizations, whereas other models used either a fixed albedo or excluded albedo altogether. It is therefore not surprising that modeled daily albedo values (calculated using these 23 models) differed between 5 and 20 percent from those actually-measured at two high-elevation reference sites in the European Alps. At the same time, the overall model performance was highly dependent on its specific albedo parameterization (cf. Blöschl, 1991; Braithwaite and Olesen, 1990a; van de Wal and Oerlemans, 1994; Arnold *et al.*, 1996; Bøggild *et al.*, 1999; Hock, 2005).

This example illustrates that many energy-balance models are in reality not true 'physical' models that can be universally applied. Instead, they have to include considerable site-specific modifications, parameterizations, and assumptions. One could therefore argue that the main difference between a simple temperature-index model and more sophisticated energy-balance melt model is simply the level and the extent to which empirical approaches are introduced into the modeling procedure (Harding, 1986; van der Veen, 1999b; Braithwaite and Zhang, 1999).

6.2.1.3 Theory and Reality of Energy-Balance Melt Models: Spatially-Distributed Energy-Balance Melt Models

Energy-balance models require (as input) very detailed and comprehensive measurements of a wide variety of meteorological and glaciological variables, including air temperature gradients, vapor pressure gradients, wind speed gradients, radiation balance/albedo, and precipitation. Those input data are difficult, time-consuming, and costly to measure accurately in-situ (cf. Ahlman, 1936; Hock, 2005), even at a single point on a glacier or in a watershed (for example at a weather station). Therefore, the necessary input data for such "data hungry" (Hanna *et al.*, 2005) energy-balance models are often only available for relatively short periods of time during dedicated field measurement campaigns and/or at especially-equipped reference sites (e.g. Arnold *et al.*, 1996; Ohmura *et al.*, 1996a; Jin *et al.*, 1999; Etchevers *et al.*, 2004; Hock, 2005).

An even bigger problem arises when attempting to distribute an energy-balance model across space and time, for example across an entire glacier (e.g. Murray Ice Cap) or region (e.g. Hazen Plateau) (cf. Plüss and Mazzoni, 1994). This requires a substitution of the in-situ measured meteorological input data and empirical model parameters with parameterized or prescribed values, which have to be determined for each point across the glacier or region, as a function of time, using some kind of interpolation or extrapolation algorithm, based on some (empirical) assumptions and/or other independent data (e.g. Oerlemans, 1991; Brock *et al.*, 2000b; Arnold. 2005). This is often simply not possible (in a robust manner, van der Veen, 1999a; Blöschl, 2006) or not practical, given the circumstances or objectives of a particular study or question (cf. Ferguson, 1999; Marshall, 2002). In fact, Beven (1996) and Luce *et al.* (1999) noted that spatially-distributed energy-balance models may have too many degrees of freedom to be properly calibrated (cf. Oerlemans *et al.*, 1991/1992; Wilcox *et al.*, 1991; Oerlemans, 1998; van der Veen, 1999b; Braithwaite and Zhang, 2000; Essery and Etchevers, 2004). This effectively means that energy-balance models are not actually validated during the modeling procedure, but instead tuned to fit whatever short-term observations and measurements are available (van der Veen, 2002b; Greuell and Genthon, 2003; Etchevers *et al.*, 2004; Hanna *et al.*, 2005).

The two most 'popular' tuning parameters in energy-balance modeling are precipitation and snow/ice albedo (Raper *et al.*, 2000; Braithwaite and Raper, 2002; Braithwaite *et al.*, 2002; Greuell and

Genthon, 2003; Hock, 2005). Unfortunately, the choice of these tuning parameter(s) affects the sensitivity of the modeled glacier mass balance to climate change. The climatic sensitivity increases, in general, with the amount of precipitation (Oerlemans and Fourtin, 1992), but also decreases with increases in ice albedo, because a smaller contrast between snow and ice albedo reduces the effectiveness of the albedo feedback process. Therefore, whether a model is tuned by means of precipitation or ice albedo has an opposite effect on the resultant climatic sensitivity of the modeled glacier (Greuell and Genthon, 2003).

6.2.1.4 Theory and Reality of Energy-Balance Melt Models: Uncertainty of Energy-Balance Melt Models

The measurement and estimation error of each meteorological and glaciological input variable, model parameter, and model assumption involved in the solution the energy-balance equation is eventually propagated into the residual term of interest, in this case the estimate of snow and ice melt (Wendler *et al.*, 1988; Hinzman *et al.*, 1991; van den Broeke, 1996; Oerlemans, 1998). It is therefore not surprising to find errors associated with the determination of daily melt rates of 40 percent or more (e.g. Hay and Fitzharris, 1988; Braithwaite and Olsen, 1990a) using energy-balance models. Favier *et al.* (2004) showed that monthly ice ablation calculated using their energy-balance model was about 30 percent greater than measured monthly ablation. Schneider (1999) reported an uncertainty of the energy balance calculation of 25 percent. Etchevers *et al.* (2004) concluded that five of the seven 'best' snowmelt models in their intercomparison of 23 models were able to predict seasonal snowmelt totals "with reasonable accuracy (error < 15 percent)". The two other 'best' models underestimated snowmelt by 18 to 32 percent. On the other hand, Brock *et al.* (2000b) reported differences between measured and modeled daily ablation rates of only 1 to 2 percent (albeit under 'ideal' conditions on the Haut Glacier d'Arolla, Switzerland).

It is obvious that the implementation of an energy-balance model raises a series of questions and problems, particularly regarding the many model assumptions and parameters involved in the formulation of the model. Those issues have to be addressed properly during the modeling experiment (Oerlemans, 2001). There is, however, a vast amount of scientific literature available about energy-balance models to offer guidance and accepted 'standard approaches' to many of the necessary model parameterizations

(e.g. Paterson, 1994; Brock and Arnold, 2000; Brock *et al.*, 2000b; Greuell and Genthon, 2003; Braun and Hock, 2004; Hock, 2005). For example, Pollard and Kasting (2005) used an energy-balance model to model a 'snowball' or 'slushball' Earth some 600 to 800 Myr ago. Energy-balance melt models have the unique ability to describe and quantify the snow/ice melt processes and associated energy exchanges (Hinzman *et al.*, 1997). But it appears that for assessing regional snowmelt and glacier-wide mass balance changes that may occur in response to past and future climate change, a simple temperature-index model is the more appropriate tool (Braithwaite and Zhang, 1999; Schneeberger *et al.*, 2003; Wild *et al.*, 2003; Hock, 2005). Such studies have been performed using energy-balance melt models (e.g. Oerlemans and Fourtin, 1992; Oerlemans, 1993; Fleming *et al.*, 1997). In the process, the energy-balance models had to be drastically simplified and parameterized, since the required input data were simply not available. Hence, they barely used more than air temperature and precipitation as independent input data (Braithwaite and Zhang, 1999). Blöschl (2006), for example, argued that:

> "...excessive model complexity will defy identification of the model parameters and it will be unclear whether feedback mechanisms (between processes, places, and scales) are represented well. Because of this, increasing model complexity may in fact decrease the modelers confidence in the model at some stage."

At this point (and for this study), it seems therefore more appropriate to 'lump' all empiricism and parameterizations into one single grand assumption (see below) and use a simple and robust temperature-index melt model to assess the sensitivity of snow and ice cover on the Hazen Plateau and North Coast to climate change (rather than hiding them deep within the sub-routines of an energy-balance model; cf. Harding, 1986; van der Veen, 1999b; Braithwaite and Zhang, 1999). This conclusion follows the arguments presented by Paterson (1994) and van der Veen (2002b) who noted that there is no inherent reason why energy-balance models should produce more reliable estimates of future glacier mass balance than simple temperature-index melt models.

6.2.2 Temperature-Index Melt Models

Temperature-index melt models (or 'degree-day models') were introduced into glaciology more than 100 years ago by Finsterwalder and Schunk (1887) (after Braithwaite, 1984 and Hock, 2005) and were probably first used in the Canadian High Arctic by Andrews *et al.* (1970). This particular class of

models uses air temperature alone as an integrated 'index' for snow and ice melt, in the sense that a known variable (in this case air temperature) is used to parameterize a phenomena of interest (in this case snow and ice melt) in a statistical or conceptual, rather than in a physical, sense (Paterson, 1994; Bøggild *et al.*, 1999; Wild *et al.*, 2003). The choice of air temperature as index variable is however not arbitrary (cf. Orvig, 1951; see below) – air temperature is also the fundamental meteorological variable used in surface energy-balance calculations (Lang and Braun, 1990). In fact, operational energy-balance models (e.g. Fourtin and Oerlemans, 1990) are often highly parameterized and primarily use air temperature and precipitation as the two independent forcing variables (Braithwaite and Zhang, 1999). Furthermore, air temperature data are often readily available and fairly easily interpolated or extrapolated across a wide range of temporal and spatial scales (Braithwaite, 1981; Fourtin and Oerlemans, 1990; Blöschl, 1991; Ferguson, 1999; Hanna *et al.*, 2002; Wild *et al.*, 2003).

Temperature-index models are based on an assumed linear relationship between snow/ice melt and air temperature, which is usually expressed in the form of positive temperature sums or cumulative melting degree-days (MDD) (Paterson, 1994), although some authors have used mean summer temperature instead (e.g. Ahlmann, 1924; Krenke, 1975; Ohmura *et al.*, 1992, Wild *et al.*, 2003). In their most basic formulation, the amount of snow and ice melt over a certain time interval is related linearly to the sum of positive air temperatures for the same time interval. The proportionality factor in this case is referred to as degree-day factor (DDF), expressed in mm weq d^{-1} $°C^{-1}$. Generally, a daily time step is used for the melt and temperature integration (Hook, 2003), although any other time interval, such as seasonal (e.g. Braithwaite and Olesen, 1989), monthly (e.g. Lang and Braun, 1990), or hourly (e.g. Wolfe and English, 1995; Hock, 1999) have also been used in the past. The total amount of snow/ice melt (Melt; mm weq) at any point, for any period of days, is then given by (e.g. Hock, 2003):

Equation 6.2 $$\text{Melt (snow/ice)} = \text{DDF (snow/ice)} * \text{MDD}$$

Here, MDD (°C * d) is the sum of positive air temperatures measured at the same point for the same period of days. Typically, mean daily air temperatures are used to calculate seasonal or annual melting degree-day totals, even though that may not be the most appropriate approach (Arnold and

MacKay, 1964; Bradley and England, 1978; Braithwaite, 1984). The basic assumption in a modeling situation is that appropriate values for the DDF (snow) and DDF (ice) can be determined (cf. Section 6.3.2) for a period/point when/where snow and ice melt has been actually measured, and then applied to other periods or points with unmeasured snow/ice melt (i.e. past and/or future).

It is worth mentioning that net radiation is the only available energy source early in the melt season, when air temperature is still below freezing and the turbulent energy fluxes are negative. Any mass loss that occurs when mean daily air temperature is below 0°C (e.g. sublimation) can obviously not be captured by a temperature-index melt model (Greuell and Genthon, 2003). But this limitation is insignificant in many climatic environments, especially when calculating seasonal, or annual, melt totals for an entire glacier, ice cap or region.

6.2.2.1 The 'Physical Basis' of Temperature-Index Melt Models

Many studies have revealed a very high correlation between snow/ice melt and air temperature (Hock, 2003). For example, Sagar (1964) noted that air temperature exhibited a "direct and systematic relation with ablation" on the Gilman Glacier, Ellesmere Island. This is intuitively not surprising – yet it is also well-established that net radiation represents often (e.g. Braithwaite, 1981; Ohmura *et al.*, 1992), though not always (e.g. Takeuchi *et al.*, 1999; Schneider, 1999), the single largest source of available melt energy. The predictive capabilities of air temperature as a single index of snow and ice melt is therefore generally attributed to its own high correlation with several of the energy-balance components, especially sensible heat flux (Martinec and Rango, 1986; Ambach, 1988; Hock, 2003; 2005), and their associated temporal variability. Oerlemans (2005) also noted that glacier mass balance fluctuations from year-to-year are mainly due to air temperature and precipitation variability, even though net radiation is often the primary source of melt energy (cf. Ahlman, 1936; Mark and Seltzer, 2005). The 'physical basis' of temperature-index models has been investigated over the years by a number of researchers; their pertinent results and conclusions are highlighted below.

6.2.2.1.1 Tangborn (1980)

Tangborn (1980) presented two simple empirical models for estimating the relationships between climate and glacier mass balance in the North Cascades mountains of Washington State. He noted:

> "Although an attempt has been made to develop a physically real system, the limitation imposed by using only measured temperature creates an unavoidably empirical means of estimating ablation. It is hoped that neglecting such important ablation factors as albedo and its changes with time, surface roughness, condensation, humidity, and wind is compensated for by extreme simplicity of this method of estimating total ablation."

Tangborn (1980) also provided perhaps the simplest, and most elegant, explanation for the high correlation between air temperature and snow/ice melt:

> "The fact that temperature appears to be closely related to ablation is probably caused more by similarity of air temperature and ablation as functions of the energy processes producing ablation and air warming – namely the radiation balance – than by any direct effects."

6.2.2.1.2 Braithwaite (1981)

Braithwaite (1981) attempted to reconcile the fact that there are often high correlations between snow/ice melt and air temperature, while net radiation was in fact usually the main source of available melt energy. His study is particularly relevant in the context of this study, as it included glaciological and meteorological data collected in the Canadian High Arctic (on the White Glacier and Devon Ice Cap). Braithwaite (1981) was able to show that, although net radiation is the largest individual energy source, glacier ice ablation is much better correlated with sensible heat flux, as both ablation and sensible heat flux are much more variable in time than net radiation (cf. Sato, 1984; Plüss and Mazzoni, 1994). Furthermore, he showed that sensible heat flux was strongly correlated with air temperature variability. Braithwaite and Olesen (1990b) showed very similar results using field data from two glaciers located in southern Greenland.

Braithwaite (1981) concluded that modeling snow and ice melt exclusively as a function of air temperature "achieves simplicity at the cost of accuracy", but is appropriate for the estimation of seasonal or annual ablation totals, as the random errors involved in estimating the daily melt rates tend to

compensate over periods of weeks to months (cf. Blöschl, 1991). Furthermore, air temperature measurements can be fairly easily extrapolated from distant, low-lying weather station (as is the case in the Canadian High Arctic, cf. Chapter 5) and temperature-index models are therefore very useful in such remote environments (Ferguson, 1999) using lapse-rate adjustments.

6.2.2.1.3 Lang and Braun (1990)

Lang and Braun (1990) offered a comprehensive discussion of the 'information content' of air temperature in the context of snowmelt. They argued that air temperature variability is caused by two different mechanisms: (1) variations in the energy-balance of the underlying ground surface, and (2) variation in heat supply associated with the advection of 'outside' warm or cold air masses. Assuming a linear relationship between snow/ice melt and air temperature therefore implies a constant relative contribution of each of the energy-balance components and external heat advection (cf. Braithwaite, 1984). It follows that, as long as the energy-balance components and heat advection term do not change "substantially" in their averages over a given time period, variations in air temperature as averaged over the same period will effectively represent a useable 'index' of the available melt energy (cf. Greuell and Genthon, 2003).

In reality, any spatial and temporal variations in weather, climate, and surface conditions will influence the partitioning of the surface energy-balance (e.g. Koizumi and Naruse, 1992). It thus follows that temperature-index models perform best at time scales long enough to capture all 'typical' weather conditions, and at spatial scales large enough to minimize the effect of localized changes in the surface conditions. Lang and Braun (1990) therefore considered temperature-index models as most appropriate to assess 'average conditions' (Martinec and Rango, 1986; Kustas *et al.*, 1994; Bøggild *et al.*, 1999) (Fig. 6.1), defined spatially by the watershed or glacier scale, and temporally by time intervals of a few days or more (Hock, 2003; Konya *et al.*, 2004).

6.2.2.1.4 Ohmura (2001)

Ohmura (2001) analyzed what he called the 'physical basis' of temperature-index models and stressed the importance of longwave atmospheric radiation in the context of snowmelt. Combined with

the sensible heat flux, longwave atmospheric radiation provided about 75 percent or more of the energy available for snow and ice melt (his Table 2) (cf. Hanna *et al.*, 2002). Both of these energy sources are highly affected by air temperature variability (cf. Braithwaite, 1981; Kuhn, 1993), which provides one possible explanation of the close relationship between air temperature and snow/ice melt (Hock, 2003; 2005). Ohmura (2001) concluded that a (linear) parameterization of snowmelt, based exclusively on air temperature, provides sufficient accuracy for most practical glaciological and climate change applications.

6.2.2.1.5 Greuell and Genthon (2003)

Greuell and Genthon (2003) argued that temperature-index melt models can be considered a simplification of the energy-balance approach (cf. Lang and Braun, 1990). For a melting snow or ice surface, the sum of net longwave radiation and turbulent heat fluxes can be approximated linearly as a function of air temperature (cf. Ohmura, 2001). Net shortwave radiation over the course of a melt season is also positively correlated with cumulative melting degree-days, or, as they simply put it: "sunny summers are warmer" and lead to more melting (Hoinkes, 1968). Their underlying argument follows Hoinkes (1955), who already argued 50-years ago that summer air temperature (and precipitation) can be considered as useful substitutes for radiation and surface albedo (cf. Hoinkes, 1968).

6.2.2.1.6 Synopsis

It is quite obvious from all of these studies that snow and ice melt are two inherently non-linear and highly spatially-variable processes (cf. Wilcox *et al.*, 1991). The proven effectiveness of temperature-index models therefore implies that much of the non-linearity and spatial variability associated with snow and ice melt can be adequately approximated linearly by air temperature variability (Braithwaite and Olesen, 1990c; Williams and Tarboton, 1999). This in turn makes air temperature a very complex, yet at the same time very 'integrating', variable (Orvig, 1951; Oerlemans and Hoogendoorn, 1989; Lang and Braun, 1990). The successful implementation of a temperature-index model, therefore, depends (1) on an appropriate choice of the degree-day factor (DDF), and (2) on the choice of an appropriate spatial and temporal modeling scale (Lang and Braun, 1990) (Fig 6.1).

6.2.2.2 The Degree-Day Factor in Temperature-Index Melt Models

It is obvious that the success of a temperature-index melt model relies heavily on an appropriate choice of degree-day factors (DDF's) used, as they implicitly incorporate all surface energy balance information (Ohmura, 2001). In fact, Zweck and Huybrechts (2005) showed that, of all the model parameters involved in dynamic three-dimensional ice sheet modeling, the degree-day factors exerted the strongest influence on modeled ice sheet volume (cf. Ritz *et al.*, 1997; Oerlemans, 2000; Ridley *et al.*, 2005). The main criticism facing temperature-index models is precisely the assumption of a constant and linear relationship between air temperature and snow/ice melt, expressed by the use of constant degree-day factors (Lang and Braun, 1990). The variability of degree-day factors in time and space has been assessed qualitatively by Schytt (1964), Ambach (1988), and Lang and Braun (1990), analyzed quantitatively by Braithwaite (1995), and summarized comprehensively most recently by Hock (2003).

Degree-day factors, in reality, vary with time and space across a glacier or region, as they effectively integrate and parameterize the energy-balance of the melting snow and ice surface (Martinec and Rango, 1986). Most of the variability in the degree-day factor can therefore be traced back to changes in the relative contribution of the individual energy-balance components to total snow and ice melt (Lang and Braun, 1990; Hock, 2003). For example, snow generally has a lower degree-day factor than ice because of its higher surface albedo (i.e. more energy is reflected and thus not available as melt energy) (Ahlman, 1936; Greuell and Genthon, 2003). The DDF (snow) may also increase during the snowmelt season due the ripening of the snow pack and associated decline in surface albedo (Martinec, 1976; Kuunisto, 1980; Martinec and Rango, 1986; Hock, 2003). Martinec and Rango (1986), for example, showed DDF (snow) increases from about 4 (April) to about 6 (August) for three large watersheds in the European Alps and Rocky Mountains. It should be noted however that the progression of snowmelt and ablation is not universally linked to calendar months, as in a warm climate or year, April may be comparable to June in a cold climate or year (Martinec and Rango, 1986). Over ice, seasonal variations in surface albedo, and hence degree-day factor, tend to be less pronounced (Schaper *et al.*, 1999; Singh *et al.*, 2000; Hock, 2003).

Degree-day factors are also subject to considerable small-scale variability. For example, Braithwaite *et al.* (1998b) compared degree-day factors measured at several different ablation stakes

installed within a few meters of each other and found a ±10 percent variation between the ablation stakes. Singh *et al.* (2000) showed that the presence of dust on the snow or ice surface can increase the respective degree-day factor by about 10 percent. Degree-day factors also tend to vary annually, or seasonally, due to annual/seasonal cycles in the relevant climatic variables (e.g. humidity; Lang and Braun, 1990). Degree-day factors may also vary to some extent with summer temperature, which obviously would lead to an over- or underestimation of snowmelt and glacier mass balance under warmer or colder climates (van der Veen, 2002b). Unfortunately, there are currently no appropriate models or parameterizations available to account for the possible temperature dependence of the degree-day factors (van der Veen, 2002b).

On the other hand, Johannesson *et al.* (1995) remarked that degree-day factors in fact exhibit a high degree of stability with time and across a wide range of different climatic regimes. Braithwaite and Olesen (1993) and Schaper *et al.* (1999), for example, detected no distinct seasonal variations in the degree-day factors. Braithwaite (1995) showed that the degree-day factor of snow remained almost constant, despite considerable variations in wind speed, for air temperatures between 1°C and 5°C, which is a crucial temperature range during snowmelt (Ohmura, 2001). Braithwaite and Olesen (1990c) showed, using a simplified energy-balance model, that ablation along the margin of the Greenland Ice Sheet shows a nearly linear response to summer temperature increases or decreases by 5°C relative to present conditions (cf. Wild *et al.*, 2003).

An appropriate degree-day factor for a temperature-index melt model should be obviously based on 'typical' conditions in terms of time and space (Lang and Braun, 1990; Martinec and Rango, 1986). If the period or area of interest is too long or too large, one has to account for possible inter-annual and/or regional variations of the degree-day factor (Lang and Braun, 1990). If the period or area of interest is too short or too small, one may need to account for the influence of different weather and local topographic conditions (Braithwaite *et al.*, 1998b). The question of degree-day factor variability, and its effect on melt model performance, comes back to the issue of appropriate spatial and temporal scales for snow and ice melt modeling (Fig. 6.1). If the objective or question allows an integration of snow and ice melt over sufficient (long) time and (large) space, then the uncertainty introduced by assuming a linear and constant

relationship between air temperature and snow/ice melt will be (hopefully) reduced to the level of "acceptable noise" (Lang and Braun, 1990).

6.2.2.3 Spatial and Temporal Scales in Temperature-Index Melt Models

Any spatial variability of snow and ice melt (beyond simple linear gradients as a function of elevation = air temperature lapse rate) cannot be captured by traditional temperature-index models, since the degree-day factors are generally assumed to be constant in space (Greuell and Genthon, 2003). In reality, melt rates can vary considerably across a glacier or region, for example due to topographic effects such as shading, surface slope, and surface aspect. Nevertheless, many studies have shown that the ablation gradient with elevation on glaciers and ice caps is more-or-less linear, at least up to the ELA (e.g. Hattersley-Smith *et al.*, 1961; Mercer, 1961; Rosqvist and Østrem, 1989; Pelto *et al.*, 1990; Cogley *et al.*, 1996; Jansson, 1999; Fountain and Vecchia, 1999; Benn and Lehmkuhl, 2000; Hagen *et al.*, 2003; Arnold, 2005). However, this linearity may not necessarily be stable under changing climatic conditions (e.g. warmer summers and reduced winter snowfall) (Arnold, 2005).

There have been a number of interesting attempts in recent years to 'enhance' the traditional temperature-index model by incorporating some measure or index of the radiative fluxes, distributed across the glacier or watershed on the basis of a digital elevation model (e.g. Kustas *et al.*, 1994; Cazorzi and Fontana, 1996; Hock, 1999; Williams and Tarboton, 1999; Pellicciotti *et al.*, 2003; Marshall *et al.*, 2004). The challenge is obviously to find an appropriate model enhancement that improves the predictive capabilities of the traditional temperature-index model without invoking additional input data requirements. The model presented by Hock (1999), for example, varies the degree-day factors at every time step for each grid cell according to the spatial and temporal variability of potential clear-sky direct solar radiation, a quantity that strongly affects melt and varies considerably in complex topography. This 'radiation index' can be computed internally from standard algorithms on solar geography using a digital elevation model, without the need for any additional meteorological data or model parameters. This enhanced model was able to improve the simulation of spatial melt patterns on Storglaciären, Sweden, compared to a traditional temperature-index melt model (Hock, 1999; 2005).

Spatially-distributed temperature index melt models are clearly superior in high-relief, mountainous areas, where topographic shading is an important factor determining the amount of snow and ice melt (e.g. Kustas *et al.*, 1994; Marshall and Clarke, 1999; Hock *et al.*, 2002; Marshall *et al.*, 2004). They are also a requirement if the spatial dynamics of melt have to be accounted for in the modeling experiment (e.g. Hock, 1999). However, if the primary goal is to determine reliable annual or seasonal totals of snow and ice melt over an entire glacier or region, a traditional temperature-index model is perfectly adequate (Hock, 1999; 2005). For this study, topographic shading is not an important issue for snow and ice melt across the wide-open Hazen Plateau and North Coast of Ellesmere Island.

6.2.3 Modeling Cryospheric Changes Associated with Climate Change

Many modeling studies have focused on predicting the response of glacier mass balance to past and future climate change (e.g. Oerlemans, 1991/1992; Lauman and Reeh, 1993; Bøgghild *et al.*, 1994; Johannesson *et al.*, 1995; Braithwaite and Zhang, 1999; Engeset *et al.*, 2000; Schneeberger *et al.*, 2003; Wild *et al.*, 2003; Zweck and Huybrechts, 2005; Ridley *et al.*, 2005). There is however one fundamental caveat associated with asking and answering this type of question: Unless one uses a fully physically-based model, it is somewhat questionable if variability beyond the range of 'normal' cryospheric and climatic conditions can be reliably forecasted (or hindcasted) (Sellers, 1973; Braithwaite and Olesen, 1990c; van der Veen, 1999a, b; 2002; Arnold, 2005; Nordli *et al.*, 2005). At first glance, this appears to be a much bigger concern for a purely empirical temperature-index model than for a more physically-based surface energy-balance melt model (cf. Oerlemans, 2001). However, many of the necessary model parameters (e.g. aerodynamic roughness length), as well as many of the needed input variables (e.g. snow/ice albedo or cloud cover), are often not measured directly, and have to be parameterized or prescribed in an energy-balance model (e.g. Oerlemans, 1993; Oerlemans and Fourtin, 1992). This is an even greater issue when attempting to implement an energy-balance model in a spatially-distributed manner across a glacier, watershed, or region.

The basic assumption in a temperature-index model is that appropriate values for the DDF (snow) and DDF (ice) can be determined for a period when snow and ice melt are measured directly, and then applied to past or future periods with unmeasured snow and ice melt. This assumption is certainly

problematic (Marsiat, 1995; Marshall and Clarke, 1999), although Braithwaite and Olesen (1990c) have shown, using an energy-balance model, that ablation along the margin of the Greenland Ice Sheet shows a nearly linear response when summer temperature is increased or decreased by 5°C relative to present conditions (cf. Wild *et al.*, 2003). Bøggild *et al.* (1994) also concluded that it is reasonable to ignore any possible temperature influence on the degree-day factors, as the direct effect of temperature change on ablation is much larger in comparison.

An obvious drawback of temperature-index models in this context is that they can only be used to assess the sensitivity of snow and ice melt to variations in air temperature and precipitation – variations in other important climatic variables such as cloudiness, surface albedo, or solar radiation cannot be considered. On the other hand, the energy-balance models commonly used in climate sensitivity studies (e.g. Oerlemans and Fourtin, 1992; Fleming *et al.*, 1997; Oerlemans *et al.*, 1998) are so highly parameterized that they barely use more than temperature and precipitation as independent forcing variables (Braithwaite and Zhang, 1999). Furthermore, past or future climate change scenarios are typically simplified in terms of changes in air temperature and precipitation over a given time period (e.g. Oerlemans *et al.*, 1998; Engeset *et al.*, 2000; Bradley *et al.*, 2003; Johannesson *et al.*, 2004). Wild *et al.* (2003) presented the following simple equation to calculate summer ablation of snow and ice on the Greenland and Antarctic Ice Sheet, based exclusively on mean summer air temperature:

Equation 6.3 Ablation (mm/year) = $514 * T_{JJA} + 930$; for $T_{JJA} > -1.8°C$

Equation 6.4 Ablation (mm/year) = 0; for $T_{JJA} < -1.8°C$

This simple linear melt parameterization is based on extensive in-situ measurements and observation on the Greenland Ice Sheet (Ohmura *et al.*, 1996a, 1996b). Ohmura (2001) reviewed the physical reasoning behind this melt parameterization and argued that this equation includes an uncertainty of about 2.5 percent, which is comparable in relative magnitude to the standard error of typical melting degree-day calculations (Braithwaite, 1984; 1995). Bromwich *et al.* (2002), for example, used this approach to illustrate the relative importance of summer temperature and winter precipitation in the context of the initiation of the Laurentide Ice Sheet. The climatic sensitivity (514 mm weq/°C change in

mean summer temperature) included in the Equation 6.3 is somewhat higher than global estimates provided by Dyurgerov and Meier (2000), Oerlemans (1993), and Braithwaite and Raper (2002) of 370, 390, and 410 mm/year * °C, respectively. Similar empirical approaches have also been successfully adopted by Sutherland (1984), Ballantyne (1990, 2002), Lie *et al.* (2003a, b), and Bakke *et al.* (2005) to estimate the responses of glaciers in Norway and Scotland to climate change during the Holocene.

Finally, Oerlemans (1991, 1998, 2000, 2001) cautioned against overestimating the predictive capabilities of any snowmelt and/or glacier mass balance model (cf. van der Veen, 2002b). He argued that it is currently impossible to make an absolute quantitative assessment of the balance state of a natural system (such as a glacier) unless that particular system is very insensitive to changes in the input parameters or variables (cf. van der Veen, 1999a; Hubbard *et al.*, 2005). For example, since snowmelt and glacier mass balance are very sensitive to air temperature variations, a snowmelt or glacier mass balance model cannot be used to assess the absolute amount of snowmelt or mean specific mass balance of a glacier say in the year 1672 or 2032. Even if the model itself were (almost) perfect, the uncertainty associated with the climatological input data would produce an error bar large enough to make the model predictions inconclusive in reality (cf. van de Wal and Oerlemans, 1994; Bugnion, 1999):

> "As the mean annual air temperature on Greenland is certainly not known to an accuracy of better than 1 K, one must conclude that it is impossible to obtain the present state of balance from climatological data." (Oerlemans, 1991) (cf. Cogley, 2004)

> "The use of a mass balance model, no matter how sophisticated, will probably not solve the problem of the current state of balance of the [Greenland] ice sheet." (Oerlemans, 1991) (cf. Cogley, 2004)

Oerlemans concluded that the most appropriate snowmelt and glacier mass balance modeling approach, at least for today, is to conduct sensitivity experiments (i.e. prescribed changes relative to some defined initial conditions) with a carefully calibrated and tuned model that explicitly incorporates the relevant physical processes in an appropriate manner (e.g. Walsh, 2005). Oerlemans opinion was more recently echoed and discussed by van der Veen (1999a; 2002b). Blöschl (2006) extended this argument into the realm of public policy and argued that "...the best model is not the most accurate one but the one that serves best the purpose of reaching a consensus among the players." (cf. Section 6.3.1).

6.2.4 Synopsis

Many studies have compared the performance of energy-balance and temperature-index melt models in terms of their overall predictive capabilities (e.g. Braithwaite, 1981; van der Wal, 1996; Hock, 1999; 2005; Essery and Etchevers, 2004). Such studies are certainly interesting and important – but an absolute ranking of the two very different modeling approaches is in reality not particularly useful (cf. Paterson, 1994; van der Veen, 1999a). Energy-balance models are uniquely able to describe and quantify the snow/ice melt process and associated energy exchanges – the total amount of melt for an entire glacier, watershed, or time interval is merely a secondary by-product of the modeling exercise. In contrast, temperature-index melt models can only provide such totals (van der Veen, 2002b), but offer essentially no insight into the melt processes and associated energy exchanges at the glacier surface. It seems therefore more appropriate to critically evaluate the objectives and questions of a given study, and then decide what type of model is most suitable to provide the desired answers given the specific circumstances and limitations (cf. Braithwaite, 1996; Greuell and Genthon, 2003; Etchevers *et al.*, 2004; Hock, 2005).

Despite (or rather because of) their simplicity, temperature-index melt models have proven to be effective and efficient tools for snow and ice melt modeling (Martinec and Rango, 1986), often outperforming more sophisticated energy-balance melt models in suitable applications (Bøggild *et al.*, 1999; Wild *et al.*, 2003; Hook, 2003). Temperature-index models are most appropriate to assess 'average conditions' (Fig. 6.1), defined spatially by the watershed or glacier scale, and temporally by time intervals of a few days or more (Martinec and Rango, 1986; Laumann and Reeh, 1993; Johannesson *et al.*, 1995; Bøggild *et al.*, 1999; Hock, 2003, 2005). However, their predictive capabilities decrease with increased spatial and temporal resolution (Lang and Braun, 1990). Finally, air temperature data are generally readily available from a variety of sources (for example weather station data, climate model data, and gridded climatologies), whereas the necessary data to implement an energy-balance model are often simply not available.

It is clear, after an exhaustive literature review, that temperature-index melt models perform very well for snowmelt and glacier mass balance modeling in a wide variety of different environments, for example on the Greenland and Antarctic Ice Sheet (Reeh, 1991; Wild *et al.*, 2003; Ridley *et al.*, 2005), on

the Antarctic Ice Shelves (Sheperd *et al.*, 2003), in the European Alps (Kuhn *et al.*, 1999; Braithwaite and Zhang, 2000), on glaciers in Sweden, Norway, Iceland, Canada, and Greenland (Lundquist, 1982; Young, 1982; Laumann and Reeh, 1993; Johannesson *et al.*, 1995; Hock, 1999; Engeset *et al.*, 2000), on glaciers in the Canadian High Arctic (Andrews *et al.*, 1970; Wolfe and English, 1995; Ardent, 1997; Mair *et al.*, 2005), and for global studies (Martinec and Rango, 1986; Braithwaite and Zhang, 1999; Braithwaite and Raper, 2002; Braithwaite *et al.*, 2002; Schneeberger *et al.*, 2003; Raper and Braithwaite, 2006). Bradley and England (1978) showed that the mass balance of the Devon Ice Cap is very closely related to annual melting degree-day totals measured at Resolute Bay, regardless of variations in winter snowfall. Their results also match the findings of Hooke *et al.* (1987) for the Barnes Ice Cap on Baffin Island and the results presented by Oerlemans and Reichert (2000) for the White Glacier on Axel Heiberg Island. It is difficult to quantitatively assess the uncertainty associated with such modeling experiments, although a value of about ±20 percent of the modeled annual melt totals seems to be appropriate (van der Veen, 2002b). However, in the interest of full disclosure, it is also instructive to briefly discuss the one single study (that I am aware of) where a temperature-index melt model failed to yield satisfactory results.

6.2.4.1 Harding (1986) 'Exchanges of Energy and Mass associated with a Melting Snowpack'

Harding (1986) compared the performance of an energy-balance and a temperature-index melt model in the context of snowmelt modeling on a small snow field in southern Norway. The temperature-index model in this test was unable to predict reasonable daily and seasonal snowmelt totals. Harding (1986) explained this highly unusual result by the dominance of net radiation as available energy source for snowmelt. But this is a fairly typical situation, and usually does not lead to a complete failure of a temperature-index model (cf. Braithwaite, 1981).

More importantly, air temperature during his field experiment was remarkably constant, both on a daily basis and in terms of its day-to-day variability. Consequently, variations in turbulent heat flux were mainly a function of wind speed variability (cf. Koizumi and Naruse, 1992). If air temperature does not change appreciably over time, but snowmelt and ice ablation do, then a temperature-index model obviously cannot perform well. This may be an issue for the more maritime Ward Hunt Ice Rise and Ice Shelf, but should not be a significant concern for the very continental Hazen Plateau.

Lotz (1961a) commented precisely on the absence of strong correlation between air temperature and ablation on the Ward Hunt Ice Shelf in 1959 and noted:

> "This is strikingly at variance with Sagar's conclusions [Sagar, 1962] on the [very strong] relation between ablation and meteorological factors [i.e. air temperature] on Gilman Glacier."

Summer temperatures in coastal locations, which are surrounded by sea ice or open water for much of the year, show relatively little day-to-day variability (cf. Jonsson and Hansson, 1990), especially when compared to very continental locations such as the Hazen Plateau. Therefore, one might expect a relatively weak correlation between summer temperatures and net annual mass balance for coastal ice masses (Jonsson and Hansson, 1990). Instead, mean annual temperature might be of greater importance, as superimposed ice can only form as long as the underlying ice surface is sufficiently cold (cf. Woodward *et al.*, 1997). In addition, annual precipitation and ablation season length may also be of some importance (Jonsson and Hansson, 1990). Hattersley-Smith and Serson (1970) also commented on the lack of "close correlation" between summer ablation on the Ward Hunt Ice Rise/Ice Shelf and corresponding summer temperatures at Alert, but also emphasized the importance of "the correlation between more than average warm summers and more than average cold summers in the two areas" and their respective influence on the mass balance of the Ward Hunt Ice Rise/Ice Shelf.

6.3 A Temperature-Index Melt Model for the Hazen Plateau and North Coast

6.3.1 Model Overview

The snow and ice melt sequence used in this model follows the popular approach first introduced by Rech (1991), which is considered the 'best available' modeling procedure in this context (van der Veen, 1999b). The total melting degree-days available for any given year are used to melt snow, superimposed ice, and glacier ice in the following order (Fig. 6.2):

1. Snow is melted first with a constant DDF (snow). It is assumed that all meltwater percolates initially down into the snow pack and refreezes to form

superimposed ice (spi) until the superimposed layer thickness is equal to a fixed fraction of the available winter snow accumulation (P-max).

2. Superimposed ice is melted with a constant DDF (spi), which is assumed to be identical to the DDF (ice) used in Step 3 (Huybrechts *et al.*, 1991).
3. Glacier ice is melted with a constant DDF (ice).

This snow and ice melt process can stop at any time, depending on the magnitude of annual melting degree-days and annual snow accumulation. Snowmelt on the ice-free Hazen Plateau only involves Step 1, without superimposed ice formation (cf. Section 6.5). This snow and ice melt model requires two independent input variables: annual melting degree-days and annual snow accumulation (cf. Chapter 5). The model includes three specific model parameters: DDF (snow), DDF (ice), and P-max. In addition, a digital-elevation model is required to provide the spatial reference frame in two or three dimensions. The details of the snow/ice melt model will be developed and discussed in the following sections.

The fundamental assumption in this modeling exercise is that most of the variability in snow and ice melt can be accounted for exclusively by air temperature variability (cf. Section 6.2). This modeling philosophy has been eloquently summarized by Bergström (1992) and Lindström *et al.* (1997) with respect to the well-established and widely-used HBV snowmelt runoff model (cf. Blöschl, 2006):

> "The goal was a conceptual model...of reasonable complexity, and with a requirement on input data that could be met in most...basins."

> "The model shall be based on a sound scientific foundation...[but]...complexity must be justified by model performance ...[and]...the model must be understandable by users."

The goal of these modeling experiments is therefore not to quantify all possible or even all important mass and energy exchanges associated with snowmelt and ice ablation. There is obviously some trade-off between simplicity and physical accuracy (cf. Braithwaite, 1981; van der Veen, 2002b), but a temperature-index melt model at least avoids most of the largely unsolved problems related to the spatial distribution and sub-grid parameterizations of melt processes that make spatially-distributed

energy-balance models often impractical (Ferguson, 1999; Blöschl, 2006). Predictions from a temperature-index melt model may include errors because of the (1) imperfections and simplifications inherent in the modeling approach, (2) uncertainties included in the climatological input data, and (3) uncertainties regarding the correct choice of the required model parameters (Ferguson, 1999; van der Veen, 1999a, 2002b). It is difficult to quantitatively assess the uncertainty associated with such modeling experiments, although a value of about ±20 percent of the modeled annual melt totals seems to be appropriate (van der Veen, 2002b).

6.3.2 Degree-Day Factors for Snow and Ice Melt

The single most important model parameter used in a temperature-index melt model (cf. Zweck and Huybrechts, 2005) is the degree-day factor (DDF), which provides the essential link between atmospheric energy input to the melting snow and ice surface (parameterized as melting-degree days) and resultant snow or ice melt (cf. Section 6.2.2.2). Appropriate values for the DDF (snow) and DDF (ice) for a modeling study can be obtained using four different approaches (Martinec and Rango, 1986):

1. Degree-day factors previously reported in the scientific literature (Section 6.3.2.1).
2. Degree-day factors determined using available simple (empirical) equations (e.g. Martinec, 1976; Kuunisto, 1980) (Section 6.3.2.2).
3. Degree-day factors measured in-situ on the Hazen Plateau (1999 to 2001) and North Coast (Section 6.3.2.3 and 6.3.2.4).
4. Degree-day factors derived during the model tuning/calibration phase of the experiment (Hock, 2003) (Section 6.3.2.5).

6.3.2.1 Degree-Day Factors: Values from the Literature

It is generally assumed in a temperature-index melt model that the amount of snow or ice melt at any given location is linearly proportional to the corresponding melting degree-day total. The proportionality factor (or degree-day factor (DDF)) depends primarily upon whether melting is calculated

for a snow or an ice surface (Table 6.1). The degree-day factor for snow is usually much lower than that for ice (Ahlman, 1936; Braithwaite, 1995; Hock 2003), as a melting snow surface has generally a much higher albedo than a melting ice surface (Reeh, 1991). Previous studies, for example, have simply fixed the DDF (snow) at 40 percent of the DDF (ice) (e.g. Bøgghild *et al.*, 1994) for the Greenland Ice Sheet, although that percentage appears to increase to about 70 percent for some of the Scandinavian glaciers (Braithwaite, 1996) or decrease to about 30 percent for some glaciers in the Himalayas (Singh *et al.*, 2000). The most recent compilation by Braithwaite *et al.* (2002) puts the 'global' average percentage at about 53 percent. Other studies have instead assumed a 'lumped' degree-day factor for both snow and ice (e.g. Podlech *et al.*, 2004).

The most commonly observed and used values for the DDF (snow) and the DDF (ice) overall in the scientific literature are 3 to 5 and ~7 mm weq d^{-1} $°C^{-1}$ respectively (Braithwaite, 1996; Raper *et al.*, 2000; Lefebre *et al.*, 2002). Table 6.1 lists values for DDF (snow) and DDF (ice) for selected 'Arctic' and 'High Arctic' locations around the world. The value for DDF (ice) of 6.3±1.0 mm weq d^{-1} $°C^{-1}$ (Braithwaite, 1981) is perhaps the most applicable in the context of this study, as it is based on three years of data collection on the White Glacier (1960 to 1962) and one year of data collection on the Devon Ice Cap (1963). DDF (snow) values tend to be somewhat lower (~2.8 mm weq d^{-1} $°C^{-1}$) for the 'true' High Arctic locations (= cold and dry), and slightly higher (~4.7 mm weq d^{-1} $°C^{-1}$) for the more moderate or maritime (= warmer and wetter) Arctic locations (Fig. 6.3). This difference is much less pronounced for the DDF (ice), since the physical properties of ice are less variable in time and space (Singh *et al.*, 2000).

Braithwaite (1995; his Fig. 5) tested the sensitivity of degree-day factors and predicted overall lower values for the DDF (snow) under colder and dryer climatic conditions. His model predicted a DDF (snow) of about 2 to 2.5 mm weq d^{-1} $°C^{-1}$ for the Hazen Plateau, given the measured summer air temperatures between 1999 and 2001. Braithwaite and Raper (2002) determined the DDF (snow) for 67 glaciers around the world and calculated a 'global' average of 3.6±1.1 mm weq d^{-1} $°C^{-1}$, which is (coincidentally?) identical to the overall average and standard deviation shown in Table 6.1. The only study that explicitly mentioned a value for the degree-day factor of superimposed ice (DDF (spi)) is Huybrechts *et al.* (1991), who set the DDF (spi) equal to the DDF (ice), but without any further

discussion. It seems reasonable to assume that other studies (e.g. Reeh, 1991), if they explicitly accounted for superimposed ice formation in their model, also set the DDF (spi) equal to the DDF (ice).

6.3.2.2 Degree-Day Factors: Simple (Empirical) Equations

A (perhaps) more robust approach than merely choosing what appears to be an 'appropriate' value for the degree-day factor from the scientific literature might be to use a simple (empirical) equation to parameterize the degree-day factor internally within the melt model (cf. Martinec and Rango, 1986). There are two different empirical equations published today in the scientific literature, both relating the DDF (snow) directly to snow density (Martinec, 1976; Kuunisto, 1980). These equations allow a determination of the DDF (snow) if the snow density is either known, or itself internally prescribed/parameterized within the melt model. But, why should it be appropriate to use snow density as an 'index' or 'proxy' for the degree-day factor of snow?

1. Greater snow density generally means 'older' snow with greater density, lower albedo, and higher liquid water content (Martinec, 1976; Martinec and Rango, 1986; Barry, 1996; Jin *et al.*, 1999).
2. Snow density is also a useful 'index' to describe the overall thermal properties of the snow pack (Martinec, 1976; Jin *et al.*, 1999).

These empirical equations can provide realistic values for DDF (snow) in the absence of specific on-site snowmelt measurements (Schaper *et al.*, 1999). Similar equations do not exist to estimate the degree-day factor of ice, which is much less variable in time and space (Singh *et al.*, 2000). On the other hand, Hock (2003) considered such parameterization approaches as fundamentally "problematic" and argued instead that degree-day factors are best determined internally by model calibration and tuning (cf. Section 6.3.2.4).

Martinec (1976) presented a simple empirical equation relating the DDF (snow) to snow density, based on extensive field measurements between 1958 and 1963 in the Swiss Alps:

Equation 6.5 $DDF\ (snow) = 11 * \rho_{snow} / \rho_{water}$

(Units: DDF (snow) in mm d^{-1} $°C^{-1}$; $\rho_{snow} / \rho_{water}$ in g cm^{-3})

Kuunisto (1980) presented two different empirical equations, one valid for forested sites, the other valid for open (i.e. un-forested) sites, based on data collected between 1959 and 1978 at 12 sites across Finland:

Equation 6.6 Forested sites: $DDF\ (snow) = (10.4 * \rho_{snow}) - 0.70$

Equation 6.7 Open sites: $DDF\ (snow) = (19.6 * \rho_{snow}) - 2.39$

(Units: DDF (snow) in mm d^{-1} $°C^{-1}$; $\rho_{snow} / \rho_{water}$ in g cm^{-3})

Figure 6.4 shows DDF (snow) variations for a range of typical snow densities (0.1 to 0.5), calculated using Equations 6.5 to 6.7. The Kuunisto (1980) equation for forested sites (Equation 6.6; dotted line in Fig. 6.4) is probably not appropriate in High Arctic situations. For typical dry snow densities between 0.3 and 0.35 g cm^{-3} (cf. Hattersley-Smith and Serson, 1972; Bradley and England, 1977; Jeffries and Krouse, 1987; Braun *et al.*, 2004a, b) on the Hazen Plateau and North Coast, the Martinec (1976) and the Kuunisto (1980) equations predict DDF (snow) values between 3.3 and 4.4 mm weq d^{-1} $°C^{-1}$. Overall, these values compare well with those measured on different Arctic glaciers around the world (Table 6.1). One problem with using those equations is that snow density obviously increases during the snowmelt season (Martinec and Rango, 1986). Of course, the main goal of these equations is precisely to allow for an adjustment of the DDF (snow) in response to such increases (e.g. Schaper *et al.*, 1999). Such an adjustment, however, requires detailed, comprehensive, and reliable snow density measurements throughout the entire melt season (or an appropriate internal model parameterization), which are in reality difficult to obtain for a melting snow pack (cf. Braithwaite *et al.*, 1994; Hock, 2003).

It is difficult to assess how representative these equations are for specific High Arctic conditions (cold and dry), as they were originally developed in and for more temperate Arctic (Kuunisto, 1980) or high-elevation alpine environments (Martinec, 1976). Kuunisto's measured DDF (snow) for his northernmost station (Inari) was 2.8 mm weq d^{-1} $°C^{-1}$, whereas the measured DDF (snow) at his

southernmost and most coastal station (Jokioinen) was 4.9 mm weq d^{-1} $°C^{-1}$. This pattern – lower overall DDF (snow) values in colder and drier environments – has also been noted more quantitatively by Braithwaite (1995). Table 6.1 and Figure 6.4 also shows this general spatial pattern (High Arctic vs. moderate Arctic).

The Martinec (1976) and Kuunisto (1980, 'open') equations are used in Table 6.2 to parameterize the DDF (snow) with snow densities actually measured in-situ on the Hazen Plateau and North Coast of Ellesmere Island. The equations predict a DDF (snow) of about 2.8 mm weq/DD using the measured dry snow densities for Simmons Ice Cap (2000 and 2001). The predicted DDF (snow) values for greater snow densities (e.g. Ward Hunt Ice Rise) are obviously higher (cf. Fig. 6.4). Overall, the predicted values compare well with those from other studies listed in Table 6.1.

6.3.2.3 Degree-Day Factors: Measurements on the Hazen Plateau

The degree-day factors for snow and ice measured on Murray Ice Cap and the Hazen Plateau are discussed in detail in Section 6.5.2.

6.3.2.4 Degree-Day Factors: Measurements on the North Coast

Lotz (1961a, b) presented snowmelt measurements on the Ward Hunt Ice Rise conducted in 1959, which allow a crude determination (cf. Section 6.4.1.1) of the DDF (snow) for that particular melt season of about 4.98 mm weq d^{-1} $°C^{-1}$. The mean snow density specified by Lotz (1961a, b) from 24 June 1959 at six ablation stakes was 0.366, which gives a DDF (snow) of 4.78 mm weq d^{-1} $°C^{-1}$ using Equation 6.7. This suggests that the Kuunisto (1980) 'open' DDF (snow) parameterization is appropriate for the North Coast. Likewise, the measurements presented by Lotz (1961a, b) allow for a crude estimation of the DDF (ice) on the Ward Hunt Ice Rise of about 6.5 mm weq d^{-1} $°C^{-1}$ (cf. Section 6.4.1.2). Both values compare well with those determined by other scientific studies (Table 6.1).

6.3.2.5 Degree-Day Factors: Model Calibration/Tuning

Hock (2003) proposed a radically different approach to determine appropriate degree-day factors (and melt model parameters in general) by suggesting they are best determined by model calibration and

tuning (cf. van der Veen, 1999a). This approach immediately raises concerns about its scientific validity, as it introduces a distinct element of subjectivity into the analysis. Presumably, several different combinations of model parameters will give similar fits of model output to measured data (Braithwaite and Zhang, 1999; 2000; Mair *et al.*, 2005). In other words, there may not be a unique calibration solution (Braithwaite *et al.*, 1998a; Oerlemans, 1998; Greuell and Genthon, 2003; Essery and Etchevers, 2004). For example, an increase in precipitation (i.e. external climatic forcing) can be compensated for by internally increasing the DDF (snow) or by reducing the temperature lapse rate to yield higher air temperatures (and thus increased melt) at a given elevation on the glacier or ice cap. Nonetheless, Hock (2003) argued that degree-day factors (and other melt model parameters) are sufficiently variable in time and space across a glacier or watershed that any other approach (such as simple parameterizations or limited on-site point measurements) is not able to capture this variability in a meaningful manner. In other words, degree-day factors measured at discrete points during short field campaigns are not representative at larger and longer spatial and temporal scales (cf. van der Veen, 1999a; 2002b; Blöschl, 2006). Instead, Hock (2003) argued that model tuning and calibration "within reasonable limits" represents actually a more objective and robust procedure to determine the degree-day factors and other required model parameters in general (cf. Oerlemans, 1998; Bøggild *et al.*, 1999; Ferguson, 1999; van der Veen, 1999a; Mair *et al.*, 2005).

6.3.2.6 Degree-Day Factors: Comparison of the Different Approaches

The Hock (2003) approach would be entirely reasonable if there was no uncertainty about the other components of the temperature-index melt model, such as the climatological forcing or the superimposed ice formation parameterization. In reality, there is considerable uncertainty about all aspects of the melt model and therefore the Hock (2003) approach may mask more fundamental problems with the model (Braithwaite *et al.*, 1998a; Braithwaite and Zhang, 1999; van der Veen, 2002b; Siddall, 2005). One possible solution for this problem is to evaluate the degree-day factors and their climatic sensitivity first at the point scale (e.g. at AWS G3 and AWS T3), where climatological forcing and resultant snow/ice melt were measured directly. Such an assessment can then provide the necessary 'reasonable limits' (cf. Hock, 2003) for spatial parameter optimization during model calibration and

tuning. The paucity of published melt process data from the North Coast precludes this approach for the Ward Hunt Ice Rise and Ice Shelf. Here, the available values from the scientific literature and empirical parameterizations have to provide the necessary 'reasonable limits' (cf. Section 6.4). Lefebre *et al.* (2002) modeled DDF (snow) values on the Greenland Ice Sheet of up to 15 mm weq d^{-1} $°C^{-1}$ and corresponding DDF (ice) values of up to 40 mm weq d^{-1} $°C^{-1}$ (cf. Bøggild *et al.*, 1994; Braithwaite, 1995; Morris, 1999; Morris and Mulvaney, 2004; Mair *et al.*, 2005). The DDF (snow) and DDF (ice) frequency distributions values, however, strongly peaked at 3 and 8 mm weq d^{-1} $°C^{-1}$ respectively and those values were used by Ridley *et al.* (2005) to model the mass balance (and complete disappearance) of the Greenland Ice Sheet under a high CO_2 climate. Braithwaite *et al.* (2002) 'picked' a DDF (snow) value of 3.7 mm weq d^{-1} $°C^{-1}$ and a DDF (ice) value of 7.0 mm weq d^{-1} $°C^{-1}$ for a global glacier mass balance sensitivity study.

6.3.3 Superimposed Ice Formation

Superimposed ice formation has long been recognized as an important process affecting the mass balance especially of sub-polar and polar glaciers (e.g. Schytt, 1949; Baird *et al.*, 1952; Koerner, 1970; Wakahama *et al.*, 1976; Hagen and Liestol, 1990; Braithwaite, 1996; Woodward *et al.*, 1997; Wadham and Nuttall, 2002; Obleitner and Lehning, 2004). For example, superimposed ice formation contributed an additional 0.1 to 0.2 m weq mass accumulation (about 10 to 30 percent of the winter snow accumulation) (Hagen and Liestol, 1990) on some glaciers in Svalbard. On temperate glaciers, superimposed ice formation either does not occur at all or only represents an insignificant process in the context of snowmelt or glacier mass balance (Oerlemans, 2001; Braithwaite *et al.*, 2002). Superimposed ice formation therefore needs to be incorporated into any quantitative attempt to predict glacier mass balance changes in the Arctic associated with past and future climate change (Huybrechts *et al.*, 1991; Pollard and Thompson, 1997; Woodward *et al.*, 1997; Braithwaite and Zhang, 1999; Wadham and Nuttall, 2002; Ridley *et al.*, 2005; Wright *et al.*, in press).

Superimposed ice forms typically at the base of the (winter) snow pack on glaciers, when percolating meltwater refreezes upon contact with the underlying cold glacier ice (Schytt, 1949; Ward, 1954; Koerner, 1970; Ambach, 1985). In High Arctic regions, where winter air temperatures are continually below 0°C, virtually all superimposed ice formation occurs during the summer melt season,

but more maritime Arctic glaciers (e.g. on Svalbard) may also experience superimposed ice formation during the spring, fall, and even winter (Wadham and Nuttall, 2002). On some High Arctic glaciers, superimposed ice formation accounts for much or all of their annual mass accumulation (e.g. Baird *et al.*, 1952; Paterson, 1969; Blatter and Kappenberger, 1988; Jonsson and Hansson, 1990). Superimposed ice formation thus represents a unique 'mass buffer' for the glacier (Obleitner and Lehning, 2004), as superimposed ice has to be melted again before it can runoff the glacier, effectively reducing net glacier ablation produced by a given energy input to the glacier surface over a melt season. As a result, the energy required to remove the accumulated winter snow from the glacier surface is considerably higher, since the snow pack has to be melted effectively twice: first as snow, and subsequently again as superimposed ice (Paterson, 1990; Bøggild *et al.*, 1994). In other words, the glacier can effectively 'absorb' a certain amount of energy input or melting before any net mass loss occurs (Schytt, 1964; Boike *et al.*, 2003). Or, in the precise words of Schytt (1949):

> "...the ablation must first scale of a layer...of superimposed ice before it comes down to the real glacier ice." (see Schytt (1949, Fig. 6) for a beautiful picture of this 'new' superimposed ice 'superimposed' on 'old' glacier ice below)

Superimposed ice formation can be therefore regarded as a unique 'survival mechanism' for High Arctic glaciers or ice caps. In general, superimposed ice formation occurs preferentially on those parts of a glacier or ice cap where meltwater drainage is somehow impeded (Hattersley-Smith, 1960c; Koerner, 1970), such as flat summit plateaus or areas with enhanced snow accumulation (e.g. along the ice margins). Superimposed ice formation thus may be able to compensate for some of the enhanced ablation experienced along the ice margins due to the advection of warm air from the surrounding ice-free terrain (Hattersley-Smith *et al.*, 1961; Wendler, 1974; van de Wal *et al.*, 1992; Wolfe and English, 1995).

Glacier mass balance models typically treat superimposed ice formation (if at all) in a highly schematic fashion. The most common approach is to set some fixed limit to the thickness of superimposed ice that can develop during the annual snowmelt before runoff occurs (e.g. Reeh, 1991; Pollard and Thompson, 1997; Braithwaite and Zhang, 1999; Janssens and Huybrechts, 2000; Marshall *et al.*, 2004). This is generally accomplished by introducing a dedicated model parameter, P-max, which represents the proportion of annual snowfall or (winter) snow pack water equivalent which melts to form

superimposed ice at a given site on the glacier (Reeh, 1991). Appropriate values for P-max can be obtained using three different approaches (cf. Martinec and Rango, 1986):

1. P-max values previously published in the scientific literature (Section 6.3.3.2).
2. P-max values determined using simple (empirical) equations (Section 6.3.3.3).
3. P-max values measured in-situ on the Hazen Plateau (Section 6.3.3.4) and North Coast (Section 6.3.3.5).

There is obviously no reason to expect that the amount of superimposed ice formed across a glacier or ice cap is spatially-homogeneous. In reality, many factors can influence the amount of superimposed ice formation at a given location, including snow depth and density, ablation season length, snow/ice temperature, topography of the glacier surface, and availability of ponded meltwater at the ice surface (Schytt, 1949; Koerner, 1970; Obleitner and Lehning, 2004). It is therefore important to realize any simple parameterization of superimposed ice formation represents a drastic simplification of reality. There are more sophisticated approaches to model meltwater percolation and refreezing within the snow pack and associated superimposed ice formation, employing more physically-based snow pack models (e.g. Pfeffer *et al.*, 1990; Janssens and Huybrechts, 2000; Obleitner and Lehning, 2004; Wright *et al.*, in press; and references therein), but those approaches are not useable in the context of this study (cf. Marshall *et al.*, 2004). The challenge is therefore to find an appropriate, yet simple, superimposed ice parameterization that can be incorporated into a temperature-index melt model without the need for any additional input data.

Ambach (1985) was the first to develop several simple parameterizations for superimposed ice formation, based on his longtime work on the Greenland Ice Sheet. He also emphasized that superimposed ice formation is "of decisive importance" for the mass and energy balance of an arctic ice sheet or ice cap, especially near the equilibrium line of the ice mass (cf. Braithwaite, 1996). Ambach (1985) determined a value for P-max of 0.66, based simply on the conservation of mass during snowmelt

and an assumed (but realistic) initial snow density of 0.3 and superimposed ice density of 0.9. His approach provided the basis for the popular P-max value of 0.6 used frequently in the scientific literature (see below). Ambach (1985) continued the conservation of mass argument and determined that, at the glacier equilibrium line, the ratio of the number of days with a melting snow surface and with melting superimposed ice is 2:1 (cf. Boike *et al.*, 2003). In other words: snowmelt typically takes twice as long as superimposed ice melt, because of the lower albedo (i.e. higher degree-day factor) of an exposed superimposed ice surface (Ambach, 1985).

6.3.3.1 The Importance of Superimposed Ice Formation: Some Simple Considerations

Table 6.3 presents a simple 'back-of-the-envelope' calculation to illustrate the importance of superimposed ice formation in the context of snowmelt and glacier mass balance.

- It takes 15 additional melting degree-days (or 30 percent) to remove all mass accumulation from a glacier compared to the ice-free tundra, which is equivalent to about three very warm summer days on the Hazen Plateau.
- A glacier can experience 90 mm weq melt (or 30 MDD) without actually loosing any net mass, as 30 MDD are simply consumed in the conversion of snow to superimposed ice.
- On the ice-free tundra, 30 MDD are able to melt and remove 90 mm weq snow, leaving only 60 mm weq behind for the remainder of the snowmelt season.

This simple calculation shows that a glacier can initially 'buffer' 30 MDD without any net mass loss, simply through superimposed ice formation. Overall, at the end of the melt season, superimposed ice requires 15 additional MDD to be removed. This simple calculation illustrates that superimposed ice formation is an important process and therefore has to be incorporated into a snow and ice melt model for the Hazen Plateau and North Coast.

6.3.3.2 Superimposed Ice Formation: Values from the Literature

Table 6.4 presents a comprehensive compilation of all directly or indirectly reported values of P-max in the scientific literature about Arctic glaciers. Values generally range between 0.4 and 0.6 (Fig. 6.5) (cf. Janssens and Huybrechts, 2000). This considerable variation is not surprising, given the many variables that are actually involved in superimposed ice formation (Koerner, 1970) and obviously presents a challenge when attempting to develop a simple and robust superimposed ice formation parameterization. Overall, higher values of P-max (> 0.4) appear to be characteristic for colder and drier locations (e.g. Greenland Ice Sheet), whereas lower values (P-max < 0.4) appear to be characteristic of more moderate, maritime Arctic environments (e.g. Svalbard). The P-max values for the Ward Hunt Ice Rise and Ice Shelf are of particular interest in the context of this study. In 1959, P-max was 0.41, whereas in 1960, P-max was 0.57 (cf. Section 6.3.3.5). Winter snow accumulation in 1960 was considerably greater than in 1959, suggesting a dependence of P-max on total available snow accumulation (cf. Section 6.3.3.3).

If superimposed ice formation is parameterized in a glacier mass balance model, the most common approach is to use a constant value of P-max = 0.6 (e.g. Reeh, 1991; Woodward *et al.*, 1997; Janssens and Huybrechts, 2000; Marshall *et al.*, 2004) following the considerations by Ambach (1985), even when the climatic boundary conditions are altered substantially from those of the present. The simple mean P-max of this compilation is 0.44±0.14 (Table 6.4) which is consistent with the conclusions by Arendt (1997) and Janssens and Huybrechts (2000) that the popular value of P-max = 0.6 is actually too high in many cases. For example, Janssens and Huybrechts (2000) reported an 'optimized' value of P-max of about 0.3 for the Greenland Ice Sheet as a whole. The data presented by Hattersley-Smith *et al.* (1961) suggested a value of P-max for one location on the Gilman Glacier in 1961 of about 0.2. Fujita *et al.* (1996) and Fujita and Ageta (2000) reported P-max values between 0.2 and 0.26 for a high-elevation glacier on the Tibetan Plateau. Fortunately, Janssens and Huybrechts (2000) and van der Veen (2002b) were able to show that the overall modeled mass balance of the Greenland Ice Sheet was not very sensitive to the specific choice of P-max (cf. van der Veen, 1999b; Marshall *et al.*, 2004; Ridley *et al.*, 2005).

6.3.3.3 Superimposed Ice Formation: Simple (Empirical) Equations

A perhaps more robust approach than arbitrarily choosing what may appear as an 'appropriate' P-max value from the scientific literature might be to incorporate a simple internal parameterization for superimposed ice formation into the temperature-index melt model. There are basically three different types of simple equations available in the scientific literature today: one type determines the amount of superimposed ice formation based exclusively on mean annual temperature (e.g. Woodward *et al.*, 1997) whereas another type relates superimposed ice formation to snow pack water equivalent and snow/superimposed ice density (e.g. Braithwaite *et al.*, 1994). A third approach presented more recently by Janssens and Huybrechts (2000) incorporates both air temperature and precipitation into a simple superimposed ice parameterization.

Woodward *et al.* (1997) essentially simplified the simple heat flux approach originally introduced by Ward and Orvig (1953), combined with more recent field measurements on Ellesmere Island by Wolfe (1995), and presented an empirical equation that relates the maximum amount of superimposed ice formation that can occur at a point on a glacier for a given year (in cm ice thickness, not water equivalent) to the mean annual temperature (MAT) at that particular point on the glacier:

Equation 6.8 $SPI\ (cm) = (-0.69 * MAT) + 0.0096$

Equation 6.9 $P\text{-}max = (SPI * \rho_{SPI}) / SWE$

(SWE = snow water equivalent of winter snow accumulation)

This simple superimposed ice formation parameterization was most recently used by Mair *et al.* (2005) in the context of a mass balance reconstruction for the Devon Ice Cap. The Woodward *et al.* (1997) approach is very convenient, as it only requires MAT as an input variable, which is often readily available from climate stations or borehole ice temperatures. It is also possible to investigate changes in superimposed ice formation (Fig. 6.6; Table 6.5) as a function of climate change, prescribed as changes in MAT over time (Woodward *et al.*, 1997). The slope of the line relating superimposed ice thickness to MAT (Fig. 6.6) can therefore be viewed as a measure of the climatic sensitivity of superimposed ice formation. Superimposed ice formation decreases by 6.9 cm for every 1°C increase in MAT. It is

interesting to note that an almost identical climatic sensitivity for superimposed ice formation (7 cm decrease per 1 °C air temperature increase) has been calculated by Obleitner and Lehning (2004) for a glacier on Svalbard (Kongsvegen), using a sophisticated physically-based snow pack evolution and energy balance model.

The fundamental problem with the Woodward *et al.* (1997) approach is that it does not incorporate the actually available amount of (winter) snow accumulation on the glacier or ice cap into the superimposed ice parameterization. Rather, it determines a (maximum possible) thickness for superimposed ice that can form each year exclusively as a function of the MAT. For example, the predicted superimposed ice thickness for Murray Ice Cap (MAT = –17.0°C; cf. Chapter 5 or Table 6.5) is 11.7 cm or 106 mm weq. Normal levels of winter snow accumulation on the Hazen Plateau are only about 125 mm weq (±25 percent) (cf. Chapter 5). The predicted superimposed ice thickness for the Ward Hunt Ice Rise and Ice Shelf (MAT = –19.9°C; cf. Chapter 5) is 13.7 cm or 124 mm weq. Normal levels of winter snow accumulation on the North Coast are only about 160 mm weq (±25 percent) (cf. Chapter 5). The Woodward *et al.* (1997) model can therefore easily produce more superimposed ice than actual winter snow accumulation available for a given year (i.e. P-max ≥ 1) (Fig. 6.7). This is especially a concern for cold and dry areas, such as the Canadian High Arctic (cf. Jonsson and Hansson, 1990). Obviously, the fundamentally limiting factor for superimposed ice formation is the amount of (winter) snow accumulation, as the amount of refreezing meltwater and superimposed ice formation cannot exceed the amount of snow available in the first place (cf. Koerner, 1970; Ambach, 1985; Bøgghild *et al.*, 1994), no matter how cold the underlying ice surface is.

Braithwaite *et al.* (1994) presented a simple equation based on earlier work by Shumskii (1964), Ambach (1985), and Pfeffer *et al.* (1991) that can be used to determine the maximum amount of superimposed ice formation (and associated value for P-max) based on snow density, superimposed ice density, and water equivalent of the available winter snow pack:

Equation 6.10 $$\text{P-max} = (\rho_{SPI} - \rho_{snow}) / \rho_{SPI}$$

The maximum amount of superimposed ice formation (mm weq) can then be determined by combining total (winter) snow accumulation (SWE; mm weq) and P-max, as calculated by Equation 6.10:

Equation 6.11 SPI (mm weq) = SWE * P-max

Braithwaite *et al.* (1994) used field data collected in West Greenland (measured snow density = 0.375; assumed superimposed ice density = 0.890) to calculate a P-max value of 0.58 (Table 6.4). They concluded that this simple equation is applicable in the ablation and accumulation zone of the Greenland Ice Sheet, provided that appropriate densities are available for snow and superimposed ice. Braithwaite (1996) argued that this approach is "probably good enough" given the other large uncertainties in snowmelt and glacier mass balance modeling (cf. Braithwaite *et al.*, 2002). Braithwaite and Zhang (1999) subsequently used a value of P-max = 0.58 in a global glacier mass balance modeling study that included the White Glacier and Devon Ice Cap. Figure 6.8 shows the amount of superimposed ice formation (expressed as P-max) as a function of snow density using the Braithwaite *et al.* (1994) equation. Superimposed ice density was set to 0.9 (cf. Table 6.6). The Braithwaite *et al.* (1994) equation predicted P-max values between 0.61 and 0.67 for typical range of dry snow densities between 0.3 and 0.35 (e.g. Braun *et al.*, 2004b), consistent with reported P-max values for cold and dry Arctic locations in Table 6.4. P-max values calculated using the Braithwaite *et al.* (1994) equation for snow densities measured on the Hazen Plateau and North Coast are listed in Table 6.7.

Janssens and Huybrechts (2000) presented a third superimposed ice formation parameterization that is based on a simple thermodynamic parameterization of the meltwater refreezing process within the snow pack (cf. Huybrechts and de Wolde, 1999):

Equation 6.12 P-max = min (0.003 * (MAT/total annual precipitation); 1)

This equation assumes a thickness of about 0.5 m for the thermally-active layer that is raised to the melting point by latent heat release associated with superimposed ice formation. It can be used to predict superimposed ice formation (expressed as P-max) based on mean annual air temperature (°C) and

total annual precipitation (m weq) (e.g. Hanna *et al.*, 2002; 2005, Ridley *et al.*, 2005). Figure 6.9 presents a contour plot of the equation for a range of mean annual temperatures and annual totals of precipitation. For the Hazen Plateau ice caps (AWS G3*), the model predicts a P-max value of 0.41 (assuming MAT = –17°C and annual precipitation = 125 mm weq; cf. Chapter 5 or Table 6.5). For the North Coast (WHIRWHIS*), the model predicts a P-max value of 0.37 (assuming MAT = –19.9°C and annual precipitation = 160 mm weq; cf. Chapter 5).

6.3.3.4 Superimposed Ice Formation: Measurements on the Hazen Plateau

Superimposed ice formation and applicable measurements on Murray Ice Cap are presented in detail in Section 6.5.2.

6.3.3.5 Superimposed Ice Formation: Measurements on the North Coast

Superimposed ice formation represents the most important mode of annual mass accumulation on the maritime Meighen Ice Cap (Arnold, 1965; Paterson, 1969). It is therefore reasonable to assume that superimposed ice formation is also an important process on the Ward Hunt Ice Rise (WHIR) and Ward Hunt Ice Shelf (WHIS). Superimposed ice formation has been measured and reported by Sagar (1962) and Lister (1962) for two years of measurements in 1959 and 1960 (cf. Table 6.4). Their data allow formulation of several conclusions:

- The amount of superimposed ice formation each year is very similar on the ice rise and ice shelf.
- The mean P-max value measured in 1959 (0.41) was considerably less than the corresponding value in 1960 (0.57).
- Mean snow accumulation in 1959 (170 mm weq) was also considerably less than the corresponding value in 1960 (240 mm weq).
- The 1960 P-max value of 0.38 (for a different section of the ice shelf with reduced winter snow accumulation of ~170 mm weq) was similar to the 1959 P-max value of 0.41.

- Superimposed ice formation on the ice shelf is somewhat enhanced inside the ice shelf troughs as opposed to the ice shelf ridges.

6.3.3.6 Basal Ice Formation

A very similar process to superimposed ice formation on glaciers has also been described on unglaciated tundra surfaces and stream channel beds and is commonly referred to as 'basal ice formation' (Woo and Heron, 1981; Woo *et al.*, 1982; Boike *et al.*, 2003). Basal ice formation, in general, represents a much more localized process (Woo *et al.*, 1982), typically restricted to stream channels, topographic depressions, and thick snow drifts/banks (cf. Østrem, 1963). We did not observe any evidence for spatially-extensive basal ice formation on the Hazen Plateau between 1999 and 2001. Presumably, the spring snow cover is typically too thin and the tundra surface of the Hazen Plateau too permeable to allow for significant basal ice formation. On the Hazen Plateau, the tundra surface is mainly coarse gravel, rocks, and boulders. The meltwater reaching the bottom of the snow pack during snowmelt is thus able to infiltrate readily into the ground below before refreezing (Woo and Heron, 1981). In contrast, glacier ice is impermeable, thus the meltwater can refreeze readily on top of the underlying glacier ice to form superimposed ice. Eventually, the available pore space of the tundra surface may fill-up completely with refrozen meltwater. But by that time, the refreezing process has likely warmed the ground surface sufficiently, and the snow cover has melted enough, to prevent significant and widespread basal ice formation (Woo *et al.*, 1982).

6.3.3.7 Superimposed Ice Formation: Comparison of the Different Approaches

It is clearly necessary to incorporate superimposed ice formation into the temperature-index melt model for the Hazen Plateau and North Coast of Ellesmere Island. The complex process of superimposed ice formation as detailed for example by Pfeffer *et al.* (1991) and Obleitner and Lehning (2004) however needs to be drastically simplified and parameterized by assuming that all percolating meltwater during the early snowmelt period refreezes within the inter-grain pore space at the bottom of the snow pack to form a solid layer of superimposed ice at the snow/ice interface. Therefore, a portion of the initial snowmelt has to be melted again (i.e. twice) before producing runoff and glacier mass loss (Bøggild *et al.*, 1994).

The simple superimposed ice parameterization proposed by Woodward *et al.* (1997) is very appealing at first, as it only requires mean annual air temperature (MAT) as input variable. The exclusion of any snow information (e.g. water equivalent or density), however, creates a peculiar problem, especially in cold and dry environments. The Woodward *et al.* (1997) model effectively determines an upper limit of superimposed ice formation (= maximum refreezing potential, cf. Bøggild *et al.*, 1994), using ice temperature (parameterized as MAT) to describe the coldness or refreezing potential of the underlying ice. Simply speaking, the colder the ice, the more superimposed ice can form during snowmelt. In reality, available snow accumulation is (also) a (more) limiting factor, since the amount of superimposed ice formation cannot exceed the amount of snow available, no matter how cold the ice is (cf. Koerner, 1970; Ambach, 1985; Bøgghild *et al.*, 1994). The superimposed ice parameterizations that instead require snow and superimposed ice densities rely heavily on the correct choice of those densities, which in reality is not straightforward at all (Braithwaite *et al.*, 1994). The approach proposed by Janssens and Huybrechts (2000) is perhaps the most appealing, as it incorporates both the availability of snow and coldness of the ice into the superimposed ice parameterization. Their model has been used successfully by Hanna *et al.* (2002, 2005), Ridley *et al.* (2005), and Zweck and Huybrechts (2005) based on climate model data for MAT and annual precipitation.

Janssens and Huybrechts (2000) also compared several different meltwater refreezing and superimposed ice formation parameterizations for the Greenland Ice Sheet and concluded that a simple approach, using a realistic value for P-max (e.g. 0.3; cf. Zweck and Huybrechts, 2005), is perfectly appropriate for glacier mass balance sensitivity studies (all superimposed ice parameterizations compared in their study yielded very similar overall totals and sensitivities for a +1°C warming scenario) (cf. Marshall *et al.*, 2004; Zweck and Huybrechts, 2005). Nevertheless, a major flaw affecting all currently available superimposed ice formation parameterizations is that they neglect the surface topography of the glacier or ice cap, which in reality has a considerable effect on the amount, rate, and spatial distribution of superimposed ice formation (cf. Hattersley-Smith, 1960c; Koerner, 1970).

6.3.4 Summer Snowfall Events

Summer snowfall events have an obvious and direct influence on glacier mass balance, since they simply 'add' snow (i.e. mass) to the glacier during the summer and thus represent an additional source of accumulation (e.g. Ageta and Higuchi, 1984), although the total amounts of summer snowfall in the Canadian High Arctic may be too small to begin with to have a significant effect on glacier mass balance (Braithwaite and Olesen, 1988; Favier *et al.*, 2004). However, summer snowfall events also tend to reduce ablation by increasing the surface albedo of the glacier and surrounding ice-free terrain for sometime following the actual snowfall event (Hattersley-Smith, 1960a; Hattersley-Smith and Serson, 1970; Alt, 1979; Jonsson, 1982; Brock *et al.*, 2000b; Fujita and Ageta, 2000).

About 27 percent (or 52.5 mm weq) of the annual snowfall at Alert typically occurs during the three summer months (June, July, and August) (Table 6.8). The relative contribution and absolute amounts are considerably less at Eureka (14 percent and 11.1 mm weq, respectively). Summer snowfall contributes about 20 percent of the total annual snowfall at Lake Hazen and on the Gilman Glacier (cf. Chapter 5). Oerlemans and Klok (2004) derived a simple empirical approach to parameterize the direct consequences (= mass addition) and indirect effects (= albedo increase) of summer snowfall events on the mass balance of the Morteratsch Glacier in the Swiss Alps. They showed that it took about five days for the particular summer snowfall event used in their case study to melt and the associated albedo increase to disappear again. They then defined a feedback factor F as the ratio between the resultant change in glacier mass balance and the direct mass addition to the glacier due to the studied snowfall event. They found that a typical feedback factor F in the ablation zone of the Morteratsch Glacier is between 3 and 4 (Fig. 6.10), depending on the precise methodology used in its parameterization. For the entire glacier, they found that a much smaller value was more appropriate (F~1.6), since the influence of the indirect albedo effect diminishes at higher elevations (= accumulation area) of the glacier.

The Oerlemans and Klok (2004) summer snowfall parameterization is illustrated in Figure 6.10 for a winter snow accumulation of 100 mm weq and a summer snow accumulation of 25 mm weq (= precipitation climatology for the Hazen Plateau; cf. Chapter 5). Assuming a feedback factor F of 3 (4), 25 mm weq summer snowfall translates into 75 (100) mm weq 'effective' summer mass accumulation for the glacier when accounting for the indirect albedo effect of the summer snowfall events. However, this

parameterization is not applicable for a temperature-index melt model, since the degree-day factor for snow implicitly incorporates these indirect albedo effects. Consider, for example, a winter snow accumulation of 100 mm weq. Assuming a DDF (snow) of 2.5 mm weq d^{-1} deg^{-1}, it would take 40 melting degree-days to melt the entire winter snow pack during the spring snowmelt period. Now, consider a situation where a large summer snowfall event leads to an additional 100 mm weq summer snow accumulation, effectively turning the landscape back to late winter, pre-melt conditions (i.e. 100 percent snow cover on the glacier and surrounding ice-free terrain). Such a snowfall event would translate to 300 or 400 mm weq 'effective' mass accumulation according to the Oerlemans and Klok (2004) parameterization, which would require 120 or 160 additional melting degree-days to melt. Furthermore, if the summer melt season were to end before the entire parameterized 'effective' mass accumulation was melted again, the glacier would gain more mass than it actually accumulated over the course of its mass balance year.

The situation may be slightly different for very small amounts of summer snowfall and/or other types of 'trace' solid precipitation (e.g. rime, hoar frost, frozen fog, etc.). Such events may be able to reduce ablation appreciably by increasing the surface albedo of the glacier and surrounding ice-free terrain, albeit without registering as significant or measurable mass accumulation events (cf. Jonsson, 1982). Hattersley-Smith and Serson (1970), in fact, implied that such indirect effects may amplify the mass balance response of the Ward Hunt Ice Rise and Ice Shelf to relatively small changes in air temperature.

6.3.5 Climatic Forcing

It is worth noting that the effects of a changing climate on glaciers will not solely manifest themselves through changes in air temperature and/or precipitation. Changes in atmospheric moisture, cloud cover, radiation balance, and atmospheric circulation patterns are other potentially significant climatic factors influencing the mass balance of glaciers (e.g. Alt, 1979; Østrem and Tvede, 1986; Cline, 1997; Cawkwell and Bamber, 2002; Nesje and Dahl, 2003; Pielke *et al.*, 2004; Maasch *et al.*, 2005; Mark and Seltzer, 2005; Nordli *et al.*, 2005). However, the spatial and temporal variations of these (secondary?) climatic variables are not (yet?) reliably resolved by existing global climate models at the regional or

local scale (Ohmura *et al.*, 1996a; Oerlemans *et al.*, 1998), limiting their usability in the context of cryospheric modeling mainly to assess future or past air temperature and precipitation changes (e.g. Schneeberger *et al.*, 2001, 2003; Wild *et al.*, 2003; Oerlemans *et al.*, in press). Furthermore, estimates of past climatic conditions in the Canadian High Arctic (and elsewhere around the world) based on paleoclimatic proxy records are essentially limited to (largely) qualitative summer temperature and annual precipitation changes (Bradley, 1990).

6.3.5.1 'Modern' Climatic Conditions (1951 to 2000)

The modern climatologies of the North Coast and Hazen Plateau were developed and comprehensively discussed in Chapter 5 – here only a short summary table (Table 6.9) is included. In terms of mean summer temperature, the climatic conditions along the North Coast (0 m asl) are fairly similar to those of the Hazen Plateau (~1100 m asl) . The Arctic Ocean/Continentality effect becomes most pronounced in July, when the North Coast is considerably colder than the Hazen Plateau. Air temperatures in July are frequently used as generalized indices for glaciation and glacier mass balance (e.g. Bradley, 1973, 1975; Vaughn and Doake, 1996; Dahl *et al.*, 1997; Hostetler and Clark, 2000; Porter, 2001) and it is therefore not surprising at all that the long-term mass balance of the Hazen Plateau ice caps has been much more negative than the corresponding surface mass balance of the Ward Hunt Ice Rise and Ice Shelf (Braun *et al.*, 2004a, b).

6.3.5.2 Climate Sensitivity: Temperature and/or Precipitation

Glacier mass balance changes in response to climate change are typically assessed for a ±1°C warming or cooling and/or a ±10 percent increase or decrease in annual or winter precipitation (e.g. Oerlemans and Fourtin, 1992; Oerlemans *et al.*, 1998). The choice of these particular values is somewhat arbitrary (cf. Chapter 2), but provides a useful reference frame to compare the climatic sensitivity of different glaciers worldwide (Braithwaite and Zhang, 1999; Oerlemans, 2001). It is important to note, however, that the mass balance response of a glacier to a positive or negative climate perturbation is not necessarily entirely symmetrical (Schytt, 1964; van de Wal and Oerlemans, 1994; cf. Section 6.4).

However, it is also reasonable to assume that the net effect of any change in air temperature on glacier mass balance will be (at least in part) offset by corresponding changes in precipitation (= negative feedback process) (e.g. Miller and de Vernal, 1992; Greene *et al.*, 1999; Weber and Oerlemans, 2003; Morris and Mulvaney, 2004; de Woul and Hock, 2004; Chinn *et al.*, 2005; Davis *et al.*, 2005; Johannessen *et al.*, 2005). For example, Bøggild *et al.* (1994) and Janssens and Huybrechts (2000) determined a 5 percent increase in annual precipitation for a +1°C increase of monthly or seasonal air temperature on the Greenland Ice Sheet. Oerlemans (1991) determined a very similar value (4 percent) for the precipitation change associated with a 1°C temperature change. Kattsov *et al.* (2005) reported values between 3 and 3.5 percent annual precipitation increase per degree warming for the next 100 years in the Arctic as a whole. Other values in the scientific literature typically range from 3 to 9 percent increases in annual precipitation per 1°C increase in annual mean temperature (Oerlemans, 1991; Morris and Mulvaney, 2004). For global studies, precipitation increases/decreases between 10 and 20 percent per degree warming/cooling appear to be more appropriate (Oerlemans *et al.*, 1998; Braithwaite and Zhang, 1999).

However, the projected increases in annual precipitation do not necessarily imply that the total annual amount of solid precipitation (i.e. snowfall) will increase proportionally. Woo and McCann (1994), for example, concluded that snowfall under a double CO_2 climate will probably constitute a smaller portion of the annual precipitation. This does not, however, necessarily imply that the total amount of annual snowfall will decrease in the future, but that the relative contribution of annual snowfall to annual precipitation will decline in favor of rainfall. On the other hand, Zhang *et al.* (2000) argued that most of the projected temperature and associated precipitation changes in the Arctic will occur during the fall and winter season, when air temperatures are still well-below freezing (cf. Serreze *et al.*, 2000; Przybylak, 2002; Johannessen *et al.*, 2004). The phase of precipitation (i.e. liquid vs. solid) is usually determined in snowmelt, glacier mass balance, and climate models by defining a fixed threshold temperature ranging typically between 0° and 2°C (e.g. Oerlemans, 1991, 1993; Fierz *et al.*, 2003; Marshall *et al.*, 2004; Strasser *et al.*, 2004). Ohmura *et al.* (1999) employed a somewhat more sophisticated approach and parameterized the proportion of solid precipitation each month (in percent) by mean monthly air temperature and an empirical higher-order regression equation (cf. Ageta and Higuchi,

1984). Either way, summer temperatures on northern Ellesmere Island today (Table 6.9) fall very close or even within these commonly-used threshold temperature ranges, suggesting that only small changes in summer temperature can determine whether summer precipitation falls as snow or as rain (cf. Hattersley-Smith, 1969; Hattersley-Smith and Serson, 1970). The direct heat advection associated with liquid precipitation is usually negligible and thus typically neglected in energy-balance models (cf. Section 6.2.1.1), although summer rainfall events, especially when of high-intensity, can have a significant impact on the physical properties of the (melting) snow pack (Hattersley-Smith, 1969; Male and Gray, 1981; Hay and Fitzharris, 1988; Greuell and Genthon, 2003). Summer rainfall events of sufficient intensity can also drastically alter the surface conditions of an Arctic glacier or ice cap by 'flushing' away the weathering crust (Mueller and Keeler, 1969) typically formed at the ice surface (cf. Jonsson, 1982).

6.3.5.3 Past Climatic Conditions: The Early Holocene, the 'Little Ice Age', and the early 20th century

The overall climatic variability throughout the Holocene in the Canadian High Arctic was characterized by warmer than present conditions during the early Holocene (~8 to 10 kyr BP), followed by a gradual cooling trend that culminated in the so-called 'Little Ice Age' between about 1250 and 1900 (Bradley, 1990; Koerner and Fisher, 2002; Bradley *et al.*, 2003; Gajewski and Atkinson, 2003). It is also worth emphasizing that even the mains phase of the 'Little Ice Age' (~1600 to 1900) was not a uniformly cold period, but also included a period of relative warmth in the 1700s (Fisher *et al.*, 1998; Gajewski and Atkinson, 2003). Williams (1978a) determined, via a simple mass and energy balance modeling experiment, that summer air temperatures during the 'Little Ice Age' were about 1.5°C lower than present on Baffin Island. This value compares well with other independent estimates from ice core records (e.g. Koerner, 1989a) and logs of Royal Navy ships wintering in the Northwest Passage between 1819 and 1859 (Dowdeswell, 1995) (Table 6.10).

In general, modern air temperatures (from 1951 to 2000) are (still) somewhat lower than those of the early Holocene (Koerner and Fisher, 2002). There is additional evidence from snow-pit and firn-core studies (Hattersley-Smith, 1963; 1969, Holdsworth, 1984) for further elevated summer temperatures (~1 to 2°C), increased glacier melting, and glacier recession in the period from about 1925 to 1961 (cf.

Diamond, 1960; Davies and Krinsley, 1962; Warren, 1990; Bengtsson *et al.*, 2004; Johannessen *et al.*, 2004). This suggests overall more negative glacier mass balances in the Canadian High Arctic during the first part of the 20th century (cf. Thorarinsson, 1940), compared to the last 40 years of direct glaciological measurements (Koerner, 1996). However, Bengtsson *et al.* (2004) noted more recently that the present warming trend (with respect to mean annual temperatures) in the Arctic has now (just) reached the peak warming values of the 1940s (cf. Davies and Krinsley, 1962; Warren, 1990).

6.3.5.4 Future Climatic Conditions: The 21st century

Walsh *et al.* (2002) presented a comprehensive assessment and discussion of current and future Arctic climate simulations by currently available state-of-the-art global climate models (cf. Johannessen *et al.*, 2004). These simulations consistently predicted increases in air temperature and precipitation during the twenty-first century in the Arctic as a whole. The absolute magnitudes of the projected changes, however, differed significantly between the different climate models (especially for precipitation, see below), but the relative changes appeared to be more-or-less consistent (Walsh *et al.*, 2002) across the different models.

The Arctic Climate Impact Assessment (ACIA, 2004) also included projections of 21st century climate change in the Arctic, using a composite of five state-of-the-art global climate models forced by the IPCC SRES B2 emissions scenario (Kattsov *et al.*, 2005). The global gridded data (for air temperature and precipitation only at 2.5° latitude by 2.5° longitude resolution) are available at http://igloo.atmos.uiuc.edu/ACIA/index.html from January 1980 to December 2099 at monthly resolution (n = 1440 month).

Mean monthly air temperatures from January 1980 to December 2099 (n = 1440 months or 120 years) were extracted from the global data set for the 2.5° latitude by 2.5° longitude grid box centered on 82. 5°N and 70°W ('Hazen Plateau grid box'; Table 6.12). The predicted temperature changes are greatest, as expected, during the fall and winter months (Fig. 6.11, Fig 6.12), which is presumably related to reduced Arctic Ocean sea ice cover (extent and thickness; Serreze *et al.*, 2000). These model predictions also indicate that the assumption of a uniform temperature increase or decrease throughout the year in response to climate change (e.g. ±1°C, cf. Chapter 2), which is commonly used in cryospheric

modeling studies (e.g. Reeh, 1991; Oerlemans *et al.*, 1998; Braithwaite and Zhang, 1999), is actually not valid (cf. Payne and Sugden, 1990). It may also be inappropriate, since most glaciers are more sensitive to summer than to non-summer warming (Gregory and Oerlemans, 1998). This particular uniform change assumption is also implicitly included in the Reeh (1991) melting degree-day model (cf. Chapter 5), suggesting that it is indeed more appropriate to use the Braithwaite (1984) approach as it uses mean monthly air temperatures (and their associated variability) to model monthly melting degree-day totals (cf. Chapter 5).

Modeled total monthly precipitation values from January 1980 to December 2099 (n = 1440; 120 years) were also extracted from the global data set for the 2.5° latitude by 2.5° longitude grid box centered on 82.5°N and 70°W ('Hazen Plateau grid box'). Total modeled annual precipitation is plotted between 1980 and 2099 in Figure 6.13. It is quite obvious that the absolute annual precipitation amounts for northern Ellesmere Island are overestimated by a factor of three to five by the ACIA model composite (cf. Section 6.5.1.3). This may explain the common practice of climate modelers (e.g. Walsh *et al.*, 2002; Kattsov *et al.*, 2005) to express modeled precipitation changes (and even temperature changes, e.g. Ridley *et al.*, 2005) in relative (i.e. anomalies), rather than absolute, values (cf. Bintanja and Oerlemans, 1995). Mean annual modeled precipitation (between 1980 to 1999) was 635 mm weq and is predicted to increase by 145 mm weq (or 23 percent) to 780 mm weq within the next 100 years (until 2080 to 2099) (Fig. 6.13). These predicted relative changes (in percent) can be combined with the actual precipitation climatology for the Hazen Plateau and North Coast (cf. Chapter 5) to yield more realistic regional estimates of future precipitation than the absolute model predictions (cf. Section 6.4).

6.4 Climatic Sensitivity of the North Coast

Section 6.4 presents a temperature-index melt and mass balance model for the North Coast of Ellesmere Island, specifically for the Ward Hunt Ice Rise and Ice Shelf. This model is essentially limited to a one-dimensional point model, since the available long-term mass balance from the ice rise and ice shelf are not spatially-distributed (i.e. they represent so-called 'index' or 'stake-farm' mass balances, Koerner, 1996; Braun *et al.*, 2004b) and the lack of any significant vertical relief on the ice rise and ice shelf.

The model therefore ignores or indirectly incorporates at least two previously documented spatial mass balance patterns on the Ward Hunt Ice Rise and Ice Shelf (Braun *et al.*, 2004b; or Chapter 3).

1. Ablation at lower elevations and closer to the ice margin has been consistently greater than ablation towards the interior and higher elevations of the Ward Hunt Ice Rise (Braun *et al.*, 2004b). This spatial mass balance pattern is consistent with the nature of the ice rise surface observed in 2002 and 2003. Considerable accumulations of wind-blown dust, together with well-developed cryoconite holes, are characteristic at lower elevations near the ice margin, whereas the ice surface towards the center and higher elevations of the Ward Hunt Ice Rise is very clean, white ice. Lotz (1961a, b) commented on the different localized climatic conditions that he observed across the ice rise in 1959 (cf. Chapter 5) which may provide an explanation for these observed spatial ablation patterns (M. Jeffries, 2001, pers. comm.).
2. The characteristic ridge and trough topography (i.e. 'corrugated' surface, Debenham, 1954) of the Ward Hunt Ice Shelf (Koenig *et al.*, 1952) leads to the formation of elongated sub-parallel meltwater lakes on the ice shelf surface each summer (cf. Peary, 1907). Ablation within these meltwater lakes is enhanced relative to the surrounding ice shelf ridges (or the ice rise) by the continuous presence and flow of liquid melt water (Hattersley-Smith, 1955, 1957; Lister, 1962). Detailed ablation measurements over melting sea ice in Tanquary Fjord by Langleben (1966) suggested that the DDF (ice) underneath standing or running meltwater may be between 12 and 20 mm weq/DD, about twice or three times as much as the 'normal' degree-day factor of exposed glacier or sea ice (cf. Section 6.3.2.1).

It is also worth emphasizing that the long surface mass balance record for the Ward Hunt Ice Shelf does not provide any useable information about mass gains or losses occurring at the bottom of the

floating ice shelf through melting and/or accretion of sea water (Hattersley-Smith and Serson, 1970). Recent evidence from the ice shelves along the Antarctic Peninsula, however, suggests that mass losses at the bottom of ice shelves related to warmer ocean water temperatures might be more significant than the surface mass balance in terms of the overall ice shelf mass balance and stability (Shepherd *et al.*, 2003; Braun *et al.*, 2004b; Grosfeld and Sandhäger, 2004; Scambos *et al.*, 2004). Unless otherwise noted, Section 6.4 presents and discusses only the surface mass balance of the Ward Hunt Ice Rise and Ice Shelf (cf. Section 6.4.4.5).

6.4.1 Melt Model Parameters: Reasonable Limits

Despite the long-term surface mass balance record for the Ward Hunt Ice Rise and Ice Shelf (Braun *et al.*, 2004b), the paucity of published melt process studies precluded a detailed quantitative evaluation of the required melt model parameters. Therefore, model parameters have to be determined through model calibration (cf. Section 6.4.3), with the limited in-situ measurements, values from the scientific literature, and the available empirical parameterization (cf. Section 6.3) providing the aforementioned 'reasonable limits' (Hock, 2003) for the model parameters.

6.4.1.1 Degree-Day Factors for Snow

The very limited data presented by Lotz (1961a, b) suggested a DDF (snow) value of about 5 mm weq d^{-1} deg^{-1} for the 1959 snowmelt period on the Ward Hunt Ice Rise (cf. Section 6.3.2.4). This single value compares well with the mean of the scientific literature values of 4.7±0.8 mm weq d^{-1} deg^{-1} for 'maritime' Arctic locations (Table 6.1). The data presented by Lotz (1961a, b) also implies that the Kuunisto (1980) 'open' degree-day factor parameterization (i.e. Equation 6.7) is the probably the most appropriate for the North Coast (cf. Section 6.3.2.4), which predicts a DDF (snow) of 4.1±0.8 mm weq d^{-1} deg^{-1} (Fig. 6.14). The above considerations, summarized in Table 6.12, suggest that a DDF (snow) value of about 4.6±0.8 mm weq d^{-1} deg^{-1} can be considered as an appropriate initial value and range for the northern coast of Ellesmere Island.

6.4.1.2 Degree-Day Factors for Ice

The very limited data presented by Lotz (1961a, b) suggested a DDF (ice) value of about 6.5 mm weq d^{-1} deg^{-1} for the 1959 summer melt season on the Ward Hunt Ice Rise (cf. Section 6.3.2.4). This single value exactly matches (by coincidence) the mean of the scientific literature values of 6.5±0.8 mm weq d^{-1} deg^{-1} reported previously for 'maritime' Arctic locations (Table 6.1). However, detailed ablation measurements over melting sea ice in Tanquary Fjord by Langleben (1966) suggested that the DDF (ice) underneath standing or running meltwater may be between 12 and 20 mm weq d^{-1} deg^{-1}, about twice or three times as much as the 'normal' degree-day factor of exposed glacier or sea ice (cf. Section 6.3.2.1).

6.4.1.3 Superimposed Ice Formation (P-max)

Superimposed ice formation can be calculated based exclusively on mean annual temperature (MAT) (Table 6.13), using the parameterization presented by Woodward *et al.* (1997) (i.e. Equations 6.8 and 6.9). This particular approach could therefore be used to calculate a specific P-max value for each year of interest, based simply on its MAT. The Braithwaite *et al.* (1994) superimposed ice parameterization (Table 6.13), in contrast, requires the density of the winter snow accumulation and the density of the newly formed superimposed ice (~0.9; cf. Table 6.6) as the two input variables. It is therefore possible to determine a specific P-max value for each year for which reliable snow density and snow accumulation measurements are available. Finally, the superimposed ice formation parameterization presented by Janssens and Huybrechts (2000) requires MAT and annual snow accumulation as its two required input variables (Fig. 6.15, Table 6.13).

The mean of the scientific literature values (cf. Table 6.4) was 0.44±0.14, which is consistent with the conclusions by Arendt (1997) and Janssens and Huybrechts (2000) that the popular value of P-max = 0.6 may actually be too high in many cases. The measured P-max on the Ward Hunt Ice Rise and Ice Shelf was 0.57 for an 'above-average' winter snow accumulation of 240 mm weq (Table 6.13). In contrast, the measured P-max for more 'normal' levels of winter snow accumulation (170 mm weq) was about 0.40 (cf. Section 6.3.3.5). The above considerations, summarized in Table 6.13, suggest that a P-max value of about 0.40±0.13 can be considered as an appropriate initial value and range for the northern coast of Ellesmere Island.

6.4.2 A Mass Balance Model for the Ward Hunt Ice Rise and Ice Shelf

Figure 6.16 presents the surface mass balance model for the Ward Hunt Ice Rise and Ice Shelf and illustrates the assumed snow and ice melt process as a function of increasing melting degree-days and a range of initial values for winter snow accumulation (i.e. 0 to 300 mm weq at 50 mm weq increments). This figure can be interpreted as the annual temporal progression of melt (i.e. how does, for example, 160 mm weq snow (green curve) melt over the course of a single summer melt season as a function of time or increasing melting degree-days). However, Figure 6.16 can also be interpreted on inter-annual time scales by predicting how much melting (i.e. b_n) would occur for any given combination of annual melting degree-day totals and winter snow accumulation, although that particular aspect is better illustrated in Figure 6.20 as an interpolated contour plot (see below).

Figures 6.17 and 6.18 are identical to Figure 6.16, albeit enlarged and expanded to better illustrate the annual snow and ice melt process for a winter snow accumulation of 160 mm weq. The fact that the model predicts a more-or-less neutral annual mass balance (b_n = +1 mm weq) for 41 annual melting degree-days is completely coincidental and simply a function of the assumed melt model parameters. Figures 6.16, 6.17, and 6.18 highlight several interesting features of the assumed snow and ice melt process on the Ward Hunt Ice Rise and Ice Shelf incorporated into the melt model:

1. A 'threshold' situation is evident during the annual melt process (i.e. the horizontal section of the curve(s) for 0 to 12.8 MDD for a winter snow accumulation of 160 mm weq). This section of the melt process curve represents superimposed ice formation (here assuming a P-max of 0.4), where melting (of accumulated winter snow) occurs and melting degree-days are thereby consumed, but no net mass is lost from the snow pack due to superimposed ice formation (cf. Section 6.3.3).
2. The first sloped section of the annual melt process curve represents the spring snowmelt period (here assuming a DDF (snow) = 5 mm weq d^{-1} deg^{-1}).
3. The second (steeper) sloped section of the annual melt process curve represents subsequent superimposed ice and glacier ice melt (here assuming a DDF (ice) =

DDF (spi) = 7 mm weq d^{-1} deg^{-1}). The steeper slope of this section is due to the higher degree-day factor for superimposed ice and glacier ice melt compared to snowmelt (cf. Section 6.3.2).

Figure 6.16 also emphasizes the importance of the 'ice-cap cooling' effect (cf. Chapter 5) in promoting and prolonging the survival of the ice rise and ice shelf under current climatic conditions. The annual mass balance for the mean climatic conditions on the Ward Hunt Ice Rise and Ice Shelf between 1951 and 2003 (annual melting degree-day totals 40.9±15.4; SWE 160±40 mm weq) is +1 mm weq. In contrast, for the mean climatic conditions on the adjacent ice-free Ward Hunt Island (annual melting degree-day totals 76.7±23.1; SWE 160±40 mm weq), the model predicts a much more negative mean annual surface mass balance of –251 mm weq.

6.4.2.1 Asymmetry of Mass Balance Response to Changes in Annual Melting Degree-Days

Figures 6.16 to 6.18 also reveal an interesting feature of the snow/ice melt process on the Ward Hunt Ice Rise and Ice Shelf (and elsewhere): the mass balance response to a given change in climate (i.e. increases or decreases in annual melting degree-day totals and/or winter snow accumulation) is not symmetrical (cf. Schytt, 1964; van de Wal and Oerlemans, 1994). For example, assume that the long-term mean annual melting degree-day total is 41 MDD and is normally-distributed (Fig. 6.17).

- If the annual melting degree-day totals are high enough to be well within the ice melt section of the melt process curve and/or the normal distribution is 'narrow' enough (Case #1; 'Global Warming' situation), then it effectively does not matter whether annual melting degree-day totals are increased or decreased by a given value – the resultant change in mass balance will be symmetrical (i.e. identical relative mass gains or losses for the same relative change in annual melting degree-day totals).
- If annual melting degree-day totals are low enough, and/or their normal distribution is 'wide' enough to also encompass snowmelt (i.e. the first sloped

section of the melt process curve), then the mass balance response will not be entirely symmetrical (Case #2 = 'normal' conditions). For example, adding 20 melting degree-days would cause much more overall mass losses than subtracting 20 melting degree-days would lead to reduced mass losses (since ice melt is more energy-efficient than snowmelt because of its higher degree-day factor).

- If annual melting degree-day totals are very low (e.g. Case #3; 'Little Ice Age') and/or the normal distribution is particularly 'wide', then the annual melt process may include a threshold situation, leading to years with no net annual mass loss at all (due to superimposed formation), whereas warmer years are characterized by increased mass losses from snowmelt and possibly ice melt.

The above considerations have interesting implications for the mass balance sensitivity of the Ward Hunt Ice Rise and Ice Shelf (cf. Section 6.4.4). An annual melting degree-day total of 41 MDD, combined with 160 mm weq winter snow accumulation, leads to an annual mass gain of +1 mm weq, according to the model. However, this does not imply that the cumulative mass balance between 1951 and 2003 (n = 53 years) is +53 mm weq, since the mass balance response to changes in annual melting degree-day totals is characterized by the aforementioned asymmetry and non-linearity (Schytt, 1964; van de Wal and Oerlemans, 1994). This particular aspect is illustrated schematically in Figure 6.17 using generalized bell curves, and in Figure 6.18 using box-whisker plots of WHIRWHIS* annual melting degree-day totals (1951 to 2003). Ultimately, annual mass gains of the ice rise and ice shelf are also fundamentally limited by the available winter snow accumulation (e.g. 160 mm weq), whereas annual mass losses are, at least theoretically, unlimited if the summer melt season becomes warm and/or long enough (Bradley and England, 1978; Koerner, 1979; Adams *et al.*, 1998) (i.e. Case #1, 'Global Warming' situation).

6.4.2.2 Asymmetry of the Mass Balance to Changes in Snow Accumulation

A similar asymmetry argument can be developed for the mass balance response of the Ward Hunt Ice Rise and Ice Shelf to changes in winter snow accumulation (Fig. 6.19). For example, assume again that the long-term mean annual melting degree-day total is 41 MDD and investigate how the annual mass balance of the ice rise and ice shelf responds to changes in winter snow accumulation.

- If winter snow accumulation increases to over 500 mm weq, all the available melting degree-days for a given year are consumed exclusively by superimposed ice formation. There is no annual net mass loss in this particular case (i.e. b_n = SWE).
- The first change in slope occurs at the transition from ice melt to snowmelt (here at 200 mm weq). If winter snow accumulation is less than 200 mm weq, more melting degree-days will be available after snowmelt and superimposed ice melt to melt additional ice (relatively). Limited winter snow accumulation also results in reduced superimposed ice formation (relatively).
- Between 200 to 500 mm weq winter snow accumulation, relatively more melting degree-days are consumed by the less energy-efficient snowmelt and superimposed ice formation. Therefore, less melting degree-days (relatively) will be available after the snowmelt period for additional ice melt.

In essence, if winter snow accumulation doubles, for example, to over 300 mm weq, there will be (relatively) much more of the less energy-efficient snowmelt consuming the available melting degree-days (in addition to enhanced superimposed ice formation). If winter snow accumulation decreases, for example, to below 100 mm weq, relatively more melting degree-days will be available for the more energy-efficient ice melt (in addition to reduced superimposed ice formation).

In summary, it is necessary to determine the mass balance of the Ward Hunt Ice Rise and Ice Shelf on an annual basis in order to arrive at accurate cumulative totals or means over time. Both asymmetry aspects and the model threshold situation are combined when plotting the annual net surface

mass balance as a function of summer melt (i.e. annual melting degree-day totals) and winter snow accumulation as a contour plot (Fig. 6.20). Here, the distance between the contour lines increases the more positive the modeled annual mass balance becomes, reflecting the aforementioned mass balance asymmetry. The horizontal sections of the contour lines indicate the threshold situation due to superimposed ice formation. Figure 6.20 allows the determination of the annual net surface mass balance of the Ward Hunt Ice Rise and Ice Shelf for any given combination of annual melting degree-day totals and winter snow accumulation. The grey rectangle marks the mean climatology 'space' for the Ward Hunt Ice Rise and Ice Shelf (1951 to 2003). This shows that it is possible for the ice rise and ice shelf to experience positive mass balance years under 'normal' climatic conditions. However, the mass balance response to changes in annual melting degree-day totals is characterized by the aforementioned asymmetry and non-linearity, which is consistent with the overall mass losses of the ice rise and ice shelf over the last 50 years (Braun *et al.*, 2004b). However, as discussed before, a mean annual balance, based on mean values for air temperature and precipitation, is not meaningful in reality (van de Wal and Oerlemans, 1994).

6.4.3 Model Verification: Validation, Calibration, and Confirmation

> "Given the interaction between predictions based on glaciological modeling and public policy, it is surprising that the subject of model verification or validation has received little attention in the glaciological literature...If glaciologists are to be taken seriously in the process of formulating public policy, it is imperative that such an evaluation be initiated." (van der Veen, 1999a)

Van der Veen (1999a) provided an eloquent, almost philosophical assessment of the issues surrounding cryospheric models and, more specifically, surrounding the objective evaluation of their performance and predictive capabilities. His discussion focused largely on cryospheric models of varying complexity, but the presented concepts are applicable to any type of model describing any natural system or process. It is therefore useful at this point to highlight some of most relevant points discussed by van der Veen (1999a) in the context of this particular modeling exercise. Another useful discussion about cryospheric modeling, and its underlying assumptions and parameterizations, has been provided by Hindmarsh (1993) and Ferguson (1999). A recent paper by Lahsen (2005) presented an interesting and

somewhat sobering discussion about the professional, psychological, and political relationships between (climate) modelers, their models, reality, and the public, based on 'fieldwork' conducted over six years at the U.S. National Center for Atmospheric Research (NCAR) in Boulder, Colorado.

Van der Veen (1999a) argued that it is impossible to objectively verify a cryospheric model (or any model that describes an 'open' natural system or process, cf. Oerlemans, 1991, 1998, 2000, 2001). Instead, he proposed a formal, sequential three-step modeling assessment, consisting of (1) model validation, (2) model calibration, and (3) model confirmation (cf. Hindmarsh, 1993).

Model validation requires that the mathematical model used in the experiment is consistent with the associated conceptual model for the natural system or process. This consistency, however, only confirms the validity of the mathematical model with respect to the conceptual model, but does not imply that the conceptual model is an appropriate, albeit simplified, description of the natural system or process. Model calibration refers to an (iterative) procedure by which unknown or poorly-constrained model parameters are adjusted or 'tuned' to improve the match between observations and model predictions (cf. Ferguson, 1999; Hock, 2003). In fact, model calibration is usually necessary to achieve adequate prediction by most models (Wilcox *et al.*, 1991). Model calibration, therefore, does not assess how well a mathematical model is able to describe a natural system or process. Model confirmation, in an absolute sense, is again impossible when modeling an 'open' natural system or process. Therefore, a common approach is to compare model predictions with independent observations that were not already incorporated into the model during its calibration process (e.g. Greene *et al.*, 1999; Nordli *et al.*, 2005). The situation is obviously more problematic when the glaciers of interest either no longer exist today (e.g. Glasser, 1995; Glasser and Siegert, 2002; Brugger, 2005; Laabs *et al.*, 2005) or are not in equilibrium with current climatic conditions (e.g. Braun *et al.*, 2004a).

6.4.3.1 Model Validation, Calibration, and Confirmation: General Considerations

The snow/ice melt model for the North Coast has been comprehensively validated in Section 6.4.2 in the sense that it represents a mathematically accurate description of the assumed snow and ice melt process. However, this does not imply that the conceptual melt process is an appropriate simplification of reality (cf. van der Veen, 1999a). The model, however, is well-established today in the

scientific literature (cf. Section 6.3.1) and matches well the observed snow and ice melt processes on the Ward Hunt Ice Rise and Ice Shelf (Lotz, 1961 a, b; Lister, 1962; Sagar, 1962; Hattersley-Smith and Serson, 1970).

In theory, model calibration should be a simple and straight-forward process: one simply compares the model predictions with the available observations and adjusts the model parameters (within reasonable limits) until the model predictions 'fit' the observations (cf. Hock, 2003). However, such an approach assumes that a high-quality set of observations is available for the model calibration and confirmation process (e.g. sufficient length of the record, low enough measurement uncertainty, lack of systematic bias, etc.). Unfortunately, the available long-term mass balance measurements on the Ward Hunt Ice Rise and Ice Shelf are far from perfect (cf. Cogley *et al.*, 1996; Cogley and Adams, 1998; Cogley, 2004). The problems and assumptions associated with these records are described in detail in Braun *et al.* 2004b (i.e. Chapter 3). Here, only the most relevant aspects are discussed:

- The two records contain many multi-year mass balances (i.e. they are not true annual time series).
- The latter parts of both records may progressively underestimate the actual surface mass losses, as the total number of stakes contributing to each annual or multi-year average decreased, with those at (locally) high melt locations (e.g. stakes inside ice shelf meltwater lakes) likely to have been lost earlier (leading to an increasing systematic bias over time).

It seems therefore prudent to restrict the model calibration and confirmation process (see below) to the 'best' part of the two mass balance records, which is the period from 1959 to 1985, as meticulously compiled by the late Harold Serson (cf. Chapter 3). Another concern is the reliability of the available winter snow accumulation measurements on the ice rise and ice shelf. First, actual winter snow accumulation measurements are only available for about half of all measured years between 1959 and 2003. Furthermore, the winter snow accumulation measurements occurred at a more-or-less arbitrary date, sometimes months before the onset of snowmelt along the North Coast (cf. Section 6.5.2.1).

Therefore, it may be more appropriate and realistic to follow the approach of Bradley and England (1978) and Hooke *et al.* (1987) and treat winter snow accumulation as a constant, thereby attributing all annual mass balance variability exclusively to differences in summer melting.

It is also worth re-emphasizing at this point the concerns raised by Oerlemans (1991, 1998, 2000, 2001) in the context of glacier mass balance modeling. It is obviously tempting to calibrate the model by comparing the predicted annual mass balance values with the available measured annual mass balance values. But such a calibration procedure is unrealistic. The model itself, the required model input data, the model parameters, and the available mass balance observations all contain too much inherent uncertainty to expect the model to predict accurate absolute annual values (cf. Cogley *et al.*, 1996; Cogley and Adams, 1998; Cogley, 2004). A more appropriate and robust calibration procedure would be to run the model for an extended period of time (e.g. 20 years) and to optimize the modeled cumulative mass balance against the measured cumulative mass balance for that particular time period (cf. Williams, 1979). Such a calibration procedure seems more appropriate in the context of this particular study, given the quality of the long-term mass balance data and the overall predictive capabilities of this model, or any other glacier mass balance model for that matter (cf. Oerlemans, 1991, 1998, 2000, 2001).

Finally, it is very important to recognize that the mass balance observations from the Ward Hunt Ice Rise and Ice Shelf do not represent consistent, annual time series. Therefore, the 'shape' of the modeled cumulative balance curves (cf. Fig. 6.23) cannot be compared directly to the shape of the measured cumulative mass balance curve, as those include many multi-year balances where each annual value simply represents the mean of the respective multi-year balance (cf. Chapter 3). Thus, the model calibration and confirmation process is limited to a comparison of the cumulative mass balances for a given time period, rather than their inter-annual variability.

6.4.3.2 A Simple Model Calibration and Confirmation

Given the above considerations, the simple model calibration procedure adopted in this study involved the determination of which combination of the three model parameters (P-max, DDF (snow), and DDF (ice)) resulted in the best prediction of the cumulative mass balance of the Ward Hunt Ice Rise and Ice Shelf for the time period from 1966 to 1985 (n = 20 years), assuming a constant value for winter

snow accumulation of 160 mm weq. The time period from 1959 to 1965 (n = 7 years) was used afterwards for model confirmation. More specifically, values for P-max were adjusted iteratively between 0 (i.e. no superimposed ice formation) and 1 (i.e. 100 percent superimposed ice formation) for different combinations of DDF (snow) and DDF (ice), maintaining a relative difference between the DDF (snow) and the DDF (ice) values of two (i.e. 4/6, 4.5/6.5, 5/7, 5.5/7.5, etc) (cf. Braithwaite *et al.*, 2002; Mair *et al.*, 2005; Wang *et al.*, 2005). These model parameter adjustments effectively alter the position and shape of the melt process curves shown in Figure 6.16. Increases (decreases) of superimposed ice formation (i.e. P-max parameter) shifts the melt process to the right (left) by increasing (decreasing) the length of the horizontal section. Changes in the two degree-day factors obviously influence the slopes of the snowmelt and ice melt sections of the annual melt process.

As expected, several different model parameter combinations produced very similar results (i.e. there was not a unique 'best' calibration solution; cf. Braithwaite and Zhang, 1999, 2000; Hock 2003; Mair *et al.*, 2005). The decision of which combination of model parameters (Table 6.14, 6.17) to adopt was therefore not completely straight-forward and objective, although the 'reasonable limits' for the model parameters determined in Section 6.4.1 offered some guidance (cf. Hock, 2003). In addition, the optimized melt model parameters have to be consistent in a relative sense between the ice rise and the ice shelf, and relative to each other (cf. Braithwaite *et al.*, 2002).

The optimized values for P-max (Table 6.14, 6.17) are slightly lower than expected (cf. Section 6.4.1), but fall well within the range of values previously reported in the scientific literature (Table 6.4). The higher P-max value for the ice shelf is also quite reasonable, as superimposed ice formation is presumably enhanced inside the ice shelf troughs due to impeded meltwater drainage during snowmelt. The values for the DDF (snow) and DDF (ice) are slightly higher than expected (cf. 6.4.1), but also fall well within the range of values and ratios previously reported in the scientific literature (Table 6.1; cf. Braithwaite *et al.*, 2002). Higher degree-day factors are also reasonable, given the influence of summer snowfall events on the measured annual mass balances (cf. Section 6.3.4). This additional mass accumulation is implicitly accounted for in the measured annual mass balances, but not in the annual model predictions. Therefore, the degree-day factors in the model have to be increased to account for this unknown amount of mass accumulation associated with summer snowfall events. Perhaps the most

surprising optimized model parameter is the unusually high DDF (ice) for the Ward Hunt Ice Shelf (Table 6.14, 6.17). However, as noted before, the characteristic ridge and trough topography of the Ward Hunt Ice Shelf (Koenig *et al.*, 1952) leads to the formation of elongated, sub-parallel meltwater lakes on the ice shelf surface each summer (Peary, 1907). Ablation within these meltwater lakes is enhanced relative to the surrounding ice shelf ridges (or the ice rise) by the continuous presence and flow of liquid melt water (Hattersley-Smith, 1957; Lister, 1962). Measurements over melting sea ice in Tanquary Fjord by Langleben (1966) suggested that the DDF (ice) underneath standing or running meltwater may be between 12 and 20 mm weq d^{-1} deg^{-1}, about twice or three times as much as the 'normal' degree-day factor of glacier or sea ice (cf. Section 6.3.2.4). The optimized model parameters for the combined record ('combo'; Table 6.14, 6.17) are consistent relative to the calibrated values for the ice rise and ice shelf.

Table 6.14 also shows the results of the simple model confirmation procedure. The seven years from 1959 to 1965 were not used in the model calibration process and can therefore be used to confirm the robustness of the model calibration (van der Veen, 1999a). This shows that the calibrated model produces reasonable cumulative mass balances between 1959 and 1965, albeit with a slight tendency to overestimate the mass losses for that particular time period. For reference, Table 6.15 lists the optimized model parameters for the entire 1959 to 1985 reference period (n = 27 years). These model parameter values are, as expected, almost identical to those shown in Table 6.14, and may be considered as the 'best' overall calibration solution (Hock, 2003).

It would be certainly feasible to perform a more sophisticated model calibration, or to enhance the temperature-index melt model by, for example, incorporating internal model parameter parameterizations, based on snow density, mean air annual temperature, and snowpack water equivalent (cf. Section 6.3.2 and 6.3.3). However, those required snow data are only available for less than half of the years on record (cf. Chapter 3), and there are questions about their reliability and usability (cf. Section 6.4.3.1). Such an 'enhancement' would therefore necessitate additional assumptions (beyond the assumption of constant winter snow accumulation of 160 mm weq) which makes it doubtful whether or not it would actually represent an improvement of the predictive capabilities of the model (cf. van der Veen, 1999a).

6.4.4 Sensitivity of the North Coast to Climate Change

This section uses the calibrated temperature-index melt model for the Ward Hunt Ice Rise and Ice Shelf to assess the sensitivity of their surface mass balance in the context of the modern climatic conditions (Section 6.4.4.1) and in the context of arbitrary (Section 6.4.4.2), past (Section 6.4.4.3), and future (Section 6.4.4.4) climate change. The implications of this assessment in the context of the long-term stability of the ice rise and ice shelf are discussed and compared in Section 6.4.4.5.

6.4.4.1 The Ward Hunt Ice Rise and Ice Shelf: Modern Conditions

Figure 6.21 illustrates the modern snow and ice melt process on the Ward Hunt Ice Rise (blue) and Ward Hunt Ice Shelf (red), using the calibrated model parameters as listed in Table 6.15. The different lengths of the horizontal sections of the two melt process curves reflect the different amounts of superimposed ice formation, whereas the different slopes of the snowmelt and ice melt sections reflect the different degree-day factors. For an annual melting degree-day total of 40.9 MDD (1951 to 2003 mean), the model predicts an annual mass balance of –50 mm weq (–116 mm weq) for the ice rise (ice shelf). Figure 6.21 again includes a box-whisker plot of the long-term melting degree-day climatology (WHIRWHIS*, 1951 to 2003). The 'width' of this box-whisker plot, combined with the model asymmetry (cf. Section 6.4.2), explains why the mean modeled annual mass balance of the Ward Hunt Ice Rise between 1951 and 2003 (–54 mm weq) and Ward Hunt Ice Shelf (–123 mm weq) are slightly higher than the respective 'mean' mass balances predicted simply using the mean of the long-term melting degree-day climatology (40.9 MDD).

Figure 6.22 depicts the annual mass balance of the Ward Hunt Ice Rise and Ward Hunt Ice Shelf as a function of summer melting (i.e. annual melting degree-day totals) and winter snow accumulation. The asymmetry of the melt process is more pronounced for the ice shelf, because of the greater relative difference between the calibrated degree-day factors for snow and ice (Table 6.15). This graph can be interpreted in the context of the modern climatic conditions (as indicated by the gray shading). However, perhaps more interestingly, one can determine the mass balance for any given year based on its annual melting degree-day total and winter snow accumulation and what changes in annual melting degree-day totals and winter snow accumulation are required to bring the mass balance of the ice rise and ice shelf

into equilibrium for any given year (cf. Bromwich *et al.*, 2002). For the ice rise (ice shelf), annual melting degree-day totals would have to decrease by about 6 (9) to achieve mass equilibrium under unchanged winter snow accumulation conditions. Conversely, winter snow accumulation would have to increase by about 30 (45) mm weq to achieve mass equilibrium under unchanged summer melting conditions on the ice rise (ice shelf). These temperature and precipitation changes are put into a climatic context in Section 6.4.4.2 (climatic sensitivity), 6.4.4.3 ('Little Ice Age'), and 6.4.4.4 (21st century).

Figure 6.23, finally, compares the measured cumulative mass balance (solid curve) of the Ward Hunt Ice Rise and Ice Shelf with the modeled cumulative mass balance (dashed curve) between 1959 and 2003. The match between model predictions and observations is obviously excellent until 1985 (i.e. the end of the calibration period, cf. Section 6.4.3). However, between 1986 and 2003, the model predictions far exceed the measured cumulative mass balances of the Ward Hunt Ice Rise and Ice Shelf. The measured (modeled) cumulative annual mass balance of the ice rise between 1959 and 2003 was –1677 mm weq (–2151 mm weq). For the ice shelf, the measured (modeled) cumulative annual mass balance between 1959 and 2003 was –3101 mm weq (–5108 mm weq). As noted before, the actual shape of the cumulative balance curves do not have to be identical, since the mass balance measurements are characterized by many multi-year balances.

These discrepancies between model predictions and observations can be explained by an increasing systematic bias of the mass balance measurements (cf. Chapter 3). Mass balance measurements began initially at 45 (100) ablation stakes on the ice rise (ice shelf), but the number of ablation stakes measured each year decreased over time, as stakes melted out of the ice or were otherwise lost (Serson, 1979). This obviously reduced the stake density and spatial coverage of the stake network, but the accurate number or location of stakes used to determine each yearly value is largely unknown. In 2002, only 16 (6) useable ablation stakes remained on the ice rise (ice shelf). The latter parts of both records (i.e. 1986 to 2003) may therefore progressively underestimate actual surface mass losses, as the total number of stakes contributing to each annual average decreased, with those at (locally) high melt locations (e.g. stakes inside ice shelf meltwater lakes) likely to have been lost earlier.

Nevertheless, both the predicted and measured overall mass losses of the Ward Hunt Ice Rise and Ice Shelf between 1959 and 2003 imply that the ice rise and ice shelf are not currently in equilibrium

with the climatic conditions along the North Coast. On the other hand, both model predictions and measurements indicate that positive mass balance years have occurred in the past, for example during the mid-1960s and mid-1970s, when much of the Canadian High Arctic experienced overall colder summers, perhaps slightly increased winter snowfall, and positive glacier mass balances (Bradley and Miller, 1972; Bradley, 1973; Bradley and England, 1978; Alt, 1987; Braun *et al.*, 2004a, b). This, in turn, suggests that relatively small variations in summer melting and/or winter snow accumulation can lead to annual mass gains of the ice rise and ice shelf (Hattersley-Smith and Serson, 1970; Serson, 1979). More importantly, the recent documented break-up and alleged instability of the Ward Hunt Ice Shelf (Mueller *et al.*, 2003) are difficult to reconcile with only the measured (~3 m weq) or modeled (~5 m weq) surface mass losses over the last 45 years. This suggests that some other process or mechanism is operating at the same time, enhancing the overall mass losses of the ice shelf and reducing its stability at the same time (cf. Section 6.4.4.5).

6.4.4.2 The Ward Hunt Ice Rise and Ice Shelf: Temperature and Precipitation Sensitivity

The climatic sensitivity of glaciers is often discussed (and simplified; cf. Chapter 2) in terms of their specific mass balance response to changes in air temperature (i.e. ±1°C) and/or precipitation (i.e. ±10 percent) (e.g. Oerlemans and Fourtin, 1992; Oerlemans *et al.*, 1998; Bromwich *et al.*, 2002). The choice of a ±1°C air temperature change or ±10 percent annual precipitation change is more-or-less arbitrary, but represents a useful standard reference for the comparison of different glaciers around the world (e.g. Oerlemans and Fourtin, 1992; Oerlemans, 1993, 2001; Braithwaite and Zhang, 1999, 2000).

6.4.4.2.1 Temperature Sensitivity

The air temperature sensitivity of the Ward Hunt Ice Rise and Ice Shelf was determined by adding/subtracting 1°C and 2°C from the WHIRWHIS* mean monthly air temperature climatology before the conversion to monthly melting degree-day totals using the Braithwaite (1984) degree-day model (assuming a σ value of 2.2°C, cf. Chapter 5). Then, the mean annual mass balance for the ice rise and ice shelf for the 1951 to 2000 (n = 50 years) reference period was calculated under modern climatic conditions and under the ±1°C/±2°C changed climatic conditions (Fig. 6.24, Table 6.16).

The mass balance sensitivity both for the ice rise and ice shelf is, as expected, greater for a 1 or 2°C warming then for a 1 or 2°C cooling, which is a function of the threshold condition included in the model (due to superimposed ice formation) and the model asymmetry associated with the different energy efficiencies of snowmelt as opposed to ice melt (cf. Schytt, 1964; van de Wal and Oerlemans, 1994). The mass balance sensitivity of the ice rise and ice shelf is more-or-less identical for a 1 or 2°C cooling situation. In fact, the climatic sensitivity of the ice shelf to a climate cooling is slightly greater due to its higher P-max parameter. In contrast, a warmer climate will have a larger relative effect on the mass balance of the ice shelf than on the mass balance of the ice rise, because of the much larger DDF (ice) for the ice shelf included in the melt model.

6.4.4.2.2 Precipitation Sensitivity

The precipitation sensitivity of the Ward Hunt Ice Rise and Ice Shelf was determined by increasing/decreasing winter snow accumulation by 10, 20, 30, 40, and 50 percent relative to the modern conditions (160 mm weq) (Fig. 6.25) and calculating the mean annual mass balance for the 1951 to 2000 reference period under those changed precipitation conditions (using the WHIRWHIS* melting degree-day climatology). Figure 6.25 shows that the mass balance response to changes in precipitation is not perfectly linear, which is consistent with the aforementioned model asymmetry to changes in snow accumulation (cf. Section 6.4.2). Overall, the ice shelf exhibits a greater precipitation sensitivity than the ice rise (Table 6.16) because of its higher DDF (snow) and P-max model parameters. Table 6.16 also shows that the precipitation sensitivity for the Ward Hunt Ice Rise and Ice Shelf is, as expected, much smaller than their respective sensitivities to air temperature changes (cf. Chapter 2). However, one has to keep in mind that the prescribed temperature (i.e. ±1 °C) and precipitation changes (i.e. ±10 percent) do not necessarily represent an 'equal' climate or mass balance forcing relative to each other, but instead more-or-less arbitrary changes.

6.4.4.2.3 Temperature and Precipitation Sensitivity

Following the consideration in Section 6.3.5, the combined temperature and precipitation sensitivity of the Ward Hunt Ice Rise and Ice Shelf was determined for a +1°C/+10 percent, +2°C/+20

percent, –1°C/–10 percent, and –2°C/–20 percent climate change situation (e.g. Oerlemans *et al.*, 1998) (Table 6.16).

As expected, the prescribed precipitation changes are able to reduce the climatic sensitivity of the ice rise and ice shelf to a climate warming and cooling. Under a warming scenario, the increased precipitation is able to compensate for some of the enhanced melting due to the air temperature increase. The inverse is obviously the case for a cooling scenario, when the reduced precipitation acts as a limiting factor for the possible mass gains associated with reduced melting (e.g. Bradley and England, 1978; Koerner, 1979; Adams *et al.*, 1998).

6.4.4.2.4 The Climatic Sensitivity of the Ward Hunt Ice Rise and Ice Shelf: Regional Context

The predicted temperature sensitivity (precipitation sensitivity) of the Ward Hunt Ice Rise and Ice Shelf, using the two empirical equations presented by Oerlemans (2001) (cf. Chapter 2) is –91 mm weq/°C and 3 mm weq/10 percent precipitation change (assuming an annual precipitation of 160 mm weq). These values are much smaller than the climatic sensitivities of the ice rise and ice shelf determined here using the temperature-index melt model (Table 6.16). This suggests that the Oerlemans (2001) equations are not able to capture the specific climatic and glaciologic conditions that characterize the Ward Hunt Ice Rise and Ice Shelf.

A similar situation has been described previously in Chapter 2 for the White and Baby Glacier on Axel Heiberg Island. There, the actual climatic sensitivity of the Baby Glacier (~300 mm weq/°C) is much larger than its predicted climatic sensitivity (~73 mm weq/°C) and the climatic sensitivity of its neighbor, the much larger White Glacier (74 mm weq/°C). In fact, the ±1°C climatic sensitivities determined here for the Ward Hunt Ice Rise and Ice Shelf are quite similar to that of the Baby Glacier. Baby Glacier is situated in a particularly sensitive topographic and climatic position, where relatively small changes in summer climate can put the entire glacier either above, or below, the ELA. This situation is somewhat analogous to the location of the ice rise and ice shelf with respect to their ELA. It is therefore not surprising that a climate cooling of merely 1°C can lead to an overall positive mass balance of the Ward Hunt Ice Rise and Ice Shelf. In contrast, the (larger) White Glacier spans a much greater

elevation range (~50 to 1800 m asl), thus small changes in summer climate have a much less drastic effect on its accumulation/ablation area ratio and overall mass balance (cf. Chapter 2).

6.4.4.3 The Ward Hunt Ice Rise and Ice Shelf: 'Little Ice Age' Conditions

It is arguably much more interesting to evaluate the climatic sensitivity of the Ward Hunt Ice Rise and Ice Shelf relative to 'real' past or future (cf. Section 6.4.4.4) changes in climate, rather than relative to some arbitrary changes as prescribed in the previous section. Specifically, it would be interesting to assess if the climatic conditions during the so-called 'Little Ice Age' (LIA) were sufficiently 'severe' to allow for a thickening and expansion of the ice rise and ice shelf during that time period. A series of distinct, sub-parallel ridges and lichen trim lines on the north side of Ward Hunt Island, interpreted to represent a series of lateral moraines and associated ice rise expansion, provide some geomorphic evidence for a larger and thicker Ward Hunt Ice Rise at some point within the recent past. However, such a modeling exercise is not entirely straight-forward, since the climatic conditions during the 'Little Ice Age' in the Canadian High Arctic are not well-defined, even for temperature and precipitation changes.

6.4.4.3.1 'Little Ice Age' Climatology: Precipitation

There are no quantitative estimates of precipitation changes on northern Ellesmere Island during the 'Little Ice Age' available in the scientific literature (cf. Section 6.5). Ice core evidence from the Canadian High Arctic, however, does not indicate any consistent or distinct increases or decreases in precipitation during the 'Little Ice Age' (Fisher and Koerner, 1994; Fisher *et al.*, 1995). It is therefore reasonable to assume that precipitation along the North Coast during the 'Little Ice Age' was not significantly different from today, even though the availability of local moisture sources was presumably somewhat reduced due to more persistent, and thicker, Arctic Ocean sea ice cover. On the other hand, the colder air temperatures during the 'Little Ice Age' (see below) presumably further reduced the amount of annual rainfall in favor of snowfall (cf. Table 6.8) (Zhang *et al.*, 2000), but increased snowfall amounts do not necessarily imply increased snow accumulation on the ground (cf. Chapter 5).

6.4.4.3.2 'Little Ice Age' Climatology: Temperature

The generally accepted range for reduced air temperatures during the 'Little Ice Age' in the Canadian High Arctic is somewhere between 1.5 and 2.5°C relative to today, although the precise definition of 'today' has not been explicitly defined in the sources listed in Table 6.10 (cf. Section 6.5). It seems therefore reasonable and conservative to simply assume that every month of the year was 1.5°C colder during the 'Little Ice Age' than during the 1951 to 2000 reference period on northern Ellesmere Island.

The next question is whether to use the WHI AWS* (ice-free tundra) or WHIRWHIS* (with ice-cap cooling) climatology from 1951 to 2000 as reference climatology for the 'Little Ice Age', as there may have been sufficiently little summer melting during the 'Little Ice Age' to make the ice-cap cooling effect relative to the ice-free tundra a negligible process (cf. Bradley and Serreze, 1987b). On the other hand, reduced summer melting may actually reduce or eliminate the 'ice-free tundra warming effect' on the island relative to the ice rise and ice shelf (cf. Serreze, 1987). The 'Little Ice Age' climatology was therefore constructed by subtracting 1.5°C from each mean monthly air temperature value between 1951 and 2000 to yield a reconstructed 'Little Ice Age' monthly air temperature climatology between, for example, 1801 to 1850 (Table 6.17). The temperature climatology was then converted into a monthly melting degree-day climatology using the Braithwaite (1984) model (cf. Chapter 5). This resulted in a mean annual melting degree-day total of about 31 on the ice-free Ward Hunt Island (WHIAWS*_LIA), which may be regarded as 'minimum' 'Little Ice Age' cooling (Table 6.17). Assuming a DDF (snow) of about 5 to 6 (Table 6.15) implies that it was barely, or almost, possible for snow to survive a 'normal' summer melt season during the 'Little Ice Age' (assuming an unchanged winter snow accumulation of 160 mm weq). The mean annual melting degree-day total for the ice rise and ice shelf (which incorporates the ice-cap cooling effect; cf. Chapter 5) was only about 13 (Table 6.17). This may be regarded as a 'maximum' 'Little Ice Age' cooling climatology.

6.4.4.3.3 The Ward Hunt Ice Rise during the 'Little Ice Age'

Figure 6.26 compares the modern cumulative mass balance (1951 to 2000) of the Ward Hunt Ice Rise (blue) with its cumulative mass balance during the 'Little Ice Age' (1801 to 1850). The cumulative

mass balance of the ice rise, today, is obviously negative (cf. Section 6.4.4.1). In contrast, its cumulative mass balance during the 'Little Ice Age' (i.e. from 1801 to 1850) was clearly positive, no matter which of the two 'Little Ice Age' cooling climatologies is prescribed as model forcing. It is important to note that this modeled mass balance represents the mass balance of the Ward Hunt Ice Rise at or near the current ice margins. It is therefore reasonable to assume that the mass balance of the entire Ward Hunt Ice Rise was positive (cf. Chapter 2) during the 'Little Ice Age', which would presumably lead to a gradual thickening and possible expansion of the ice rise over time. In addition, with a maximum of 31 MDD on the currently ice-free island (Table 6.17), it is very likely that at least some perennial snow cover formed and persisted on Ward Hunt Island during the 'Little Ice Age'. It is therefore reasonable to conclude that the moraines found today on the island represent evidence for a larger Ward Hunt Ice Rise, most likely during the 'Little Ice Age'. The lichen trim lines may also be indicative of an expansion of the ice rise (Ives, 1962), but may also record the formation and persistence of (almost) perennial snow cover in its immediate vicinity (cf. Koerner, 1980b).

6.4.4.3.4 The Ward Hunt Ice Shelf during the 'Little Ice Age'

The situation is slightly different for the Ward Hunt Ice Shelf. Its cumulative mass balance was also clearly positive, and very similar to that of the ice rise, under the prescribed 'maximum' 'Little Ice Age' cooling climatology (Fig 6.26; red curves). However, the 'minimum' 'Little Ice Age' cooling climatology alone was not sufficiently severe to lead to an overall positive surface mass balance of the ice shelf. The modeling situation for the Ward Hunt Ice Shelf is further complicated by the presence (at least today, cf. Table 6.15) of large, elongated summer meltwater lakes inside the ice shelf troughs, which lead to an usually high DDF (ice) for the ice shelf (at least today). It is reasonable to assume that the size and depth of these meltwater lakes, and thus their impact on the mass balance of the ice shelf, was much reduced during the 'Little Ice Age', no matter which of the two 'Little Ice Age' climatologies is prescribed. This implies that the DDF (ice), calibrated against the modern melt and climate conditions, is probably too high for the colder climate during the 'Little Ice Age'. In a sense, under a colder climate, the ice shelf becomes more-and-more similar to the ice rise in terms of their respective model parameters and melt process curves (cf. Fig. 6.21; Section 6.4.4.2). The opposite is obviously the case for a climate

warming scenario (see below). Therefore, it is reasonable to conclude that the overall mass balance of the Ward Hunt Ice Shelf was positive during the 'Little Ice Age' and similar to that of the Ward Hunt Ice Rise.

6.4.4.4 The Ward Hunt Ice Rise and Ice Shelf in the 21st Century

As previously discussed in Section 6.3.5.4, mean monthly surface air temperatures and total monthly precipitation were extracted from the global ACIA 5-GCM composite data set for the 2.5° latitude by 2.5° longitude grid box centered at 85°N and 70°W ('North Coast grid box'). This grid box falls entirely into the Arctic Ocean north of Ellesmere Island, but presumably provides a better estimate for the climatic conditions along the North Coast than the grid box located just below, which encompasses essentially all land up to an elevation of about 2500 m asl (centered at 82.5°N and 70°W; 'Hazen Plateau grid box'; cf. Section 6.3.5.4).

6.4.4.4.1 Air Temperature (1951 to 2099)

The ACIA 5-GCM composite mean monthly surface air temperatures (1980 to 2099) for the grid box centered at 85°N and 70°W were 'merged' with the WHIRWHIS* mean monthly air temperature climatology using the period from 1980 to 1999 (n = 20 years) as overlap period and using the respective monthly means to determine an appropriate monthly offset between the two time series. Total monthly melting degree-days were then calculated for each month between 1980 and 2099 using the Braithwaite (1984) degree-day model (assuming a σ value of 2.2°C, cf. Chapter 5) (Fig. 6.27).

The mean annual melting degree-day totals for the 1980 to 1999 overlap period corresponded well between the WHIRWHIS* data set (38.6 MDD) and the 'adjusted' ACIA 5-GCM composite data set (35.2 MDD). Yet, Figure 6.27 also reveals that the ACIA 5-GCM composite data set for this particular grid box is not able to capture some of the more 'unusual' inter-annual climatic variability (e.g. the exceptionally warm summers of 1998, 2002, and 2003). This represents a problem when using those model data for glacier mass balance modeling, since the impact of an unusually warm summer on the mass balance of a glacier is enhanced (or proportionally greater) due to the model asymmetry (cf. Schytt,

1964; van de Wal and Oerlemans, 1994) and the low total annual precipitation amounts (cf. Bradley and England, 1978; Koerner, 1979; Adams *et al.*, 1998).

6.4.4.4.2 Precipitation (1951 to 2099)

Following the considerations in Section 6.3.5.4, annual precipitation anomalies (in percent) from the 1980 to 1999 reference period (n = 20 years) were applied to the precipitation climatology of the North Coast (160 mm weq, cf. Chapter 5) to determine total winter snow accumulation on the North Coast between 1951 and 2099 (Fig. 6.27). The so-determined mean winter precipitation between 1980 and 1999 was 161 mm weq, very similar to the original precipitation climatology for the North Coast of 160 mm weq.

The 'merged' time series for annual melting degree-day totals and winter precipitation (Fig. 6.27) consist of the original WHIRWHIS* climatology developed in Chapter 5 (from 1951 to 2003) and the adjusted ACIA 5-GCM composite data afterwards (2004 to 2099). It would be possible to merge the two data sets, at, for example, 1980 (or any other date between 1980 and 2003 for that matter). 2004 has the advantage to be most compatible with the analysis and results already presented in this section (i.e. Section 6.4.4.1).

6.4.4.4.3 Surface Mass Balance the Ward Hunt Ice Rise and Ward Hunt Ice Shelf (1951 to 2099)

It is now possible to calculate the surface mass balance of the Ward Hunt Ice Rise and Ward Hunt Ice Shelf from 1951 to 2099 (Fig. 6.28; note that mass balance units now expressed in m weq rather than mm weq). The model predicts a cumulative surface mass loss for the ice rise (ice shelf) between 1951 and 2099 of 17.46 (33.85) m weq. Such mass losses would translate into an ice surface lowering (i.e. thinning) of 19.4 m for the Ward Hunt Ice Rise and 37.6 m for the Ward Hunt Ice Shelf between 1951 and 2099. The effects of such a thinning are discussed below in the context of the overall stability of the ice shelf and ice rise.

6.4.4.4.4 Stability of the Ward Hunt Ice Rise

The old Defense Research Board meteorological camp on the Ward Hunt Ice Rise, which was located more-or-less in the center of the old ablation stake network (cf. Chapter 3), was in 1959 at an elevation of 47 feet (~14 m) asl (Sagar, 1962). In 2003, the elevation of this camp was about 11 m asl (based on uncorrected GPS measurements). This implies an overall ice surface lowering of about 3 m between 1959 and 2003 in this particular location. This value compares well with the model predictions between 1959 and 2003 (~2.4 m; Fig. 6.28). Between 2004 and 2099, the model predicts an overall mass loss for the ice rise of about 14.6 m weq, which would translate to an ice surface lowering of about 16.2 m. Such a thinning would put significant parts of the Ward Hunt Ice Rise, including the old research camp and the old ablation stake network, below sea level (Fig. 6.29). However, the highest elevations of the ice rise today reach elevations between 30 and 50 m asl and should therefore still be well-above sea level by the end of the 21st century (cf. Fig. 6.28).

6.4.4.4.5 Stability of the Ward Hunt Ice Shelf

Figure 6.30 puts the modeled ice surface lowering of the Ward Hunt Ice Shelf due to its surface mass losses in the context of the overall thickness of the ice shelf, using all available ice shelf thickness measurements as compiled by Vincent *et al.* (2001) and Mueller *et al.* (2003). The most recent ice shelf thickness measurement (~25 m) was provided by Mueller *et al.* (2003) for a single location south of Ward Hunt Island. Assuming this particular ice shelf thickness is representative of the larger ice shelf, and future thinning only due to surface mass losses, the ice shelf would disappear by about 2090 (case #1). If one accounts for parallel ice shelf thickness reductions due to bottom mass losses and assumes that the five available thickness measurements can be used to approximate this process, then the ice shelf is likely to disappear several decades earlier (cases #2 and #3). However, the disappearance of the Ward Hunt Ice Shelf is presumably not a entirely gradual or linear process. At some point, the ice shelf may become too thin to be stable as it floats on the surface of the Arctic Ocean, leading to an abrupt disintegration, rather than a gradual disappearance (cf. Vaughan and Doake, 1996; Cooke *et al.*, 2005) (see below).

6.4.4.5 The Ward Hunt Ice Rise and Ice Shelf: Sensitivity to Climate Change

The Ward Hunt Ice Rise and Ice Shelf, together, represent an unusual juxtaposition of two very different ice masses, even though the ice rise initially formed as a part of the larger ice shelf. However, the (grounded) ice rise is today effectively 'decoupled' dynamically from the (floating) ice shelf (cf. Weertman, 1957; Warren, 1990; Hindmarsh, 1993), which has interesting implications for their respective overall mass balances, stabilities, and future survival prospects (cf. Chapter 2).

The ice shelves along the northern coast of Ellesmere Island probably began to form some 3000 to 4000 years ago (Evans and England, 1992; Jeffries, 1994), as climatic conditions in the Canadian High Arctic deteriorated from the early/mid Holocene warm phase (Bradley, 1990). The Ward Hunt Ice Rise is thought to have formed only within the last ~1500 years when the ice shelf thickened and grounded on the isostatically-uplifted seafloor north of Ward Hunt Island (Lyons *et al.*, 1972). The ice rise and ice shelf probably reached their maximum extent and thickness towards the end of the 19th century (cf. Section 6.4.4.3), when the entire northern coastline of Ellesmere Island appears to have been fringed by a continuous ice shelf some 500 km in length (Koch, 1926; Vincent *et al.*, 2001). Since that time, quasi-continuous mass losses have led to a thinning and recession of the Ward Hunt Ice Rise, which was paralleled by a thinning and progressive disintegration of the Ward Hunt Ice Shelf over the course of the 20th century. These processes are likely to continue in the 21st century (Fig. 6.28, 6.30).

However, it quite possible that the Ward Hunt Ice Shelf has reached a critical 'threshold' ice thickness in recent years in terms of its overall stability (Fig. 6.31). Past ice thickness estimates for the ice shelf have ranged between 40 and 60 m (Crary, 1958; Lyons and Ragle, 1962; Jeffries and Krouse, 1984; Jeffries, 1994), but Mueller *et al.* (2003) have recently provided evidence for a substantial thinning (down to ~25 m) since 1980 (Fig. 6.30). This ~50 percent reduction in overall ice shelf thickness is difficult to reconcile with the available surface mass balance data and the model predictions (cf. Fig. 6.30; Section 6.4.4.1), which suggests that mass losses occurring at the bottom of the floating ice shelf related to higher sub-ice water temperatures are more significant than the surface mass losses (cf. Debenham, 1954; Wexler, 1960; Lyons and Ragle, 1962; Shepherd *et al.*, 2003; Braun *et al.*, 2004b; Grosfeld and Sandhäger, 2004; Scambos *et al.*, 2004; Alley *et al.*, 2005; Smedsrud *et al.*, 2006). However, this is very much a speculation, since 'hard' data regarding sub-ice processes and ocean water temperatures (still) do

not exist for the Ward Hunt Ice Shelf (cf. Debenham, 1954). Ice shelves along the Antarctic Peninsula influenced by polar water masses typically experience basal melt rates below 0.5 m/a (Payne *et al.*, 1989), whereas ice shelves affected by sub-polar water can experience basal melt rates of up to 2 m/a (Bishop and Walton, 1981; Marshall *et al.*, 2004; Smedsrud *et al.*, 2006). Modeling studies summarized by Hindmarsh (1993) suggest that large amounts of basal melting (up to 10 m/a) or freezing (up to 1 m/a) are possible, the magnitude and sign of which can vary rapidly in space and time.

In conclusion, it is reasonable to hypothesize that the gradual, but continuous, mass losses over the last ~100 years have by now weakened the Ward Hunt Ice Shelf sufficiently to induce an irreversible disintegration in the near future. The ice shelf fractured into two distinct pieces just to the south of Ward Hunt Island between 2000 and 2002, after experiencing some 20 years of relative stability (Mueller *et al.*, 2003). The floating ice shelf is particularly sensitive to climatic variability (cf. Weidick, 1984), as its mass balance is not 'buffered' by mass input from associated upstream land glaciers (cf. Debenham, 1954; Hattersley-Smith, 1960a). It also seems likely that dynamic stresses on the ice shelf related to wave, wind, and tidal action have also increased in recent years, as open water conditions on the Arctic Ocean have become more prevalent (cf. Koenig *et al.*, 1952; Mueller *et al.*, 2003). In addition, sea ice may actually have a stabilizing effect on the ice shelf (cf. van der Veen, 2002a) by buttressing and supporting the floating front of the Ward Hunt Ice Shelf. Once the ice shelf disintegrates, it cannot readily reform, unless climatic conditions deteriorate dramatically (hysteresis effect; cf. Fig. 6.31). This may leave the Ward Hunt Ice Rise stranded as one of the last remnants of the once much more extensive ice shelves along the northern coast of Ellesmere Island (Fig. 6.29), although its long-term survival is also threatened by current and predicted future climatic conditions.

6.5 Climatic Sensitivity of the Hazen Plateau

It is interesting to investigate the climatic sensitivity of a 100 percent ice-free (i.e. fully unglaciated) Hazen Plateau, which obviously ignores the current existence (or persistence) of the four Hazen Plateau ice caps. However, these ice caps are (at least) today out-of-equilibrium with contemporary climatic conditions (Miller *et al.*, 1975; Bradley and Serreze, 1987a; Braun *et al.*, 2004a), and can therefore be effectively ignored in the context of the larger Hazen Plateau and its overall

sensitivity to climate change (cf. Miller *et al.*, 1975; Williams, 1978a; Bradley and Serreze, 1987a). The objective of this section is therefore to determine the climatic conditions (specifically in terms of temperature and precipitation changes) that are necessary to allow snow to survive a given summer melt season on the Hazen Plateau, similar to the recent study by Hock *et al.* (2002) (cf. Section 6.1). The formation and existence of such perennial snow cover obviously requires that annual ablation is less than annual accumulation (Loewe, 1971; Williams, 1978a). These climatic conditions, in turn, can be viewed as defining the basis for the initiation of glaciation of the Hazen Plateau (cf. Ives *et al.*, 1975; Bromwich *et al.*, 2002; Hock *et al.*, 2002; Ruddiman *et al.*, 2005) and can be evaluated in the context of reconstructed past and modeled future climate change.

At the most basic level, it is possible to reduce the entire ice-free Hazen Plateau to only one single point, represented appropriately in this case by AWS T3, located on the (currently) unglaciated Hazen Plateau, or by AWS G3, located on the summit plateau of Murray Ice Cap. AWS T3 was located on the currently unglaciated Hazen Plateau at about 1025 m asl (Fig. 6.32). This site represents one of the highest ice-free points on the Hazen Plateau today, although there are some ice-free plateau hill tops a few tens of meters higher in elevation elsewhere in the extended study area. Detailed meteorological observations and snowmelt measurements are available between 1999 and 2001 from this single point. AWS G3 was located on the summit plateau of Murray Ice Cap at about 1100 m asl (Fig. 6.32). This site represents the highest elevation of the Hazen Plateau within the immediate and extended study area. Detailed meteorological observations and snow/ice melt measurements are available between 1999 and 2001 from this single point, the summit plateau of Murray Ice Cap, and Murray Ice Cap as a whole.

The temperature-index modeling strategy employed here focuses on the two primary climatic controls on snowmelt and glacier mass balance in the High Arctic (i.e. temperature and precipitation) and ignores (or indirectly incorporates, cf. Section 6.2.2.2) any 'secondary' climatic influences (cf. Plummer and Phillips, 2003; Raper and Braithwaite, 2006). The model therefore requires only two climatic input variables: (1) SWE (mm weq) of the accumulated winter/annual snow pack, and (2) melting degree-day totals for each (summer) melt season, spatially-distributed across the area of interest using a digital elevation model and does not attempt to incorporate all relevant physical processes involved in snow- and ice melt on the Hazen Plateau. It would be also possible to use an even simpler melt parameterization as

introduced by Wild *et al.* (2003) or Abdalati *et al.* (2004) to model annual snowmelt based exclusively on mean summer air temperature (cf. Ohmura, 2000; Bromwich *et al.*, 2002). Gregory and Oerlemans (1998) and Raper and Braithwaite (2006), for example, excluded the effects of precipitation changes on future glacier mass balance during the 21st century, consistent with the model results of van de Wal and Wild (2001).

6.5.1 Background Information: Climatic and Regional Context

Obviously, a study of the climatic sensitivity of Ellesmere Island's Hazen Plateau is an interesting and worthwhile scientific endeavor in its own right. However, such a study becomes (perhaps) more relevant and applicable when viewed in the larger context of glacial inception, ice sheet formation, and associated climate change in the Canadian High Arctic (e.g. Barry *et al.*, 1975) as discussed in the scientific literature over the last 30 years.

6.5.1.1 The 'Little Ice Age' on Baffin Island

Andrews *et al.* (1972) included the following elegant quotation by R.S. Tarr at the beginning of their paper on the past and present glaciological responses to climate change as seen on Baffin Island:

> "The point I wish chiefly to make is that the climatic conditions of Baffin Island and Labrador are wonderfully near those which produce glaciation." (Tarr, 1897, p. 320).

Surprisingly, the Scottish Highlands, especially the mountainous areas around Ben Nevis (the highest peak in Scotland), appear to be approximately as near to glaciation today as Baffin Island, Labrador, and the rest of the Canadian High Arctic (Hubbard, 1999; Golledge and Hubbard, 2005).

Ives (1962), Andrews *et al.* (1972, 1976), and Locke and Locke (1977) noted the pervasive presence of lichen-free areas on the interior Baffin Island plateau and interpreted them as direct evidence of former permanent snow or ice cover during the 'Little Ice Age' (cf. Chapter 1). Based on the spatial and elevational distribution of these lichen-free zones, Andrews *et al.* (1976) concluded that the regional snow line on Baffin Island lowered between 100 and 400 m during the 'Little Ice Age' and thus extensive areas of the interior Baffin Island plateau above about 600 m asl (Table 6.18) were mantled by a thin, but

permanent, snow or ice cover at that time (cf. Ives, 1962; Andrews *et al.*, 1972; Miller, 1976). In fact, Locke and Locke (1977) argued that the 'Little Ice Age' essentially "provides a possible portrayal of the events that led to the initiation of the Laurentide Ice Sheet".

Koerner (1980b), on the other hand, argued instead that lichen-free zones surrounding present-day ice masses, or covering currently unglacierized plateau hilltops, are not indicative at all of permanent snow and ice cover during the 'Little Ice Age' (cf. Levesque and Svoboda, 1999). In his view, lichen-free areas or zones with reduced lichen coverage typically occur (or develop) throughout the Canadian High Arctic when seasonal snow cover persists for a longer part of the summer than elsewhere in the vicinity (or than before). In other words:

> "...lichen-free zones are coincident with snow cover that persists through a large part of, but not all, the melt season. These snow covers inhibit lichen growth by drastically reducing their growth season."

Koerner (1980b) also cautioned against the use of lichen-free areas as a paleoclimate proxy in the Canadian High Arctic in general:

> "I want to stress strongly that we cannot yet (if ever) use lichen-free areas to measure the degree of past climatic change and glacierization in the High Arctic."

Nevertheless, Ives *et al.* (1975) linked the climatic and glaciologic conditions during the 'Little Ice Age' on Baffin Island (as interpreted by Andrews *et al.*, 1976) directly to their recently developed theory of 'Instantaneous Glacierization' as follows:

> "It is reasonable to speculate that had the Little Ice Age persisted longer, not only would north-central Baffin Island have 'jumped' into ice-sheet formation whilst the glaciers and ice caps along the mountainous east coast would have hardly expanded, but that a widespread snow bank threshold situation would have been achieved shortly thereafter over the Labrador-Ungava and Keewatin plateaus and uplands. Melville Peninsula and the high islands of the Canadian Arctic Archipelago would have shown a comparable and semi-contemporaneous response."

Ives *et al.* (1975) and Andrews *et al.* (1976) continued to speculate that the 'Little Ice Age' had the climatic potential to shift Baffin Island (and North America as a whole) into a full glaciation mode in terms of its magnitude of cooling. However, its duration was insufficient and it thus represents merely an

'abortive glaciation' (Flohn, 1974) in the context of the Quaternary glaciations. Koerner (1980b), on the other hand, felt that is inappropriate to use Flohn's term 'abortive glaciation' to describe the glaciologic and climatic conditions in the Canadian High Arctic during the 'Little Ice Age':

> "We still do not know how close Baffin Island itself was to complete glacierization 300 yr ago, let alone what this effect could have on developing another North American ice sheet."

Koerner (1980b), however, acknowledged that summer conditions were *"substantially colder"* during the 'Little Ice Age' and that "...new permanent snowfields may well have developed then and even covered areas much larger than the lichen-free zones, without killing the lichens above the present trimlines". Miller (1976) noted that the activity of local glaciers on Baffin Island was actually reduced during the last glaciation due to the prevailing cold and arid climate. In contrast, the climatic cooling during much of the 'Little Ice Age' occurred during a time of relatively high precipitation, which allowed some local glaciers to expand to their Holocene maxima (cf. Miller *et al.*, 2005). In fact, some of the local glaciers on Baffin Island may have been larger during the 'Little Ice Age' than during the Last Glacial Maximum or the Younger Dryas (Miller, 1976) because of the much more abundant precipitation in the region.

In summary, the 'Little Ice Age' on Baffin Island was clearly characterized by glacier expansion (Ives, 1962; Løken and Andrews, 1966; Miller, 1976) and perhaps/probably by the formation of extensive perennial snow and ice cover across the previously unglaciated interior Baffin Island plateau (Andrews *et al.*, 1976), although some of the geomorphic evidence for its existence (i.e. lichen-free zones) is debatable (Koerner, 1980b; Wolken *et al.*, 2005). This represents, at first glance, a reasonably coherent (and frequently cited) story about climate change and resultant changes in glaciation. However, the 'Little Ice Age' was mainly a (summer) temperature anomaly in the Canadian High Arctic; there is no evidence, mechanism, or reason to suggest or expect significantly increased precipitation during the 'Little Ice Age' (e.g. Lamb and Woodroffe, 1970; Loewe, 1971; Andrews and Mahaffy, 1976; Fisher and Koerner, 1994; Fisher *et al.*, 1995; Dowdeswell *et al.*, 1997; Bromwich *et al.*, 2002). Yet, Andrews *et al.* (1972), Barry *et al.* (1975), as well as many other authors at the time (and today, e.g. Marshall, 2002), always stressed the special importance of precipitation in the context of Arctic glaciation:

> "In our view, the glaciation of arctic areas must rely primarily on an increase in solid precipitation."

The 'Little Ice Age' and its effect on glaciation on northern Ellesmere Island is primarily defined today by much less available data and much less precipitation compared to Baffin Island (Table 6.18).

6.5.1.2 The 'Little Ice Age' on northern Ellesmere Island

The generally accepted notion is that most glaciers all across the Canadian High Arctic (and elsewhere around the world, cf. Grove, 2004; Matthews and Briffa, 2005) expanded in size and volume to reach a distinct Holocene maximum towards the end of the 'Little Ice Age' (Koerner, 1989a, 2002; Dowdeswell *et al.*, 1997; Koerner and Fisher, 2002; Miller *et al.*, 2005). It is also worth emphasizing that the 'Little Ice Age' was not a uniformly cold period, but also included a period of relative warmth in the 1700s (Fisher *et al.*, 1998; Gajewski and Atkinson, 2003). However, actual quantitative studies on northern Ellesmere Island of this recent change in glaciation are sparse. Hattersley-Smith (1969) concluded that many glaciers and ice caps on northern Ellesmere Island appear to have reached their maximum Neoglacial extents perhaps as late as the early 20th century, similar to most glaciers in Scandinavia (Nesje and Dahl, 2003) and glaciers along the coast of Greenland (Weidick, 1984):

> "...recent looped moraines off all side glaciers seen in the area are believed to be due to glacial retreat since about 1925, as inferred from glaciological studies on the central ice cap of northern Ellesmere Island." (In fact, these 'Little Ice Age' terminal and lateral moraines are ubiquitous today on the landscape of northern Ellesmere Island).

Koerner (1989a, 2002) proposed an approximate ice cap size/age relationship for the Canadian High Arctic. The largest ice caps in the area (e.g. the Agassiz Ice Cap or Devon Ice Cap) probably did not survive the last Interglacial period and therefore began their latest growth phase during the early stages of the last glacial period. Some of the larger stagnant ice caps (e.g. the Meighen Ice Cap) probably disappeared completely during the Holocene warm period between about 9000 and 4500 years ago (Bradley, 1990; Koerner and Fisher, 1990) and thus are less than about 4500 years old today. Another marked cooling step occurred in the Canadian High Arctic about 1500 years ago (e.g. Koerner, 1968; Lyons *et al.*, 1972). Ice caps formed at that time are today about 10 km in diameter and perhaps between

30 and 50 m thick. The smallest ice caps existing on the landscape today (e.g. Hazen Plateau ice caps, diameter <5 km, thickness 10 to 30 m) probably began their (most recent) growth phase only during the 'Little Ice Age' some 300 to 400 years ago.

Hattersley-Smith (1969) also noted the presence of lichen-free zones around many of the receding ice margins on northern Ellesmere Island:

> "Because of the virtual absence of lichens and the very sparse colonization by flowering plants and mosses between the ice ramps and the moraine edges, it is concluded that the ground has been uncovered with the last few decades."

Evidence for increased snow and ice cover on the Hazen Plateau at some point in the recent past, probably during the 'Little Ice Age', is provided by a well-defined lichen trim line surrounding Murray Ice Cap today (cf. Chapter 3). A similar lichen trim line is also evident around Simmons Ice Cap and around the St. Patrick Bay ice caps, but has not been mapped in detail so far. A lichen-free 'patch' is also present on the unglaciated plateau between Murray and Simmons Ice Cap (near AWS T3; cf. Chapter 3), as well as on other currently unglaciated plateau hilltops of similar elevation in the larger vicinity. The 'standard' interpretation of this evidence, following Andrews *et al.* (1976) and Locke and Locke (1977), would attribute these lichen-free areas to the presence of permanent snow and ice cover on the Hazen Plateau during the 'Little Ice Age' (cf. Wolken *et al.*, 2005). Alternatively, following Koerner (1980b), these lichen-free zones may not provide any direct evidence of more extensive snow cover and increased glaciation during the 'Little Ice Age' (cf. Section 6.5.5.3). It is important to remember in this context that modern-day precipitation on northern Ellesmere Island is three to four times less than precipitation on the interior Baffin Island plateau (Table 6.18).

6.5.1.3 The Innuitian Ice Sheet: Fact or Fiction?

The spatial extent of ice cover (i.e. ice sheet size) in the Canadian High Arctic during the Last Glacial Maximum used to be the subject of an intense scientific debate between the supporter of a so-called 'big-ice' model (= Innuitian Ice Sheet; e.g. Blake, 1970; 1992) and the supporters of a so-called 'small-ice' model (= Franklin Ice Complex; e.g. England, 1976). Much of this controversy revolved around the contentious mapping, dating, and interpretation of old glacial-geomorphic features on the

landscape. However, glaciological and climatological considerations, as well as a series of large-scale modeling experiments, also provide(d) strong independent support for the small-ice model (see below).

The early work of John Andrews and colleagues remains, to this day, the most detailed studies of the inception of the Laurentide Ice Sheet (Marshall and Clarke, 1999). These original modeling experiments conducted by Barry *et al.* (1975), Andrews and Mahaffy (1976), and Johnson and Andrews (1979) succeeded in growing large-scale ice cover on Baffin Island, but their models required a maximum mass input of 0.9 m weq annually during the ice sheet inception and expansion phase, a value that is two to three times more than the annual mass accumulation today on Baffin Island (cf. Marshall and Clarke, 1999; Table 6.18). Pollard and Thompson (1997) coupled a high-resolution (relatively speaking) dynamic ice sheet model with GCM climate simulations to investigate northern hemisphere ice–sheet initiation and expansion at the start of the last glacial cycle (116 kyrs BP). Their coupled model was able to predict ice-sheet initiation, expansion, and persistence over the interior Baffin Island highlands and the rest of the Canadian Arctic island archipelago, but only with "relatively anemic growth over northeastern Canada" (i.e. northern Ellesmere Island), presumably due to the lack of available precipitation. Marshall and Clarke (1999) incorporated additional parameterizations to account for sub-grid topography into their model and were able to achieve full glaciation of much of the Canadian Arctic Archipelago (including northern Ellesmere Island) after prescribing a 6°C temperature reduction and a doubling of annual precipitation (cf. Loewe, 1971; Andrews and Mahaffy, 1976).

More recently, Bintanja *et al.* (2002) modeled global ice volume variations through the last glacial cycle using a 3-D ice-dynamical model forced by a combination of paleoclimatic data and complementary GCM output. Ice-sheet nucleation in North America occurred at about 118 kyrs BP (following a ~4°C cooling) on Baffin Island, northern Quebec-Labrador, and in the western parts of the Cordilleran (cf. Williams, 1979; Marsiat, 1995; Kleman *et al.*, 2002). However "no ice forms on Ellesmere Island" as "the northern Arctic Islands of Canada are probably too dry to become glaciated in our model". Furthermore, Bintanja *et al.* (2002), after conducting a comprehensive series of sensitivity tests, concluded that "very dry regions such as the northern Canadian Arctic islands remain free of ice [during the LGM] even for the strongest forcing considered here."

The modeling results of Marsiat (1995), Bintanja *et al.* (2002), Kleman *et al.* (2002), and Ruddiman *et al.* (2005, see below) are consistent with the conclusions reached by England and Bradley (1978) some 30 years ago. They argued, based largely on intuitive grounds, that it was simply too dry during the Last Glacial Maximum (and perhaps during the 'Little Ice Age') to allow for the formation and existence of extensive permanent snow and ice cover on northern Ellesmere Island (= 'Siberia Effect'):

> "...as such a topographic barrier [i.e. the Laurentide Ice Sheet] would effectively restrict advection of moisture from the south into the arctic archipelago and result in 'starvation' of the ice bodies to the north."

On the other hand, Blake (1992) argued that even reduced precipitation does not necessarily prohibit the (slow) initiation or expansion of glaciers in the Canadian High Arctic, as long as summer melting is sufficiently reduced to allow for a positive annual mass balance (cf. Hattersley-Smith, 1960a; England, 1999). Similarly, Koerner *et al.* (1987) concluded, based on ice core data from the Agassiz Ice Cap and simple ice flow modeling experiments, that the currently-existing ice caps on northern Ellesmere Island were no more than 200 m thicker than today at the time of the Last Glacial Maximum.

In summary, many modeling studies were able to initiate and sustain the Laurentide Ice Sheet on Baffin Island (e.g. Bintanja *et al.*, 2002; Ruddiman *et al.*, 2005), although all models had to be 'forced' by large (i.e. unrealistic) increases in precipitation (e.g. Barry *et al.*, 1975; Andrews and Mahaffy, 1976; Johnson and Andrews, 1979; Marshall and Clarke, 1999). In contrast, most model experiments and basic climatological/glaciological considerations consistently suggest that northern Ellesmere Island was too dry during the last glacial cycle to support a large Innuitian Ice Sheet. One aspect of the 'small-ice' vs. 'big-ice' controversy has been resolved in recent years when John England abruptly revised his interpretation of the available geomorphic evidence compiled over two decades in favor of the existence of the Innuitian Ice Sheet during the Last Glacial Maximum (England, 1998; 1999). Still, the inception of Northern Hemisphere ice sheets at the start of the last glacial period is still not well understood today (e.g. Andrews and Mahaffy, 1976; Marshall 2002; Marshall *et al.*, 2004), especially when considering the rates of ice expansion that are required to account for the changes in global sea level. Yet, there are certainly parts of the world (e.g. the mountains of Utah) where the climate of the Last Glacial Maximum (LGM) was characterized by colder and much wetter conditions (Munroe and Mickelson, 2002). Laabs *et*

al. (2005), furthermore, related marked spatial differences in the amount of glacier expansion during the LGM to the localized availability of lake-effect moisture derived from the surface of Lake Bonneville.

The generally-accepted notion of severe aridity in the Canadian High Arctic during the Last Glacial Maximum was recently challenged by Bromwich *et al.* (2004), who, using a regional climate model, produced enhanced precipitation in the Canadian High Arctic in association with the northern branch of the split jet stream (cf. Barry, 2002). According to England *et al.* (2006), this altered atmospheric circulation would have led to a substantial increase in annual precipitation across the Queen Elizabeth Islands (by 1.5 to 4 times modern), thus providing the necessary moisture to grow and sustain a large-scale Innuitian Ice Sheet.

6.5.1.4 The 'Overdue Glaciation' Hypothesis

Ruddiman *et al.* (2005) attempted to test Ruddiman's 'Overdue Glaciation' hypothesis, which represents essentially a prediction or outcome of his controversial hypothesis that human activities and associated emissions of carbon dioxide and methane starting some 5000 to 8000 years ago had a significant (i.e. warming) impact on global climate. In their model, in the absence of those early anthropogenic greenhouse gas emissions, summer temperatures over northern Canada (50 to 80°N) decreased by about 1.2°C and several model grid boxes on Baffin Island were able to retain perennial snow cover (= incipient glaciation, cf. Ives *et al.*, 1975; Bromwich *et al.*, 2002; Hock *et al.*, 2002). Portions of Labrador and Hudson Bay were able to retain their seasonal snow cover for 11 months of the year. In contrast, northern Ellesmere Island did not experience similar conditions, presumably due to the lack of available precipitation (Ruddiman *et al.*, 2005):

> "The last place [i.e. the Barnes Ice Cap] from which the Laurentide ice melted – Baffin Island – is the first (and only) place where it reappears in our simulation. The next-to-last place the ice sheet melted — the high terrain in central Labrador – is the region poised very near a state of incipient glaciation in this experiment."

This particular study represents the latest attempt in a long series of modeling studies (as summarized above) to grow permanent large-scale ice cover in the Canadian High Arctic in response to climate change. The high plateaus of Baffin Island consistently emerge as a suitable location for

glacier/ice sheet inception and expansion, whereas northern Ellesmere Island appears to be too dry (today and in the past) to respond sensitively to climate change (cf. Oerlemans and Fourtin, 1992), despite the availability of a suitable plateau topography.

6.5.2 Measurements on the Hazen Plateau (1999, 2000, and 2001)

The mass balance measurements conducted between 1999 and 2001 on Murray Ice Cap and the adjacent Hazen Plateau provide an opportunity to estimate in-situ values for some of the necessary parameters required by the snowmelt/mass balance model (cf. Section 6.5.3), specifically the degree-day factors for snow and ice and the amount of superimposed ice formation (P-max). It is, however, worth reiterating the argument presented by Hock (2003) that the degree-day factors for snow and ice, and model parameters in general, measured at discrete points during short field campaigns may not representative at larger spatial and longer temporal scales (cf. van der Veen, 1999a; 2002b), for example across an entire glacier or watershed (cf. Section 6.3.2.5) and that model parameters are, therefore, best determined by model calibration 'within reasonable limits'. In some respect, the calculations detailed below already represent (part of) the model calibration step further discussed in Section 6.5.3.5.

6.5.2.1 Measurements on Murray Ice Cap in 1999

1999 was a reconnaissance field season in terms of quantitative mass balance measurements on Murray Ice Cap and elsewhere on the Hazen Plateau. Manual snow accumulation measurements focused on the broad summit plateau of Murray Ice Cap and it is therefore prudent to restrict the 1999 mass balance analysis and discussion mainly to this particular area. 25 ablation stakes were installed during the 1999 field season, the majority of which too late to capture the 1999 melt season. These stakes, however, provided the spatial framework for the mass balance measurements in the following two years.

Winter snow accumulation, as measured initially in late May 1999 (~92 mm weq), was considerably less than the actual amount of (winter) snow accumulation on the ice cap prior to the onset of snowmelt (135 mm weq) (Table 6.19) in late June. This highlights one of the fundamental problems inherent in glacier mass balance measurements (cf. Section 6.4.3.1): measured winter snow accumulation is not necessarily the same as actual snow accumulation available for summer snowmelt or annual snow

accumulation (cf. Østrem and Brugman, 1991). Two snow depth transects conducted on 2/3 and 14 June 1999 across the ice cap revealed only very little consistent spatial snow depth variability, except for localized increases near the ice margins and on the terminus of the ice cap. This is a fairly typical situation on small, low-relief glaciers or ice caps (e.g. Paterson, 1969; Rosqvist and Østrem, 1989; Wolfe and English, 1995; Adams *et al.*, 1998), and in situations where the wind re-deposition of snow is of similar magnitude as the direct snowfall amounts (Messel, 1971; Fountain and Vecchia, 1999). At the local level, snow accumulation is typically greatest near and along the ice margin ('wind-drift wedge'; cf. Hooke *et al.*, 1987), without having any significant impact on the overall amount of snow accumulation on the glacier or ice cap (e.g. Hattersley-Smith, 1960; Hooke *et al.*, 1987; Wolfe and English, 1995; Hock, 1999; Jansson, 1999; Fountain and Vecchia, 1999). Snowmelt on the Murray Ice Cap summit plateau commenced 1 July 1999 and ended 8 days later on 9 July 1999, when all accumulated winter snow was melted and the newly formed superimposed ice was exposed at the surface (i.e. the surface of the ice cap 'rose' in elevation relative to the initial measurements in late May 1999) (Table 6.19). The remainder of the summer melt season was interrupted twice by multi-day cold periods, but summer snowfall events did not lead to any measurable additional summer snow accumulation in 1999.

The winter snow accumulation (135 mm weq) melted between 30 June and 9 July, consuming a total of 28.05 melting degree-days, which corresponds to a DDF (snow) value of 4.8 mm weq d^{-1} deg^{-1}. This value is somewhat greater than the values previously reported in the scientific literature (Table 6.1) and the corresponding values bases on measurements at AWS T3 (cf. Section 6.5.2.4).

Between 20 July and 8 August, a total of 612 mm weq ice ablation was measured at ablation stake M11, located at about 970 m asl near the end of the ice cap terminus (cf. Chapter 3). This amount corresponded to a cumulative melting degree-day total at that particular elevation over the same time period of 72.81, assuming an air temperature lapse rate of 5.5°C/1000 m (cf. Chapter 5), which implies a DDF (ice) value of 8.4 mm weq d^{-1} deg^{-1}. This value is somewhat greater than those previously reported in the scientific literature (Table 6.1), which is reasonable given that the ice cap terminus at and around ablation stake M11 is very dirty ice. It is also possible to compare the amount of ice ablation and associated melting degree-day totals on the summit plateau and at ablation stake M11 by choosing a slightly shorter time period (i.e. 26 July to 8 August 1999). At M11, 35.35 cumulative melting degree-

days were responsible for 315 mm weq ice ablation, which corresponded to a DDF (ice) of 8.9 mm weq d^{-1} deg^{-1}. On the summit plateau, 25.34 cumulative melting degree-days were responsible for 150 mm weq ice ablation (mean of stakes M1 to M8), implying a DDF (ice) of 5.9 mm weq d^{-1} deg^{-1}. This suggests that the DDF (ice) is not necessarily constant across the ice cap, an issue that is further explored below in Sections 6.5.2.2, 6.5.2.3, and 6.5.3.4 for 2000 and 2001, when the ablation gradients across the ice cap were better defined by a transect of stake measurements.

Values for the P-max model parameter required to parameterize superimposed ice formation in the snowmelt/mass balance model were determined for each individual ablation stake on the summit plateau (M1 to M8) by comparing the amount of (winter) snow accumulation as measured 30 June 1999 and the amount of superimposed ice formed on the summit plateau by 9 July 1999 (Table 6.19). It is interesting to note the relatively high degree of spatial variability of superimposed ice formation, even on the relatively homogenous summit plateau of Murray Ice Cap (i.e. without any systematic differences in surface slope, snow depth, etc.). This variability was presumably related to more subtle differences in the ice cap surface between the eight ablation stakes (e.g. localized topographic lows vs. topographic highs; cf. Koerner, 1970).

6.5.2.2 Measurements on Murray Ice Cap in 2000

The 2000 winter snow pack on Murray Ice Cap was characterized by an exceedingly hard and dense basal layer, which was almost impossible to measure and sample given the equipment available in the field. This certainly led to some systematic biases in the snow accumulation measurements and presumably also influenced the progression of snowmelt and superimposed ice formation in 2000. Hattersley-Smith (1960b) previously described an exceptionally hard and dense wind-packed snow layer near the bottom of the winter snow pack in 1959 on the Gilman Glacier and Lake Hazen, which appears to be analogous to the 'Dole-Layer' (unofficial term) found on Murray Ice Cap in 2000.

The maximum amount of winter snow accumulation was measured 14 June 2000 on the summit plateau of the ice cap, just prior to the onset of snowmelt (Table 6.20). The initial snowmelt period ended 25 June, when the newly-formed superimposed ice became exposed at the surface of the ice cap. An extended period of bad weather, punctuated by two significant summer snowfall events, occurred

between 9 July to 24 July. The (summer) snow accumulation associated with this period was measured 23/24 July (Table 6.20) and had melted again by 29 July. It is interesting to note that summer snow accumulation actually exceeded winter snow accumulation for the 2000 mass balance year on Murray Ice Cap.

84 mm weq winter snow accumulation melted on the summit plateau of Murray Ice Cap until/including 24 June, consuming a total of 49.24 MDD for a DDF (snow) value of 1.7 mm weq d^{-1} deg^{-1}. This value is somewhat lower than expected (Table 6.1), which may be related to the presence of the aforementioned dense 'Dole-Layer' on the ice cap. Measurements on 23/24 July 2000 showed about 92 mm weq summer snow accumulation over the period starting 9 July (Table 6.20). Melting of this summer snow accumulation until/including July 29 consumed 20.99 MDD, implying a DDF (snow) value of 4.4 mm weq d^{-1} deg^{-1}.

A linear ablation gradient was defined for 20 m elevations bands across the ice cap between 25 June and 2 July 2000 (cf. Chapter 3; Cogley *et al.*, 1996), which corresponded to a 'textbook' ablation period, characterized by consistently warm, sunny weather and perfectly bracketed by matching ablation stake measurements. This ablation gradient can be compared to the corresponding cumulative melting degree-day gradient over the same time period, calculated from the point measurements at AWS G3, assuming an air temperature lapse rate of 5.5°C/1000 m (cf. Chapter 5). Figure 6.32 shows that the degree-day factor for ice in 2000 was not constant across the ice cap, but rather varied as a function of elevation, with higher DDF (ice) values occurring at lower elevations. This result is reasonable, given the surface conditions and topography of Murray Ice Cap. The albedo of the ice surface increases markedly from the 'white' summit plateau towards the much dirtier and darker ice margins. In addition, on the flat summit plateau, the majority of the meltwater is not able to readily produce runoff from the ice cap, thus meltwater ponding and possible re-freezing can occur, especially in colder nights during cold intervals and/or towards the end of the summer melt season. In contrast, the steeper sections of the ice cap are able to better 'shed' the produced meltwater (cf. Hattersley-Smith, 1960c). Using the detailed digital elevation model used in Chapter 3 for the mass balance integration, it was possible to calculate an average (i.e. area/elevation-weighted) DDF (ice) value of 5.78 mm weq d^{-1} deg^{-1}, which is reasonably in line with the values previously published in the scientific literature (cf. Table 6.1).

Values for the P-max model parameter were again determined for each individual ablation stake on the summit plateau (M1 to M8) by comparing the amount of (winter) snow accumulation as measured 14 June 2000 and the amount of superimposed ice formed by 25 June 2000 (Table 6.20). Overall, less superimposed ice formed in 2000 compared to 1999, but the mean P-max value was nevertheless greater because of the lower amount of associated snow accumulation.

6.5.2.3 Measurements on Murray Ice Cap in 2001

2001 should have been the 'best' and most comprehensive of the three field season, benefiting from the experiences gained in 1999 and 2000. To some extent, that was the case, however, the field site was left unoccupied between 28 June and 12 July 2001. Fortunately, this was a period of consistently cold weather and summer snow accumulation, hence actual ice ablation was minimal.

The maximum amount of winter snow accumulation (Table 6.21) was measured between 10 and 12 June 2001, just prior to the onset of snowmelt on the ice cap. The accumulated winter snowfall melted from the summit plateau and the rest of the ice cap by 18 June 2001, exposing the newly formed superimposed ice at its surface (Table 6.21). A significant summer snowfall/ snow accumulation event occurred in early July 2001, the amount of which was measured at all 29 ablation stakes across the ice cap on 13 July (Table 6.21). This 'additional' summer snow accumulation had melted again by 16 July 2001. Measurements and observations ended 7 August 2001.

AWS G3 on the summit plateau of Murray Ice Cap recorded 12.86 cumulative melting degree-days until/including 18 June 2001, which correspond to a DDF (snow) values associated with the melting of the winter snow accumulation on the summit plateau of 4.1 mm weq d^{-1} deg^{-1}. This value is somewhat greater than those previously reported in the scientific literature (Table 6.1) and the corresponding values from AWS T3 (cf. Section 6.2.3.4). Between 13 and 16 July 2001, 18.40 cumulative melting degree-days were recorded at AWS G3, which correspond to a DDF (snow) value of 2.4 mm weq d^{-1} deg^{-1} associated with the melting of the summer snow accumulation on the summit plateau of the ice cap. This lower value closely matches those measured at AWS T3 between 1999 and 2001 (cf. Section 6.5.2.4).

A linear ablation gradient was again defined for 20 m elevation bands on the ice cap between 19 June and 5 August 2001 (cf. Chapter 3; Cogley *et al.*, 1996). This gradient represents the total amount of

(ice) ablation over this time interval (i.e. it includes the 2001 superimposed ice formation/ablation on the ice cap). This ablation gradient can be compared (Fig. 6.32) to a corresponding cumulative melting degree-day gradient for the same time period, calculated from the point measurements at AWS G3, assuming an air temperature lapse rate of 5.5°C/1000 m (cf. Chapter 5) and excluding the amount of melting degree-days required to melt the summer snow accumulation between 13 and 16 July 2001. As in 2000, the DDF (ice) values varied across the ice cap as a function of elevation. Using the detailed digital elevation model used in Chapter 3 for the mass balance integration, it is possible to calculate an average (i.e. area/elevation-weighted) DDF (ice) value of 5.77 mm weq d^{-1} deg^{-1}, which is reasonably in line with the values previously published in the scientific literature (cf. Table 6.1). It is interesting to note that the elevational DDF (ice) gradients were not exactly the same in 2000 and 2001 (Fig. 6.32), even though the area-elevation weighted DDF (ice) means for 2000 and 2001 were virtually identical (cf. Section 6.5.3.4)

Superimposed ice formation was observed all across the entire ice cap and at all of the 29 ablation stakes in 2001. Values for the P-max model parameter were determined for each individual stake by comparing the amount of (winter) snow accumulation as measured 11 June 2001 and the amount of superimposed ice formed by 18/19 June 2001 (Table 6.21). Superimposed ice formation was, as expected, highly variable across the ice cap, with some stakes showing essentially no superimposed ice formation at all, while others showed P-max values approaching and exceeding 1 (i.e. 100 percent refreezing). The highest P-max values occurred, overall, on the flat summit plateau and on the terminus of the ice cap (both areas where meltwater drainage is impeded either by topography or increased snow accumulation), and the lowest P-max values on the steepest sections of the ice cap (cf. Hattersley-Smith, 1960c; Koerner, 197; Adams *et al.*, 1998). The mean values shown in Table 6.21 compare well with those previously reported in the scientific literature (Table 6.4).

6.5.2.4 Measurements at AWS T3 between 1999 and 2001

Detailed meteorological observations and snowmelt measurements at AWS T3 between 1999 and 2001 allowed the determination of three site-specific values for the degree-day factor of snow (Table 6.22). This process is effectively equivalent to model calibration (cf. Section 6.5.3.5). The DDF(snow) value for 1999 (2.9 mm weq d^{-1} deg^{-1}) has to be viewed somewhat with caution, as the winter snow

accumulation measurements in 1999 were not as comprehensive as in 2000 and 2001 (1999 was more-or-less a reconnaissance field season in terms of quantitative glacier mass balance measurements) and AWS T3 was not operational during much of the 1999 snowmelt period (cf. Chapter 5) due to a technical malfunction. Nevertheless, it is encouraging that the three calculated values for the 1999, 2000, and 2001 snowmelt period compare quite well with each other, and with values previously published in the scientific literature.

6.5.3 The Snowmelt and Mass Balance Model

The snowmelt and mass balance model used here is essentially an extension used in Section 6.4 to estimate the surface mass balance of the Ward Hunt Ice Rise and Ice Shelf. However, the model is run on the basis of a digital elevation model to account for the spatial variability of snowmelt and mass balance across the Hazen Plateau and starts (initially) with an unglaciated surface. In essence, the model illustrates the changing climatic conditions required for the formation of perennial snow/ice cover and glaciation initiation on the ice-free Hazen Plateau as a function of climate change, time, and location (i.e. elevation) on the Hazen Plateau. This more-sophisticated, three-dimensional approach, obviously, does not improve the validity or applicability of the underlying conceptual model (cf. van der Veen, 1999a; Braithwaite *et al.*, 2002). The model, for example, ignores ice dynamics (e.g. ice flow), in essence limiting the analysis to the static sensitivity of the Hazen Plateau and its ice cover to climate change (cf. Chapter 2). Support for this simplification comes from basic glaciological considerations and the ice sheet modeling studies by Andrews and Mahaffy (1976) and Johnson and Andrews (1979), where ice flow was largely insignificant until ice sheet growth on Baffin Island exceeded about 5000 years.

6.5.3.1 The Model Structure and Assumptions

This snowmelt/mass balance model determines changes in the amount of snow and ice accumulation across the Hazen Plateau over time simply as a function of air temperature and precipitation, similar to the approaches most recently used by Braithwaite *et al.* (2002; and references therein) and Raper and Braithwaite (2006). The basic assumption inherent to this model is that all spatial variability of snowmelt and mass balance (i.e. melting/ablation) across the Hazen Plateau can be

attributed solely to the surface elevation and surface characteristics of a particular grid cell. This assumption obviously ignores any other possible causes of spatial variability, such as radiation receipt (i.e. slope and aspect; cf. Hock, 1999). Support for this assumption (cf. Section 6.2) comes, most recently, from a study by Wang *et al.* (2005), who found that the length of the summer melt season (i.e. the annual melt duration) on the large Canadian High Arctic ice caps (e.g. Devon Ice Cap, Agassiz Ice Cap, etc.) is largely a function of surface elevation on the ice cap.

An unglaciated surface behaves, at least initially, differently from an already established glacier in the sense that it has no immediate 'memory' effect from year-to-year: once the snow is melted in a given summer, any 'excess' snowmelt does not (further) influence the 'mass balance' of an unglaciated surface in subsequent years (in contrast to an existing glacier). However, the snow cover that is able to survive a given (first) summer melt season (= firn) presumably begins to form a largely impervious layer of 'old' basal firn/ice on the ground surface, upon which the 'new' snowfall accumulates during the following fall, winter, and spring (see Boike *et al.*, 2003, Fig. 6 or Woo and Heron, 1981, Fig. 1 for photographs showing basal ice formation at the base of a seasonal snow pack). Basal ice formation during the subsequent spring/summer melt season then may lead to an additional basal ice layer forming 'superimposed' on this older basal firn/ice (Woo *et al.*, 1982; Koerner, 1989b; 1997). A continuation of this process over several years may therefore lead to the formation of perennial snow cover/pack with a base or core consisting of multiyear basal ice (Woo *et al.*, 1982). Thus, the initial formation, expansion, and thickening of snow fields during glaciation initiation is intimately linked to this basal/superimposed ice formation process (Koerner, 1989b). The standard assumption used here is that snow that is able to survive a given (single) summer melt season is transformed into impervious (basal/superimposed) ice the following year (Marshall and Clarke, 1999). This obviously represents a double-positive feedback (i.e. mass and energy) for the existing and expanding snow cover (cf. Section 6.3.3):

> "Moreover, ablation is [often] equated with melting; this ignores the refreezing of surface meltwater in cold firn. As a result of this process, the heat required to remove a polar snow cover is significantly greater than that needed to melt it once." (Paterson, 1990)

This 'internal' feedback process obviously does not make it any 'easier' to initiate a perennial snow cover – this basic first step still requires at least one summer/year where the amount of annual snow

accumulation exceeds the amount of annual melting (Williams, 1978a). However, once established (even for a single year), this positive feedback process facilitates the persistence and thickening of the snow pack over time due to basal ice/superimposed ice formation in the subsequent year(s). The model therefore calculates the amount of mass (in mm weq) accumulated on each grid cell at the end of each summer melt season as a function of annual snow accumulation and annual melting degree-day totals:

1. If there was no snow 'left over' at the end of the previous summer melt season, then the annual 'mass balance' of the ice-free grid cell (i.e. tundra) is determined using the simple snowmelt model.
2. If there was snow 'left over' at the end of the previous summer melt season, then the annual 'mass balance' is determined for that particular year using the mass balance model and the resultant annual balance added to, or subtracted from, the amount of mass (i.e. ice) already accumulated in that particular grid cell.

However, one side of this process (i.e. the mass loss side) is fundamentally limited by zero for an ice-free grid cell (i.e. a tundra surface). In other words, the 'potential' annual mass balance calculated for any given year/grid cell might be highly negative, but, in contrast to an ice-covered grid cell (i.e. an existing glacier), the amount of annual mass loss cannot exceed the amount of mass already accumulated.

6.5.3.2 The Spatial Reference Frame: The Digital Elevation Model

The most precise (i.e. highest-spatial resolution) commercially-available digital elevation model (DEM) for northern Ellesmere Island is the Canadian Digital Elevation Dataset (CDED), which is derived from the elevation contour lines included in the National Topographic Date Base (NTDB). The NTDB is based on the Canadian National Topographic System (NTS) 1:250,000 map sheets, which, in turn, are based on aerial photographs from 1959 and 1960 (cf. Braun *et al.*, 2004a). The accuracy of the CDED elevations has not been officially specified (Cogley and Jung-Rothenhäusler, 2004), although Burgess and Sharp (2004) claim a vertical accuracy of ±20 m over bedrock and ±50 m towards the centers of the larger High Arctic ice caps (e.g. Devon Ice Cap). Cogley and Jung-Rothenhäusler (2004) argued for a

more conservative DEM elevation uncertainty of about one half of the elevation contour interval (152 m) of the associated topographic parent map (i.e. ±75 m in this case). This DEM seamlessly covers the entire Canadian landmass, including the Queen Elizabeth Islands, and is therefore frequently used (e.g. Copland *et al.*, 2003; Burgess and Sharp, 2004; Mair *et al.*, 2005) for more regional glacier mass balance and recession studies in the Canadian Arctic.

The CDED DEM captures the large-scale (i.e. regional) topographic variability across the Hazen Plateau very well, but does not adequately represent the local-scale topography found in the vicinity of Murray and Simmons Ice Cap (and presumably elsewhere). For example, the CDED DEM includes frequent north-to-south trending linear features, which do not exist in reality on the landscape. These digital 'artifacts' are presumably related to the spatial interpolation algorithms interacting with the coarse (1:250,000) topographic base data. In addition, the absolute elevations of topographic features (and their relative differences) differ significantly from those printed on the more-detailed 1:50,000 topographic map sheets and those actually measured in the field between 1999 and 2001.

Therefore, a more accurate and precise 'local' DEM (Fig. 6.33, 6.34) was created by hand-digitizing the elevation contour lines (contour interval = 40 m) of the appropriate 1:50,000 topographic map sheet (NTS 120 C/6) in the vicinity of Murray and Simmons Ice Cap. The digitizing methodology and interpolation algorithms were identical to those used to create the two very detailed DEMs for Murray and Simmons Ice Cap used for the spatial mass balance integrations in Chapter 3. This DEM is able to capture the detailed local-scale topographic variability on and around the ice caps very well, but has problems at elevations below sea level (e.g. negative elevations in Archer Fjord) due to the nature of the interpolation algorithm used (i.e. it allows 'overshoots' and 'undershoots' to create a smoother interpolated surface). Therefore, all elevations less than 0 m asl are automatically set to zero in the snowmelt/mass balance model. The only other noticeable discrepancy between the DEM and reality occurs in the vicinity of AWS T3 (~1025 m asl), where the DEM includes a maximum surface elevation of only about 1013 m asl (the elevations of all other plateau hilltops in the vicinity of Murray and Simmons Ice Cap are within ±2 m between the DEM, the topographic base map, and the in-situ elevation measurements).

It is also important to remember that the DEM, obviously, includes the two ice caps in its surface elevations, as they represent(ed) the actual topography of the land surface as it existed when the aerial photographs were acquired in 1959. However, for this modeling experiment, it was necessary to 'remove' Murray and Simmons Ice Cap from the unglaciated plateau surface in order to derive the 'actual' ice-free topography of the Hazen Plateau and the spatial extent and thickness of the ice caps. This is achieved within the snowmelt/mass balance model simply by selecting an appropriate threshold elevation (e.g. 1070 m asl), defining essentially the maximum elevation of the ice-free terrain underneath the two ice caps. This obviously creates an ice-free topography with two horizontal hilltops at 1070 m asl, and two corresponding ice caps with a horizontal base, an ice thickness equal to the original DEM elevation minus the selected threshold elevation, and a more-or-less parabolic cross-section (cf. Paterson, 1981; Raper and Braithwaite, 2006). In reality, the ice caps are probably more 'draped' across the underlying, non-horizontal, topography (cf. Pollard and DeConto, 2004, their Fig. A1), but this should not present a significant issue in this context.

Koerner (1979) emphasized that a linear change in climate (for example, changes in the ice cap ELA, cf. Bradley, 1973) will, in reality, lead to a non-linear change in the mass balance of the High Arctic ice caps because of their highly non-linear area-elevation distribution (or hypsography) (cf. Adams *et al.*, 1998; Hagen *et al.*, 2003; Hoelzle *et al.*, 2003). This notion (albeit combined with additional positive feedback processes) is also an integral part of Ives *et al.* (1975) theory of 'Instantaneous Glacierization' (cf. Andrews *et al.*, 1976; Chapter 2) of high-latitude plateau areas, such as the Hazen Plateau. Figure 6.34a shows very well the highly non-linear area-elevation distribution of the Hazen Plateau, as illustrated for a SW-to-NE transect from Lower Murray Lake to the summit of Murray Ice Cap. This is not a true area-scaled hypsography (cf. Fig. 6.34b), thereby highlighting and amplifying the distinct topographic transition from the incised fjord to the main plateau surface at about 900 m asl along that particular transect.

6.5.3.3 The Climatology: Temperature and Precipitation

6.5.3.3.1 Mean Climatic Conditions (1951 to 2000)

The simplest way to define a climatology for the Hazen Plateau (cf. Chapter 5) is to calculate the mean annual air temperature cycle over a given time period (Table 6.23), distributed across the DEM as a function of grid cell elevation, assuming a constant air temperature lapse rate of 5.5°C/1000 m in time and space. These 12 monthly mean values are then converted to corresponding monthly melting degree-day totals using the Braithwaite (1984) degree-day model (assuming a σ value of 3.7°C/4.0°C depending on surface conditions; cf. Chapter 5) and combined to yield a mean annual melting degree-day total (between 1951 to 2000) as a function of elevation. Such a 'mean' climatology obviously smoothes out some of the existing inter-annual variability, therefore leading to less annual melting degree-totals (and thus snowmelt) on average.

6.5.3.3.2 Inter-annual Variability

Prescribing a 'mean' climatology is obviously a simplification of reality, and the issues of inter-annual and multi-year variability may become significant when considering the formation and preservation of perennial snow cover during the transition phase from an ice-free to an ice-covered locality. Bromwich *et al.* (2002), for example, concluded that merely a change in the frequency distribution of certain climatic events (i.e. unusually warm summers) is all that is needed today on Baffin Island to initiate glaciation (cf. Koerner, 1980a; Alt, 1987; Marshall, 2002). This is, not surprisingly, not a new idea in the context of glacier mass balance and glacier expansion in the Canadian High Arctic. Hattersley-Smith (1969) concluded that only small changes in summer temperature, "if continued over a number of years", are all that is necessary for significant glacier and ice caps expansion on northern Ellesmere Island (cf. Hattersley-Smith, 1960a). Bradley and England (1978) noted an interesting asymmetry of glacier mass balance in the Canadian High Arctic with respect to climatic variability and change. Annual mass gains of a typical High Arctic glacier are fundamentally limited by the very low and more-or-less constant amounts of annual precipitation (cf. Hooke *et al.*, 1987), whereas annual mass losses are (at least theoretically) unlimited. In other words: Glaciers and ice caps in the Canadian High

Arctic can loose substantial amounts of mass in exceptionally warm summers (e.g. 1962, 1998, or 2003), but cannot gain more mass than they accumulate in any given mass balance year (Koerner, 1977a; Adams *et al.*, 1998). However, annual snowfall amounts are today, on average, so low that even a few 'good' years of net accumulation can be easily obliterated by a single 'normal' negative mass balance year (cf. Bromwich *et al.*, 2002). Koerner (1980a) thus concluded that a decreased variability of summer climate, specifically the disappearance of anomalously warm summers, is necessary prerequisite for glaciation initiation, in addition to an overall climate cooling (cf. Alt, 1987; Bromwich *et al.*, 2002).

It is certainly reasonable to assume that the inter-annual and multi-year variability of climate (e.g. summer temperatures) was somewhat reduced during the so-called 'Little Ice Age' (and/or any other past cold periods). For example, Koerner (1977a, 1980a) and Alt (1987) argued that the paucity of summer melt layers in the Devon Ice Cap ice cores during parts of the 'Little Ice Age' (e.g. 1827 to 1857) indicated the complete absence of (very) warm summers during that particular time period. On the other hand, it is also well-established today that the 'Little Ice Age' was not uniformly cold for its entire duration (Luckman, 2000; Grove, 2001; Bradley *et al.*, 2003; Gajewski and Atkinson, 2003; Matthews and Briffa, 2005). The mean climatic conditions during the 'Little Ice Age' were apparently sufficiently 'severe', on average, to allow for significant glacier expansion around the world. Yet, superimposed on this overall cooling, was also sufficient temporal variability to lead to periods of glacier recession and re-advance within the overall time interval of the 'Little Ice Age' (Luckmann, 2000; Grove, 2001; Casely and Dugmore, 2004). For example, the 'Little Ice Age' in the Canadian Arctic apparently included a period of relative warmth in the 1700s, bracketed by colder conditions in the 1600s and 1800s (Gajewski and Atkinson, 2003). Koerner and Lundgaard (1995; their Fig. 6) showed considerable multi-decadal summer melt variability on the Agassiz and Devon Ice Caps, with a pronounced melt maxima occurring over the second half of the 16th century.

6.5.3.3.3 Climate Change Scenarios

Climate change scenarios (i.e. cooling or warming), in terms of a temperature sensitivity analysis, can be prescribed by simply adding or subtracting 0.5°C, 1°C, 1.5°C, etc. from each mean monthly air temperature (Braithwaite *et al.*, 2002; Raper and Braithwaite, 2006) before the conversion to

monthly melting degree-day totals using the Braithwaite (1984) degree-day model (assuming a σ value of 3.7°C (ice) or 4.0°C(tundra); cf. Chapter 5). This approach is applicable to either the 'mean' climatology or the 'inter-annual variability' climatology. The 'mean' climatology, as noted before, smoothes out some of the existing inter-annual variability, therefore leading to less annual melting degree-totals (and thus snowmelt) on average (cf. Fig. 6.35). Therefore, the climate change scenarios were prescribed relative to the AWS T3* mean monthly air temperature climatology (1951 to 2000) in order to retain the inter-annual variability and the 50-year time series was simply repeated 10 times to yield a 500-year time series for the 'Little Ice Age' (cf. Section 6.5.6.2).

6.5.3.3.4 The Ice-Cap Cooling Effect

The 'ice-cap cooling effect' has been discussed and quantified in Chapter 5. Here, Table 6.23 illustrates one possible approach to parameterize the ice-cap cooling effect by comparing the mean annual air temperature cycle at AWS G3* and AWS T3* for the last 50 years (1951 to 2000). These values (i.e. column ΔT) compare very well with those shown in Chapter 5, but also include an elevation difference of about 75 m, which is equivalent to an air temperature difference of 0.41°C (assuming a lapse rate of 5.5°C/1000 m). The altitude-adjusted ice cap cooling effect used here for May to September is shown in column ΔT 'lapsed'; for the remainder of the year the ice-cap cooling effect was set to 0 (cf. Braithwaite *et al.*, 2002).

It would be also possible to use the empirical ice-cap cooling effect parameterization recently presented by Braithwaite *et al.* (2002), which is based on Braithwaite's own dissertation research on the Sverdrup Glacier (Devon Ice Cap) and White Glacier in the late 1970s (Braithwaite, 1977). This parameterization predicts slightly greater values for the ice cap cooling effect, which is reasonable given that it was calibrated against the influence of much larger ice masses (cf. Chapter 5).

6.5.3.3.5 Snow Accumulation

Snow accumulation is assumed to be constant in time and across the spatial domain (i.e. 20 by 20 km) of the model at 125 weq, thus attributing differences in melting/ablation solely to air temperature (cf. Hooke *et al.*, 1987). This value can be increased or decreased to assess the sensitivity of snow and ice

on the Hazen Plateau to precipitation changes. All precipitation is assumed to occur in solid form (cf. Braithwaite *et al.*, 2002), a reasonable assumption given the observations between 1999 and 2001 and the overall climatic and topographic setting (cf. Fristrup, 1951). However, this assumption may become progressively invalid over the course of the 21st century as temperatures increase (cf. Section 6.3.4). Unfortunately, the 'Arctic Climate Impact Assessment' (ACIA, 2005) projections of 21st century climate change in the Arctic (cf. Section 6.3.5.4) only include total monthly precipitation. Braithwaite *et al.* (2002), for example, simply assumed that all rainfall on Arctic glaciers refreezes to form additional mass accumulation.

6.5.3.4 The Model Parameters

The snowmelt/mass balance model includes three major assumptions with respect to the required model parameters (in addition to the many additional assumptions implicit within the assumed melt process):

- The air temperature lapse rate is constant in time and space (cf. Chapter 5).
- The degree-day factors for snow and ice are constant in time and space (cf. Sections 6.2.2 and 6.3.2).
- Superimposed ice formation is constant in time and space (cf. Section 6.3.3)

The validity of these and other assumptions cannot be objectively tested, but they are, most likely, not valid (cf. Fig. 6.32), but represent (hopefully) reasonable approximations. Furthermore, since the precise spatial and temporal variability of these model parameters is largely unknown, it seems most appropriate to follow the lead of other researchers in the field and assume constancy (e.g. Braithwaite *et al.*, 2002, and references therein, Raper and Braithwaite, 2006) in time and space. It is also difficult (cf. Ferguson, 1999), perhaps even inappropriate (Mair *et al.*, 2005), to interpret these model parameters and their variability in a truly physical sense, which is presumably why many similar studies simply choose or assume their model parameters 'within reasonable limits' (cf. Hock, 2003), for example:

> "We therefore chose to prescribe the degree-day factors for ice and snow as constant values of 7.0 and 3.7 mm weq d^{-1} deg^{-1} respectively." (Braithwaite *et al.*, 2002)

This statement is especially noteworthy since it (more-or-less arbitrarily) 'chooses' model parameter values different from those that the authors compiled and discussed just a few sentences earlier in the paper (Braithwaite *et al.*, 2002; their Table 2). Another example is the study by Abdalati *et al.* (2004), who simply assumed that degree-day factors "generally assumed" for the Greenland Ice Sheet are appropriate for the ice caps in the Canadian High Arctic, despite empirical evidence to suggest otherwise (e.g. Braithwaite, 1981).

6.5.3.4.1 The Degree-Day Factor for Snow: Reasonable Limits

Table 6.24 compiles all relevant values of the degree-day factor for snow, including those published previously in the scientific literature (cf. Table 6.1), those calculated using the applicable empirical equations (cf. Section 6.3.2.2), and those measured in-situ on Murray Ice Cap and the adjacent Hazen Plateau between 1999 and 2001 (cf. Section 6.5.2). The simple mean of 3.1±0.4 mm weq d^{-1} deg^{-1} is, not surprisingly, very close to the mean used in the scientific literature for 'High Arctic' conditions (2.8±0.2 mm weq d^{-1} deg^{-1}) but somewhat lower than the value most recently used by Braithwaite *et al.* (2002) (3.7 mm weq d^{-1} deg^{-1}) for the White Glacier and Devon Ice Cap as part of a global study.

6.5.3.4.2 Degree-Day Factor for Ice: Reasonable Limits

Table 6.25 compiles all relevant values of the degree-day factor for ice, including those published previously in the scientific literature (cf. Table 6.1) and those measured in-situ on Murray Ice Cap between 1999 and 2001 (cf. Section 6.5.2). The simple mean of 6.8±0.4 mm weq d^{-1} deg^{-1} is slightly lower than the value most recently used by Braithwaite *et al.* (2002) (7.0 mm weq d^{-1} deg^{-1}) for the White Glacier and Devon Ice Cap as part of a global study. On the other hand, it is also slightly greater than the frequently used 'benchmark' value for the Canadian High Arctic (6.3±1.0 weq d^{-1} deg^{-1} is) as calculated by Braithwaite (1981) for the White Glacier and Devon Ice Cap as part of his dissertation research (Braithwaite, 1977).

However, it is also clear that the DDF (ice) was not constant across the Murray Ice Cap in 2000 and 2001, with higher values at lower elevations due to the lower albedo of the (dirty) ice surface (Fig. 6.32). The snow and basal firn/ice that accumulates initially on the Hazen Plateau will be, presumably, fairly dirty due to wind-blown particles and dust from the surrounding snow-free terrain (cf. Østrem, 1963; Koerner, 1989b; Souchez, 1997), which, in turn, will have an amplifying effect on the rate of melting. In addition, this material tends to collect during years of net mass loss on the (ablation) surface of the snow/ice cover, forming cryoconite holes (e.g. Hattersley-Smith and Serson, 1973) and/or (dark) surface dirt layers. Hattersley-Smith (1961) noted with respect to the ablation effects of wind-blown dust:

> "The rock material in the snow aided the early onset of ablation by decreasing the albedo of the snow surface".

This 'melt enhancement' presumably becomes less efficient over time, as the snow/ice fields expand and the areal extent of the surrounding or surrounded ice-free areas becomes more-and-more restricted (Koerner, 1989b). It is therefore reasonable to expect comparatively high degree-day factors for snow and ice in this initial transition period from a snow/ice-free to a snow/ice-covered land surface. Singh *et al.* (2000) attempted to quantify the effects of surface dust on the degree-day factors for snow and ice in a field experiment conducted at about 4000 m asl in the Himalayas. They covered small blocks of snow/firn and ice with a 2 mm thick layer of 'natural fine dust' and collected the meltwater runoff from several adjacent 'dusty' and 'clean' blocks. Surprisingly, the presence of the surface dust layer increased the measured DDF (snow) values only by about 12 percent and the DDF (ice) values only by about 9 percent. Their study remains today the only published attempt to quantify this 'melt enhancement' due to the presence of surface dust in the context of a temperature-index melt model, even though their values (i.e. 12 and 9 percent) appear, at least intuitively, somewhat too small.

It was also interesting to note that the elevational DDF (ice) gradients were not exactly the same in 2000 and 2001 (Fig. 6.32). The reason for this, presumably, lies in the fact that the 2001 DDF (ice) gradient captured the entire summer melt season (encompassing superimposed ice melt, ice melt, cold/warm days, days with temperatures around freezing, nights below freezing, unmeasured trace precipitation events, etc.), whereas the 2000 gradient covered only eight days with air temperatures consistently well-above freezing across the entire ice cap. Thus, it is reasonable that the same amount of

melting degree-days in a situation like 2000 would lead to more melting and ablation than in a situation like 2001, where some 'warmth' was 'wasted' at times to re-start melting after period of melt shut-down and to melt small amounts of (unmeasured) summer snowfall. However, it is encouraging to see that the area-elevation weighted DDF (ice) means for 2000 and 2001 were virtually identical (Table 6.25).

6.5.3.4.3 Superimposed Ice Formation: Reasonable Limits

Table 6.26 compiles all relevant values for P-max, including those published previously in the scientific literature (Table 6.4) and those measured in-situ on Murray Ice Cap between 1999 and 2001 (cf. Section 6.5.2). The simple mean (0.50±0.04) is somewhat higher than the mean of the values reported in the scientific literature, but falls well within the range of values shown in Table 6.4.

It is impossible to objectively judge if the mean P-max values for superimposed ice formation as compiled in Tables 6.5 and 6.28 are appropriate values to use for an initial basal firn/ice formation parameterization in this particular context. The data presented by Woo and Heron (1981; their Table 1) suggest P-max values for the (annual) basal ice formation on ice-free High Arctic tundra surfaces ranging from about 0.22 to 0.50 (mean = 0.35), a range and mean that correspond reasonably well with the values for annual superimposed ice formation on glaciers listed in Table 6.4. Perhaps most applicable in this context is the P-max value of 0.33 determined from the data shown by Woo and Heron (1981) for the annual basal ice formation over annual lake ice, where meltwater seepage losses to the underlying substrate are more-or-less negligible because of the low permeability of the lake ice.

It would be easily possible to parameterize superimposed ice formation within the snowmelt/mass balance model using any one of the available simple empirical parameterizations as reviewed in Section 6.3.3.3. The choice is not obvious, as every research group appears to have their own preference as to which parameterization to use (usually, their own; cf. Section 6.3.3.3). The one thing that all available parameterizations have in common is that they require some additional input data to define a value for P-max, be it mean annual temperature, snow density, superimposed ice density, snow accumulation, or some combination thereof. In turn, one can assess the sensitivity of superimposed ice formation to changes in these input variables, which, in essence, almost represents circular reasoning. It seems unnecessary, and the studies by Janssens and Huybrechts (2000), Marshall *et al.* (2004), and

Zweck and Huybrechts (2005) certainly support this notion, to replace one assumption (i.e. that of which particular constant P-max value to use) with another set of assumptions (i.e. those related to the necessary input data and their spatial and temporal variability). As a historical note, the paper by Schytt (1949) probably included the first description of superimposed ice formation and its double-influence on glacier mass balance. His P-max value was about 0.47.

6.5.3.5 Model Verification (Validation/Calibration/Confirmation) and Uncertainty

The snowmelt/mass balance model used here has been comprehensively validated in Sections 6.3 and 6.4 in the sense that it represents a mathematically accurate description of the assumed snow and ice melt process. However, this does not necessarily imply that the conceptual melt process is an appropriate simplification of reality today, in the past, or in the future (cf. van der Veen, 1999a; Braithwaite *et al.*, 2002). The model, however, is well-established today in the scientific literature (cf. Section 6.3.1) and matches well the observed snow and ice melt processes on the Hazen Plateau ice caps (e.g. Hattersley-Smith and Serson, 1973; Bradley and England, 1977; Bradley and Serreze, 1987a; Braun *et al.*, 2004a).

The model was calibrated with respect to the in-situ measurements on Murray Ice Cap and the adjacent Hazen Plateau in Section 6.5.2, and with respect to 'reasonable limits' as previously reported in the scientific literature and determined using empirical parameterization in Section 6.5.3.4 (cf. Tables 6.26 to 6.28). It is worth noting that some researchers (e.g. Braithwaite *et al.*, 2002) at this point continue to further tune their models by adjusting precipitation on the glacier as a function of elevation to optimize the predictive accuracy of the model.

A robust model confirmation is impossible, since all directly applicable observations and measurements were already 'used-up' during the model calibration step (cf. van der Veen, 1999a). There are, however, three independent lines of evidence that can be used to increase one's confidence in the model and its predictive capabilities:

1. The model parameters are quite reasonable and fall well within the range of generally-accepted values (Tables 6.26. to 6.28).

2. This type of model has been used successfully in the Canadian High Arctic (e.g. Andrews *et al.*, 1970; Braithwaite, 1981; Woodward, 1995; Wolfe and English, 1995; Arendt, 1997; Boon, 2005, Mair *et al.*, 2005).

It is also possible to test the performance of the snowmelt/mass balance model on the nearby Simmons Ice Cap in 2000 and 2001 (cf. Chapter 3), since those data have not been used in the model calibration so far (assuming that the AWS G3 measurements are representative for the Simmons Ice Cap). However, it is worth remembering in this context the opinion expressed by Oerlemans (1991, 1998, 2000, 2001) that this type of model confirmation test is very, perhaps too, stringent (cf. Section 6.1 and 6.4.3.1) given the circumstances and uncertainties involved in glacier mass balance modeling. Table 6.27 summarizes the test results for 2000 and 2001, which involved the calculation of a modeled ablation gradient, determined by forcing the model with a corresponding linear melting degree-day gradient based on the measurements at AWS G3 for the entire snowmelt and ice ablation period in 2000 and 2001. The performance of the snowmelt/mass balance model using the preferred set of model parameters (case #2) was adequate in both years. The differences between the measurements and the model predictions were well-within the uncertainty of the actual mass balance measurements (cf. Chapter 3) and are of similar magnitude as the expected model uncertainties (see below). The model overestimation of the amount of mass loss in 2000 (case #2) could be compensated for by decreasing the degree-day factors for snow and ice (case #3, #4) or by accounting for the unusual amount of summer snow accumulation (case #5, #6). In 2001, the model underestimated the amount of mass loss, which could be compensated for by increasing the degree-day factors for snow and ice, or by reducing the amount of snow accumulation to 105 mm weq. Accounting for the summer snowfall in 2001 slightly increases the discrepancies between the model predictions and actual measurements. Sensitivity tests indicated that the model is quite sensitive to changes in the degree-day factors (cf. Zweck and Huybrechts, 2005), but rather insensitive to changes in P-max (i.e. superimposed ice formation) (cf. Janssens and Huybrechts, 2000; Marshall *et al.*, 2004; Zweck and Huybrechts, 2005).

Significant uncertainties obviously exist in all aspects of this snowmelt/mass balance model and therefore the associated model results (e.g. temperature and precipitation sensitivities, ice thickness

estimates, snowline elevations, ice extent, etc.) because of the myriad of uncertainties and biases associated with the conceptual model, the model parameters, and the model input data. Model uncertainty is presumably especially a concern right at the transition from unglaciated to glaciated conditions, when a small change in the model input or model parameters may have a large impact on the model results. However:

> "...we cannot make definitive statements about errors and uncertainties in the modeling..." (Braithwaite *et al.*, 2002)

It is therefore not surprising that most similar modeling studies either do not discuss the associated model uncertainty at all, or mention it only briefly in passing. Braithwaite *et al.* (2002), in fact, provided the only comprehensive uncertainty assessment of an operational temperature-index melt model (at least in the context of glacier mass balance modeling). They ran their model after prescribing plausible ranges for the degree-day factors and air temperature lapse rate 'centered' on their preferred values to test the sensitivity of the model results to the uncertainties in the model parameters and concluded that their model results (e.g. glacier mass balance (amplitude), temperature sensitivity, etc.) were accurate to within about 10 to 20 percent due to the various uncertainties included in all aspects of the model input (e.g. climatology, model parameters, calibration data, etc.). This range compares well with the ±20 percent uncertainty in the modeled annual melt totals as suggested by van der Veen (2002b). Overall, model results are affected more by the uncertainty associated with the degree-day factors than with the air temperature lapse rate or superimposed ice formation (cf. Braithwaite *et al.*, 2002; Zweck and Huybrechts, 2005). Similar sensitivity tests conducted by Plummer (2002) in a similar modeling study suggested a 'combined' or 'resultant' uncertainty in the calculated temperature sensitivities of about ±0.5°C and in the calculated precipitation sensitivities of about ±30 percent (Laabs *et al.*, 2005). In other words, a range of plausible ice extents can be produced by their model within a corresponding range of ±0.5°C temperature and ±30 percent precipitation change.

The resultant model uncertainty is illustrated in Table 6.28 for a 'middle-of-the-road' climate change scenario of 2.0°C cooling and a 100 percent increase in annual snow accumulation (250 mm weq), by varying the DDF (snow), DDF (ice), and P-max model parameters around their respective 'preferred' values. The model results are most sensitive to changes in DDF (snow) and P-max,

presumably since most of the available melting degree-days are consumed during snowmelt and superimposed ice formation. This implies that the resultant model uncertainty is best determined specifically for each climate change scenario of interest, since the relative importance of each model parameter will change depending on the prescribed climate change scenario (e.g. amount of temperature change, amount of snow accumulation change, and amount of time considered). Unfortunately, the impact of uncertainty is greatest right at the climatic transition from ice-free to ice-covered conditions, when small changes in temperature, snow accumulation, and/or model parameters will have the proportionally greatest impact on the model results (e.g. ice area or volume).

6.5.4 Sensitivity of the Hazen Plateau to Climate Change: Temperature and Precipitation Sensitivity

6.5.4.1 Temperature or Precipitation Sensitivity

Figure 6.35 (a, b) shows the amount of plateau area and associated thickness covered by ice (after 50 years) within the spatial domain of the model as a function of a series of cooling steps (i.e. –0.5°C, –1°C, etc.). About 8 km^2 of the plateau surface (~2 percent) begin to support permanent ice cover (i.e. ice existed at the end of the 50 year period) once the prescribed cooling reaches 2.5°C. The amount of ice-covered area then increases rapidly as the ice cover expands across the flat, high-elevation parts of the plateau. Once the ice cover reaches the transition to the steeper terrain (cf. Fig. 6.34), the amount of area increase for each cooling step decreases due to topographic constraints. The entire 400 km^2 domain becomes ice-covered once the prescribed cooling exceeds –9°C. The maximum ice thickness (Fig. 6.35b) also increases rapidly once the cooling exceeds –2.5°C and reaches its maximum of 6.25 m weq (which is equivalent to 125 mm weq per year for 50 years) beyond a –9°C cooling. The mean ice thickness (i.e. the ice volume divided by the corresponding ice area) increases more gradually, but eventually 'catches' up to its associated maximum ice thickness beyond a prescribed cooling of –14°C.

The 'threshold' and non-linear response of the model (i.e. predicted ice area/thickness) is an expression of the highly non-linear plateau hypsography of the study area (cf. Marshall and Clarke, 1999). Koerner (1979), for example, emphasized that a linear change in climate will, in reality, lead to a

non-linear change in the mass balance of the High Arctic ice caps because of their highly non-linear area-elevation distribution (or hypsography) (cf. Adams *et al.*, 1998; Hagen *et al.*, 2003; Hoelzle *et al.*, 2003). This notion (albeit combined with additional positive feedback processes) is also an integral part of Ives *et al.* (1975) theory of 'Instantaneous Glacierization' (cf. Andrews *et al.*, 1976; Chapter 2). In essence, the model is able to create a thin, 'crêpe-like' layer of ice across the Hazen Plateau as the climatic cooling allows the snow to persist and accumulate at lower and lower elevations. However, significant mass accumulation (in terms of volume and thickness) is fundamentally limited by the low amounts of annual snow accumulation (i.e. 125 mm weq), no matter how much cooling is prescribed, or for how long (cf. Section 6.5.4.2).

This precipitation limitation is well-illustrated when increasing the amount of annual snow accumulation (Fig. 6.35c, d; note the difference in y-axis scale compared to Fig. 6.35b). For example, a similarly-sized ice cover of about 130 km^2 (~32 percent of the spatial domain) can be created in the model, after 50 years, either with a 3.5°C cooling (maximum thickness ~3.2 m weq) or by increasing annual snow accumulation to 400 mm weq (maximum thickness ~8.8 m weq). Therefore, the model can either create a large and thin ice cover by reducing air temperatures or an equally extensive, but much thicker ice cover by increasing precipitation. Of course, there is no unique solution, both with respect to the prescribed forcing (i.e. temperature or precipitation change) and with respect to the resultant volume of ice that each forcing generates.

6.5.4.2 Temperature and Precipitation Sensitivity

The sensitivity of snow and ice cover on the Hazen Plateau is therefore best evaluated as a (combined) function of temperature change, precipitation change, and (elapsed) time, as illustrated with a series of contour plots in Figure 6.36 after 50 years (top row), after 250 years (middle row), and after 500 years (bottom row). The reference lines and circle in each plot mark the modern climatic conditions on the Hazen Plateau (i.e. 0°C temperature change; 125 mm weq annual snow accumulation). A (simplified) change in the mean climatic conditions is therefore essentially equivalent to shifting the circle to the left/right (i.e. representing a colder/warmer climate) or up/down (i.e. representing a wetter/drier climate), or any combination thereof (cf. Hock *et al.*, 2002). It is therefore possible to determine a specific value

for ice area and ice thickness for any combination of temperature change, precipitation change, and elapsed time of interest.

The amount of plateau area covered by ice remains essentially constant for a specific climate change scenario (i.e. a given combination of temperature and snow accumulation change) at the three different time steps, while the associated thickness of the ice cover continues to increase as a function of time. This result is expected, given that the magnitude of the ice-cap cooling effect parameterized in the model does not depend on the amount of ice-covered area. As noted before, the model is able to create more-or-less the same area of ice (e.g. 200 km^2) at the end of 50, 250, or 500 years with a range of different climate change scenarios (e.g. 0°C/450 mm weq, –2°C/250 mm weq, or –4°C/125 mm weq), but with much different associated ice thicknesses. Given a sufficient amount of time and magnitude of cooling (e.g. –6°C for 500 years), the model creates a large (~300 km^2) and reasonably thick (~60 m weq) ice cover, even with the relatively low modern amounts of annual snow accumulation (125 mm weq). Ice-covered area and thickness for a –6°C cooling obviously increases dramatically if annual snow accumulation is increased as well. Under modern temperature conditions (i.e. 0°C temperature change), an annual snow accumulation of at least 300 mm weq is required for the model to create a permanent ice cover after 50, 250, or 500 years. Under a warmer climate, (i.e. +2°C), more than 500 mm weq annual snow accumulation are required to initiate glaciation on the Hazen Plateau.

This very simplistic assessment, which follows the approach taken, for example, by Arnold (1965), Hock *et al.* (2002), and most recently Bromwich *et al.* (2002) in similar studies, implies that it is today (1) too warm and/or (2) too dry to sustain permanent snow and ice cover on the Hazen Plateau, or to initiate glaciation. This, obviously, also implies that the Hazen Plateau ice caps could not (re)form today under current climatic conditions, which is analogous to the condition of the Barnes Ice Cap on Baffin Island (cf. Chapter 2) or the Greenland Ice Sheet (Weidick, 1975). On the other hand, there appears to be no need to increase annual snow accumulation in order to slowly glaciate the Hazen Plateau under much colder (i.e. glacial) climatic conditions (cf. Hattersley-Smith, 1960a; Blake, 1992; England, 1999). A renewed glaciation of the Hazen Plateau under a warmer 'greenhouse' climate (cf. Miller and de Vernal, 1992), however, seems highly unlikely (cf. Braithwaite *et al.*, 2002), given that annual snow accumulation would have to increase dramatically.

6.5.5 The Hazen Plateau during the 'Little Ice Age'

It is arguably much more interesting to evaluate the climatic sensitivity of the Hazen Plateau relative to some 'real' changes in climate, rather than relative to some arbitrary changes as prescribed in the previous section. In this context, the 'Little Ice Age' provides the most recent 'case study' of climate change and associated glaciation change on northern Ellesmere Island. Specifically, the objective was to assess if the climatic conditions during the so-called 'Little Ice Age' were sufficiently 'severe' to allow for the (latest) formation of the Hazen Plateau ice caps, which is a widely-held assumption today (e.g. Koerner, 1989a; Wolken *et al.*, 2005).

6.5.5.1 Model Setup

The model setup for the 'Little Ice Age' climate change experiment was identical to temperature and precipitation sensitivity experiment in Section 6.5.3. The AWS T3* climatology (1951 to 2000) was repeated 10 times to yield a 500 year time series of mean monthly air temperatures, thus retaining all the temporal variability of the last 50 years, including the warm and variable 1950s to early 1960s, the subsequent 'melt suppression decade' (Alt, 1987), and the warming phase starting sometimes during the 1980s (cf. Sections 6.5.3.3 and 6.5.6.2). The climatic sensitivity of the Hazen Plateau was evaluated by reducing mean monthly air temperatures at 0.5°C steps between –1°C and –3°C (cf. Table 6.10) for a range of annual snow accumulation values ranging from 25 to 600 mm weq at 25 mm weq increments. The sensitivity of the model results to changes in the model parameters was considered using a specific 'middle-of-the-road' climate change scenario (–2°C; 200 mm weq).

6.5.5.2 Model Results

6.5.5.2.1 Climatic Sensitivity

The high-degree of climatic sensitivity of the modeled ice cover (in terms of ice area and maximum ice thickness after 500 years) is well-illustrated in Figures 6.37 and 6.38. For example, the same magnitude of prescribed cooling (e.g. –2°C) can lead to drastically different ice configurations on the Hazen Plateau simply by varying annual snow accumulation between 100 and 250 mm weq (Fig.

6.37). Likewise, the modeled area of ice and its associated maximum thickness for a prescribed annual snow accumulation of, for example, 200 mm weq, changes considerably depending on the magnitude of the associated temperature cooling (Fig. 6.38). These model results can be interpreted as confirmation of the original hypothesis of this study that the Hazen Plateau is a climatically-sensitive area, where relatively small changes in the climatic conditions (e.g. temperature and/or precipitation) can lead to large changes in the amount of glaciation (cf. Chapter 1). However, these results also immediately raise concerns about the predictive capabilities of the model (or any other model for that matter, cf. Oerlemans, 1991, 1998, 2000, 2001) under such extremely sensitive circumstances. This 'climatic' sensitivity or uncertainty of the model is (schematically) illustrated in Figures 6.37 and 6.38 by the grey shading and the associated red reference lines (i.e. ±0.5°C around –2°C and ±25 mm weq around 200 mm weq) and implies that a wide range of equally plausible ice configuration can be modeled on the Hazen Plateau during the 'Little Ice Age' simply by minor adjustments to the specific climate change scenario considered (e.g. ±0.5°C and/or ±25 mm weq; cf. Table 6.29). At the same time, it is realistically only possible to define a rather broad 'reasonable' range for the amount of cooling during the 'Little Ice Age' on northern Ellesmere Island (i.e. –1 to –3°C; cf. Table 6.10). The situation in terms of precipitation changes is even less well-defined beyond the general consensus that there is no clear evidence for consistent or distinct increases or decreases in precipitation during the 'Little Ice Age' (e.g. Fisher and Koerner, 1994; Fisher *et al.*, 1995). The modeled ice configurations in terms of absolute ice area and thickness are therefore a function of the prescribed temperature and precipitation changes, but a strict comparison of the highly-sensitive model results for different climate change scenarios does not seem appropriate given the large model sensitivity (cf. Marshall and Clarke, 1999).

6.5.5.2.2 Model Parameter Sensitivity

This situation further is exasperated by the sensitivity of the model results to changes in the three main model parameters (DDF (snow); DDF (ice); P-max) as illustrated in Figure 6.39 for a 'middle-of-the-road' 'Little Ice Age' climate change scenario of –2°C and 200 mm weq annual snow accumulation. The black curves represents the model results for the preferred model parameter values, while the upper (lower) bounds of the surrounding grey shading are defined by a respective model parameter combination

leading to a 'minimum melt' ('maximum melt') scenario (Table 6.29). Figure 6.39 illustrates that the model results are very sensitive to the specific choice of the three main model parameters (Table 6.29). The 'minimum melt'/ 'maximum melt' scenarios can be regarded as 'worst case' situations, as all three model parameters were systematically adjusted towards producing either minimum or maximum melting. The resultant model parameter sensitivity/uncertainty is of similar magnitude, in fact somewhat smaller, than the model sensitivity/uncertainty associated with ±0.5°C or ±25 mm weq variations in the specific climate change scenario considered (cf. Fig. 6.37, 6.38). Overall, the extent of ice-covered area increases slowly over time (due to the elevation-mass balance feedback, cf. Section 6.5.6.1), but a high-degree of inter-annual and multi-year variability dominates the time series (cf. Section 6.5.6.2). This is, on one hand, a reflection of the plateau topography (Fig. 6.34), where any small changes in summer melting can either include or exclude relatively large areas of the plateau (cf. Marshall and Clarke, 1999). In addition, a grid cell is considered ice-covered in the model if it retains any amount of snow at the end of a given summer melt season, thus the immediate increase or decrease in ice-covered area from year-to-year can be quite dramatic.

This high-degree of model sensitivity does not imply a fundamental flaw of the model or the associated modeling experiment, but instead is a reflection of the 'real world' climatic sensitivity of the Hazen Plateau. Unfortunately, in a modeling context, this also translates to a comparatively high level of model sensitivity or uncertainty associated with the specific choice of the required model parameters. This conclusion was entirely expected, given the arguments eloquently presented, for example, by Oerlemans (1991, 1998, 2000, 2001), Hindmarsh (1993), and van der Veen (1999a, b) (cf. Section 6.2.3). In essence, they simply considered the obvious: it is fundamentally impossible to make an absolute, quantitative assessment of the state of a natural system (e.g. extent/thickness of ice cover on the Hazen Plateau at any given time) to changes in climate forcing, model parameters, feedback processes, etc., unless the system considered is very insensitive to such changes, even if the underlying model were (almost) perfect. In such a scenario, the spatial extent and thickness of ice cover on the Hazen Plateau would be fairly stable over time (i.e. insensitive to changes in the climate forcing, model parameters, feedback processes, etc.), but would be "...of no interest" according to Oerlemans (1998). The situation

of the Hazen Plateau is obviously very sensitive to changes in climate forcing, model parameters, feedbacks, etc., and the model used here is far from perfect.

Laabs *et al.* (2005; their Fig. 7) presented a set of three non-linear equations expressing the extent of glacier cover within their three study areas, at the Last Glacial Maximum (LGM), as a function of temperature change and precipitation change relative to modern conditions. What is striking about their results is that a wide range of temperature changes (–3 to –10°C), combined with an equally wide range of precipitation changes (–75 to +450 percent), were able together to produce equally-plausible ice extents for the LGM in their model. Sensitivity tests conducted by Plummer (2002), in a very similar study, suggested that model parameter variability is approximately equivalent to a ±0.5°C temperature change or a ±30 percent precipitation change in terms of the specific climate change scenario considered. Taken together, this implies that a wide range of plausible climate change scenarios can equally satisfy the glaciological evidence (which itself is very uncertain), while model parameter uncertainty contributed about ±0.5°C/ ±30 percent uncertainty to each climate change scenario (which may be viewed as a measure of the precision of the model results). Laabs *et al.* (2005) noted:

> "...this would greatly expand the paleoclimate constraints discussed previously, probably even to the extent that many combinations of temperature depression and precipitation change could have produced all three LGM glaciers."

At a larger scale, the study by Marshall and Clarke (1999; their Fig. 2) provided another 'extreme' example of ice sheet model sensitivity. Predicted ice sheet thickness approximately doubled for each 0.5°C cooling step beyond a given threshold temperature, with a similar sensitivity and threshold response to slight changes in precipitation. This implies that small uncertainties in the prescribed climatic conditions, or model assumptions, can lead to extremely different modeled ice configurations, especially at the end of long model runs. At an even larger scale, a similar problem is well-illustrated in the 2005 'Arctic Climate Impact Assessment' Scientific Report (ACIA, 2005). Here, the projected changes in glacier mass balance over the 21st century vary widely between the different models considered, to the extent that not even the sign of the contribution of Arctic glaciers to projected sea level changes agrees amongst the different models, especially at the regional scale (ACIA, 2005; their Fig. 6.19). Again, this is

presumably a reflection of both the actual climatic sensitivity of the Arctic cryosphere, as well as of model sensitivity, differences in model assumptions, and model uncertainty.

Such a situation, however, does not diminish the validity of the model(s) and its/their results in the context of sensitivity tests. The absolute values for ice-covered area and ice thickness at any given time may include a (too) large uncertainty due to model sensitivity, but it is reasonable to assume that the relative changes are much more robust (Oerlemans, 1991, 1998, 2000, 2001). Therefore, it seems reasonable to conclude that there (probably) was extensive, permanent ice cover on the Hazen Plateau during the 'Little Ice Age', but not unless substantial increases in annual snow accumulation (~20 to 60 percent; cf. Fig. 6.37; 6.38) occurred at the same time. Such a significant relative precipitation increase at a time of overall colder climatic conditions seems highly unlikely, but only represents 25 to 75 mm weq in absolute numbers. On the other hand, the availability of local moisture sources was probably significantly reduced during the 'Little Ice Age' due to more extensive sea ice cover on the Arctic Ocean and in the inter-island channels (cf. Alt, 1987). Thus, increased precipitation during the 'Little Ice Age', if there was any, was probably associated with some external process(es). Bradley and Miller (1972) analyzed the unusual climatic conditions on Baffin Island (and much of Canadian High Arctic in general, cf. Alt, 1987) during the 1960s, with reduced summer temperatures, increased winter temperatures, slightly increased summer precipitation (~7.2 percent), and significantly increased winter precipitation (~33.7 percent) and speculated as to their climatic causes:

> "So it is possible that the recent climatic fluctuation which has occurred on Baffin Island since the late 1950s is related to atmospheric teleconnexions resulting from the inception of a new climatic regime which in turn can be related to large scale seasonal ocean-atmosphere interactions in the Pacific." (cf. Bradley, 1973)

Alt (1987) took this idea one step further and suggested that this particular time period (i.e. her 'melt suppression decade') can be regarded as an approximate modern-day analogue for the climatic conditions during the 'Little Ice Age'. That raises an interesting possibility: perhaps the High Arctic cooling during the 'Little Ice Age' was mainly a summer phenomena (cf. Section 6.5.1.1), but was accompanied by a relative warming during the winter month, which led to increased winter/annual precipitation and snow accumulation (cf. Zhang *et al.*, 2000). Nesje and Dahl (2003) recently concluded

that changes in large-scale atmospheric circulation patterns led to increased winter precipitation, lower summer temperatures, and glacier expansion in southern Norway during the first half of the 18th century (i.e. during the so-called 'Little Ice Age') (cf. Nordli *et al.*, 2005). Many other authors have in the past speculated or implied that similar types of atmospheric circulation changes may have resulted in significant precipitation increases across the Canadian High Arctic during climatic cooling phases (e.g. Barry, 1966; Barry *et al.*, 1971, 1975; Lamb and Woodroffe, 1970; Loewe, 1971; Johnson and Andrews, 1979; Zhang *et al.*, 2000; Bromwich *et al.*, 2002; Marshall, 2002), albeit without further quantification or discussion as to the precise mechanism(s) involved. Bradley and England (1979; their Fig. 7, 8) classified synoptic-scale atmospheric circulation patterns across the Canadian High Arctic and argued that a simple change in the relative frequency of certain types (e.g. warm/dry vs. cold/wet patterns) could have significant consequences for High Arctic climate, especially with respect to summer melting and precipitation (cf. Chapter 7). Alt (1987) subsequently linked these atmospheric circulation patterns (albeit based on a slightly different classification system) directly to glacier mass balance variability in the Canadian High Arctic.

6.5.5.3 Glaciological Considerations

One can consider two complementary lines of evidence to define 'reasonable limits' for the extent and thickness of ice on the Hazen Plateau during the 'Little Ice Age' based on independent glaciological evidence. First, the maximum thickness of Murray Ice Cap today is probably no more than about 30 m (~27 m weq), given topographic considerations and the results of a simple equation presented by Paterson (1981, p. 163) relating the ice thickness at a point along an ice sheet/cap profile to its distance from the ice margin (assuming a basal shear stress of zero). In fact, one of the basic model assumptions included in the digital elevation model is that the maximum elevation of the (initially) ice-free Hazen Plateau is 1070 m asl (cf. Section 6.5.3.2). It is therefore reasonable to assume that the maximum ice thickness of the 'Little Ice Age' ice cover must have been at least greater than about 30 m (~27 m weq), given that the ice cap has lost significant area and volume since that time (cf. Chapter 3).

The second line of evidence consists of a subtle, but well-defined lichen trimline found today on the Hazen Plateau surrounding Murray Ice Cap and on the unglaciated plateau in the vicinity of AWS T3

and towards the Simmons Ice Cap (Fig. 6.40). It is traditional and common practice in the scientific literature to utilize the presence or absence of lichen, or their respective differences in size, as quantitative tools to reconstruct the position of past ice margins and to derive estimates of past ice thickness, ice volume, and even past ELAs (e.g. Karlen, 1973; Andrews *et al.*, 1976; Locke and Locke, 1977; Furbish and Andrews, 1984; Edlund, 1985; Matthews, 2005; Wolken *et al.*, 2005) both in the Canadian High Arctic and elsewhere around the world.

6.5.5.3.1 A Traditional Interpretation of the Lichen Evidence

The traditional interpretation would consider the lichen trimline found today on the Hazen Plateau in vicinity of Murray and Simmons Ice Cap as depicting their most recent maximum spatial extent, probably towards the end of the 'Little Ice Age' around the end of the 19th century (e.g. Ives, 1962; Andrews *et al.*, 1972, 1976; Locke and Locke, 1977). It is interesting to note that the lichen trimline around Murray Ice Cap follows more-or-less consistently the 990/995 m asl contour line (Fig. 6.40). Around the plateau hilltop of AWS T3 and towards the Simmons Ice Cap, the lichen trimline descends to somewhat lower elevations (~950/960 m asl), especially on north-facing slopes. Similar lichen-free zones are also found today on other plateau hilltops in the vicinity (e.g. Point A in Fig. 6.40), but have not been mapped in detail. The plateau hilltop just southwest of the Simmons Ice Cap (Point A in Fig. 6.40) is of particular interest in this context, as it represents the highest plateau elevation in the vicinity (~1030 m asl) and apparently supported a small remnant ice patch as late as 1959 (Bradley and England, 1977). The lichen trimline as mapped around Murray Ice Cap is much better defined than the lichen trimline mapped around AWS T3 and towards the Simmons Ice Cap, as it is based on a careful and comprehensive mapping program over three field seasons with a variety of different field partners. In contrast, the lichen trimline around AWS T3 and towards the Simmons Ice Cap was mapped during one (rushed) day towards the end of the 2001 field season.

Figure 6.40 shows two possible ice cover configurations during the 'Little Ice Age'. The 'minimum' ice extent scenario (black outlines) is based on a 'strict' interpretation of the lichen trimline around Murray Ice Cap, assuming that all elevations within the spatial domain of the model greater than 990/995 m asl supported permanent ice during the 'Little Ice Age'. This corresponds to a total ice-

covered area of about 20 to 23 km^2, with an approximate maximum thickness of about 35 m (~32 m weq). The corresponding 'maximum' ice extent scenario (blue outlines) is based on a more 'generous' interpretation of the lichen trimline as mapped in the vicinity of AWS T3 and towards the Simmons Ice Cap, assuming that all elevations within the spatial domain of the model greater than 950/960 m asl supported permanent ice cover during the 'Little Ice Age'. This interpretation corresponds to a total ice-covered area of about 40 to 48 km^2, with an approximate maximum thickness of about 40 m (~36 m weq).

Koerner (1980a), in contrast, argued that the simplest explanation for (most) lichen-free zones in the Canadian High Arctic is simply the presence of long-lasting, but still annual, snow cover, especially in topographic situations where snow accumulation is (locally) enhanced due to snow drifting (cf. Section 6.5.1.1). Wolken *et al.* (2005) offered an interpretation of lichen trimlines which satisfies both the traditional interpretation as well as Koerner's challenge. They concluded that lichen trimlines surrounding thin, stagnant, cold-based ice caps typically mark the spatial extent of long(er)-lasting, or perhaps perennial, 'snow aprons' accumulated around the actual ice perimeter of the ice caps (cf. Hattersley-Smith and Serson, 1973). This 'snow apron' hypothesis can explain why the lichen trimline found today along the north-facing, steeper slopes in the vicinity of AWS T3 and towards the Simmons Ice Cap is located a few tens of meters lower in elevation than around Murray Ice Cap, where all steeper slopes face either south or east. If this interpretation is correct, then the lichen trimline around Murray Ice Cap should represent a better proxy for the maximum spatial extent of actual ice cover (~20 to 23 km^2) at some point in the recent past, presumably the 'Little Ice Age'.

Figure 6.41 puts the extent and thickness of ice during the 'Little Ice Age', as recorded by the lichen evidence (black and blue rectangles), into the context of the different modeled ice configurations (i.e. area of modeled ice plotted as a function of its corresponding thickness for different levels of climate cooling). The graphs reveal a consistent mismatch between the model results and the lichen evidence in the sense that the model is not able to produce an ice configuration on the Hazen Plateau during the 'Little Ice Age' that matches the one(s) that may have existed at that time based on a traditional interpretation of the lichen evidence: if the modeled ice area (after 500 years) matches the ice area as recorded by the lichen trimline, then the resultant modeled ice caps are much too thin. Likewise, if the

respective ice thicknesses agree (after 500 years), then the modeled ice cover is much too large. It is also important to remember that the different modeled ice configurations shown in Figure 6.41 are not all equally plausible from a climatic perspective (i.e. the ice configurations for a –1 °C cooling require a much larger increase in annual snow accumulation than the ice configurations for a –3 °C cooling). In addition, whatever ice configuration is being considered, it is very sensitive to even small changes in its associated climate change scenario, the specific choice of the model parameters, and the amount of time considered (cf. Figs. 6.37 to 6.39). It is therefore most conservative to view the entire spread of the five curves as an uncertainty envelope – still, the ice cover as recorded by the lichen evidence falls outside the entire range of model possibilities. It is theoretically possible that there is some specific combination of prescribed temperature change, precipitation change, and model parameter values that leads to a modeled ice cover whose dimensions perfectly match the lichen evidence. But such a unique solution would not be very meaningful in reality (cf. Marshall and Clarke, 1999; Blöschl, 2006), as it still is affected by the climatic sensitivity of the model (e.g. ±0.5°C/ ±30 percent; Laabs *et al.*, 2005) and the model uncertainty due to model parameter uncertainty.

6.5.5.3.2 An Alternative Interpretation

It seems intuitively much too simplistic to assume an entirely static margin of Murray and Simmons Ice Cap during the 'Little Ice Age', i.e. one that remained essentially fixed at a given position for (much) of its duration. Instead, it seems much more probable that the position of the ice margin 'proper', and the spatial extent of the surrounding snow apron, fluctuated considerably from year-to-year in response to variations in summer melting (cf. Fig. 6.39). The lichen trimline as mapped on the Hazen Plateau in vicinity of Murray and Simmons Ice Cap does not (as it frequently does on Baffin Island) represent an abrupt transition from completely lichen-free terrain to completely lichen-covered terrain (e.g. Ives, 1962; Falconer, 1966; Wolken *et al.*, 2005). Instead, it marks what Koerner (1980b) referred to as a 'diffuse boundary' between areas 100 percent devoid of lichens and vegetation, and surrounding areas with very sparse lichen and vegetation cover. The extent/degree of lichen/vegetation coverage (or landscape maturity) increases with increased distance from the modern ice margin and/or decreased elevation. Koerner (1980b) explained the formation of such diffuse lichen boundaries by arguing:

> "This is because permanent snow and ice fields expand and contract areally in response to the varying intensity of melting from summer to summer. A permanent snowfield 1 to 2 m thick would disappear every few years after a particularly warm summer to reform a year or so later."

Diffuse trimlines are frequently found today on carbonate bedrock in the Canadian High Arctic, according to Wolken *et al.* (2005), on low-angle slopes or plateau uplands, where a small change in the magnitude of summer melting can lead to a large horizontal displacement of the position of the snowline/ice margin at the end of a given summer. Accordingly, the zone or 'moat' of completely lichen-free ground adjacent to Murray Ice Cap, covering the currently ice-free plateau in the vicinity of AWS T3, towards the Simmons Ice Cap, and found on other plateau hilltops of similar elevations (cf. Fig. 6.40), may be interpreted to mark the spatial extent of 'Little Ice Age' ice cover that was "sufficiently thick to withstand variations in the annual melt rate long enough to kill the plant cover to that [i.e. inside that] limit." (Wolken *et al.*, 2005). In other words, it records a minimum ice extent that existed more-or-less continuously for the entire duration of the 'Little Ice Age'. The diffuse boundary, or surrounding areas with reduced lichen/vegetation cover, would then be indicative of the expansion and retraction of the 'Little Ice Age' ice cover and its surrounding snow apron, which limited, but not necessarily prohibited, lichen growth and survival. In essence, there is an abrupt boundary recorded on the landscape between no lichen coverage and sparse lichen coverage (reflecting minimum ice extent), followed by a gradual transition into a terrain that was progressively less and less influenced by snow/ice cover during the 'Little Ice Age'. Ultimately, there should be another noticeable transition at some lower elevation to a much more mature ground surface that remained free-of-ice and snow throughout the entire 'Little Ice Age' (= maximum ice extent).

Figure 6.42 shows the 500-year time series of ice extent (top) and maximum ice thickness (bottom) for three different climate change scenarios: –1°C/250 mm weq (red); –2°C/200 mm weq (black); and –3°C/150 mm weq (blue). Again, this is not meant to imply that these three selected climate change scenarios are equally probable to have actually occurred during the 'Little Ice Age'; rather they illustrate a range of different possibilities. The areal extent of ice, as expected, fluctuated considerably over time (cf. Koerner, 1980b), yet the minimum amount of ice-covered area is broadly consistent with this alternative interpretation of the lichen evidence, especially for the –1°C/250 mm weq and the —

2°C/200 mm weq climate change scenario. Again, it would be possible to define a specific climate change scenario that optimizes the match, or rather minimizes the mismatch, with the lichen evidence, but, given the large uncertainties involved in all aspects of such a comparison, such a 'best-fit' solution is not especially meaningful (cf. Marshall and Clarke, 1999; Blöschl, 2006). Nevertheless, it is instructive to visualize how one of these climate change scenarios (e.g. –2°C/200 mm weq) might have been expressed on the landscape of the Hazen Plateau (Fig. 6.43) in terms of ice extent and ice thickness. The total colored (i.e. ice-covered) area, at the end of 500 years, is about 115 km^2, extending in elevation down to about 890 m asl. However, the green colors denote ice thicknesses of less than about 3 m weq and the transition to yellow occurs at about 950 m asl (~48 km^2), which corresponds approximately to the most recent minimum ice extent for this particular climate change scenario (cf. Fig. 6.42; model year 462; ~51.5 km^2). Obviously, the particular choice of color scale can be used here to emphasize or achieve the desired visual perception.

6.5.6 Discussion

The generally-accepted Holocene glacial history of the Hazen Plateau holds that the Hazen Plateau was essentially ice-free for much of the Holocene and that the Hazen Plateau ice caps (re)-formed most recently during the 'Little Ice Age' to reach their maximum Holocene extent towards the end of the 19th century. However, this sequence of events is difficult to reconcile with the modeling results and the complementary climatic and glaciologic evidence. The model is able to glaciate the Hazen Plateau during the 'Little Ice Age', assuming a range of reasonable temperature reductions, but not without increasing annual snow accumulation between at least 20 and 60 percent (Fig. 6.37 and 6.38). Such a precipitation increase has not been documented so far and seems unlikely, unless indeed changes in the large-scale atmospheric circulation patterns and global tele-connections did result in increased moisture advection into the Canadian High Arctic. This remains an interesting hypothesis, which (still) awaits testing (cf. Chapter 7). The model was able to produce an ice configuration that is broadly consistent with the lichen trimline evidence (Fig. 6.43) and the basic glaciological requirement that the Hazen Plateau ice caps during the 'Little Ice Age' must have been (at least) thicker than today's ice caps, but the success of such

a model result vs. 'reality' comparison depends entirely on one's interpretation of the lichen trimline and its glaciological meaning.

6.5.6.1 Modeling Considerations

The modeling experiments in the preceding section did not explicitly include many of the possibly important positive or negative feedback processes, for example the snow/ice-albedo-temperature feedback loop (cf. Chapter 2). This is a quite common situation today in the available climate change and snow/ice cover modeling literature (e.g. Souchez, 1997; Marshall and Clarke, 1999; Marshall, 2002; Marshall *et al.*, 2004; Bromwich *et al.*, 2002; Ruddiman *et al.*, 2005). For example, Loewe (1971), in a paper entitled 'Considerations on the origin of the Quaternary ice sheet of North America' stated:

> "Once established, an ice sheet grows to higher and generally colder levels; it will tend to preserve itself. Hence, the conditions which allow an ice sheet to start will generally be more stringent than those which allow its survival."

Loewe (1971) specifically singled out the height-mass balance feedback (cf. Oerlemans, 2002; Pollard and DeConto, 2004) in the context of ice sheet formation and expansion. Bromwich *et al.* (2002), in a recent paper entitled 'Meteorological perspective on the initiation of the Laurentide Ice Sheet' treated the snow/ice-albedo-temperature feedback process simply as follows:

> "Once a persistent snowfield is established and can grow sufficiently large, positive feedback mechanisms (i.e. albedo related cooling) would become significant factors for atmospheric circulation."

In fact, the snow/ice-albedo-temperature feedback process is (albeit crudely) parameterized within the model in the form of a constant ice-cap cooling effect (Table 6.23), which does not actually represent a proper dynamic feedback process since it does not interact with the surrounding ice-free terrain, no matter how large or thick an ice cover is generated in the model. More broadly, it is obviously difficult (or perhaps impossible) to distinguish precisely between cause (i.e. external climate change) and effect (i.e. internal feedback process) in this context (Koerner, 1980b; Hall, 2004; Blöschl, 2006). For example, a cooling/glaciation trend manifests itself by extending the period (i.e. time) and the area (i.e. space) of snow and ice cover each year, which, at some point, begins to create a positive feedback

mechanism upon itself. At the local scale, this positive feedback begins essentially immediately once snow/ice cover is able to persist for a slightly longer time period than before (Takahara and Higuichi, 1985; Marsh *et al.*, 1997). The strength/magnitude of the positive feedback, in turn, is a function of the spatial extent and thickness of the snow cover (amongst other things). At the regional or global scale, the snow/ice cover presumably has to reach some (unknown) longer temporal and larger spatial scale to have a significant impact on the surrounding environment (Williams, 1978b; Ridley *et al.*, 2005). Either way, it becomes progressively more and more difficult to separate the (initial) external forcing (e.g. climatic cooling) from the secondary internal process(es), especially since both are also continuously associated with, and/or modified by, local, regional, and global climatic variability (cf. Hall, 2004). At some point, an initially positive feedback process may also 'morph' into a negative feedback process, for example once the amount of cooling and the size of the ice cover begins to restrict moisture availability (cf. England and Bradley, 1978).

The simplicity of the modeling experiments presented here largely prohibits an understanding of the precise partitioning between external forcing and internal response/feedback (Marshall, 2002; Blöschl, 2006), but rather refers to a 'net' change in the climatic conditions (cf. Bromwich *et al.*, 2002; Winton, 2006). The most appropriate way to interpret some of the presented results is therefore to assume that a given amount of prescribed (or real) cooling would implicitly include a variety of internal feedback processes not explicitly included in the model. In other words, a 'net' 2°C cooling during the 'Little Ice Age' might, in reality, be achieved via a 1.5°C 'direct' climate cooling and an additional 0.5°C cooling 'equivalent' supplied, for example, by a variety of positive feedback processes, such as the snow/ice-albedo-temperature feedback process (cf. Marshall, 2002).

6.5.6.2 Issues of Inter-Annual and Multi-Year Variability

The climate change scenario used in this modeling experiment consisted of a simple repetition of the modern-day climatology (AWS T3*, 1951 to 2000), albeit 'cooled' by a fixed monthly offset (e.g. 0.5°C, 1.0°C, etc.). Therefore, the prescribed climatology during the 'Little Ice Age' retained all the temporal variability of the last 50 years every 50 years (i.e. repeated 10 times; cf. Fig. 6.44). This is certainly a more realistic approach (cf. Marshall and Clarke, 1999) than simply prescribing a constant

cooling relative to some mean climatic conditions (cf. Section 6.5.3.3), but also leaves the model results, on purpose, susceptible to inter-annual and multi-year climatic variability.

This is significant in this context since an 'anomalously' warm year or period of years can have a disproportionate effect on glacier mass balance in areas with low annual precipitation amounts (Schytt, 1964; Bradley and England, 1978; Adams *et al.* 1998). Essentially, the amount of potential mass loss during a given year/period is theoretically unlimited, whereas the maximum possible mass gains are fundamentally limited by the low amounts of annual snow accumulation. Koerner (1980a), for example, stressed that a decreased variability of summer climate, specifically the disappearance of anomalously warm summers, would be very beneficial for glaciation initiation, in addition to an overall climate cooling (cf. Alt, 1987; Bromwich *et al.*, 2002).

Figures 6.44 to 6.46 illustrate the sensitivity of the modeled ice cover on the Hazen Plateau, in terms of its area and maximum thickness, to adjustments in the input climatology in the form of three case studies for the same climate change scenario (–2°C; 200 mm weq annual snow accumulation). Case #1 (black curves) represents, as before, the 50 year AWS T3* climatology simply repeated 10 times. In case #2 (red curves), the 50 year AWS T3* climatology was randomized individually 10 times and then combined to yield a 500 year time series. Case #3 (blue) is identical to case #2, except that the two warmest years on record (i.e. 1957 and 1960 in the original AWS T3* time series) were replaced with the long-term mean in order to simulate a 'Little Ice Age' without anomalously warm summers (cf. Alt, 1987). This obviously has an indirect effect of lowering the long-term mean from –0.39°C to –0.53°C (Fig. 6.44), which may be interpreted as a positive feedback mechanism (cf. Section 6.5.6.1), adding to the 'direct' climatic forcing. This is reflected in the model results, for example, by an overall increase in ice extent and thickness from case #2 to case #3 (Fig. 6.45, 6.46). The influence of persistent, multi-year warm or cold periods dominates the temporal variability of ice-covered area and thickness in case #1. For example, the warm period of the 1950s to early 1960s always (i.e. in each of the 10 cycles) leads to a prolonged period of shrinking and thinning ice cover, only to recover during the relatively cold and less variable mid-1960s to late 1970s. In contrast, the lack of consistent, multi-year warm or cold periods in the two randomized climatologies allowed for the establishment of a reasonably stable ice configuration

(in terms of its spatial extent) – the effect of single warm years is therefore much more muted than the effect of a single cold year (cf. Section 6.5.5.2).

It is probably unrealistic to assume that the temporal variability observed over last 50 years will repeat itself exactly 10 times over 500 years during the 'Little Ice Age' and in that sense, a randomized time series represents probably a more appropriate climatology, especially for sensitivity tests. On the other hand, multi-year persistence was clearly an important feature of the climate of the last 50 years in the Canadian High Arctic and the climate during the 'Little Ice Age' (cf. Koerner and Lundgaard, 1995; their Fig. 6), with a high-degree of (random?) inter-annual variability superimposed to top of it. It is interesting to note that the modeled ice extent for the randomized climatology, and its temporal variability, appears to match the lichen evidence much better than the original climatology used (Fig. 6.45).

6.5.6.3 Climatic Considerations

In the Canadian High Arctic (and elsewhere in polar regions), the question of glaciation (or rather lack thereof) always comes back to the amount of available precipitation (or rather lack thereof), which is perceived by many to prohibit the past existence of large ice masses. Loewe (1971), for example, discussed the likelihood that a climatic cooling trend in the Arctic would be accompanied by simultaneous and substantial increases in solid precipitation and dismissed this notion as 'unlikely'. Ice sheet and global climate models typically adopt/assume existing present-day spatial precipitation patterns, albeit scaled to incorporate the increased aridity during colder (glacial) climates (Tarasov and Peltier, 1997; Marshall *et al.*, 2004). This assumption is almost certainly wrong (e.g. Kapsner *et al.*, 1995; Marshall *et al.*, 2004), especially for the mid-latitudes (e.g. Hostetler *et al.*, 2000). For example, Nesje and Dahl (2003) recently concluded that changes in large-scale atmospheric circulation patterns led to increased winter precipitation, lower summer temperatures, and glacier expansion in southern Norway during the first half of the 18th century (i.e. during the so-called 'Little Ice Age') (cf. Nordli *et al.*, 2005). Several authors have in the past speculated or implied that similar types of atmospheric circulation changes may have resulted in significant precipitation increases across the Canadian High Arctic during climatic cold/cooling phases (e.g. Barry, 1966; Barry *et al.*, 1971; Lamb and Woodroffe, 1970; Bradley

and Miller, 1972; Loewe, 1971; Johnson and Andrews, 1979; Bromwich *et al.*, 2002; Marshall, 2002), although Barry *et al.* (1975) noted that "It is hard [for them] to visualize appropriate [i.e. atmospheric and oceanic] circulation regimes to provide the necessary input of snow accumulation recurring over thousands of years."

However, this paradigm of severe glacial aridity in the Canadian High Arctic (cf. England and Bradley, 1978) was challenged recently by Bromwich *et al.* (2004), who showed, using a regional climate model, that the presence of the Laurentide Ice Sheet 'split' the jet stream and deflected its northern branch directly into the Canadian High Arctic (cf. Manabe and Broccoli, 1985). England *et al.* (2006), citing Bromwich *et al.* (2004), argued that "...the strength of a split jet stream was linearly related to the height of the Laurentide Ice Sheet, which by the LGM [Last Glacial Maximum] would have occasioned a substantial increase in precipitation across the QEI (by 1.5 – 4 times modern; Bromwich *et al.*, 2004).", thus providing a moisture transport mechanism and the moisture necessary to grow a large and thick Innuitian Ice Sheet at that time. However, this proposed 'wetter-than-today' Last Glacial Maximum still needs to be reconciled with the existing ice core evidence from the Canadian High Arctic and Greenland, which actually shows reduced accumulation rates during the Last Glacial Maximum (e.g. Fisher *et al.*, 1983; Koerner, 1989a; Cuffey and Clow, 1997; Alley, 2000).

Marshall (2002) noted with respect to the formation and expansion of glaciers in the Canadian High Arctic at the transition from the last Interglacial to the Last Glacial period:

> "Cold temperatures need to be accompanied by substantial increases in precipitation in the North Atlantic and polar regions in order to accrue continental ice at the rate demanded by sea level reconstructions."

This is, not surprisingly, a new idea (see above and below) – in fact this issue of ice sheet expansion, sea level decreases, and climate change is still one of the grand problems of Quaternary geosciences. There is simply no direct evidence or mechanism to suggest, or give reason to believe, that there were any (substantial) increases in precipitation either at the onset of, and/or during, significant cold intervals such as the 'Little Ice Age' and the Last Glacial period (cf. Chapter 7). However, this does not necessarily prohibit the (slow) initiation and (slow) expansion of glaciers, ice caps, and even ice sheets across the Canadian High Arctic as long as summer melting is sufficiently and consistently reduced to

allow for positive annual mass balances (cf. Hattersley-Smith, 1960a; Blake, 1992; England, 1999). The rates of ice cover expansion under such a scenario are, however, probably not compatible with those required to explain the sea level reconstructions. Bromwich *et al.* (2004) provided a plausible mechanism for increased precipitation in the Canadian High Arctic during the Last Glacial Maximum, but their presented mechanism is not applicable at times when the Laurentide Ice Sheet was not in existence (i.e. the 'Little Ice Age' or the last Interglacial/Glacial transition) and is not supported by the ice core evidence from the Canadian High Arctic. This leaves the glaciation hypothesis developed by Ruddiman and McIntyre (1981), eloquently summarized in Bradley (1985), who argued that ice sheet formation is favored at times when Northern Hemisphere summers are relatively cold (due to orbital forcing), but sea surface temperatures are (still) relatively high, thus providing abundant moisture for the growing ice sheets. In an earlier paper (Ruddiman and McIntyre, 1979), they offered "strong evidence" (Bradley, 1985) from the sub-polar North Atlantic that indeed sea surface temperatures remained relatively high during periods of substantial ice growth. In fact, sea surface temperature cooling lagged ice sheet growth by about 1000 to 5000 years (Bradley, 1985).

6.5.6.4 An Alternative Sequence of Events on the Hazen Plateau

Perhaps the simplest way to reconcile the model results, the climatic considerations, and the glaciological evidence is to consider the possibility that the Hazen Plateau ice caps may have existed continuously throughout the entire Holocene as remnants of the Innuitian Ice Sheet, which would be analogous to the association of the Barnes Ice Cap and the Laurentide Ice Sheet (Ward, 1954; Dyke and Prest, 1987; Andrews, 2002). Support for this interpretation comes from the work of Rod Smith (1999, 2002) who showed that plateau ice caps persisted on the Hazen Plateau between Lake Hazen and Fort Conger well into the mid-Holocene (~5 ka BP) (cf. England, 1986; Bell, 1996). These plateau ice caps would have occupied an elevation range between about 300 and 800 m asl, significantly lower than Murray and Simmons Ice Cap.

The most recent reconstruction of Late Glacial ice cover across the Canadian High Arctic (England, 1998; 1999; England *et al.*, 2006) showed the Innuitian Ice Sheet maintaining its maximum configuration until about 11 ka BP, with a continuous, thick ice cover all along the entire east coast of

Ellesmere Island until about 8.5 ka BP. The Innuitian Ice Sheet remained in contact with the Greenland Ice Sheet across Nares Strait until about 7.5 ka BP before breaking up into several large, residual ice caps. At the same time, there is also clear evidence for high levels of summer melting between about 11.5 and 8 ka BP, which may have led to several short intervals of net ablation on the Agassiz Ice Cap summit (Fisher *et al.*, 1995). At the same time, England *et al.* (2006) speculated that the retreating Innuitian Ice Sheet by about 8.5 ka BP opened up additional moisture sources in the western parts of the Queen Elizabeth Islands, leading to a cooler summer climate, increased cloud cover, and increases in precipitation over its remnants located over eastern and north-eastern Ellesmere Island. Summer temperatures have in fact been decreasing continuously over the last 8000 years, particularly during the last 5000 years (Koerner and Fisher, 2002). The 'Little Ice Age', according to this longer temporal perspective, does not represent a distinct or unusual cold period, but instead "...may be nothing more than a slight cooling variation within that [5000 year cooling] trend." (Koerner, 2002).

It therefore does not seem unreasonable to consider the possibility that the Hazen Plateau ice caps survived the warmth of the Early Holocene as remnants of the Innuitian Ice Sheet, thus existing continuously since its initial formation some 20000 years ago (England *et al.*, 2006). Plateau ice caps apparently existed on the Hazen Plateau, at much lower elevations, well into the mid-Holocene (Smith, 1999; 2002). Cooling over the last 5000 years would have promoted/enabled their continued survival and possible expansion, similar to other glaciers and ice caps in the Canadian High Arctic (Fisher and Koerner, 2002; Koerner, 2002), to reach a period of stability during, and a (relative) maximum towards the end of, the 'Little Ice Age', the extent of which is marked today on the landscape by the lichen trimline.

Table 6.1 Positive degree-day factors (DDF) for snow, ice, and superimposed ice (in mm weq d^{-1} $°C^{-1}$) from selected 'Arctic' and 'High Arctic' locations around the world (cf. Fig. 6.3). See Braithwaite and Zhang (2000) and Hock (2003) for more comprehensive global degree-day factor compilations.

#	DDF (snow)	DDF (ice)	DDF (spi)	Location	Reference
1	3.0	7.0		Greenland Ice Sheet	Reeh (1991)
2	3.0	8.0	8.0	Greenland Ice Sheet	Huybrechts *et al.* (1991) Zweck and Huybrechts (2005)
3	3.0	8.0		Sth. Greenland Ice Sheet	Lefebre *et al.* (2002)
4	2.8	7.3		Greenland	Johannesson *et al.* (1995)
5	2.5	7.2		Nordboglacier (Greenland)	Braithwaite and Olesen (1988)
6		6.3±1.0		Arctic Canada	Braithwaite (1981)
7	2.5±0.5			JEG 1996(Arctic Canada)	Arendt (1997)
8		5.5		JEG 1996(Arctic Canada)	Arendt and Sharp (1999)
9	3.0	7.0		JEG 2002 (Arctic Canada)	Boon (2004)
10	2.8±1.0			Larsen Ice Shelf	Shepherd *et al.* (2003)
11	2.7	7.2		Greenland Ice Sheet	Janssens & Huybrechts (2000)
	2.8±0.2	7.0±0.8		'High Arctic' Locations	Cold and Dry
12	4.4	6.4		Nigardsbreen (Norway)	Johannesson *et al.* (1995)
13	4.4	6.3		Storglaciären (Sweden)	Hock (1999)
14	4±0.5	5.75±0.25		Three glaciers (Norway)	Laumann and Reeh (1993)
15	5.6	7.7		Satujökull (Iceland)	Johannesson *et al.* (1995)
16	~4.0			'Maritime' Arctic climates	Harding (1986)
17	5.7			Labrador (humid, windy)	Essery and Etchevers (2004)
	4.7±0.8	6.5±0.8		'Low Arctic' Locations	Warmer and Wetter
	3.6±1.1	6.9±0.8		All Arctic Locations	

Notes

- The first half of the table represents 'true' High Arctic locations, characterized by cold and dry climatic conditions. The second half represents more moderate, maritime Arctic locations with a relatively warmer and wetter climate.
- JEG: John Evans Glacier
- Mair *et al.* (2005) recently reported tuned degree-day factors for the Devon Ice Cap of 3.5 to 4 mm weq d^{-1} $°C^{-1}$ for the DDF (snow) and 6/14 mm weq d^{-1} $°C^{-1}$ for the DDF (ice).
- Braithwaite *et al.* (2002) determined almost identical 'mean' values: DDF (snow) = 3.8±0.9 mm weq d^{-1} $°C^{-1}$; DDF (ice) = 6.7±0.9 mm weq d^{-1} $°C^{-1}$.

Table 6.2 Snow densities measured on Murray Ice Cap (MIC), Simmons Ice Cap (SIC), St. Patrick Bay ice cap NE (STPBIC_NE), and on the Ward Hunt Ice Rise (WHIR) and Ice Shelf (WHIS) and associated DDF (snow) (in mm weq d^{-1} deg^{-1}) values based on Equations 6.5 and 6.7 (Martinec, 1976; Kuunisto, 1980).

Location/Year	Type of Snow	Snow Density	Martinec (1976)	Kuunisto (1980; 'open')
MIC (1999)	Winter snow accumulation	0.294	3.23	3.37
MIC (2000)	Winter snow accumulation	0.313	3.44	3.74
MIC (2001)	Winter snow accumulation	0.273	3.00	2.96
SIC (1976)[1]	Winter snow accumulation	0.300	3.30	3.49
SIC (2000)	Winter snow accumulation	0.266	2.93	2.82
SIC (2001)	Winter snow accumulation	0.256	2.82	2.63
STPBIC_NE[2]	Winter snow accumulation	0.300	3.30	3.49
WHIR[3]	Winter snow accumulation	0.350	3.85	4.47
WHIS[3]	Winter snow accumulation	0.310	3.41	3.69

Notes

1. Bradley and England (1977)
2. Hattersley-Smith and Serson (1972)
3. Braun *et al.* (2004b)

- See Tables 6.21 to 6.23 for Murray Ice Cap snow densities.

Table 6.3 The importance of superimposed ice formation for snowmelt and glacier mass balance: A simple example and calculation for a glacier and ice-free tundra surface.

	SWE	SPI	Total_accu	MDD_needed
Glacier surface	150	90	240	65
Tundra surface	150	0	150	50

Notes

- SWE: Water equivalent of the winter snow accumulation (mm weq) on the glacier or tundra.
- SPI: Amount of superimposed ice formation (mm weq), assuming a P-max of 0.6 (cf. Table 6.4).
- Total_accu: Total mass accumulation (= SWE + SPI) on the glacier or tundra surface.
- MDD_needed: MDD needed to melt the total mass accumulation. (assuming a DDF (snow) = 3 mm weq d^{-1} deg^{-1} and a DDF (ice) = 6 mm weq d^{-1} deg^{-1}; cf. Section 6.3.2.1)

Table 6.4 Values for P-max reported by other relevant Arctic glacier mass balance studies or calculated from data reported therein.

#	P-max	Location
1	0.60	Greenland Ice Sheet
2	0.44	Storstrømmen, Northeast Greenland
3	0.58	West Greenland, White Glacier, Devon Ice Cap
4	0.67	Quviagivaa Glacier, Ellesmere Island
5	0.47	John Evans Glacier, Ellesmere Island (1996)
6	0.60	John Evans Glacier, Ellesmere Island (2002)
7	0.1 to 0.3	Glaciers on Svalbard
8	0.16 to 0.25	Midtre Løvenbreen, Svalbard (1999 and 2000)
9	0.50	McCall Glacier, Alaska
10	0.35	Kongsvegen, Svalbard
11	0.38	Barnes Ice Cap (1976)
12	0.39	Storöyjökulen, Svalbard
13	0.26	Penny Ice Cap (1953)
14	0.49	Barnes Ice Cap (1950)
15	0.41	Ward Hunt Ice Rise and Ice Shelf (1959)
16	0.57	Ward Hunt Ice Rise and Ice Shelf (1960)
17	0.38	Ward Hunt Ice Shelf (1960)
18	0.4 to 0.6	Greenland Ice Sheet
19	0.3	Greenland Ice Sheet 'optimized'
20	0.4	Penny Ice Cap
21	0.66	Greenland Ice Sheet
22	0.37	Midtre Løvenbreen, Svalbard (last 30 years)
Mean	0.44±0.14	(all 22 values)

Continued next page

Table 6.4 continued: Notes

1. Value used for superimposed ice parameterization for the entire Greenland Ice Sheet (Reeh, 1991; Huybrechts *et al.*, 1991).
2. Bøggild *et al.* (1994).
3. Value originally determined from field measurements in West Greenland (Braithwaite *et al.*, 1994) and subsequently applied to the White Glacier and Devon Ice Cap (Braithwaite and Zhang, 1999).
4. Wolfe (1995).
5. Value calculated using an energy-balance model (Arendt, 1997).
6. Value used by Boon (2005).
7. Range of values determined from long-term glacier mass balance measurements on two glaciers on Svalbard (Hagen and Liestol, 1990).
8. Range of values measured in-situ by Wadham and Nuttall (2002) in 1999 and 2002.
9. Wakahama *et al.* (1976).
10. Obleitner and Lehning (2004).
11. Value calculated from data reported by Hooke *et al.* (1987).
12. Value calculated from data reported by Jonsson (1982).
13. Calculated from data reported by Ward and Baird (1954), assuming a superimposed ice density of 0.9 (cf. Table 6.6).
14. Calculated from data reported by Baird *et al.* (1952), assuming a superimposed ice density of 0.9 (cf. Table 6.6).
15. Value calculated from data reported by Sagar (1962).
16. Value calculated from data reported by Sagar (1962). Note the winter snow accumulation in 1960 was considerably greater than in 1959.
17. Value calculated from data reported by Lister (1962) for a different section of the ice shelf with less winter snow accumulation (~170 mm weq; similar to Sagar's 1959 SWE values (Sagar, 1962)).
18. Janssens and Huybrechts (2000). A P-max of 0.4 was used at low-elevations in southern Greenland, where up to 1/3 of the annual precipitation was rainfall.
19. Janssens and Huybrechts (2000); 'optimized' P-max value (i.e. tuned to fit mass balance data).
20. Value reported by Fisher *et al.* (1998).
21. Value reported by Ambach (1985).
22. Wright *et al.* (in press), modeled value based on a snowpack energy-balance model, parameterized using 30 years of climate data and corresponding glacier mass balance measurements.

Table 6.5 Superimposed ice thickness (SPI, in cm ice thickness) calculated using the Woodward *et al.* (1997) parameterization (Equation 6.8) based on mean annual temperature measurements (MAT, °C) at different locations on northern Ellesmere Island.

Location	MAT (°C)	SPI (cm)	Comment
Murray Ice Cap (~1100 m asl)	–16.4	11.3	AWS G3, Sept. 1999 to August 2000
Murray Ice Cap (~1100 m asl)	–17.0	11.7	1951 to 2000 climatology[3]
Ward Hunt Island (~0 m asl)	–19.9	13.7	1951 to 2000 climatology[4]
Gilman Glacier (~1040 m asl)	–18.4	12.7	10 m borehole ice temperature[1]
Agassiz Ice Cap (~1700 m asl)	–22.0	15.2	10 m borehole ice temperature[2]
Mt. Oxford (~1805 m asl)	–24.2	16.7	10 m borehole ice temperature[1]

Notes

1. Hattersley-Smith (1960c)
2. Fisher and Koerner (1994)
3. 1951 to 2000 climatology for AWS G3 (cf. Chapter 5), January to December.
4. 1951 to 2000 climatology for WHIRWHIS (cf. Chapter 5), January to December.

Table 6.6 Superimposed ice densities: Values previously used or reported in the scientific literature.

SPI density	Reference
0.7 to 0.8	Østrem and Brugman (1991)
0.8 to 0.9	Koerner (1970)
0.82 to 0.87	Hattersley-Smith (1963)
0.88	Wolfe and English (1995)
0.89	Braithwaite *et al.* (1994)
0.9	Jonsson (1982)
0.9	Bøggild *et al.* (1994)
0.9	Ward and Orvig (1953)
0.9	Sagar (1966)
0.9	Wakahama *et al.* (1976)
0.9	Ambach (1985)
0.9	Wadham and Nuttall (2002)
0.87±0.04	Fujita *et al.* (1996)
0.85	Schytt (1949)

Notes

- Koerner (1970) described two different characteristic 'modes' of superimposed ice formation on the Devon Ice Cap. Rapid refreezing and incomplete saturation of the snow pack (typical for superimposed ice formation during the very early melt season) will give superimposed ice densities between 0.8 and 0.86. Complete saturation of the snow pack, slush formation, and ponded meltwater on the ice surface will yield superimposed ice densities of about 0.9. Hattersley-Smith (1963) and Pohjola *et al.* (2005) described similar melt processes and resultant superimposed ice densities on glaciers and ice caps on northern Ellesmere Island and northern Sweden. Both superimposed ice formation processes were observed on Murray and Simmons Ice Cap between 1999 and 2001, hence 0.9 was chosen as superimposed ice density in this study.

Table 6.7 Snow densities measured on Murray Ice Cap (MIC), Simmons Ice Cap (SIC), St. Patrick Bay ice cap NE (STPBIC_NE), and on the Ward Hunt Ice Rise (WHIR) and Ice Shelf (WHIS) and the associated P-max value using the Braithwaite *et al.* (1994) parameterization (Equation 6.10).

Location/Year	Type of Snow	Snow Density	P-max (Braithwaite *et al.*, 1994)
MIC (1999)	Winter snow accumulation	0.294	0.67
MIC (2000)	Winter snow accumulation	0.313	0.65
MIC (2001)	Winter snow accumulation	0.273	0.70
SIC (1976)[1]	Winter snow accumulation	0.300	0.67
SIC (2000)	Winter snow accumulation	0.266	0.70
SIC (2001)	Winter snow accumulation	0.256	0.72
STPBIC_NE[2]	Winter snow accumulation	0.300	0.67
WHIR[3]	Winter snow accumulation	0.350	0.61
WHIS[3]	Winter snow accumulation	0.310	0.66

Notes

1. Bradley and England (1977)
2. Hattersley-Smith and Serson (1972)
3. Braun *et al.* (2004b)

• See Tables 6.21 to 6.23 for Murray Ice Cap snow densities

Table 6.8 Fall/winter/spring, summer, and annual precipitation/snow/rain at Alert and Eureka (1952 to 2001 averages; cf. Chapter 5), using the corrected monthly Canadian precipitation data set (cf. Mekis and Hogg, 1999).

Alert (1952 to 2001, in mm weq and percent)

Fall/Winter/Spring			Summer			Annual		
Precip	Snow	Rain	Precip	Snow	Rain	Precip	Snow	Rain
142.6	141.8	0.8	75.7	52.5	23.2	218.3	194.3	24.0
65%	73%	3%	35%	27%	97%	100%	100%	100%

Eureka (1952 to 2001, in mm weq and percent, 1991 missing)

Fall/Winter/Spring			Summer			Annual		
Precip	Snow	Rain	Precip	Snow	Rain	Precip	Snow	Rain
67.5	66.5	1.0	42.9	11.1	31.8	110.4	77.6	32.8
61%	86%	3%	39%	14%	97%	100%	100%	100%

Table 6.9 Modern climatology of the North Coast and Hazen Plateau (1951 to 2000 reference period). Details of the respective climatologies are available in Chapter 5.

	JJA T (°C)	July T (°C)	Annual MDD	July MDD	Snowfall (mm weq)
WHI AWS*	–0.55	1.00	74	47	160
WHIRWHIS*	–1.51	–0.36	39	23	160
AWS T3*	–0.32	2.18	165	95	125
AWS G3*	–1.29	1.15	116	71	125

Notes

- JJA T = June/July/August mean temperature.
- July T = July mean temperature.
- MDD = melting degree-days.

Table 6.10 Quantitative estimates of Holocene climate variability from the Canadian High Arctic.

Time period	'Change' in summer air temperature	Reference/Source
Early Holocene (8 to 10 kyr BP)	+2.5°C +2 to 2.5°C +1.5 to 3.5°C	Hattersley-Smith (1969) Fisher *et al.* (1995) Koerner and Fisher (2002)
'Little Ice Age' (~1400 to 1900)	–1.5 to –2.5°C –1.0 to –3.0°C –1.5°C	Koerner (1989a) Dowdeswell (1995) Dowdeswell *et al.* (1997) Dowdeswell and Hagen (2003) Williams (1978a) Kerwin *et al.* (2004) Alt (1987)
Early 20th century (~1925 to 1960)	+1 to 2°C	Hattersley-Smith (1963) Hattersley-Smith (1969)

Notes

- 'Change' refers to summer air temperature differences from 'current' climatic conditions, although the precise meaning of 'current' is usually not explicitly defined in the literature sources. The warmer conditions from 1925 to 1961 were presumably expressed relative to the average temperatures of the 1960s as a whole (Hattersley-Smith, 1963, 1969). Bengtsson *et al.* (2004) noted that present warming in the Arctic has just now reached the peak warming values of the 1940s (cf. Davies and Krinsley, 1962; Warren, 1990). Bradley *et al.* (2003) noted that the magnitude of the early 20th century warmth appears to have been greatest in records from northern Greenland and the northern parts of the Canadian High Arctic.
- Bradley *et al.* (2003) define the 'Little Ice Age' between about 1250 and 1900, with its main phase occurring after about 1550.
- It is also worth emphasizing that even the main phase of the 'Little Ice Age' was not a uniformly cold period, but also included a period of relative warmth in the 1700s (Fisher *et al.*, 1998; Bradley *et al.*, 2003; Gajewski and Atkinson, 2003). Koerner and Lundgaard (1995; their Fig. 6) showed considerable multi-decadal summer melt variability on the Agassiz and Devon Ice Caps, with a pronounced melt maxima occurring over the second half of the 16th century.

Table 6.11 5-GCM composite mean monthly air temperature data (January 1980 to December 2099; n = 1440 months or 120 years) from ACIA (2004) (http://igloo.atmos.uiuc.edu/ACIA/index.html) (cf. Kattsov *et al.*, 2005). Values were extracted from the global gridded data set for the 2.5 by 2.5° grid box centered at 82.5°N and 70°W ('Hazen Plateau grid box').

Month	1980 to 1999 mean (°C)	2080 to 2099 mean (°C)	Change (°C)	Trend (°C/year)	P-value
January	−38.54	−33.28	+5.26	0.0525	<0.0001
February	−39.13	−34.13	+5.00	0.0505	<0.0001
March	−36.89	−32.27	+4.62	0.0481	<0.0001
April	−26.41	−22.59	+3.82	0.0411	<0.0001
May	−10.51	−7.16	+3.35	0.0347	<0.0001
June	−1.35	−0.29	+1.06	0.0105	<0.0001
July	0.55	3.36	+2.81	0.0278	<0.0001
August	−0.26	2.39	+2.65	0.0268	<0.0001
September	−10.33	−6.89	+3.44	0.0309	<0.0001
October	−22.73	−16.77	+5.96	0.0638	<0.0001
November	−31.42	−25.92	+5.50	0.0570	<0.0001
December	−36.29	−31.13	+5.16	0.0550	<0.0001
Spring (MAM)	−24.60	−20.67	+3.93	0.0413	<0.0001
Summer (JJA)	−0.35	1.82	+2.17	0.0217	<0.0001
Fall (SON)	−21.49	−16.53	+4.96	0.0505	<0.0001
Winter (DJF)	−37.99	−32.87	+5.12	0.0529	<0.0001
Annual (MAT)	−21.11	−17.06	+4.05	0.0415	<0.0001

Notes

- Trend = simple linear trend calculated for the entire 120 year data set (cf. Fig. 6.11).
- Winter = December (of the previous year), January, and February; the seasonal mean for Winter 1980 is thus not defined.

Table 6.12 Degree-day factors for snow (mm weq d^{-1} deg^{-1}) determined for the North Coast of Ellesmere Island (cf. Fig. 6.14).

Method	DDF (snow)	Comment
Measurements (1959)	~5	After Lotz (1961a, b)
Literature	4.7±0.8	'maritime' Arctic (Table 6.1)
Kuunisto (1980) 'open'	4.1±0.8	Using Equation 6.7
'Mean'	~4.6±0.8	

Notes

- Using a mean snow density of 0.330±0.043, which is the mean of all reported snow densities for the Ward Hunt Ice Rise and Ice Shelf combined, Equation 6.7 predicts a DDF (snow) of 4.1±0.8 mm weq d^{-1} deg^{-1}.
- Using a mean snow density of 0.346±0.047, which is the mean of all reported snow densities for the Ward Hunt Ice Rise, Equation 6.7 predicts a DDF (snow) of 4.4±0.9 mm weq d^{-1} deg^{-1}.
- Using a mean snow density of 0.306±0.023, which is the mean of all reported snow densities for the Ward Hunt Ice Shelf, Equation 6.7 predicts a DDF (snow) of 3.6±0.4 mm weq d^{-1} deg^{-1}.

Table 6.13 Appropriate P-max values for the Ward Hunt Ice Rise and Ice Shelf, compiled using simple empirical parameterizations (cf. Section 6.3.3.3), values from the scientific literature (cf. Section 6.3.3.2), and the limited available in-situ superimposed ice measurements (cf. Section 6.3.3.5). Superimposed ice density was assumed at 0.9 (cf. Table 6.6).

Method	P-max	Comment
Woodward *et al.* (1997)	0.77±0.03	1
Braithwaite *et al.* (1994)	0.63±0.05	2
Janssens and Huybrechts (2000)	0.37 (range ~0.29 to 0.52)	3
Literature values	0.45±0.13	4
Measurements (1960)	0.57	5
Measurements (1959 and 1960)	0.40	6
'Mean'	~0.40±0.13	

Notes

1. Using MAT of −19.8±0.81°C (WHIRWHIS* climatology, 1951 to 2002 mean and associated standard deviation).
2. Using a snow density of 0.330±0.043 (Braun *et al.*, 2004b) and a corresponding superimposed ice density of 0.9.
3. See Figure 6.15 for P-max ranges (indicated by the grey shading), depending both on MAT (−19.8±0.81°C) and annual precipitation (160±40 mm weq).
4. See Table 6.4.
5. P-max for 'above-average' amounts of winter snow accumulation (cf. Section 6.3.3.5).
6. P-max for 'normal' amounts of winter snow accumulation (cf. Section 6.3.3.5).

Table 6.14 Model parameter calibration (1966 to 1985; n = 20 years) and confirmation (1959 to 1965; n = 7 years) for the Ward Hunt Ice Rise (WHIR), Ward Hunt Ice Shelf (WHIS), and the combined mass balance record ('combo'). DDF (snow) and DDF (ice) in mm weq d^{-1} deg^{-1}.

	Calibrated melt model parameters			Calibration period		Confirmation period	
	P-max	DDF (snow)	DDF (ice)	1966/85 model[1]	1966/85 meas.[1]	1959/65 model[2]	1959/65 meas.[2]
WHIR	0.23	5.5	7.5	–343	–340	–375	–331
WHIS	0.33	6.0	12.0	–1276	–1284	–859	–818
'combo'	0.28	6.0	9.0	–813	–812	–574	–593

Notes
1. Cumulative annual mass balance (mm weq) between 1966 and 1985.
2. Cumulative annual mass balance (mm weq) between 1959 and 1965.

Table 6.15 Model parameter calibration (1959 to 1985; n = 27 years) for the Ward Hunt Ice Rise (WHIR), Ward Hunt Ice Shelf (WHIS), and the combined mass balance record ('combo'). DDF (snow) and DDF (ice) in mm weq d^{-1} deg^{-1}.

	Calibrated melt model parameters			Calibration period	
	P-max	DDF (snow)	DDF (ice)	1959/85 model[1]	1959/85 meas.[1]
WHIR	0.24	5.5	7.5	–674	–671
WHIS	0.34	6.0	12.0	–2091	–2102
'combo'	0.28	6.0	9.0	–1405	–1386

Notes
1. Cumulative annual mass balance (mm weq) between 1959 and 1985.

Table 6.16 Temperature and precipitation sensitivity (mm weq/year) of the Ward Hunt Ice Rise (WHIR) and Ward Hunt Ice Shelf (WHIS) for the 1951 to 2000 reference period (n = 50 years).

Parameter	Forcing	WHIR	WHIS
Temperature Sensitivity			
+2°C climatology	118 MDD	–626	–1038
+1°C climatology	71.2 MDD	–277	–480
Modern climatology	39.3 MDD	–42	–104
–1°C climatology	19.5 MDD	+90	+92
–2°C climatology	8.2 MDD	+146	+151
Precipitation Sensitivity			
+20 percent precipitation	192 mm weq	+6	–38
+10 percent precipitation	176 mm weq	–18	–71
Modern precipitation	160 mm weq	–42	–104
–10 percent precipitation	144 mm weq	–66	–128
–20 percent precipitation	128 mm weq	–90	–173
Temperature and Precipitation Sensitivity			
+2°C and +20 percent		–575	–963
+1°C and +10 percent		–252	–442
Modern climatology		–42	–104
–1°C and –10 percent		+70	+67
–2°C and –20 percent		+110	+114

Notes

- ±1/2°C temperature and ±10/20 percent precipitation sensitivities calculated after Oerlemans (2001).

Table 6.17 Climatic conditions 'today' (i.e. 1951 to 2000) and during the so-called 'Little Ice Age'' (e.g. 1801 to 1850) on the ice-free Ward Hunt Island (top) and on the Ward Hunt Ice Rise and Ice Shelf (which incorporates the ice-cap cooling effect) (bottom).

WHIAWS* climatology

	'Modern' Conditions		'Little Ice Age' Conditions Minimum Climatology	
	Mean T (1951 to 2000)	Tot. MDD (1951 to 2000)	Mean T (1801 to 1850)	Tot. MDD (1801 to 1850)
May	–12.19°C	0.0	–13.69°C	0.0
June	–1.89°C	9.2	–3.39°C	2.5
July	1.00°C	46.6	–0.50°C	21.5
August	–0.77°C	18.7	–2.27°C	6.8
September	–10.03°C	0.0	–11.53°C	0.0
JJA	–0.55°C	74.4	–2.05°C	30.7

WHIRWHIS* climatology

	'Modern' Conditions		'Little Ice Age' Conditions Maximum Climatology	
	Mean T (1951 to 2000)	Tot. MDD (1951 to 2000)	Mean T (1801 to 1850)	Tot. MDD (1801 to 1850)
May	–12.19°C	0.0	–13.64°C	0.0
June	–2.63°C	5.0	–4.13°C	1.1
July	–0.36°C	23.1	–1.86°C	8.7
August	–1.55°C	11.2	–3.05°C	3.3
September	–10.03°C	0.0	–11.53°C	0.0
JJA	–1.51°C	39.3	–3.01°C	13.1

Notes

- This assumes that the 'Little Ice Age' (e.g. 1801 to 1850) temperature conditions can be approximated by subtracting 1.5°C from each monthly air temperature between 1951 and 2000.
- Monthly melting degree-day totals calculated from the monthly climatology using the Braithwaite (1984) model, assuming a σ value of 2.2°C (cf. Chapter 5).

Table 6.18 Comparison between the Hazen Plateau (Ellesmere Island) and the interior Baffin Island plateau today and during the 'Little Ice Age' (LIA).

	Hazen Plateau	Baffin Plateau	Comment
Glaciation Level: Today	> 1000 m asl	> 1000 m asl	'very similar' (Miller *et al.*, 1975)
Glaciation Level: LIA	???	~600 m asl	Andrews *et al.* (1976)
Summer Temp.: Today	~similar		
Summer Temp.: LIA	~1 to 3°C colder		cf. Table 6.10
Annual Snowfall: Today	~125 mm weq	~430 mm weq	See below and Chapter 5
Annual Snowfall: LIA	???	???	Not significantly different from today (Fisher *et al.*, 1995)

Notes

Precipitation on the interior Baffin Island plateau:

- 442 mm weq (Barnes Ice Cap winter balance, 1975 to 1982, n = 6 yrs, Hooke *et al.*, 1987).
- 510 mm weq (Barnes Ice Cap annual accumulation at 750 m asl in 1950; Ward, 1954).
- 437 mm weq (Penny Ice Cap winter snow accumulation, 1952/53, mean between ~400 and 2000 m asl, Orvig, 1954).
- 420 mm weq annual snowfall (Bromwich *et al.*, 2002).
- 430 mm weq (Annual net accumulation, Penney Ice Cap, 1949 to 1979, Holdsworth, 1984)
- Similar values have been reported by Løken and Andrews (1966), Sagar (1966), Loewe (1971), and Jacobs *et al.* (1993).

Table 6.19 Summary of mass accumulation measurements (winter snow accumulation and superimposed ice) on the summit plateau of Murray Ice Cap in 1999.

Winter snow accumulation	Depth	~40 cm
(late May 1999)	Density	~0.230
	SWE	~92 mm weq
Winter snow accumulation	Depth	45.9±5.2 cm
(30 June 1999)	Density	0.294
	SWE	135±15 mm weq
Superimposed ice formation	Thickness	7.4±1.6 cm
(9 July 1999)	Density	0.9
	SWE	67±15 mm weq
	P-max	0.50±0.11

Notes

- The 30 June 1999 winter snow accumulation measurements represent the mean of two short transects conducted in the vicinity of AWS G3.
- The 9 July 1999 superimposed ice formation measurement represents the mean of the eight ablation stakes located on the summit plateau of Murray Ice Cap (M1 to M8).

Table 6.20 Summary of mass accumulation measurements (winter snow, summer snow, and superimposed ice) on the summit plateau of Murray Ice Cap in 2000.

Winter snow accumulation	Depth	26.8±8.2 cm
(14 June 2000)	Density	0.313±0.1
	SWE	84±26 mm weq
Superimposed ice formation	Thickness	5.5±0.6 cm
(25 June 2000)	Density	0.9
	SWE	50±5 mm weq
	P-max	0.59±0.07
Summer snow accumulation	Depth	27.3 cm
(23 July 2000)	Density	0.328
	SWE	90 mm weq
Summer snow accumulation	Depth	28.7 cm
(24 July 2000)	Density	0.328
	SWE	94 mm weq

Notes

- The 14 June 2000 winter snow accumulation represents the mean of measurements at ablation stakes M1 to M8 on the summit plateau of the ice cap. The snow density value represents the mean of 11 actual measurements, some including the 'Dole-Layer', some limited to only the 'Dole-Layer', and some not including the 'Dole-Layer'.
- The 25 June 2000 superimposed ice formation measurements represents the mean of the eight ablation stakes located on the summit plateau of Murray Ice Cap (M1 to M8).
- The 23 July 2000 measurement of summer snow accumulation measurement represents the mean of a long transect across the summit plateau of the ice cap.
- The 24 July 2000 measurement of summer snow accumulation represents the mean of the measurements at ablation stakes M1 to M8 on the summit plateau of the ice cap.

Table 6.21 Summary of mass accumulation measurements (winter snow, summer snow, and superimposed ice) on Murray Ice Cap in 2001.

Type of mass accumulation and date	Location	Depth (cm)	Density	SWE (mm weq)
Winter snow accumulation				
10 June 2001	summit plateau	19.9±7.1	0.277	55±20
11 June 2001	summit plateau	19.0±3.7	0.273	52±13
12 June 2001	summit plateau	19.0±6.1	0.273	52±17
	'Mean' 10-12 June			53±17
11 June 2001	Murray Ice Cap			86±45
Summer snow accumulation				
13 July 2001	summit plateau	14.9±5.4	0.292	44±16
13 July 2001	Murray Ice Cap			39±17
Superimposed ice formation				
18/19 June 2001	summit plateau	P-max	0.54±0.27	
18/19 June 2001	Murray Ice Cap	P-max	0.62±0.21	

Notes

- The 10 June 2001 winter snow accumulation measurement represents the mean of a long transect across the summit plateau of the ice cap.
- The 11 June 2001 winter snow accumulation measurement represents the mean of the measurements at ablation stakes M1 to M8 on the summit plateau of the ice cap.
- The 12 June 2001 winter snow accumulation measurement represents the mean of a shorter transect in the vicinity of AWS G3.
- The 11 June 2001 winter snow accumulation measurement for the entire ice cap represents the simple mean of the measurements at the 29 ablation stakes across the ice cap.
- The 13 July 2001 measurements of the summer snow accumulation represent the respective simple means of the measurements at the eight summit plateau ablation stakes (M1 to M8) and at the 29 ablation stakes across the ice cap.

Table 6.22 The degree-day factor of snow (DDF(snow)) for the unglaciated Hazen Plateau (1999 to 2001), measured at AWS T3.

Snow Accumulation (prior to snowmelt)	Snowmelt Period	DDF (snow)
24 June 1999 Snow depth = 31 cm Snow density = 0.295 SWE = 91 mm weq	~24 June to ~8 July 1999 31 MDD	1999 winter snow accumulation 2.9 mm weq/MDD
17 June 2000 Snow depth = 19 cm Snow density = 0.289 SWE = 55 mm weq	~17 June to ~20 June 2000 27 MDD	2000 winter snow accumulation 2.0 mm weq/MDD
12 June 2001 Snow depth = 17 cm Snow density = 0.348 SWE = 59 mm weq	~June 12 to ~June 19 2001 23 MDD	2001 winter snow accumulation 2.6 mm weq/MDD

Notes

- Snow depth on 24 June 1999 was determined as the difference between the SR50 measurements at AWS T3 on 24 June (1.996 m) and 13 July (2.3055 m). Snow density is based on snow pit measurements on Murray Ice Cap (cf. Chapter 6). Finally, AWS T3 was not actually operational between 24 June and 12 July 1999, hence the melting degree-days were determined using the patched AWS T3 record (cf. Chapter 5). Based on photographs and field notes, the Hazen Plateau in vicinity of AWS T3 became snow-free by about 8 July 1999.
- Snow depth and density for 17 June 2000 are based on a long snow depth transect near AWS T3. Based on photographs, field notes, and AWS T3 data, the Hazen Plateau in vicinity of AWS T3 became snow-free by about 20 June 2000.
- Snow depth and density for 12 June 2001 are based on a short snow depth transect near AWS T3. Based on photographs, field notes, and AWS T3 data, the Hazen Plateau in vicinity of AWS T3 became snow-free by about 19 June 2001.

Table 6.23 The 'mean' annual air temperature climatology for the Hazen Plateau.

Month	AWS T3* (°C)	AWS T3* MDD	AWS G3* (°C)	AWS G3* MDD	ΔT (°C)	ΔT (°C) 'lapsed'	ΔMDD	ΔMDD 'lapsed'
Jan	–28.14	0.0	–28.40	0.0	0.26	–0.16	0.0	0.0
Feb	–28.96	0.0	–29.20	0.0	0.24	–0.18	0.0	0.0
Mar	–28.10	0.0	–28.36	0.0	0.26	–0.15	0.0	0.0
Apr	–21.81	0.0	–22.23	0.0	0.42	0.01	0.0	0.0
May	–12.70	0.0	–13.35	0.0	0.65	0.24	0.0	0.0
June	–2.78	18.0	–3.69	9.0	0.91	0.49	9.0	6.0
July	2.18	89.9	1.15	68.2	1.03	0.62	21.7	15.5
Aug	–0.55	40.3	–1.51	24.8	0.96	0.55	15.5	10.3
Sept	–9.26	0.0	–10.00	0.0	0.74	0.33	0.0	0.0
Oct	–18.07	0.0	–18.59	0.0	0.51	0.10	0.0	0.0
Nov	–23.29	0.0	–23.67	0.0	0.38	–0.03	0.0	0.0
Dec	–26.87	0.0	–27.16	0.0	0.29	–0.12	0.0	0.0
Mean	–16.53	NA	–17.08	NA	0.55	0.14	NA	NA
Total	NA	148.2 (100%)	NA	102.0 (68.8%)	NA		46.2 (31.2%)	31.8 (21.5%)

Notes

- AWS T3* (1951 to 2000) mean annual air temperature cycle, using monthly means based on 50 years of data (elevation 1025 m asl). (cf. Chapter 5)
- AWS T3* monthly melting degree-day totals calculated using the Braithwaite model and assuming a σ value of 4.0°C. (cf. Chapter 5)
- AWS G3* (1951 to 2000) mean annual air temperature cycle, using monthly means based on 50 years of data (elevation 1100 m asl). (cf. Chapter 5)
- AWS G3* monthly melting degree-day totals calculated using the Braithwaite model and assuming a σ value of 3.7°C. (cf. Chapter 5)
- 'Lapsed': adjusted AWS T3* and AWS G3* to the same elevation, assuming a lapse rate of 5.5°C/1000 m and an elevation difference of 75 m.
- The inter-annual variability climatologies are defined by the AWS T3* 50-year monthly time series (1025 m asl; 1951 to 2000) and the AWS G3* 50-year monthly time series (1100 m asl; 1951 to 2000). Missing monthly values were replaced with the means shown above.

Table 6.24 The degree-day factor for snow (mm weq d^{-1} deg^{-1}): reasonable limits for the snowmelt and mass balance model.

Location/Source	DDF (snow)	Comment
'High Arctic'	2.8±0.2	Table 6.1
Kuunisto 'open'	3.4±0.6	cf. Section 6.3.2.2
Martinec	3.2±0.4	cf. Section 6.3.2.2
AWS T3	2.5±0.4	Table 6.22
Murray Ice Cap	3.5±1.2	cf. Section 6.5.2
Mean (all)	3.1±0.4	

Notes

- The two empirical parameterizations (Kuunisto 'open' and Martinec; cf. Section 6.3.2.2) used the mean of the snow density measurements listed in Tables 6.21 to 6.24 (0.294±0.032).
- The value listed for Murray Ice Cap is the simple mean of the five DDF (snow) values discussed in Section 6.5.2.

Table 6.25 The degree-day factor for ice (mm weq d^{-1} deg^{-1}): reasonable limits for the snowmelt and mass balance model.

Location/Source	DDF (snow)	Comment
'High Arctic'	7.0±0.8	Table 6.1
MIC 1999	8.7	dirty ice (terminus)
MIC 1999	5.9	clean ice (summit plateau)
MIC 2000	5.78	area/elevation-weighted mean
MIC 2001	5.77	area/elevation-weighted mean
Murray Ice Cap	6.5±1.4	Mean of above
Mean	6.8±0.4	Murray Ice Cap and 'High Arctic'

Notes

- The MIC 1999 DDF (ice) value for dirty ice on the terminus is the mean of the two values discussed in Section 6.5.2.1.

Table 6.26 Superimposed ice formation (i.e. P-max): reasonable limits for the snowmelt and mass balance model.

Location/Source	P-max	Comment
Scientific literature	0.44±0.14	Table 6.4
Murray Ice Cap	0.56±0.05	Tables 6.21 to 6.23
Mean	0.50±0.08	

Table 6.27 Model tests on the Simmons Ice Cap. 2000: 6 June to 9 August; 2001: 27 May to 1 August, i.e. including snowmelt, superimposed ice formation/melt, glacier ice melt, and summer snow accumulation.

SIC (2000)	#1	#2	#3	#4	#5	#6
SWE	125	125	125	125	167	200
DDF(snow)	2.8	3.1	2.2	3.1	3.1	3.1
DDF(ice)	7.0	6.8	6.8	5.5	6.8	6.8
P-max	0.44	0.50	0.50	0.50	0.50	0.50
b_n (model)	–507	–512	–400	–400	–400	–310
b_n (meas.)	–395	–395	–395	–395	–395	–395
SIC (2001)	#1	#2	#3	#4	#5	#6
SWE	125	125	125	125	105	140
DDF(snow)	2.8	3.1	3.8	3.1	3.1	3.1
DDF(ice)	7.0	6.8	6.8	7.5	6.8	6.8
P-max	0.44	0.50	0.50	0.50	0.50	0.50
b_n (model)	–461	–468	–518	–523	–522	–428
b_n (meas.)	–520	–520	–520	–520	–520	–520

Notes

Four different combinations of model parameter were chosen for this table:

- #1: Means of scientific literature (cf. Tables 6.26 to 6.28).
- #2: Preferred values for this study (cf. Tables 6.26 to 6.28).
- #3: 'Tuning' by adjusting the DDF (snow).
- #4: 'Tuning' by adjusting the DDF (ice).
- #5: 'Tuning' by adjusting the amount of snow accumulation (cf. Braithwaite *et al.*, 2002).
- #6: Best estimate for actual snow accumulation on Simmons Ice Cap. In 2000, winter snow accumulation on the Simmons Ice Cap was measured 16 June for a simple mean of 108±16 mm weq. Adding the amount of summer snow accumulation as measured on Murray Ice Cap 23/24 July 2000 (~92 mm weq; cf. Table 6.20) gives a total mass balance year snow accumulation of about 200 mm weq in 2000. Winter snow accumulation was measured on Simmons Ice Cap on 27 May 2001 for a simple mean of 103±17 mm weq. Adding the amount of summer snow accumulation measured on Murray Ice Cap on 13 July 2001 (39±17 mm weq) yields a total 'mass balance year' snow accumulation of about 140 mm weq.
- b_n: mean (i.e. area-elevation weighted) specific net mass balance of the Simmons Ice Cap in 2000 and 2001 (cf. Chapter 3).

Table 6.28 Model sensitivity tests for a 'middle-of-the-road' climate change scenario (–2°C, 250 mm weq, 50 years) for a range of different model parameter values.

Model Parameter	Area	Mean Thickness	Max. Thickness
DDF (snow)	±14%	±15%	±12%
DDF (ice)	±3%	±1%	±1%
P-max	±6%	±10%	±9%

Notes

- The DDF (snow) parameter was varied between 2.8 and 3.4 mm weq d^{-1} deg^{-1}. The percent uncertainty values are expressed relative to results using the preferred DDF (snow) value of 3.1 mm weq d^{-1} deg^{-1}.
- The DDF (ice) parameter was varied between 6.3 and 7.3 mm weq d^{-1} deg^{-1}. The percent uncertainty values are expressed relative to results using the preferred DDF (ice) value of 6.8 mm weq d^{-1} deg^{-1}.
- The P-max parameter was varied between 0.44 and 0.6. The percent uncertainty values are expressed relative to results using the preferred P-max value of 0.5.

Table 6.29 The climatic sensitivity of the model results and their sensitivity to changes in the model parameters (for a prescribed cooling of –2°C and an annual snow accumulation of 200 mm weq): Maximum ice thickness and ice area at the end of 500 years.

Scenario	Maximum ice thickness (m weq)	Area of ice cover (km^2)
different cooling same precipitation		
–1.5°C; 200 mm weq	11.2	37.8
–2.0°C; 200 mm weq	41.0	114.9
–2.5°C; 200 mm weq	61.1	174.8
same cooling different precipitation		
–2.0°C; 175 mm weq	16.4	54.0
–2.0°C; 200 mm weq	41.0	114.9
–2.0°C; 225 mm weq	62.8	156.1
–2°C; 200 mm weq different parameters		
'max. melt' parameters	22.3	62.6
'preferred' parameters	41.0	114.9
'min. melt' parameters	59.9	162.5

Notes

- The 'min. melt' model parameters: DDF (snow) = 2.8 mm weq d^{-1} deg^{-1}, DDF (ice) = 6.3 mm weq d^{-1} deg^{-1}, P-max = 0.60.
- The 'max. melt' model parameters: DDF (snow) = 3.4 mm weq d^{-1} deg^{-1}, DDF (ice) = 7.3 mm weq d^{-1} deg^{-1}, P-max = 0.44.
- The 'preferred' model parameters: DDF (snow) = 3.1 mm weq d^{-1} deg^{-1}, DDF (ice) = 6.8 mm weq d^{-1} deg^{-1}, P-max = 0.50.
- Data and parameters in \model_2\ (for the –2°C; 200 mm weq model parameter sensitivity test). Data and parameters in \model_4\ )for the different/same cooling/precipitation sensitivity test). Other model parameters as noted in Figure 6.35.

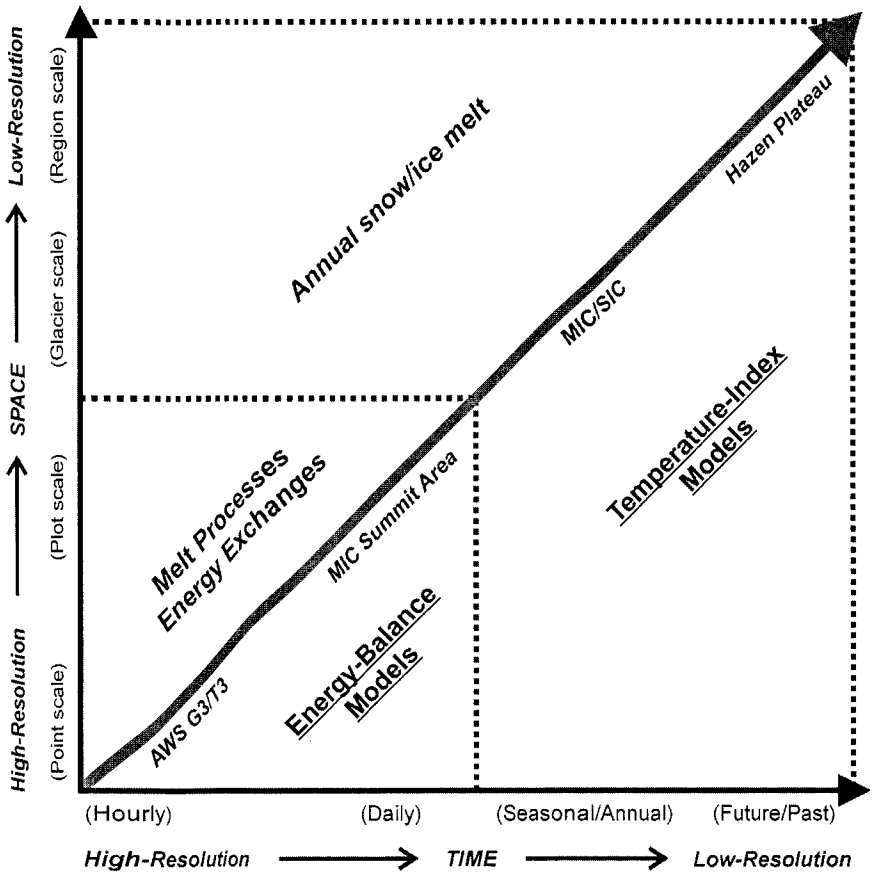

Figure 6.1 Schematic illustration of the spatial and temporal scales involved in energy-balance or temperature-index modeling. The basic argument is that the spatial and temporal scales associated with a specific objective or question should determine the appropriate snowmelt or glacier mass balance modeling technique. For example, it is inappropriate to use an energy-balance model to predict the extent of snow and ice cover changes on the Hazen Plateau during the so-called 'Little Ice Age' or under a future greenhouse warming scenario. On the other hand, a detailed quantification of the melt processes and the associated energy-exchanges at hourly to daily time scales on the summit plateau of Murray Ice Cap requires a more physically-based energy-balance model.

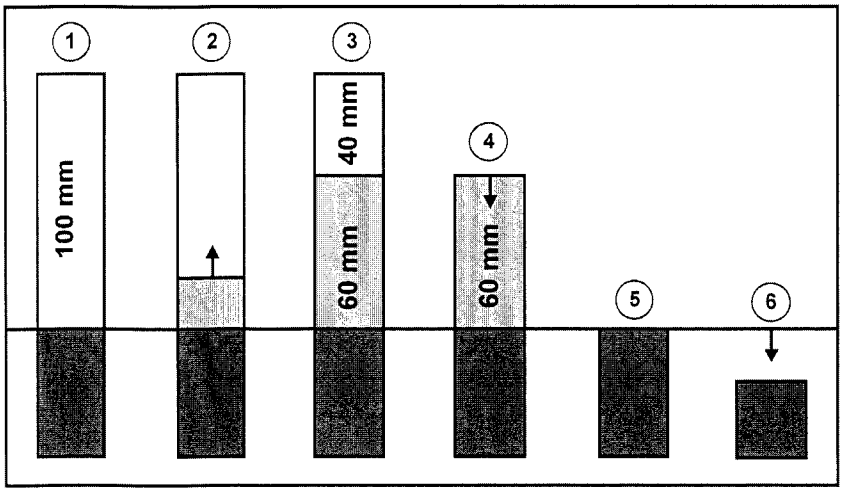

Figure 6.2 Schematic illustration of the snow and ice melt model (after Reeh, 1991). The winter snow pack (1) begins to melt and the percolating meltwater refreezes on the underlying glacier ice surface to form a layer of superimposed ice (2). This process stops once P-max (cf. Section 6.3.3) is reached (3). The remaining snow begins to melt, eventually exposing the superimposed ice (4), which begins to disappear to eventually expose 'real' glacier ice (5) below. At this point, the annual net glacier mass balance (for this particular location) is zero. If melting continues, the glacier ice surface starts to lower (6), leading to a progressively more negative mass balance. This process can stop anytime once the available melting degree-days for a given mass balance year are consumed. This model is obviously a drastic simplification of reality, but matches well the documented melt processes on the Ward Hunt Ice Rise and Ice Shelf (Lister, 1962; Sagar, 1962) and the observed melt processes on the Hazen Plateau ice caps.

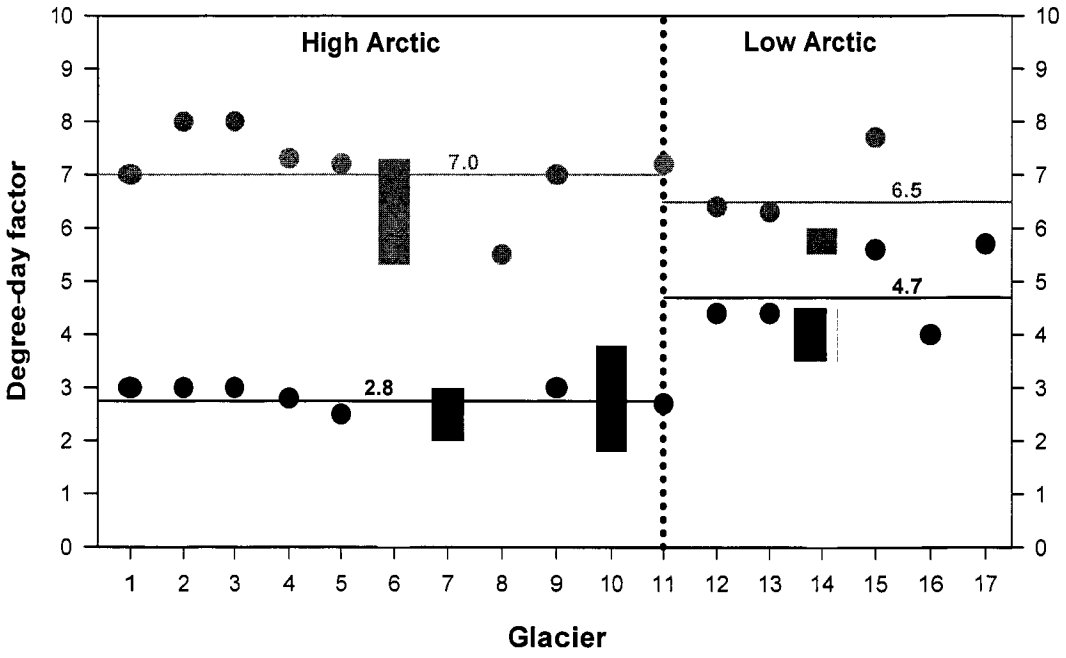

Figure 6.3 Variability of the positive degree-day factor (DDF) for snow (black) and ice (grey), as reported previously in the scientific literature (cf. Table 6.1). The numbers on the x-axis refer to the different sites as listed in Table 6.1.

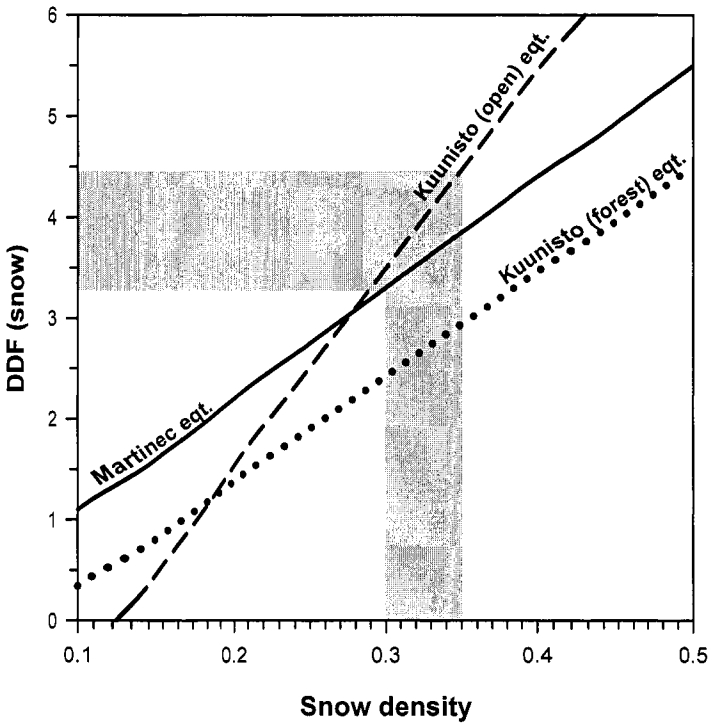

Figure 6.4 The degree-day factor for snow (DDF (snow)) plotted as a function of snow density, based on the empirical equations presented by Martinec (1976) and Kuunisto (1980). The grey shading marks the snow density range between 0.3 and 0.35, as measured previously for the winter snowpack on the Hazen Plateau ice caps (Hattersley-Smith and Serson, 1972; Bradley and England, 1977) and on the Ward Hunt Ice Rise and Ice Shelf (Braun *et al.*, 2004b).

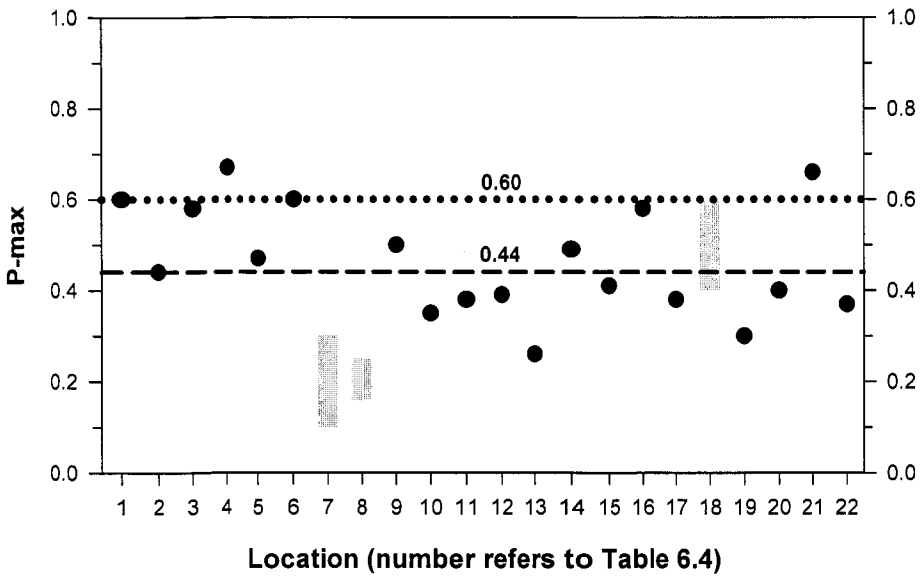

Figure 6.5 Values of P-max previously reported in the scientific literature (cf. Table 6.4). The numbers on the x-axis refer to the location numbers in Table 6.4. The commonly used value for P-max of 0.6 is shown by a dotted line. The simple mean of Table 6.4 (P-max = 0.44±0.14) is shown by the dashed line.

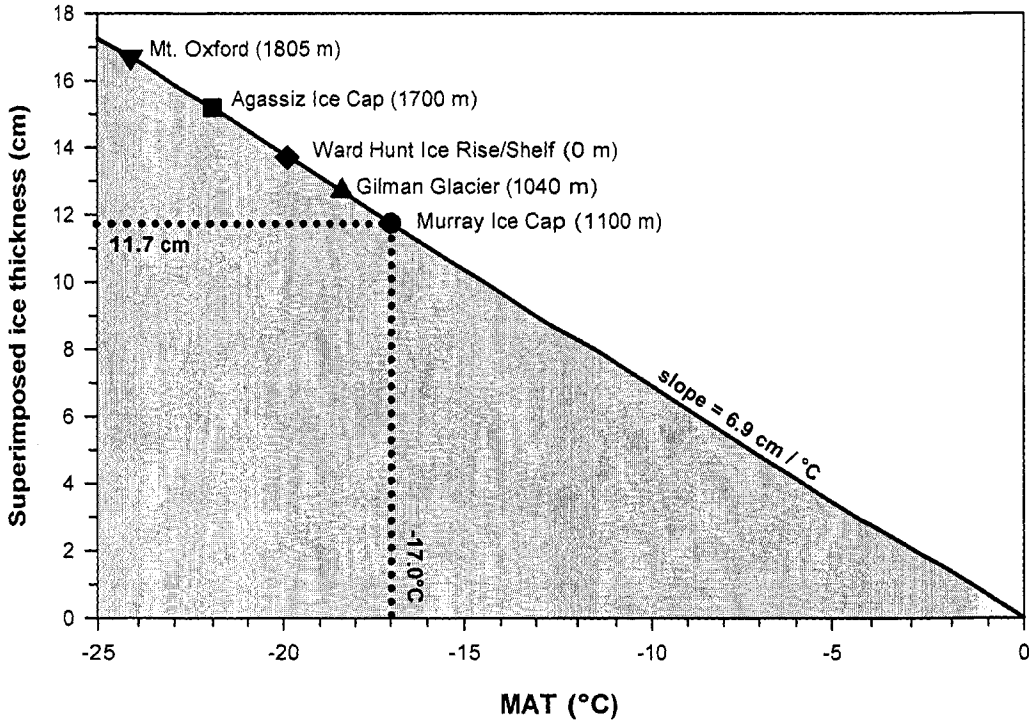

Figure 6.6 Superimposed ice formation (in cm ice thickness, not water equivalent) calculated as a function of mean annual air temperature (MAT) using the Woodward *et al.* (1997) equation (cf. Table 6.5).

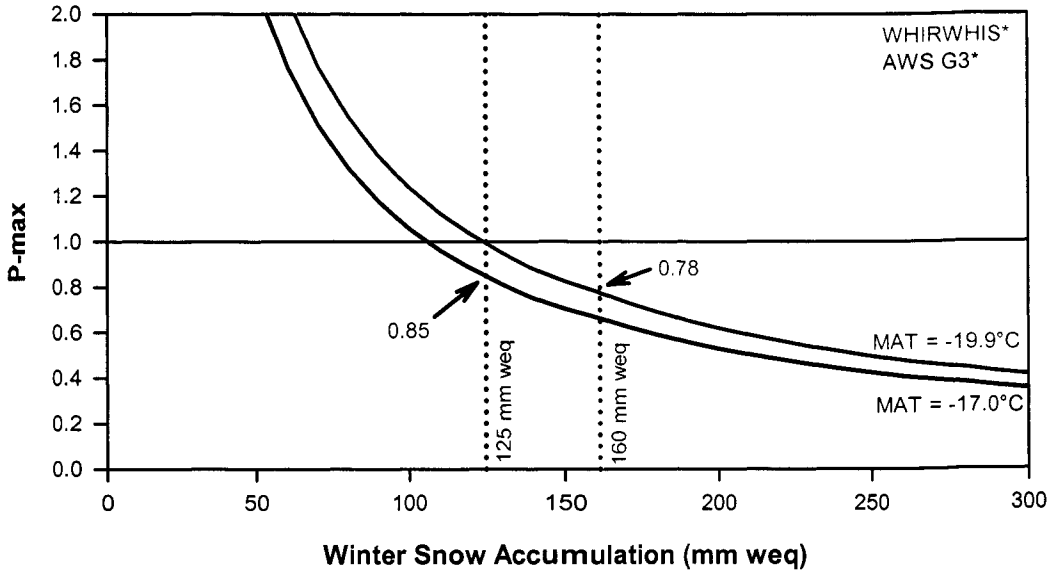

Figure 6.7 P-max calculated as a function of winter snow accumulation (mm weq) for a mean annual air temperature of –17.0°C (AWS G3*, 1951 to 2000, red) and –19.9°C (WHIRWHIS*, 1951 to 2000, blue) using the Woodward *et al.* (1997) equation (cf. Table 6.5). The dotted lines indicate normal levels of annual snow accumulation on the Hazen Plateau (125 mm weq) and North Coast (160 mm weq) (cf. Chapter 5).

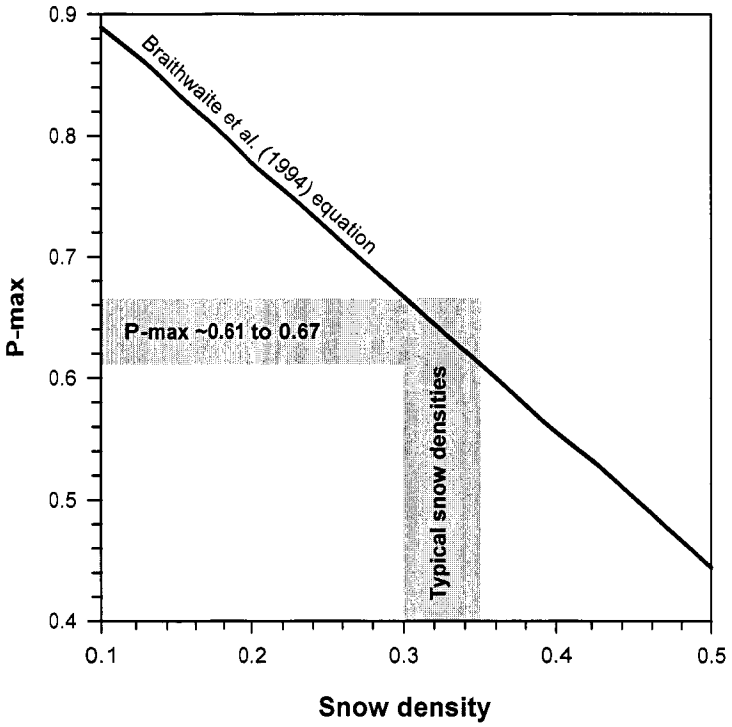

Figure 6.8 P-max calculated using the superimposed ice parameterization presented by Braithwaite *et al.* (1994). The grey shading indicates a range of typical snow densities on the Hazen Plateau (Hattersley-Smith and Serson, 1972; Bradley and England, 1977) and the Ward Hunt Ice Rise and Ice Shelf (Braun *et al.*, 2004b).

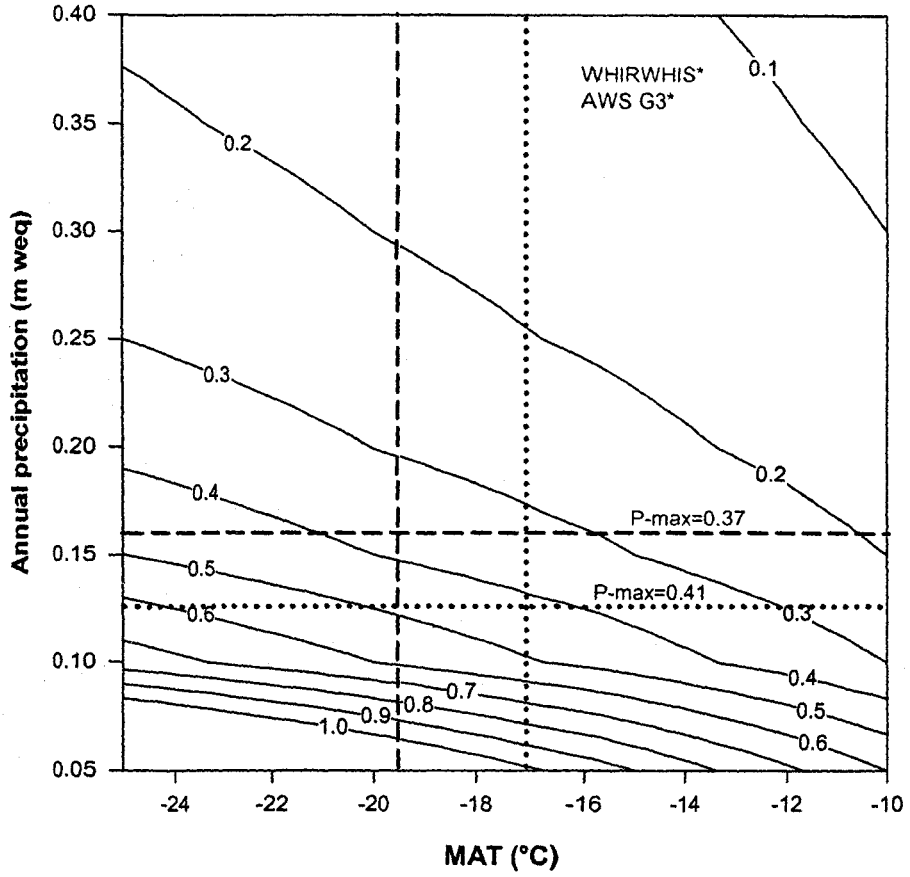

Figure 6.9 Contour plot of P-max calculated as a function of mean annual temperature (MAT, °C) and annual total precipitation (mm weq), following one of the parameterizations presented by Janssens and Huybrechts (2000). Red dotted line: AWS G3* climatology (1951 to 2000). Blue dashed line: WHIRWHIS* climatology (1951 to 2000) (cf. Table 6.5).

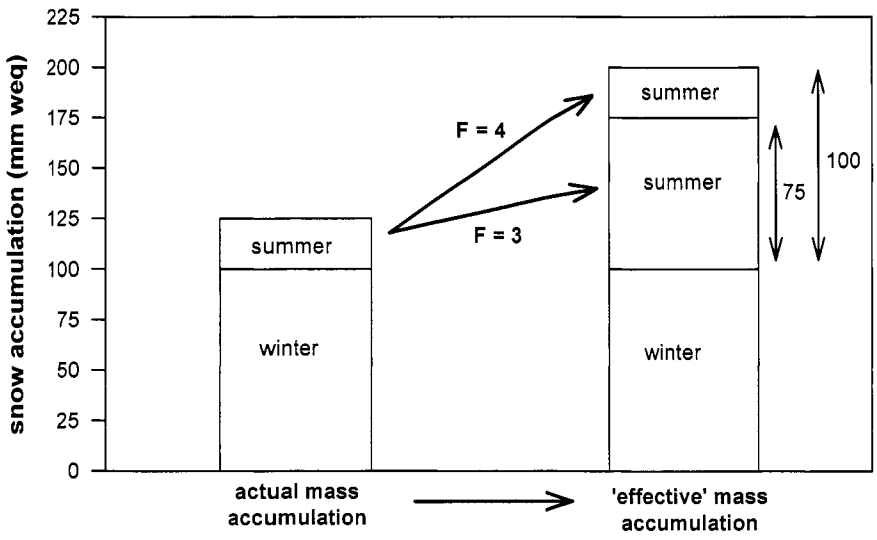

Figure 6.10 Summer snowfall 'amplification' (after Oerlemans and Klok, 2004) (cf. Section 6.3.4).

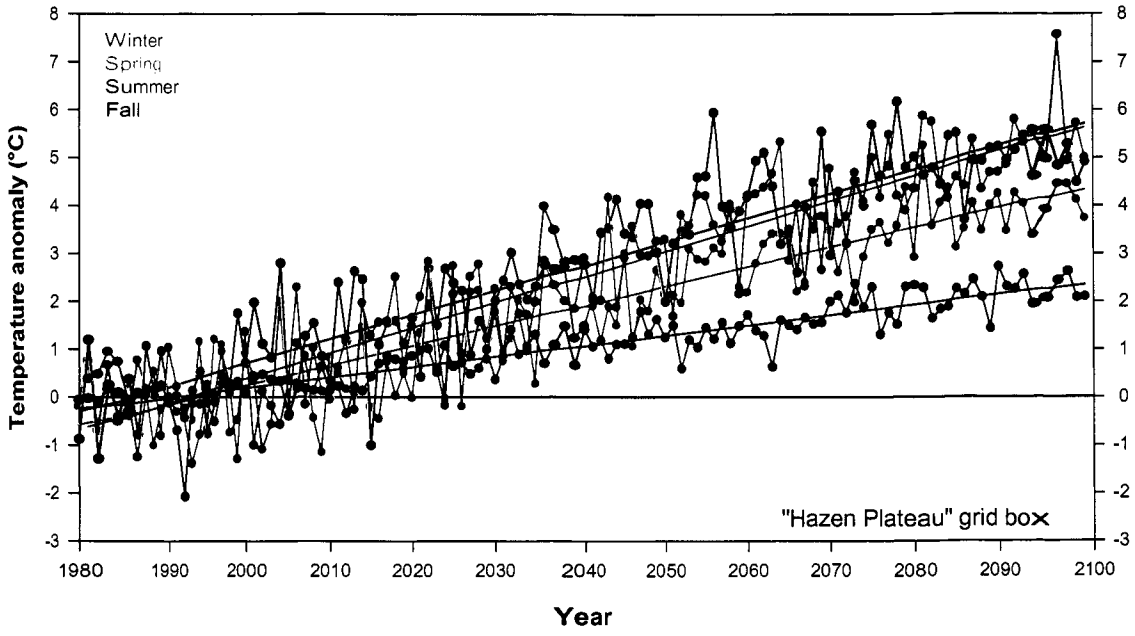

Figure 6.11 ACIA 5-GCM composite mean seasonal air temperature anomalies and trends, relative to the 1980 to 1999 (n = 20 years) reference period. Red curve = summer (JJA); black curve = fall (SON), blue curve = winter (DJF), and green curve = spring (MAM) (cf. Table 6.12). The four trend lines denote the linear trends for the respective full records (i.e. 1980 to 2099; n = 120 years). Data are shown for the 2.5 by 2.5° grid box centered at 82.5°N and 70°W ('Hazen Plateau grid box').

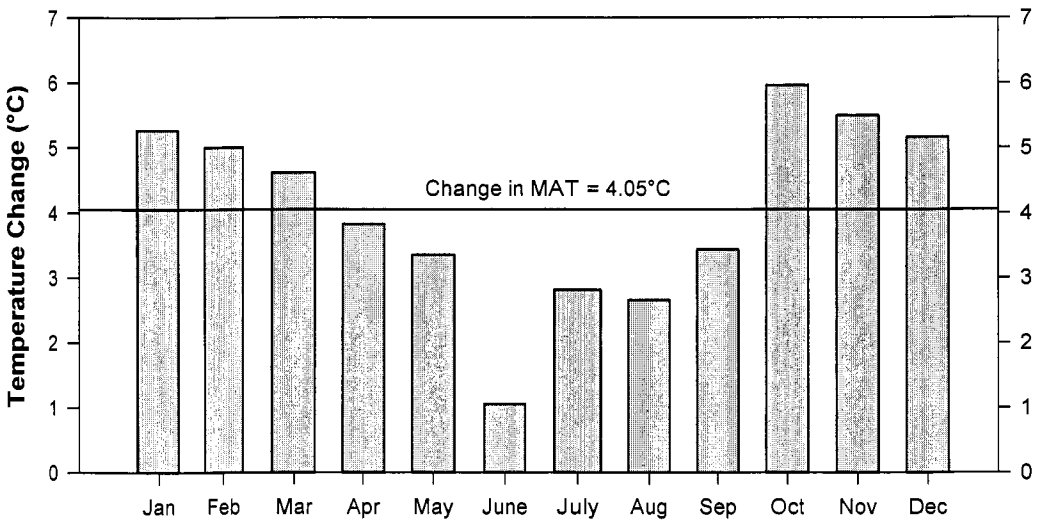

Figure 6.12 ACIA 5-GCM composite mean monthly air temperature difference between 'today' (i.e. 1980 to 1999) and the greenhouse 'future' (i.e. 2080 to 2099) (cf. Table 6.12). Data are shown for the 2.5 by 2.5° grid box centered at 82.5°N and 70°W ('Hazen Plateau grid box').

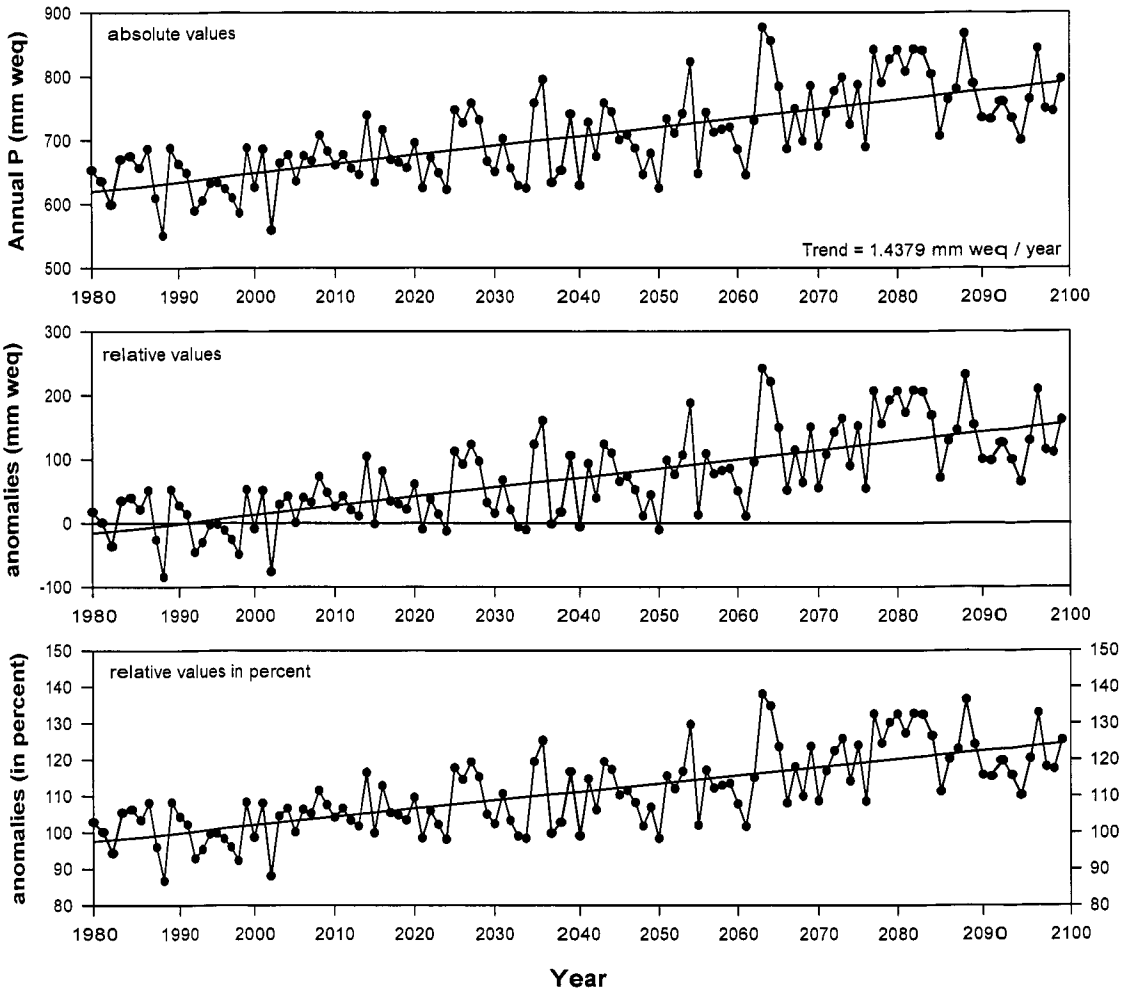

Figure 6.13 ACIA 5-GCM composite total annual precipitation. (A) Absolute modeled values; (B) modeled anomalies; and (C) modeled percent anomalies relative to the 1980 to 1999 reference period. Data are shown for the 2.5 by 2.5° grid box centered at 82.5°N and 70°W ('Hazen Plateau grid box').

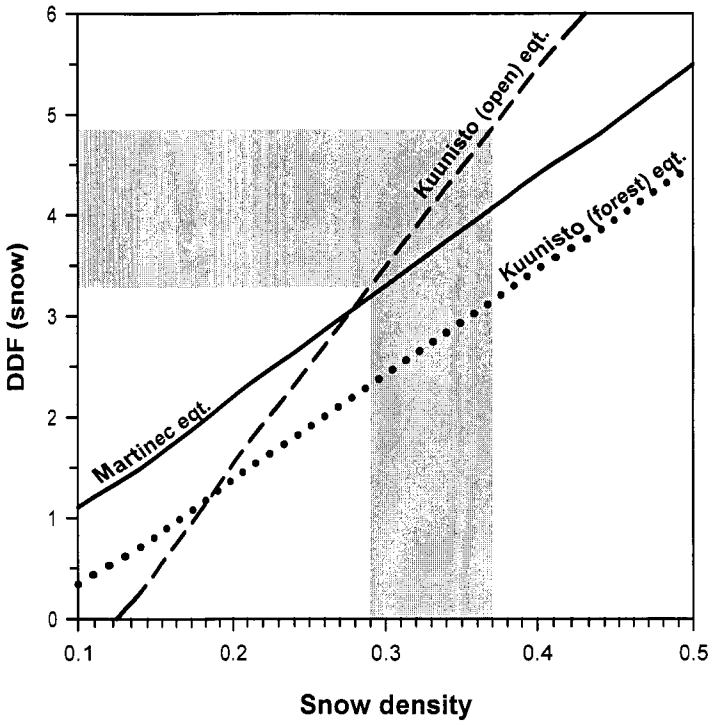

Figure 6.14 The DDF (snow) plotted as a function of snow density, using the three empirical parameterizations presented by Martinec (1976) and Kuunisto (1980) (Equations 6.5 to 6.7) (cf. Section 6.3.2.2). The grey shading indicates a range of snow densities (0.330±0.043), which represents the mean and standard deviation of all reported snow densities for the Ward Hunt Ice Rise and Ice Shelf (cf. Braun *et al.*, 2004a).

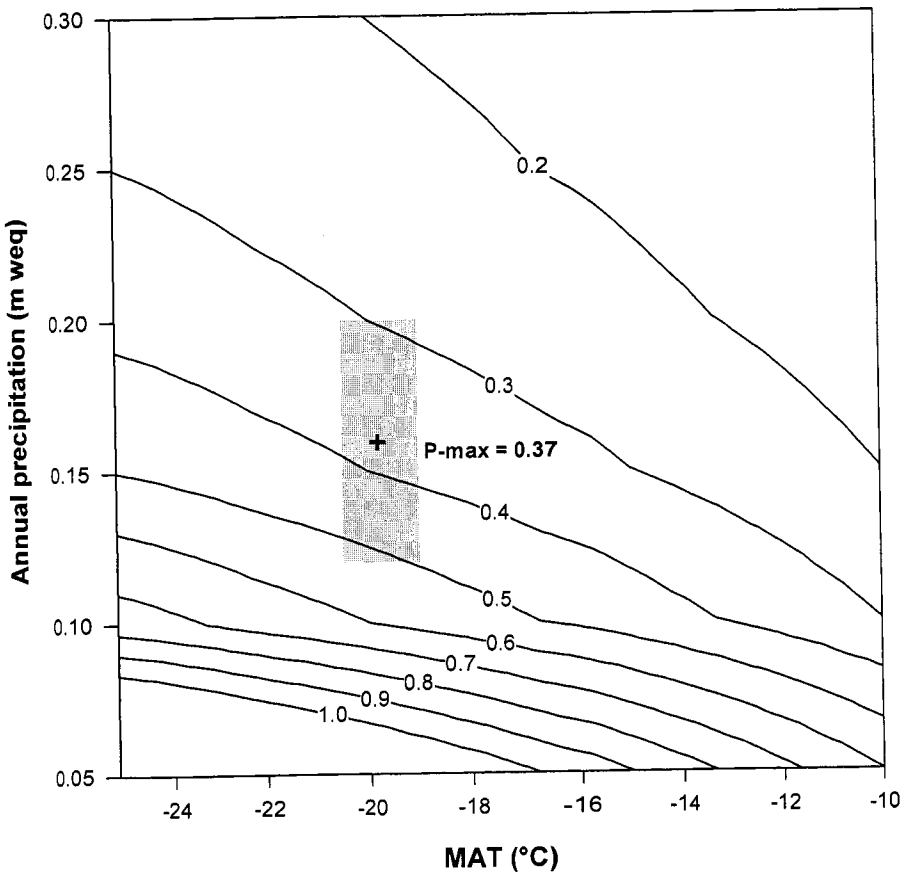

Figure 6.15 Superimposed ice formation (i.e. P-max) plotted as a function of mean annual temperature (MAT, °C) and winter snow accumulation (mm weq) (after Janssens and Huybrechts, 2000). The grey box and black cross indicate P-max values for a range of MAT values (–19.8±0.81°C) and winter snow accumulation (160±25 percent = 40 mm weq) (cf. Chapter 5), which represent the temperature and precipitation climatology for the North Coast (1951 to 2003).

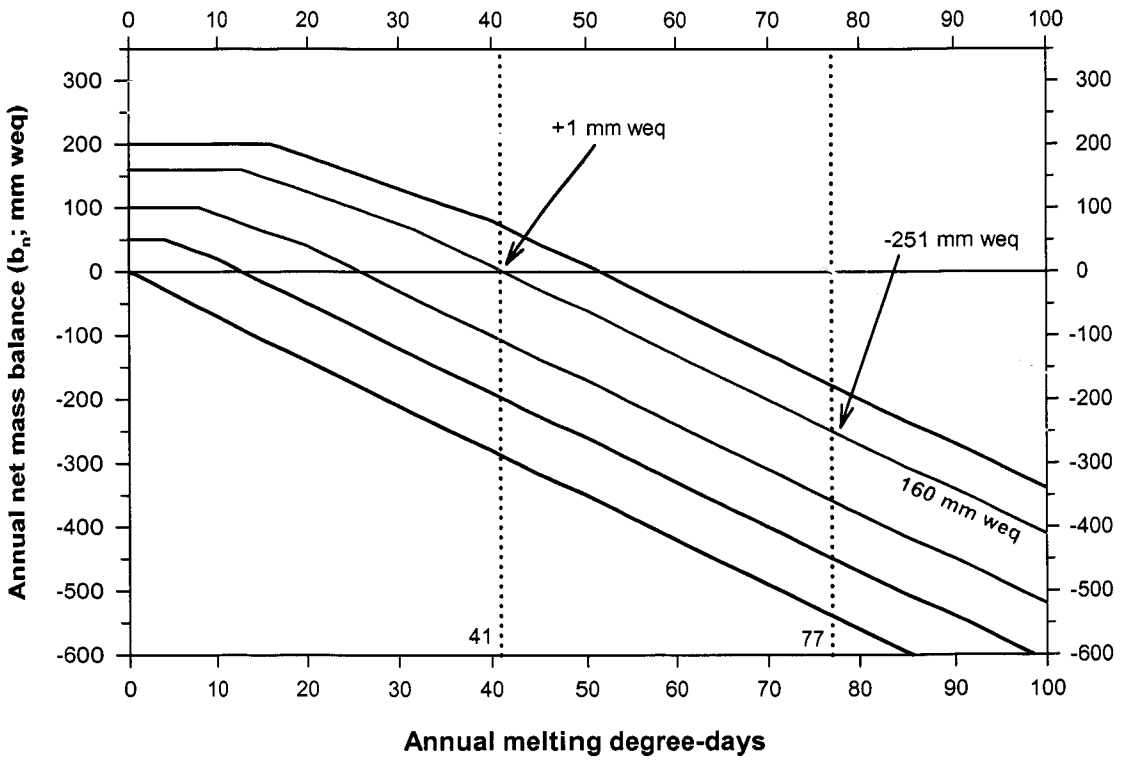

Figure 6.16 The assumed snow and ice melt process/progression for different values of winter snow accumulation (0, 50, 100,..., 300 mm weq), assuming a DDF (snow) = 5 mm weq d^{-1} deg^{-1}, a DDF (ice) = 7 mm weq d^{-1} deg^{-1}, and a P-max = 0.4 (cf. Section 6.4.1). The green curve depicts the melt process for a winter snow accumulation of 160 mm weq. The two vertical dotted lines denote the mean summer conditions on the Ward Hunt Ice Rise and Ice Shelf (WHIRWHIS*, 1951 to 2003, 41 MDD) and the adjacent ice-free island (WHI AWS*, 1951 to 2003, 77 MDD). The line colors are arbitrary.

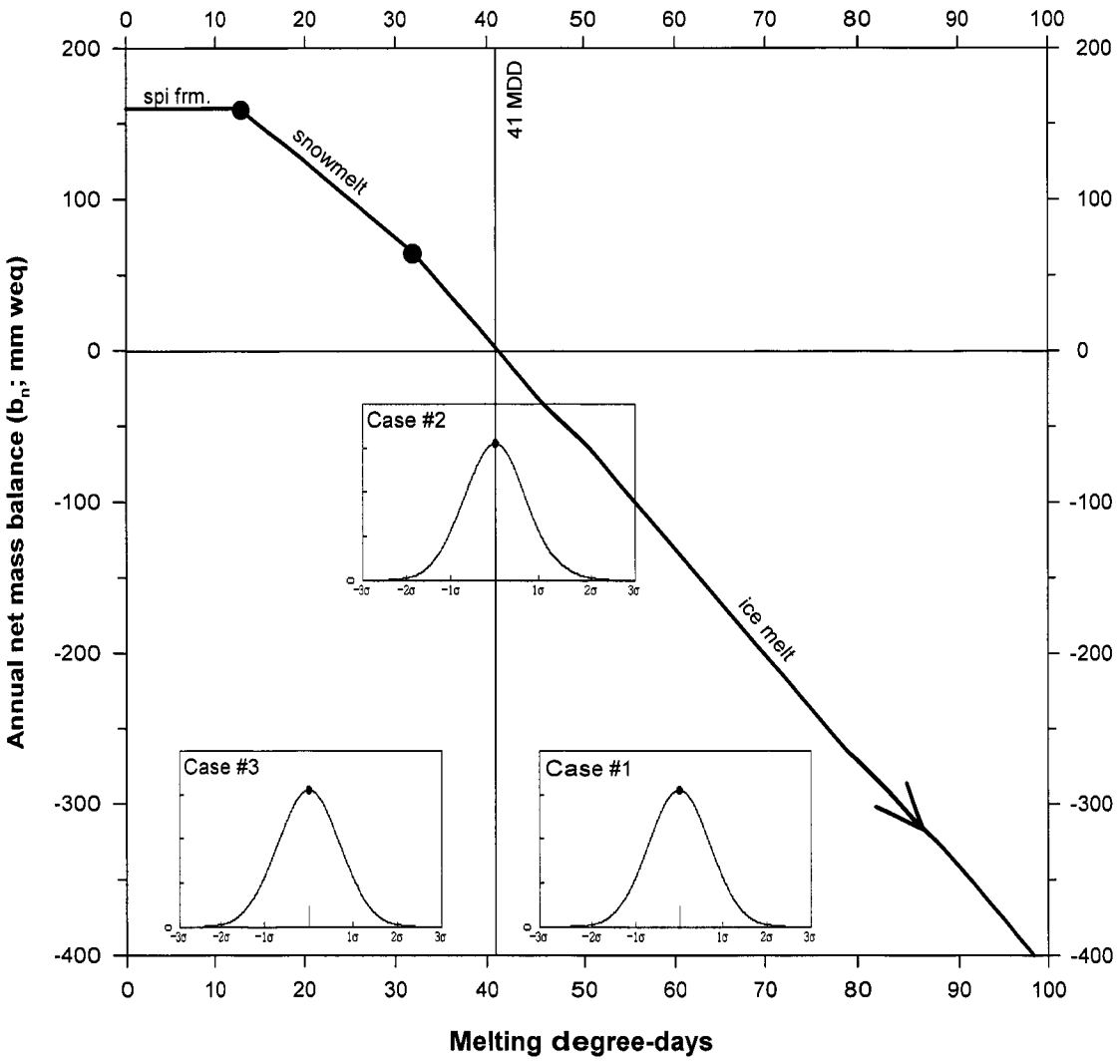

Figure 6.17 As Figure 6.16, but now enlarged and expanded for a winter snow accumulation of 160 mm weq. The three generalized bell curves highlight the three model asymmetry cases discussed in the text and are centered, respectively, at 21, 41, and 61 annual melting degree-days totals.

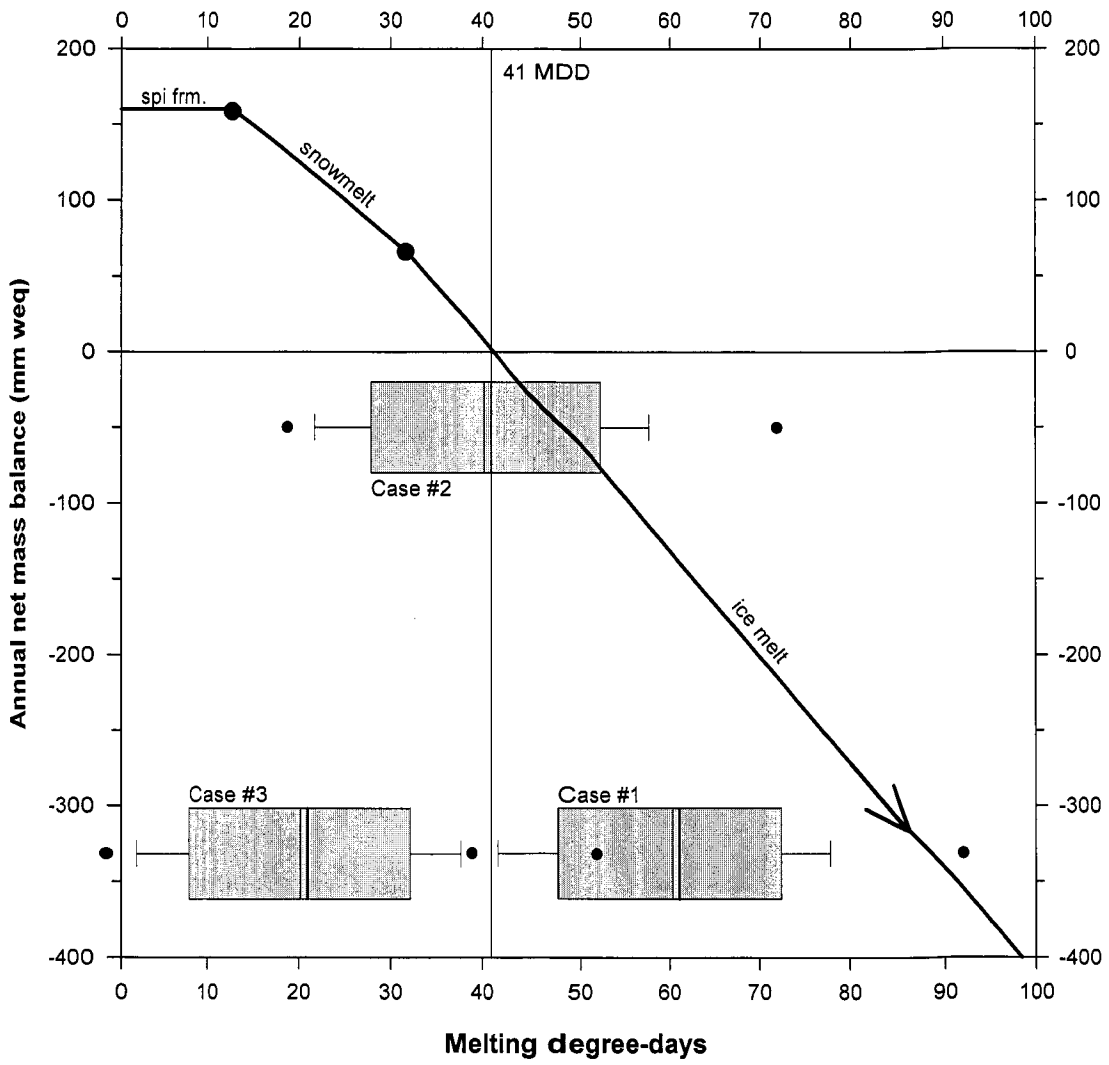

Figure 6.18 As Figure 6.17, but now showing three box-whisker plot of WHIRWHIS* annual melting degree-day totals from 1951 to 2003 (n = 53 years) instead of the three generalized bell curves. The thin solid line in each box-whisker plot denotes the median, the thick solid line the respective mean (e.g. 41 MDD). The three box-whisker plots are centered, respectively, at 21, 41, and 61 annual melting degree-day totals.

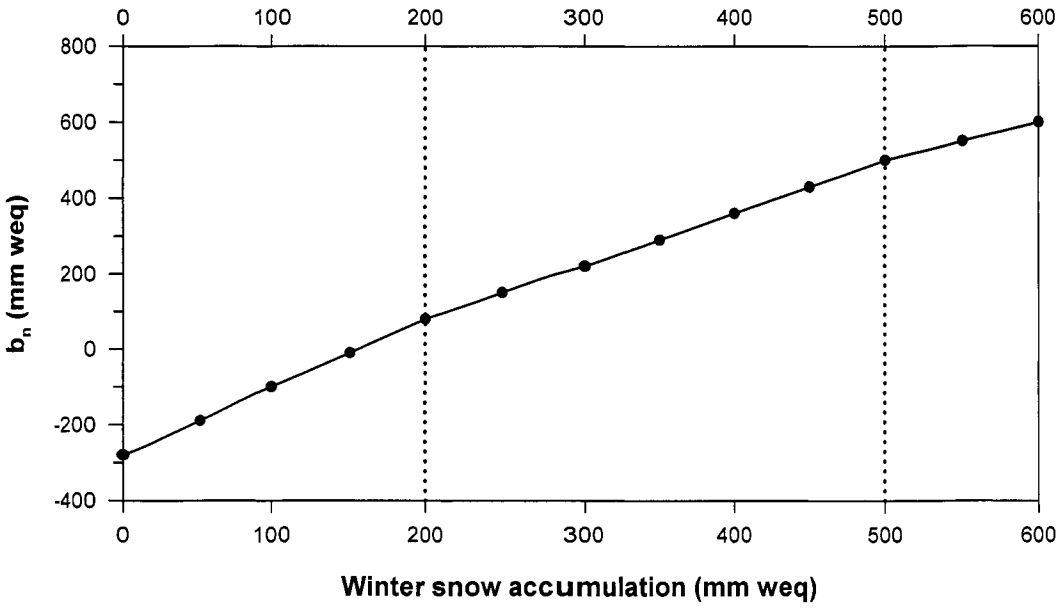

Figure 6.19 Asymmetry of modeled annual mass balance to changes in winter snow accumulation (plotted for an annual melting degree-day total of 41 MDD), assuming a DDF (snow) = 5 mm weq d^{-1} deg^{-1}, a DDF (ice) = 7 mm weq d^{-1} deg^{-1}, and a P-max = 0.4 (cf. Section 6.4.1).

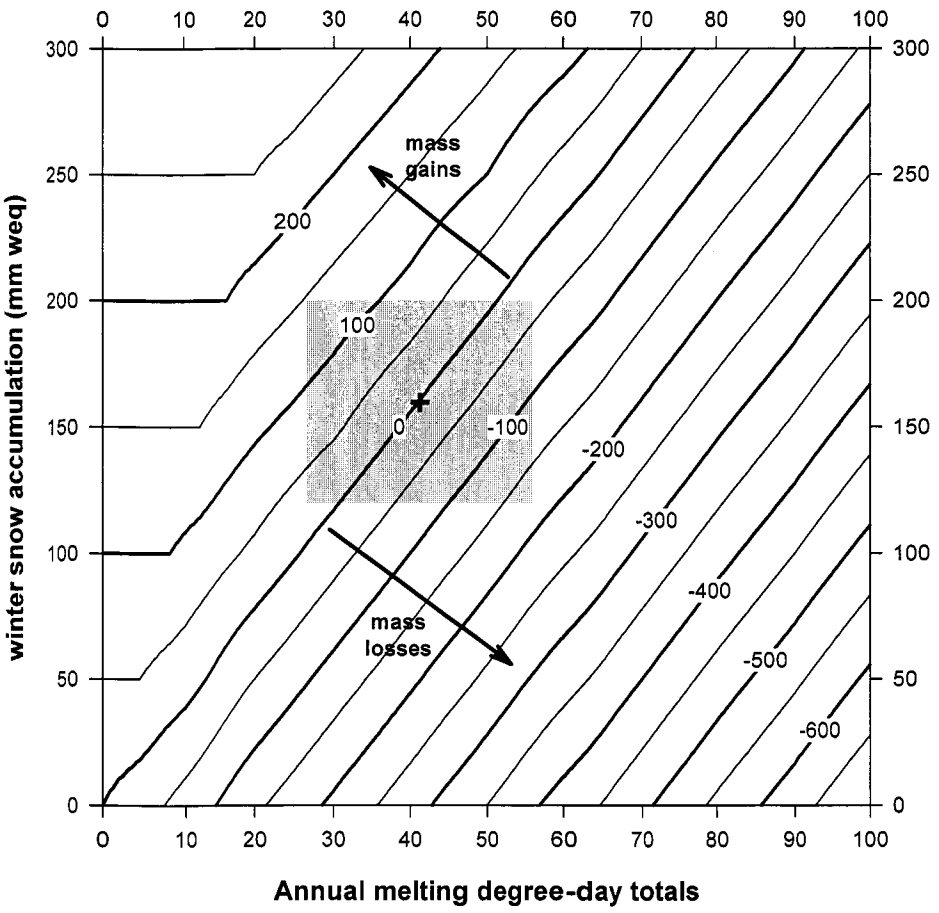

Figure 6.20 As Figure 6.16, but the annual net mass balance is now shown in matrix form as a function of annual melting degree-day totals and snow accumulation. The grey shading and black cross indicate the mean climatology 'space' of the Ward Hunt Ice Rise and Ice Shelf (WHIRWHIS* climatology, 1951 to 2003, 41±15 MDD, 160±40 mm weq).

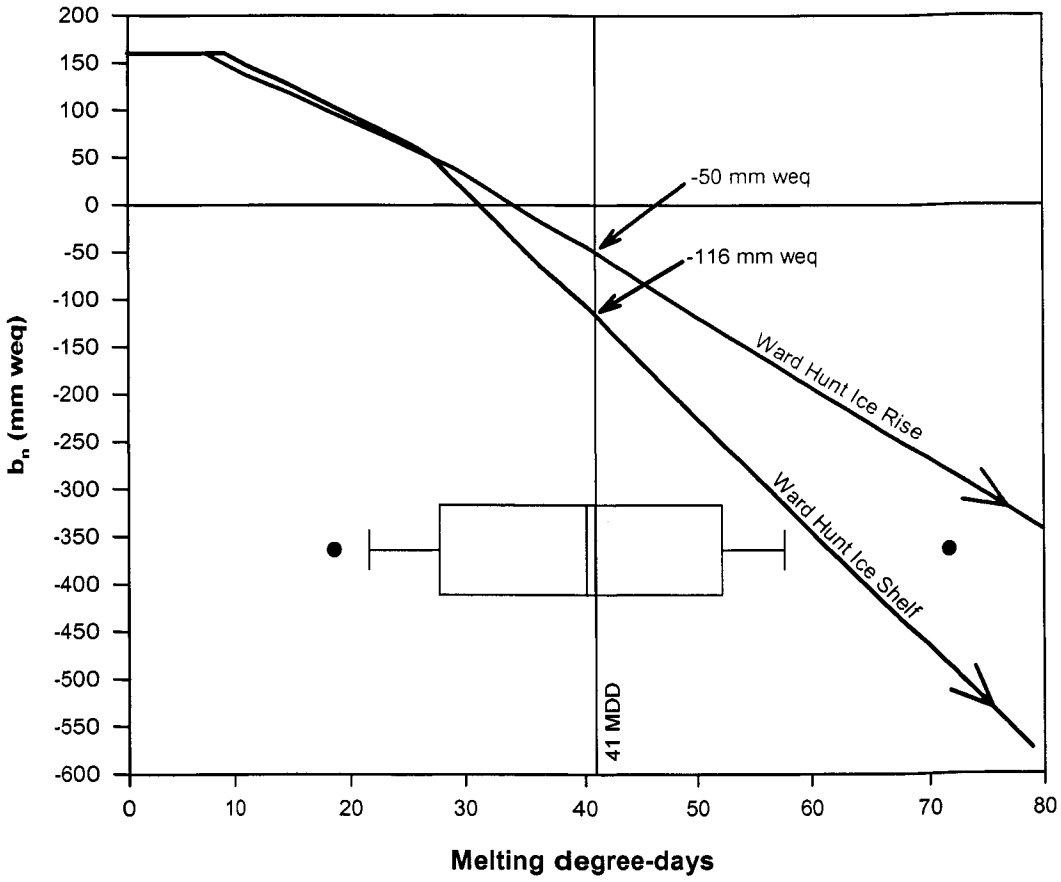

Figure 6.21 The modeled snow and ice melt process on the Ward Hunt Ice Rise (blue curve) and Ice Shelf (red curve) as a function of melting degree-days, assuming a winter snow accumulation of 160 mm weq. Model parameters (DDF (snow)/DDF (ice)/P-max): WHIR (5.5/7.5/0.24); WHIS (6/12/0.34). The vertical line denotes the mean annual melting degree-day total for the WHIRWHIS* melting degree-day climatology (41 MDD; 1951 to 2003), which is shown as a box-whisker plot, centered at 41 MDD (cf. Fig. 6.18).

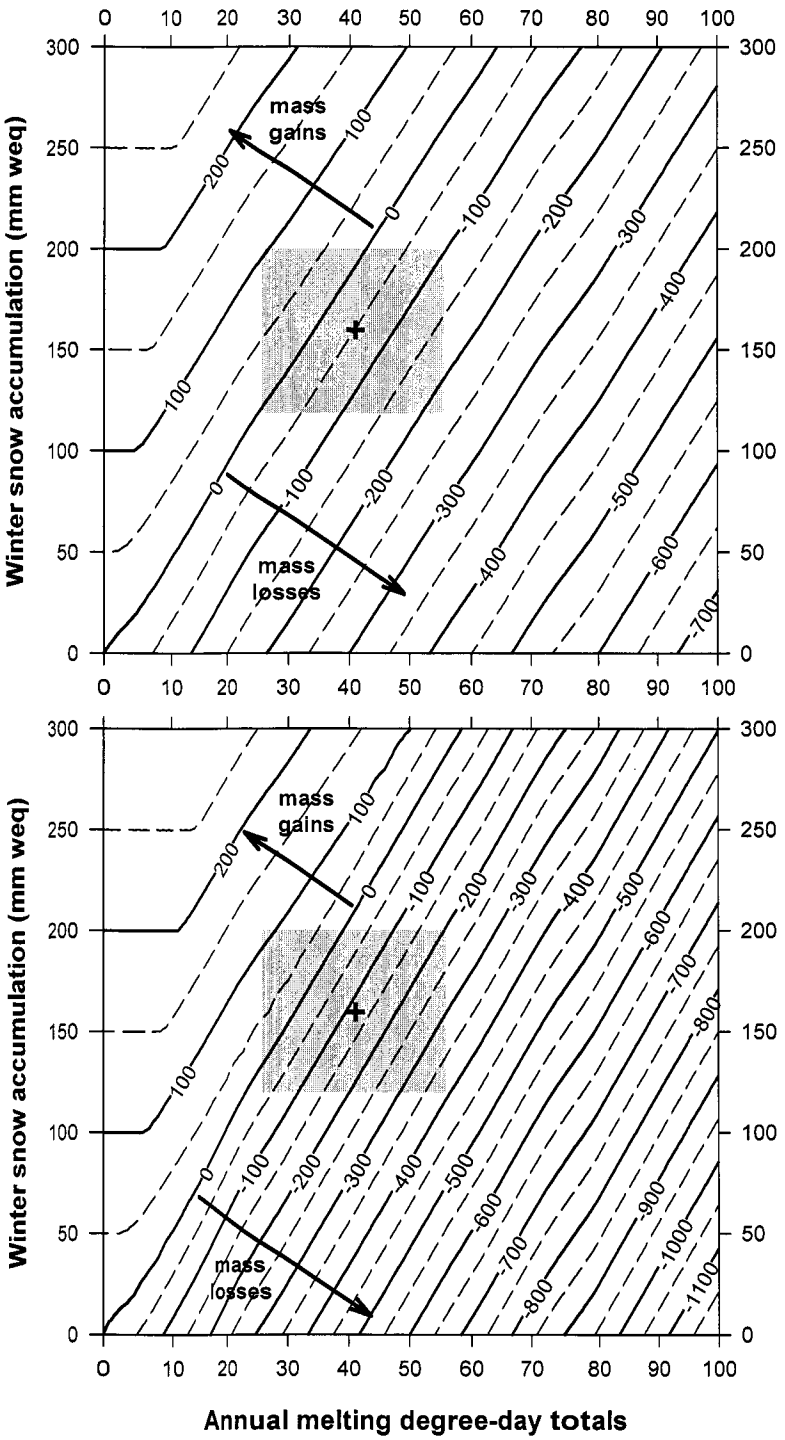

Figure 6.22 Modeled mean annual mass balance of the Ward Hunt Ice Rise (top) and Ice Shelf (bottom) as a function of annual melting degree-day totals and winter snow accumulation (cf. Fig. 6.20). Model parameters (DDF (snow)/DDF (ice)/P-max): WHIR (5.5/7.5/0.24); WHIS (6/12/0.34). The grey shading and black cross indicate the mean climatology 'space' for the Ward Hunt Ice Rise and Ice Shelf (WHIRWHIS* climatology, 1951 to 2003, 41±15 MDD, 160±40 mm weq).

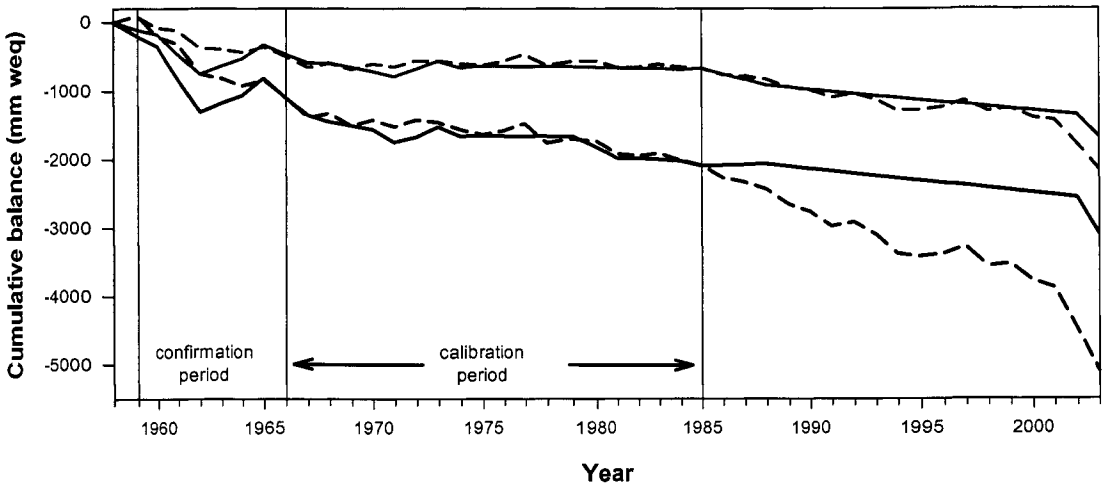

Figure 6.23 Measured (solid curve) and predicted (dashed curve) cumulative annual mass balance for the Ward Hunt Ice Rise (blue) and the Ward Hunt Ice Shelf (red) between 1959 and 2003 (referenced to 1958 = 0), assuming constant winter snow accumulation of 160 mm weq and using the WHIRWHIS* melting degree-day climatology. Model parameters (DDF (snow)/DDF (ice)/P-max): WHIR (5.5/7.5/0.24); WHIS (6/12/0.34). The three vertical lines denote the model calibration period (1966 to 1985; n = 20 years) and the model confirmation period (1959 to 1965; n = 7 years) (cf. Section 6.4.3.2).

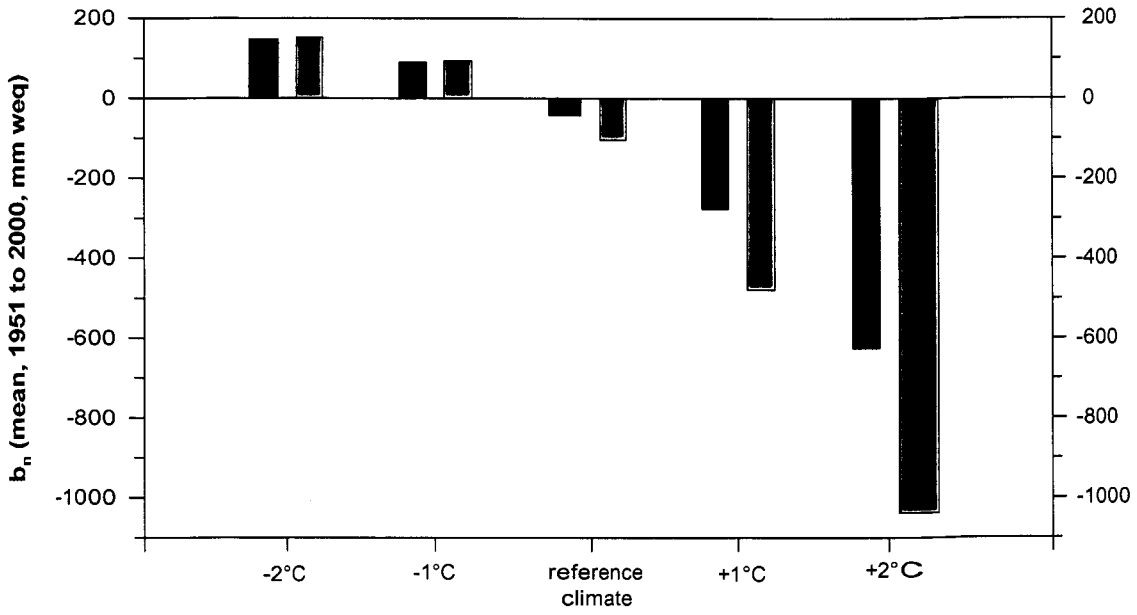

Figure **6.24** Temperature sensitivity (for ±1 and 2°C relative changes) of the Ward Hunt Ice Rise (red bars) and Ice Shelf (orange bars) relative to the 1951 to 2000 reference climate. Model parameters (DDF (snow)/DDF (ice)/P-max): WHIR (5.5/7.5/0.24); WHIS (6/12/0.34). Plotted is the mean annual mass balance for the 1951 to 2000 reference period.

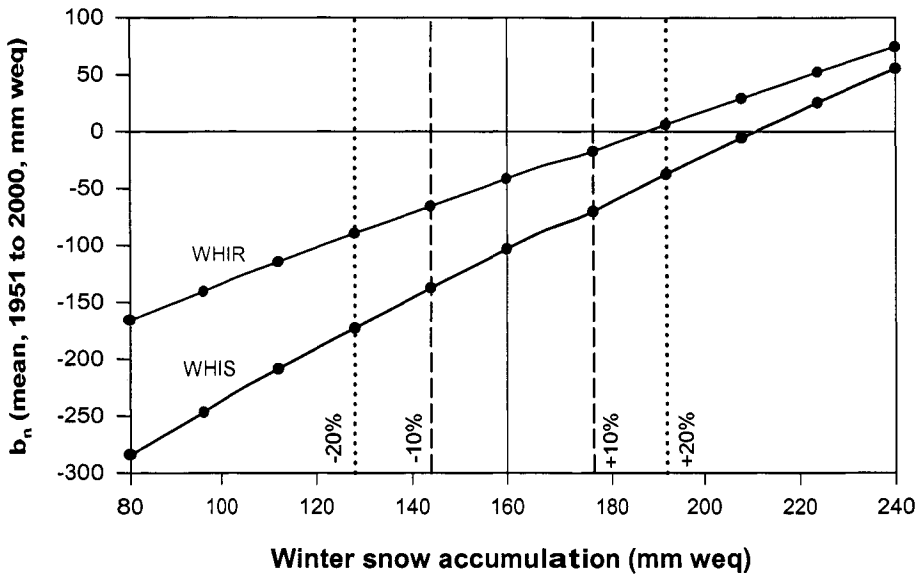

Figure 6.25 Precipitation sensitivity of the Ward Hunt Ice Rise (blue curve) and Ice Shelf (red curve) relative to the 1951 to 2000 reference period. The precipitation sensitivity was determined by increasing/decreasing winter snow accumulation by 10, 20, 30, 40, and 50 percent relative to the modern conditions (160 mm weq), and calculating the mean annual mass balance for the 1951 to 2000 reference period using the WHIRWHIS* melting degree-day climatology. Model parameters (DDF (snow)/DDF (ice)/P-max): WHIR (5.5/7.5/0.24); WHIS (6/12/0.34). The vertical lines denote the assumed mean winter snow accumulation (160 mm weq) and the ±10/20 percent envelope.

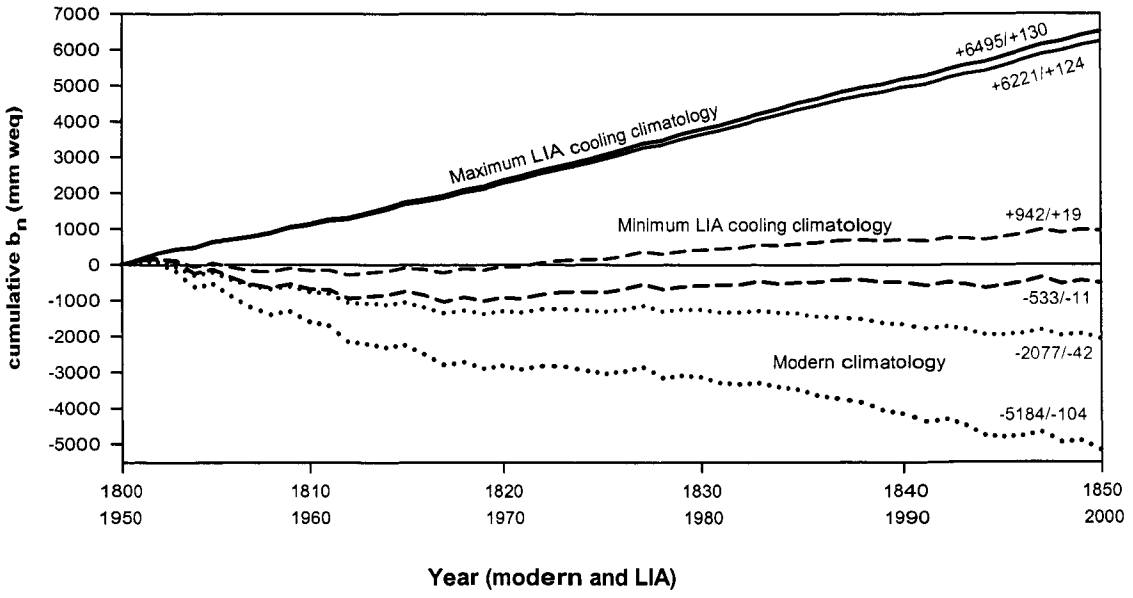

Figure 6.26 The mass balance of the Ward Hunt Ice Rise (blue curves) and Ice Shelf (red curves) today (i.e. 1951 to 2000; dotted) and during the so-called 'Little Ice Age' (LIA), using a minimum 'Little Ice Age' cooling climatology (dashed curves) and a maximum 'Little Ice Age' cooling climatology (solid curves) (cf. Section 6.4.4.3).

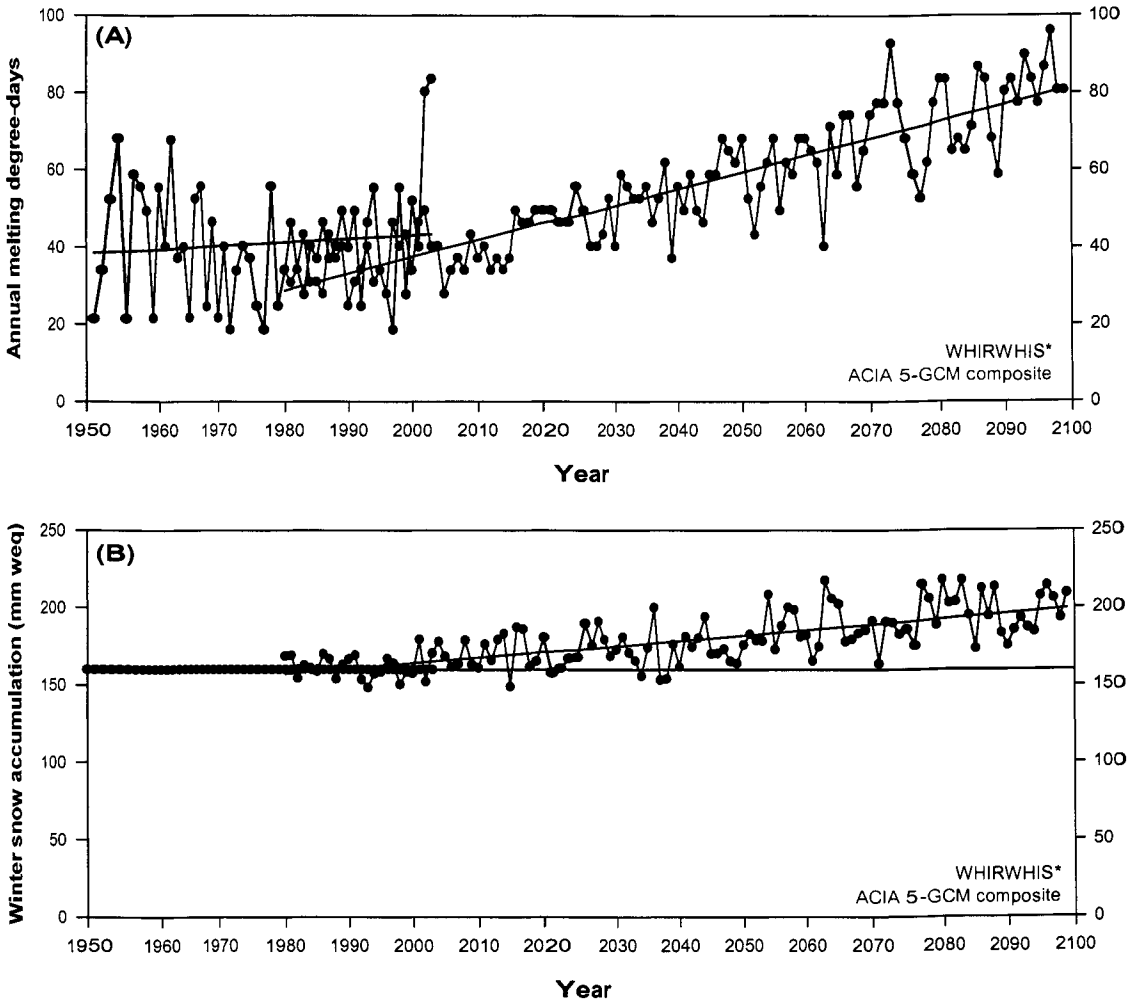

Figure 6.27 (A) Annual melting degree-day totals and (B) total annual precipitation climatology for the North Coast. Black curve: WHIRWHIS* climatology (1951 to 2003). Red curve: ACIA 5-GCM composite data set for the 2.5° latitude by 2.5° longitude grid box centered at 85°N and 70°W ('North Coast grid box'). See text for data adjustments (cf. Section 6.4.4.4). The lines are simple linear trend lines.

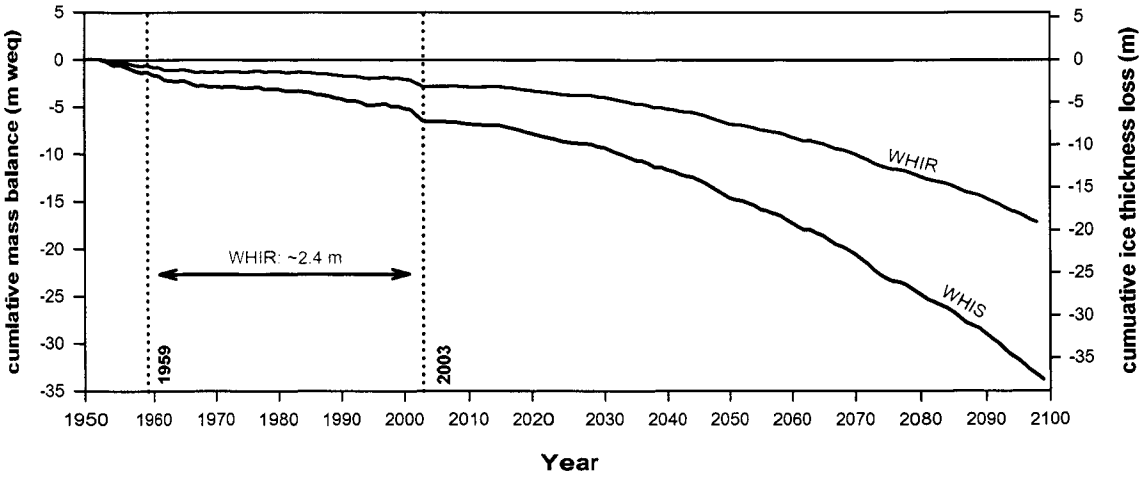

Figure 6.28 Cumulative surface mass balance and resultant ice thickness changes of the Ward Hunt Ice Rise (blue curve) and Ice Shelf (red curve) between 1951 and 2099, using the merged climatology shown in Figure 6.27. Model parameters (DDF (snow)/DDF (ice)/P-max): WHIR (5.5/7.5/0.24); WHIS (6/12/0.34).

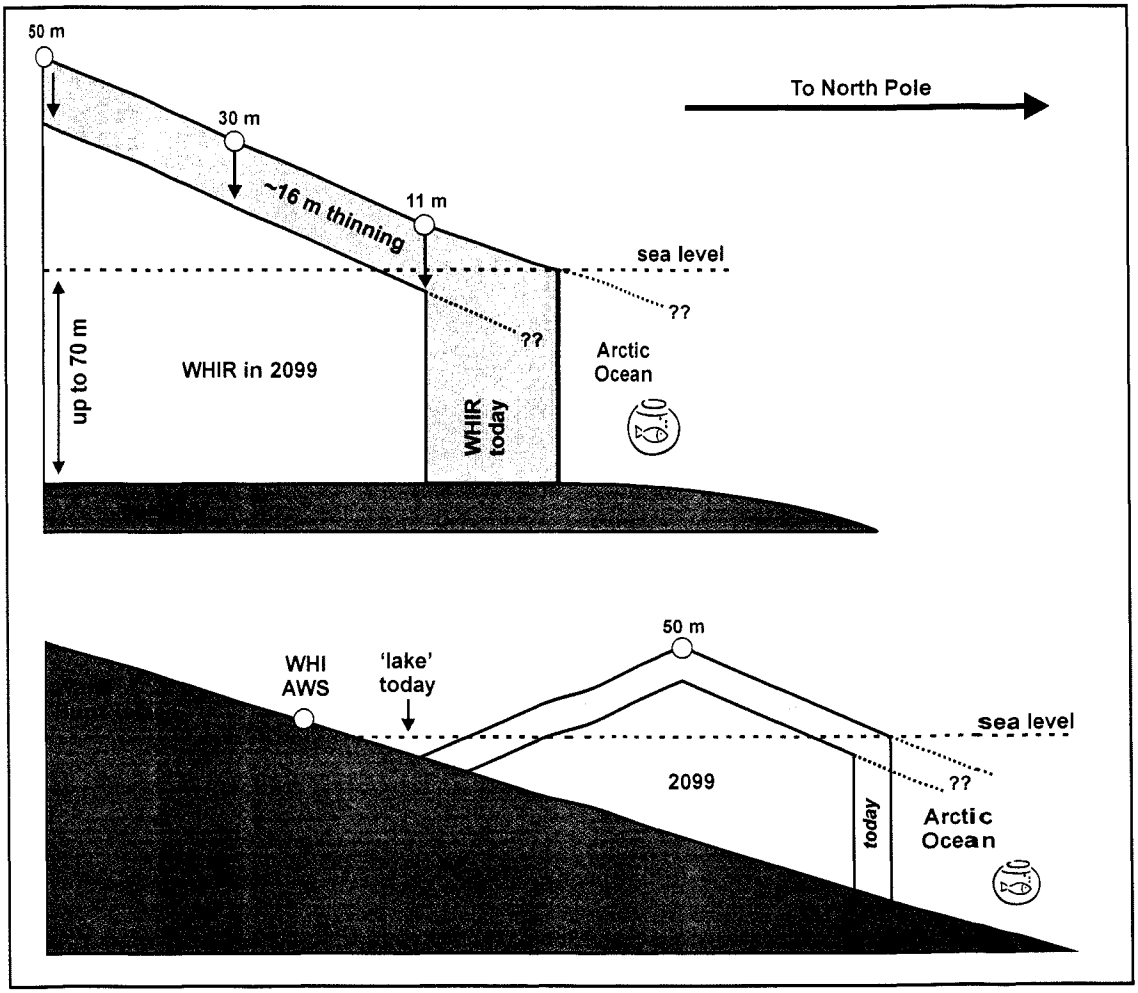

Figure 6.29 The future stability of the (highly generalized) Ward Hunt Ice Rise. Lyons *et al.* (1972) showed that the ice rise extends up to 70 m below sea-level. The grey outline depicts the Ward Hunt Ice Rise 'today'; the white outline the ice rise in 2099, after a thinning of about 16 m (cf. Section 6.4.4.4). The 30/50 m asl elevations are equivalent to the highest points of the eastern/western lobe of the Ward Hunt Ice Rise (cf. Chapter 3). The 'topography' of the sea floor and the ice rise below sea level is obviously unknown.

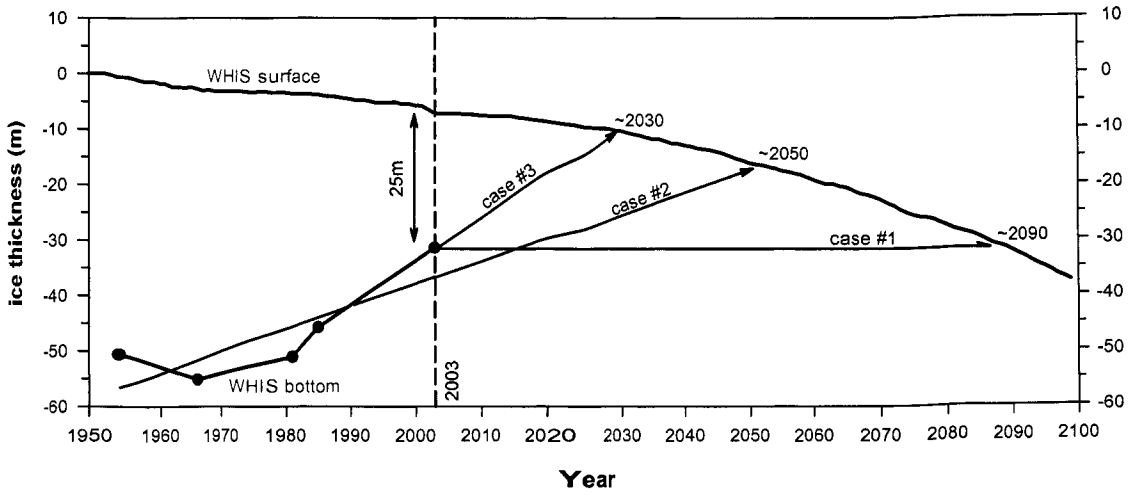

Figure 6.30 The future stability of the Ward Hunt Ice Shelf. The overall thickness (and hence stability) is obviously influenced both by processes occurring at its upper surface (i.e. surface mass losses/gains) as well as processes at its bottom surface (i.e. bottom mass losses/gains). The five ice shelf thickness measurements shown were compiled from the scientific literature by Vincent *et al.* (2001) and Mueller *et al.* (2003).

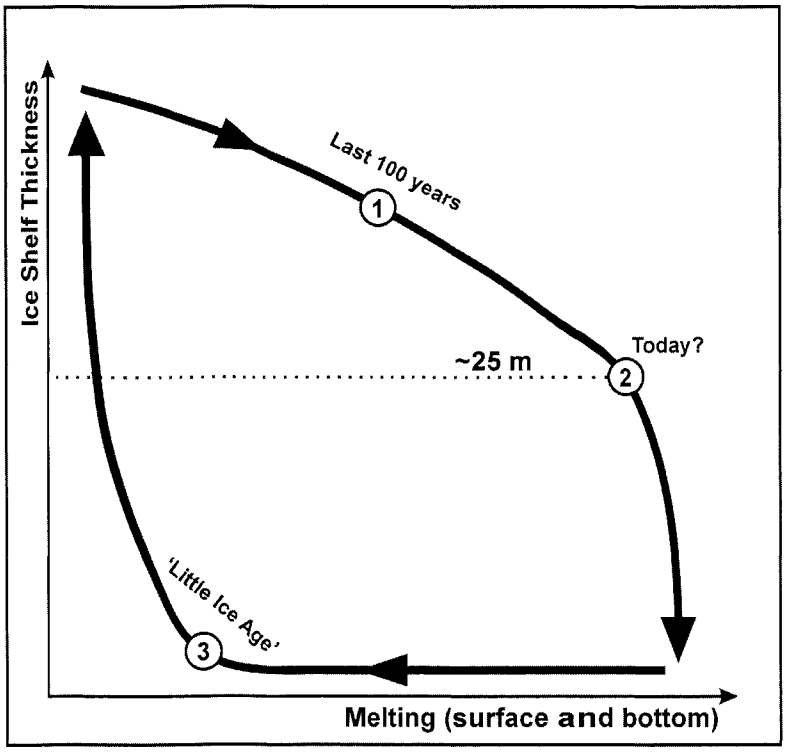

Figure 6.31 Schematic hysteresis-response of the Ward Hunt Ice Shelf to climate change. Continuous decreases (1) in ice shelf thickness (= mass losses), even if relatively slow and gradual, may lead to an abrupt break-up and collapse of the ice shelf (2) once a critical threshold is reached (cf. Vaughan and Doake, 1996; Cooke *et al.*, 2005). Once the ice shelf disintegrates, it cannot reform again (3) unless climatic conditions deteriorate dramatically (Hattersley-Smith *et al.*, 1955).

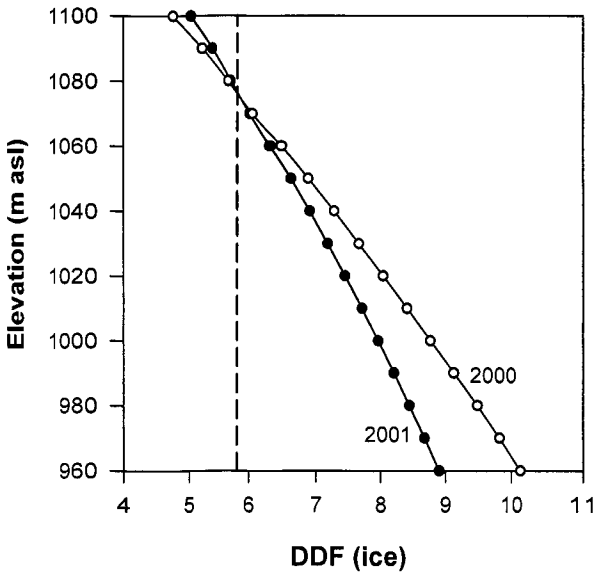

Figure 6.32 The degree-day factor for ice (DDF (ice); mm weq d^{-1} deg^{-1}) for Murray Ice Cap in 2000 (open circles; 25 June to 2 July) and 2001 (closed circles; 19 June to 5 August) plotted as a function of elevation by comparing the ablation gradient with the corresponding melting degree-day gradient (cf. Section 6.5.2.2, 6.5.2.3, and 6.5.3.4).

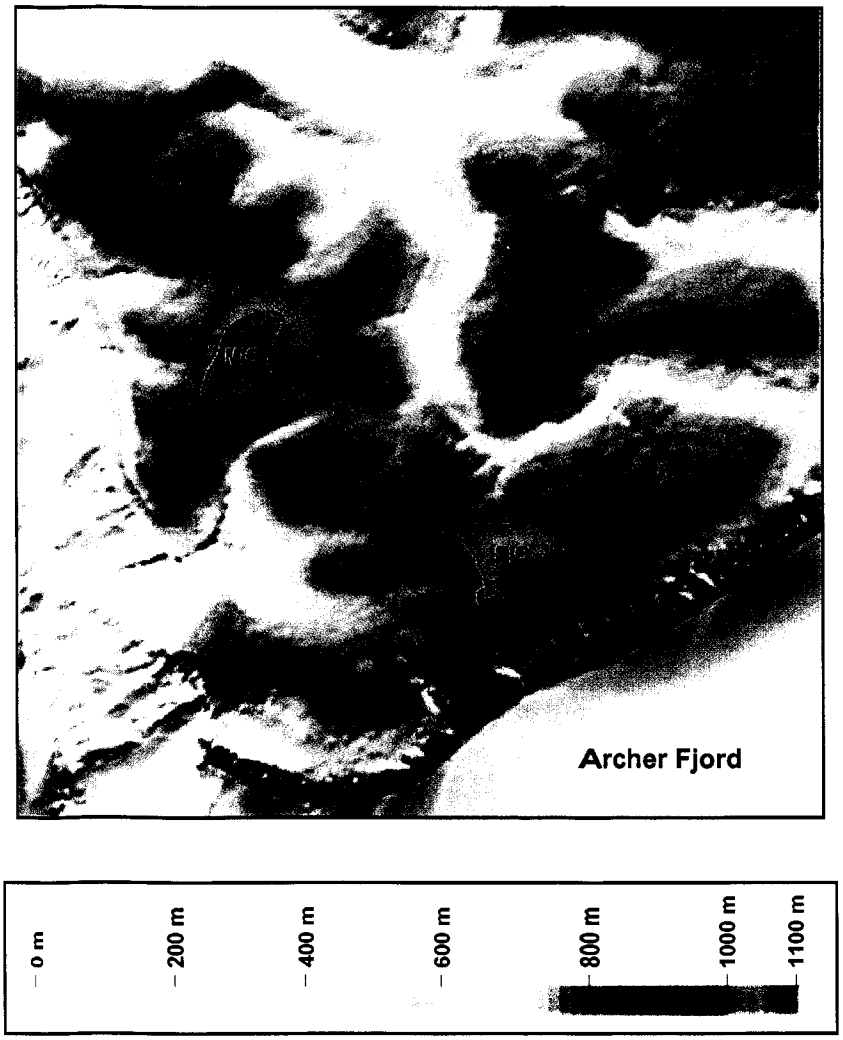

Figure 6.33 The digital elevation model used in the modeling experiment (cf. Section 6.5.3.2). The black lines depict the outlines of Murray and Simmons Ice Cap in 2003. The black stars denote the position of the lichen trim line mapped in vicinity of the ice caps.

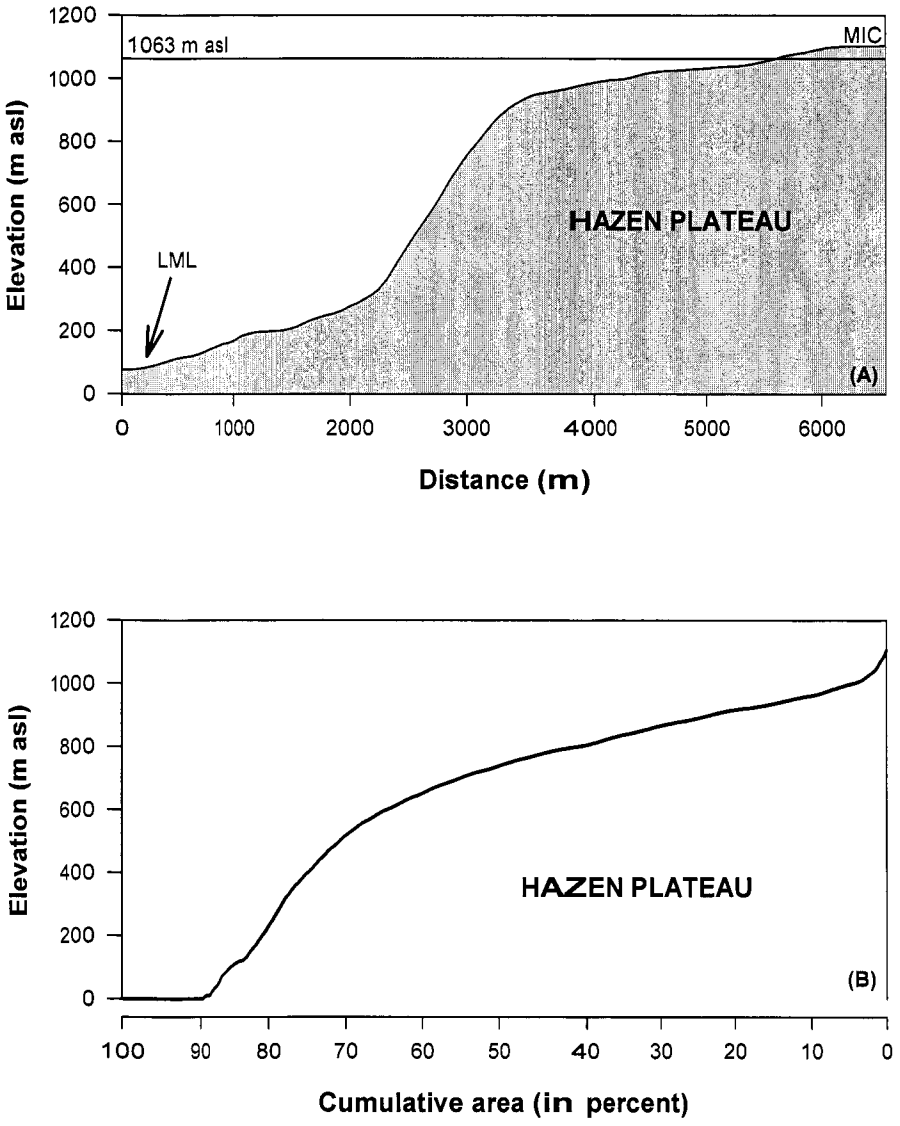

Figure 6.34 (A) Cross-section of the Hazen Plateau along a northeast to southwest transect from Murray Ice Cap down to Lower Murray Lake (LML). The edge of the ice cap along this transect was at about 1063 m asl in 2003. (B) Hypsography of the Hazen Plateau within the spatial domain of the model (cf. Fig. 6.33).

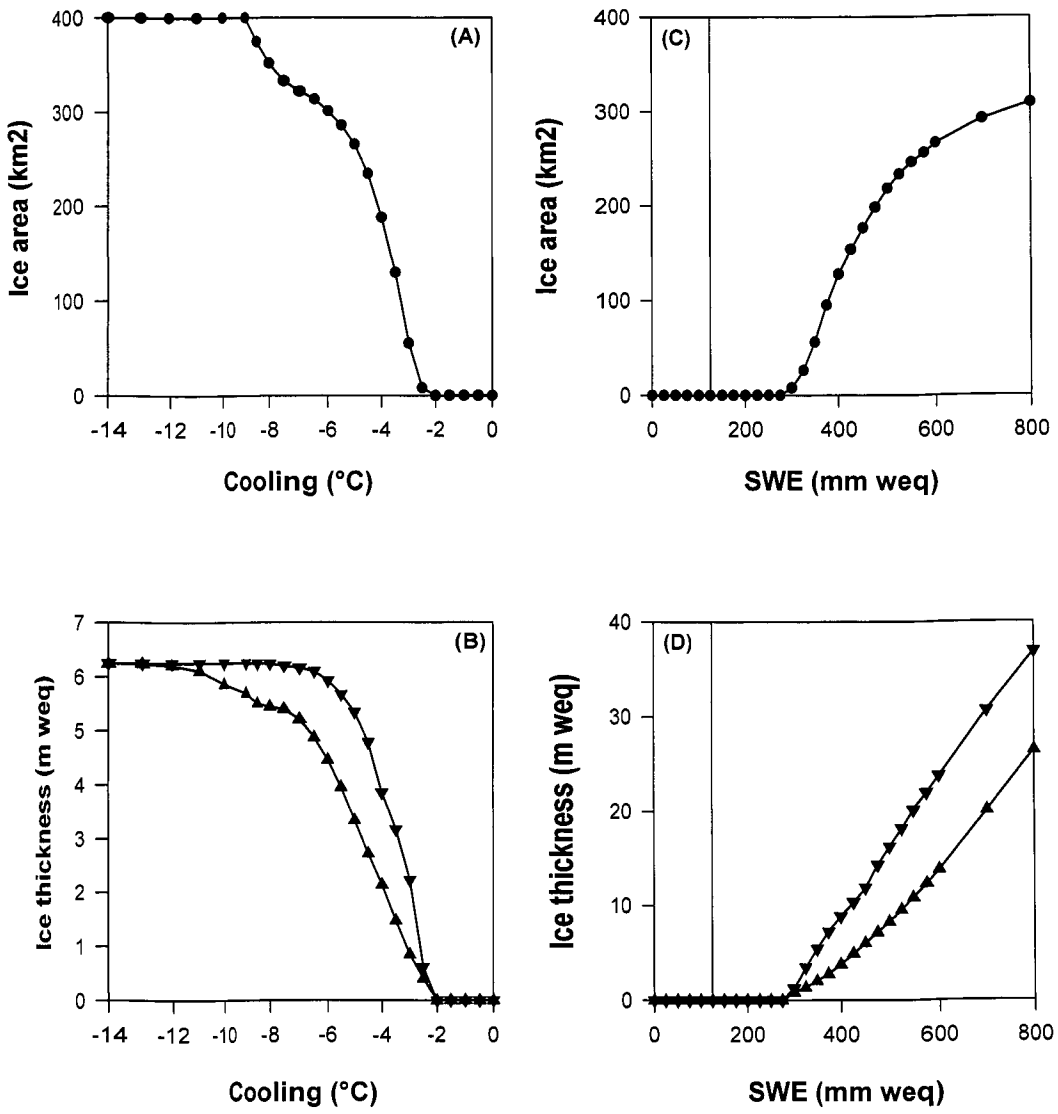

Figure 6.35 Sensitivity of snow and ice cover to changes in air temperature (a, b) or annual snow accumulation (c, d) at the end of a 50 year time period (i.e. a 'snap shot' at model year 50). The downward triangles denote the maximum ice thickness (m weq), whereas the upward triangles denote the mean ice thickness (m weq) at the end of 50 years. Data and parameters in \model_1\. Air temperature lapse rate 5.5°C/1000 m, DDF (snow) = 3.1 mm weq d^{-1} deg^{-1}; DDF (ice) = 6.8 mm weq d^{-1} deg^{-1}; P-max = 0.5; σ (over bare ground) = 4.0°C; σ (over ice) = 3.7°C; maximum elevation of the (initially) ice-free Hazen Plateau within the spatial domain = 1070 m asl, spatial domain ice-free at the start of the 50 year integration, ice-cap cooling effect as shown in Table 6.23. Using AWS T3* climatology, 1951 to 2000, missing monthly values were replaced with the respective long-term means.

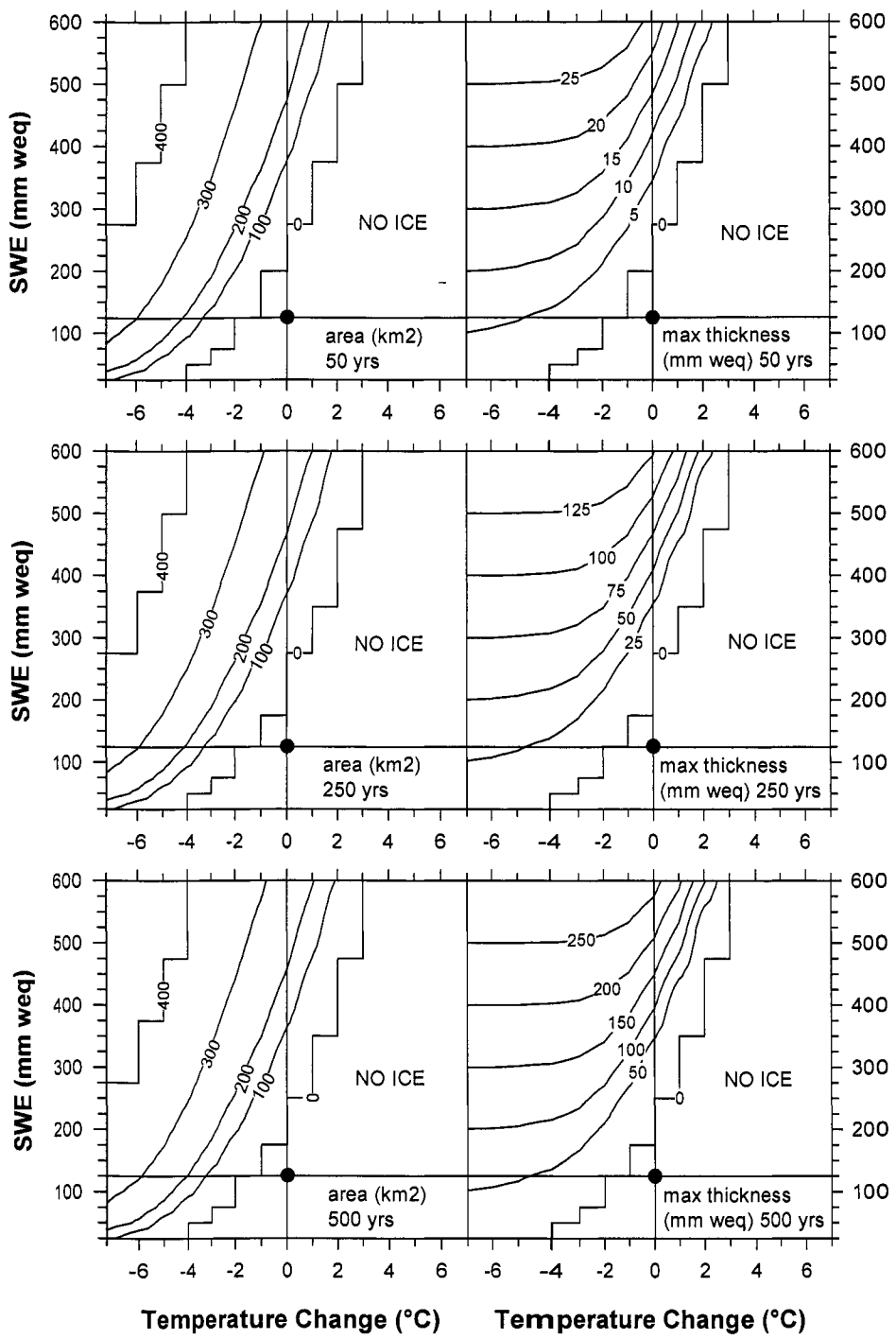

Figure 6.36 Sensitivity of snow and ice cover to changes in air temperature and annual snow accumulation at the end of 50 years (top row), 250 years (middle row), and 500 years (bottom row). The reference lines and circle in each contour plot denote the modern climatic conditions (i.e. 0°C/125 mm weq). Data and parameters in \model_3\. Model parameters as in Figure 6.35. Using AWS T3* climatology, 1951 to 2000, missing monthly values were replaced with the respective long-term means, repeated once for 50 years, five times for 250 years, and 10 times for 500 years.

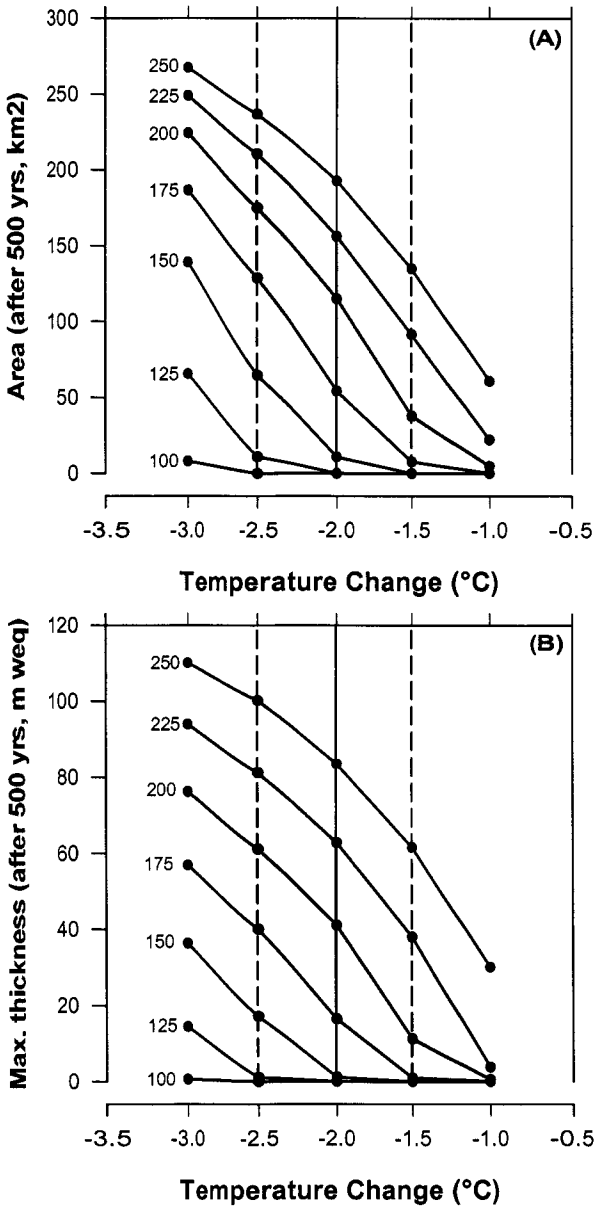

Figure 6.37 The sensitivity of snow and ice cover as a function of air temperature change (from –1°C to –3°C) and annual snow accumulation change (100 to 250 mm weq). (A) Ice area (km^2) and (B) maximum ice thickness (m weq) as a function of temperature change for a different amounts of annual snow accumulation at the end of 500 years. The grey shading (±25 mm weq) and red reference lines (±0.5°C) schematically illustrate the sensitivity of the model results to minor changes in the specific climate change scenario considered. Metadata, data, and figure in \model_4\. Model parameters as in Figure 6.35. Using AWS T3* climatology, 1951 to 2000, missing monthly values were replaced with the respective long-term means, repeated 10 times to yield a 500 year climatology.

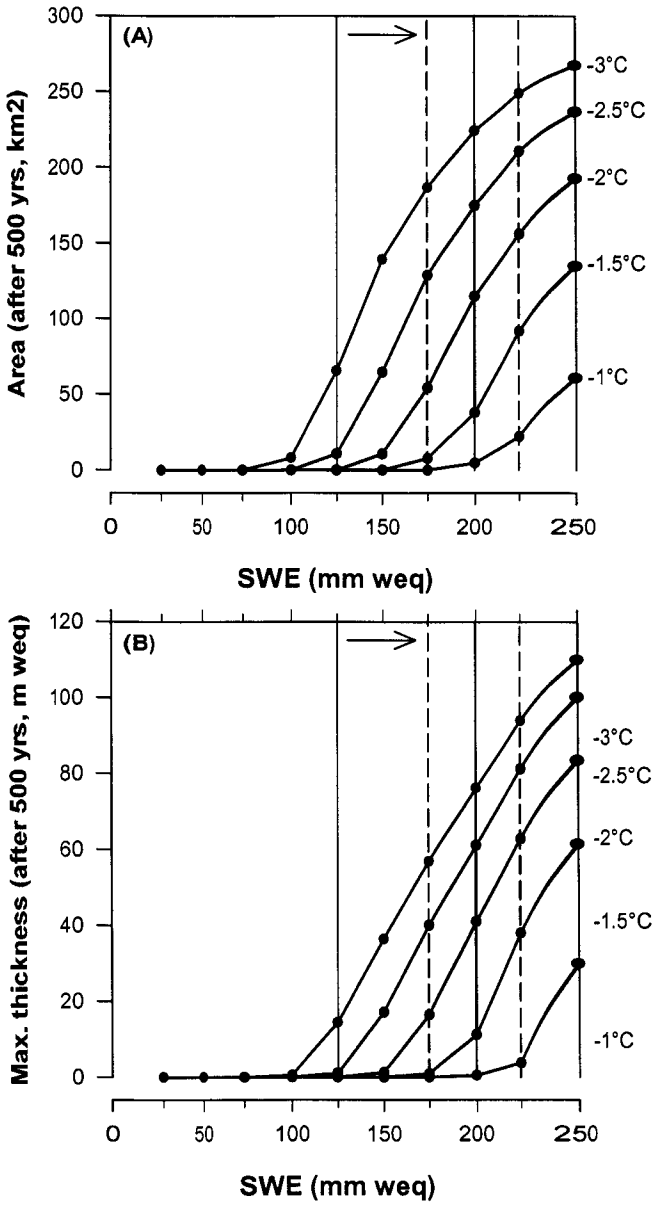

Figure 6.38 As Figure 6.37, except the model results are plotted for different amounts of annual snow accumulation as a function of different levels of cooling.

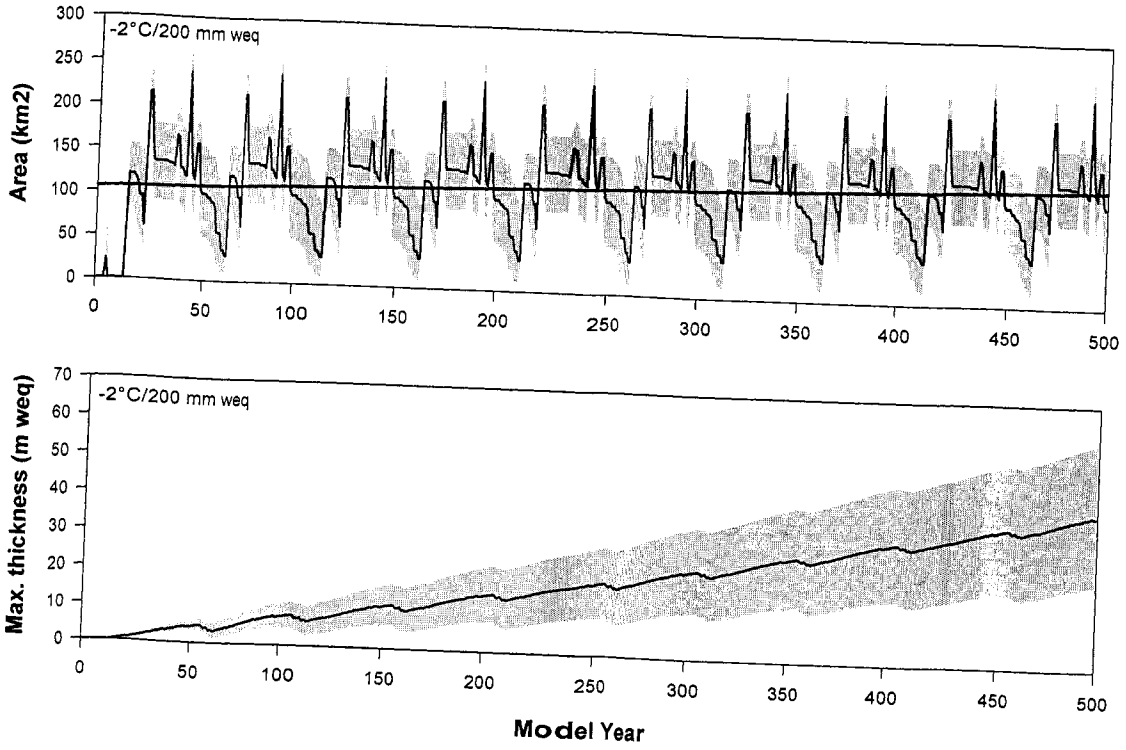

Figure 6.39 Top: Area of ice (km^2), with simple linear trend line; Bottom: Maximum ice thickness (m weq) as a function of time for a climate change scenario of –2°C and 200 mm weq annual snow accumulation. The inter-annual variability of ice area appears 'amplified' since it includes any grid cell that retains any amount of snow in a particular year. Metadata, data, and figure in \model_2\. The black curve represents the model results for the preferred model parameter values, while the upper (lower) bounds of the surrounding grey shading are defined by a respective model parameter combination leading to a 'minimum melt' ('maximum melt') scenario (cf. Table 6.29). Other model parameters as in Figure 6.35. Using AWS T3* climatology, 1951 to 2000, missing monthly values were replaced with the respective long-term means, repeated 10 times to yield a 500 year climatology.

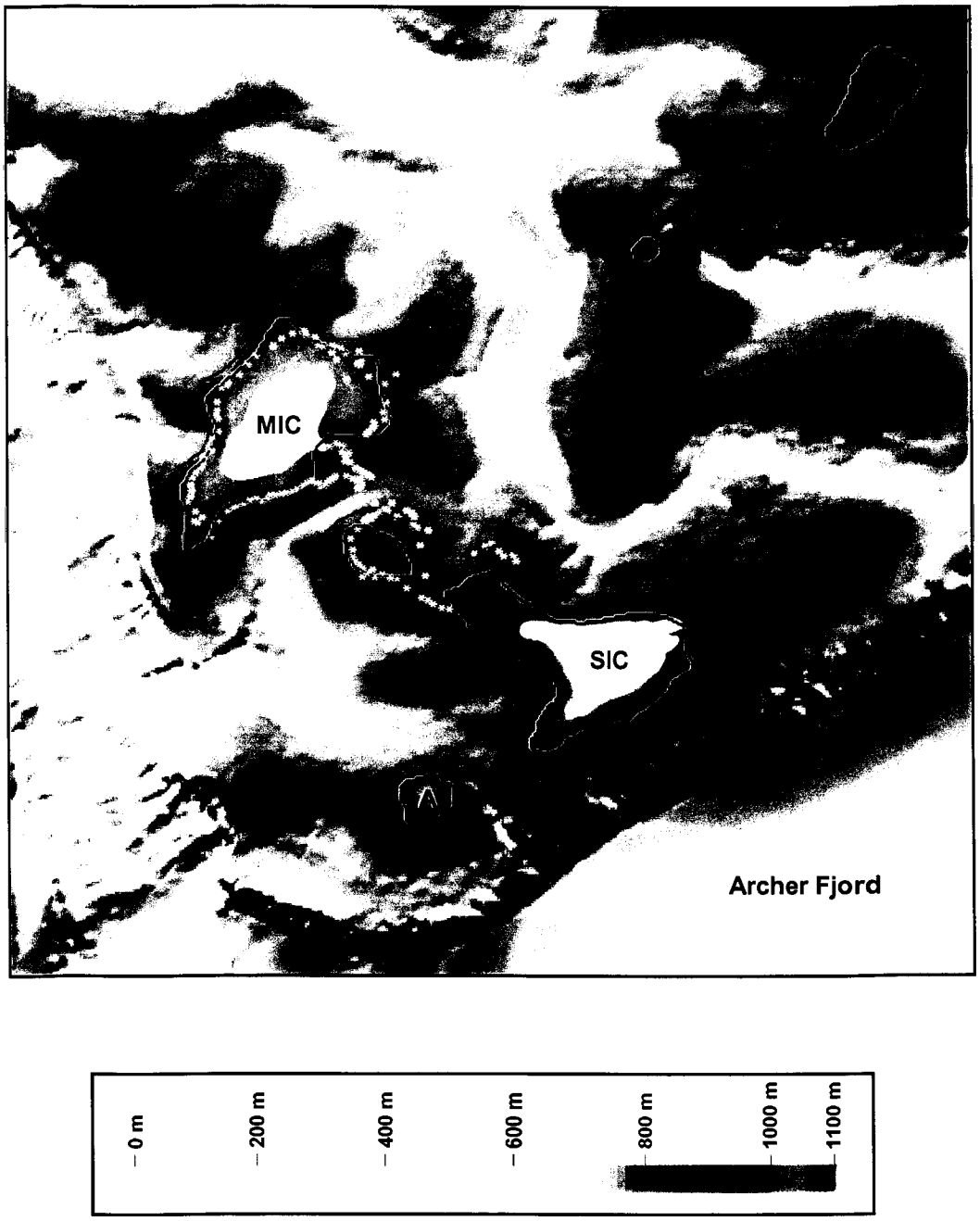

Figure 6.40 Screenshot of the Hazen Plateau GIS showing the digital elevation model (cf. Fig. 6.33) and several area polygons. White polygons: Murray Ice Cap (~2.9 km^2) and Simmons Ice Cap (~3.3 km^2) as mapped in 2003 from a helicopter; dark blue line: 950 m asl elevation contour line (plateau area above hat elevation ~48 km^2); black line: 990 m asl elevation contour line (plateau area above that elevation ~23 km^2). The grey stars mark the actual GPS positions of the lichen trimline as mapped between 1999 and 2001. The plateau hilltop marked as Point A apparently supported a small remnant ice patch as late as 1959 (Bradley and England, 1977) and is devoid of lichen and vegetation cover today (though not mapped in detail).

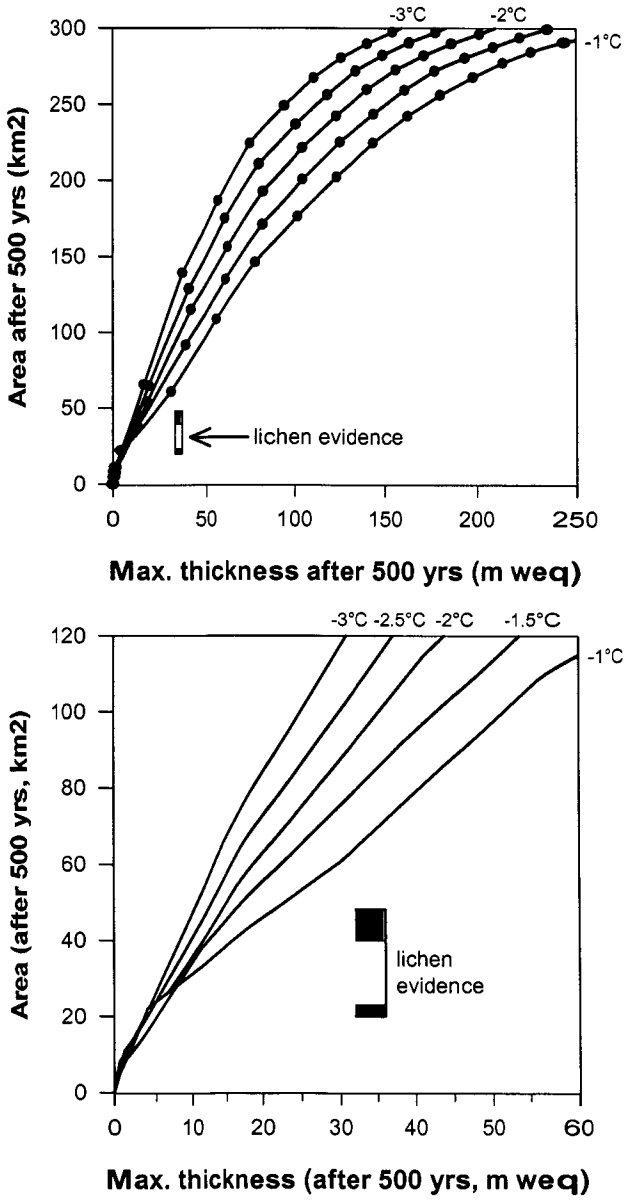

Figure 6.41 (A): Area of modeled ice plotted as a function of its corresponding maximum thickness (after 500 years) for different levels of temperature and precipitation change (cf. Fig. 6.37, 6.38). (B): Close-up of (A) to highlight the mismatch between the modeled ice configurations and the lichen evidence. The grey shading and omission of symbols depicting the actual model results in (B) is meant to illustrate that the spread of the five curves can be viewed as a conservative uncertainty envelope (see text). The black and blue rectangles correspond to the minimum and maximum ice extent scenarios following the traditional interpretation of the lichen evidence as discussed in the text and depicted in Figure 6.40. Metadata, data, and figure in \model_4\. Model parameters as in Figure 6.35. Using AWS T3* climatology, 1951 to 2000, missing monthly values were replaced with the respective long-term means, repeated 10 times to a 500 year climatology.

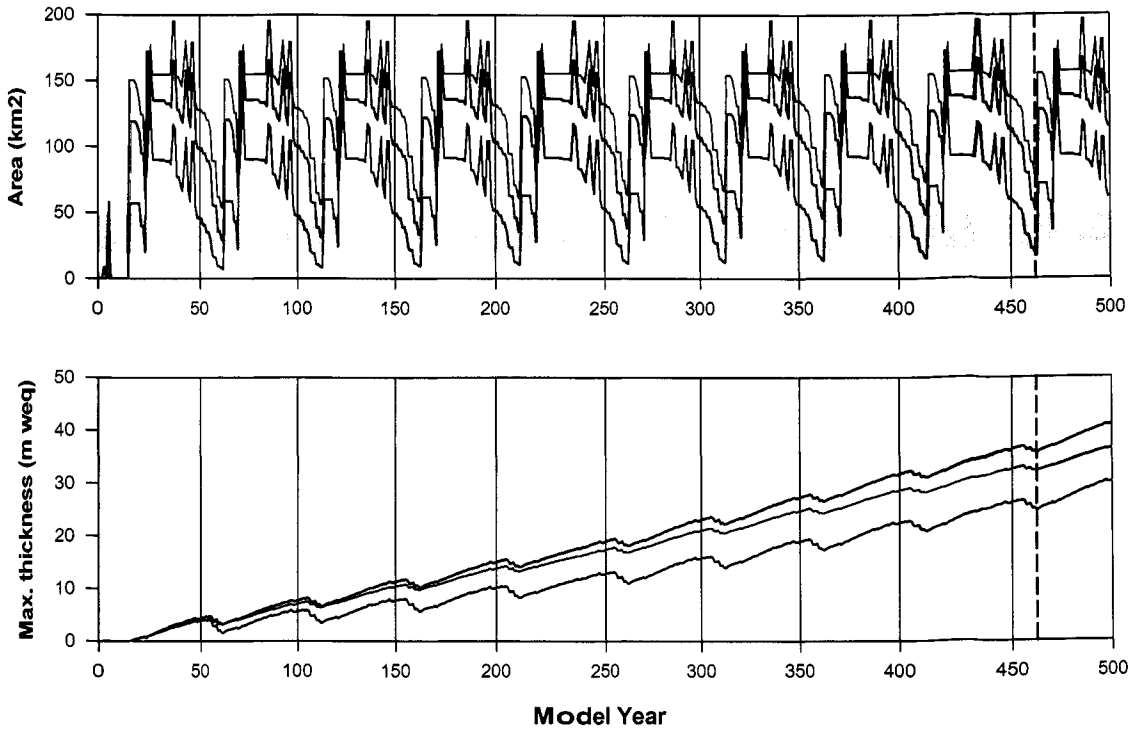

Figure 6.42 Ice area (km^2) and maximum ice thickness (m weq) for three selected climate change scenarios: –1°C/250 mm weq (red curves); –2°C/200 mm weq (black curves); and –3°C/150 mm weq (blue curves). The grey shading denotes the minimum extent of ice (20 to 48 km^2; 32 to 36 m weq) during the 'Little Ice Age', following the alternative interpretation of the lichen trimline found on the Hazen Plateau today (cf. Fig. 6.41). Metadata, data, and figure in \model_2\. Model parameters as in Figure 6.35. Using AWS T3* climatology, 1951 to 2000, missing monthly values were replaced with the respective long-term means, repeated 10 times to yield a 500 year climatology.

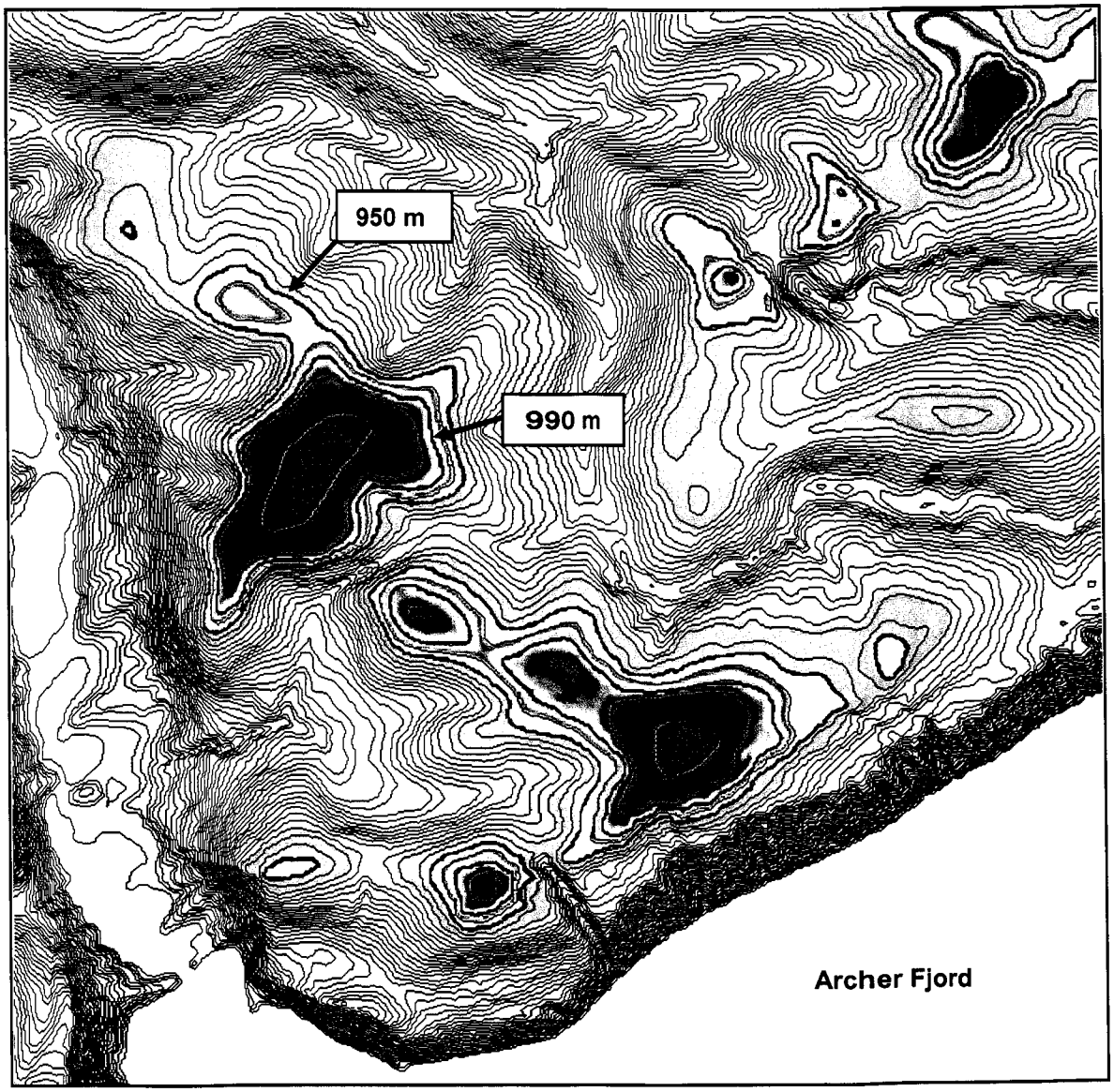

Figure 6.43 Screenshot of the Hazen Plateau GIS showing a grid of ice thickness (m weq) at the end of a 500 year model run for a –2°C/200 mm weq climate change scenario. Metadata, data, and figure in \model_2\. Model parameters as in Figure 6.35. Using AWS T3* climatology, 1951 to 2000, missing monthly values were replaced with the respective long-term means, repeated 10 times to yield a 500 year climatology. Contour interval 20 m. The 950 m and 990 m contour line are shown as thicker lines (black and blue).

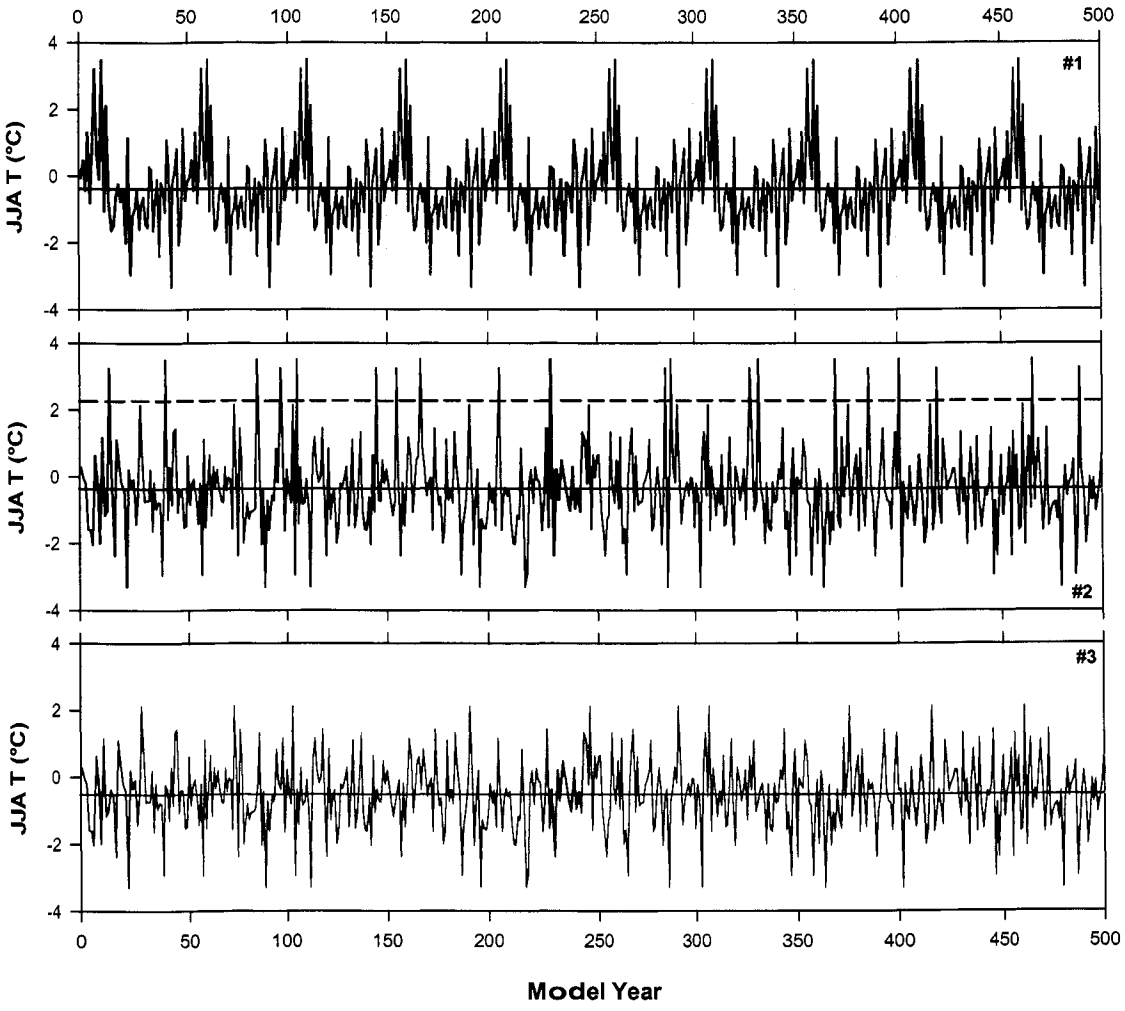

Figure 6.44 Three alternative climatologies for the 'Little Ice Age'. Case #1: AWS T3* climatology, repeated 10 times; Case #2: randomized AWS T3* climatology; Case #3: randomized AWS T3* climatology without anomalously warm summers. The dashed line for case #2 denotes the +1 standard deviation line, used to define anomalous warm summer for case #3. Shown are mean summer (i.e. June/July/August) temperatures, which are highly correlated with annual melting degree-day totals (cf. Chapter 5). The respective means are also shown.

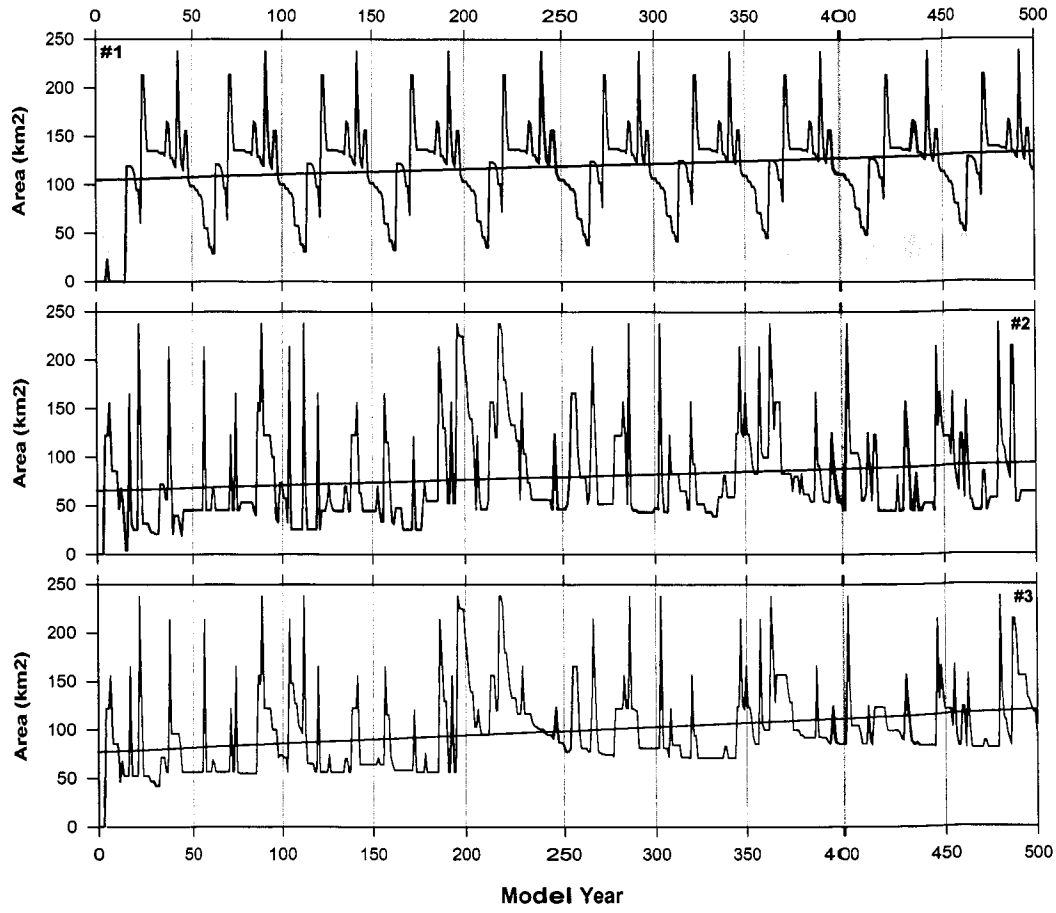

Figure 6.45 Modeled ice area over time and their respective linear trend lines for a climate change scenario of –2°C and 200 mm weq annual snow accumulation for the three climatologies shown in Figure 6.44. The grey shading denotes the minimum extent of ice (20 to 48 km^2) during the 'Little Ice Age', following the alternative interpretation of the lichen trimline found on the Hazen Plateau today (cf. Fig. 6.41). Metadata, data, and figure in \model_2\. Model parameters as in Figure 6.35.

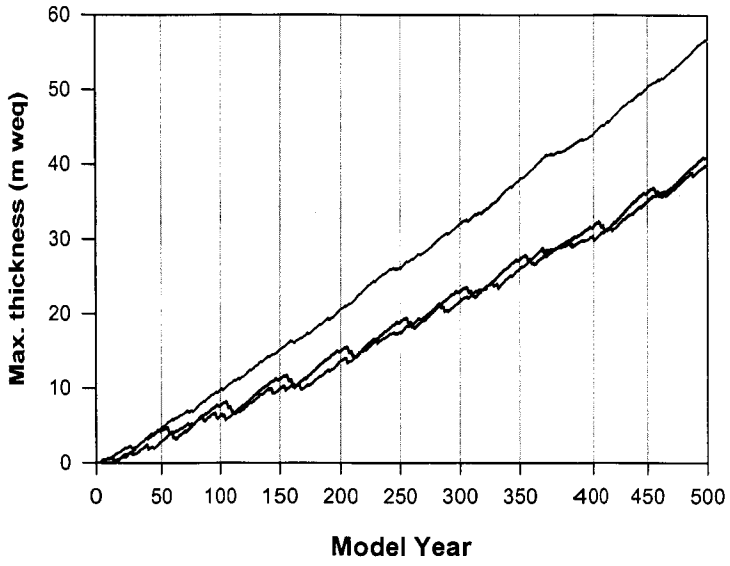

Figure 6.46 As Figure 6.46, but showing modeled maximum ice thickness (m weq). The grey shading denotes the minimum thickness of ice (32 to 36 m weq) during the 'Little Ice Age', following the alternative interpretation of the lichen trimline found on the Hazen Plateau today (cf. Fig. 6.41).

CHAPTER 7

SUMMARY AND CONCLUSIONS

The preceding six chapters represented a subjective attempt to assess and quantify the sensitivity of the Hazen Plateau and North Coast, Ellesmere Island, Nunavut, Canada to climate change. This analysis was focused specifically on the sensitivity of glaciers in those localities to climate change, even though that obviously encompasses only a small fraction of the entire Arctic's ecosystem response to one specific flavor of environmental change (i.e. climate change). For example, the 2005 'Arctic Climate Impact Assessment' Scientific Report (ACIA, 2005) contains a total of 18 chapters, spread over 1042 pages, covering every (currently) conceivable aspect of the 'Changing Arctic', as well as their associated local, regional, and global impacts. For a shorter perspective, see Serreze *et al.* (2000) or Käyhkö and Talve (2002).

7.1 The Climatic Sensitivity of Glaciers

> "The only at present available way of obtaining any knowledge of this aspect of the nature and life of glaciers is by investigating their economy [i.e. mass balance]." (Ahlman, 1936)

Chapter 2 ('Glaciation of the Hazen Plateau and North Coast, Ellesmere Island, Nunavut, Canada') presented a comprehensive, albeit subjective, discussion of the climatic sensitivity of glaciers, with a focus on those occurring today in high latitudes. The global recession of glaciers is frequently used today to provide qualitative (e.g. Houghton *et al.*, 2001) and sometimes even quantitative (e.g. Oerlemans, 2005; Raper and Braithwaite, 2006) support to the observed rise in global temperatures and sea level since the late 19th century. In this context, the statement by Ahlman (1936) quoted above remains as true today as it was some 70 years ago. Techniques and methodologies used regularly in glaciological research have certainly advanced over the years, although that did/does not necessarily expand our fundamental understanding of glaciers and their climatic sensitivities, as we are today, perhaps, frequently too pre-occupied with the technical and methodological aspects of this type of

research. Furthermore, the number of operational glacier mass balance programs have been decreasing world-wide in recent years (Dyurgerov, 2002), sometimes terminating invaluable long-term mass balance series. This is certainly an ongoing concern with respect to the glacier mass balance measurement program currently operational in the Canadian High Arctic.

In the future, sophisticated remote sensing techniques may provide an operational, truly global, 'Earth Information System' (Karl and Trenberth, 2003) in real-time, but for now such measurement techniques are effectively limited to a small number of dedicated (and specially equipped) glaciers or watersheds (e.g. Molotch *et al.*, 2004), or case studies (e.g. Adam *et al.*, 1997; Arendt *et al.*, 2002; Smith *et al.*, 2003; Abdalati *et al.*, 2004; Rignot and Kanagaratnam, 2006). Ahlman (1936) already realized a long time ago that a more complete understanding of the relationships between glaciers and climate will require much more detailed and comprehensive process measurements at appropriate spatial and temporal scales:

> "Glaciology needs meteorological observations of a special kind, and can no longer be content with the ordinarily developed schedule." (Ahlman, 1936)

Today, it is quite possible, even trivial, to routinely measure and communicate whatever data are desired by glaciologists, even in/from remote and extreme environments, using automated weather stations and instruments, even though the necessary data quality control still represents considerable challenges. However, the spatial distribution of these detailed point measurements across a watershed, glacier, or region still presents significant and largely unsolved problems, which is why this study relied solely on air temperature and precipitation for the snow/ice melt parameterization. It is currently impossible to quantify, in a truly robust and operational manner, appropriate interpolation and extrapolation algorithms in this context, especially given the wide ranges of spatial and temporal variability and scales involved. Blöschl (2006), for example, took this notion one step further and argued that the information required for robust up-scaling procedures "...may be unknowable". Thus, a more promising observational strategy should emphasize data collection already at the appropriate spatial and temporal scales (cf. Blöschl, 2006), rather than relying on some ill-defined integration or extrapolation techniques (e.g. Moore *et al.*, 2002).

The existing glacier mass balance data are strongly (spatially) biased towards Western Europe, North America, and the former USSR, with too few measurements from other parts of the world (Braithwaite, 2002). They are also biased in a temporal sense, as most available glacier mass balance series span less than 15 years, with varying degree of temporal overlap mainly between 1960 and 1990 (Dyurgerov and Meier, 1997; Braithwaite, 2002). The existing mass balance data are also skewed towards maritime climatic conditions and do not adequately capture the cold-dry climates found in many glaciated polar regions (Braithwaite, 2002). Finally, there is also a glacier-size bias to the exclusion of very small and very large glaciers and ice caps (Dyurgerov and Meier, 1997; Cogley and Adams, 1998; Meier *et al.*, 2003; Raper and Braithwaite, 2005a).

At the same time, the climatic sensitivity of a given glacier or ice cap is very much a function of its specific internal characteristics (e.g. size, slope, flow, hypsography, etc., cf. Fig. 2.9) as well as its specific climatic setting. This situation makes it obviously difficult to compare different glaciers from around the world, and their respective climatic sensitivities, in order to derive a robust global signal or pattern. This particular issue is well illustrated by the study presented by Raper and Braithwaite (2005a), the resultant challenge (Meier *et al.*, 2005), and the response of the authors (Raper and Braithwaite, 2005b). That particular argument essentially revolved around the appropriate statistical treatment of very small or very large glaciers in a global compilation and the inclusion (or rather the exclusion) of the many glaciers and ice caps that surround the two big ice sheets today. These glaciers are typically "lumped" into the Greenland and Antarctic Ice Sheets in modeling studies, even though their climatic sensitivity is presumably much greater. On the other hand, given a sufficient number of samples and an appropriate classification system (cf. Blöschl, 2006), the uniqueness of each glacier can be used to assess their specific responses to climate change across a wide variety of spatial and temporal scales (e.g. Hoelzle *et al.*, 2003). The observational strategy of the 'Global Terrestrial Network of Glaciers' (GTN-G; http://www.fao.org/gtos/gt-netGLA.html), a component of the Global Terrestrial Observing System (GTOS; http://www.fao.org/gtos/), therefore, calls for long-term observations of (at least) glacier length changes at a minimum of 10 spatially-representative sites within each mountain range around the world.

Last year's 'Arctic Climate Impact Assessment' Scientific Report (ACIA, 2005) defined the following four (broad) critical research objectives with respect to (Arctic) glacier mass balance:

1. Compilation of an up-to-date global glacier mass balance inventory.
2. Additional glacier mass balance observations in regions of particular sparse coverage.
3. Continuation of on-going mass balance measurement programs.
4. Development of more sophisticated glacier mass balance models that capture the spatial variability of the cryosphere through time.

These recommendations are, not surprisingly, consistent with those of other studies (e.g. Dyurgerov and Meier, 1997; Braithwaite, 2002; Dyurgerov, 2002), as well as common sense, but may prove to be difficult to implement given the current political and economic reality. Braithwaite (2002) thus concluded his review of the first 50 years of international glacier mass balance monitoring by noting:

> "Direct mass-balance measurements, using stakes and snowpits, is a very laborious [i.e. expensive] way of detecting climate change and should be increasingly combined with modern geodetic methods and remote sensing, especially laser profiling, in the future."

7.2 The Climatic Sensitivity of Northern Ellesmere Island

7.2.1 The North Coast

Hattersley-Smith and Serson (1970) started their paper, which summarized the first 10 years of mass balance measurements on the Ward Hunt Ice Rise and Ice Shelf, by stating:

> "Since the recognition in 1950 that ice shelves occur off the north coast of Ellesmere Island (Koenig and others, 1952), there has been speculation on whether they should be considered as relict features or as essentially the product of present climatic conditions."

The answer to that particular question is quite clear today: the Ward Hunt Ice Rise and Ice Shelf are not in equilibrium with current climatic conditions, currently have no mass accumulation (area), and will disappear at some point in the near future unless climatic conditions deteriorate dramatically. This answer, unfortunately, stands in contrast with the answer provided by Hattersley-Smith and Serson (1970) in the last sentence of their paper that "...neither the ice rise nor ice shelf should be considered as a relict

glacial feature." Their conclusion was consistent with Hattersley-Smith's first impressions after his first reconnaissance field season in 1953:

> "However, it was the impression of the writer last summer [i.e. 1953] that the ice shelf is wasting very slightly, on average perhaps only a few centimeters a year with some years scarcely any surface loss at all." (Hattersley-Smith, 1954)

This statement is noteworthy for two reasons in that (1) it expresses a (subjective) feeling that the ice shelf was fairing quite well in term of its annual surface mass balance, and (b) it already alludes to the fact that the processes (i.e. mass gains or mass losses) at the bottom of the floating ice shelf are entirely unknown (cf. Hattersley-Smith and Serson, 1970). However, in the very next sentence, he already implies that the situation may not be quite as favorable (on average):

> "Where pits were dug in the ice shelf last summer [i.e. in 1953], there were usually 0.3 to 0.6 m, sometimes less, of last winter's snow resting on a weathered and pitted surface of old ice." (Hattersley-Smith, 1954)

This particular finding was very significant, as it immediately implied that there is not net mass accumulation on the ice shelf, which is identical to the situation discovered by Baird *et al.* (1952) on the Barnes Ice Cap on Baffin Island (cf. Chapter 2), who commented upon this finding: "This was disconcerting." It remains the situation today on the Ward Hunt Ice Rise/Shelf and Hazen Plateau ice caps. Also significant in this context was the discovery of an old camp site from Peary's 1906 expedition, which implies that there was no net accumulation of mass for the first half of the 20th century. Debenham (1954) was also of the opinion that the ice shelf "continues to lose from the top and gain from the bottom", which would provide an explanation for the occurrence of marine mud, sand, and even sponges on the surface of the ice shelf. It is therefore not surprising that his subsequent paper (Hattersley-Smith *et al.*, 1955) paints a much more pessimistic picture with respect to the long-term stability of the Ward Hunt Ice Shelf. However, that perception changed again in the mid-1960s, when much of the Canadian High Arctic experienced overall colder summers, increased precipitation, positive glacier mass balance, and glacier expansion (e.g. Hattersley-Smith and Serson, 1970; Bradley and Miller, 1972; Alt, 1987).

In the early-to-mid 1980s, Martin Jeffries and colleagues spent several field seasons investigating the physical and chemical properties of the ice shelves along the North Coast (e.g. Jeffries

and Krouse, 1984, 1987; Jeffries, 1994, 2002), but without publishing any especially noteworthy concerns about their stability. The Ward Hunt Ice Rise and Ice Shelf were literally forgotten until the beginning of the 21st century when biologists from Laval University, Quebec, became interested in the unique microbial communities that live inside and around the summer meltwater lakes on the ice shelf. Papers by Vincent *et al.* (2001), entitled 'Ice-shelf collapse, climate change, and habitat loss in the Canadian high Arctic' and Mueller *et al.* (2003), entitled 'Break-up of the largest Arctic ice shelf and associated loss of an epishelf lake' raised considerable public concerns about the alleged immanent loss of the Ward Hunt Ice Shelf and its associated rare ecosystems. The fundamental 'take-home' message that comes out of this review of the past research on the Ward Hunt Ice Rise and Ice Shelf is to not over-interpret the results of a single year, single field season, or single observation (cf. Braun *et al.*, 2004b).

The (possible) (in)stability of the Earth's ice shelves has received increased scientific and public attention in recent years (e.g. Mueller *et al.*, 2003; Rignot *et al.*, 2004, Scambos *et al.*, 2004, Thomas *et al.*, 2004), since the ice shelves are believed by some to provide an important 'footing' or 'buttress' for some of the large inland glaciers in Antarctica (Hindmarsh, 1993; Dupont and Alley, 2005). At still larger scales, the catastrophic break-up of the ice shelves, that may have fringed Canada's east coast at times of extreme cold and disintegrated during periods of relative warmth, may have been an/the iceberg source during Heinrich events (Hulbe *et al.*, 2004).

The main indirect conclusion from this study is the realization that that mass losses occurring at the bottom of the floating ice shelf are probably more significant in terms of its stability than the associated surface mass losses. This conclusion concurs with the evidence from the Antarctic ice shelves (cf. Section 6.4.4.5). It is also certainly not a new idea with respect to the Ward Hunt Ice Shelf (e.g. Debenham, 1954; Hattersley-Smith and Serson, 1970). Debenham (1954) in fact already identified 50 years ago two significant gaps in available data and understanding with respect to the long-term stability of the Ward Hunt Ice Shelf:

1. Debenham concluded that most (if not all) of the ice shelf's mass gains must come "from increments from below", but "...we don't know the much about the thermal conditions there." Unfortunately, not much has changed over the last 50

years in terms of our understanding of the processes occurring at the bottom of floating ice shelves. This is obviously one of the most inaccessible places anywhere on Earth, thus requiring advanced remotely-operated vehicles to gain access (http://www.rov.org/). But even these high-tech 'robots' can only provide a very short temporal 'snap shot' of the sub-ice shelf conditions and processes and should be therefore combined with permanently moored systems at key locations, which can provide continuous process measurements over many years.

2. Debenham also suggested that, in order to ascertain the stability of the ice shelf, a transect of ice shelf thickness measurements from the coast line to the outer ice shelf edge would be very useful. Again, even 50 years later, we are still working with only a handful of discrete point measurements (cf. Fig. 6.30) of ice shelf thickness. It would be useful to develop a three-dimensional model of the current ice shelf and sea floor geometry to provide a basis for assessing any future changes that might lead to the break-up of the remaining ice shelf.

Beyond that, a wide range of additional measurements and observations would be desirable, many of which have already been formalized in a (rejected) proposal to the National Science Foundation. At the very least, the automated weather station operated by Parks Canada on Ward Hunt Island should be complemented by similar instrumentation at a suitable location on the Ward Hunt Ice Rise and the Ward Hunt Ice Shelf.

7.2.2 The Hazen Plateau

The entire issue of the climatic sensitivity of the Hazen Plateau and the Hazen Plateau ice caps can be synthesized into one single question: How old are the Hazen Plateau ice caps?

Unfortunately, this study was not able to provide a definitive answer to this question. The mass balance history of the Hazen Plateau ice caps was compiled and reviewed in Chapter 3 (i.e. Braun *et al.*,

2004a). Hattersley-Smith and Serson (1973) came to the following two main conclusions after two short reconnaissance visits to the St. Patrick Bay ice caps in the summer of 1972:

1. "It is shown that, after a period of net wastage, this ice cap [i.e. the larger of the two St. Patrick Bay ice caps] is now thickening slightly and extending its margin."
2. "The present regime of the ice cap [i.e. the larger of the two St. Patrick Bay ice caps] is a direct result of the generally cooler summers in the last decade."

This general opinion was echoed a few years later by Bradley (1975), who suggested that between 1963 and 1972, "...a large upland area in the Canadian High Arctic [i.e. the Hazen Plateau] experienced predominantly positive mass-balance years." Unfortunately, this period of apparent glacier health came to an end shortly thereafter and the Hazen Plateau ice caps have since experienced predominately negative mass balance years and a considerable reduction in their volume and area. At current down-wasting rates, they will completely disappear by, or soon after, the mid-21st century.

The modeling results did confirm the original hypothesis of the study (cf. Chapter 1) that the Hazen Plateau is indeed an environmentally-sensitive region, and small changes in the climatic conditions can lead to large changes in the extent and persistence of snow and ice cover. A formation of the Hazen Plateau ice caps during the so-called 'Little Ice Age' is entirely possible, given reasonable levels of cooling, but not without significant increases in annual snow accumulation. There is certainly no empirical evidence today for a colder and wetter 'Little Ice Age' climate, yet the possibility remains that so far unidentified changes in atmospheric circulation patterns may have resulted in increased precipitation during the 'Little Ice Age' (cf. Section 7.3). For example, it is possible that the High Arctic cooling during the 'Little Ice Age' was mainly a summer phenomena (cf. Section 6.5.1.1), but was accompanied by a relative warming during the winter month, which may have led to increased annual precipitation and snow accumulation (cf. Zhang *et al.*, 2000). This speculation is not without empirical evidence: during the 'melt suppression decade' (Alt, 1987) (~1963 to 1972), summer temperatures decreased, July freezing levels dropped, winter temperatures increased, and winter/annual precipitation increased (Bradley and Miller, 1972; Bradley, 1973).

Another intriguing possibility to resolve this question would involve an ice-core drilling campaign on the four remaining Hazen Plateau ice caps. It is very doubtful that such ice cores could

provide a useable record of past climatic variability (cf. Koerner, 1997; Pohjola *et al.*, 2005; Henderson *et al.*, 2006), but the isotopic and physical characteristics of the (basal) ice may indicate whether the ice was formed at a time of severe cold (i.e. the Last Glacial Maximum, cf. England *et al.*, 2006) or at a time of relative warmth (i.e. the mid to late Holocene) (cf. Koerner, 1989b; Koerner and Fisher, 2002). Alternatively, the lake sediments in Murray Lake should contain some evidence reflecting the extent and timing of ice cover on the surrounding Hazen Plateau (e.g. Karlen, 1981; Miller *et al.* 2004). That, in fact, was the original impetus behind coring Murray Lake.

Beyond that, it does not seem particularly useful to continue an intensive glaciological measurement program on the Hazen Plateau ice caps. For example, Bradley and Serreze (1987a) concluded:

> "Overall, the ice caps today are wasting away and will eventually disappear if contemporary conditions are any guide to the climate of the next century or two. In the sense that they provide no long-term record of climate, they do not really provide any better indication of climatic variability than the Alert instrumental record."

However, the Hazen Plateau ice caps will be probably amongst the first victims of 'Global Warming' in the High Arctic, thus tracking their demise by aerial or satellite surveys on an annual basis would provide a valuable (and very visual) documentation of environmental change.

7.3 The Future of the High Arctic Cryosphere

> "The modern period [i.e. the warm late 1950s] may represent a break before another small deterioration of climate sets in and upward growth of the [Ward Hunt] ice shelf is resumed; or, if climatic conditions remain the same or improve further, the frequent calving of ice islands in late years may mark the beginning of complete disintegration and disappearance of the [Ward Hunt] ice shelf, an event which might be the precursor of an open Arctic Ocean." (Hattersley-Smith, 1960a)

> "At the present rate of change, a summer ice-free Arctic Ocean within a century is a real possibility, a state not witnessed for at least a million years." (Overpeck *et al.*, 2005)

The 2005 'Arctic Climate Impact Assessment' Scientific Report (Chapter 4; Kattsov and Källen, 2005) estimated an Arctic-wide annual temperature increase by 2050 of about +2.5°C, and a +5°C

increase by the end of the 21st century (assuming the IPCC B2 emission scenario). Spatially, the greatest temperatures increases are predicted to occur in parts of the Canadian High Arctic and Russian Arctic. Seasonally, the greatest temperature increases are expected during the fall and winter season because of reduced Arctic Ocean sea ice cover and thickness. By contrast, projected temperature increases over the Arctic Ocean and surrounding land areas in the summer remain below about 1°C throughout much of the 21st century because of the moderating influence of melting sea ice. Projected precipitation increases by the end of the 21st century range from about 5 to 10 percent to as much as 35 percent in some High Arctic locations. Seasonally, the largest precipitation increases are predicted for the fall and winter season because of reduced Arctic Ocean sea ice cover and thickness.

In terms of glacier mass balance, the ACIA (2005) model projections indicated a continuation of the already observed trends (e.g. mass losses and recession) throughout the 21st century, although the rates of the projected changes vary widely between the different models (ACIA, 2005, their Fig. 6.19). This model spread is presumably on one hand a reflection of the high-degree of climatic sensitivity of the Arctic cryosphere, and on the other hand a reflection of model sensitivity, model assumptions, and model uncertainty. One model (CSM_1.4), for example, projects a large enough precipitation increase over the next 100 years to fully compensate for the enhanced ablation associated with its modest projected temperature increase. This type of 'greenhouse-induced' glacier expansion has been speculated on before (e.g. Miller and de Vernal, 1992), but is not supported by any empirical evidence (cf. Chapter 2) or the vast majority of modeling studies (e.g. Braithwaite *et al.*, 2002).

Going back in time, there is solid evidence from snow-pit and firn-core studies (Hattersley-Smith, 1963; 1969) and instrumental observations for elevated summer temperatures, increased glacier melting, and glacier recession in the period from about 1925 to 1961 (Diamond, 1960; Davies and Krinsley, 1962; Holdsworth, 1984; Koerner, 1996, 2001; Bengtsson *et al.*, 2004; Johannessen *et al.*, 2004). This suggests overall more negative glacier mass balances in the Canadian High Arctic and northern Greenland during the first part of the 20th century, compared to the last 40 years of direct glaciological measurements (Fristrup, 1951; Koerner, 1996). However, Bengtsson *et al.* (2004) noted more recently that present warming in the Arctic has now surpassed the peak warming values of the

1940s (cf. Davies and Krinsley, 1962; Warren, 1990), a situation not witnessed in the Canadian High Arctic since perhaps the Early Holocene.

Given the above considerations, it is clearly prudent to not over-interpret inter-annual variability into a temporal trend and results of a single, site-specific study (or model) into a coherent, large-scale pattern. However, given the consistency of the observed and (most of) the predicted changes, especially when viewed in the context of the last 50 to 100 years, one cannot help being quite pessimistic about the future of the High Arctic or global cryosphere. Entering the field of glaciology may not be a wise career choice today! (unless one plans to work on the Greenland or Antarctic Ice Sheet). Nevertheless, there are plenty of exciting opportunities for future research that go beyond merely documenting the demise of High Arctic glaciers. Time is a limiting factor here given the rate(s) of the observed and predicted cryospheric change(s), which not only endanger the physical existence of glaciers, but also threaten the preservation of future paleoclimatic records recovered from glaciers (Koerner, pers. comm.; Henderson *et al.*, 2006).

7.3.1 High Arctic Glacier Mass Balance Measurements

It is obviously imperative to continue and expand the existing glacier mass balance measurement programs in the Canadian High Arctic, which may prove to be a problem given the advanced age of some of the main players involved and the apparent disinterest of funding agencies to commit any/sufficient resources for this type of environmental monitoring. Eight glaciers are currently being monitored in the Canadian High Arctic on a regular (i.e. annual) basis:

- Devon Ice Cap, Melville South Ice Cap, Meighen Ice Cap, and Drambuie Glacier (Agassiz Ice Cap), monitored under the auspices of the Geological Survey of Canada.
- White and Baby Glacier (Axel Heiberg Island, net annual mass balance only), monitored under the auspices of Trent University, Ontario.

- Ward Hunt Ice Rise and Ward Hunt Ice Shelf (net annual mass balance only), monitored under the auspices of Parks Canada and the University of Massachusetts.

Additional observation should be initiated on one of the large 'maritime' glaciers on northern Ellesmere Island (e.g. Disraeli Glacier) and on one of the large 'continental' glacier on the other side of the Grantland Mountains (e.g. Gilman Glacier). Simple mass balance measurement on the Hazen Plateau ice caps should be continued in conjunction with annual area surveys. It will be probably possible at some point in the future to measure the mass balance of the High Arctic glaciers remotely (e.g. Adam *et al.*, 1997; Arendt *et al.*, 2002; Abdalati *et al.*, 2004) but, until then, manual measurements need to be continued (cf. Braithwaite, 2002) in order to ensure a complete and consistent baseline of observations.

7.3.2 Climatic Controls on High Arctic Glacier Mass Balance

Many authors have in the past implied or speculated that changes in large-scale atmospheric circulation patterns may, ultimately, be responsible for changes in glacier mass balance and glaciation in the Canadian High Arctic (e.g. Barry, 1966, Barry *et al.*, 1971; Lamb and Woodroffe, 1970; Bradley and Miller, 1972; Bradley, 1973; Loewe, 1971; Johnson and Andrews, 1979). This (obvious) notion continues to be mentioned today in the literature (e.g. Bromwich *et al.*, 2002; Marshall, 2002; ACIA, 2005), albeit without any further elaboration as to the precise processes and mechanisms involved.

Bradley and England (1979) and Bradley and Eischeid (1985) already linked synoptic-scale atmospheric circulation patterns over the Canadian High Arctic to summer temperature and annual precipitation variability and argued that small changes in the frequency of these synoptic patterns can have a marked climatic consequences. Alt (1979, 1987) extended this approach by relating 'extreme' mass balance conditions as measured on the Canadian High Arctic glaciers to specific patterns or types of atmospheric circulation. Boon *et al.* (2003) revisited Alt's approach and explained an extreme melt event 28 to 30 July 2000 on John Evans Glacier with the occurrence of an unusual 'chinook-type' atmospheric circulation pattern. Finally, Wang *et al.* (2005) linked inter-annual variations in melt duration on the large

Canadian High Arctic ice caps between 2000 and 2004 to the height of the 500 hPa atmospheric pressure level.

Elsewhere in the world, numerous studies (e.g. Ebbesmeyer *et al.*, 1991; McCabe and Fountain, 1991; Hodge *et al.*, 1998; McCabe *et al.*, 2000; Meier *et al.*, 2003; Fealy and Sweeney, 2005; Nordli *et al.*, 2005) have linked contemporary glacier mass balance variability to atmospheric circulation variability, expressed, for example, by the Arctic Oscillation (AO), the North Atlantic Oscillation (NAO), the Southern Oscillation Index (SOI), and the Pacific Decadal Oscillation (PDO). Nesje and Dahl (2003) recently concluded that changes in large-scale atmospheric circulation patterns (i.e. the NAO) led to increased winter precipitation, lower summer temperatures, and glacier expansion in southern Norway during the first half of the 18th century (i.e. during the so-called 'Little Ice Age') (cf. Nordli *et al.*, 2005). At the same time, Shabbar *et al.* (1997) showed that winter temperature variability in northeastern Canada, is closely related to the corresponding variability of the NAO (cf. Bradley and England, 1979; Zhang *et al.*, 2000).

The link between glacier mass balance and synoptic atmospheric circulation patterns has already been established by Bea Alt in the 1980s. This approach could be easily extended to the present, given that some 20 years of additional data (and additional types/sources of data) are now available (e.g. Andrews, 2001). What is missing is the link between glacier mass balance, synoptic-scale atmospheric circulation patterns, and the relatively recently discovered characteristic modes of atmospheric variability, specifically the AO and the related NAO. Unfortunately, both are best expressed during the wintertime (Serreze *et al.*, 2000; Bradley *et al.*, 2003), a season that is not particularly important in terms of glacier mass balance variability in the Canadian High Arctic at inter-annual time scales. Nevertheless, such a study could provide an important link (or lack thereof) between the local climatic conditions (expressed as glacier mass balance variations in time and space) across the High Arctic and the larger-scale climatic conditions, and its associated variability, in the Northern Hemisphere. As noted in Chapter 2, precipitation (i.e. snowfall) can be viewed as an important 'background' control on glaciation, upon which the inter-annual glacier mass balance variability due to summer melting is superimposed.

Bromwich *et al.* (2004) recently presented a plausible mechanism that would be able to substantially increase precipitation in the Canadian High Arctic during the Last Glacial Maximum. Their

study, if independently confirmed, would represent a major paradigm shift and remove one of the main arguments (that of severe aridity) against the existence of a vast and thick Innuitian Ice Sheet during the Last Glacial Maximum (cf. England *et al.*, 2006). However, this proposed 'wetter-than-today' Last Glacial Maximum still needs to be reconciled with the existing ice core evidence from the Canadian High Arctic and Greenland, which shows reduced accumulation rates during the Last Glacial Maximum (e.g. Fisher *et al.*, 1983; Koerner, 1989a; Cuffey and Clow, 1997; Alley, 2000).

7.3.3 The Role of the Arctic Ocean in Glaciation of the High Arctic

Hattersley-Smith (1960a) raised some intriguing points about climate change and glaciation changes, and the role of the Arctic Ocean in providing a link between the two of them. He argued that substantial increases in glaciation on northern Ellesmere Island require greater amounts of solid precipitation (i.e. snowfall), an opinion that is today very much accepted in the scientific community. He also argued that the only conceivable way to increase precipitation on northern Ellesmere Island is by removing the (perennial) sea ice cover from the Arctic Ocean, thus increasing atmospheric humidity, cyclonic activity, and precipitation in general. There may be other mechanisms that can also lead to increased precipitation in the region (e.g. Barry, 1960; Lamb and Woodroffe, 1970; Johnson and Andrews, 1979; Bromwich *et al.*, 2004), but it is very reasonable to assume that "removing the lid" from the Arctic Ocean must be among the most efficient, certainly with respect to northern Ellesmere Island and northern Greenland. Hattersley-Smith continued to speculate that the (initial) development of "heavy glacierization" (i.e. ice sheets) would therefore have been favored by a relatively warm and ice-free Arctic Ocean over long periods of time, for example at the end of an interglacial or at the beginning of a glacial phase. The same argument should be applicable, for example, for the transitions from warm period such as the 'Holocene Climatic Optimum' or the 'Medieval Warm Period' to the colder conditions of the last 5000 years or the 'Little Ice Age'. Finally, Hattersley-Smith linked climate change and Arctic Ocean sea ice by making the (obvious) argument that an open Arctic Ocean would lead to a milder and moister climate on northern Ellesmere Island (or vice-versa). Such a situation would be, presumably, very detrimental to the ice shelves and low-elevation ice rises along the North Coast, since they respond quite sensitively to changes in summer temperature. In contrast, the large, high-elevation regions of northern

Ellesmere Island or northern Greenland may remain largely unaffected by such a milder climate, but would greatly benefit from the increased precipitation associated with a moister climate. In some respect, such a situation already exists further south on Baffin Island and along the east coasts of Devon and southern Ellesmere Island, where snowfall/glaciation are much greater/extensive due to a local 'snow gun' (cf. Prentice and Matthews, 1991) sitting directly offshore in Baffin Bay (i.e. the 'North Water' polynya) (Miller *et al.*, 1975; Koerner, 1977; 1979).

This hypothesis could be tested, for example, by recovering a new ice core from the highest elevations of northern Ellesmere Island, specifically from the area around Mt. Oxford, which would provide a wealth of information about the climate and sea ice conditions on the Arctic Ocean in the past (e.g. Grumet *et al.*, 2001; Moore *et al.*, 2002), including:

- Summer temperatures (melt layers, isotopes)
- Precipitation (accumulation rate)
- Moisture source/history (isotopes)
- Sea ice cover (ice chemistry)
- Atmospheric composition (gas bubbles)

Results could then be compared with the studies by Dyke *et al.* (1996, 1997) who documented sea ice variations within the Canadian Arctic Archipelago and Tremblay *et al.* (1997) who linked driftwood patterns and their variability to changes in atmospheric circulation. Or, we can just wait and see, since the experiment that tests Geoff Hattersley-Smith's hypothesis is currently ongoing: the climate is warming, the ice shelves along the North Coast are disintegrating, and the Arctic Ocean is becoming ice-free in the summer.

BIBLIOGRAPHY

Abdalati, W. Krabill, W.B., Frederick, E.B., Manizade, S., Martin, C., Sonntag, J., Swift, R., Thomas, R.H., Yungel, J., and R. Koerner (2004), Elevation changes of ice caps in the Canadian archipelago. Journal of Geophysical Research, 109(F04007), doi: 10.1029/2003JF000045.

Abe-Ouchi, A., and H. Blatter (1993), On the initiation of ice sheets. Annals of Glaciology, 18, 203-207.

ACIA (2005), *Arctic Climate Impact Assessment – Scientific Report.* Cambridge University Press, New York, 1042 pp.

Adam, S., Pietroniro, A., and M. Brugman (1997), Glacier Snow Line Mapping Using ERS-1 SAR Imagery. Remote Sensing of Environment, 61, 46-54.

Adams, W.P., Cogley, J.G., Ecclestone, M.A., and M.N. Demuth (1998), A small glacier as an index of regional mass balance: Baby Glacier, Axel Heiberg Island, 1959-1992. Geografiska Annaler, 80A(1), 37-50.

Ageta, Y., and K. Higuchi (1984), Estimation of mass balance components of a summer-accumulation type glacier in the Nepal Himalaya. Geografiska Annaler, 66A(3), 249-255.

Ahlmann, H.W. (1924), Le niveau de glaciation comme function de l'accumulation d'humidite sous forme solide. Geografiska Annaler, 6(3-4), 223-272.

Ahlmann, H.W. (1936), Variations of glaciers and measurements of ablation. International Association of Hydrological Sciences (IAHS) Publication, 22, 417-429.

Ahlmann, H.W. (1948), Glaciological research on the North Atlantic Coast. Royal Geographical Society, Research Series, No. 1, London, UK, 83 pp.

Ahlmann, H.W. (1953), Glacier variations and climatic fluctuations. Bowman Memorial Lecture, Series 3, American Geographical Society, New York, 51 pp.

Alley, R.B. (2000), The Younger Dryas cold interval as viewed from central Greenland. Quaternary Science Reviews, 19, 213-226.

Alley, R.B., Clark, P.U., Huybrechts, P., and I. Joughin (2005), Ice sheets and sea-level change. Science, 310, 456-460.

Allen, T.R. (1997), Topographic context of glaciers and perennial snowfields, Glacier National Park, Montana. Geomorphology, 21, 207-216.

Alt, B.T. (1979), Investigation of Summer Synoptic Climate Controls in the Mass Balance of Meighen Ice Cap. Atmosphere-Oceans, 17(3), 181-199.

Alt, B.T. (1987), Developing Synoptic Analogs for Extreme Mass Balance Conditions on Queen Elizabeth Island Ice Caps. Journal of Climate and Applied Meteorology, 26(11), 1605-1623.

Ambach, W. (1985), Characteristics of the heat balance of the Greenland Ice Sheet for modeling. Journal of Glaciology, 31(107), 3-12.

Ambach, W. (1988), Interpretation of the Positive-Degree-Days Factor by Heat Balance Characteristics – West Greenland. Nordic Hydrology, 19, 217-224.

Anderson, M.P., and W.W. Woessner (1992), *Applied Groundwater Modeling: Simulation of Flow and Advective Transport*. Academic Press, San Diego, California, 381 pp.

Andrews, J.T. (2002), Glaciers on Baffin Island. In *Satellite Image Atlas of Glaciers of the World*, edited by R.S. Williams and J.G. Ferrigno, U.S. Geological Survey Professional Paper 1386-J-1.

Andrews, J.T., and M.A.W. Mahaffy (1976), Growth Rate of the Laurentide Ice Sheet and Sea Level Lowering (with Emphasis on the 115,000 BP Sea Level Low). Quaternary Research, 6, 167-183.

Andrews, J.T., and R.G. Barry (1978), Glacial Inception And Disintegration During The Last Glaciation. Annual Reviews Earth Planetary Science, 6, 205-228.

Andrews, J.T., Barry, R.G., and L. Drapier (1970), An inventory of the present and past glacierization of Home Bay and Okoa Bay, east Baffin Island, N.W.T., Canada, and some climatic and paleoclimatic considerations. Journal of Glaciology, 9(57), 337-362.

Andrews, J.T., Barry, R.G., Bradley, R.S., Miller, G.H., and L.D. Williams (1972), Past and Present Glaciological Responses to Climate in Eastern Baffin Island. Quaternary Research, 2, 303-314.

Andrews, J.T., Davis, P.T., and C. Wright (1976), Little Ice Age permanent snow cover in the eastern Canadian Arctic: Extent mapped from LANDSAT-1 satellite imagery. Geografiska Annaler, 58A(1-2), 71-81.

Andrews, S. (2001), Synoptic Climatology of the Canadian High Arctic. 7th Annual Undergraduate Conference, co-sponsored by the Massachusetts Public System of Higher Education and the Commonwealth College at the University of Massachusetts Amherst. April 27, 2001, Sturbridge Host Conference Center, Sturbridge, Massachusetts.

Arendt, A.A. (1997), Approaches to Modelling the Mass Balance of High Arctic Glaciers. M.Sc. thesis, University of Alberta, Edmonton, Alberta, Canada, 222 pp.

Arendt, A.A., and M. Sharp (1999), Energy balance measurements on a Canadian high arctic glacier and their implications for mass balance modeling. International Association of Hydrological Sciences (IAHS) Publication, 256, 165-172.

Arendt, A.A., Echelmeyer, K.A., Harrison, W.D., Lingle, C.S., and V.B. Valentine (2002), Rapid Wastage of Alaska Glaciers and Their Contribution to Rising Sea Level. Science, 297, 382-386.

Armstrong, T.E., and B.B. Roberts (1956), Illustrated ice glossary. Polar Record, 8(52), 4-12.

Arnold, K.C. (1965), Aspects of the glaciology of Meighen Island, Northwest Territories, Canada. Journal of Glaciology, 5(40), 399-410.

Arnold, K.C., and D.K. MacKay (1964), Different methods of calculating mean daily temperatures, their effects on degree-day totals in the high Arctic and their significance to glaciology. Geographical Bulletin, 21, 123-129.

Arnold, N.S. (2005), Investigating the Sensitivity of Glacier Mass-Balance/Elevation Profiles to Changing Meteorological Conditions: Model Experiments for Haut Glacier D'Arolla, Valais, Switzerland. Arctic, Antarctic, and Alpine Research, 37(2), 139-145.

Arnold, N.S., Willis, I.C., Sharp, M.J., Richards, K.S., and W.J. Lawson (1996), A distributed surface energy-balance model for a small valley glacier. I. Development and testing for Haut Glacier d'Arolla , Valais, Switzerland. Journal of Glaciology, 42(140), 77-89.

Atkinson, D.E. (2002), High spatial resolution mean July air temperature data for the Canadian Arctic Archipelago, 1957-2001: A research note. Polar Geography, 26(4), 321-324.

Atkinson, D.E., and K. Gajewski (2002), High-Resolution Estimation of Summer Surface Air Temperature in the Canadian Arctic Archipelago. Journal of Climate, 15, 3601-3614.

Atkinson, D.E., Alt, B., and K. Gajewski (2000), A New Database of High Arctic Climate Data from the Polar Continental Shelf Project Archives. Bulletin of the American Meteorological Society, 81(11), 2621-2629.

Bahr, D.B., Pfeffer, W.T., Sassolas, C., and M.F. Meier (1998), Response time of glaciers as a function of size and mass balance: 1. Theory. Journal of Geophysical Research, 103(B5), 9777-9782.

Baird, P.D., Ward, W.H., and S. Orvig (1952), The glaciological studies of the Baffin Island Expedition, 1950. Parts 1 & 2. Journal of Glaciology, 2(11), 2-23.

Bakke, J., Dahl, S.O., Paasche, O., Løvlie, R., and A. Nesje (2005), Glacier fluctuations, equilibrium-line altitudes and paleoclimate in Lyngen, northern Norway, during the Lateglacial and Holocene. The Holocene, 15(4), 518-540.

Ballantyne, C.K. (1990), The Holocene glacial history of Lyngshalvöya, northern Norway: chronology and climatic implications. Boreas, 19, 93-117.

Ballantyne, C.K. (2002), The Loch Lomond Readvance on the Isle of Mull, Scotland: glacier reconstruction and palaeoclimatic implications. Journal of Quaternary Science, 17(8), 759-771.

Bamber, J., Krabill, W., Raper, V., and J. Dowdeswell (2004), Anomalous recent growth of part of a large Arctic ice cap: Austfonna, Svalbard. Geophysical Research Letters, 31(L12402), doi: 10.1029/2004GL019667.

Barnett, T.P., Adam, J.C., and D.P. Lettenmaier (2005), Potential impacts of a warming climate on water availability in snow-dominated regions. Nature, 438, 303-309.

Barry, R.G. (1960), The application of synoptic studies in paleoclimatology: A case study for Labrador-Ungava. Geografiska Annaler, 42, 36-44.

Barry, R.G. (1992), *Mountain Weather and Climate, 2nd edition.* Routledge, London, UK, 432 pp.

Barry, R.G. (1996), The parameterization of surface albedo for sea ice and its snow cover. Progress in Physical Geography, 20(1), 63-79.

Barry, R.G. (2002), The Role of Snow and Ice in the Global Climate System: A Review. Polar Geography, 26(3), 235-246.

Barry, R.G., and C.I. Jackson (1969), Summer weather conditions at Tanquary Fjord, N.W.T., 1963-1967. Arctic and Alpine Research, 1(3), 169-180.

Barry, R.G., Ives, J.D., and J.T. Andrews (1971), A Discussion of Atmospheric Circulation during the Last ice Age. Quaternary Research, 1, 415-418.

Barry, R.G., Andrews, J.T., and M.A. Mahaffy (1975), Continental Ice Sheets: Conditions for Growth. Science, 190(4218), 979-981.

Bednarski, J. (1994), Geomorphology. In *Resource Description and Analysis – Ellesmere Island National Park Reserve*, Natural Resource Conservation Section, Parks Canada, Department of Canadian Heritage, Winnipeg, Manitoba, Canada.

Bengtsson, L., Semenov, V.A, and O.M. Johannessen (2004), The Early Twentieth-Century Warming in the Arctic – A Possible Mechanism. Journal of Climate, 17, 4045-4057.

Benn, D.I., and F. Lehmkuhl (2000), Mass balance and equilibrium-line altitudes of glaciers in high-mountain environments. Quaternary International, 65/66, 15-29.

Bergström, S. (1992), The HBV model – its structure and applications. *SMHI Hydrology Report RH4*, Swedish Meteorological and Hydrological Institute, Norrkoping, Sweden.

Beven, K.J. (1996), A discussion of distributed hydrological modeling. In *Distributed Hydrological Modelling*, edited by M.B. Abbott and J.C. Refsgaard, Kluwer, Dordrecht, Netherlands, 255-278.

Bigelow, N.H., and 26 others (2003), Climate change and Arctic ecosystems: 1. Vegetation changes north of 55°N between the last glacial maximum, mid-Holocene, and present. Journal of Geophysical Research, 108(D19), doi: 10.1029/2002JD002558.

Bingham, R.G., Hulton, N.R.J., and A.J. Dugmore (2003), Modelling the southern extent of the last Icelandic ice-sheet. Journal of Quaternary Science, 18(2), 169-181.

Bintanja, R., and J. Oerlemans (1995), The influence of the albedo-temperature feed-back on climate sensitivity. Annals of Glaciology, 21, 353-360.

Bintanja, R., van de Wal, R.S.W., and J. Oerlemans (2002), Global ice volume variations through the last glacial cycle simulated by a 3-D ice-dynamical model. Quaternary International, 95-96, 11-23.

Birchfield, G.E., and J. Weertman (1983), Topography, Albedo-Temperature Feedback, and Climate Sensitivity. Science, 219, 284-285.

Birchfield, G.E., Weertman, J., and A.T. Lunde (1982), A Model Study of the Role of High-Latitude Topography in the Climatic Response to Orbital Insolation Anomalies. Journal of the Atmospheric Sciences, 39, 71-87.

Bishop, J.F., and J.L.W. Walton (1981), Bottom melting under George VI Ice Shelf, Antarctica. Journal of Glaciology, 27, 429-447.

Blake, W., Jr. (1970), Studies of glacial history in arctic Canada. I. Pumice, radiocarbon dates, and differential postglacial uplift in the eastern Queen Elizabeth Islands. Canadian Journal of Earth Sciences, 7, 634-664.

Blake, W., Jr. (1992), Holocene emergence at Cape Herschel, east-central Ellesmere Island, Arctic Canada: implications for ice sheet configuration. Canadian Journal of Earth Sciences, 29, 1958-1980.

Blatter, H., and G. Kappenberger (1988), Mass balance and thermal regime of Laika Ice Cap, Coburg Island, N.W.T., Canada. Journal of Glaciology, 34(116), 102-110.

Blöschl, G. (1991), The Influence of Uncertainty in Air Temperature and Albedo on Snowmelt. Nordic Hydrology, 22, 95-108.

Blöschl, G. (2006), Hydrologic synthesis: Across processes, places, and scales. Water Resources Research, 42(W03S02), doi: 10.1029/2005WR004319.

Bogdanova, E.G., Ilyin, B.M., and I.V. Dragomilova (2002), Application of an improved bias correction model to precipitation measured at Russian North Pole drifting stations. Journal of Hydrometeorology, 3, 700-713.

Bogen, J., Wold, B., and G. Østrem (1989), Historic glacier variations in Scandinavia. In *Glacier Fluctuations and Climatic Change*, edited by J. Oerlemans, Kluwer, Dordrecht, Netherlands, 109-128.

Bøggild, C.E., Reeh, N., and H. Oerter (1994), Modelling ablation and mass-balance sensitivity to climate change of Storstrømmen, Northeast Greenland. Global and Planetary Change, 9, 79-90.

Bøggild, C.E., Knudby, C.J., Knudsen, M.B., and W. Starzer (1999), Snowmelt and runoff modeling of an Arctic hydrological basin in west Greenland. Hydrological Processes, 13, 1989-2002.

Boike, J., Roth, K., and O. Ippisch (2003), Seasonal snow cover on frozen ground: Energy balance calculations of a permafrost site near Ny-Alesund, Spitsbergen. Journal of Geophysical Research, 108(D2), doi: 10.1029/2001JD000939.

Boon, S. (2005), Hydrometeorology of a High Arctic Glacier. Ph.D. dissertation, University of Alberta, Edmonton, Alberta, Canada, 230 pp.

Boon, S., Sharp, M., and P. Nienow (2003), Impact of an extreme melt event on the runoff and hydrology of a high Arctic glacier. Hydrological Processes, 17, 1051-1072.

Boulton, G.S., Hulton, N., and M. Vautravers (1995), Ice-sheet models as tools for palaeoclimatic analysis: the example of the European ice sheet through the last glacial cycle. Annals of Glaciology, 21, 103-110.

Bradley, R.S. (1972), The problem of inversions in estimating the height of glaciation limits in Arctic regions. Arctic and Alpine Research, 4, 359-360.

Bradley, R.S. (1973), Recent Freezing Level Changes and Climatic Deterioration in the Canadian Arctic Archipelago. Nature, 243, 398-400.

Bradley, R.S. (1975), Equilibrium-line altitudes, mass balance, and July freezing-level heights in the Canadian High Arctic. Journal of Glaciology, 14(71), 267-274.

Bradley, R.S. (1985), *Quaternary Paleoclimatology – Methods of Paleoclimatic Reconstructions*. Allen and Unwin, Winchester, Massachusetts, 472 pp.

Bradley, R.S. (1990), Holocene Paleoclimatology of the Queen Elizabeth Islands, Canadian High Arctic. Quaternary Science Reviews, 9(4), 365-384.

Bradley, R.S., and G.H. Miller (1972), Recent Climatic Change and Increased Glacierization in the Eastern Canadian Arctic. Nature, 237, 385-387.

Bradley, R.S., and J. England (1977), The Simmonds Ice Cap. In *Past glacial activity in the High Arctic*, edited by R.S. Bradley and J. England, Contribution No. 31, Department of Geology and Geography, University of Massachusetts, Amherst, Massachusetts, 177-182.

Bradley, R.S., and J. England (1978), Recent climatic fluctuations of the Canadian High Arctic and their significance for glaciology. Arctic and Alpine Research, 10(4), 715-731.

Bradley, R.S., and J. England, J. (1979), Synoptic climatology of the Canadian High Arctic. Geografiska Annaler, 61A(3-4), 187-201.

Bradley, R.S., and J.K. Eischeid (1985), Aspects of the precipitation climatology of the Canadian High Arctic. In *Glacial and Glacio-Climatic studies in the Canadian High Arctic*, edited by R.S. Bradley, Contribution No. 49, Department of Geology and Geography, University of Massachusetts, Amherst, Massachusetts, 240-271.

Bradley, R.S., and M.C. Serreze (1987a), Mass balance of two High Arctic plateau ice caps. Journal of Glaciology, 33(113), 123-128.

Bradley, R.S., and M.C. Serreze (1987b), Topoclimatic studies of a High Arctic plateau ice cap. Journal of Glaciology, 33(114), 149-158.

Bradley, R.S., Retelle, M.J., Ludlam, S.D., Hardy, D.R., Zolitschka, B., Lamoureux, S.F., and M.S.V. Douglas (1996), The Taconite Inlet Lakes Project: a systems approach to paleoclimatic reconstruction. Journal of Paleolimnology, 16, 97-110.

Bradley, R.S., Briffa, K.R., Cole, J., Hughes, M.K., and T.J. Osborn (2003), The climate of the last millennium. In *Paleoclimate, Global Change and the Future*, edited by K. Alverson, R.S. Bradley and T.F. Pederson, Springer Verlag, Berlin, Germany, 105-141.

Braithwaite, R.J. (1977), Air temperature and glacier ablation – a parametric approach. Ph.d. dissertation, McGill University, Montreal, Quebec, Canada.

Braithwaite, R.J. (1981), On glacier energy balance, ablation, and air temperature. Journal of Glaciology, 27(97), 381-391.

Braithwaite, R.J. (1984), Calculation of degree-days for glacier-climate research. Zeitschrift für Gletscherkunde und Glazialgeologie, 20, 1-8.

Braithwaite, R.J. (1995), Positive degree-day factors for ablation on the Greenland ice sheet studied by energy-balance modeling. Journal of Glaciology, 41(137), 153-160.

Braithwaite, R.J. (1996), Models of ice-atmosphere interactions for the Greenland ice sheet. Annals of Glaciology, 23, 149-153.

Braithwaite, R.J. (2002), Glacier mass balance: the first 50 years of international monitoring. Progress in Physical Geography, 26(1), 76-95.

Braithwaite, R.J., and O.B. Olesen (1988), Winter accumulation reduces summer ablation on Nordbogletscher, South Greenland. Zeitschrift für Gletscherkunde und Glazialgeologie, 24(1), 21-30.

Braithwaite, R.J., and O.B. Olesen (1989), Calculation of Glacier Ablation from Air Temperature, West Greenland. In *Glacier Fluctuations and Climatic Change*, edited by J. Oerlemans, Kluwer, Dordrecht, Netherlands, 219-233.

Braithwaite, R.J., and O.B. Olesen (1990a), A simple energy-balance model to calculate ice ablation at the margin of the Greenland Ice Sheet. Journal of Glaciology, 36(123), 222-228.

Braithwaite, R.J., and O.B. Olesen (1990b), Response of the energy balance on the margin of the Greenland Ice Sheet to temperature changes. Journal of Glaciology, 36(123), 217-221.

Braithwaite, R.J., and O.B. Olesen (1990c), Increased ablation at the margin of the Greenland Ice Sheet under a greenhouse-effect climate. Annals of Glaciology, 14, 20-22.

Braithwaite, R.J., and O.B. Olesen (1993), Seasonal variation of ice ablation at the margin of the Greenland ice sheet and its sensitivity to climate change, Qamanarssup sermia, West Greenland. Journal of Glaciology, 39(132), 267-274.

Braithwaite, R.J., and Y. Zhang (1999), Modelling changes in glacier mass balance that may occur as a result of climate changes. Geografiska Annaler, 81A(4), 489-496.

Braithwaite, R.J., and Y. Zhang (2000), Sensitivity of mass balance of five Swiss glaciers to temperature changes assessed by tuning a degree-day model. Journal of Glaciology, 46(152), 7-14.

Braithwaite, R.J., and S.C.B. Raper (2002), Glacier and their contribution to sea level change. Physics and Chemistry of the Earth, 27, 1445-1454.

Braithwaite, R.J., Laternser, M., and W.T. Pfeffer (1994), Variations of near-surface firn density in the lower accumulation area of the Greenland ice sheet, Pakitsoq, West Greenland. Journal of Glaciology, 40(136), 477-485.

Braithwaite, R. J., Konzelmann, T., Marty, C., and O. B. Olesen (1998a), Reconnaissance study of glacier energy balance in North Greenland, 1993-1994. Journal of Glaciology, 44(147), 239-247.

Braithwaite, R.J., Konzelmann, T., Marty, C., and O.B. Olesen (1998b), Errors in daily ablation measurements in northern Greenland, 1993-94, and their implications for glacier climate studies. Journal of Glaciology, 44(148), 583-588.

Braithwaite, R.J., Zhang, Y, and S.C.B. Raper (2002), Temperature sensitivity of the mass balance of mountain glaciers and ice caps as a climatological characteristic. Zeitschrift für Gletscherkunde und Glazialgeologie, 38(1), 35-61.

Braun, C. (1997), Streamflow and sediment transport in two High Arctic watersheds, Nunavut, Canada. M.Sc. thesis, University of Massachusetts, Amherst, Massachusetts, 167 pp.

Braun, C., Hardy, D.R., Bradley, R.S., and M.J. Retelle (2000), Hydrological and Meteorological Observations at Lake Tuborg, Ellesmere Island, Nunavut, Canada. Polar Geography, 24(2), 83-97.

Braun, C., Hardy, D.R., and R.S. Bradley (2001), Recent recession of a small plateau ice cap, Ellesmere Island, Canada. Journal of Glaciology, 47(15), 154.

Braun, C., Hardy, D.R., and R.S. Bradley (2004a), Mass Balance and Area Changes of four High Arctic Plateau Ice Caps, 1959-2002. Geografiska Annaler, 86A(1), 43-52.

Braun, C., Hardy, D.R., and R.S. Bradley (2004b), Surface Mass Balance of the Ward Hunt Ice Rise and Ice Shelf, Ellesmere Island, Nunavut, Canada. Journal of Geophysical Research, 109(D22110), doi: 10.1029/2004JD004560.

Braun, M., and R. Hock (2004), Spatially distributed surface energy balance and ablation modeling on the ice cap of King George Island (Antarctica). Global and Planetary Change, 42, 45-58.

Brock, B.W. (2004), An analysis of short-term albedo variations at Haut Glacier d'Arolla, Switzerland. Geografiska Annaler, 86A(1), 53-65.

Brock, B.W., and N.S Arnold (2000), A spreadsheet-based (Microsoft Excel) point surface energy balance model for Glacier and Snow Melt Studies. Earth Surface Processes and Landforms, 25, 649-658.

Brock B.W., Willis, I.C., and M.J. Sharp (2000a), Measurement and parameterization of albedo variations at Haut Glacier d'Arolla, Switzerland. Journal of Glaciology, 46(155), 675-688.

Brock B.W., Willis, I.C., Sharp, M.J., and N.S. Arnold (2000b), Modelling seasonal and spatial variations in the surface energy balance of Haut Glacier d'Arolla, Switzerland. Annals of Glaciology, 31, 53-62.

Brocklehurst, S.H., and K.X. Whipple (2004), Hypsometry of glaciated landscapes. Earth Surface Processes and Landforms, 29, 907-926.

Bromwich, D.H., Toracinta, E.R., and S.H. Wang (2002), Meteorological perspective on the initiation of the Laurentide Ice Sheet. Quaternary International, 95-96, 113-124.

Bromwich, D.H., Toracinta, E.R., Wei, H., Oglesby, R.J., Fastook, J.L., and T.J. Hughes (2004), Polar MM5 Simulations of the Winter Climate of the Laurentide Ice Sheet at the LGM*. Journal of Climate, 17, 3415-3433.

Brooks, C.E.P. (1926), The Causes of Glaciation. Monthly Weather Review, 54(9), 384-385.

Brown, I., and R. Ward (1996), The influence of topography on snowpatch distribution in southern Iceland: A new hypothesis for glacier formation? Geografiska Annaler, 78A(4), 197-207.

Brown, R. D., and B.T. Alt (Eds.) (2001), *The state of the Arctic cryosphere during the extreme warm summer of 1998: documenting cryospheric variability in the Canadian Arctic*. Canadian Cryospheric Information Network, University of Waterloo, Waterloo, Ontario, Canada.

Brugger, K.A., 2005, Late Pleistocene climate inferred from the reconstruction of the Taylor River glacier complex, southern Sawatch Range, Colorado. Geomorphology, in press.

Bugnion, V. (1999), Model Estimates of the Mass Balance of the Greenland and Antarctic Ice Sheets. *Report No. 54*, Massachusetts Institute of Technology Joint Program on the Science and Policy of Global Change, Cambridge, Massachusetts, 34 pp.

Burgess, D.O., and M.J. Sharp (2004), Recent Changes in Areal Extent of the Devon Ice Cap, Nunavut, Canada. Arctic, Antarctic, and Alpine Research, 36(2), 261-271.

Calov, R., and R. Greve (2005), A semi-analytical solution for the positive degree-day model with stochastic temperature variations. Journal of Glaciology, 51(172), 173-188.

Carrivick, J.L., and T.R. Brewer (2004), Improving local estimations and regional trends of glacier equilibrium altitudes. Geografiska Annaler, 86A(1), 67-79.

Casely, A.F., and A.J. Dugmore (2004), Climate changes and 'anomalous' glacier fluctuations: the southwest outlets of Myrdalsjökull, Iceland. Boreas, 33, 108-122.

Cawkwell, F.G.L., and J.L. Bamber (2002), The impact of cloud cover on the net radiation budget of the Greenland ice sheet. Annals of Glaciology, 34, 141-149.

Cazorzi, F., and D.G. Fontana (1996), Snowmelt modeling by combining air temperature and a distributed radiation index. Journal of Hydrology, 181, 169-187.

Chapin III, F.S., and 20 others (2005), Role of Land-Surface Changes in Arctic Summer Warming. Science, 310, 657-660.

Chapman, W.L., and J.E. Walsh (1993), Recent Variations of Sea Ice and Air Temperature in High Latitudes. Bulletin of the American Meteorological Society, 74(1), 33-48.

Chinn, T.J. (1999), New Zealand glacier responses to climate change of the past 2 decades. Global and Planetary Change, 22, 155-168.

Chinn, T.J., Winkler, S., Salinger, M.J., and N. Haakensen (2005), Recent glacier advances in Norway and New Zealand: A comparison of their glaciological and meteorological causes. Geografiska Annaler, 87A(1), 141-157.

Christiansen, H.H. (1998), 'Little Ice Age' nivation activity in northeast Greenland. The Holocene, 8(6), 719-728.

Church, J.E. (1924), Present methods of glacier study in the Swiss Alps. Monthly Weather Review, 52(5), 264-266.

Cia, J.C., Andres, A.J., Sanchez, M.A.S., Novau, J.C., and J.I.L. Moreno (2005), Responses to climatic changes since the Little Ice Age on Maladeta Glacier (Central Pyrenees). Geomorphology, 68, 167-182.

Cline, D.W. (1997), Snow surface energy exchanges and snowmelt at a continental, midlatitude Alpine site. Water Resources Research, 33(4), 689-701.

Cogley, J.G. (2004), Greenland accumulation: An error model. Journal of Geophysical Research, 109(D18101), doi: 10.1029/2003JD004449.

Cogley, J.G., and W.P. Adams (1998), Mass balance of glaciers other than ice sheets. Journal of Glaciology, 44(147), 315-325.

Cogley, J.G., and F. Jung-Rothenhäusler (2004), Uncertainty in Digital Elevation Models of Axel Heiberg Island, Arctic Canada. Arctic, Antarctic, and Alpine Research, 36(2), 249-260.

Cogley, J.G., Adams, W.P., Ecclestone, M.A., Jung- Rothenhäusler, F., and C.S.L. Ommanney (1996), Mass balance of White Glacier, Axel Heiberg Island, N.W.T., Canada, 1960-91. Journal of Glaciology, 42 (142), 548-563.

Comiso, J.C. (2002a), Correlation and trend studies of the sea-ice cover and surface temperatures in the Arctic. Annals of Glaciology, 34, 420-428.

Comiso, J.C. (2002b), A rapidly declining Arctic Perennial Ice Cover. Geophysical Research Letters, 29(20), doi: 10.1029/2002GL015650.

Comiso, J.C. (2003), Warming Trends in the Arctic from Clear Sky Satellite Observations. Journal of Climate, 16(21), 3498-3510.

Comiso, J.C., and C.L. Parkinson (2004), Satellite-Observed Changes in the Arctic. Physics Today, 57(8), 38-44.

Comiso, J.C., Yang, J., Honjo, S., and R.A. Krishfield (2003), Detection of change in the Arctic using satellite and in situ data. Journal of Geophysical Research, 108(C12), doi: 10.1029/2002JC001347.

Conway, H., Rasmussen, L.A., and P. Hayes (1995), On the use of radiosondes to model glacier ablation. Annals of Glaciology, 21, 245-250.

Cooke, A.J., Fox, A.J., Vaughan, D.G., and J.G. Ferrigno (2005), Retreating Glacier Fronts on the Antarctic Peninsula over the Past Half Century. Science, 308, 541-544.

Crary, A.P. (1958), Arctic ice island and ice shelf studies, Part I. Arctic, 11(1), 3-42.

Cuffey, K.M., and G.D. Clow (1997), Temperature, accumulation, and ice sheet elevation in central Greenland through the last deglacial transition. Journal of Geophysical Research, 102, 26383-26396.

Dahl, S.O., and A. Nesje (1992), Paleoclimatic implications based on equilibrium-line altitude depressions of reconstructed Younger Dryas and Holocene cirque glaciers in inner Nordfjord, western Norway. Palaeogeography, Palaeoclimatology, Palaeoecology, 94, 87-97.

Dahl, S.O., Nesje, A., and J. Ovstedal (1997), Cirque glaciers as morphological evidence for a thin Younger Dryas ice sheet in east-central Norway. Boreas, 26, 161-180.

Davis, C.H., Li, Y., McConnell, J.R., Frey, M.M., and E. Hanna (2005), Snowfall-Driven Growth in East Antarctic Ice Sheet Mitigates Recent Sea-Level Rise. Science, 308, 1898-1901.

Davies, W.E., and D.B. Krinsley (1962), The recent regimen of the ice cap margin in North Greenland. International Association of Hydrological Sciences (IAHS) Publication, 58, 119-130.

De Woul, M., and R. Hock (2004), Static mass balance sensitivity of Arctic glaciers and ice caps using a degree-day approach. Paper presented at the International Symposium on Arctic Glaciology, International Glaciological Society, Geilo, Norway, 23-27 July 2004.

Debenham, F. (1954), The ice islands of the Arctic: A hypothesis. Geographical Review, 44(4), 495-507.

DeConto, R.M., and D. Pollard (2003), Rapid Cenozoic glaciation of Antarctica induced by declining atmospheric CO2. Nature, 421, 245-249.

Denton, G.H., and T.H. Hughes (1981), *The Last Great Ice Sheets*. Wiley-Interscience, New York, 484 pp.

Diamond, M. (1960), Air temperatures and precipitation on the Greenland ice sheet. Journal of Glaciology, 3(27), 558-567.

Doake, C.S.M., Corr, H.F.J., Rott, F., Skvarca, P., and N.W. Young (1998), Breakup and conditions for stability of the northern Larsen Ice Shelf, Antarctica. Nature, 391, 778-780.

Dorsey, H.G. (1945), Some meteorological aspects of the Greenland Ice Cap. Journal of Meteorology, 2(3), 135-142.

Dowdeswell, J.A. (1995), Glaciers in the High Arctic and recent environmental change. Philosophical Transactions of the Royal Society, Series A, 352, 321-334.

Dowdeswell, J.A., and J.O. Hagen (2003), Arctic ice caps and glaciers. In *Mass Balance of the Cryosphere*, edited by J.L. Bamber and A.J. Payne, Cambridge University Press, Cambridge, New York, 527-558.

Dowdeswell, E.K., and J.A. Dowdeswell (2004), Recent changes in the dimension of the glaciers on Bylot Island, Arctic Canada. Paper presented at the International Symposium on Arctic Glaciology, International Glaciological Society, Geilo, Norway, 23-27 July 2004.

Dowdeswell, J.A., Hagen, J.O., Björnsson, H., Glazovsky, A.F., Harrison, W.D., Holmlund, P., Jania, J., Koerner, R.M., Lefauconnier, B., Ommanney, C.S.L., and R.H. Thomas (1997), The Mass Balance of Circum-Arctic Glaciers and Recent Climate Change. Quaternary Research, 48, 1-14.

Dugdale, R.E. (1972), A statistical analysis of some measures of the state of a glacier's health. Journal of Glaciology, 11(61), 73-79.

Dupont, T.K., and R.B. Alley (2005), Assessment of the importance of ice-shelf buttressing on ice-sheet flow. Geophysical Research Letters, 32(L04503), doi: 10.1029/2004GL022024.

Dyke, A.S. (1983), Quaternary geology of Somerset Island, District of Franklin. *Memoir No. 404*, Geological Survey of Canada, Ottawa, Ontario, Canada, 32 pp.

Dyke, A.S., and V.K. Prest (1987), Late Wisconsinan and Holocene History of the Laurentide Ice Sheet. Geographie physique et Quaternaire, 41, 237-263.

Dyke, A.S., Hooper, J., and J. Savelle (1996), A history of sea ice in the Canadian Arctic Archipelago based on postglacial remains of bowhead whale (*Balaena mysticetus*). Arctic, 49, 235-255.

Dyke, A.S., England, J., Reimnitz, E., and H. Jette (1997), Change in driftwood delivery to the Canadian Arctic Archipelago: the hypothesis of postglacial oscillations of the transpolar drift. Arctic, 50, 1-16.

Dyurgerov, M. (2002), Glacier mass balance and regime: Data of measurements and analysis. *Occasional Paper 55*, edited by M. Meier and R.L. Armstrong, Institute of Arctic and Alpine Research, University of Colorado, Boulder, Colorado.

Dyurgerov, M. (2003), Mountain and subpolar glaciers show an increase in sensitivity to climate warming and intensification of the water cycle. Journal of Hydrology, 282, 162-176.

Dyurgerov, M.B., and M.F. Meier (1997), Mass Balance of Mountain and Subpolar Glaciers: A New Global Assessment for 1961-1990. Arctic and Alpine Research, 29(4), 379-391.

Dyurgerov, M.B., and M.F. Meier (2000), Twentieth century climate change: evidence from small glaciers. Proceeding of the National Academy of Sciences, 97(4), 1406-1411.

Ebbesmeyer, C.C., Cayan, D.R., McLain, D.R., Nichols, F.H., Peterson, D.H., and K.T. Redmond (1991), 1976 Step in the Pacific Climate: Forty Environmental Changes between 1968-1975 and 1974-1984. *Report 26*, Proceedings of the Seventh Annual Pacific Climate Workshop, California Department of Water Resources, Interagency Ecological Studies Programm, Asilomar, California.

Edlund, S.A. (1985), Lichen-free zones as Neoglacial indicators on western Melville Island, District of Franklin. *Paper 85-1A*, Geological Survey of Canada, Ottawa, Ontario, Canada, 709-712.

Edlund, S.A., and B.T. Alt (1989), Regional congruence of vegetation and summer climate patterns in the Queen Elizabeth Islands, Northwest Territories, Canada. Arctic, 42(1), 3-23.

Elsberg, D.H., Harrison, W.D., Echelmeyer, K.A., and R.M. Krimmel (2001), Quantifying the effects of climate and surface change on glacier mass balance. Journal of Glaciology, 47(159), 649-658.

Engeset, R.V., Elvehoy, H., Andreassen, L.M., Haakensen, N., Kjøllmoen, L.A., and E. Roland (2000), Modelling of historic variations and future scenarios of the mass balance of Svartisen ice cap, northern Norway. Annals of Glaciology, 31, 97-103.

England, J. (1976), Late Quaternary glaciation of the eastern Queen Elizabeth Island, Northwest Territories, Canada: alternative models. Quaternary Research, 6, 185-202.

England, J. (1986a), A paleoglaciation level for north-central Ellesmere Island, N.W.T., Canada. Arctic and Alpine Research, 18(2), 217-222.

England, J. (1986b), Glacial Erosion of a High Arctic Valley. Journal of Glaciology, 32(110), 60-64.

England, J. (1998), Support for the Innuitian Ice Sheet in the Canadian High Arctic during the Last Glacial Maximum. Journal of Quaternary Science, 13, 275-280.

England, J. (1999), Coalescent Greenland and Innuitian ice during the Last Glacial Maximum: revising the Quaternary of the Canadian High Arctic. Quaternary Science Reviews, 18, 421-456.

England, J., and R.S. Bradley (1978), Past Glacial Activity in the Canadian High Arctic. Science, 200, 265-270.

England, J., Atkinson, N., Bednarski, J., Dyke, A.S., Hodgson, D.A., and C.O. Cofaigh (2006), The Innuitian Ice Sheet: configuration, dynamics, and chronology. Quaternary Science Reviews, 25(7-8), 689-703.

Escher-Vetter, H., and H. Rentsch (1995), The behavior of the Bavarian Glaciers: Results from surveying and mass balance modeling. Zeitschrift für Gletscherkunde und Glazialgeologie, 31, 181-187.

Essery, R., and P. Etchevers (2004), Parameter sensitivity in simulations of snowmelt. Journal of Geophysical Research, 109(D20111), doi: 10.1029/2004JD005036.

Etchevers, P., and 22 others (2004), Validation of the energy budget of an alpine snowpack simulated by several snow models (SnowMIP project). Annals of Glaciology, 38, 150-158.

Evans, D.J.A., and J. England (1992), Geomorphological evidence of Holocene climatic change from northwest Ellesmere Island, Canadian High Arctic. The Holocene, 2, 148-158.

Evans, D.J.A., Rea, B.P., Hansom, J.D., and W.B. Whalley (2002), Geomorphology and style of plateau icefield deglaciation in fjord terrains: the example of Troms-Finnmark, north Norway. Journal of Quaternary Science, 17(3), 221-239.

Falconer, G. (1962), Patterned ground under ice fields. Journal of Glaciology, 4(32), 238-239.

Falconer, G. (1966), Preservation of vegetation and patterned ground under a thin ice body in northern Baffin Island, N.W.T. Geographical Bulletin, 8(2), 194-200.

Favier, V., Wagnon, P., Chazarin, J.P., Maisincho, L., and A. Coudrain (2004), One-year measurements of surface heat budget on the ablation zone of Antizana Glacier 15, Ecuadorian Andes. Journal of Geophysical Research, 109(D18105), doi: 10.1029/2003JD004359.

Fealy, R., and J. Sweeney (2005), Detection of a possible change point in atmospheric variability in the North Atlantic and its effect on Scandinavian glacier mass balance. International Journal of Climatology, 25(14), 1819-1833.

Feddema, J.J., Oleson, K.W., Bonan, G.B., Mearns, L.O., Buja, L.E., Meehl, G.E., and W.M. Washington (2005), The Importance of Land-Cover Change in Simulating Future Climates. Science, 310(5754), 1674-1678.

Ferguson, R.I. (1999), Snowmelt runoff models. Progress in Physical Geography, 23(2), 205-227.

Fierz, C., Riber, P., Adams, E.E., Curran, A.R., Föhn, P.M.B., Lehning, M., and C. Plüss (2003), Evaluation of snow-surface energy balance models in alpine terrain. Journal of Hydrology, 282, 76-94.

Finsterwalder, S., and H. Schunk (1887), Der Suldenferner. Zeitschrift des Deutschen und Österreichischen Alpenvereins, 18, 72-89.

Fisher, D.A., and R.M. Koerner (1994), Signal and noise in four ice-core records from the Agassiz Ice Cap, Ellesmere Island, Canada: details of the last millennium for stable isotopes, melt and solid conductivity. The Holocene, 4(2), 113-120.

Fisher, D.A., Koerner, R.M., Paterson, W.S.B., Dansgaard, W., Gundestrup, N., and N. Reeh (1983), Effect of wind scouring on climatic records from ice-core oxygen-isotope profiles. Nature, 301, 205-209.

Fisher, D.A., Koerner, R.M., and N. Reeh (1995), Holocene climatic records from Agassiz Ice Cap, Ellesmere Island, NWT, Canada. The Holocene, 5(1), 19-24.

Fisher, D.A., and 12 others (1998), Penny Ice Cap cores, Baffin Island, Canada, and the Wisconsinan Foxe Dome connection: two states of Hudson Bay ice cover. Science, 279(5351), 692-695.

Fleming, K.M., Dowdeswell, J.A., and J. Oerlemans (1997), Modelling the mass balance of northwest Spitsbergen glaciers and responses to climate change. Annals of Glaciology, 24, 203-210.

Flint, R.F. (1943), Growth of the North American ice sheet during the Wisconsin Age. Geological Society of America Bulletin, 54, 325-362.

Flint, R.F. (1971), *Glacial and Quaternary Geology*. John Wiley, New York, 892 pp.

Flohn, H. (1974), Background of a geophysical model of the initiation of the next glaciation. Quaternary Research, 4, 385-404.

Föhn, P.M. (1973), Short-term snow melt and ablation measurements derived from heat- and mass-balance measurements. Journal of Glaciology, 12(65), 275-289.

Fountain, A.G., and A. Vecchia (1999), How many stakes are required to measure the mass balance of a glacier? Geografiska Annaler, 81A(4), 563-573.

Fountain, A.G., Lewis, K.J., and P.T. Doran (1999), Spatial climatic variation and its control on glacier equilibrium line altitude in Taylor Valley, Antarctica. Global and Planetary Change, 22, 1-10.

Fortuin, J.P.F., and J. Oerlemans (1990), Parameterization of the annual surface temperature and mass balance of Antarctica. Annals of Glaciology, 14, 78-84.

Fredin, O. (2002), Glacial inception and Quaternary mountain glaciations in Fennoscandia. Quaternary International, 95-96, 99-112.

Fristrup, B. (1951), Climate and glaciology of Peary Land, North Greenland. International Association of Hydrological Sciences (IAHS) Publication, 32, 185-193.

Fujita, K., Seko, K., Ageta, Y., Jianchen, A., and Y. Tandong (1996), Superimposed ice in glacier mass balance on the Tibetan Plateau. Journal of Glaciology, 42(142), 454-460.

Fujita, K., and Y. Ageta (2000), Effect of summer accumulation on glacier mass balance on the Tibetan Plateau revealed by mass-balance model. Journal of Glaciology, 46(153), 244-252.

Furbish, D.J., and J.T. Andrews (1984), The use of hypsometry to indicate long-term stability and response of valley glaciers to changes in mass transfer. Journal of Glaciology, 30(105), 199-211.

Gajewski, K., and D.A. Atkinson (2003), Climatic change in northern Canada. Environmental Reviews, 11, 69-102.

Gellatly, A.F., Whalley, W.B., and J.E. Gordon (1986), Topographic control over recent glacier changes in southern Lyngen Peninsula, North Norway. Norsk Geografisk Tidsskirft, 41(1), 211-218.

Gellatly, A.F., Gordon, J.E., Whalley, W.B., and J.D. Hansom (1987), Thermal regime and geomorphology of plateau ice caps in northern Norway: Observations and implications. Geology, 16, 983-986.

Gellatly, A.F., Whalley, W.B., Gordon, J.E., Hansom, J.D., and D.S. Twigg, (1989), Recent glacial history and climatic change, Bergsfjord, Troms-Finnmark, Norway. Norsk Geografisk Tidsskirft, 43(1), 19-30.

Glasser, N.F. (1995), Modelling the effect of topography on ice sheet erosion, Scotland. Geografiska Annaler, 77A(1-2), 67-82.

Glasser, N.F., and M.J. Siegert (2002), Calculating basal temperatures in ice sheets: an Excel spreadsheet method. Earth Surface Processes and Landforms, 27, 673-680.

Glazirin, G., and H. Escher-Vetter (1998), The existence of glaciers in Bavaria, demonstrating climatic limitations of mountain glaciation. Zeitschrift für Gletscherkunde und Glazialgeologie, 34(1), 47-56.

Glen, A.R. (1941a), A sub-arctic glacier cap: The West Ice of North East Land. The Geographical Journal, 98(2), 65-76.

Glen, A.R. (1941b), A sub-arctic glacier cap: The West Ice of North East Land (Continued). The Geographical Journal, 98(3), 135-146.

Glenday, P.J. (1989), Mass balance parameterizations, White Glacier, Axel Heiberg Island, N.W.T., 1970-1980. B.A. thesis, Trent University, Peterborough, Ontario, Canada.

Golledge, N.R., and A. Hubbard (2005), Evaluating Younger Dryas glacier reconstructions in part of the western Scottish Highlands: a combined empirical and theoretical approach. Boreas, 34, 274-286.

Gordon, J.E., Whalley, W.B., and A.F. Gellatly (1995), Fluctuations of glaciers in Lyngsdalen, Troms, Norway, during the 20th century. Zeitschrift für Gletscherkunde und Glazialgeologie, 31, 125-134.

Granger, R.J., Pomeroy, J.W., and J. Parviainen (2002), Boundary-layer integration approach to advection of sensible heat to a patchy snow cover. Hydrological Processes, 16(18), 3559-3569.

Gray, D.R. (1994), Ecology. In *Resource Description and Analysis – Ellesmere Island National Park Reserve*, Natural Resource Conservation Section, Parks Canada, Department of Canadian Heritage, Winnipeg, Manitoba, Canada.

Green, F.H.W., and R.J. Harding (1980), The altitudinal gradients of air temperature in southern Norway. Geografiska Annaler, 62A(1-2), 29-36.

Greene, A.M. (2005), A time constant for hemispheric glacier mass balance. Journal of Glaciology, 51(174), 353-362.

Greene, A.M., Broecker, W.S., and D. Rind (1999), Swiss glacier recession since the Little Ice Age: Reconciliation with climate records. Geophysical Research Letters, 26(13), 1909-1912.

Gregory, J.M., and J. Oerlemans (1998), Simulated future sea-level rise due to glacier melt based on regionally and seasonally resolved temperature changes. Nature, 391, 474-476.

Greuell, W., and J. Oerlemans (1989), Energy balance calculations on and near the Hintereisferner (Austria) and an estimate of the effect of greenhouse warming on ablation. In *Glacier Fluctuations and Climatic Change*, edited by J. Oerlemans, Kluwer, Dordrecht, Netherlands, 305-323.

Greuell, W., and R. Böhm (1998), 2 m temperatures along melting mid-latitude glaciers, and implications for the sensitivity of the mass balance to variations in temperature. Journal of Glaciology, 44(146), 9-20.

Greuell, W., and C. Genthon (2003), Modelling land-ice surface mass balance. In *Mass Balance of the Cryosphere*, edited by J.L. Bamber and A.J. Payne, Cambridge University Press, Cambridge, New York, 117-168.

Greuell, W., Knap, W.H., and P.C. Smeets (1997), Elevational changes in meteorological variables along a midlatitude glacier during summer. Journal of Geophysical Research, 102(D22), 25941-25954.

Greve, R. (2000), On the response of the Greenland Ice Sheet to Greenhouse Climate Change. Climatic Change, 46, 289-303.

Grosfeld, K., and H. Sandhäger (2004), The evolution of a coupled ice shelf-ocean system under different climate states. Global and Planetary Change, 42, 107-132.

Grove, J.M. (1988), *The Little Ice Age*. Methuen, New York, 487 pp.

Grove, J.M. (2001), The initiation of the 'Little Ice Age' in regions round the North Atlantic. Climatic Change, 48, 53-82.

Grove, J.M. (2004), *Little Ice Ages: Ancient and Modern (2 volumes)*. Routledge, London, UK, 718 pp.

Grudd, H. (1990), Small glaciers as sensitive indicators of climatic fluctuations. Geografiska Annaler, 72A(1), 119-123.

Grumet, N.S., Wake, C.F., Mayewski, P.A., Zielinski, G.A., Whitlow, S.I., Koerner, R.M., Fisher, D.A., and J.M. Woollett (2001), Variability of sea-ice extent in Baffin Bay over the last millennium. Climatic Change, 49, 129-145.

Guomundsson, S., Björnsson, H., Palsson, F., and H.H. Haraldsson (2003), Physical energy balance and degree-day models of summer ablation on Langjökull ice cap, SW-Iceland. *Report No. RH-20-2003*, Science Institute, University of Iceland and National Power Company of Iceland, Reykjavik, Iceland, 20 pp.

Haeberli, W. (1995), Glacier fluctuations and climate change detection – operational elements of a worldwide monitoring strategy. World Meteorological Organization Bulletin, 44, 23-31.

Haeberli, W. (1998), Historical evolution and operational aspects of worldwide glacier monitoring. In *Into the Second Century of World Glacier Monitoring - Prospects and Strategies*, edited by W. Haeberli, M. Hoelzle, and S. Suter, UNESCO Publishing, Paris, France, 35-51.

Haeberli, W. (2004), Glaciers and ice caps: historical background and strategies of world-wide monitoring. In *Mass Balance of the Cryosphere*, edited by J.L. Bamber and A.J. Payne, Cambridge University Press, Cambridge, New York, 559-578.

Haeberli, W., and M. Hoelzle (1995), Application of inventory data for estimating characteristics of and regional climate-change effects on mountain glaciers: a pilot study with the European Alps. Annals of Glaciology, 21, 206-212.

Haeberli, W., Mueller, P., Alean, P., and H. Boesch (1989), Glacier changes following the Little Ice Age – A survey of the International Data Basis and its perspectives. In *Glacier Fluctuations and Climatic Change*, edited by J. Oerlemans, Kluwer, Dordrecht, Netherlands, 77-101.

Hagen, J.O., and O. Liestol (1990), Long-term glacier mass-balance investigations in Svalbard, 1950-88. Annals of Glaciology, 14, 102-106.

Hagen, J.O., Melvold, K., Eiken, T., Isaksson, E., and B. Lefauconnier (1999), Mass balance methods on Kongsvegen, Svalbard. Geografiska Annaler, 81A(4), 593-601.

Hagen, J.O., Melvold, K., Pinglot, F., and J.A. Dowdeswell (2003), On the Net Mass Balance of the Glaciers and Ice Caps in Svalbard, Norwegian Arctic. Arctic, Antarctic, and Alpine Research, 35(2), 264-270.

Hall, A. (2004), The Role of Surface Albedo in Climate. Journal of Climate, 17, 1550-1568.

Hanna, E., Huybrechts, P., and T.L. Mote (2002), Surface mass balance of the Greenland ice sheet from climate-analysis data and accumulation/runoff models. Annals of Glaciology, 35, 67-72.

Hanna, E., Huybrechts, P., Janssens, I., Cappelen, J., Steffen, K., and A. Stephens (2005), Runoff and mass balance of the Greenland ice sheet: 1958-2003. Journal of Geophysical Research, 110(D13108), doi: 10.1029/2004JD005641.

Harding, R.J. (1986) Exchanges of energy and mass associated with a melting snowpack. International Association of Hydrological Sciences (IAHS) Publication, 155, 3-15.

Hardy, D.R. (1996), Climatic influences on streamflow and sediment flux into Lake C2, northern Ellesmere Island, Canada. Journal of Paleolimnology, 16(2), 133-149.

Hardy, D.R., Bradley, R.S., and B. Zolitschka (1996), The climatic signal in varved sediments from Lake C2, northern Ellesmere Island, Canada. Journal of Paleolimnology, 16, 227-238.

Harrison, W.D., Elsberg, D.H., Echelmeyer, K.A., and R.M. Krimmel (2001), On the characterization of glacier response by a single time-scale. Journal of Glaciology, 47(159), 659-664.

Harvey, L.D.D. (1988), On the role of high latitude ice, snow, and vegetation feedbacks in the climatic response to external forcing changes. Climatic Change, 13, 191-224.

Hattersley-Smith, G. (1954), Glaciological reconnaissance in northern Ellesmere Island. International Association of Scientific Hydrology (IAHS) Publication, 39, 229-235.

Hattersley-Smith, G. (1957), The rolls on the Ellesmere Ice Shelf. Arctic, 10(1), 32-44.

Hattersley-Smith, G. (1960a), Some remarks on glaciers and climate in northern Ellesmere Island. Geografiska Annaler, 43(1), 45-48.

Hattersley-Smith, G. (1960b), Glaciological Studies: Snow Cover, Accumulation and Ablation. Report D Phys R (G), Defense Research Board, Department of National Defense, Ottawa, Ontario, Canada, 13 pp.

Hattersley-Smith, G. (1960c), Studies of englacial profiles in the Lake Hazen region of northern Ellesmere Island. Journal of Glaciology, 3(27), 610-625.

Hattersley-Smith, G. (1961), Ablation effects due to wind-blown dust. Journal of Glaciology, 3(30), 1152-1153.

Hattersley-Smith, G. (1963), Climatic inferences from firn studies in northern Ellesmere Island. Geografiska Annaler, 45(2-3), 139-151.

Hattersley-Smith, G. (1968), Comment on the paper presented by Løken, O.H. and Sagar, R.B., Mass balance observations on the Barnes Ice Cap, Baffin Island, Canada. International Association of Hydrological Sciences (IAHS) Publication, 79, 282-291.

Hattersley-Smith, G. (1969), Glacial Features of Tanquary Fjord and adjoining areas of northern Ellesmere Island, N.W.T. Journal of Glaciology, 8(52), 23-50.

Hattersley-Smith, G. (1970), Barbeau Peak. Canadian Geographical Journal, 80(3), 86-91.

Hattersley-Smith, G., and H. Serson (1970), Mass Balance of the Ward Hunt Ice Rise and Ice Shelf: a 10 year record, Journal of Glaciology, 9(56), 247-252.

Hattersley-Smith, G., and H. Serson (1973), Reconnaissance of a small ice cap near St Patrick Bay, Robeson Channel, Northern Ellesmere Island, Canada. Journal of Glaciology, 12(66), 417-421.

Hattersley-Smith, G., A.P. Crary, and Christie, R.L. (1955), Northern Ellesmere Island, 1953 and 1954. Arctic, 8(1), 3-36.

Hattersley-Smith, G., Lotz, J.R., and R.B. Sagar (1961), The ablation season on Gilman Glacier, Northern Ellesmere Island. International Association of Scientific Hydrology (IAHS) Publication, 54, 152-168.

Havens, J.M., Müller, F., and G.C. Wilmot (1965), Comparative meteorological survey and a short-term heat balance study of the White Glacier, summer 1962. *Axel Heiberg Island Research Reports – Meteorology 4,* McGill University, Montreal, Quebec, Canada, 68 pp.

Hay, J.E., and B.B. Fitzharris (1988), A comparison of the energy-balance and bulk-aerodynamic approaches for estimating glacier melt. Journal of Glaciology, 34(117), 145-153.

Henderson, K., Laube, A., Gäggeler, H.W., Olivier, S., Papina, T., and M. Schwikowski (2006), Temporal variations of accumulation and temperature during the past two centuries from Belukha ice core, Siberian Altai. Journal of Geophysical Research, 111(D03104), doi: 10.1029/2005JD005819.

Hindmarsh, R. (1993), Modelling the dynamics of ice sheets. Progress in Physical Geography, 17(4), 291-312.

Hinzman, L.D., Kane, D.L., and R.E. Gieck (1991), Regional snow ablation in the Alaskan Arctic. In *Northern hydrology : selected perspectives*, edited by T.D. Prowse and C.S.L. Ommanney, National Hydrology Research Institute, Environment Canada, Saskatoon, Saskatchewan, Canada, 121-139.

Hinzman, L.D., and 34 others (2005), Evidence and implications of recent climate change in northern Alaska and other Arctic regions. Climatic Change, 72, 251-298.

Hock, R. (1999), A distributed temperature-index ice- and snowmelt model including potential direct solar radiation. Journal of Glaciology, 45(149), 101-111.

Hock, R. (2003), Temperature index melt modeling in mountain areas. Journal of Hydrology 282, 104-115.

Hock, R. (2005), Glacier melt: a review of processes and their modeling. Progress in Physical Geography, 29(3), 362-391.

Hock, R., Johannson, M., Jansson, P., and L. Bärring (2002), Modeling Climate Conditions Required for Glacier Formation in Cirques of the Rassepautasjtjåkka Massif, Northern Sweden. Arctic, Antarctic, and Alpine Research, 34(1), 3-11.

Hodge, S.M., Trabant, D.C., Krimmel, R.M., Heinrichs, T.A., March, R.S., and E.G. Josberger (1998), Climate Variations and Changes in Mass of Three Glaciers in Western North America. Journal of Climate, 11, 2161-2179.

Hoelzle, M., Haeberli, W., Dischl, M., and W. Pescke (2003), Secular glacier mass balances derived from cumulative glacier length changes. Global and Planetary Change, 36, 295-306.

Hoinkes, H.C. (1955), Measurements of ablation and heat balance on Alpine glaciers. Journal of Glaciology, 2(17), 497-501.

Hoinkes, H.C. (1968), Glacier variations and weather. Journal of Glaciology, 7(49), 3-19.

Holdsworth, G. (1984), Glaciological reconnaissance of an ice core drilling site, Penny Ice Cap, Baffin Island. Journal of Glaciology, 30(104), 3-15.

Holland, M.M., and C.M. Bitz (2003), Polar amplification of climate in coupled models. Climate Dynamics, 21, 221-232.

Holmlund P., and T. Schneider (1997), The effect of continentality of glacier response and mass balance. Annals of Glaciology, 24, 272-276.

Hooke, R.B., Johnson, G.W., Bruger, K.A., Hanson, B., and G. Holdsworth (1987), Changes in mass balance, velocity, and surface profile along a flow line on Barnes Ice Cap, 1970-1984. Canadian Journal of Earth Sciences, 24, 1550-1561.

Hostetler, S.W., and P.U. Clark (2000), Tropical climate at the last glacial maximum inferred from glacier mass-balance modeling. Science, 290, 1747-1750.

Hostetler, S.W., Bartlein, P.J., Clark, P.U., Small, E.E., and A.M. Solomon (2000), Simulated influence of Lake Agassiz on the climate of central North America 11,000 years ago. Nature, 405, 334-337.

Houghton, J.T., Ding, Y., Griggs, D.J., Noguer, M., van der Linden, P.J., and D. Xiaosu (Eds.) (2001), *Climate Change 2001: The scientific basis, Third Assessment Report, IPCC Working Group I.* Cambridge University Press, New York, 944 pp.

Hubbard, A. (1997), Modelling climate, topography and paleoglacier fluctuations in the Chilean Andes. Earth Surface Processes and Landforms, 22, 79-92.

Hubbard, A. (1999), High-Resolution Modeling of the Advance of the Younger Dryas Ice Sheet and Its Climate in Scotland. Quaternary Research, 52, 27-43.

Hubbard, A., Hein, A.S., Kaplan, M.R., Hulton, N.J., and N. Glasser (2005), A modeling reconstruction of the last glacial maximum ice sheet and its deglaciation in the vicinity of the northern Patagonian icefield, South America. Geografiska Annaler, 87A(1), 375-391.

Hulbe, C.L., MacAyeal, D.R., Denton, G.H., Kleman, J., and T.V. Lowell (2004), Catastrophic ice shelf breakup as the source of Heinrich event icebergs. Paleoceanography, 19(PA1004), doi: 10.1029/2003PA000890.

Hulton, N., Sudgen, D., Payne, A., and C. Clapperton (1994), Glacier Modeling and the Climate of Patagonia during the Last Glacial Maximum. Quaternary Research, 42, 1-19.

Humlum, O. (1985), The Glaciation Level in West Greenland. Arctic and Alpine Research, 17(3), 311-319.

Humlum, O. (1997), Younger Dryas glaciation in Soerderasen, South Sweden: an analysis of meteorologic and topographic control. Geografiska Annaler, 79A(1-2), 1-5.

Humphreys, N., Shackleton, E., and A.W. Moore (1936), Oxford University Ellesmere Land Expedition. The Geographical Journal, 87(5), 385-410.

Huybrechts, P., and J. de Wolde (1999), The dynamic response of the Greenland and Antarctic ice sheets to multiple-century climatic warming. Journal of Climate, 12(8), 2169-2188.

Huybrechts P., Letreguilly, A., and N. Reeh (1991), The Greenland ice sheet and greenhouse warming. Global and Planetary Change, 3(4), 399-412.

Ives, J.D. (1957), Glaciation of the Torngat Mountains, northern Labrador. Arctic, 10, 67-88.

Ives, J.D. (1962), Indications of recent extensive glacierization in north-central Baffin Island, N.W.T. Journal of Glaciology, 4(32), 197-205.

Ives, J.D., Andrews, J.T., and R.G. Barry (1975), Growth and decay of the Laurentide Ice Sheet and Comparison with Fenno-Scandinavia. Die Naturwissenschaften, 62, 118-125.

Jackson, C.I. (1959), The meteorology of Lake Hazen, N.W.T. – Part I: Analysis of the Observations. *Publication in Meteorology No. 15*, Arctic Meteorology Research Group, McGill University, Montreal, Quebec, Canada, 114 pp.

Jackson, C.I. (1965), The vertical profile of wind at Lake Hazen, N.W.T. Arctic, 18(1), 21-35.

Jackson, C.I. (2002), *Does anyone read Lake Hazen?* Canadian Circumpolar Institute Press, Occasional Publication Series No. 53, University of Alberta, Edmonton, Alberta, Canada, 164 pp.

Jacobs, J.D. (1991), Climate Autostations on Barnes and Penny Ice Caps. *Baffin Island and Labrador Mesoclimate Project, Research Note 91/2*, Memorial University of Newfoundland, St. John's, Newfoundland, Canada, 19 pp.

Jacobs, J.D., Heron, R., and J.E. Luther (1993), Recent Changes at the Northwest Margin of the Barnes Ice Cap, Baffin Island, N.W.T., Canada. Arctic and Alpine Research, 25(4), 341-352.

Jacobs, J.D., Simms, E.L., and A. Simms (1997), Recession of the southern part of Barnes Ice Cap, Baffin Island, Canada, between 1961 and 1993, determined from digital mapping of Landsat TM. Journal of Glaciology, 43(143), 98-102.

Janssens, I., and P. Huybrechts (2000), The treatment of meltwater retardation in mass-balance parameterizations of the Greenland ice sheet. Annals of Glaciology, 31, 133-140.

Jansson, P. (1999), Effect of uncertainties in measured variables on the calculated mass balance of Storglaciären. Geografiska Annaler, 81A(4), 633-642.

Jansson, P., Rosqvist, G., and T. Schneider (2005), Glacier fluctuations, suspended sediment flux and glacio-lacustrine sediments. Geografiska Annaler, 87A(1), 37-50.

Jeffries, M.O. (1994), Marine Ice. In *Resource Description and Analysis – Ellesmere Island National Park Reserve*, Natural Resource Conservation Section, Parks Canada, Department of Canadian Heritage, Winnipeg, Manitoba, Canada.

Jeffries, M.O. (2002), Ellesmere Island Ice Shelves and Ice Islands. In *Satellite Image Atlas of Glaciers of the World*, edited by R.S. Williams and J.G. Ferrigno, U.S. Geological Survey Professional Paper 1386-J-1.

Jeffries, M.O., and H.R. Krouse (1984), Arctic ice shelf growth, fjord oceanography and climate. Zeitschrift für Gletscherkunde und Glazialgeologie, 20, 147-153.

Jeffries, M.O., and H.R. Krouse (1987), Snowfall and oxygen-isotope variations off the north coast of Ellesmere Island, N.W.T., Canada. Journal of Glaciology, 33(114), 195-199.

Jin, J., Gao, X., Yang, Z.-L., Bales, R.C., Sorooshian, S., Dickinson, R.E., Sun, S.F., and G.X. Wu (1999), Comparative Analyses of Physically Based Snowmelt Models for Climate Simulations. Journal of Climate, 12, 2643-2657.

Johannessen, O.M., and 12 others (2004), Arctic climate change – Observed and modeled temperature and sea ice variability. Tellus, 56A, 328-341.

Johannessen, O.M., Khvorostovsky, K., Miles, M.W., and L.P. Bobylev (2005), Recent Ice-Sheet Growth in the Interior of Greenland. Science, 310, 1013-1016.

Johannesson, T., Raymond, C.F., and E. Waddington (1989), Time-scale for adjustments of glaciers to changes in mass balance. Journal of Glaciology, 35(121), 355-369.

Johannesson, T., Sigurdsson, O., Laumann, T., and Kennett, M., 1993, Degree-day glacier mass balance modeling with applications to glaciers in Iceland and Norway. *Rapport 33*, Nordic Hydrological Programme, Reykjavik, Iceland.

Johannesson, T., Sigurdsson, O., Laumann, T., and M. Kennett (1995), Degree-day glacier mass-balance modeling with applications to glaciers in Iceland, Norway and Greenland. Journal of Glaciology, 41(138), 345-358.

Johnson, R.G., and J.T. Andrews (1979), Rapid Ice-Sheet Growth and Initiation of the Last Glaciation. Quaternary Research, 12, 119-134.

Jonsson, S. (1982), On the present glaciation of Storöya, Svalbard. Geografiska Annaler, 64A(1-2), 53-79.

Jonsson, S., and Hansson, M. (1990), Identification of annual layers in superimposed ice from Storöyjökulen in northeastern Svalbard. Geografiska Annaler, 72A(1), 41-54.

Käyhkö, J., and L. Talve (Eds.) (2002), *Understanding The Global System – The Finnish Perspective.* Finnish Global Change Research Programme (FIGARE), Painosalama, Turku, Finland, 232 pp.

Kahl, J.D.W., Serreze, M.C., Stone, R.S., Shiotani, S., Kisley, M., and R.C. Schnell (1993), Tropospheric Temperature Trends In the Arctic: 1958-1986. Journal of Geophysical Research, 98(D7), 12825-12838.

Kapsner, W.R., Alley, R.B., Shuman, C.A., Anandakrishnan, S., and P.M. Grootes (1995), Dominant influence of atmospheric circulation on snow accumulation in Greenland over the past 18,000 years. Nature, 373, 52-54.

Karl, T.R., and K.E. Trenberth (2003), Modern Global Climate Change. Science, 302, 1719-1723.

Karlen, W. (1973), Holocene glacier and climatic variations, Kebnekaise Mountains, Swedish Lapland. Geografiska Annaler, 55A(1), 29-63.

Karlen, W. (1988), Scandinavian glacial and climatic fluctuations during the Holocene. Quaternary Science Reviews, 7, 199-209.

Kaser, G. (1999), A review of the modern fluctuations of tropical glaciers. Global and Planetary Change, 22, 93-103.

Kaser, G., Hardy, D.R., Mölg, T., Bradley, R.S., and T.M. Hyera (2004a), Modern glacier retreat on Kilimanjaro as evidence of climate change: Observations and facts. International Journal of Climatology, 24, 329-339.

Kaser, G., Georges, C., Juen, I., Mölg, T., Wagnon, P., and B. Francou (2004b), The Behavior of Modern Low-Latitude Glaciers. PAGES News, 12(1), 15-17.

Kattsov, V.M., and E. Källen (2005), Future Climate Change: Modeling and Scenarios for the Arctic. In *Arctic Climate Impact Assessment – Scientific Report*, Cambridge University Press, New York, 99-150.

Keeler, C.M. (1964), Relationships between climate, ablation, and runoff on the Sverdrup Glacier, 1963, Devon Island, N.W.T. *Research Paper No. 27*, Arctic Institute of North America, University of Calgary, Calgary, Alberta, Canada, 125 pp.

Kerr, A. (1993), Topography, climate and ice masses: a review. Terra Nova, 5, 332-342.

Kerr, R.A. (1994), 'Climate Modeling's Fudge Factor Comes Under Fire'. Science, 265(9), 1528.

Kerwin, M.W., Overpeck, J., Webb, R., and K.H. Anderson (2004), Pollen-based summer temperature reconstructions for the eastern Canadian Boreal Forest, Sub-Arctic, and Arctic. Quaternary Science Reviews, 23, 1901-1924.

Kinger, J.B. (1940), Relation of recent glacier recessions to prevailing temperatures. Monthly Weather Review, 68(6), 158-160.

Kleman, J. (1994), Preservation of landforms under ice sheets and ice caps. Geomorphology, 9, 19-32.

Kleman, J., Fastook, J., and A.P. Stroeven (2002), Geologically and geomorphologically constrained numerical model of the Laurentide Ice Sheet inception and build-up. Quaternary International, 95-96, 87-98.

Klingbjer, P., Brown, I.A., and P. Holmlund (2005), Identification of climate controls on the dynamic behaviour of the subarctic glacier Salajekna, northern Scandinavia. Geografiska Annaler, 87A(1), 215-229.

Klok, E.J., and J. Oerlemans (2003), Deriving historical equilibrium-line altitudes from a glacier length record by linear inverse modeling. The Holocene, 13(3), 343-351.

Knight, P.G. (1998), Glaciers. Progress in Physical Geography, 22(3), 407-411.

Koch, L. (1926), Ice cap and sea ice in North Greenland. Geographical Review, 16(1), 98-107.

Koenig, L.S., Greenaway, K.R., Dunbar, M., and G. Hattersley-Smith (1952), Arctic Ice Islands. Arctic, 5(2), 67-103.

Koerner, R.M. (1968), Fabric Analysis of a core from the Meighen Ice Cap, Northwest Territories, Canada. Journal of Glaciology, 7(51), 421-430.

Koerner, R.M. (1970), Some observations on superimposition of ice on the Devon Island Ice Cap, N.W.T., Canada. Geografiska Annaler, 52A(1), 57-67.

Koerner, R.M. (1977a), Devon Island Ice Cap: Core Stratigraphy and Paleoclimate. Science, 196, 15-18.

Koerner, R.M. (1977b), Ice thickness measurements and their implications with respect to past and present ice volumes on the Canadian High Arctic ice caps. Canadian Journal of Earth Sciences, 14, 2697-2705.

Koerner, R.M. (1979), Accumulation, ablation and oxygen isotope variations on the Queen Elizabeth Islands ice caps, Canada. Journal of Glaciology, 22(86), 25-41.

Koerner, R.M. (1980a), Instantaneous Glacierization, the Rate of Albedo Change, and Feedback Effects at the Beginning of an Ice Age. Quaternary Research, 13, 153-159.

Koerner, R.M. (1980b), The problem of lichen-free zones in Arctic Canada. Arctic and Alpine Research, 12(1), 87-94.

Koerner, R.M. (1989a), Queen Elizabeth Island glaciers. In *Quaternary Geology of Canada and Greenland*, edited by R.J. Fulton, Geological Survey of Canada, Ottawa, Ontario, Canada.

Koerner, R.M. (1989b), Ice Core Evidence for Extensive Melting of the Greenland Ice Sheet in the last Interglacial. Science, 244, 964-968.

Koerner, R.M. (1996), Canadian Arctic. In *Report on mass balance of Arctic glaciers*, edited by J. Jania and J.O. Hagen, Working Group on Arctic Glaciology, International Arctic Science Committee, Oslo, Norway, 5-8.

Koerner, R.M. (1997), Some comments on climatic reconstructions from ice cores drilled in areas of high melt. Journal of Glaciology, 43(143), 90-97.

Koerner, R.M. (2001), Glacier Mass Balance in the Canadian High Arctic: Placing the Summer of 1998 in long-term context. In *The state of the Arctic cryosphere during the extreme warm summer of 1998: documenting cryospheric variability in the Canadian Arctic*, edited by R.D. Brown and B.T. Alt, Canadian Cryospheric Information Network, University of Waterloo, Waterloo, Ontario, Canada.

Koerner, R.M. (2002), Glaciers of the High Arctic Islands. In *Satellite Image Atlas of Glaciers of the World*, edited by R.S. Williams and J.G. Ferrigno, U.S. Geological Survey Professional Paper 1386-J-1.

Koerner, R.M., and D.A. Fisher (1990), A record of Holocene summer climate from a Canadian high-Arctic ice core. Nature, 343, 630-631.

Koerner, R.M., and L. Lundgaard (1995), Glaciers and Global Warming. Geographie physique et Quaternaire, 49(3), 429-434.

Koerner, R.M., and D.A. Fisher (2002), Ice-core evidence for widespread Arctic glacier retreat in the Last Interglacial and the early Holocene. Annals of Glaciology, 35, 19-24.

Koerner, R.M., Fisher, D.A., and W.S.B. Paterson (1987), Wisconsinan and pre-Wisconsinan ice thickness on Ellesmere Island, Canada: inferences from ice cores. Canadian Journal of Earth Science, 24, 296-301.

Koizumi, K., and R. Naruse (1992), Measurements of meteorological conditions and ablation at Tyndall Glacier, southern Patagonia, in December 1990. Bulletin of Glacier Research, 10, 79-82.

Konikow, L.F., and J.D. Bredehoeft (1992), Ground-water models cannot be validated. Advances in Water Resources, 15, 75-83.

Konya, K., Matsumoto, T., and R. Naruse (2004), Surface heat balance and spatially distributed ablation modeling at Koryto Glacier, Kamchatka Peninsula, Russia. Geografiska Annaler, 86A(4), 337-347.

Kovanen, D.J., and O. Slaymaker (2005), Fluctuations of the Deming Glacier and theoretical equilibrium line altitudes during the Late Pleistocene and Early Holocene on Mount Baker, Washington, USA. Boreas, 34, 157-175.

Krabill, W., Abdalati, W., Frederick, E., Manizade, S., Martin, C., Sonntag, J., Swift, R., Thomas, R., Wright, W., and J. Yungel (2000), Greenland ice sheet: High-elevation balance and peripheral thinning. Science, 289, 428-430.

Krabill, W., Hanna, E., Huybrechts, P., Abdalati, W., Cappelen, J., Csatho, B., Frederick, E., Manizade, S., Martin, C., Sonntag, J., Swift, R., Thomas, R., and J. Yungel (2004), Greenland Ice Sheet: Increased coastal thinning. Geophysical Research Letters, 31(L24402), doi:10.1029/2004GL021533.

Krenke, A.N. (1975), Climatic conditions of present-day glaciation in Soviet Central Asia. International Association of Hydrological Sciences (IAHS) Publication, 104, 30-41.

Kuhn, M. (1984), Mass budget imbalances as criterion for a climatic classification of glaciers. Geografiska Annaler, 66A(3), 229-238.

Kuhn, M. (1993), Methods of assessing the effects of climatic changes on snow and glacier hydrology. International Association of Hydrological Sciences (IAHS) Publication, 218, 135-144.

Kuhn, M. (1995), The mass balance of very small glaciers. Zeitschrift für Gletscherkunde und Glazialgeologie, 31, 171-179.

Kuhn, M., Dreiseitl, E., Hofinger, S., Markl, G., Span, N., and G. Kaser (1999), Measurements and models of the mass balance of Hintereisferner. Geografiska Annaler, 81A(4), 659-670.

Kuhry, P., and 15 others (2002), Arctic feedbacks to global warming. In *Understanding The Global System – The Finnish Perspective*, edited by J. Käyhkö and L. Talve, Finnish Global Change Research Programme (FIGARE), Painosalama, Turku, Finland, 232 pp.

Kustas, W.P., Rango, A., and R. Uijlenhoet (1994), A simple energy budget algorithm for the snowmelt runoff model. Water Resources Research, 30(5), 1515-1527.

Kuusisto, E. (1980), On the Values and Variability of Degree-Day Melting Factor in Finland. Nordic Hydrology, 11, 235-242.

Kuusisto, E. (1986), The energy balance of a melting snow cover in different environments. International Association of Hydrological Sciences (IAHS) Publication, 155, 37-45.

Laabs, B.J.C., Plummer, M.A., and Mickelson, D.M., 2005, Climate during the last glacial maximum in the Wasatch and southern Uinta Mountains inferred from glacier modeling. Geomorphology, in press.

Lahsen, M. (2005), Seductive Simulations? Uncertainty Distribution Around Climate Models. Social Studies of Science, 35(6), 895-922.

Lamb, H.H., and A. Woodroffe (1970), Atmospheric circulation during the last Ice Age. Quaternary Research, 1, 29-58.

Lang, H., and L. Braun (1990), On the information content of air temperature in the context of snow melt estimation. International Association of Hydrological Sciences (IAHS) Publication, 190, 347-354.

Langleben, M.P. (1966), On the factors affecting the rate of ablation of sea ice. Canadian Journal of Earth Sciences, 3, 431-439.

Larocque, S.J., and D.J. Smith (2005), 'Little Ice Age' proxy glacier mass balance records reconstructed from tree rings in the Mt Waddington area, British Columbia Coast Mountains, Canada. The Holocene, 15(5), 748-757.

Laumann, T., and N. Reeh (1993), Sensitivity to climate change of the mass balance of glaciers in southern Norway. Journal of Glaciology, 39(133), 656-665.

Laxon, S.W., Walsh, J.E., Wadhams, P., Johannessen, O., and M. Miles (2003), Sea-ice observations. In *Mass Balance of the Cryosphere*, edited by J.L. Bamber and A.J. Payne, Cambridge University Press, New York, 337-366.

Lefebre, F., Gallee, H., Van Ypersele, J.P., and P. Huybrechts (2002), Modelling of large-scale melt parameters with a regional climate model in south Greenland during the 1991 melt season. Annals of Glaciology, 35, 391-397.

Lehmkuhl, F., and L.A. Owen (2005), Late Quaternary glaciation of Tibet and the bordering mountains: a review. Boreas, 34, 87-100.

Leonard, E.M. (1986), Use of lacustrine sedimentary sequences as indicators of Holocene glacial history, Banff National Park, Alberta, Canada. Quaternary Research, 26, 218-231.

Levesque, E., and J. Svoboda (1999), Vegetation re-establishment in polar 'lichen-kill' landscapes: a case study of the Little Ice Age impact. Polar Research, 18, 221-228.

Lewis, T., Gilbert, R., and S.F. Lamoureux (2002), Spatial and Temporal Changes in Sedimentary Processes at Proglacial Bear Lake, Devon Island, Nunavut, Canada. Arctic, Antarctic, and Alpine Research, 34(2), 119-129.

Lewis, T., Braun, C., Hardy, D.R., Francus, P., and R.S. Bradley (2005), An Extreme Sediment Transfer Event in a Canadian High Arctic Stream. Arctic, Antarctic, and Alpine Research, 37(4), 477-482.

Lie, O., Dahl, S.O., and A. Nesje (2003a), A theoretical approach to glacier equilibrium-line altitudes using meteorological data and glacier mass-balance records from southern Norway. The Holocene, 13(3), 365-372.

Lie, O., Dahl, S.O., and A. Nesje (2003b), Theoretical equilibrium-line altitudes and glacier buildup sensitivity in southern Norway based on meteorological data in a geographical information system. The Holocene, 13(3), 373-380.

Lindström, G., Johansson, B., Perrson, M., Gardelin, M., and S. Bergström (1997), Development and test of the distributed HBV-96 model. Journal of Hydrology, 201, 272-288.

Lister, H. (1962), Heat and mass balance at the surface of the Ward Hunt Ice Shelf, 1960. *Research Paper No. 19*, Arctic Institute of North America, University of Calgary, Calgary, Alberta, Canada, 54 pp.

Liston, G.E. (1995), Local Advection of Momentum, Heat, and Moisture during the Melt of Patchy Snow Covers. Journal of Applied Meteorology, 34, 1705-1715.

Locke, C.W., and W.W. Locke III (1977), Little Ice Age snow-cover extent and paleoglaciation thresholds: North-central Baffin Island, N.W.T., Canada. Arctic and Alpine Research, 9, 291-300.

Løken, O.H., and J.T. Andrews (1966), Glaciology and chronology of fluctuations of the ice margin at the south end of the Barnes Ice Cap. Geographical Bulletin, 8(4), 341-359.

Løken, O.H., and R.B. Sagar (1968), Mass balance observations on the Barnes Ice Cap, Baffin Island, Canada. International Association of Hydrological Sciences (IAHS) Publication, 79, 282-291.

Loewe, F. (1971), Considerations on the origin of the Quaternary ice sheet of North America. Arctic and Alpine Research, 3(4), 331-344.

Lotz, J.R. (1961a), Meteorological observations in Northern Ellesmere Island – 1959. *Scientific Report No. 11*, Arctic Institute of North America, University of Calgary, Calgary, Alberta, Canada, 74 pp.

Lotz, J.R. (1961b), Analysis of meteorological and micrometeorological observations, Northern Ellesmere Island, 1959. *Scientific Report No. 12*, Arctic Institute of North America, University of Calgary, Calgary, Alberta, Canada, 81 pp.

Lotz, J.R., and R.B. Sagar (1962), Northern Ellesmere Island – An Arctic Desert. Geografiska Annaler, 19(3-4), 366-377.

Lowell, T.V. (2000), As climate changes, so do glaciers. Proceedings of the National Academy of Sciences, 97(4), 1351-1354.

Luce, C.H., Tarboton, D.G., and K.R. Cooley (1999), Sub-grid parameterization of snow distribution for an energy and mass snow cover model. Hydrological Processes, 13, 1921-1933.

Luckman, B.H. (2000), The Little Ice Age in the Canadian Rockies. Geomorphology, 32(3), 357-384.

Lundquist, D. (1982), Modeling runoff from a glacierized basin. International Association of Hydrological Sciences (IAHS) Publication, 138, 131-136.

Lyons, J.B., and R.H. Ragle (1962), Thermal history and growth of the Ward Hunt Ice Shelf. International Association of Hydrological Sciences (IAHS) Publication, 58, 88-97.

Lyons, J.B., Ragle, R.H., and A.J. Tamburi (1972), Growth and Grounding of the Ellesmere Island Ice Rises. Journal of Glaciology, 11(61), 43-52.

Maasch, K.A., Mayewski, P.A., Rohling, E.J., Stager, J.C., Karlen, W., Meeker, L.D., and E.A. Meyerson (2005), A 2000-year context for modern climate change. Geografiska Annaler, 87A(1), 7-15.

Mackintosh, A.N., Dugmore, A.J., and A.L. Hubbard (2002), Holocene climatic changes in Iceland: evidence from modeling glacier length fluctuations at Solheimajökull. Quaternary International, 91, 39-52.

Mair, D., Burgess, D., and M. Sharp (2005), Thirty-seven year mass balance of Devon Ice Cap, Nunavut, Canada, determined by shallow ice coring and melt modeling. Journal of Geophysical Research, 110(F01011), doi: 10.1029/2003JF000099.

Male, D.H., and D.M. Gray (1981), Snowcover ablation and runoff. In *Handbook of Snow*, edited by D.M. Gray and D.H. Male, Pergamon Press, Toronto, Ontario, Canada, 360-436.

Manabe, S., and A.J. Broccoli (1985), The influence of continental ice sheets on the climate of an Ice Age. Journal of Geophysical Research, 90D, 2167-2190.

Manley, G. (1955), On the occurrence of ice-domes and permanently snow-covered summits. Journal of Glaciology, 2, 453-456.

Mark, B.G., and G.O. Seltzer (2005), Evaluation of recent glacier recession in the Cordillera Blanca, Peru (AD 1962-1999): spatial distribution of mass loss and climatic forcing. Quaternary Science Reviews, 24, 2265-2280.

Marsh, P. (1999), Snow cover formation and melt: recent advances and future prospects. Hydrological Processes, 13, 2117-21134.

Marsh, P., and J.W. Pomeroy (1996), Meltwater fluxes at an arctic forest-tundra site. Hydrological Processes, 10, 1383-1400.

Marsh, P., Pomeroy, J.W., and N. Neumann (1997), Sensible heat flux and local advection over heterogeneous landscape at an Arctic tundra site during snowmelt. Annals of Glaciology, 25, 132-136.

Marshall, S.J. (2002), Modelled nucleation centres of the Pleistocene ice sheets from an ice sheet model with subgrid topographic and glaciologic parameterizations. Quaternary International, 95-96, 125-137.

Marshall, S.J., and G.K.C. Clarke (1999), Ice sheet inception: subgrid hypsometric parameterization of mass balance in an ice sheet model. Climate Dynamics, 15, 533-550.

Marshall, S.J., Pollard, D., Hostetler, S., and P.U. Clark (2004), Coupling ice-sheet and climate models for simulation of former ice sheets. Developments in Quaternary Science, 1, 105-126, doi: 10.1016/S1571-0866(03)01006-6.

Marsiat, I. (1995), The waxing and waning of the Northern Hemisphere ice sheets. Annals of Glaciology, 21, 96-102.

Martinec, J. (1976), Snow and ice. In *Facets of Hydrology*, edited by J. Rodda, Wiley & Sons, London, UK, 85-118.

Martinec, J., and A. Rango (1986), Parameter values for snowmelt runoff modeling. Journal of Hydrology, 84, 197-219.

Matthes, F.E. (1939), Report of the Committee on Glaciers, April 1939. Transactions of the American Geophysical Union, 20, 518-523.

Matthews, J.A. (2005), 'Little Ice Age' glacier variations in Jotunheimen, southern Norway: a study in regionally controlled lichenometric dating of recessional moraines with implications for climate and lichen growth rates. The Holocene, 15(1), 1-19.

Matthews, J.A., and K.R. Briffa (2005), The 'Little Ice Age': Re-evaluation of an evolving concept. Geografiska Annaler, 87A(1), 17-36.

Maxwell, J.B. (1980), The Climate of the Canadian Arctic Islands and Adjacent Waters. Vol. 1. *Climatological Studies No.30*, Atmospheric Environment Service, Environment Canada, Downsview, Ontario, Canada, 532 pp.

Maxwell, J.B. (1981), Climatic regions of the Canadian Arctic Islands. Arctic, 34(3), 225-240.

McCabe, G.J., and A.G. Fountain (1995), Relations between Atmospheric Circulation and Mass Balance of South Cascade Glacier, Washington, U.S.A. Arctic and Alpine Research, 27, 226-233.

McCabe, G.J., Fountain, A.G., and M. Dyurgerov (2000), Variability in Winter Mass Balance of Northern Hemisphere Glaciers and Relations with Atmospheric Circulation. Arctic, Antarctic, and Alpine Research, 32, 64-72.

Meehl, G., Washington, W.M., Collins, W.D., Arblaster, J.M., Hu, A., Buja, L.E., Strand, W.G., and H. Teng (2005), How Much More Global Warming and Sea Level Rise? Science, 307, 1769-1772.

Meier, M.F. (1962), Proposed definitions for glacier mass budget terms. Journal of Glaciology, 4(33), 252-263.

Meier, M.F., Dyurgerov, M.B., and G.J. McCabe (2003), The health of glaciers: recent changes in glacier regime. Climatic Change, 59, 123-135.

Meier, M.F., Bahr, D.B., Dyurgerov, M.B., and W.T. Pfeffer (2005), Comment on 'The potential for sea level rise: New estimates from glacier and ice cap area and volume distributions'. Geophysical Research Letters, 32(L17501), doi: 10.1029/2005GL023319.

Mekis, E., and W.D. Hogg (1999), Rehabilitation and Analysis of Canadian Daily Precipitation Time Series. Atmosphere-Ocean, 37(1), 53-85.

Mengel, J.G., Short, D.A., and G.R. North (1988), Seasonal snowline instability in an energy balance model. Climate Dynamics, 2, 127-131.

Mercer, J.H. (1961a), The estimation of the regimen and former firn limit of a glacier. Journal of Glaciology, 3(30), 1053-1062.

Mercer, J.H. (1961b), The response of fjord glaciers to changes in the firn limit. Journal of Glaciology, 3(29), 850-858.

Melloh, R.A. (1999), A Synopsis and Comparison of Selected Snowmelt Algorithms. *Report 99-8*, U.S. Army Cold Regions Research and Engineering Laboratory, Hanover, New Hampshire, 17 pp.

Messel, S. (1971), Mass and heat balance of Omnsbreen – a climatically dead glacier in southern Norway. *Norsk Polarinstitut Skrifter No. 156*, Norsk Polarinstitut, Oslo, Norway, 42 pp.

Miller, G.H. (1976), Anomalous local glacier activity, Baffin Island, Canada: Paleoclimatic implications. Geology, 4, 502-504.

Miller, G.H., and A. de Vernal (1992), Will greenhouse warming lead to Northern Hemisphere ice-sheet growth? Nature, 355, 244-246.

Miller, G.H., Bradley, R.S., and J.T. Andrews (1975), The glaciation level and lowest equilibrium line altitude in the High Canadian Arctic: Maps and climatic interpretation. Arctic and Alpine Research, 7(2), 155-168.

Miller, G.H., Wolfe, A.P., Briner, J.P., Sauer, P.E., and A. Nesje (2005), Holocene glaciation of climate evolution of Baffin Island, Arctic Canada. Quaternary Science Reviews, 24, 1703-1721.

Mineter, M., and N. Hulton (2001), Parallel processing for finite-difference modeling of ice sheets. Computers and Geosciences, 27, 829-838.

Mölg, T., Hardy, D.R., and G. Kaser (2003), Solar-radiation-maintained glacier recession on Kilimanjaro drawn from combined ice-radiation geometry modeling. Journal of Geophysical Research, 108(D23), doi: 10.1029/2003JD003546.

Molotch, N.P., Painter, T.H., Bales, R.C., and J. Dozier (2004), Incorporating remotely-sensed snow albedo into a spatially-distributed snowmelt model. Geophysical Research Letters, 31(L035O1), doi: 10.1029/2003GL019063.

Moore, A.W., Bentham, R., Haig-Thomas, D., Shackleton, E., and A.J. Wilmott (1936), The Sledge Journey to Grant Land. The Geographical Journal, 87(5), 419-441.

Moore, R.D. (1983), On the Use of Bulk Aerodynamic Formulae Over Melting Snow. Nordic Hydrology, 14, 193-206.

Moore, J.C., Kekonen, T., and A. Pälli (2002), The record of rapid changes in the Arctic and their impact on glaciers in Svalbard. In *Understanding The Global System – The Finnish Perspective*, edited by J. Käyhkö and L. Talve, Finnish Global Change Research Programme (FIGARE), Painosalama, Turku, Finland, 232 pp.

Morris, E.M. (1999), Surface ablation rates on Moraine Corrie Glacier, Antarctica. Global and Planetary Change, 22, 221-231.

Morris, E.M., and R. Mulvaney (2004), Recent variations in surface mass balance of the Antarctic Peninsula ice sheet. Journal of Glaciology, 50(169), 257-267.

Moss, R. (1938), The Physics of an Ice-Cap. The Geographical Journal, 92(3), 211-227.

Müller, F. (1962), Glacier mass-budget studies on Axel Heiberg Island, Canadian Arctic Archipelago. International Association of Hydrological Sciences (IAHS) Publication, 58, 131-142.

Müller, F., and N. Roskin-Sharlin (1967), A High Arctic climate study on Axel Heiberg Island, Canadian Arctic Archipelago – summer 1961. Part 1. General meteorology. *Axel Heiberg Island Research Reports - Meteorology No.3*, McGill University, Montreal, Quebec, Canada.

Müller, F., and C.M. Keeler (1969), Errors in short-term ablation measurements on melting ice surfaces. Journal of Glaciology, 8(52), 91-105.

Mueller, D.R., Vincent, W.F., and M.O. Jeffries (2003), Break-up of the largest Arctic ice shelf and associated loss of an epishelf lake. Geophysical Research Letters, 30(20), doi: 10.1029/2003GL017931.

Munro, D.S. (1991), A surface energy exchange model of glacier melt and net mass balance. International Journal of Climatology, 11, 689-700.

Munroe, J., and D. Mickelson (2002), Last Glacial Maximum equilibrium-line altitudes and paleoclimate, northern Uinta Mountains, Utah, U.S.A. Journal of Glaciology, 48, 257-266.

Nesje, A., and S.O. Dahl (2003), The 'Little Ice Age' – only temperature? The Holocene, 13(1), 171-177.

Nesje, A., Johannessen, T., and H.J.B. Birks (1995), Briksdalsbreen, western Norway: climatic effects on the terminal response of a temperate glacier between AD 1901 and 1994. The Holocene, 5, 343-347.

Neumann, N., and P. Marsh (1998), Local advection of sensible heat in the snowmelt landscape of Arctic tundra. Hydrological Processes, 12, 1547-1560.

Nordli, O., Lie, O., Nesje, A., and R.E. Benestad (2005), Glacier mass balance in southern Norway modeled by circulation indices and spring-summer temperatures AD 1781-2000. Geografiska Annaler, 87A(1), 431-445.

North, G.R. (1984), The Small Ice Cap Instability in Diffusive Climate Models. Journal of the Atmospheric Sciences, 41(23), 3390-3395.

Nyberg, R., and L. Lindh (1990), Geomorphic features as indicators of climatic fluctuations in a periglacial environment, northern Sweden. Geografiska Annaler, 72A(2), 203-210.

Nye, J.F. (1963), The response of a glacier to changes in the rate of nourishment and wastage. Proceedings of the Royal Society, Series A, 275(1360), 87-112.

Nye, J.F. (1965), A numerical method for inferring the budget history of a glacier from its advance and retreat. Journal of Glaciology, 5(41), 589-607.

Obleitner, F., and M. Lehning (2004), Measurements and simulation of snow and superimposed ice at the Kongsvegen glacier, Svalbard (Spitsbergen). Journal of Geophysical Research, 109(D04106), doi: 10.1029/2003JD003945.

Oerlemans, J. (1989), On the response of valley glaciers to climatic change. In *Glacier Fluctuations and Climatic Change*, edited by J. Oerlemans, Kluwer, Dordrecht, Netherlands, 353-371.

Oerlemans, J. (1991), The mass balance of the Greenland ice sheet: sensitivity to climate change as revealed by energy-balance modeling. The Holocene, 1(1), 40-49.

Oerlemans, J. (1991/1992), A model for the surface balance of ice masses: part I. Alpine glaciers. Zeitschrift für Gletscherkunde und Glazialgeologie, 27/28, 63-83.

Oerlemans, J. (1993), Modelling of Glacier Mass Balance. In Ice in the Climate System, edited by W.R. Peltier, NATO ASI Series, vol. I 12, Springer Verlag, Berlin, Germany, 101-116.

Oerlemans, J. (1998), Modelling glacier fluctuations. In *Into the Second Century of World Glacier Monitoring - Prospects and Strategies*, edited by W. Haeberli, M. Hoelzle, and S. Suter, UNESCO Publishing, Paris, France, 85-96.

Oerlemans, J. (2000), Analysis of a 3 year meteorological record from the ablation zone of Morteratschgletscher, Switzerland: energy and mass balance. Journal of Glaciology, 46(155), 571-579.

Oerlemans, J. (2001), *Glaciers and Climate Change*. Swets and Zeitlinger, Lisse, Netherlands, 148 pp.

Oerlemans, J. (2002), On glacial inception and orography. Quaternary International, 95-96, 5-10.

Oerlemans, J. (2005), Extracting a Climate Signal from 169 Glacier Records. Science, 308(5722), 675-677.

Oerlemans, J., and N.C. Hoogendoorn (1989), Mass-balance gradients and climatic change. Journal of Glaciology, 35(121), 399-405.

Oerlemans, J., and J.P.F. Fortuin (1992), Sensitivity of Glaciers and Small Ice Caps to Greenhouse Warming. Science, 258, 115-117.

Oerlemans, J., and H.F. Vugts (1993), A Meteorological Experiment in the Melting Zone of the Greenland Ice Sheet. Bulletin of the American Meteorological Society, 74(3), 355-365.

Oerlemans, J., and B.K. Reichert (2000), Relating glacier mass balance to meteorological data by using a seasonal sensitivity characteristic. Journal of Glaciology, 46(152), 1-6.

Oerlemans, J., and E.J. Klok (2004), Effect of summer snowfall on glacier mass balance. Annals of Glaciology, 38, 97-100.

Oerlemans, J., Anderson, B., Hubbard, A., Huybrechts, P., Johanesson, T., Knap, W.H., Schmeits, M., Stroeven, A.P., van der Wal, R.S.W., Wallings, J., and Z. Zuo (1998), Modelling the response of glaciers to climate warming. Climate Dynamics, 14, 267-274.

Oerlemans, J., Bassford, R.P., Chapman, W., Dowdeswell, J.A., Glazovsky, A.F., Hagen, J.-O., Melvold, de Ruyter de Wildt, M., and R.S.W van de Wal (2006), Estimating the contribution from Arctic glaciers to sea-level change in the next hundred years. Annals of Glaciology, 42, in press.

Ogura, T., and A. Abe-Ouchi (2001), Influence of the Antarctic ice sheet on southern high latitude climate during the Cenozoic: Albedo vs. topography effect. Geophysical Research Letters, 28(4), 587-590.

Ohmura, A. (2000), Climate on tundra and thoughts on causes of regional climate differences. Annals of Glaciology, 31, 10-14.

Ohmura, A. (2001), Physical basis for the temperature-based melt-index method. Journal of Applied Meteorology, 40(4), 753-761.

Ohmura, A., Kasser, P., and M. Funk (1992), Climate at the equilibrium line of glaciers. Journal of Glaciology, 38(130), 397-411.

Ohmura, A., Wild, M., and L. Bengtsson (1996a), A possible change in mass balance of Greenland and Antarctic ice sheets in the coming century. Journal of Climate, 9, 2124-2135.

Ohmura, A., Wild, M., and L. Bengtsson (1996b), Present and future mass balance of the ice sheets simulated with GCM. Annals of Glaciology, 23, 187-193.

Ohmura, A., Calanca, P., Wild, M., and M. Anklin (1999), Precipitation, accumulation, and mass balance of the Greenland Ice Sheet. Zeitschrift für Gletscherkunde und Glazialgeologie, 35(1), 1-20.

Ommanney, C.S.L. (1969), A study in glacier inventory: The ice masses of Axel Heiberg Island, Canadian Arctic Archipelago. *Axel Heiberg Island Research Reports, Glaciology No. 3*, McGill University, Montreal, Quebec, Canada, 105 pp.

Ommanney, C.S.L. (1977), Quadrennial report to the Permanent Service on the Fluctuations of Glaciers on Canadian glacier variations and mass balance changes. Glaciology Division, Inland Waters Directorate, Fisheries and Environment Canada, Ottawa, Ontario, Canada.

Oreskes, N., Shrader-Frechette, K., and K. Belitz (1994), Verification, validation, and confirmation of numerical models in the earth sciences. Science, 263, 641-646.

Orvig, S. (1951), The climate of the ablation period on the Barnes Ice-Cap in 1950. Geografiska Annaler, 33(3-4), 166-209.

Orvig, S. (1954), Glacial-Meteorological Observations on Icecaps in Baffin Island. Geografiska Annaler, 36(3-4), 193-314.

Østrem, G. (1963), Comparative Crystallographic Studies on Ice from Ice-Cored Moraines, Snow-Banks and Glaciers. Geografiska Annaler, 45(4), 210-240.

Østrem, G., and A. Tvede (1986), Comparison of glacier maps – A source of climatological information? Geografiska Annaler, 68A(3), 225-231.

Østrem, G., and M. Brugman (1991), *Glacier mass-balance measurements. A manual for field and office work.* National Hydrology Research Institute Science Report 4, Environment Canada, Saskatoon, Saskatchewan, 224 pp.

Overpeck, J.T., and 20 others (2005), Arctic System on Trajectory to New, Seasonally Ice-Free State. EOS Transactions of the American Geophysical Union, 86(34), 309-313.

Owen, L.A., Finkel, R.C., Barnard, P.L., Haizhou, M., Asahi, K., Caffee, M.W., and E. Derbyshire (2005), Climatic and topographic controls on the style and timing of Lake Quaternary glaciation throughout Tibet and the Himalaya defined by ^{10}Be cosmogenic radionuclide surface exposure dating. Quaternary Science Reviews, 24, 1391-1411.

Pälli, A., Moore, J.C., Jania, J., and P. Glowacki (2003), Glacier changes in southern Spitsbergen, Svalbard, 1901-2000. Annals of Glaciology, 37, 219-225.

Paterson, W.S.B. (1969), The Meighen Ice Cap, Arctic Canada: Accumulation, Ablation and Flow. Journal of Glaciology, 8(54), 341-352.

Paterson, W.S.B. (1981), *The Physics of Glaciers. Second Edition.* Pergamon Press, Oxford, UK, 380 pp.

Paterson, W.S.B. (1990), Summary of Final Discussion. Annals of Glaciology, 14, 230-231.

Paterson, W.S.B. (1994), *The Physics of Glaciers, Third Edition.* Elsevier, Oxford, UK, 480 pp.

Payne, A., and D.E. Sugden (1990), Topography and ice sheet growth. Earth Surface Processes and Landforms, 15, 625-639.

Payne, A., Sugden, D.E., and C.M. Clapperton (1989), Modeling the Growth and Decay of the Antarctic Peninsula Ice Sheet. Quaternary Research, 31, 119-134.

Peary, R.E. (1907), *Nearest the Pole.* Hutchinson, London, UK, 410 pp.

Pellicciotti, F., Brock, B., Strasser, U., Burlando, P., Funk, M., and J. Corripio (2003), A distributed temperature index model including albedo: application to Haut Glacier d'Arolla. Geophysical Research Abstracts, 5(09101), European Geophysical Society – American Geophysical Union – European Union of Geoscientist Joint Assembly, Nice, France, 6-11 April 2003.

Pelto, M.S., Higgins, S.M., Hughes, T.J., and J.L. Fastook (1990), Modelling mass balance during a glaciation cycle. Annals of Glaciology, 14, 238-241.

Pfeffer, W.T., Illangasekare, T.H., and M.F. Meier (1991), Analysis and modeling of melt-water refreezing in dry snow. Journal of Glaciology, 36(123), 238-246.

Pfeffer, W.T., Sassolas, C., Bahr, D.B., and M.F. Meier (1998), Response time of glaciers as a function of size and mass balance: 2. Numerical Experiments. Journal of Geophysical Research, 103(B5), 9783-9789.

Pielke Sr., R.A., Davey, C., and J. Morgan (2004), Assessing 'global warming' with surface heat content. EOS Transactions of the American Geophysical Union, 85(21), 210-211.

Plüss, C., and R. Mazzoni (1994), The Role of Turbulent Heat Fluxes in the Energy Balance of High Alpine Snow Cover. Nordic Hydrology, 25, 25-38.

Plummer, M.A. (2002), Paleoclimate conditions during the last deglaciation inferred from combined analysis of pluvial and glacial records. Ph.D. dissertation, New Mexico Institute of Mining and Technology, Socorro, New Mexico, 346 pp.

Plummer, M.A., and F.M. Phillips (2003), A 2-D numerical model of snow/ice energy balance and ice flow for paleoclimatic interpretation of glacial geomorphic features. Quaternary Science Reviews, 22, 1389-1406.

Podlech, S., Mayer, C., and C.E. Bøggild (2004), Glacier retreat, mass-balance and thinning: Sermilik Glacier, South Greenland. Geografiska Annaler, 86A(4), 305-317.

Pohjola, V.A., Cole-Dai, J., Rosqvist, G., Stroeven, A.P., and L.G. Thompson (2005), Potential to recover climatic information from Scandinavian ice cores: An example from the small ice cap Riukojietna. Geografiska Annaler, 87A(1), 259-270.

Pollard, D., and S.L. Thompson (1997), Driving a high-resolution dynamic ice-sheet model with GCM climate: ice-sheet initiation at 116,000 BP. Annals of Glaciology, 25, 296-304.

Pollard, D., and R.M. DeConto (2005), Hysteresis in Cenozoic Antarctic ice-sheet variations. Global and Planetary Change, 45(1-3), 9-21.

Pollard, D., and J.F. Kasting (2005), Snowball Earth: A thin-ice solution with flowing sea glaciers. Journal of Geophysical Research, 110(C07010), doi: 10.1029/2004JC002525.

Porter, S.C. (1977), Present and past glaciation thresholds in the Cascade Range, Washington, U.S.A.: Topographic and Climatic controls, and paleoclimatic implications. Journal of Glaciology, 18(78), 101-116.

Porter, S.C. (2001), Snowline depression in the tropics during the Last Glaciation. Quaternary Science Reviews, 20, 1067-1091.

Posamentier, H.W. (1977), A new climatic model for glacier behavior of the Austrian Alps. Journal of Glaciology, 18(78), 57-65.

Prentice, M.L., and R.K. Matthews (1991), Tertiary ice sheet dynamics: The snow gun hypothesis. Journal of Geophysical Research, 96(B4), 6811-6827.

Przybylak, R. (2002), Variability of total and solid precipitation in the Canadian Arctic from 1950 to 1995. International Journal of Climatology, 22, 395-420.

Ragle, R.H., Blair, R.G., and L.E. Persson (1964), Ice core studies of Ward Hunt Ice Shelf, 1960. Journal of Glaciology, 5(37), 39-59.

Raper, S.C.B., and R.J. Braithwaite (2005a), The potential for sea level rise: New estimates from glacier and ice cap area and volume distributions. Geophysical Research Letters, 32(L05502), doi: 10.1029/2004GL021981.

Raper, S.C.B., and R.J. Braithwaite (2005b), Reply to comment by M.F. Meier *et al.* on 'The potential for sea level rise: New estimates from glacier and ice cap area and volume distributions'. Geophysical Research Letters, 32(L17502), doi: 10.1029/2005GL023460.

Raper, S.C.B., and R.J. Braithwaite (2006), Low sea level rise projections from mountain glaciers and icecaps under global warming. Nature, 439, 311-313.

Raper, S.C.B., Briffa, K.R., and T.M.L. Wigley (1996), Glacier change in northern Sweden from AD 500: a simple geometric model of Storglaciären. Journal of Glaciology, 42(141), 341-351.

Raper, S.C.B., Brown, O., and R.J. Braithwaite (2000), A geometric glacier model for sea-level change calculations. Journal of Glaciology, 46(154), 357-368.

Rea, B.R., Whalley, W.B., Evans, D.J.A., Gordon, J.E., and D.A. McDougall (1998), Plateau Ice fields: Geomorphology and Dynamics. Quaternary Proceedings, 6, 35-54.

Reasoner, M.A., Davis, P.T., and G. Osborn (2001), Evaluation of proposed early-Holocene advances of alpine glaciers in the North Cascade Range, Washington State, USA: constraints provided by palaeo-environmental reconstructions. The Holocene, 11(5), 607-611.

Reeh, N. (1991), Parameterization of melt rate and surface temperature on the Greenland ice sheet. Polarforschung, 59(3), 113-128.

Reynaud, L., Vallon, M., Martin, S., and A. Letreguilly (1984), Spatio Temporal distribution of the glacial mass balance in the Alpine, Scandinavian and Tien Shan Areas. Geografiska Annaler, 66A(3), 239-247.

Reynolds, J.M. (1981), The distribution of mean annual temperatures in the Antarctic Peninsula. British Antarctic Survey Bulletin, 54, 123-133.

Rial, J.A., Pielke Sr., R.A., Beniston, M., Claussen, M., Canadell, J., Cox, P., Held, H., de Noblet-Ducoudre, N., Prinn, R., Reynolds, J.F., and J.D. Salas (2004), Nonlinearities, feedbacks, and critical thresholds within the Earth's climate system. Climatic Change, 65, 11-38.

Ridley, J.K., Huybrechts, P., Gregory, J.M., and J.A. Lowe (2005), Elimination of the Greenland Ice Sheet in a High CO_2 Climate. Journal of Climate, 18(17), 3409-3427.

Rignot, E., and P. Kanagaratnam (2006), Changes in the Velocity Structure of the Greenland Ice Sheet. Science, 311, 986-990.

Rignot, E., Casassa, G., Gogineni, P., Krabill, W., Rivera, A., and R. Thomas (2004), Accelerated ice discharge from the Antarctic Peninsula following the collapse of the Larsen B ice shelf. Geophysical Research Letters, 31(L18401), doi: 10.1029/2004GL020697.

Ritz, C., Fabre, A., and A. Letreguilly (1997), Sensitivity of a Greenland ice sheet model to ice flow and ablation parameters: consequences for the evolution through the last climatic cycle. Climate Dynamics, 13, 11-24.

Robock, A. (1980), The Seasonal Cycle of Snow Cover, Sea Ice, and Surface Albedo. Monthly Weather Review, 108(3), 267-285.

Robock, A. (1983), Ice and Snow Feedbacks and the Latitudinal and Seasonal Distribution of Climate Sensitivity. Journal of the Atmospheric Sciences, 40, 986-997.

Rosqvist, G., and G. Østrem (1989), The sensitivity of a small ice cap to climatic fluctuations. Geografiska Annaler, 71A(1), 99-103.

Rothrock, D.A., Yu, Y., and G.A. Maykut (1999), Thinning of the Arctic sea ice cover. Geophysical Research Letters, 26(23), 3469-3472.

Ruddiman, W.F., and A. McIntyre (1979), Warmth of the subpolar North Atlantic Ocean during Northern Hemisphere ice-sheet growth. Science, 204, 173-175.

Ruddiman, W.F., and A. McIntyre (1981), Oceanic mechanism for amplification of the 23000 year ice-volume cycle. Science, 212, 617-627.

Ruddiman, W.F., Vavrus, S.J., and J.E. Kutzbach (2005), A test of the overdue-glaciation hypothesis. Quaternary Science Reviews, 24, 1-10.

Sagar, R.B. (1962), Meteorological and Glaciological Studies Ice Rise Station, Ward Hunt Island, May to September 1960. *Research Paper No. 24*, Arctic Institute of North America, University of Calgary, Calgary, Alberta, Canada, 87 pp.

Sagar, R.B. (1964), Meteorological and glaciological observations on the Gilman Glacier, northern Ellesmere Island, 1961. Geographical Bulletin, 22(1), 13-56.

Sagar, R.B. (1966), Glaciological and climatological studies on the Barnes Ice Cap, 1962-64. Geographical Bulletin, 8(1), 3-47.

Sato, A., Takahashi, S., Naruse, R., and G. Wakahama (1984), Ablation and heat balance of the Yukikabe snow patch in the Daisetsu Mountains, Hokkaido, Japan. Annals of Glaciology, 5, 122-126.

Savoskul, O.S. (1997), Modern and Little Ice Age glaciers in 'humid' and 'arid' areas of the Tien Shan, Central Asia: two different patterns of fluctuations. Annals of Glaciology, 24, 142-147.

Scambos, T.A., Hulbe, C., Fahnestock, M., and J. Bohlander (2000), The link between climate warming and break-up of ice shelves in the Antarctic Peninsula. Journal of Glaciology, 46(154), 516-530.

Scambos, T. A., Bohlander, J.A., Shuman, C.A., and P. Skvarca (2004), Glacier acceleration and thinning after ice shelf collapse in the Larsen B embayment, Antarctica. Geophysical Research Letters, 31(L18402), doi: 10.1029/2004GL020670.

Schaper, J., Martinec, J., and K. Seidel (1999), Distributed mapping of snow and glaciers for improved runoff modelling. Hydrological Processes, 13, 2023-2031.

Schneeberger, C., Albrecht, O., Blatter, H., Wild, M., and R. Hock (2001), Modelling the response of glaciers to a doubling in atmospheric CO2: a case study of Storglaciären, northern Sweden. Climate Dynamics, 17, 825-834.

Schneeberger, C., Blatter, H., Abe-Ouchi, A., and M. Wild (2003), Modelling changes in the mass balance of glaciers of the northern hemisphere for a transient 2 x CO_2 scenario. Journal of Hydrology, 282, 145-163.

Schneider, C. (1999), Energy balance estimates during the summer season of glaciers of the Antarctic Peninsula. Global and Planetary Change, 22, 117-130.

Schytt, V. (1949), Refreezing of melt water on the surface of glacier ice. Geografiska Annaler, 31, 222-227.

Schytt, V. (1964), Scientific results of the Swedish Glaciological Expedition to Nordaustlandet, Spitsbergen, 1957 and 1958. Geografiska Annaler, 46(3), 243-281.

Schytt, V. (1967), A study of 'ablation gradient'. Geografiska Annaler, 49A(2-4), 327-332.

Sellers, W.D. (1973), A New Global Climate Model. Journal of Applied Meteorology, 12(2), 241-254.

Sellers, W.D., and W. Liu (1988), Temperature patterns and trends in the upper atmosphere and lower troposphere. Journal of Climate, 1(6), 573-581.

Serreze, M.C. (1985), Topoclimatic investigations of a small, sub-polar ice cap with implications for glacierization. M.Sc. thesis, University of Massachusetts, Amherst, Massachusetts, 201 pp.

Serreze, M.C., and R.S. Bradley (1987), Radiation and cloud observations on a High Arctic plateau ice cap. Journal of Glaciology, 33(114), 162-168.

Serreze, M.C., Walsh, J.E., Chapin III, F.S., Osterkamp, T., Dyurgerov, M., Romanovsky, V., Oechel, W.C., Morison, J., Zhang, T., and R.G. Barry (2000), Observational Evidence of Recent Change in the Northern High-Latitude Environment. Climatic Change, 46(1-2), 159-207.

Serreze, M.C., Maslanik, J.A., Scambos, T.A. Fetterer, F., Stroeve, J., Knowles, K., Fowler, C., Drobot, S., Barry, R.G., and T.M. Haran (2003), A record minimum sea ice extent in 2002. Geophysical Research Letters, 30(3), doi: 10.1029/2002GL016406.

Serson, H.V. (1979), Mass Balance of the Ward Hunt ice rise and ice shelf: an 18-year record. Defence Establishment Pacific, Victoria, Victoria, British Columbia, Canada, 14 pp.

Shabbar, A., Higuchi, K., Skinner, W., and J.L. Knox (1997), The association between the BWA index and winter surface temperature variability over eastern Canada and west Greenland. International Journal of Climatology, 17, 1195-1210.

Shahgedanova, M., Stokes, C.R., Gruney, S.D., and V. Popovnin (2005), Interactions between mass balance, atmospheric circulation, and recent climate change on the Djankuat Glacier, Caucasus Mountains, Russia. Journal of Geophysical Research, 110(D04108), doi: 10.1029/2004JD005213.

Sharp, R.P. (1956), Glaciers in the Arctic. Arctic, 9(1-2), 78-117.

Shea, J.M., Marshall, S.J., and J.M. Livingston (2004), Glacier Distributions and Climate in the Canadian Rockies. Arctic, Antarctic, and Alpine Research, 36(2), 272-279.

Shepherd, A., Wingham, D., Payne, T., and P. Skvarca (2003), Larsen Ice Shelf Has Progressively Thinned. Science, 302, 856-859.

Shumskii, P.A. (1964), *Principles of Structural Glaciology*. Dover Publications, New York, 497 pp.

Siddall, M. (2005), The riddle of the sediments. Nature, 437, 39-41.

Shiklomanov, H.I., and F.E. Nelson (2003), Climatic Variability in the Kuparuk Region, North-Central Alaska: Optimizing Spatial and Temporal Interpolation in a Sparse Observation Network. Arctic, 56(2), 136-146.

Singh, P., Kumar, N., and M. Arora (2000), Degree-day factors for snow and ice for Dokriani Glacier, Garhwal Himalayas. Journal of Hydrology, 235, 1-11.

Sissons, J.B. (1979), Palaeoclimatic inferences from former glaciers in Scotland and the Lake District. Nature, 278, 518-521.

Small, E.E. (1995), Hypsometric forcing of stagnant ice margins: Pleistocene valley glaciers, San Juan Mountains, Colorado. Geomorphology, 14, 109-121.

Smedsrud, L.H., Jenkins, A., Holland, D.M., and O.A. Nost (2006), Modeling ocean processes below Fimbulisen, Antarctica. Journal of Geophysical Research, 111(C01007), doi: 10.1029/2005JC002915.

Smith, I.R. (1999), Late Quaternary glacial history of Lake Hazen Basin and eastern Hazen Plateau, northern Ellesmere Island, Nunavut, Canada. Canadian Journal of Earth Science, 36, 1547-1565.

Smith, I.R. (2002), Diatom-based Holocene paleoenvironmental records from continental sites on northeastern Ellesmere Island, high Arctic, Canada. Journal of Paleolimnology, 27, 9-28.

Smith, L.C., Sheng, Y., Forster, R.R., Steffen, K., Frey, K.E., and D.E. Alsdorf (2004), Melting of small Arctic ice caps observed from ERS scatterometer time series. Geophysical Research Letters, 30(20), doi: 10.1029/2003GL017641.

Smith, S.V., Bradley, R.S., and M.B. Abbott (2004), A 300 year record of environmental change from Lake Tuborg, Ellesmere Island, Nunavut, Canada. Journal of Paleolimnology, 32, 137-148.

Souchez, R. (1997), The buildup of the ice sheet in central Greenland. Journal of Geophysical Research, 102(C12), 26317-26323.

Steffen, K., and J. Box (2001), Surface climatology of the Greenland ice sheet: Greenland Climate Network 1995-1999. Journal of Geophysical Research, 106(D24), 33951-33964.

Strahler, A.N. (1987), *Science and Earth History: The Evolution – Creation Controversy*. Prometheus Books, Buffalo, New York, 552 pp.

Strasser, U., Corripio, J., Pellicciotti, F., Burlando, P., Brock, B., and M. Funk (2004), Spatial and temporal variability of meteorological variables at Haut Glacier d'Arolla (Switzerland) during the ablation season 2001: Measurements and simulations. Journal of Geophysical Research, 109(D03103), doi: 10.1029/2003JD003973.

Stroeven, A.P., Fabel, D., and S.J. Marshall (2002), Inceptions, mechanisms, patterns, and timing of ice sheet inceptions. Quaternary International, 95-96, 1-4.

Sugden, D.E., Hulton, N.R.J., and R.R. Purves (2002), Modelling the inception of the Patagonian icesheet. Quaternary International, 95-96, 55-64.

Sutherland, D.G. (1984), Modern glacier characteristics as a basis for inferring former climates with particular reference to the Loch Lomond Stadial. Quaternary Science Reviews, 3, 291-309.

Takahara, H., and K. Higuchi (1985), Thermal modification of air moving over melting snow surfaces. Annals of Glaciology, 6, 235-237.

Takeuchi, Y., Naruse, R., Satow, K., and N. Ishikawa (1999), Comparison of heat balance characteristics at five glaciers in the Southern Hemisphere. Global and Planetary Change, 22, 201-208.

Tangborn, W. (1980), Two models for estimating climate-glacier relationships in the North Cascades, Washington, U.S.A. Journal of Glaciology, 25(91), 3-21.

Tarasov, L., and W.R. Peltier (1997), Terminating the 100 kyr ice age cycle. Journal of Geophysical Research, 102, 21665-21693.

Tarasov, L., and W.R. Peltier (2005), Arctic freshwater forcing of the Younger Dryas cold reversal. Nature, 435, 662-665.

Tarr, R.S. (1897), Difference in the climate of the Greenland and American sides of Davis and Baffin Bay. American Journal of Science, Series 4, 3, 315-320.

Taurisano, A., Bøggild, C.E., and H.G. Karlsen (2004), A century of climate variability and climate gradients from coast to ice sheet in west Greenland. Geografiska Annaler, 86A(2), 217-224.

Thomas, R.H. (1973), The creep of ice shelves: Theory. Journal of Glaciology, 12(64), 45-53.

Thomas, R.H., and 17 others (2004), Accelerated Sea-Level Rise from West Antarctica. Science, 306, 255-258.

Thorarinsson, S. (1940), Present glacier shrinkage, and eustatic changes of sea-level. Geografiska Annaler, 22, 131-159.

Tjernström, M., Leck, C., Persson, P.O.G., Jensen, M.L., Oncley, S.P., and A. Targino (2004), The Summertime Arctic Atmosphere: Meteorological Measurements during the Arctic Ocean Experiment 2001. Bulletin of the American Meteorological Society, 85(9), 1305-1321.

Tremblay, L.B., Mysak, L.A., and A.S. Dyke (1997), Evidence from driftwood records for century-to-millennial scale variations of high latitude atmospheric circulation during the Holocene. Geophysical Research Letters, 24, 2027-2030.

van den Broeke, M. (1996), Characteristics of the lower ablation zone of the West Greenland ice sheet for energy-balance modeling. Annals of Glaciology, 23, 160-166.

van der Veen, C.J. (1999a), Evaluating the performance of cryospheric models. Polar Geography, 23, 83-96.

van der Veen, C.J. (1999b), *Fundamentals of Glacier Dynamics*. A.A. Balkema, Rotterdam, Netherlands, 472 pp.

van der Veen, C.J. (2002a), Calving glaciers. Progress in Physical Geography, 26(1), 96-122.

van der Veen, C.J. (2002b), Polar ice sheets and global sea level: how well can we predict the future? Global and Planetary Change, 32, 165-194.

van de Wal, R.S.W. (1996), Mass-balance modeling of the Greenland ice sheet: a comparison of an energy-balance and a degree-day model. Annals of Glaciology, 23, 36-45.

van de Wal, R.S.W., and J. Oerlemans (1994), An energy balance model for the Greenland ice sheet. Global and Planetary Change, 9, 115-131.

van de Wal, R.S.W., and M. Wild (2001), Modelling the response of glaciers to climate change by applying volume-area scaling in combination with a high resolution GCM. Climate Dynamics, 18, 359-366.

van de Wal, R.S.W., Oerlemans, J., and J.C. van de Hage (1992), A study of ablation variations on the tongue of Hintereisferner, Austrian Alps. Journal of Glaciology, 38(130), 319-324.

Vaughan, D.G., and C.S.M. Doake (1996), Recent atmospheric warming and retreat of ice shelves on the Antarctic Peninsula. Nature, 379, 328-331.

Vincent, W.F., Gibson, J.A.E., and M.O. Jeffries (2001), Ice-shelf collapse, climate change, and habitat loss in the Canadian high Arctic. Polar Record, 37(201), 133-142.

Vincent, C., Kappenberger, G., Valla, F., Bauder, A., Funk, M., and E. Le Meur (2004), Ice ablation as evidence of climate change in the Alps over the 20th century. Journal of Geophysical Research, 109(D10104), doi: 10.1029/2003JD003857.

Vinnikov, K.Y., Robock, A., Stouffer, R.J., Walsh, J.E., Parkinson, C.L., Cavalieri, D.J., Mitchell, J.F.B., Garrett, D., and V.F. Zakharov (1999), Global Warming and Northern Hemisphere sea ice extent. Science, 286, 1934-1937.

Wadham, J.L., and A.M. Nuttall (2002), Multiphase formation of superimposed ice during a mass-balance year at a maritime high-Arctic glacier. Journal of Glaciology, 48(163), 545-551.

Wakahama, G., Kuroiwa, D., Hasemi, T., and C.S. Benson, (1976), Field observations and experimental and theoretical studies on the superimposed ice of McCall Glacier, Alaska. Journal of Glaciology, 16(74), 135-149.

Walcher, J. (1773), *Nachrichten von den Eisbergen in Tyrol.* Joseph Kurzböck, Vienna, Austria.

Wallace, J.E., Zhang, Y., and L. Bajuk (1996), Interpretation of Interdecadal Trends in Northern Hemisphere Surface Air Temperature. Journal of Climate, 9, 249-259.

Walsh, J.E. (2005), Cryosphere and Hydrology. In *Arctic Climate Impact Assessment – Scientific Report*, Cambridge University Press, New York, 183-242.

Walsh, J.E., and M.S. Timlin (2003), Northern Hemisphere sea ice simulations by global climate models. Polar Research, 22(1), 75-82.

Walsh, J.E., Kattsov, V.M., Chapman, W.L., Govorkova, V., and T. Pavlova (2002), Comparison of Arctic Climate Simulations by Uncoupled and Coupled Global Models. Journal of Climate, 15, 1429-1446.

Walters, R.A., and M.F. Meier (1989), Variability of glacier mass balances in western North America. In *Aspects of Climate Variability in the Pacific and Western Americas, Geophysical Monograph Series*, vol. 55, edited by D.H. Peterson, American Geophysical Union, Washington, D.C., 365-374.

Wang, X., and J.R. Key (2003), Recent Trends in Arctic Surface, Cloud, and Radiation Properties from Space. Science, 299, 1725-1728.

Wang, L., Sharp, M.J., Rivard, B., Marshall, S., and D. Burgess (2005), Melt season duration on the Canadian Arctic ice caps, 2000-2004. Geophysical Research Letters, 32(L19502), doi: 10.1029/2005GL023962.

Ward, W.H. (1954), Glaciological studies in the Penny highland, Baffin Island 1953. International Association of Hydrological Sciences (IAHS) Publication, 39, 297-308.

Ward, W.H., and S. Orvig (1953), The glaciological studies of the Baffin Island Expedition, 1950. Part IV: The heat exchange at the surface of the Barnes Ice Cap during the ablation season. Journal of Glaciology, 2(13), 158-168.

Ward, W.H., and P.D. Baird (1954), A description of the Penny Ice Cap, its accumulation and ablation. Journal of Glaciology, 2(15), 342-355.

Warren, C.R. (1991), Terminal environment, topographic control and fluctuations of West Greenland glaciers. Boreas, 20, 1-15.

Weber, S.L., and J. Oerlemans (2003), Holocene glacier variability: three case studies using an intermediate-complexity climate model. The Holocene, 13(3), 353-363.

Weertman, J. (1957), Deformation of floating ice shelves. Journal of Glaciology, 3(21), 38-42.

Weidick, A. (1975), A review of Quaternary investigations in Greenland. *Misc. Papers 145*, Geological Survey of Denmark and Greenland, Copenhagen, Denmark, 161 pp.

Weidick, A. (1984), Studies of glacier behavior and glacier mass balance in Greenland – A review. Geografiska Annaler, 66A(3), 183-195.

Wendler, G. (1974), A note on the advection of warm air towards a glacier. A contribution to the International Hydrological Decade. Zeitschrift für Gletscherkunde und Glazialgeologie, 10, 199-205.

Wendler, G., Ishikawa, N., and Y. Kodama (1988), The Heat Balance of the Icy Slope of Adelie Land, Eastern Antarctica. Journal of Applied Meteorology, 27, 52-65.

Wexler, H. (1960), Heating and Melting of Floating Ice Shelves. Journal of Glaciology, 3(27), 626-645.

Whalley, W.B., Gordon, J.E., and D.L. Thompson (1981), Periglacial features on the margins of a receding plateau ice cap, Lyngen, North Norway. Journal of Glaciology, 27(97), 492-496.

Whalley, W.B., Gordon, J.E., and A.F. Gellalty (1989), Effects of topographic and climatic controls on 19th and 20th century glacier changes in the Lyngen and Bergsfjord areas, North Norway. In *Glacier Fluctuations and Climatic Change*, edited by J. Oerlemans, Kluwer, Dordrecht, Netherlands, 153-172.

Whalley, W.B., Gordon, J.E., Gellatly, A.F., and J.G. Hansom (1995), Plateau and valley glaciers in North Norway: Responses to climate change over the last 100 years. Zeitschrift für Gletscherkunde und Glazialgeologie, 31, 115-124.

Wilcox, B.P., Seyfried, M.S., and T.H. Matison (1991), Searching for Chaotic Dynamics in Snowmelt Runoff. Water Resources Research, 27(6), 1005-1010.

Wild, M., Calanca, P., Scherrer, S.C., and A. Ohmura (2003), Effects of polar ice sheets on global sea level in high-resolution greenhouse scenarios. Journal of Geophysical Research, 108(D5), doi: 10.1029/2002JD002451.

Williams, L.D. (1978a), The Little Ice Age Glaciation Level on Baffin Island, Arctic Canada. Palaeogeography, Palaeoclimatology, Palaeoecology, 25, 199-207.

Williams, L.D. (1978b), Ice-Sheet Initiation and Climatic Influences of Expanded Snow Cover in Arctic Canada. Quaternary Research, 10, 141-149.

Williams, L.D. (1979), An Energy Balance Model of Potential Glacierization of Northern Canada. Arctic and Alpine Research, 11(4), 443-456.

Williams, K.S., and D.G. Tarboton (1999), The ABC's of snowmelt: a topographically factorized energy component snowmelt model. Hydrological Processes, 13, 1905-1920.

Willis, I.C., Sharp, M.J., and K.S. Richards (1991/1992), Studies of the water balance of Midtdalsbreen, Hardangerjökulen, Norway. I. The calculation of surface water inputs from basic meteorological data. Zeitschrift für Gletscherkunde und Glazialgeologie, 27/28(1), 97-115.

Winton, M. (2006), Amplified Arctic climate change: What does surface albedo feedback have to do with it? Geophysical Research Letters, 33(L03701), doi: 10.1029/2005GL025244.

Wolfe, P.M. (1995), Hydrometeorological investigations on a small valley glacier in the Sawtooth Range, Ellesmere Island, Northwest Territories. M.A. thesis, Wilfried Laurier University, Waterloo, Ontario, Canada, 205 pp.

Wolfe, P.M., and M.C. English (1995), Mass balance of a small valley glacier in the Canadian High Arctic, Ellesmere Island, Northwest Territories. Zeitschrift für Gletscherkunde und Glazialgeologie, 31, 93-103.

Wolken, G.J., England, J.H., and A.S. Dyke (2005), Re-evaluating the relevance of vegetation trimlines in the Canadian Arctic as an indicator of Little Ice Age paleoenvironments. Arctic, 58(4), 341-343.

Woo, M-K., and R. Heron (1981), Occurrence of ice layers at the base of High Arctic snow packs. Arctic, Antarctic, and Alpine Research, 13(2), 225-230.

Woo, M-K., and S.B. McCann (1994), Climatic variability, climatic change, runoff, and suspended sediment regimes in northern Canada. Physical Geography, 15(3), 201-226.

Woo, M-K., Heron, R., and P. Marsh (1982), Basal Ice in High Arctic Snow Packs. Arctic, Antarctic, and Alpine Research, 14(3), 251-260.

Woodward, J. (1995), The influence of superimposed-ice formation on the sensitivity of glacier mass balance to climate change. M.Sc. thesis, University of Alberta, Edmonton, Alberta, Canada, 96 pp.

Woodward, J., Sharp, M., and A. Arendt (1997), The influence of superimposed-ice formation on the sensitivity of glacier mass balance to climate change. Annals of Glaciology, 24, 186-190.

Wright, J. (1940), South-East Ellesmere Island. The Geographical Journal, 95(4), 278-291.

Wright, A., Wadham, J., Siegert, M., Luckman, A., and J. Kohler (2006), Modelling the Impact of Superimposed Ice on the Mass Balance of an Arctic Glacier under Scenarios of Future Climate Change. Annals of Glaciology, 42, in press.

Yang, D., and M.-K Woo (1999), Representativeness of Local Snow Data for Large Scale Hydrologic Investigation. Hydrological Processes, 13, 1967-1978.

Young, G.J. (1982), Hydrological relationships in a glacierized mountain basin. International Association of Hydrological Sciences (IAHS) Publication, 138, 51-59.

Zeeberg, J., and S.L. Forman (2001), Changes in glacier extent on north Novaya Zemlya in the twentieth century. The Holocene, 11(2), 161-175.

Ziaja, W. (2001), Glacial Recession in Sørkappland and Central Nordenskiöldland, Spitsbergen, Svalbard, during the 20th century. Arctic, Antarctic, and Alpine Research, 33(1), 36-41.

Zweck, C., and P. Huybrechts (2005), Modeling of the northern hemisphere ice sheets during the last glacial cycle and glaciological sensitivity. Journal of Geophysical Research, 110(D07103), doi: 10.1029/2004JD005489.

Zhang, X., Vincent, L.A., Hogg, W.D., and A. Niitsoo (2000), Temperature and Precipitation Trends in Canada During the 20th Century. Atmosphere-Ocean, 38(3), 395-429.